



University of Strathclyde

Department of Pure and Applied Chemistry

**The design, synthesis and optimisation of
CCR4 antagonists for the treatment of
asthma**

Thesis submitted to the University of Strathclyde in fulfilment of the
requirements for the degree of Doctor of Philosophy

Afjal Hussain Miah

Declaration of Copyright

This thesis is the result of the author's original research. It has been composed by the author and has not been previously submitted for examination which has led to the award of a degree.

The copyright of this thesis belongs to the author under the terms of the United Kingdom Copyright Acts as qualified by University of Strathclyde Regulation 3.50. Due acknowledgement must always be made of the use of any material contained in, or derived from, this thesis.

Signed:

Date:

Acknowledgements

I would like to offer my sincere gratitude to my supervisors, Prof. Jonathan Percy and Dr Pan Procopiou for their support throughout the last few years. Their guidance with every aspect of my PhD programme has been invaluable.

I am particularly grateful to Dr Harry Kelly for giving me the opportunity to be a part of the PhD programme at GlaxoSmithKline, and I would like to express my deepest gratitude towards him and the staff at the University of Strathclyde for setting up the collaborative PhD programme and for providing their continuous support and encouragement.

I would like to thank the chemical arrays team at GlaxoSmithKline, especially Heather Barnett for her contribution to the CCR4 programme. Stephen Richards, Sean Lynn, Dr Roy Copley and Dr Bill Leavens provided their support with analytical problems and I am most grateful for all of the expertise they offered. My sincere thanks also goes to Dr Nick Barton for the computational modelling work, Rebecca Graves for the pharmacokinetic work, and Dr Alison Ford, Dr Malcolm Begg, Rob Slack and Michael Hasse for the *in vitro* and *in vivo* biological work on the programme.

I would also like to thank my fellow colleagues, lab members, past and present, for their assistance and support over the years, especially Dr Simon Hodgson, Dr John Harling, Ian Smith, Dr Sebastien Campos, Dr Chris Tame, Dr Mubina Mohammed and Dr Lena Shukla.

I would like to thank my parents, Arju Miah and Hana Begum, and all my family and friends for their continuous support and encouragement throughout the years.

Finally, I would like to thank my loving wife, Sultana Laila Begum, son, Arif Miah, and daughters, Amara Miah and Amelia Miah for sticking with me through all the good and bad times, and apologies for taking so much time away from them to write my thesis. You guys were very patient and never failed to lift my spirit.

1.0 Abstract

The 7-transmembrane chemokine receptor, CCR4 is differentially expressed on T helper type 2 (T_H2) cells; together with its endogenous ligands, CCL17 and CCL22, it promotes activation and recruitment of T_H2 cells into the lungs. Infiltration of T_H2 cells into the airways is an important characteristic of allergic asthma, so inhibition of CCR4 binding to its endogenous ligands might provide a potential therapeutic target for treating the disease.

In order to identify a potential back-up to the clinical development candidate, *N*-(3-((3-(5-chlorothiophene-2-sulfonamido)-4-methoxy-1*H*-indazol-1-yl)methyl)benzyl)-2-hydroxy-2-methylpropanamide (**6**), a library of 2,3-dichlorobenzene sulfonamides were designed. Synthesis and evaluation of the 'hits' in the primary antagonist assay (GTPγS) led to the identification of three novel templates with good potency and ligand efficiency (LE). The benzimidazolone template, exemplified by **88** (2,3-dichloro-*N*-(6-methoxy-2-oxo-2,3-dihydro-1*H*-benzo[d]imidazol-5-yl)benzenesulfonamide), demonstrated a good PK profile (low clearance, moderate to high oral bioavailability) in both rat and dog, and had better potency in the human whole blood (hWB) assay compared to the other two series, and hence was explored further. Investigation of substituents of the benzimidazolone series, and incorporation of nitrogen into the core led to the discovery of **239** (2,3-dichloro-*N*-(6-methoxy-2-oxo-2,3-dihydro-1*H*-imidazo[4,5-*b*]pyridin-5-yl)benzenesulfonamide), which had a pA₂ value of 6.0 in the hWB assay and a much improved LE (0.43) compared to indazole **6** (LE = 0.30). The azabenzimidazolone **239** provides a new starting point for further lead optimisation to develop a novel allosteric CCR4 antagonist from which a potential oral asthma drug could emerge.

A phenylpyrazole sulfonamide (*N*-(2-(1*H*-pyrazol-1-yl)phenyl)phenylsulfonamide) was also identified, where X-ray diffraction studies showed that one of the nitrogens of the pyrazole ring forms an intramolecular hydrogen bond with the sulfonamide NH and promotes a conformation that was thought to be preferred in the active site. A SAR study around the phenylpyrazole core provided pyridine analogue **115** (*N*-(3-(1*H*-pyrazol-1-yl)pyridin-2-yl)-5-chlorothiophene-2-sulfonamide) with very good potency, high LE (0.47) and excellent physicochemical properties (chromlogD_{7.4} =

2.7, MW = 340, solubility = 133 µg/mL). Pyridylpyrazole **115** also represent good starting points for a lead optimisation programme.

In addition, a novel series of 2,8-diazaspiro[4.5]decan-8-yl)pyrimidin-4-amine inhibitors, were identified using computational modelling studies, which bind to a different allosteric region on the CCR4 receptor compared to indazole **6**. Evaluation of SAR led to identification of several analogues that exhibited hWB activity superior or comparable to that of **6**. The most potent compound, **282** (*N*-(2,4-dichlorobenzyl)-2-(2-(pyrrolidin-2-ylmethyl)-2,8-diazaspiro[4.5]decan-8-yl)pyrimidin-4-amine, hWB pA₂ = 6.7) demonstrated anti-inflammatory activity in acute *in vivo* murine allergic inflammation models. After an ovalbumin challenge in mice, compound **282** showed not only significant reduction in eosinophil and lymphocyte infiltration into the bronchoalveolar lavage (BAL) fluid but also displayed a profound effect on airway hyperreactivity, returning the levels back to the control line. The *in vivo* results indicate that targeting CCR4 with a small molecule allosteric antagonist could be a potential novel way of treating allergic diseases such as asthma. Interestingly, representative compounds from the spiro-pyrimidine series were found to induce receptor internalisation of CCR4 in HUT78 cell with approximately 50% reduction of cell surface receptor. It is suggested that *in vivo* activity of **282** might be due to its ability to induce internalisation of the receptor.

Contents

2.0 Abbreviations and symbols.....	8
3.0 Introduction - Asthma	10
3.1 The allergic cascade.....	11
3.2 Complexity of asthma	13
3.3 Treatments of asthma.....	14
4.0 Chemokines and chemokine receptors.....	17
4.1 The chemokine receptor 4 (CCR4)	22
4.2 CCR4, a 7 transmembrane receptor	24
4.3 Structure of CCR4.....	25
4.4 Biological assays (see experimental section for full details)	28
5.0 Ligand efficiency and lipophilic ligand efficiency	30
6.0 Programme goals for CCR4.....	31
7.0 Results and discussion – identification of the sulfonamide ‘hits’	35
7.1 Potential uses of an intramolecular hydrogen bond	42
7.2 Introduction of intramolecular hydrogen bond interaction in phenyl sulfonamide.....	44
7.3 First approach to improving potency – 5-chlorothiophene sulfonamide analogues	51
7.4 Second approach to improving potency – introduction of a methoxy group	52
7.5 Pyrazole as hydrogen bond acceptor for the 4-aminoindazole series	68
7.6 Phenylpyrazole template	70
7.7 Pharmacokinetic studies.....	76
7.8 The pyrazolopyrimidine series	78
7.9 The benzimidazolone series	92
7.10 The azabenzimidazolone series.....	104
8.0 Extracellular allosteric CCR4 antagonists.	110
8.1 CCR4 binding Site 1	112
8.2 Design of novel Site 1 antagonists	115
8.3 SPA binding data of new analogues	122
8.4 The spiro-pyrimidine template.....	124
8.5 Changes to the terminal proline group.....	126
8.6 Variation of the benzyl group	129
8.7 Removal of the proline carbonyl group.	133
8.8 Core changes.....	137
8.9 Changes to the left wing benzylamine NH of the spiro-pyrimidine series.	141

8.10 GTP γ S and human whole blood data	144
8.11 Pharmacokinetic studies of the spiro-pyrimidine series.....	145
8.12 Site 1 antagonists induce CCR4 internalisation	146
8.13 <i>In vivo</i> studies	148
9.0 Conclusion	153
10.0 Experimental section.....	158
10.1 Biological assays.....	158
10.2 Pharmacokinetics ¹³²	159
10.3 Physicochemical assays ⁹⁰	160
10.4 <i>In vivo</i> experiments ¹⁷¹	160
10.5 Chemistry	161
References:.....	322
Appendix 1	332
Appendix 2.....	336

2.0 Abbreviations and symbols

The following list provides definitions of certain abbreviations as used herein.

7TM (7 transmembrane)

AHR (Airway hyperresponsiveness)

AMD (Age-related macular degeneration)

APC (Antigen-presenting cell)

cAMP (cyclic adenosine monophosphate)

CCR4 (CC-chemokine receptor 4)

CDI (1,1'-Carbonyldiimidazole)

CLND (ChemiLuminescent Nitrogen Detection)

cod (Cycloocta-1,5-diene)

CV (Column volume)

DEAD (Diethyl azodicarboxylate)

DIAD (*Diiso*-propyl azodicarboxylate)

dppf (1,1'-*Bis*(diphenylphosphino) ferrocene)

equiv. (Equivalent)

FDA (Food and drug administration)

GDP (guanosine diphosphate)

GPCR (G-protein coupled receptor)

GTP (guanosine triphosphate)

HAC (Heavy atom count)

HATU [*O*-(7-azabenzotriazol-1-yl)-*N, N, N', N'*-tetramethyluronium hexafluorophosphate]

HIV (Human immunodeficiency virus)

HMBC (Heteronuclear multiple bond correlation)

HMQC (Heteronuclear multiple quantum coherence)

HSA (Human serum albumin)

IgE (Immunoglobulin E)

IL-1 (Interleukin 1)

L (ligand)

LABA (Long acting β_2 adrenoreceptor agonists)

mAbs (monoclonal antibodies)

MDAP (Mass directed auto-preparative HPLC)

MDC (Macrophage-derived chemokine)

MDCK (Madin Darby canine kidney)

nd (not determined)

NOE (Nuclear Overhauser effect)

PK (pharmacokinetic)

PPB (Plasma protein binding)

RT (retention time)

SABA (Short acting β_2 adrenoreceptor agonists)

SAR (Structure-activity relationship)

SPE (Solid phase extraction)

TARC (Thymus activation-regulated chemokine)

T_H1 (T helper type 1)

T_H2 (T helper type 2)

TBAD (*tert*-butyl azodicarboxylate)

TBD (1,3,4,6,7,8-hexahydro-2*H*-pyrimido[1,2-*a*]pyrimidine)

UV (Ultra violet)

All references to ether are to diethyl ether, and brine refers to a saturated aqueous solution of NaCl.

3.0 Introduction - Asthma

Asthma is a condition that affects the airways of the lungs causing them to become inflamed and narrow. This leads to difficulty in breathing, and to wheezing, coughing and tightness in patients' chests. It affects around 300 million people worldwide and has increased considerably in prevalence over the last few years, particularly in young children.¹ When an individual comes into contact with an asthma trigger, the bronchioles of the lungs become irritated causing inflammation of the bronchiole muscle. The swelling from the inflammation narrows the airways. Also, the muscles around the walls tighten, constricting the airways further causing shortness of breath. In addition, the trigger causes the secretion of sticky mucus and phlegm to build up, which causes patients to cough, and further narrows their airways (Fig. 1). The inflammation can also damage the lining of the airways exposing sensory nerve endings; the exposure triggers the inflammatory response in asthma patients more strongly.

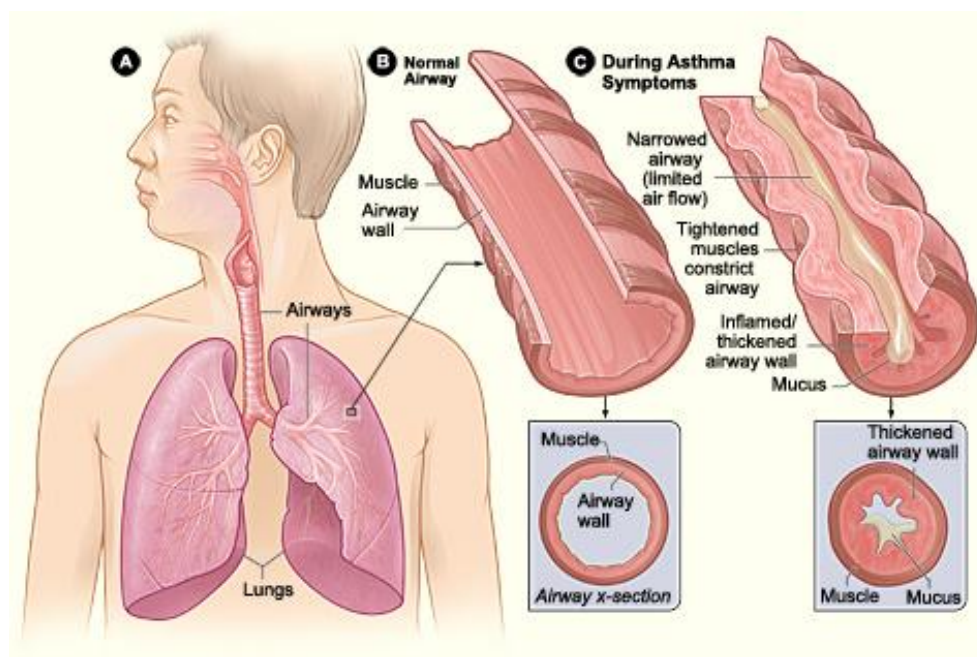


FIGURE 1. Comparison of the airways.² (A) Location of the lungs and the airways. (B) Cross-section of a normal airway. (C) Cross-section of an airway during asthma symptoms. Reproduce with permission.

Asthma is a chronic and complex disease characterised by airway inflammation, airway wall remodelling and airway hyperresponsiveness (AHR).³ AHR is an exaggerated response to stimuli in which the bronchioles constrict. The stimuli could be an allergen, or a non-specific stimulus such as cold air or moisture, or a chemical such as a synthetic choline ester, methacholine, which is commonly used to diagnose bronchial AHR.^{4,5} The stimulus usually

has little or no effect on a normal individual but in an individual with asthma, the airflow to the lungs becomes severely restricted. In addition, after a long term unresolved airway inflammation, a number of structural wall changes occur in the airways of asthma patients, including thickening of the airway epithelium. This is generally described as ‘airway remodelling’. Airway remodelling is caused by immune cells and structural cells trying to repair the damage to the lining of the airways by triggering changes in the repair process. It is still unclear how these three key features interact or whether they are dependent on each other. However, it is quite clear that all of these important hallmarks of asthma are caused by a combination of environmental and genetic factors, and that they are orchestrated by both structural cells and the immune system.⁶

There are many different forms of asthma, including allergic and non-allergic asthma. Allergic asthma can be induced by common allergens such as house dust mites, pollen, ragweed and moulds. Non-allergic asthma can be induced by several factors such as air pollutants (cigarette smoke, ozone and diesel particles), infection and even exercise. These different phenotypes have different and distinct pathogenic pathways which often coexist and can act in synergy in patients.⁴

Nonetheless, over the past 30 years most research has been focused on allergic asthma, the most common form. A hallmark of allergic asthma is the presence of inflammatory cell infiltrates, most commonly, the granular leukocytes (eosinophils and basophils), and the T helper type 2 CD4+ lymphocytes (T_H2 cells) in the airways.⁷ In the mid-1980s, it emerged that specific cells, termed T_H2 cells existed, and that they were important in the pathogenesis of allergic asthma.⁸ These T_H2 cells produce immunomodulatory agents called cytokines that regulate important features of asthma. These include the production of the cytokine interleukin 4 (IL-4) which regulates the synthesis of antibodies called immunoglobulin E (IgE), IL-5 which is involved with the recruitment of eosinophils, IL-9 which aids in the recruitment and growth of mast cells, and IL-13 which is responsible for AHR.⁷

3.1 The allergic cascade

The allergen sensitisation process and the allergic immune response in humans are poorly understood. In recent years, mouse models have helped us to understand a lot more about allergic asthma. Allergen specific T_H2 cells can be induced by sensitising mice with a number of foreign proteins such as ovalbumin or house dust mite extract. This immunisation results in a T_H2 polarised response and the production of IgE. Once sensitised, a repeated

administration of the allergen leads to recruitment of T_H2 cells into the lungs, which causes the development of eosinophilic inflammation, mucus secretion, AHR and airway remodelling.^{3,4}

The sequence of events leading to the development of airway inflammation in allergic asthma is known as the allergic cascade (Fig. 2). Initially, processed allergens are presented to naïve T cells by antigen-presenting cells (APCs). This leads to the differentiation and activation of naïve T cells into T_H2 cells. Although pro-inflammatory cells, such as the eosinophils and basophils, can act as APCs, the lung dendritic cells are the main APCs that are necessary for induction of T_H2 driven response.⁹ They are found throughout the conducting airways and express many different receptors. Dendritic cells upregulate the expression of many co-stimulatory molecules and chemokines that attract T cells, eosinophils and basophils into the lung.

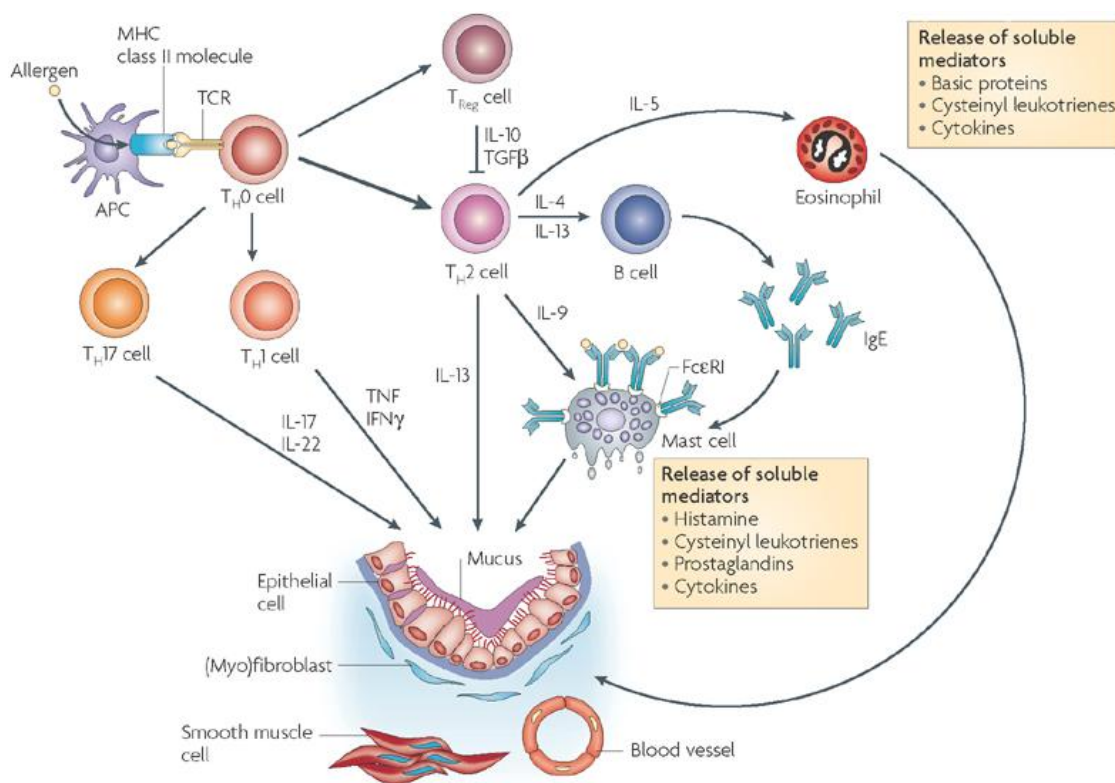


FIGURE 2. Mechanism of asthma. Reproduce with permission. (*Nature Rev. Immun.* **2008**, 8, 213-230)

Once the T_H2 cells are activated by APCs, the T_H2 cells then secrete cytokines such as IL-4, IL-5, IL-9 and IL-13. Also, IgE is synthesised (which requires IL-4 and IL-13) and both of these early processes are known as allergic sensitisation. Exposure to the same allergen again,

causes inflammatory cell recruitment and activation and the release of various hormonal mediators that are responsible for early and late allergic responses.

In the early allergic response, mast cells (which require IL-9) play a central role in the inflammatory processes.¹⁰ Mast cells express a high affinity receptor (FcεR1) for a specific region (Fc region) of IgE to bind. When naïve B cells are exposed to a particular allergen, they differentiate into an antibody producing cell called a plasma cell. The activated plasma cell secretes IgE, which binds to the FcεR1 region of the mast cell. After the sensitisation process, the mast cells remain inactive. Subsequent exposure to the allergen causes cross linking of the IgE that is bound to the mast cells FcεR1 region. This stimulates the release of granules and various bronchoconstrictor mediators such as histamine, prostaglandin D₂, leukotriene and cytokines, causing the characteristic symptoms of allergy in the so-called early phase.¹⁰ The early phase occurs within 1-30 minutes of exposure to an asthma trigger, and causes the constriction of airway smooth muscles, vascular leakages, and mucus production (Fig. 2).

The late phase allergic response is characterised by excessive inflammation of the airways resulting in further airway narrowing. This is induced by various mediators including chemoattractant cytokines called chemokines (see section 4.0), which are released by mast cells and other immune cells.¹¹ In the late allergic response, chemokines recruit eosinophils and T_H2 cells into the airways. This is a critical event that triggers and sustains the symptoms of allergic asthma.⁷ Eosinophils serve an important pro-inflammatory role by releasing soluble mediators including cysteinyl leukotrienes, basic proteins and cytokines such as IL-13, which are responsible for damaging the epithelial airway tissue. In some models of asthma (not all), eosinophils have been shown to be required for AHR.¹² However, the role of eosinophils in AHR has been controversial, as in the mouse model, it has been shown that AHR can occur without eosinophilic inflammation.¹³

3.2 Complexity of asthma

Over the past few years, there have been many clinical and experimental observations that have shown asthma to be a much more heterogeneous and complex disease than suggested by the T_H2 driven response.⁴ Non-allergic forms of asthma, triggered by environmental factors such as air pollutants, viral infections and stress, cause asthma independently of T_H2 cells. Patients with this type of asthma respond poorly to inhaled corticosteroids, the most common

therapy for asthma, which are normally highly efficacious in 90% of patients. Also, non T_H2 mediators, such as the cytokines, interferon- γ released by T_H1 cells, IL-17 and neutrophils are frequently found in the lungs of patients with asthma.⁴ These mediators are found at higher levels in patients with asthma resistant to inhaled corticosteroids also known as severe asthma. These observations suggest that it is very difficult to find a therapeutic approach that will treat all forms of asthma and it will be more valuable to identify different therapies for the different phenotypes of the disease.

3.3 Treatments of asthma

There is no cure for asthma and as symptoms for each individual can range from mild to moderate to severe, different approaches are necessary for effective management of the disease. For mild asthma sufferers, a simple and effective treatment is to identify the trigger and if possible, remove it from their environment. This works if the trigger is easily identifiable and can be avoided, such as animal hairs or cigarette smoke.

If identifying and removing the trigger is not effective, then there are many current drugs which can be used to alleviate the symptoms of asthma. In most cases, a person typically may use maintenance inhalers usually twice a day to control the inflammation and constriction of the bronchioles, and use rescue therapy when the symptom becomes worse.^{14,15}

The maintenance therapy usually contains a combination of inhaled corticosteroids and long acting β_2 adrenoreceptor agonists (LABA). The world leading asthma prevention inhaler, seretide, contains fluticasone propionate as the synthetic corticosteroid and salmeterol as the long acting β_2 agonist (Fig. 3).¹⁴

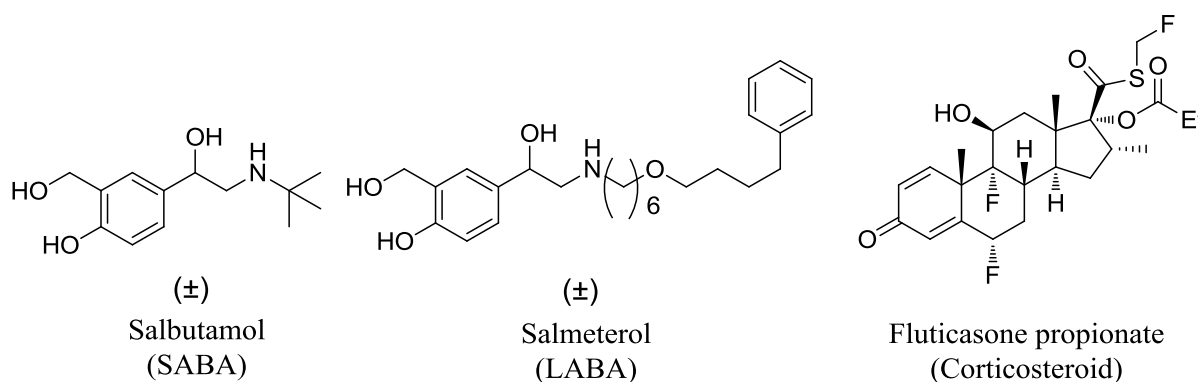


FIGURE 3. Structure of a SABA, LABA and a corticosteroid.

The corticosteroids suppress the T_H2 mediated inflammatory response and the β_2 agonist works on β_2 adrenoreceptors causing the smooth muscles surrounding the airways to relax and widen, making it easier for the patient to breathe.¹⁶ The duration of action for a LABA is around 12 hours, whereas short-acting β_2 adrenoreceptor agonists (SABA), such as salbutamol, used in rescue therapy have a rapid onset of action and relieve symptoms for 3-6 hours. Salmeterol has a long duration of action because of its long lipophilic side chain, which confers a high level of retention at the adrenergic auxiliary exosite allowing the head of the molecule to continuously bind and unbind to the active site of the β_2 receptors (Fig. 4).¹⁷

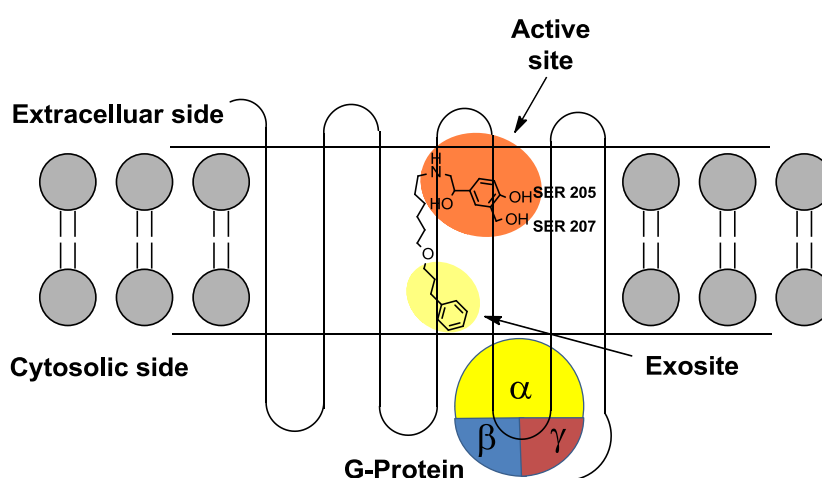


FIGURE 4. The exosite mechanism of action of salmeterol. Reproduce with permission. (*Prog. Respir. Res.* 2001, 31, 60-63)

Oral corticosteroids such as prednisolone and prednisone are used to treat severe asthma, or afford relief when symptoms worsen suddenly during an asthma attack. They are normally given at high doses for short periods of time, to avoid any of the serious side effects that are known to be caused by prolonged exposure to steroids. As corticosteroids are hormones, repeated exposure to them can cause growth retardation, suppression of the immune system, weight gain, skin thinning and osteoporosis. Common side effects of β_2 agonists include muscle tremor, peripheral vasodilation, tachycardia (increased heart rate) and headaches. Using inhalers reduces the risks, as the dosage is localised in the lung, and the amount absorbed into the systemic circulation is much lower than if taken orally. Also, as the inhalers deliver the drug directly to the lung, a lower dose (200 μ g) is sufficient for efficacy compared to oral delivery (200 mg).

There are several other treatments of varying degrees of scope and effectiveness. These include antimuscarinic agents, such as ipratropium and tiotropium, and leukotriene receptor antagonists such as the oral drug, montelukast (Fig. 5). Even immunotherapy, in which allergy desensitisation is effected over a long period of time by injecting allergens has been used.

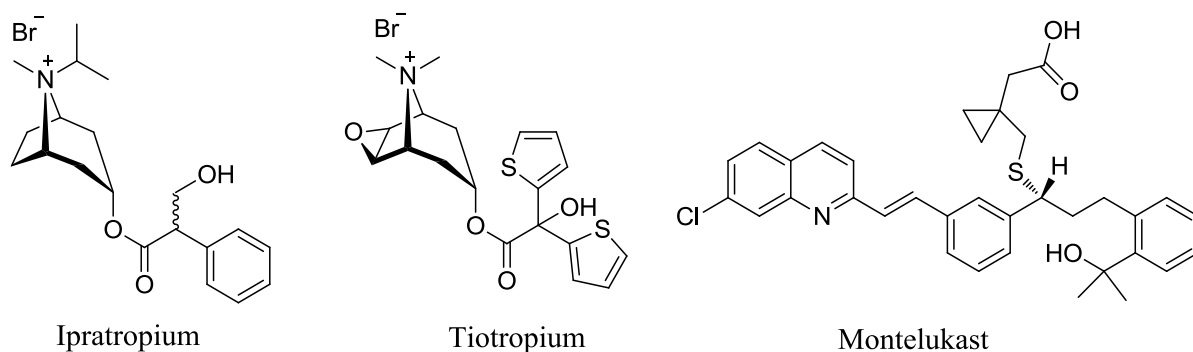


FIGURE 5. Structure of ipratropium, tiotropium, and montelukast.

Muscarinic antagonists block muscarinic receptors on the bronchial smooth muscle, which leads to bronchodilation and reduction in the secretion of mucus. Leukotriene receptor antagonists inhibit leukotriene production. Leukotriene is an inflammatory mediator that is produced in response to an immune challenge, and it triggers smooth muscle contraction and mucus secretion. Both types of these drugs can be taken separately or in combination with another asthma drug. For example, ipratropium is combined with a β_2 agonist such as salbutamol for the treatment of asthma. Nonetheless, these therapies are not as effective as β_2 agonists or corticosteroids and they also have many side effects. The common side effects of antimuscarinic agents include dry mouth, dry skin, palpitation and constipation, and leukotriene receptor antagonists are known to cause nausea, headache and gastrointestinal tract upset.

These side effects and the fact that some treatments are not effective in some moderate and severe asthmatic patients are reasons for an urgent need for new and more effective treatments. Over the past decade, chemokine receptors such as CCR3 and CCR4 have been implicated in the pathophysiology of asthma and considerable effort has gone into identifying novel inhibitors from academics and pharmaceutical companies.¹⁸ CCR4 was being investigated by our team as a potential new therapeutic target. The main goal for the CCR4 programme was to identify a novel oral non-steroidal drug to be used as an alternative to both

inhaled and oral corticosteroids for the treatment of asthma. The drug needed to demonstrate greater efficacy than the current oral drug, montelukast, and it should be applicable to asthma conditions of all degrees of severity.

4.0 Chemokines and chemokine receptors

Chemotaxis is the movement of cells towards or away from a concentration gradient of a chemical stimulus. Chemokines are a group of chemotactic cytokines that are involved in directing leukocytes to the site of inflammation and play an important role in host defence.¹⁹ They are complex protein molecules (8-16 kDa) that are secreted by many immune and non-immune cells. In a normal immune response, chemokines orchestrate the migration and activation of the leukocytes to the site of injury or infection. This is a normal defence mechanism to help the body fight off invading microorganisms such as bacteria and viruses.¹⁹ However if the immune system is inappropriately activated, then it turns rogue and the leukocytes target the body's own tissue, which leads to autoimmune and chronic inflammatory diseases such as multiple sclerosis, rheumatoid arthritis and asthma.

Chemokines are categorised into four subfamilies (C, CC, CXC and CX3C) according to the position of their first two cysteine residues in the polypeptide chain.²⁰ The C chemokine family lacks one cysteine residue; the CC chemokines have the cysteine pair adjacent to each other, whilst the CXC and CX3C subfamilies have the cysteine pair separated by a single (X), or 3 amino acid residues (X3), respectively. To date, over 50 chemokines and 20 chemokine receptors have been identified in humans.^{11,21} In addition to the chemokines binding to their own receptors, most chemokines can bind to multiple receptors, and to add complexity, multiple ligands can bind to most chemokine receptors. For example, CCR3 binds a number of chemokines including CCL5, CCL7, CCL11, CCL13, CCL15, CCL24, CCL26 and CCL28, whereas the chemokine CCL5 for example, can bind with high affinity to the chemokine receptors, CCR1, CCR2, CCR3 and CCR5.²² This promiscuous nature of chemokines and their receptors has made chemokine research complicated. Despite the redundancy of chemokine and chemokine receptors, and disease heterogeneity, so far two small molecule inhibitors that selectively bind to single chemokine receptors are registered drugs. These include the anti-retroviral CCR5 antagonist from Pfizer, maraviroc, for the treatment of multi-drug resistance CCR5-trophic human immunodeficiency virus (HIV) type-1 infection,²³ and the CXCR4 antagonist from AnorMed, plerixafor, for the treatment of non-Hodgkin lymphoma and multiple myeloma²⁴ (Fig.6). Maraviroc was the first chemokine

receptor-targeting drug to be approved by the FDA.²⁵ It is an entry inhibitor for macrophage-tropic strains of HIV-1, the virus that causes AIDS.²⁶ The HIV-1 strain enters cell by attaching itself to the host cellular receptors on the surface of CD4+ cell.²⁷ The virus uses its glycoprotein, gp120 to interact with the host CD4+ T-cell receptor, and in combination with the co-receptors, CCR5 and CXCR4, attaches to the cell surface before fusion and entry into the host cell. Maraviroc blocks CCR5 by binding to an allosteric site, and consequently prevents the virus to attach to the cell surface effectively, prohibiting its entry.^{25,28}

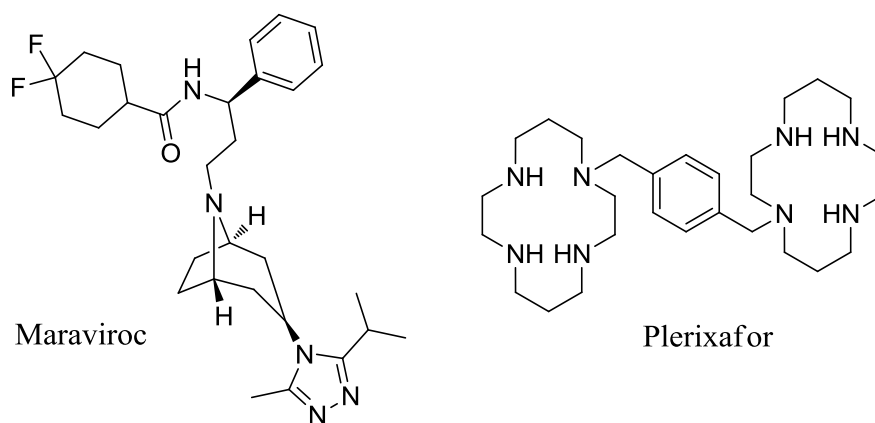


FIGURE 6. Structure of maraviroc and plerixafor.

Owing to the success of maraviroc, many companies have invested in finding novel CCR5 antagonists, and a number of these small molecule inhibitors went into clinical trials for the treatment of AIDS, and these have been reviewed recently.^{22,29}

In addition, approval of maraviroc greatly accelerated research into finding an antagonist for CXCR4.³⁰ As the chemokine receptor, CXCR4, along with CCR5, plays an important co-receptor role for the entry of HIV-1, it is also considered to be a highly promising therapeutic target for the treatment of AIDS.^{26,30} Anormed were the first company, with their CXCR4 bicyclam-containing antagonist, plerixafor (Fig. 6), to go into phase I clinical trials for the treatment of AIDS.³¹ Although, plerixafor showed positive results *in vitro*, the compound suffered from poor oral bioavailability.³¹ New findings that CXCR4 and its endogenous ligand, SDF-1 (CCCL12) are important in homing hematopoietic stem cells to the bone marrow,³² led Anormed to change direction, and go into clinical trials with plerixafor for the treatment of blood cell cancers, such as non-Hodgkin lymphomas.^{30,31} It has been shown that plerixafor, when dosed subcutaneously, inhibits CXCR4, and mobilises hematopoietic stem cells from the bone marrow into circulation as peripheral blood stem cells.³³ These stem cells

can then be harvested, and after a successful treatment of high dose chemotherapy, given back to patients suffering from white blood cell cancers. As with CCR5 inhibitors, many CXCR4 antagonists are currently in different stages of clinical development for AIDS, non-Hodgkin lymphoma, and multiple myeloma, and are awaiting clinical trial outcomes.^{29,30}

At the time this project started, there were several small molecule inhibitors targeting chemokine receptors in clinical trials for a wide range of inflammatory disorders and autoimmune diseases, including asthma, allergic rhinitis, AIDS, diabetes, rheumatoid arthritis and even cancer.^{29,34} Horuk and Pease have published an excellent review on the successes and failures of chemokine receptor antagonists from discovery to clinic²⁹ making it an essential read for a more in-depth background around the various inhibitors so far identified.

Unfortunately, as the authors have pointed out, a lot of the earlier compounds have failed in the clinic due to lack of efficacy, promiscuity of the drug target, toxicity, sufficient receptor occupancy and poor pharmacokinetics.^{22,29,35} The promiscuity of the drug targets, especially in the inflammatory area, meant that targeting single chemokine receptors proved to be challenging. This was the case for targeting CCR3 for the treatment of allergic rhinitis and asthma, where it has been extremely difficult to demonstrate clinical efficacy with a specific antagonist to a single receptor.¹⁸ For example, one of the most advanced CCR3 candidates in clinical trial, GW76694 (Fig. 7), which had good oral bioavailability and showed complete blockade of CCR3 *in vivo*, failed to show efficacy in a phase II study for the treatment of asthma.³⁶ Although there is strong evidence that CCR3 plays an important role in rodent models of asthma and allergic rhinitis,^{34,37} it has been suggested that in human, the receptor may play a minimal role, or the redundancy within the complex chemokine system makes it difficult to demonstrate clinical efficacy.^{18,36} For this reason, a number of authors have suggested that for chemokine targets where promiscuity could be an issue, it may be beneficial to target more than one receptor for the next wave of drug development.^{18,22,29} However, it should be pointed out that interest of pharmaceutical companies to progress CCR3 small molecule antagonists has not reached a dead end.¹⁸ Recently it has been identified that CCR3 appears to play a key role in the development of blood vessels within the choroid (vascular layer of the eye, which contains connective tissue), and has been proposed as a drug target for age-related macular degeneration (AMD), a common cause of serious visual impairment in elderly people.³⁸ Encouraging data have emerged from animal models of AMD,³⁸ and there appears to be a lot of interest in taking current CCR3 antagonists

into the clinic for this alternative indication. In addition, GSK's CCR3 antagonist, GW76694 was found to be efficacious in an animal model of AMD.³⁹

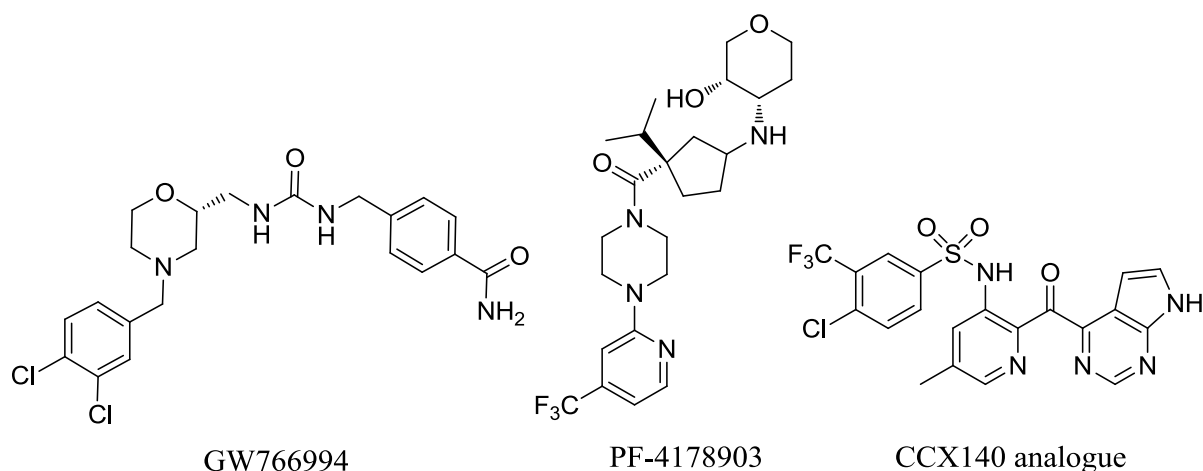


FIGURE 7. Structure of clinical candidates, GW76694, PF-4178903 and an analogue of CCX14 .

A number of small molecule compounds targeting chemokine receptors have failed because of off-target activities. For example, the CCR2 antagonist from Pfizer, PF-4178903 (Fig. 7) was selected as a candidate for its favourable pharmacokinetics data; however it had cardiovascular liabilities, leading to its termination.⁴⁰ With this class of compounds, the mechanism of action could not be investigated and the failure was due to poor selection of the compound, and not the target. In addition progression of a lot of candidates were halted because of limited oral bioavailability in humans leading to poor occupancy of the target to elicit an effect.²²

Despite the early failures, a number of candidates currently in late stage clinical trials are trying to overcome some of these hurdles and are progressing well.^{22,29,35,41} Now that companies are realising the requirement of greater levels of occupancy of chemokine receptors for translation into good efficacy, significant progress has been made in the inflammatory field to successfully target a single receptor, and achieve a positive clinical outcome.²² For example, ChemoCentryx had a long interest in CCR9 inhibitors, and their latest antagonist, CCX507 (structure not disclosed) was shown to be well tolerated and effective in blocking CCR9 on circulating leukocytes (99% occupancy) in a phase I study for the treatment of inflammatory bowel disease and ulcerative colitis.⁴² The positive results have given ChemoCentryx confidence to move forward with CCX507 in to a phase II clinical trial.

Another example is the selective antagonism of the CCR2 receptor, where 7 small molecule antagonists have advanced to clinical trials for a range of disorders including allergic rhinitis, rheumatoid arthritis, multiple sclerosis, type 2 diabetes, and neuropathic pain associated with type 2 diabetes.²² Unfortunately, a number of these compounds have failed, again due to cardiovascular liabilities and poor pharmacokinetic properties,²² including the first compound from ChemoCentryx, CCX915 (structure not disclosed), which was terminated during phase I clinical trials due to lack of oral bioavailability.²⁹ ChemoCentryx's current candidate, CCX140 (structure not disclosed, although it is likely to belong to the class of compound exemplified in Fig.7) has been reported to have favourable pharmacokinetic properties, lacked inhibition of hERG at 100 μ M (patch clamp technique), had no cytochrome p450 issues, and was selective against a panel of 142 other receptors.⁴³ In 2012, CCX140 has shown favourable results in phase II studies for the treatment of type 2 diabetes,⁴⁴ and more recently, the company has announced that they have seen positive outcomes with CCX140 for diabetic nephropathy in a phase II clinical trial.⁴⁵

There is also growing interest in using novel approaches to target chemokine receptors including the use of monoclonal antibodies, as exemplified by mogamulizumab for the treatment of cancer.^{41,46} It has been shown that CCR4 is expressed on tumour cells from patients with adult T-cell leukaemia, which is a rare cancer of the immune system's own T-cell caused by the virus, human T-cell lymphotropic virus type-1 (HTLV-1).⁴⁷ A Japanese company, Kyowa Hakko Kirin has developed a humanised monoclonal antibody, mogamulizumab, directed against CCR4, which was approved in Japan in 2012 for demonstrating clinical anti-tumour activity in patients with relapsed or refractory CCR4-positive adult T-cell leukaemia/lymphoma.^{41,48} In addition, a phase I clinical trial is currently being conducted with mogamulizumab for the treatment of asthma.⁴¹ A lot of effort has also gone into identifying small molecule inhibitors for CCR4,¹⁸ and some of this work will be discussed in the next section. It should be pointed out that the endogenous chemokine ligands, CCL17 & CCL22 solely bind to CCR4 in comparison to chemokine such as CCL5, which binds to several chemokine receptors such as CCR1, CCR2, CCR3 and CCR5. Therefore it is expected that a small molecule antagonist for CCR4 should be specific in blocking the action of its cognate chemokines. These findings together with the success of the monoclonal antibody mogamulizumab highlight that a small molecule antagonist for CCR4 is more likely to be successful in the clinic, if the right compound with good *in vivo* potency, high level of receptor occupancy and good pharmacokinetic properties could be developed.

In the chemokine field there is growing optimism that by tackling some of the issues observed in the clinic with some of the earlier compounds, and with better understanding of the role of chemokines and their receptors in different disease models, the inhibitors currently in clinical trials, and future development compounds, are more likely to reach their goal of becoming marketed drugs.

4.1 The chemokine receptor 4 (CCR4)

CCR4 receptors are mainly expressed on the membrane of T_H2 cells that produce IL-4, IL-5 and IL-13, the cytokines responsible for the recruitment of eosinophils, and production of high levels of serum IgE and activation of mast cells.^{11,49} The endogenous ligands for CCR4 are CC chemokine ligand 17 (CCL17), also known as thymus activation-regulated chemokine (TARC), and CCL22, also known as macrophage-derived chemokine (MDC). The mechanism of chemokine-mediated recruitment of leukocytes to drive an allergic response is a complex process and involves a sub-set of immune cells to orchestrate the inflammatory process. Initially, inhaled allergens or antigens on the surface of the endothelium are processed by dendritic cells, which produce and release the chemokines, TARC and MDC (Fig. 8).⁵⁰ Although these chemokines are produced mainly by dendritic cells in tissue, they are also produced by endothelial cells after being exposed to antigens.⁵⁰ The chemokine gradient of TARC and MDC causes the T_H2 cells to migrate from the blood into the tissue upon activation by binding to the chemokine receptor, CCR4. The T_H2 cells then interact with APCs, such as dendritic cells, in the tissue of the allergic airways to induce a T_H2 driven allergic response,⁷ which contributes to eosinophilia, airway hyperresponsiveness, and mucus production by releasing cytokines such as IL-4, 5, 10, 11 and 13 (as previously mentioned in section 3.1). In addition, upon maturation, the dendritic cells migrate from the inflamed tissues to local lymph nodes where the chemokines (MDC and TARC) recruit further T-cells to maintain the allergic response. Furthermore, there is clinical evidence suggesting that activated CCR4-positive cells and the expression of CCR4 ligands (MDC and TARC) are upregulated in the airways after an allergen challenge in mildly asthmatic patients.⁵¹

As the T_H2 cells play an important role in the allergic inflammatory response, it is suggested that inhibiting CCR4 with an antagonist will provide an attractive new therapeutic intervention for allergic inflammatory diseases such as asthma⁵² and atopic dermatitis.⁵³

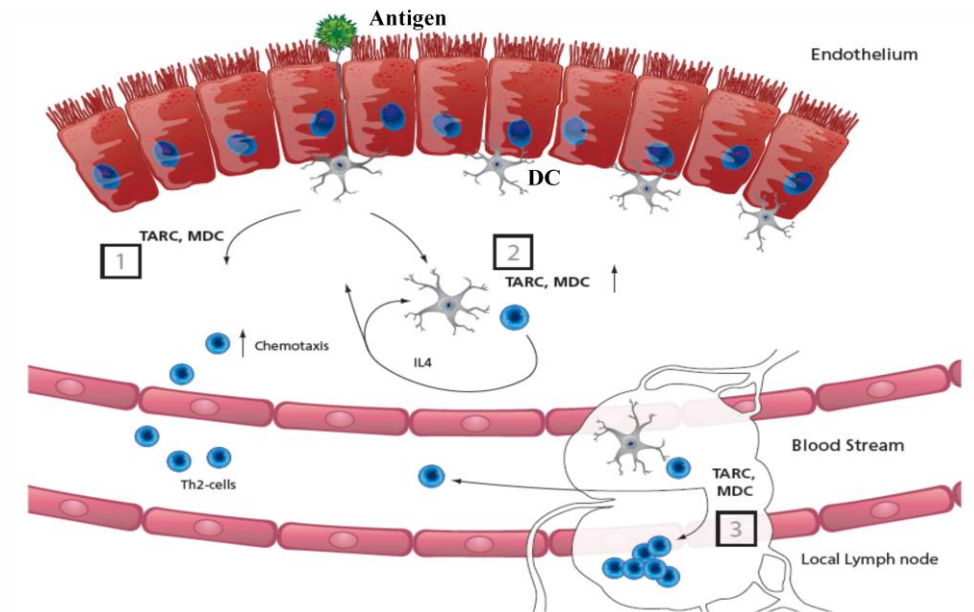


FIGURE 8. Chemotaxis of T_H2 -cells toward a concentration gradient of chemokines (TARC & MDC), followed by interaction of the T-cells with dendritic cell (DC). Hypothesis that a CCR4 antagonist will (1) reduce migration of T-cell into the tissue, (2) reduce local DC/T-cell interaction, (3) reduce the generation of T-cell memory towards allergens and also reduce the CCR4-driven self amplifying loop between T-cells and dendritic cells.

CCR4 antagonists could also provide novel therapy for when CCR4 and its endogenous ligands participate in the pathogenesis of disease such as allergic bronchopulmonary aspergillosis,⁵⁴ inflammatory bowel disease⁵⁵ and cancer.⁴⁷ As mentioned earlier, CCR4 is also expressed on tumour cells from patients with adult T-cell leukaemia,⁴⁷ and a humanised monoclonal antibody, mogamulizumab, directed against CCR4 has been approved in Japan for demonstrating clinical anti-tumor activity in patients with relapsed or refractory adult T-cell leukaemia/lymphoma.^{41,48}

Significant effort has also gone into discovering small molecule CCR4 antagonists in pharmaceutical companies,⁵⁶⁻⁶⁰ but so far only one candidate molecule, GSK2239633A from GSK has progressed to phase I clinical trials for asthma.⁶¹ Although GSK2239633A demonstrated good pharmacokinetic data in preclinical animal studies (bioavailability in rats and beagle dogs 85% and 97% respectively),⁶² it suffered from low solubility, poor bioavailability in humans (16%) and weak *ex vivo* potency preventing it from being progressed further,^{48,61} despite the fact that at the highest dose of 1500 mg/kg, GSK2239633A was found to be safe and demonstrated 74% CCR4 receptor occupancy. The approval of mogamulizumab and the lack of small molecule candidates clearly highlight the

needs for identifying efficacious CCR4 antagonists, with improved potency, solubility and good pharmacokinetic properties that are capable of engaging CCR4 at lower doses.

4.2 CCR4, a 7 transmembrane receptor

CCR4 receptor is a 7 transmembrane (7TM) receptor. 7TM receptors are integral membrane proteins known as G-protein coupled receptors (GPCR). They are characterised by an amino acid sequence containing seven α -helical hydrophobic domains which span the membrane seven times (Fig. 9). They have an extracellular N-terminal sequence, three sets of alternate extracellular and intracellular loops, and an intracellular C-terminal sequence. 7TM receptors respond to a wide range of endogenous ligands including lipid analogues, amino acid derivatives, small peptides, and stimuli such as light and odour.

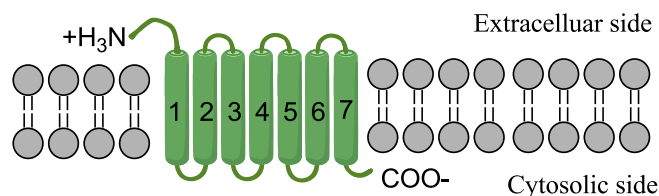


FIGURE 9. Structure of 7TM receptor.

7TM receptors are involved in signal transmission from the exterior of the cell to the interior through interaction with a heterotrimeric protein known as guanine nucleotide-binding protein (G-protein) (Fig. 10). A G-protein consists of an α , β and γ -subunit bound to guanosine diphosphate (GDP). Once a 7TM receptor is stimulated, a loop on the cytosolic side chain is involved in activating the G-protein and replaces GDP with guanosine triphosphate (GTP). This results in the dissociation of the subunits. The activated α -subunit still bound to GTP, stimulates adenylate cyclase to form cyclic adenosine monophosphate (cAMP) from adenosine triphosphate (ATP). The cAMP acts as secondary messenger within the cell to mediate and further amplify the intracellular effects. Besides cAMP, the dissociated subunits can also activate a variety of other signalling molecules including inositol triphosphate and calcium ions. Activation of the secondary messengers results in downstream signalling and the expression of biological effects; for example, the binding of chemokine receptors causes the firm adhesion of leukocytes to endothelial cells, and the migration towards a concentration gradient of chemokines into the tissue.²¹ Hydrolysis of the bound GTP at the α -subunit brings the G-protein back to its inactive state stopping the signal transduction.

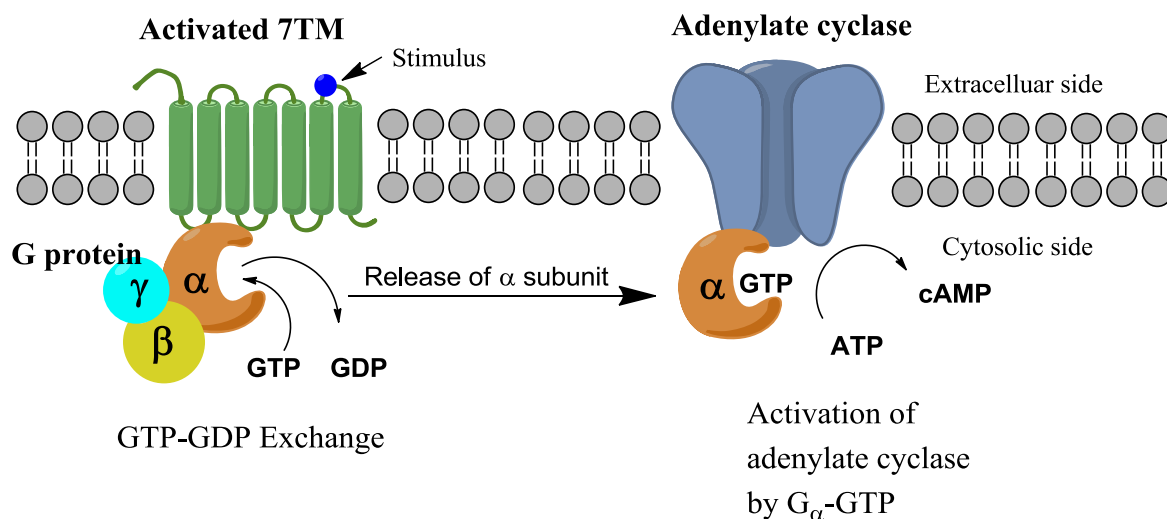


FIGURE 10. Signal transduction of 7TM receptors.

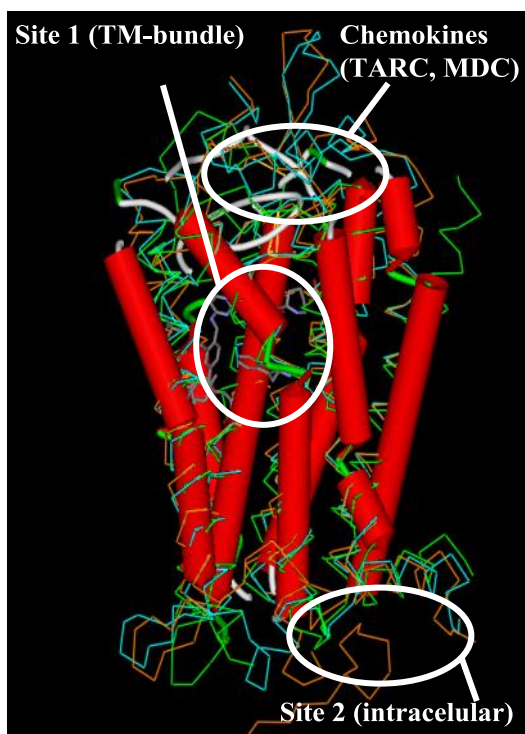
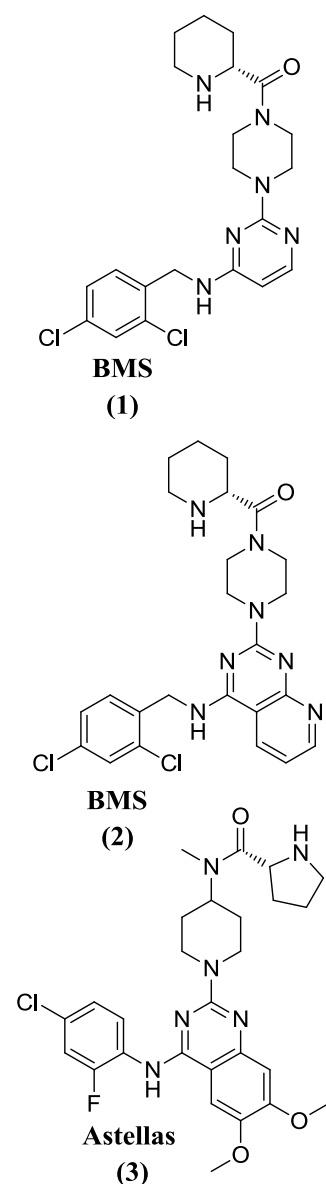
4.3 Structure of CCR4

Very little is known about the actual structure of the CCR4 receptor. As membrane bound 7TM receptors are conformationally flexible, it is very difficult to obtain a crystal structure of CCR4. Most of the structural information has been obtained from pharmacological studies and homology models based on the resolved 7TM crystal structure of rhodopsin.⁶³ Since 2007, other 7TM crystal structures have been resolved, including β_1 and β_2 adrenergic GPCR.^{64,65} More recently, the X-ray crystal structure of CCR5 was also resolved in complex with the antagonist maraviroc.⁶⁶ Although the overall structure of CCR5 shares similar architecture to those of earlier reported resolved 7TM receptors, a key difference was the presence of an additional shorter α -helix termed helix VIII on the intracellular side of the membrane.⁶⁶ It is suggested that the structure of CCR4 resembles more the structure of CCR5 than those GPCRs determined previously. However, it should be noted that the homology model work described in this thesis was carried out before the X-ray structure of CCR5 was known.

Initially, it was thought that CCR4 had two binding sites. However, recent advances in pharmacology, based on competitive ligand binding studies from two recent papers published by AstraZeneca,⁶⁷ and our group,⁶⁸ has confirmed three binding sites (Fig. 11). The endogenous ligands, MDC and TARC, bind to an extracellular region called the orthosteric site. The binding pocket of chemokine receptors for the orthosteric site is fairly large, and as synthetic ligands are in general much smaller (<600 Da) compared to chemokines (8-16 kDa), small molecule antagonists often bind to a distinct allosteric site from where the

orthosteric ligands bind.^{67,69,70} Over the past decade, numerous small-molecule CCR4 allosteric antagonists have been reported in the literature.^{56,58,62,71-75} and these antagonists are divided between two different chemotypes that bind to two different allosteric regions of the CCR4 receptor.^{67,68}

Site 1 Compounds



Site 2 Compounds

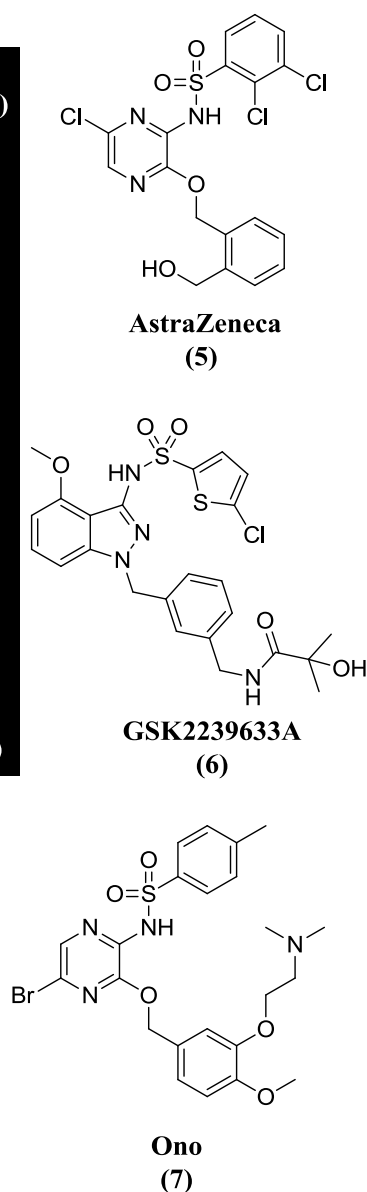


FIGURE 11. Ligand binding sites of CCR4 with examples of small molecule antagonists.

Basic small molecule antagonists such as the published compound from Bristol Myers Squibb (BMS), compounds **1** and **2**,⁵⁸⁻⁷³ Astellas' compound **3**^{59,76} and Daiichi Sankyo's compound **4**,⁷¹ bind to an extracellular allosteric region.⁶⁸ Aryl sulfonamide compounds such as AstraZeneca's pyrazine sulfonamide **5**,⁶⁰ GSK's candidate indazole **6**,^{62,77} and Ono's

sulfonamide **7**,⁷⁸ bind to an intracellular allosteric region of the 7-transmembrane CCR4 receptor.^{67,68} It is noteworthy that the compounds that bind to the intracellular region need to have properties such as good membrane permeability to access this site. In-house, the allosteric extracellular site is termed Site 1, and the intracellular site is termed Site 2.

Site 1 inhibitors are generally basic lipophilic amines (e.g. **1**, **2**, **3** and **4**); they are thought to interact with a conserved glutamate residue at the extracellular site. Whilst good potency could be achieved in the *in vitro* GTP γ S assay and the whole blood assay (see section 4.4), this class of compounds has poor pharmacokinetic properties with negligible bioavailability (Table 1). Most of the known Site 2 antagonists are weakly acidic sulfonamides. These compounds generally have good pharmacokinetic properties; however, higher molecular weights are required to achieve the whole blood activity. The in-house indazole compound **6** is active in whole blood, whilst the AstraZeneca compound (**5**) was found to be inactive.

There is also growing evidence of multiple ligand binding sites for other chemokine receptors.^{67,69,70} The general pharmacophore of Site 1 compounds featuring a basic amine is well represented in many other chemokine small molecule antagonists, including maraviroc for CCR5, and a number of CCR2 antagonists.^{66,79} For this class of compounds, the positively charged nitrogen interacts with a conserved glutamic acid residue in the TM7 α -helix, which is located in the extracellular allosteric region of the chemokine receptor.⁸⁰⁻⁸² There are several inhibitors of chemokine receptors that do not contain a basic nitrogen, and it has been confirmed through mutagenesis and radioligand binding studies that this class of molecules bind to a different allosteric site on the receptor.^{67,69,79} Andrews and co-workers have reported that the AstraZeneca CCR4 antagonists, which were also weakly active for CCR5, bind to an allosteric region of CCR5 in the intracellular side of the receptor.⁶⁷ Furthermore, Salchow and co-workers introduced ten single point mutation into CXCR2 using site-directed mutation, which helped them to identify the location of the intracellular allosteric site.⁶⁹ The mutagenesis studies revealed that a lysine residue (K320) located in the intracellular side of CXCR2 was important for making a key interaction with an acidic moiety on the small molecule antagonists.^{69,83}

More recently, Heitman and co workers with a selection of radiolabelled CCR2 antagonists in a competitive binding and whole cell assay provided further evidence of a chemically distinct allosteric site.⁷⁹ Although the location of this new CCR2 allosteric site is yet to be determined, the authors have suggested based on the similarity of the pharmacophore of the

antagonists to the CCR4, CCR5 and CXCR2 intracellular binders, that the allosteric pocket is likely to be located in the intracellular side of the receptor in the C-terminal domain.

These new insights into receptor pharmacology will no doubt lead to development of compounds, with distinct properties, targeting different allosteric sites of chemokine receptors. Identification of the two allosteric sites for CCR4 has not only helped explain the difference in structure-activity relationship observed with the two class of antagonists, but has also aided the design of new templates, including the ones reported in this thesis.

The in-house *in vitro* potency, physicochemical and rat pharmacokinetic data for the CCR4 antagonists, BMS compound, **1**, AstraZeneca's compound, **5** and the in-house indazole compound **6** are summarised below in Table 1.

TABLE 1. Biological profile of in-house compounds and published CCR4 antagonists.

Compound NO.	BMS (1)	AstraZeneca (5)	GSK (6)
GTPγS (pIC₅₀):	8.1	8.2	7.9
LE / LLE _{AT} :	0.37/0.27	0.38/0.21	0.30/0.27
I¹²⁵ TARC pK_i	8.6	8.5	8.1
LE / LLE _{AT} :	0.39/0.30	0.40/0.32	0.31/0.27
HWB Actin polym. (pA₂):	6.7	<5	6.2
MW :	449	475	549
clogP :	4.5	4.0	3.7
Chrom logD _{7.4} :	3.5	nd	4.3
CLND solubility:	132 μ g/mL	153 μ g/mL	162 μ g/mL
PPB (HSA)	93.4%	99.8%	96.5%
Rat oral PK (dose 1 mg/kg)			
Bioavailability:	Negligible	40 %	85 %
Clearance:		2.3 mL/min/kg	14 mL/min/kg
t _{1/2} :		2.1 h	2.5 h
Vd:		0.4 L/kg	1.9 L/kg

nd = not determined

4.4 Biological assays (see experimental section for full details)

Competitive radioligand binding assay is one of the most common methods used to measure inhibitory activity of small molecule antagonists against target proteins. The human CCR4

antagonist *in vitro* potency was determined by [³⁵S]-GTP γ S radioligand competition functional assay and/or [¹²⁵I]-TARC radioligand binding assay.⁸⁴ Both the assays used recombinant CCR4-expressing CHO cell membranes adhered to WGA-coated Leadseeker scintillation proximity assay (SPA) beads. The SPA beads contain scintillants that emit light when stimulated, for example, during binding of the radiolabelled ligand or when the ligand is in close proximity to the bead, and the output is measured on a scintillation counter. In the GTP γ S assay, binding of the endogenous ligand MDC changes the conformation of the receptor on the membrane from an inactive to an active form, which subsequently results in binding of [³⁵S]-GTP γ S, and stimulation of the SPA beads to emit light. In the presence of an increased concentration of antagonist, the bead becomes less bound to the radiolabelled molecule and therefore, reducing the amount of light emitted. Hence, the GTP γ S assay measures the degree to which human MDC-derived [³⁵S]-GTP γ S was prevented from binding to the receptor in the presence of an antagonist. The potency was expressed as the negative logarithm of the concentration of the test molecule that produced 50% inhibition of the target protein (pIC₅₀). The radioligand [¹²⁵I]-TARC binding assay measured the inhibition of radiolabelled TARC binding directly to CHO-CCR4 membranes in the presence of an antagonist, and the potency was expressed as the negative logarithm of the inhibitory constant, pK_i. It should be noted that indazole **6** had a pK_i of 8.1 in the [¹²⁵I]-TARC SPA binding assay and a pIC₅₀ of 7.9 in the GTP γ S assay respectively; compound **1** and **5** are 0.5 log unit more potent than **6** in the SPA assay but no significant difference was observed in the GTP γ S assay (Table 1). All three compounds were performing close to the tight-binding limit of the GTP γ S assay, so a significant difference in potency was not observed (Note. later in the thesis, the structure-activity relationship of the more potent spiro-pyrimidine template is discussed (section 8.2 – 8.13), and for these analogues, the [¹²⁵I]-TARC binding assay data were more relevant compared to the GTP γ S assay data to distinguish between the relative potency of compounds). The human whole blood (hWB) actin polymerisation assay was used as a secondary screen to determine potency against the native receptor for the more potent compounds in the primary assay.⁸⁵ The assay quantified cytoskeletal reorganisation (formation of filamentous (F-) actin) which occurs in a variety of cells in response to chemoattractants and is a surrogate for chemotaxis. This was achieved by staining the F-actin with a fluorescent derivative of phalloidin, which binds with high affinity and specificity to the interface between actin monomers in F-actin. The response was measured as an increase in the fluorescence intensity of the target cell population in a flow cytometer and was

expressed as a pA₂ value. In this assay, human CD4⁺ CCR4⁺ lymphocytes were identified by staining with antibodies to CD4 and CCR4. The GSK candidate **6** had a pIC₅₀ of 7.9 in the GTPγS assay and a pA₂ of 6.2 in the human whole blood actin polymerisation assay (Table 1). AstraZeneca's compound **5** had a pIC₅₀ of 8.2 in the GTPγS assay but was inactive in the human whole blood assay. This may be due to higher plasma protein binding (PPB = 99.8%) observed with compound **5**, which indicates that less unbound fraction is available to exert a biological response. By comparison, the Site 1 BMS compound **1** had pIC₅₀ of 8.1 in the GTPγS assay, and a pA₂ value of 6.7 in the human whole blood assay.

5.0 Ligand efficiency and lipophilic ligand efficiency

Compounds with high molecular weights (> 500 Da) and high lipophilicity (logP > 5) have been shown to possess poor drug-like properties,⁸⁶ and tend to have an increased rate of attrition in the clinic. In order to reduce the risk, ligand efficiency (LE) and ligand-lipophilicity efficiency (LLE) are used as new measures to ensure desired physicochemical profiles are maintained. LE estimates the efficiency of binding interaction with respect to the size of the ligand.⁸⁷ It is calculated by converting the K_d, which is approximated using an IC₅₀ value, into the free energy of binding (ΔG), and dividing by the number of heavy atoms in a molecule (HAC = heavy atom count) (equation 1). Based on a typical drug profile, an LE of greater than 0.3 is accepted as a good value representing an effective binding ligand. LLE estimates the ligand efficiency by taking into account the contribution to binding lipophilicity, and it is calculated by subtracting clogP from the pIC₅₀ value (equation 2).⁸⁶ In-house however, rather than using LLE, medicinal chemists prefer to use an LLE index derived from Astex Therapeutics, termed LLE_{AT} (equation 3).⁸⁸ A component of ligand binding to a protein involves transfer of ligand from an aqueous to a hydrophobic environment. The free energy change associated with this process is termed ΔG_{lipo}, which is more favourable for lipophilic compounds. In the calculation of LLE_{AT}, the free energy change of specific binding (ΔG_{specific}) of ligand to a protein is used, where the non-specific lipophilic component is subtracted from the total free energy change (ΔG_{total}) associated with the binding process.⁸⁸ The advantage of using LLE_{AT} is that it can be used for candidate compounds as well as small fragments, and the values are easier to compare with the conventional LE. An ideal LLE_{AT} value will be 0.3 or greater but in reality this depends on the target.

$$LE = - \Delta G / HAC = -RT \ln(IC_{50}) / HAC = 1.36 \times pIC_{50} / HAC \quad (\text{equation 1})$$

$$\text{LLE} = \text{pIC}_{50} - \text{clogP} \quad (\text{equation 2})$$

$$\text{LLE}_{\text{AT}} = 0.111 - (\Delta G_{\text{specific}} / \text{HAC}) \quad (\text{equation 3})$$

$$\text{where } \Delta G_{\text{specific}} = \Delta G_{\text{total}} - \Delta G_{\text{lipo}} = -1.36 \times \text{LLE}$$

6.0 Programme goals for CCR4

The overall goal for the programme was to identify a new backup series to the clinical development indazole candidate series (**6**) that was more potent in the whole blood assay and demonstrated improved pharmacokinetic properties in two preclinical species (rat and dog). Previous efforts to identify novel start points using high throughput screening, focused set screening such as the chemokine set, and rational design, have all been unsuccessful. The chemokine set contained similar analogues of compounds that are known to inhibit other homologous chemokine receptors such as CCR2, CCR3 and CXCR2. Although few initial ‘hits’ were identified from all these different approaches, triaging through them in an attempt to identify start points with desired potency, physicochemical and pharmacokinetic properties was unsuccessful.

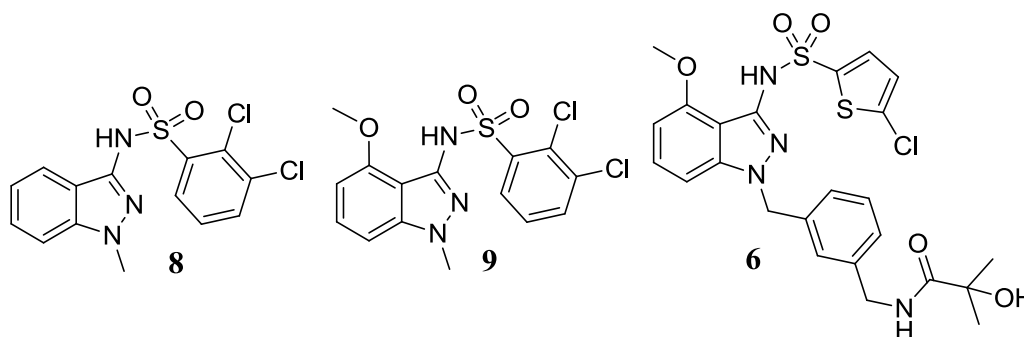
The first aim of the project was to identify a backup sulfonamide series targeting the Site 2 intracellular region of the CCR4 receptor. From previous in-house experience on the indazole series, as exemplified by **6**,^{62,77} and knowledge from other Site 2 antagonists in the literature,^{60,78} it is known that most of the advanced CCR4 inhibitors possessing good pharmacokinetic properties in rats have a common 2,3-dichlorobenzenesulfonamide moiety. It is thought that the 2,3-dichlorobenzenesulfonamide group binds to a lipophilic pocket in the intracellular region of the CCR4 receptor (Site 2) and has been found to be important for activity.

On previous occasions, it has proved difficult to identify a novel non-sulfonamide template, with the desired profile that binds in the Site-2 allosteric pocket. The possibility that the 2,3-dichlorobenzenesulfonamide moiety could be used as an anchor to identify an alternative core, prompted the design of a focused set of compounds containing the 2,3-dichlorobenzenesulfonamide (see section 7.0).

In order to maximise the chance of success in identifying a backup sulfonamide molecule with greater potency and better profile than the indazole series, a benchmark was set for ‘hit’ identification with the un-optimised indazole, **8** (Table 2). The indazole **8** had a potency of 5.7 in the GTP γ S assay and had good LE and reasonable LLE_{AT}. Indazole **7** also had good

solubility (124 $\mu\text{g/mL}$), as measured in the high throughput ChemiLuminescent Nitrogen Detection (CLND) solubility assay.^{89,90} The CLND assay involves the addition of aqueous buffer to a test compound in DMSO solution over a period of time until the compound precipitates. During investigation of structure-activity relationship of indazole **7**, it was discovered that introduction of a methoxy group at the 4-position to give indazole **9** resulted in half a log unit increase in activity in the GTP γ S assay, and this compound showed encouraging pharmacokinetic profile in rat with moderate bioavailability ($F = 24\%$) and clearance ($Cl = 17 \text{ mL/min/Kg}$). Encouraged by this data, indazole **9** was declared as a ‘lead’ and optimisation of the series led to the first candidate GSK2239633A (**6**).

TABLE 2. Biological profile of indazole ‘hit’ **8, ‘lead’ compound **9** and indazole candidate **6**.**



Compound NO.	8	9	6
GTPγS (pIC₅₀):	5.7	6.2	7.9
LE / LLE _{AT} :	0.35/0.25	0.35/0.26	0.30/0.27
MW :	356	386	549
clogP :	3.5	3.5	3.7
Chrom logD _{7.4} :	4.6	5.3	4.3
CLND solubility:	124 $\mu\text{g/mL}$	116 $\mu\text{g/mL}$	162 $\mu\text{g/mL}$
Rat PK (dose 1 mg/kg)			
Bioavailability:	nd	24%	85 %
Clearance:	nd	17 mL/min/kg	14 mL/min/kg
t _{1/2} :	nd	1.2 h	2.5 h
Vd:	nd	0.5 L/kg	1.9 L/kg

nd = not determined

Strict criteria were now set for identifying new ‘hits’ from the focused sulfonamide set. It was decided that the ‘hits’ selected must have potency, LE and LLE_{AT} comparable or greater than the indazole compound **8** ($\text{pIC}_{50} \geq 5.5$, $\text{LE} > 0.35$, $\text{LLE}_{\text{AT}} > 0.25$) and before being progressed

to lead optimisation, the templates must demonstrate potency, LE and LLE_{AT} greater than the indazole compound **9** (pIC₅₀ > 6.2, LE > 0.35, LLE_{AT} > 0.3), have high oral bioavailability (> 30%) and low clearance (< 1/3 liver blood flow) in rat.

The first part of the thesis will describe the work carried out to identify novel sulfonamide ‘hits’ and then focus on the investigation and progression of the three main series, phenylpyrazole, pyrazolopyrimidine and benzimidazolone towards a possible lead compound for further optimisation.

It should be noted that although the indazole candidate **6** showed good solubility in the CLND assay (162 µg/mL), the molecule had low equilibrium solubility in a range of physiologically relevant media, such as simulated gastric fluid (SGF, pH_{1.6} = 1 µg/mL), fed-state simulated intestinal fluid (FeSSIF pH_{6.5} = 23 µg/mL) and fasted-state simulated gastric fluid ((FaSSIF pH_{6.5} = 10 µg/mL).⁵⁷ In recent publications, it has been suggested that a high number of aromatic rings in a molecule impacts negatively on solubility owing to the π stacking nature of the flat rings.^{89,91,92} The indazole candidate has relatively high MW (549) with 4 aromatic rings, and in order to increase the chance of obtaining a backup series with better solubility, it was essential that these parameters were kept within a recommended range (MW < 500, aromatic ring count \leq 3). The ligand efficiency measures discussed earlier were used to ensure that the MW, lipophilicity and aromatic ring count were kept to an acceptable physicochemical range for an oral drug.

The second objective of the project was to discover a new Site 1 template that demonstrated good potency in hWB and has acceptable pharmacokinetic properties. As mentioned earlier, numerous small-molecule CCR4 allosteric antagonists targeting the Site 1 region have been reported in the literature (discussed later in section 8.0).^{58,59,71,73,76} This class of small-molecule antagonists however possess insufficient oral bioavailability for progression as an oral drug. The pharmacophore of the Site 1 inhibitors suggests that an interaction between a basic moiety on the ligand, and a glutamate residue on the receptor was important for potency. It is thought that the basic nature of these antagonists impacts negatively on the permeability of these molecules, resulting in poor oral absorption. It was postulated that if the basicity could be attenuated slightly than it should be possible to improve the permeability of the compounds, and hence, the oral absorption. Section 8.0 – 8.10 of the thesis will describe the work carried out to design, synthesise and identify novel Site 1 templates, and the

discussion will then focus on investigation of the structure-activity relationship around the novel spiro-pyrimidine series to improve potency and pharmacokinetic properties.

The final aim of the project was to demonstrate the *in vivo* potential of the lead compounds in different pre-clinical model of asthma. The *in vivo* result of the spiro-pyrimidine compounds will be discussed in a view to demonstrate a differentiating pharmacological effect upon binding to the allosteric Site 1, compared to Site 2 on the CCR4 receptor.

7.0 Results and discussion – identification of the sulfonamide ‘hits’

In order to identify novel sulfonamide ‘hits’ for CCR4, a focused set of 2,3-dichlorobenzenesulfonamide compounds was designed based on a knowledge driven approach, and ensuring that the set contained novel start points with desired physicochemical properties. A virtual library of compounds was prepared using computational tools (Adept), where in-house and commercially available amine monomers were enumerated with 2,3-dichlorobenzenesulfonyl chloride to give a set of ~1600 sulfonamides. Physicochemical properties were calculated (Adamantis) and the data were plotted on 2D graphs using Spotfire (Fig. 12).

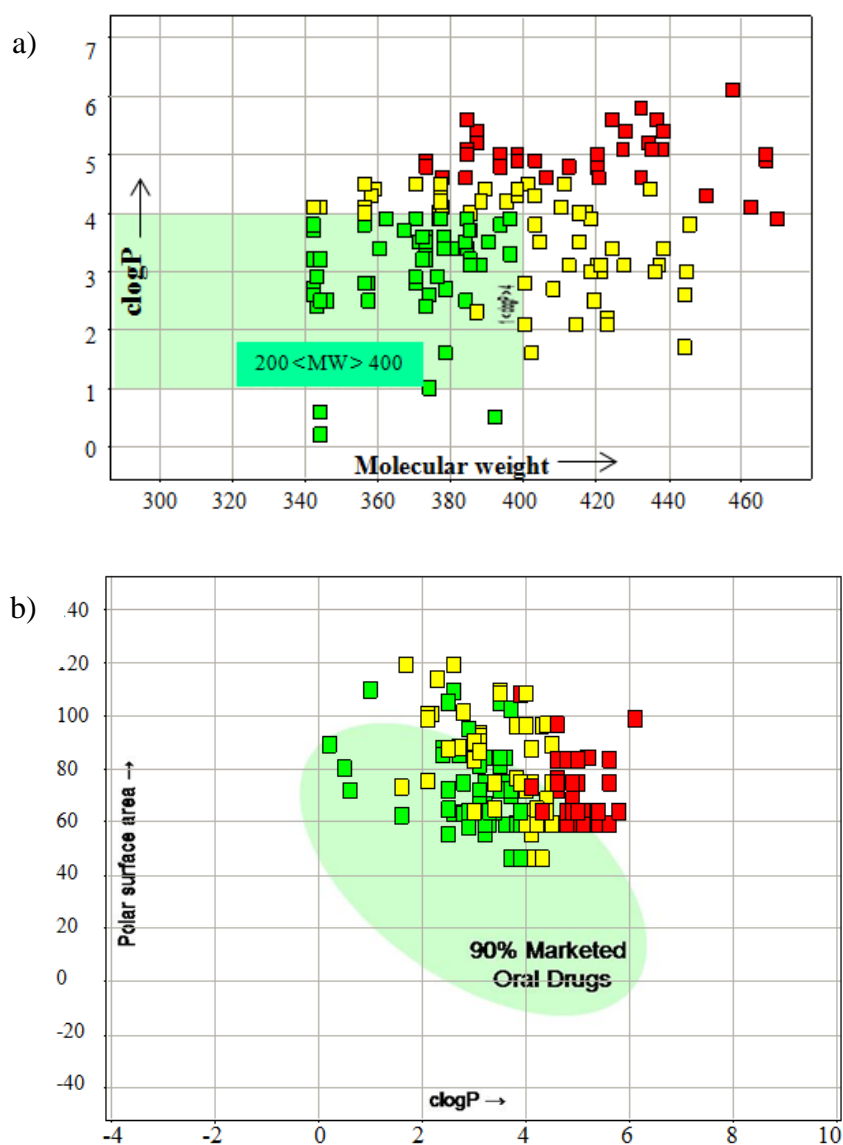


FIGURE 12. Calculated properties of sulfonamide compounds. (a) Plot of clogP vs MW (b) Plot of polar surface area vs clogP. Compounds indicated by green were selected and yellow and red were rejected. Note. For clarity of visualisation not all 1600 compounds are plotted.

The light green box in graph (a) and the ellipsoid shape in graph (b) shows the space where 90% of all marketed oral drugs lie. The range where 90% of all the marketed oral drugs lie was used as a cut off, so the compounds with undesired properties for a lead (MW > 400, clogP > 4, polar surface area > 100, H-bond acceptor > 10, H-bond donor > 5) were rejected to give a set of ~500 compounds. The cut off range selected was stricter than Lipinski's 'rule of five', which states that poor absorption or permeability are more likely when two or more of the following criteria are true: MW > 500, clogP > 5, H-bond acceptor > 10, H-bond donor > 5.⁹³ In the search for finding a drug with high potency, the optimisation process of lead molecules to candidates generally results in inflation of molecular properties (i.e. increase in molecular mass and clogP).⁹² Recent analysis based on patent data from several pharmaceutical companies has shown that medicinal chemistry efforts are producing late stage compounds with much higher molecular weight and clogP compared to historical drugs.⁹¹ This trend has resulted in the final optimised compounds (candidate molecules) having physicochemical properties outside the Lipinski's 'rule of five', and this has been implicated as an important factor in contributing to high levels of attrition in drug discovery. It is much more desirable to start with lead compounds with low molecular weight and low lipophilicity compared to a drug to maximise the chance of success.^{86,92}

In order to reduce the number of compounds for synthesis, these compounds were then grouped together based on framework clustering methods using in-house computational tools (SIV property calculation). This is a fingerprint-based method pioneered by Bermis and Murcko,⁹⁴ in which a set of compounds is grouped together based on their framework of 2D molecular structures (Fig. 13). The program carries out three levels of clustering to group the compounds together: (i) detail frame clustering removes the side chain; (ii) bond frame clustering removes atom types but the bond frame is kept; and (iii) graph frame clustering removes the side chains, atom types and bond types. In the interest of carrying out the reactions in a parallel array fashion (using a 96-well plate), a set of 96 compounds was chosen from the clusters based on lead-likeness; this is a ranking method based on physicochemical properties of historical leads that were developed into oral drugs. Higher scores are given to compounds which meet more desired criteria, e.g. low clogP, low MW etc. Tractability of chemistry and the number of vectors available for incorporating a methoxy group and if necessary, a third substituent were also important considerations.

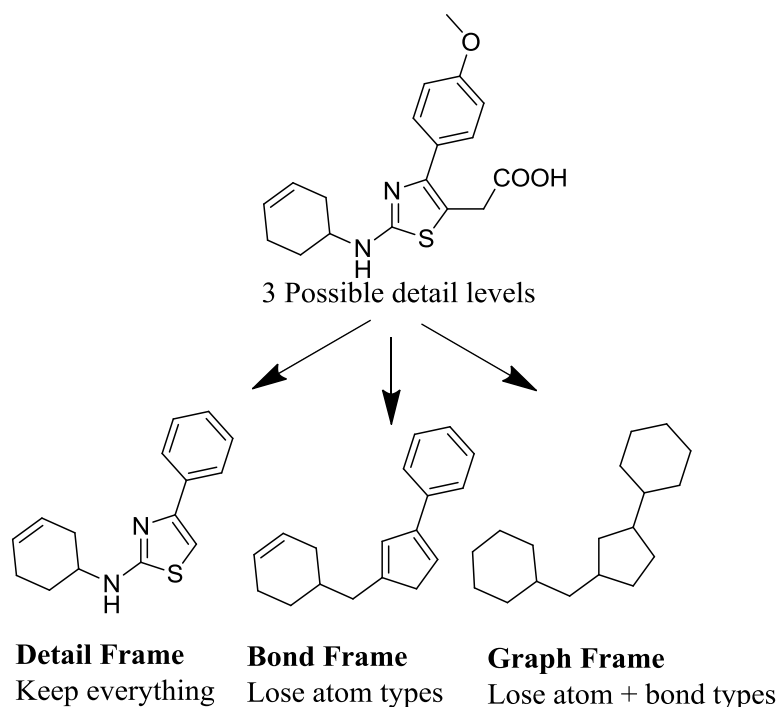
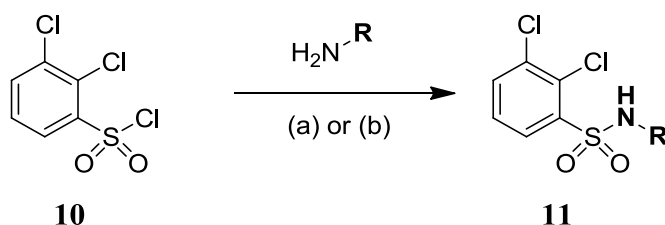


FIGURE 13. Clustering of compounds using framework cluster generation. Note: exemplar compounds are for illustrative purposes only.

The synthesis of the target sulfonamide compounds were carried out by the in-house Chemical Array Team (CAT) in a 96-well plate format. They reacted the chosen set of 96 commercially available amines with 2,3-dichlorobenzenesulfonyl chloride under identical conditions to give the corresponding sulfonamides (Scheme 1).

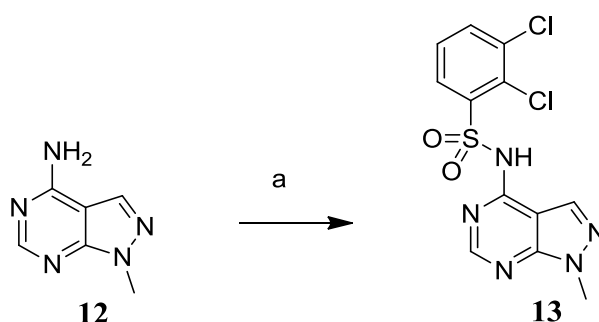


Reagents & Conditions: (a) pyridine, 18 h (b) NaH, DMF

SCHEME 1. Preparation of the sulfonamides.

After purification, they delivered 61 compounds for screening in the primary GTP γ S assay. Some of the heterocyclic amino sulfonamides proved more difficult to synthesise, so these were prepared by treatment of the amines with sodium hydride, followed by reaction with 2,3-dichlorobenzenesulfonyl chloride. This method provided a further 12 compounds for screening. For example, the pyrazolopyrimidin-4-amine **12** was commercially available and reaction with 2,3-dichlorobenzenesulfonyl chloride, in the presence of sodium hydride,

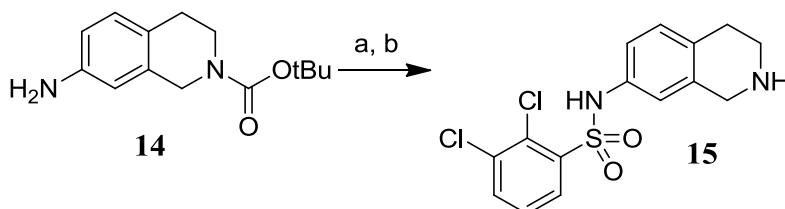
afforded the desired sulfonamide product **13** in 21% yield (Scheme 2). LCMS showed the reaction went to completion with no starting material remaining, but due to the poor recovery on the mass directed auto-preparative system (MDAP), the product was obtained in a low yield. It should be noted that purification on the MDAP often gives poor recovery with less soluble compounds. MDAP is mainly used as it provides a quick method to purify a large number of compounds with greater than 95% purity. As only 3-5 mg of compound were required for the initial biological testing, the purification methods were not optimised until an active compound, which required resynthesis was obtained.



Reagents & Conditions: (a) 2,3-dichlorobenzene sulfonyl chloride, NaH, DMF, 21%.

SCHEME 2. Synthesis of pyrazolopyrimidine **13**.

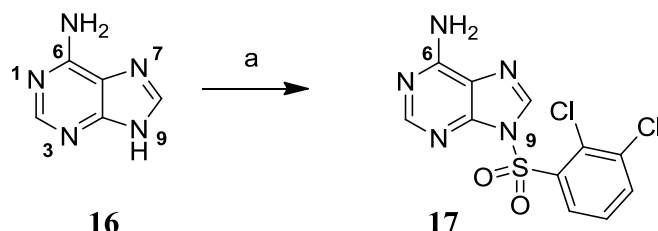
Among the set of compounds, 5 monomers had two possible amino groups the sulfonyl chloride could react with. For four of these monomers, the desired mono Boc-protected amines were commercially available. These were reacted with 2,3-dichlorobenzene sulfonyl chloride and the Boc group was cleaved with TFA before purification and submission for screening. An exemplar reaction for the preparation of 2,3-dichloro-*N*-(1,2,3,4-tetrahydroisoquinolin-7-yl)benzenesulfonamide **15** is shown in Scheme 3.



Reagents & Conditions: (a) 2,3-dichlorobenzene sulfonyl chloride, pyridine, 18 h; (b) TFA, DCM, 2 h, 55 % over two steps.

SCHEME 3. Preparation of 2,3-dichloro-*N*-(1,2,3,4-tetrahydroisoquinolin-7-yl)benzenesulfonamide **15**.⁹⁵

However, for one of the monomers, adenine (**16**), the desired mono-protected starting materials were not readily available (Scheme 4). There were few precedents for the formation of the sulfonamide on the 6-position of the adenine **16**.⁹⁶ In most of these examples, phenyl or tosyl sulfonyl chlorides were heated with adenine **16** at 60-90 °C in pyridine for 2-4 days to give mixtures of regioisomeric products.

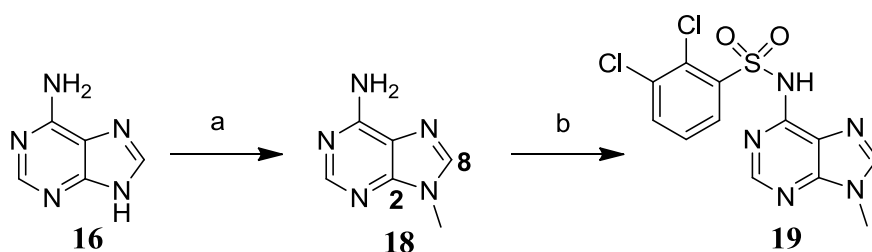


Reagents & Conditions: (a) 2,3-dichlorobenzenesulfonyl chloride, pyridine, 96 h, 22%.

SCHEME 4. Sulfonylation of adenine **16**.

However, attempts to carry out the reaction with 2,3-dichlorobenzenesulfonyl chloride failed. After heating for 96 h at 60 °C, the reaction only gave the undesired regioisomer **17**, with the sulfonamide at the 9-position of adenine **16**. As there were no obvious HMBC or NOE correlations in the 2D NMR to confirm the regioselectivity of the *N*-sulfonylation, a combination of ¹⁵N HMBC spectra and comparison against a similar literature compound, 9-tosyl-9*H*-purine-6-amine,⁹⁷ were used to confirm the structure.

In the interests of time, a decision was taken to prepare the target compound with the NH group at the 9-position of the adenine methylated to avoid the problems with regioselectivity. 2,3-Dichloro-*N*-(9-methyl-9*H*-purin-6-yl)benzenesulfonamide **19** was prepared by alkylation of adenine **16** with methyl iodide using conditions described by Cristalli and co-workers,⁹⁸ followed by reaction with 2,3-dichlorobenzenesulfonyl chloride (Scheme 5).



Reagents & Conditions: (a) MeI, Cs₂CO₃, DMF, 48 h, 39%; (b) 2,3-dichlorobenzenesulfonyl chloride, NaH, DMF, 32%.

SCHEME 5. Synthesis of 2,3-dichloro-*N*-(9-methyl-9*H*-purin-6-yl)benzenesulfonamide **19**.

The alkylation reaction in the presence of cesium carbonate gave only the desired monomethylated product **19**. This was confirmed using an HMBC experiment where two cross peaks were observed from the methyl protons (3.67 ppm) to C-2 (149.8) and C-8 (141.3) corresponding to $^3J_{C-H}$ couplings (Fig. 14).

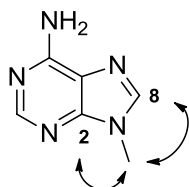


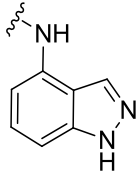
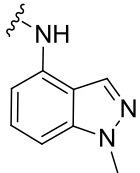
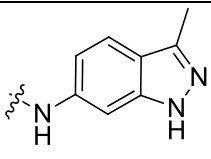
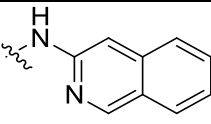
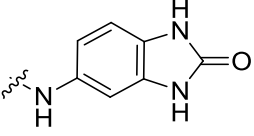
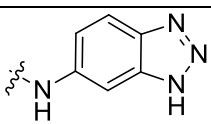
FIGURE 14. HMBC confirmation of the N9-methyl regioisomer.

In total, 83 compounds were submitted to the GTP γ S assay but only 9 compounds showed potency greater than 5.5 and LE greater than 0.35. The ‘hits’ from the focused set are summarised in Table 3. The LE, LLE_{AT}, clogP, the measured chromatographic logD at pH 7.4 (Chrom logD)^{89,90} and the measured stability data in simulated gastric fluid (SGF - an artificial dissolution medium that is intended to represent stomach acid) are included for all the active compounds.

TABLE 3. ‘Hits’ identified from the focused screen.



Cmpd	Structure	GTP γ S (pIC ₅₀)	LE	LLE _{AT}	MW	clogP	Chrom logD _{7.4}	Stability in SGF
13		5.9	0.36	0.36	358	1.8	1.7	Stable
19		5.9	0.37	0.36	358	1.9	1.0	Stable
20*		5.8	0.38	0.22	360	4.1	4.4	unstable

21*		5.8	0.38	0.25	342	3.7	3.7	stable
22*		5.5	0.34	0.23	356	3.5	4.6	stable
23*		6.0	0.37	0.24	356	3.9	4.2	stable
24*		5.6	0.35	0.21	353	4.0	5.2	unstable
25*		5.6	0.35	0.27	358	3.0	2.7	stable
26*		5.8	0.38	0.27	343	3.4	3.0	stable

*Note. Compounds **20-26** are not in the experimental as they were prepared by the CAT team.⁹⁵

The biological activity of the sulfonamide **22** is on the borderline of the set criteria (GTP γ S pIC₅₀: 5.5, LE: 0.34) but the ‘hit’ sulfonamide **21** without the *N*-methyl group was found to be slightly more potent. As both of these compounds are analogues, they were grouped together as one ‘hit’ series for further profiling.

These templates need to be stable when taken orally and so the number of ‘hits’ was further reduced by testing chemical stability of compounds in physiologically relevant media, such as the simulated gastric fluid (SGF). The sulfonamides **20** and **24** were found to be unstable and so these compounds were rejected.

Although the rest of the ‘hits’ showed reasonable potency, it was decided that a limited amount of chemistry should be carried out to demonstrate initial SAR and attempt to increase potency in order to further reduce the number of templates progressing to *in vivo* pharmacokinetic studies.

7.1 Potential uses of an intramolecular hydrogen bond

In principle, there are two methods of improving the potency based on the SAR from the indazole series and the published sulfonamide CCR4 antagonists.^{57,60,62} Firstly, the SAR has shown that replacing the 2,3-dichlorophenyl group with a 5-chlorothiophenyl group generally improves the potency in the candidate indazole series.⁶² In addition, the LLE_{AT} also improves, as the $clogP$ and MW of the 5-chlorothiophenyl group are lower compared to the 2,3-dichlorophenyl group. Secondly, the SAR also suggests that introducing a methoxy group next to the sulfonamide enhances the potency.⁵⁷ It is thought that the oxygen atom of the methyl ether functions as a hydrogen bond acceptor, which allows an intramolecular hydrogen bond to form with the NH of the sulfonamide forming a five or six-membered ring (Fig. 15).

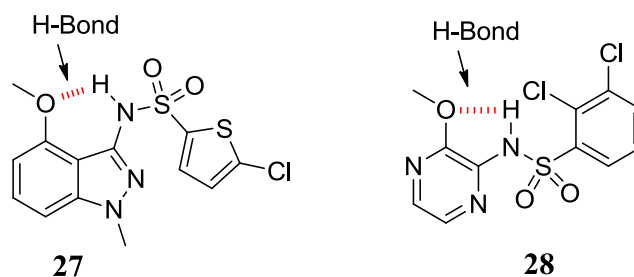


FIGURE 15. Intramolecular H-bond in the indazole (27) and AstraZeneca (28) series thought to be important for potency.

The intramolecular hydrogen bonding could have two effects; firstly, it could reduce the acidity of the sulfonamide; this could be important if there is a relationship between acidity and potency. However, earlier work on the indazole series has not shown conclusively that there is any real correlation between measured pK_a of the sulfonamide with the potency.^{57,62} Alternatively, the effect could be to allow the molecule to adopt a conformation in which it fits better in the active site. The intramolecular hydrogen bond will reduce conformational freedom, consequently resulting in loss of entropy. This hypothesis appears to be more plausible. There have been several publications demonstrating the importance of intramolecular hydrogen bond in conformationally locking small molecules to align favourably in the receptor.^{99,100} For example, Harter and co-workers designed a series of sulfonamide inhibitors with improved potency for caspase 1, a cysteine protease, by rigidifying the molecule through an intramolecular hydrogen bond.¹⁰⁰ An X-ray crystal structure of an analogue bound to the active site of caspase 1 confirmed the presence of an intramolecular hydrogen bond.

A small molecule X-ray crystal structure of **27** from the candidate indazole series was obtained (Fig. 16).⁵⁷ The low energy conformation based on the crystal structure confirmed that an intramolecular hydrogen bond exists, forming a six-membered ring, which is coplanar with the central indazole core. The intramolecular hydrogen bond allows the aryl sulfonamide to be positioned, approximately making a right angle with the plane normal of the indazole core [83.7(7)°].⁵⁷ It is presumed that this orthogonal conformation is preferred in the Site 2 allosteric site of CCR4, resulting in the increase in binding strength.

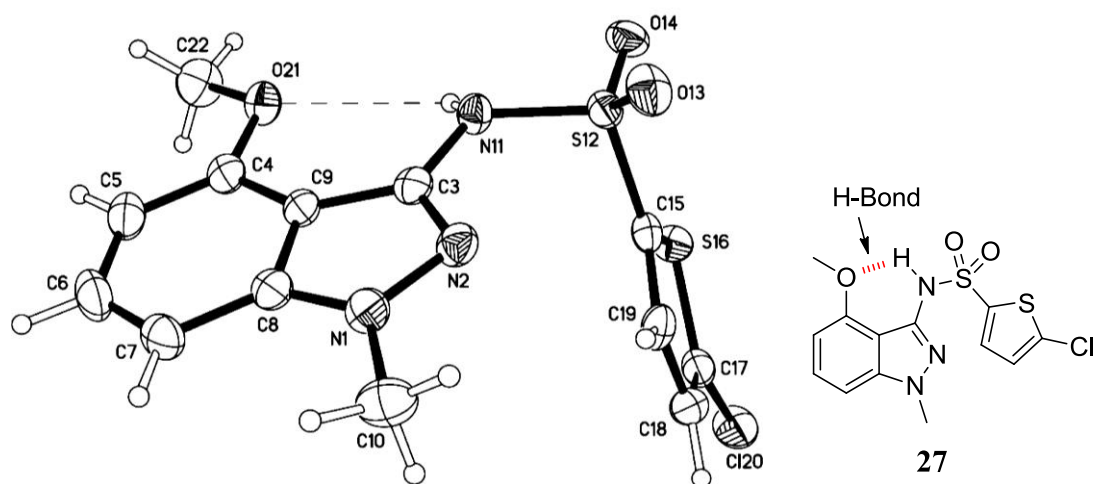


FIGURE 16. X-ray crystal structure of indazole **27** showing the intramolecular hydrogen bond between the NH of the sulfonamide and oxygen atom of the methoxy group with a dashed line. Distance from hydrogen of sulfonamide NH (N11) to oxygen (O21) = 2.52 Å [N–H, 0.80(3) Å; H···O, 2.52(3) Å; N···O, 3.036(3) Å; and \angle N–H···O, 124(3)°].

An X-ray crystal structure of the reference indazole sulfonamide compound **8**, containing a 2,3-dichlorobenzene sulfonamide substituent was also obtained (Fig. 17). The crystal structure of **8** contained two crystallographically independent molecules, where the conformations of the two compounds are related by a pseudo-inversion centre. Both of the independent molecules of **8** contained intramolecular hydrogen bonds between the sulfonamide NH and the oxygen atom of the methoxy group. This consequently allowed the plane normals of the indazole core rings and the 2,3-dichlorobenzene rings to be approximately orthogonal [81.7 (5)° and 75.9(5) °] as previously observed with the 5-chlorothiophenyl analogue **27**.

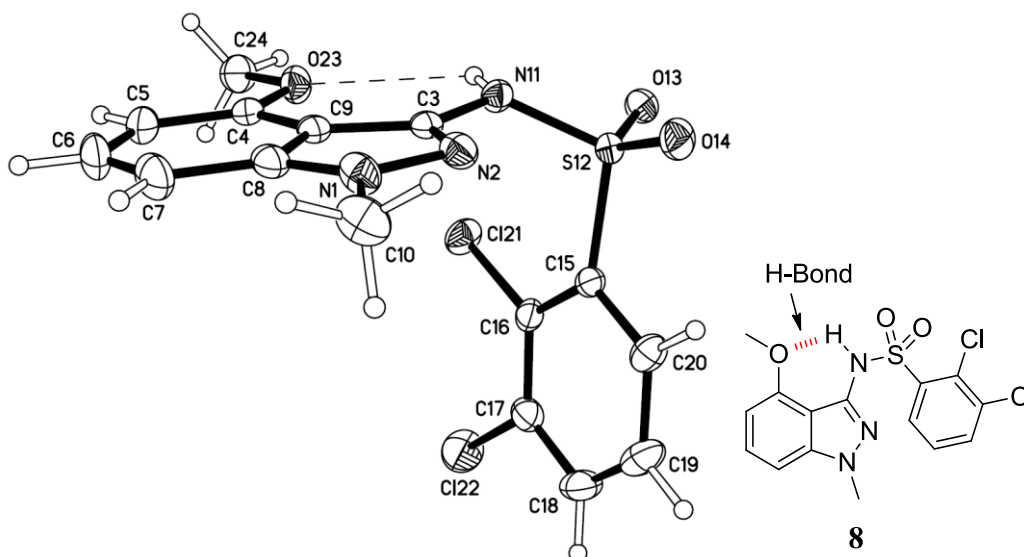


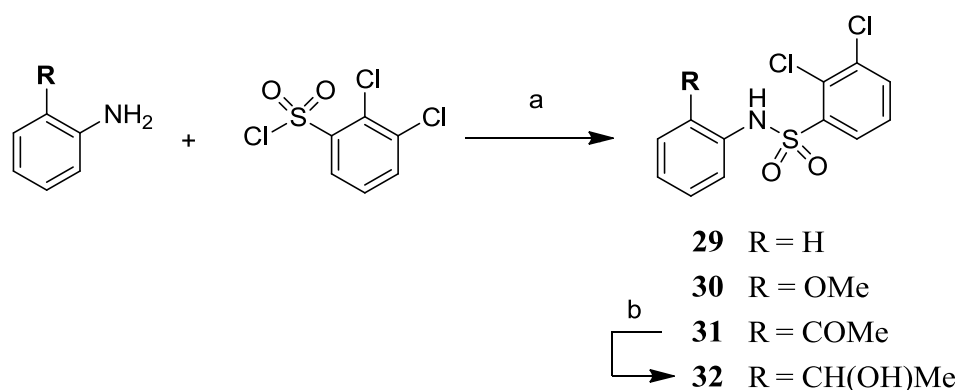
FIGURE 17. X-ray crystal structure of one of the independent molecules of indazole **8** showing the intramolecular hydrogen bond between the NH of the sulfonamide and oxygen atom of the methoxy group with a dashed line. Distance from hydrogen of sulfonamide NH (N11) to oxygen (O23) for the first molecule (shown above) = 2.49 Å. Metric details for the first molecule (shown above), N-H 0.80(2) Å, H...O 2.49(2) Å; N...O 3.011(2) Å; and \angle N-H...O 124(2) °; and for the second molecule, N-H 0.79(2) Å, H...O 2.47(2) Å; N...O 3.0238(19) Å; and \angle N-H...O 129(2) °.

In addition to enhancing the potency, by improving receptor binding, intramolecular hydrogen bonds could also have beneficial effect on the physicochemical properties of the molecules.¹⁰¹ For example, Cho and co-workers have demonstrated that for luteinising hormone-releasing receptor antagonists, an intramolecular hydrogen bond donor was important for oral absorption.¹⁰² They suggested that the intramolecular hydrogen bond shielded the hydrogen bond donor (NH) from solvent, and therefore increased the apparent lipophilicity of the molecule, allowing increased membrane permeability.

7.2 Introduction of intramolecular hydrogen bond interaction in phenyl sulfonamide

In order to identify other ‘hit’ series, the intramolecular hydrogen bond hypothesis was investigated further by introducing substituents at the *ortho*-position of a simple aniline, 2,3-dichlorobenzenesulfonamide **29**, that could potentially form a hydrogen bond with the NH sulfonamide (Table 4). Initially **29** and three analogues, **30-32** were prepared; sulfonamides **29**, **30** and **31** were synthesised from their corresponding commercially available substituted anilines, and compound **32** was synthesised by reducing sulfonamide **31** with sodium borohydride. All four compounds were tested in the GTP γ S assay and the results are shown below in table 4.

TABLE 4. Phenylsulfonamide analogues



Reagents & Conditions: (a) 2,3-dichlorobenzoyl chloride, pyridine, 18 h, **29** 69%, **30** 79%, **31** 71%; (b) NaBH₄, MeOH, 2 h, 53%.

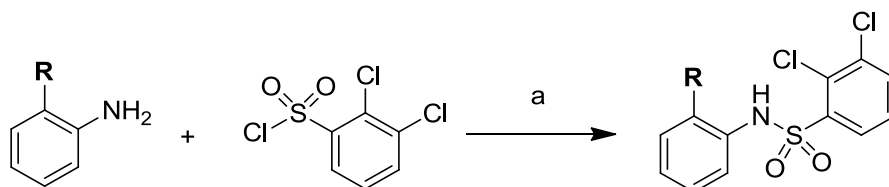
Cmpd	R group	GTP γ S (pIC ₅₀)	LE	LLE _{AT}	MW	clogP	Chrom logD _{7.4}	CLND sol μ g/mL
29	H	5.3	0.40	0.21	322	4.0	5.8	3
30	OMe	6.2	0.42	0.27	322	3.9	6.1	20
31		<4.5	-	-	344	4.0	6.5	5
32		5.2	0.34	0.27	346	2.7	5.0	132

The inhibitory activity of the sulfonamide **29** was 5.3 in the GTP γ S assay, whereas introducing a methoxy group at the *ortho*-position (**30**) resulted in a ten-fold increase in potency confirming earlier findings. Although sulfonamide **30** is equipotent to indazole **8** (GTP γ S pIC₅₀ = 6.2), it is more lipophilic (clogP = 3.9, chromlogD_{7.4} = 6.1 vs. **8**, clogP = 3.5, chromlogD_{7.4} = 5.3) and less soluble in the CLND assay (20 μ g/mL vs. **8**, 116 μ g/mL). Replacement of the methoxy group of **30** with ketone (compound **31**) or a secondary alcohol (compound **32**) was detrimental for activity in the GTP γ S assay.

Following these encouraging results, it was decided to search for alternative hydrogen bond interacting groups, which may provide benefit in terms of potency, reduced lipophilicity and improved solubility. It was envisaged that the methoxy group of **30** could be replaced with 5-membered heteroaryl rings containing heteroatoms that can act as hydrogen bond acceptors to the sulfonamide NH. It is expected this may favour the adoption of the orthogonal conformer

found in the X-ray structures of **8** and **2**. A number of commercially available aniline monomers with different 5-membered heterocyclic rings on the 2-position were reacted with 2,3-dichlorobenzenesulfonyl chloride. The results are summarised in Table 5.

TABLE 5. Preparation of phenylsulfonamide analogues with 5-membered heterocyclic groups.



Reagents & Conditions: (a) 2,3-dichlorobenzenesulfonyl chloride, pyridine, 18 h, **33** 71%, **34** 60%, **35** 47%, **36** 61%, **37** 29%, **38** 35%.

Cmpd	R group	GTP γ S (pIC ₅₀)	LE	LLE _{AT}	clogP	Chrom logD _{7.4}	CLND sol μ g/mL	pK _a measured
33		6.6	0.39	0.25	4.0	6.4	48	7.22
34		5.8	0.34	0.28	3.0	3.3	180	nd
35		5.9	0.35	0.27	3.2	2.9	233	5.28
36		5.1	0.30	0.19	3.8	4.4	123	6.87
37		<4.5	-	-	3.7	nd	10	7.68
38		<4.5	-	-	2.8	6.3	8	7.29

nd = not determined

Replacing the methoxy group of **30** with a pyrazole ring (**33**) resulted in nearly half a log unit improvement of potency in the GTP γ S assay. However, replacement of the methoxy group with oxazole (**37**) and oxadiazoles (**38** and **39**) were found to be detrimental for activity, whereas the potency only slightly reduced when the methoxy group was replaced with a tetrazole (**34**) or triazole (**35**). A possible explanation could be that that the pyrazole ring was the most effective intramolecular hydrogen bond acceptor in this set of five compounds. It

should be noted that the lipophilicity of the phenylpyrazole **33** was high ($\text{clogP} = 4.0$, $\text{chromlogD}_{7.4} = 6.4$), and although the CLND solubility of **33** is twofold better ($48 \mu\text{g/mL}$) than the methoxy analogue **30** ($20 \mu\text{g/mL}$), it was still unacceptably low. The pK_a were measured using a spectroscopic method, see experimental section for detail,⁹⁰ and appendix 1 for correlation between measured pK_a and calculated pK_a of few of the aryl sulfonamide analogues reported in this thesis. As with the indazole series, there appears to be no real correlation between acidity of the sulfonamide and the potency. At first, comparing the pyrazole analogue **33**, which has a relatively neutral pK_a value (7.22) to the more acidic tetrazole **35** (5.28), there appears to be some correlation between the pK_a of the sulfonamide and the potency. It is expected that at neutral pH, the former would be less ionised (50% neutral and 50% anion) than the latter (100% anion), which could explain why there is an intramolecular hydrogen bond in the pyrazole analogue **33** and not in the tetrazole **35**. However, both the pyrazole analogue **33** and oxadiazole analogue **38** have similar measured pK_a (7.22 and 7.29 respectively) and measured chromlogD , but the oxadiazole **38** was inactive. In addition, oxadiazole **37** is less acidic (pK_a 7.68), and if there was any relationship between acidity and pK_a , **37** would be expected to be more active, but it was found to be inactive.

The binding result from the GTP γ S assay further reinforced the idea that both the pyrazole and methoxy group were acting as hydrogen bond acceptors, fixing the molecule in a conformation allowing the 2,3-dichlobenzene group to be orthogonal to the core ring, and therefore, enhancing the potency. A small molecule crystal structure of the phenylpyrazole **33** was obtained, which also confirmed the presence of an intramolecular hydrogen bond between the NH (N9) of the sulfonamide to one of the nitrogen (N17) of the pyrazole ring (Fig. 18).¹⁰³

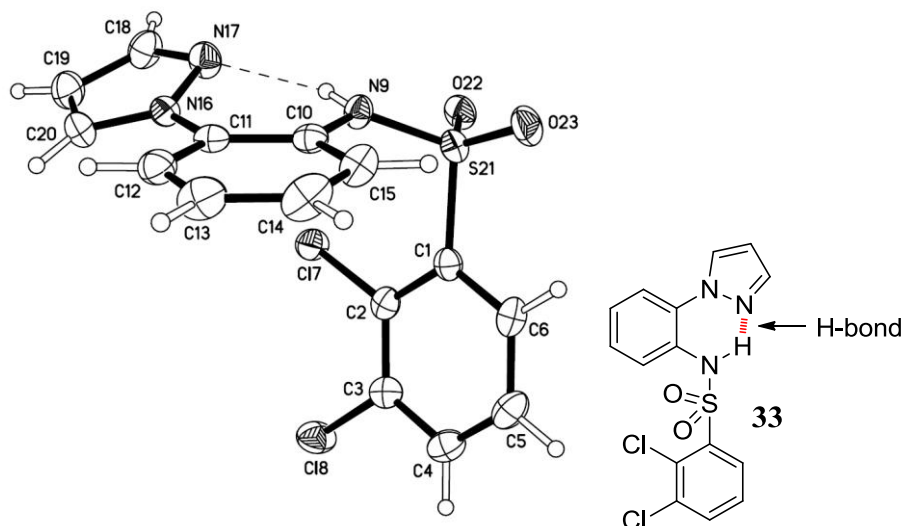


FIGURE 18. X-ray crystal structure of phenyl pyrazole **33** showing the intramolecular hydrogen bond between the NH of the sulfonamide and nitrogen of the pyrazole with a dashed line. Distance from hydrogen of sulfonamide NH (N9) to pyrazole nitrogen (N17) = 1.95 Å, torsional angle of sulfonamide NH (N9) to pyrazole nitrogen (N17) = 19°. [N-H 0.81(2) Å, H...N 1.95(2) Å; N...N 2.638(3) Å; and \angle N-H...N 143(2) °]. Plane normals to the two phenyl rings were inclined at 76.65(7) °.

The X-ray structure of phenylpyrazole **33** was overlaid with indazole **8** (the independent molecule shown in Fig. 17) using a least-squares fit for the non-hydrogen atoms in the 2,3-dichlorobenzene sulfonamide side chains, and is shown below in Fig. 19. It is quite clear from the overlay how the remainder of the two molecules occupy a similar region of space relative to the atoms fitted. It is postulated that these conformations are potentially driven by the intramolecular hydrogen bonding interactions.

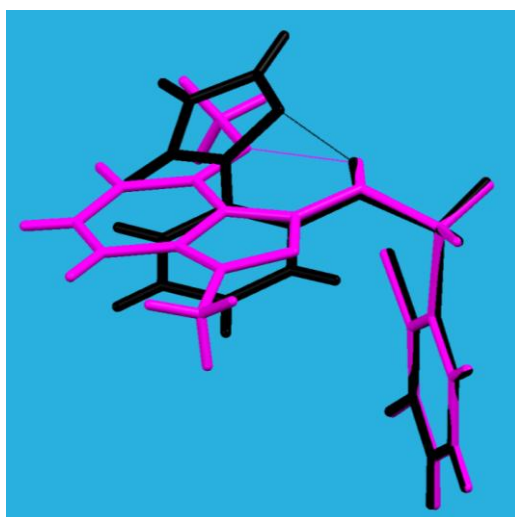


FIGURE 19. Overlay of X-ray structures of indazole **8** and phenylpyrazole **33**. Least-squares fit (RMS = 0.05 Å) of the 12 non-hydrogen atoms in the sulfonamide side-chain of indazole **8** (magenta) and phenylpyrazole **33** (black). The intramolecular hydrogen bonds are depicted as dotted lines.

In order to understand why the other compounds were not as active as the phenylpyrazole **33**, an X-ray crystal structure of one of the less active compounds, phenyltetrazole **35**, was obtained (Fig. 20).¹⁰³

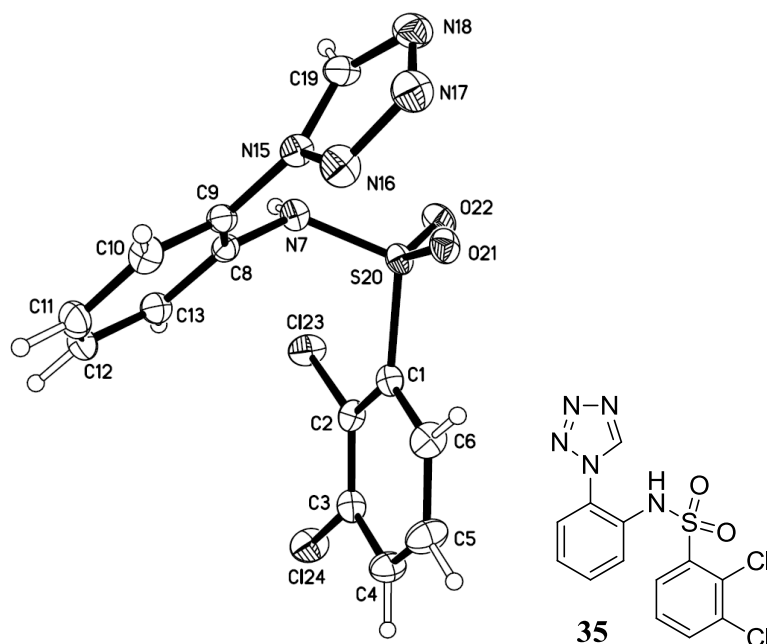


FIGURE 20. X-ray crystal structure of phenyltetrazole **35** showing no intramolecular hydrogen bond between the NH of the sulfonamide and the nitrogen of the tetrazole ring. Distance from hydrogen of sulfonamide NH (N7) to tetrazole nitrogen (N16) = 4.8 Å. The sulfonamide NH did not take part in an intramolecular hydrogen bond but instead was associated with an intermolecular hydrogen bond to N17 [N-H 0.80(2) Å, H...N 2.34(2) Å; N...N 3.107(2) Å; and \angle N-H...N 161(2)°].

The X-ray crystal structure of **35** showed that the tetrazole ring is out of the plane of the phenyl core, and the 2,3-dichlorobenzene ring is somewhat less orthogonal (normal inclined at 65.7(7)°) to the phenyl core compared to the X-ray structure of **33**. None of the nitrogens on the tetrazole ring is acting as a hydrogen bond acceptor for the NH of the sulfonamide. The unit cell of the crystal structure of tetrazole **35** showed that the hydrogen at N7 has an intermolecular hydrogen bond to another molecule of tetrazole (N17 atom, which is exposed to the outside).

The structures of **33** and **35** were overlaid as before on the basis of a least-squares fit for the non-hydrogen atoms in the 2,3-dichlorobenzene sulfonamide side-chains (Fig. 21). The overlays shows that the 2,3-dichlorobenzene moiety of both X-rays are more or less identical but the rest of the molecules are now occupying a different region of space relative to each other. Geometrically, the tetrazole nitrogens are more exposed to the outside surface, therefore, favouring other hydrogen bonding partners, whereas the pyrazole is more inward

facing, favouring intramolecular interaction. These data further validate the theory that the intramolecular hydrogen bond is important for locking the conformation in a fixed position, which is believed to be important for biological activity. However, it is important to highlight that in physiological systems in solution, the conformation could be completely different to the X-ray crystal structure.

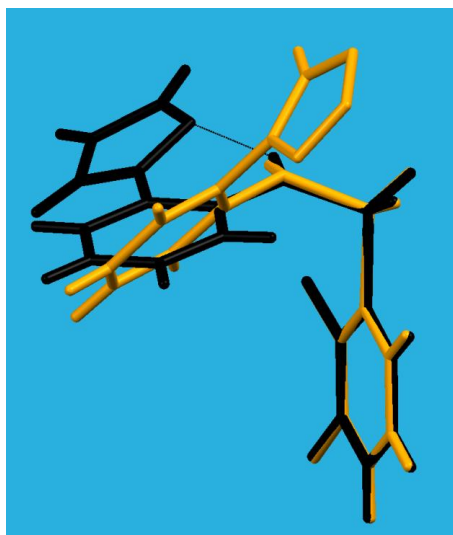


FIGURE 21. Overlay of X-ray structures of phenylpyrazole **33** and phenyltetrazole **35**. Least-squares fit (RMS = 0.05 Å) of the 12 non-hydrogen atoms in the sulfonamide side-chain of phenylpyrazole **33** (black) and phenyltetrazole **35** (orange). The intramolecular hydrogen bond in the former is depicted as a dotted line.

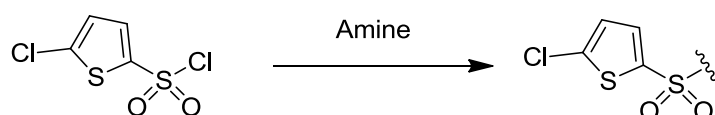
Electronic structure calculations were carried out in order to determine if the conformations observed in the small molecule X-ray crystal structures were in agreement with those expected in solutions.^{103,104} Monte Carlo conformational searching using the PM3 semi empirical method and geometry optimisation calculations (B3LYP/6-31G* in water) identified clip-shaped or orthogonal conformations corresponding to the conformers revealed in the crystal structures of **8** and **33**, and to a lesser extent **35**. For the indazole **8** and phenylpyrazole **33**, the two lowest energy conformers in solutions were found to be clip or orthogonal, and were in good agreement with the conformers observed in the small molecule crystal structures. However, for the phenyltetrazole **35**, the lowest energy clip-shaped conformation that was in the same orientation as the minima for **8** and **33**, was found to be 0.7 kcal mol⁻¹ higher in energy. The conformation of **35** found in the crystal structure (with no intramolecular hydrogen bond) was also identified in the electronic analysis, at 5.1 kcal mol⁻¹ higher than the global minimum. This suggests that the conformer of **35** observed in the crystal structure may have resulted due to packing forces, and may not be populated in

solution. The order of preference for the clip or orthogonal conformation found in the X-ray crystal structures of **8**, **33** and **35** were in accordance with the order of potency (**33** > **8** > **35**) in the GTP γ S assay.^{103,104}

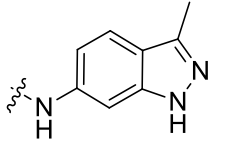
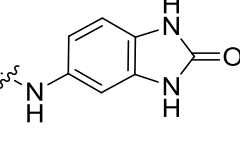
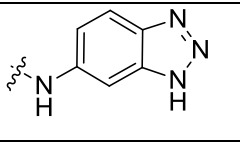
7.3 First approach to improving potency – 5-chlorothiophene sulfonamide analogues

As mentioned previously, based on the work on the indazole series, it is known that replacing the 2,3-dichlorophenyl group with a 5-chlorothiophenyl group generally increases the potency and helps improve ligand efficiency. As the amine monomers and 5-chlorothiophenesulfonyl chloride were readily available, the initial chemistry focused on replacing the 2,3-dichlorophenyl group of all the remaining ‘hits’ with a 5-chlorothiophenyl group. The amine monomers were reacted with 5-chlorothiophenesulfonyl chloride either in pyridine or with sodium hydride in DMF to give the target compounds. The biological results are shown below in Table 6.

TABLE 6. Preparation and biological data of 5-chlorothiophene sulfonamide products.



Cmpd	Structure Reg. no.	GTP γ S (pIC ₅₀)	LE	LLE _{AT}	MW	clogP	Chrom logD	Yield
39		5.7	0.39	0.41	329	1.3	1.3	16%
40		5.7	0.39	0.41	329	1.3	0.9	48%
41		6.7	0.43	0.32	339	3.5	6.3	78%
42		5.6	0.40	0.29	313	3.1	3.3	67%

43		5.8	0.39	0.26	327	3.6	3.8	40%
44		5.0	0.34	0.29	330	2.4	2.2	64%
45		5.7	0.41	0.32	315	2.8	2.3	53%

In most of the examples, replacement of 2,3-dichlorophenyl with 5-chlorothiophenyl did not improve the potency but as the clogP and MW were reduced, the LE and LLE_{AT} of the compounds did improve. The chromlogD of the 5-chlorothiophenyl analogues were also lower than those of the corresponding 2,3-dichlorophenyl analogues. The benzimidazolone series, as exemplified by sulfonamide **44**, was the only compound that showed half a log unit reduction in potency when the 2,3-dichlorophenyl group was replaced with a 5-chlorothiophenyl group.

The phenylpyrazole series, as exemplified by sulfonamide **41**, did show a slight improvement and with the reduced clogP and MW, the compound appeared as an attractive starting point. Although, it should be noted that the measured chromlogD value of both the 2,3-dichlorophenyl (compound **33**) and 5-chlorothiophenyl analogue (compound **41**) from the phenylpyrazole series are high (6.5 and 6.3 respectively). One of the main priorities for the phenylpyrazole series will be to reduce lipophilicity and this is discussed later in section 7.6 of the thesis.

7.4 Second approach to improving potency – introduction of a methoxy group

The second approach to improving the potency of the remaining active templates from the focused array was to introduce a methoxy group adjacent to the sulfonamide substituent on the core. The sulfonamides **21**, **23**, **25** and **26** have two positions free and the focus of the chemistry was to introduce methoxy groups on both of these positions (Fig. 22).

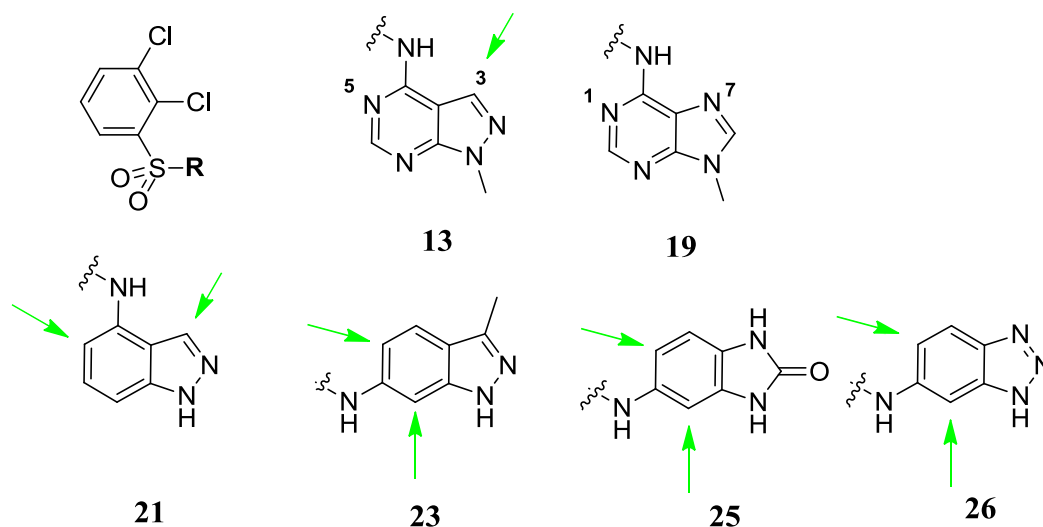


FIGURE 22. Possible positions to introduce an H-bond acceptor on the new templates.

However, the pyrazolopyrimidine **13** has only one position, and the adenine **19** has no positions free next to the sulfonamide substituent to introduce the methoxy group, as they are flanked with nitrogen (Fig. 22). One possibility would be to remove one of the nitrogens and replace it with a carbon to allow a position to incorporate a methoxy group. For the adenine **19**, replacement of the nitrogen on the 7-position with a carbon will give an azaindole derivative. From previous in-house experience, it is known that indoles are not active, so this only leaves the N1-position to introduce the methoxy group. However, before introducing the methoxy group, it was decided to replace the nitrogen with a carbon first, to determine if the compound remained potent. This will allow the biological activity to be compared with the reference indazole compound **7** and other sulfonamide ‘hits’ which lack the methoxy group.

The target sulfonamide compound **53** was prepared following the previously published route, converting commercially available azabenzimidazole **46** to 7-nitroazabenzimidazole **49** (Scheme 6).¹⁰⁵ This was carried out by reacting azabenzimidazole **46** with hydrogen peroxide to give the *N*-oxide derivative **47**. The *N*-oxide activates the 7-position of **47** for electrophilic aromatic substitution. Selective nitration at the 7-position with nitric acid in TFA, followed by reduction of the *N*-oxide with phosphorus trichloride, gave the deoxygenated derivative **49**. The ¹H NMR spectrum of the nitration product **48**, contained a pair of doublets corresponding to the protons on H5 and H6 with a ³*J* coupling constant of 7.0 Hz. These results conclusively proved that the nitration occurred at the 7-position. Alkylation of **49** with methyl iodide gave the alkylated regioisomeric products **50** and **51** (ratio 1:3). These were separated by HPLC, and the structures were confirmed by a combination of ¹³C and ¹⁵N

HMBC (Fig. 23). For compound **50**, key ^1H - ^{15}N HMBC correlations were observed between the N1-nitrogen (145 ppm) to the *N*-methyl protons (4.09 ppm) and the proton at the 2-position (8.58 ppm). In addition, key ^1H - ^{13}C HMBC correlations were observed between the *N*-methyl protons (4.09 ppm) to the carbon at the 8-position (117.6 ppm) and 2-position (151.3 ppm). For compound **51**, key ^1H - ^{13}C HMBC correlations were observed between the carbon at the 9-position (151.0 ppm) to the *N*-methyl protons (3.97 ppm), and the protons at the 2 and 5-positions (8.90 - 8.38 ppm).

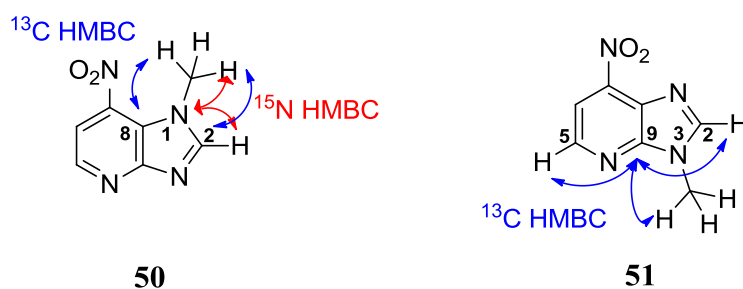
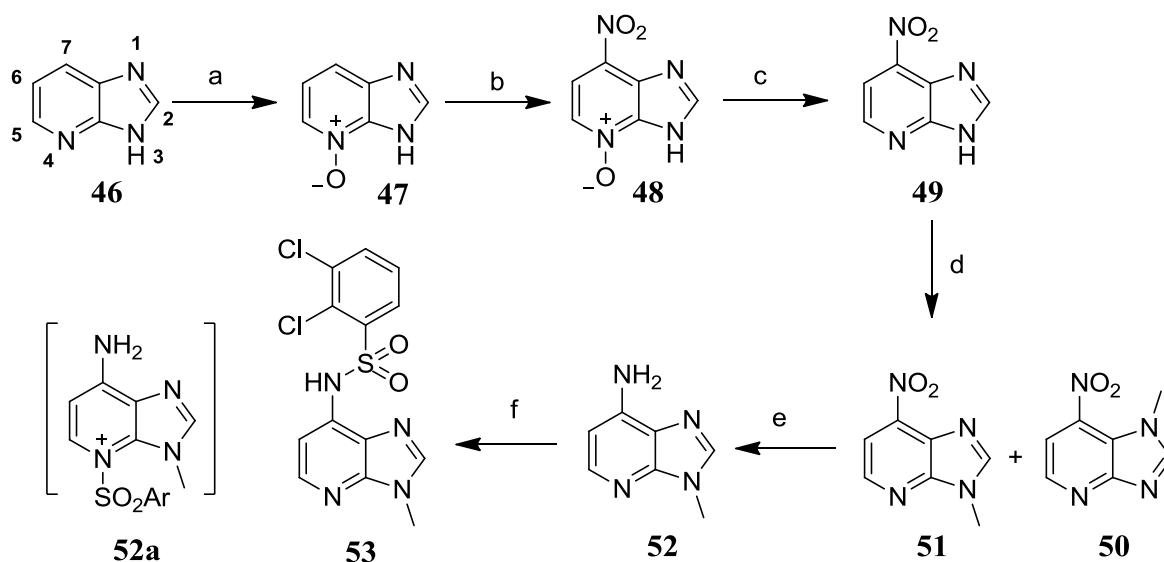


FIGURE 23. HMBC confirmation of the regioisomers 50 and 51.

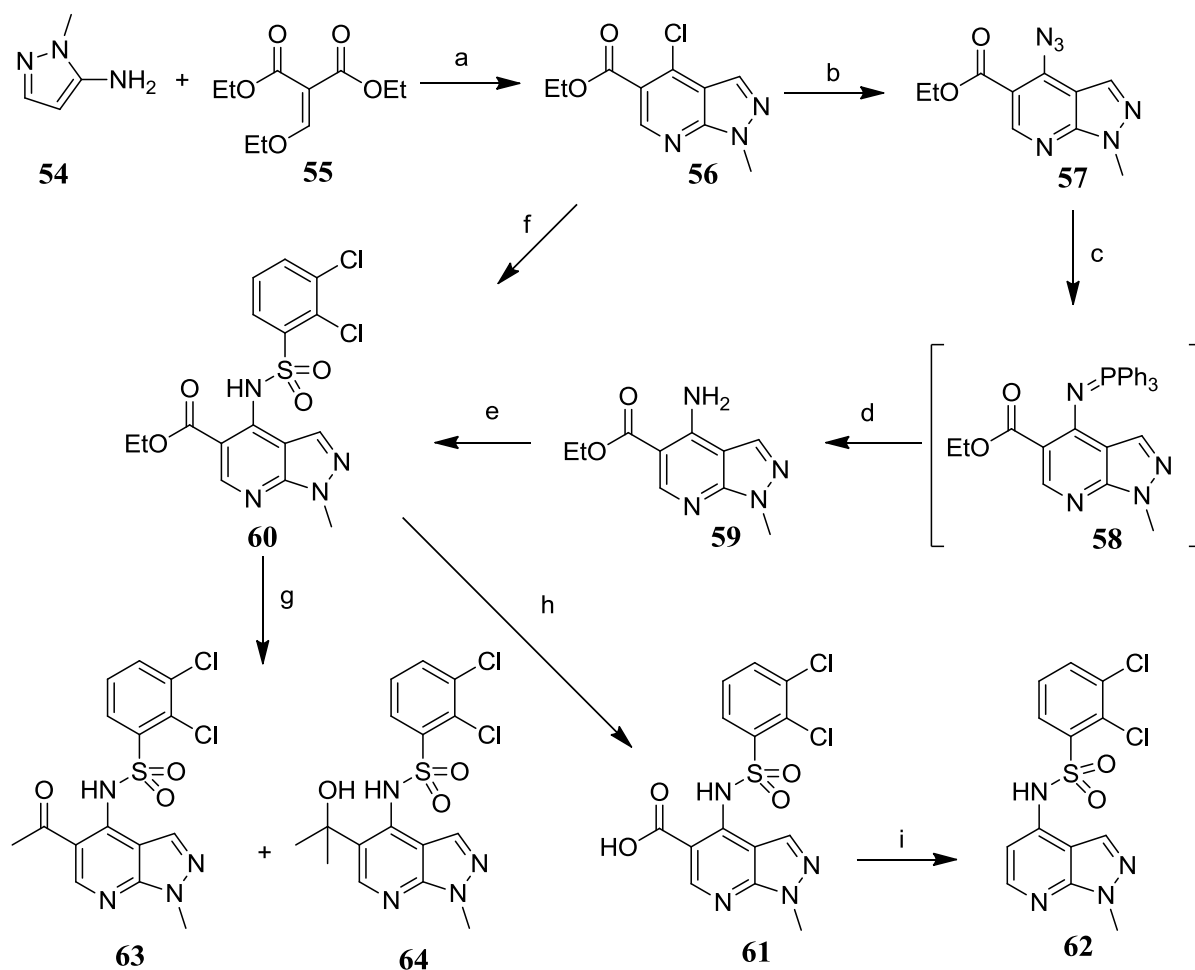
Azabenzimidazole **51** was reduced over a 10% Pd/C catalyst under a hydrogen atmosphere, to afford amine **52**. The final reaction with 2,3-dichlorobenzenesulfonyl chloride proved problematic. In the LCMS, a very small amount of product was observed, with the main peak arising from the starting material **52**, and the hydrolysed sulfonyl chloride. Even when reagents were used in excess, the reaction provided only 10% of the desired product **53**. In the reaction, amine **52** could act like DMAP where the sulfonyl chloride reacts on the pyridine nitrogen, which hydrolyses during work-up to provide the acid.¹⁰⁶ Normally, species like the acylated DMAP acts as a reactive intermediate (nucleophilic catalysis is in operation) and would react quickly with the amine to give the acylated product.¹⁰⁶⁻¹⁰⁸ It is noteworthy that in this instance, the acylated species **52a** is presumably quite stable and does not react with the amine **52** (calc. $\text{pK}_a = 8.0$, ACD software, version 12). It is not clear why the amine **52** is not very reactive. However, as enough material was recovered to get the initial *in vitro* data, the reaction was not optimised.



Reagents & Conditions: (a) H_2O_2 , AcOH, 80 °C, 8 h, 64%; (b) 70% fuming HNO_3 , TFA, 90 °C, 3 h, 22%; (c) PCl_3 , MeCN, 80 °C, 2 h, 40%; (d) MeI, Cs_2CO_3 , DMF, 18 h, **51** 61%, **50** 25%; (e) H_2 , Pd/C (10%), EtOH, 3h, 77%; (f) NaH, DMF, 18h, 10%.

SCHEME 6. Preparation of 2,3-dichloro-*N*-(3-methyl-3*H*-imidazo[4,5-*b*]pyridin-7-yl)benzenesulfonamide **53.**

The pyrazolopyridine template, exemplified by **13** does have a free 3-position at which the methoxy group could be introduced (Fig. 22), but the nitrogen at the 5-position could also be replaced with a carbon to allow another position to incorporate a methoxy group. The pyrazolopyridine analogue of **13**, with replacement of the nitrogen on the 5-position with a carbon, was prepared to check if the compound still remains active (Scheme 8). A common 4-aminopyrazolopyridine ester intermediate **59** was prepared by following a previously published procedure.¹⁰⁹ Condensation of *N*-1-ethyl-5-aminopyrazole **54** with diethylethoxy methylenemalonate **55** was followed by treatment with phosphoryl chloride to give the 4-chloropyrazolopyridine ester intermediate **56**. Nucleophilic substitution with sodium azide and reduction under Staudinger conditions¹¹⁰ afforded the 4-aminopyrazolopyridine ester intermediate **59**.



Reagents & Conditions: (a) i. 110 °C, 1.5 h, ii. POCl₃, 110 °C, 3.5 h, 54%; (b) NaN₃, DMF, 72 h, 89%; (c) PPh₃, THF, 2.5 h; (d) conc HCl, 4 h, 68%; (e) 2,3-dichlorobenzoyl chloride, pyridine, 90 °C, 18 h, 2%; or K₂CO₃, DMF, 50 °C, 72 h, 37%; (f) 2,3-dichlorobenzoyl chloride, Pd(OAc)₂, Xantphos, Cs₂CO₃, Dioxane, 150 °C, 30 min, μ wave, 63%; (g) MeMgBr (2.5 equiv.), THF, -78 °C, **63** 8%, **64** 23%; (h) NaOH, EtOH, 18 h, 82%; (i) DMF, 190 °C, μ wave, 28%.

SCHEME 7. Preparation of pyrazolopyridine analogues **62**, **63** & **64**.

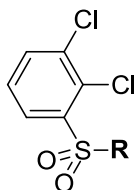
As with the aminoadenine **52**, the reaction with 2,3-dichlorobenzoyl chloride in pyridine proved problematic, only providing the sulfonamide product **60** in 2% yield. An alternative method using potassium carbonate in DMF improved the yield, but only to 37%. A Buchwald coupling reaction was carried out between 2,3-dichlorobenzoyl chloride and 4-chloropyrazolopyridine ester **56** to afford the desired product **60** in 63% isolated yield. Saponification of sulfonamide **60**, followed by decarboxylation of the acid **61** upon microwave heating at 190 °C in DMF, provided the desired target sulfonamide compound **62**.

The 4-aminopyrazolopyridine ester intermediate **60** was also used to prepare both the ketone **63** and tertiary alcohol **64** by treatment with methyl Grignard reagent at low temperature

(Scheme 7). Along with the desired target compounds, both the ketone **63** and alcohol **64** were submitted for test in the GTP γ S assay as the oxygen atom on both of these compounds could form an intramolecular hydrogen bond to the sulfonamide hydrogen through a 6-membered ring.

The results from these compounds are shown below in Table 7.

TABLE 7. GTP γ S data for adenine and pyrazolopyrimidine analogues.



Cmpd	R group	GTP γ S (pIC ₅₀)	LE	LLE _{AT}	MW	clogP	Chrom logD _{7.4}
53		5.4	0.33	0.27	356	2.8	1.8
60		5.1	0.26	0.21	428	3.2	3.4
62		4.9	0.31	0.25	356	2.7	1.7
63		<4.5	-	-	398	2.8	2.4
64		<4.5	-	-	415	1.8	nd

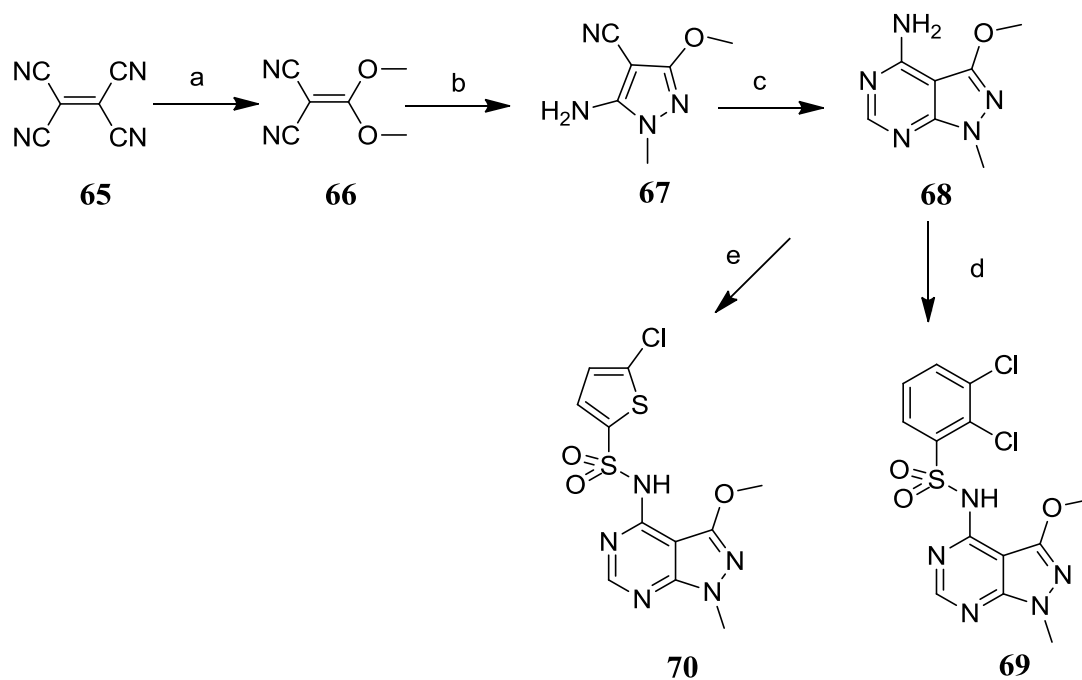
nd = not determined

It appears that half a log unit of potency was lost in the GTP γ S by replacing the nitrogen with carbon to give the sulfonamide **53** ($pIC_{50} = 5.4$) (Table 7) compared to the adenine **19** ($pIC_{50} = 6.0$) (Table 3). Generally, incorporating a methoxy group improves the potency by half a log unit so this suggests that, in terms of potency, it will not be worth removing the nitrogen to introduce a methoxy group. As the adenine template (**19**) without an activating group is not potent enough in the GTP γ S assay, this series was abandoned.

In the pyrazolopyrimidine series, exemplified by sulfonamide **13** ($pIC_{50} = 5.4$) (Table 3), replacing the nitrogen with carbon to give the sulfonamide **62** was detrimental for activity, resulting in loss of potency by 100-fold (Table 7). The activity was not improved by introducing an ethyl ester (compound **60**), ketone (compound **63**) or tertiary alcohol (compound **64**). Although, the methoxy group was not introduced, the SAR based on the indazole series⁶² suggests that incorporating the methoxy group at the 5-position will not improve the potency above that of sulfonamide **13**.

Nonetheless, the pyrazolopyrimidine sulfonamide **13** does have the 3-position free to accommodate a methoxy group, which could potentially accept a hydrogen bond from the NH of the sulfonamide (Fig. 22). The 3-methoxypyrazolopyrimidine **69** was prepared from commercially available tetracyanoethylene (**65**) in four steps (Scheme 8).

The synthetic route involved preparation of a key intermediate, 4-amino-3-methoxypyrazolopyrimidine **68** according to literature and patent procedures.¹¹¹⁻¹¹³ Reaction of tetracyanoethylene (**65**) with MeOH and urea afforded the dimethoxymethylene malononitrile **66**. Subsequent reaction with methylhydrazine, followed by condensation with formamide afforded 4-amino-3-methoxypyrazolopyrimidine **68** in moderate yield. Finally, reaction with either 2,3-dichlorobenzenesulfonyl chloride or 5-chlorothiophenesulfonyl chloride in the presence of sodium hydride afforded the desired target pyrazolopyrimidine compounds **69** and **70** in 39% and 47% yield respectively from **68**.

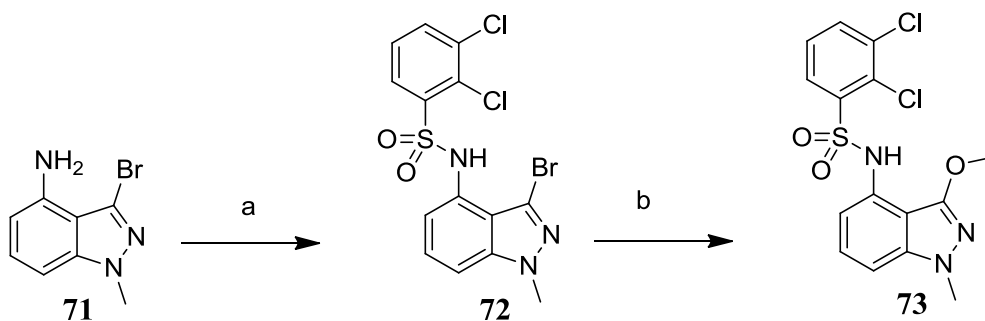


Reagents & Conditions: (a) urea, MeOH, 50 °C, 0.5 h, 29%; (b) methylhydrazine, MeOH, reflux, 2.5 h, 58%; (c) formamide, 185 °C, 4 h, 39%; (d) 2,3-dichlorobenzenesulfonyl chloride, NaH, DMF, rt, 39%; (e) 5-chlorothiophene-2-sulfonyl chloride, NaH, DMF, rt, 47%.

SCHEME 8. Preparation of pyrazolopyrimidine 69 and 70.

There were no similar examples of pyrazolopyrimidine sulfonamide with a methoxy group at the 3-position (**69**) in the literature, and in order to determine if the compound will be stable if taken orally, the compound was submitted for a stability test in simulated gastric fluid. Fortunately, the compound was found to be stable but it was also found to be photolabile. At this stage of the programme, this did not appear to be a problem for further progression, as there are many ways to solve this problem such as placing the active drug molecule in a capsule to avoid photochemical decomposition.

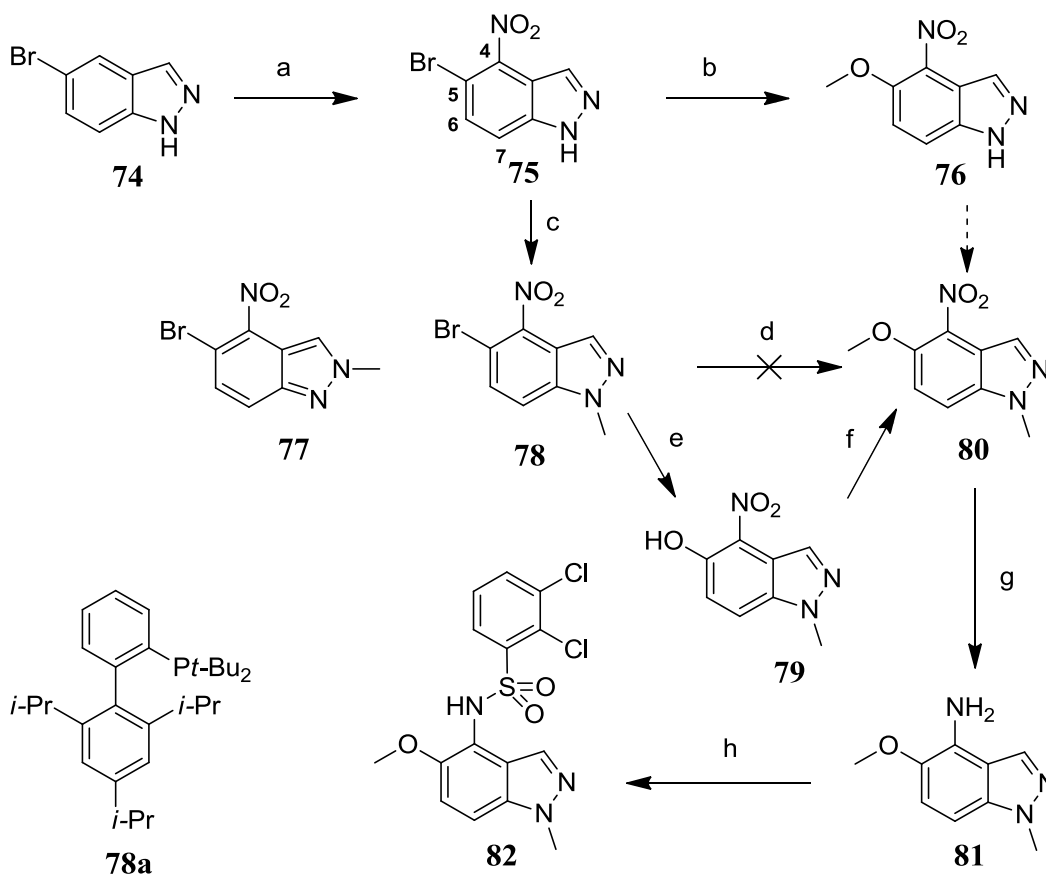
The 4-aminoindazole **21** has two positions free next to the sulfonamide substituent to introduce the methoxy group (Fig. 23). The methoxy group at the 3-position was introduced by a coupling reaction between 3-bromoindazole sulfonamide **72** and methanol, using copper as a catalyst, to afford the 3-methoxyindazole sulfonamide **73** in 39% yield after MDAP purification (Scheme 9). The 3-bromoindazole sulfonamide **72** was prepared from reaction of commercially available 4-amino-3-bromoindazole **71** with 2,3-dichlorobenzenesulfonyl chloride in pyridine giving the product in 67% yield.



Reagents & Conditions: (a) 2,3-dichlorobenzene sulfonyl chloride, pyridine, rt, 18 h, 67%; (b) NaO^tBu, MeOH, Cu powder, sealed tube, 150 °C, 18 h, 39%.

SCHEME 9. Preparation of 4-aminoindazole sulfonamide 73.

The introduction of the methoxy group at the 5-position of the 4-aminoindazole series is described in Scheme 10.



Reagents & Conditions: (a) 70% fuming HNO₃, conc. H₂SO₄, 0 °C, 1 h, 90%; (b) NaOMe, CuBr, MeOH, DMF, 120 °C, 2%; (c) NaH, MeI, DMF, **77** 23% and **78** 46%; (d) Cu, NaO^t-Bu, MeOH, **82** 0% and **79** 56%; (e) KOH, Pd₂dba₃, **78a**, 110 °C, 0.5 h, μ wave, 80%; (f) MeI, K₂CO₃, DMF, 98%; (g) SnCl₂, conc. HCl, MeOH, 52%; (h) 2,3-dichlorobenzene sulfonyl chloride, pyridine, 43%.

SCHEME 10. Preparation of 4-aminoindazole sulfonamide 82.

Nitration of commercially available 5-bromoindazole **74** at 0 °C occurred exclusively at the 4-position affording 4-nitroindazole **75** in excellent yield. The ^1H NMR spectrum of **75** contained a pair of doublets corresponding to the H-6 (7.77 ppm) and H-7 (7.87 ppm) protons with a 3J coupling constant of 8.8 Hz, confirming that the nitration occurred at the 4-position. Nucleophilic displacement of the bromine of **75** with sodium methoxide using various conditions, including conventional heating to high temperature, and heating in the microwave reactor failed. The coupling of **75** with sodium methoxide, using copper bromide as the catalyst, only gave 2% of 5-methoxyindazole **76**. Various copper coupling reactions were attempted to introduce the methoxy group, including the use of copper bromide, copper iodide, and the catalysts with different bases and different ligands, but the reactions did not give any 5-methoxyindazole product, **76**.¹¹⁴⁻¹¹⁷ It should be noted that in the LCMS of few of the reactions, a peak was observed for an *N*-arylation product (not isolated), where the NH of indazole **75** couples to the 5-bromo-position of another molecule of **75**. There are vast numbers of literature precedents for the copper-catalysed *N*-arylation of indazole at the N1 or N2-position with aryl halides,¹¹⁸⁻¹²¹ and it is thought that this may be competing with the desired C-O bond formation. In order to avoid any unwanted side reactions, a decision was taken to alkylate the N1-position of indazole **75** before carrying out the coupling reaction. The reaction of **75** with methyl iodide, using sodium hydride as base, gave a mixture of regioisomers, **77** and **78**, with the desired 1-methylindazole **78** predominating (ratio 1:2). The regiochemistry of the two isomers was determined using ^{13}C HMBC experiment, where for regioisomer **77**, a correlation was observed between the *N*-methyl protons (4.24 ppm) and the carbon at the 3-position (125.6 ppm), and for regioisomer **78** a cross peak was observed between the *N*-methyl protons (4.14 ppm) and the carbon at the 8-position (141.4 ppm) corresponding to $^3J_{\text{C-H}}$ couplings (Fig. 24).

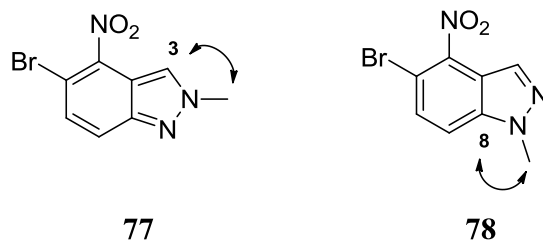
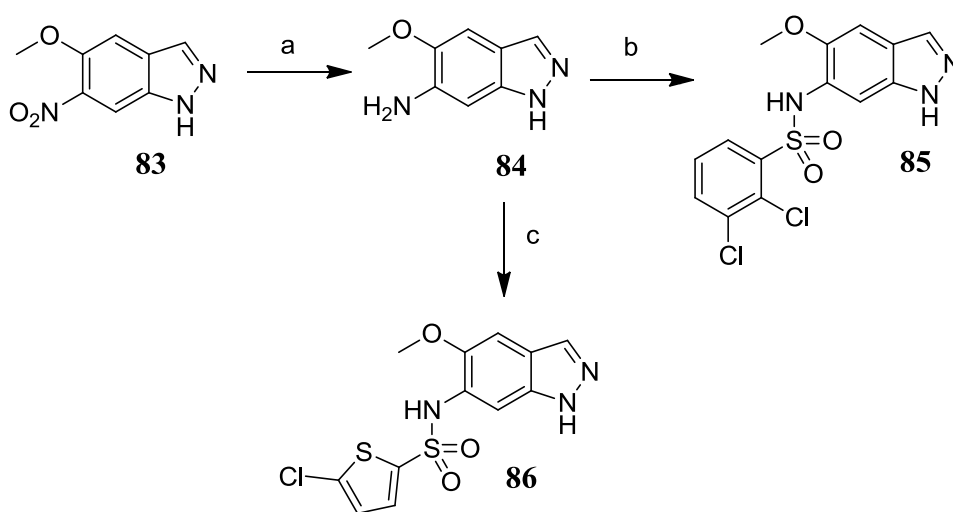


FIGURE 24. HMBC confirmation of the regioisomers 77 and 78.

Attempts to replace the bromine of the indazole **78** with a methoxy group, using sodium methoxide under conventional heating, and coupling with the copper-catalysed conditions described above, were all found to be unsuccessful. A decision was taken to prepare the 5-

hydroxyindazole **79** using palladium-catalysed hydroxylation. Among the reactions screened, Buchwald and co-workers' method,¹²² employing bulky monodentate phosphine ligand **78a** with KOH, and Pd₂dba₃ as the pre-catalyst, was found to be very effective, affording the product **79**, in 80% yield. The 5-hydroxyindazole **79** was alkylated with methyl iodide under basic conditions, and was reduced with tin(II) chloride to give 4-amino-5-methoxyindazole **81**. Finally, reaction with 2,3-dichlorobenzenesulfonyl chloride in pyridine afforded the desired 5-methoxyindazole sulfonamide **82**.

Incorporation of a methoxy group at the 5-position of the 6-aminoindazole series is outlined in Scheme 11.

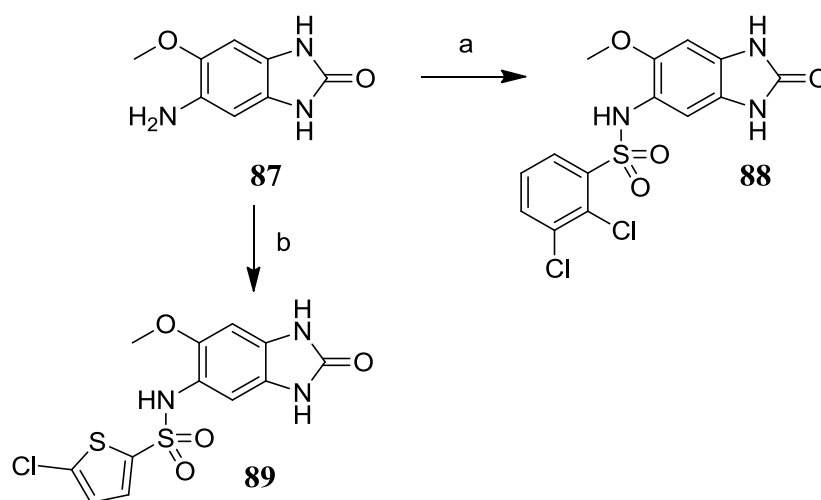


Reagents & Conditions: (a) H₂, Pd/C, rt, 18 h, 97%; (b) 2,3-dichlorobenzenesulfonyl chloride, pyridine, rt, 61%; (c) 5-chlorothiophene-2-sulfonyl chloride, pyridine, rt, 42%.

SCHEME 11. Preparation of 2,3-dichloro-N-(5-methoxy-1H-indazol-6-yl)benzenesulfonamide **85 and 5-chloro-N-(5-methoxy-1H-indazol-6-yl)thiophene-2-sulfonamide **86**.**

Catalytic hydrogenation of commercially available 5-methoxy-6-nitroindazole **83** over 10% palladium-on-carbon gave the 5-methoxy-6-aminoindazole **84** in 97% yield. Reaction with either 2,3-dichlorobenzenesulfonyl chloride or 5-chlorothiophenesulfonyl chloride in pyridine provided the desired 5-methoxyindazole sulfonamides **85** and **86** respectively.

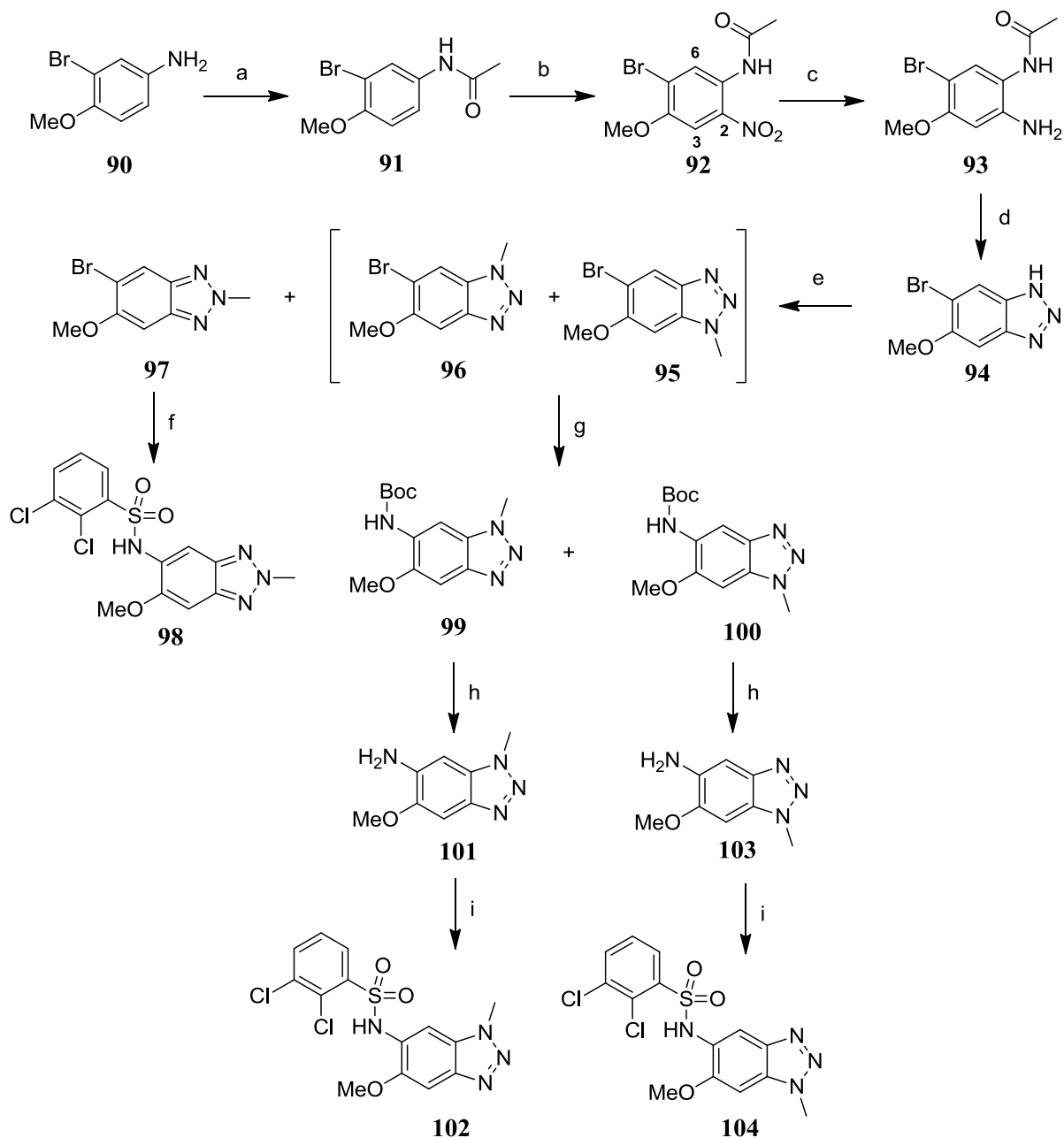
For the introduction of the methoxy group in the benzimidazolone series, 5-methoxy-6-nitrobenzimidazolone (**87**) was commercially available and reaction with either 2,3-dichlorobenzenesulfonyl chloride or 5-chlorothiophenesulfonyl chloride in pyridine afforded the desired 5-methoxybenzimidazolone sulfonamides **88** and **89** in 54% and 70% yield respectively (Scheme 12).



Reagents & Conditions: (a) 2,3-dichlorobenzoyl chloride, pyridine, rt, 3 h, 54%; (c) 5-chlorothiophene-2-sulfonyl chloride, pyridine, rt, 3 h, 70%.

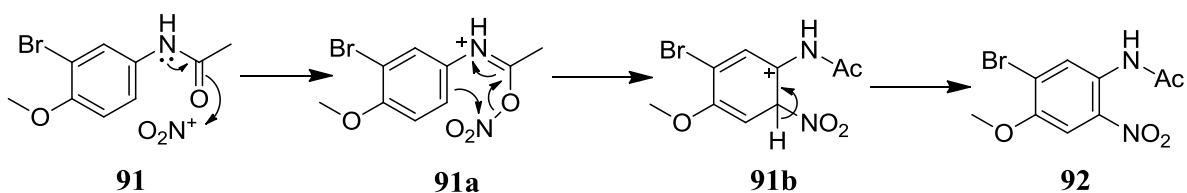
SCHEME 12. Preparation of benzimidazolone sulfonamides 88 and 89.

The introduction of the methoxy group at the 6-position of the benzotriazole series is described in Scheme 13. Commercially available 3-bromo-4-methoxyaniline **90** was treated with acetic anhydride in the presence of triethylamine to give the acetamide **91** in excellent yield. Nitration of the acetamide **91** using a modified procedure described by Shi and co-workers¹²³ with nitronium tetrafluoroborate at 0 °C occurred exclusively at the 2-position affording 2-nitrophenyl acetamide **92** in 87% yield. In this reaction, the methoxy group is expected to be the stronger activator of the ring towards electrophilic attack at the *ortho*-position (C3), compared to the acetamido group directing at the 2-position. However, the observed regioselectivity in the nitration of **91** can be explained by the formation of an intermediary *O*-nitro imidate, **91a** (Scheme 14). Evidence for the formation of these *O*-nitro imidates have been reported by Iley and co-workers.¹²⁴ Under the reaction conditions, the acetamido group reacts with the nitronium species to form the charged intermediate **91a**, which subsequently undergoes intramolecular rearrangement through a six-membered cyclic transition state to favour electrophilic aromatic substitution at the *ortho*-position to the acetamide group.^{124,125} As the 6-position is more hindered because of the bulky bromine, the nitration only occurs at the 2-position. The ¹H NMR spectrum of **92** contained a pair of singlets corresponding to the H-3 and H-6 protons, confirming the regiochemistry of the product.



Reagents & Conditions: (a) Ac_2O , Et_3N , DCM, rt, 30 min, 94%; (b) NO_2BF_4 , CH_3CN , 2 h, 87%; (c) Fe, AcOH, 50°C , 1h, 99%; (d) NaNO_2 , HCl, H_2O , 0°C – rt, 89%; (e) MeI, KOH, DMSO, rt, **96:95** (3:2) 14%, **97** 12%; (f) 2,3-dichlorobenzene sulfonamide, Pd_2dba_3 , Xantphos, Cs_2CO_3 , dioxane, 100°C , 48 h, 34%; (g) *tert*-butylcarbamate, Pd_2dba_3 , Xantphos, Cs_2CO_3 , dioxane, 100°C , 18 h, **99** 33% and **100** 32%; (h) 4N HCl in dioxane, rt, 18 h, **101** 99% and **103** 99%; (i) 2,3-dichlorobenzene sulfonyl chloride, pyridine, rt, 1 h, **102** 52% and **104** 59%.

SCHEME 13. Synthetic route to prepare benzotriazole sulfonamide **98**, **102** and **104**.



SCHEME 14. Proposed mechanism for regioselective *ortho*-nitration of acetanilide **91**

Reduction of **92** with iron, followed by diazotisation gave the cyclised methoxy benzotriazole **94** (Scheme 13). The benzotriazole **94** was alkylated with methyl iodide using sodium hydride as base to give a mixture of three regioisomers: inseparable **95** and **96** (ratio ~ 2:3), and the separable **97**. The regiochemistry of the isomers were determined using a combination of HMBC and ROESY experiments (Fig. 25). In the ROESY experiment for regioisomer **95**, an NOE correlation was observed between the aromatic hydrogen at the 7-position to two methyl groups, the *N*-methyl protons at 3.97 ppm and *O*-methyl proton at 4.26 ppm, whereas regioisomer **96** showed an NOE correlation between the aromatic hydrogen at the 4-position to the *N*-methyl protons at 3.93 ppm only. A ^{15}N HMBC experiment was used to confirm the structure of regioisomer **97**, where correlations were observed between the *N*-methyl protons and all three nitrogens of the triazole. Buchwald coupling of **97** with 2,3-dichlorobenzenesulfonamide afforded the sulfonamide **98** in good yield.

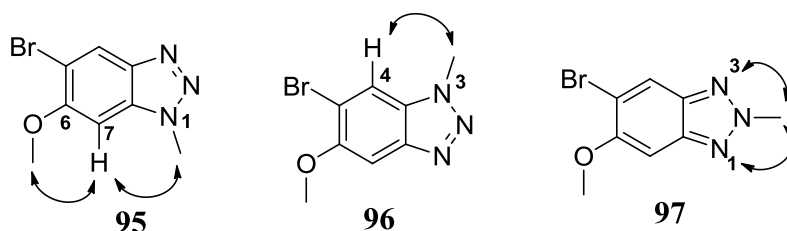


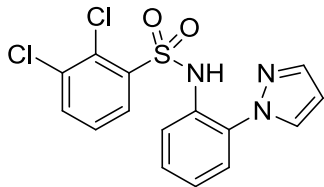
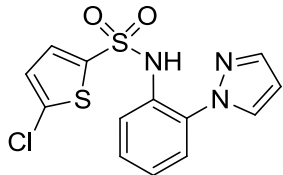
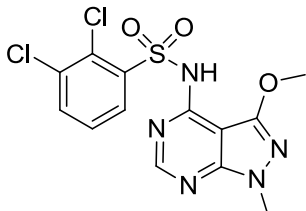
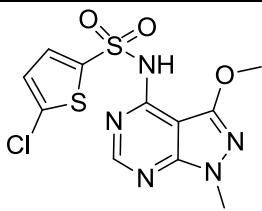
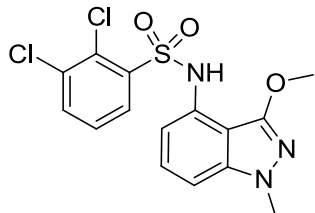
FIGURE 25. HMBC and ROESY confirmation of the regioisomers **95**, **96** and **97**.

Attempts to couple the mixture of regioisomers, **95** and **96** with 2,3-dichlorobenzene-sulfonamide was slow, requiring prolonged reaction (Scheme 13). Only 10% conversion to product was observed by LCMS after heating the reaction at 100 °C for 96 h. The mixture of regioisomers, **95** and **96** was therefore, coupled with *tert*-butylcarbamate, which also allowed the separation of the regioisomers by column chromatography to give **99** and **100** in 33% and 32% yield respectively. The Boc groups of both **99** and **100** were cleaved with 4 N HCl in dioxane and then amines **101** and **103** were reacted with 2,3-dichlorobenzene-sulfonyl chloride to afford the sulfonamides **102** and **104** respectively. The Buchwald coupling of **97**

with primary aryl sulfonamides, such as 2,3-dichlorobenzenesulfonamide, is a good synthetic strategy to explore the diversity of the template. However, many primary aryl sulfonamides are not commercially available and therefore require synthesis from their corresponding aryl sulfonyl chlorides, introducing an additional step. In contrast, the use of *tert*-butylcarbamate, followed by deprotection is an attractive approach, as it introduces an amino group, which could be reacted with aryl sulfonyl chlorides to introduce the diversity as the final step in the reaction.

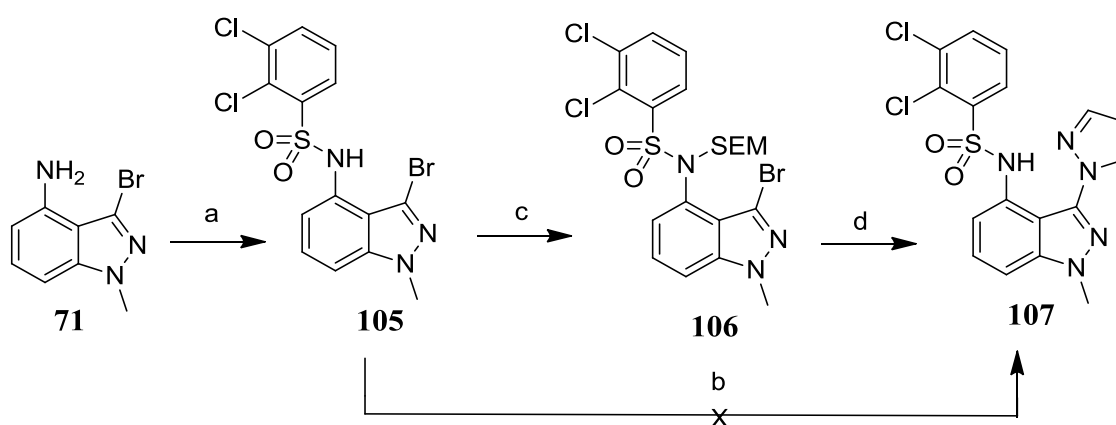
The results from all the methoxy containing analogues are shown below in Table 8, along with those from phenylpyrazoles **33** and **41**.

TABLE 8. Biological data of activated sulfonamide compounds.

Cmpd	Structure	GTP γ S (pIC ₅₀)	LE	LLE _{AT}	Chrom logD _{7.4}	HWB pA2
33		6.5	0.38	0.25	6.5	5.3
41		6.7	0.43	0.32	6.3	5.2
69		7.1	0.41	0.39	2.5	< 5
70		7.1	0.44	0.45	1.6	< 5
73		6.1	0.35	0.26	6.5	< 5

82		5.0	0.28	0.20	5.0	nd
85		7.5	0.45	0.34	4.6	5.8
86		7.3	0.47	0.38	3.9	5.4
88		6.6	0.38	0.31	3.2	5.3
89		5.9	0.36	0.32	2.7	< 5
98		5.6	0.32	0.24	5.1	< 5
102		6.0	0.33	0.27	4.4	< 5

hours. Protection of the amino group of the 3-bromo-indazolyl sulfonamide **105** with a SEM group, followed by the same copper coupling reaction afforded 11% of the free sulfonamide product, **107** after MDAP purification. It is quite unusual that the SEM group cleaves under the coupling reaction conditions, as the SEM group is typically deprotected using a fluoride ion source such as TBAF, or by strong acidic conditions, such as TFA or H₂SO₄.¹²⁶ It is not clear how the SEM group cleaved but it may be that HBr was produced in the coupling reaction, which under the harsh reaction conditions cleaves the SEM group. Although one equivalent of base was used in the reaction, it presumably was not enough to mop up all the HBr generated in the reaction. The copper-coupling reaction may be very slow because of the steric hindrance between the bulky sulfonamide substituent and the approaching pyrazole. Nonetheless, enough final material was recovered for submission to the GTP γ S assay.



Reagents & Conditions: (a) 2,3-dichlorobenzoyl chloride, pyridine, rt, 18 h, 67%; (b) pyrazole, CuI, *L*-proline, K₂CO₃, DMSO, 110 °C, 96 h, sealed tube (~2% by LCMS) (c) SEMCl, NaH, DMF, 0 °C, 15 min, rt, 3 h, 98%. (d) pyrazole, CuI, *L*-proline, K₂CO₃, DMSO, 110 °C, 72 h, sealed tube, 11%.

SCHEME 15. Preparation of 2,3-dichloro-*N*-(1-methyl-3-(1*H*-pyrazol-1-yl)-1*H*-indazol-4-yl)benzenesulfonamide **107.**

The 3-pyrazolylindazole **107** was found to be completely inactive in the GTP γ S assay ($pIC_{50} < 4.5$). This may be because the pyrazole ring cannot be co-planar with the 5,6-membered heterocyclic template as a result of steric clashes. Consequently, the nitrogen from the pyrazole ring cannot now form an intramolecular hydrogen bond with the NH of the sulfonamide, which is important for activity in the GTP γ S assay. Also, if the pyrazole could form an intramolecular hydrogen bond, it has to form an interaction through a seven-membered ring instead of the smaller (six-membered) ring observed with the phenyl pyrazole series (Fig. 18). One way to circumvent this problem would be to introduce the pyrazole ring at the 5-position of the 4-aminoindazole template. However, examining the physicochemical

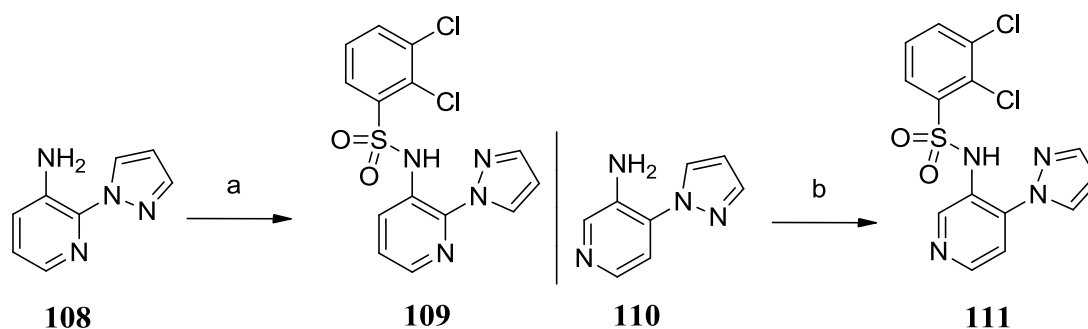
properties of **107** (MW = 422, chromlogD_{7.4} = 7.3, CLND solubility = 14 µg/mL), incorporating a pyrazole ring on a fused 5,6-membered heterocyclic core does not appear to be ideal, as it increases the number of aromatic rings without showing a great deal of improvement in potency. A higher number of aromatic rings is generally associated with poor physicochemical properties, including poor solubility, permeability and absorption.⁸⁹

After introducing the methoxy groups, only 3 templates plus the phenylpyrazole template, remained for further exploration and possible progression towards lead optimisation. Eight of the active compounds (**33**, **41**, **69**, **70**, **85**, **178**, **86** and **89**) were submitted to the human whole blood actin polymerisation assay and it was promising to see some initial activity for these un-optimised templates (Table 8). The pyrazolopyrimidine series, as exemplified by **69** and **70**, was the only series that did not show any activity in the whole blood assay. At this stage, without preparing further analogues, it is difficult to rationalise this result.

7.6 Phenylpyrazole template

The phenylpyrazole template exemplified by **33** is active in the human whole blood polymerisation assay but as mentioned earlier, the compound has poor solubility (CLND solubility = 53 µg/mL) with a clogP of 4.5 and an unacceptably high chromlogD of 6.5. Initial chemistry was focused on improving the clogP and chromlogD of the phenylpyrazole template (**33**). In addition, the current core of **33** is an aniline, which is not very attractive as a drug candidate because of potential genotoxicity issues.¹²⁷ One way to resolve both these problems is to introduce nitrogen atom into the phenyl core, as this will reduce the risk of genotoxicity, as well as lower the clogP and improve the solubility.

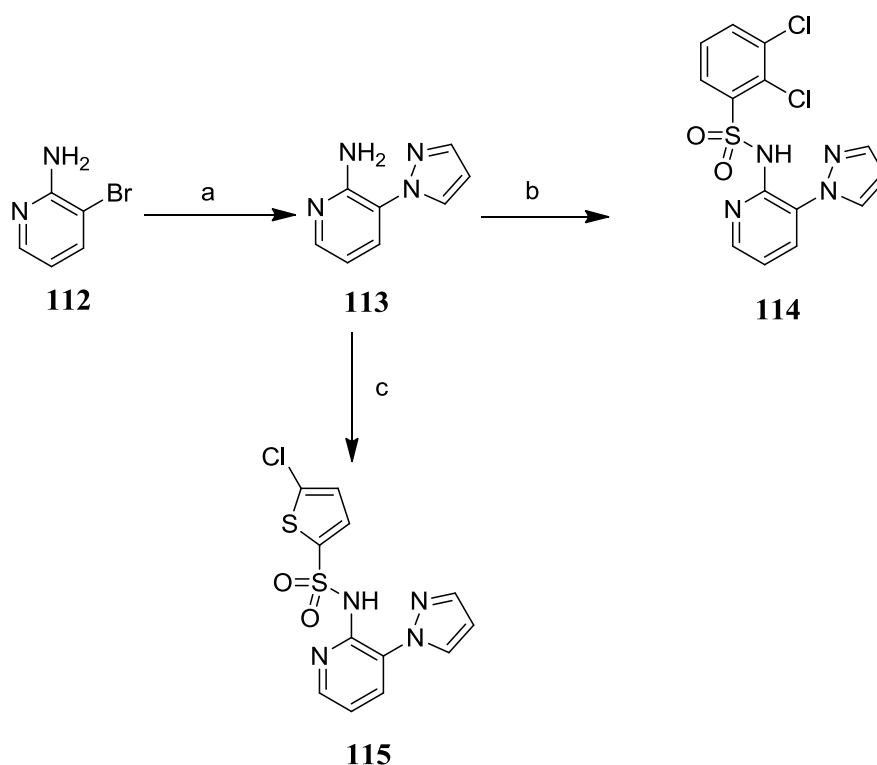
The syntheses of pyridine analogues containing a nitrogen at each of the four available positions were undertaken. 2-(1*H*-Pyrazol-1-yl)pyridin-3-amine (**108**) and 4-(1*H*-pyrazol-1-yl)pyridin-3-amine (**110**) were commercially available and reaction with 2,3-dichlorobenzenesulfonyl chloride afforded the desired sulfonamides **109** and **111** in 60% and 47% yield respectively (Scheme 16).



Reagents & Conditions: (a) 2,3-dichlorobenzenesulfonyl chloride, pyridine, rt, 18 h, 60%; (b) 2,3-dichlorobenzenesulfonyl chloride, pyridine, rt, 18 h, 47%.

SCHEME 16. Preparation of pyrazolylpyridine sulfonamide 109 and 111.

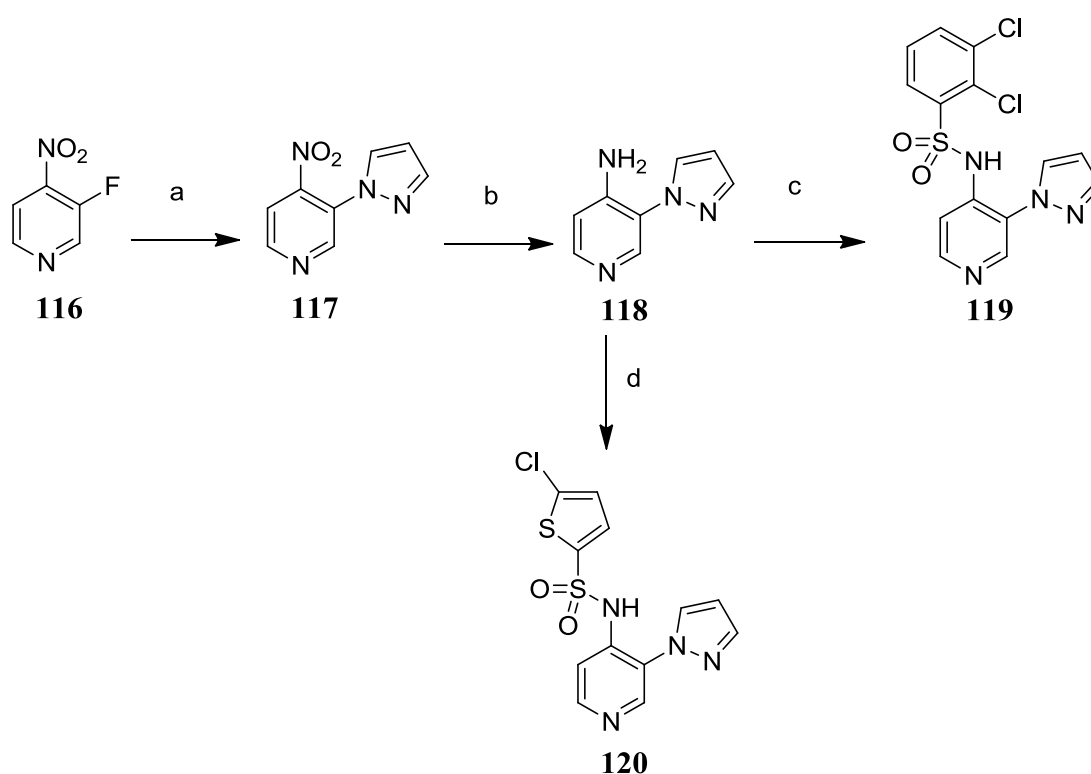
The pyrazolyl-5-pyridine sulfonamides **114** and **115** were prepared from coupling reaction of 3-bromopyridin-2-amine **112** with pyrazole, using copper iodide as a catalyst, to afford 3-(1*H*-pyrazol-1-yl)pyridin-2-amine **113** in 50% yield (Scheme 17).¹²⁸ Reaction with either 2,3-dichlorobenzenesulfonyl chloride or 5-chlorothiophenesulfonyl chloride in pyridine afforded the desired sulfonamides **114** and **115** in 41% and 57% yield.



Reagents & Conditions: (a) Pyrazole, K_2CO_3 , CuI, *N,N*-dimethylethane-1,2-diamine, *p*-xylene, 50%; (b) 2,3-dichlorobenzenesulfonyl chloride, pyridine, rt, 3 h, 41%; (c) 5-chlorothiophene-2-sulfonyl chloride, pyridine, rt, 3 h, 57%.

SCHEME 17. Preparation of pyrazolyl-5-pyridine sulfonamide 114 and 115.

The first step in the preparation of the pyrazolyl-3-pyridine sulfonamides involved nucleophilic displacement of 3-fluoro-4-nitropyridine **116** with pyrazole under basic conditions, employing a modification of a method described by Lemoine and co-workers¹²⁹ (Scheme 18). Reduction of the nitro group of pyrazolylpyridine **117** in the presence of tin(II) chloride, utilising conditions described in the literature,^{130,131} followed by reaction with either 2,3-dichlorobenzenesulfonyl chloride or 5-chlorothiophene-2-sulfonyl chloride in pyridine afforded the desired sulfonamides **119** and **120** in 51% and 53% yield respectively. It should be noted that both **118** and amine **52** (Scheme 6) have a similar aminopyridine core but the sulfonylation of **118** works much better than that of **52**.

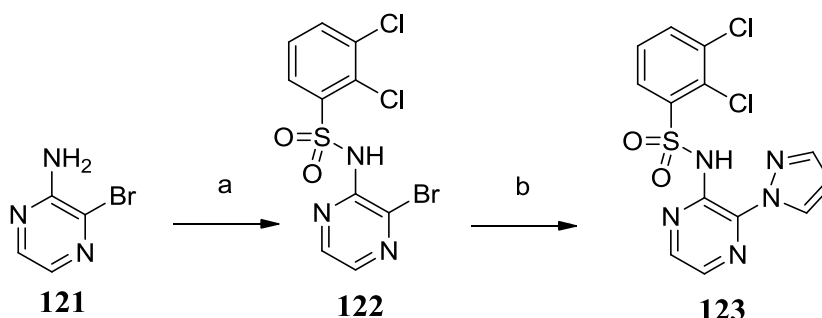


Reagents & Conditions: (a) NaH, pyrazole, NMP, 0-100 °C, 18 h, 64%; (b) SnCl₂, conc HCl, MeOH, rt, 48 h, 68%; (c) 2,3-dichlorobenzenesulfonyl chloride, pyridine, rt, 8 h, 51%; (c) 5-chlorothiophene-2-sulfonyl chloride, pyridine, rt, 4 h, 53 %.

SCHEME 18. Preparation of pyrazolyl-3-pyridine sulfonamide **119 and **120**.**

The phenyl core of the phenylpyrazole **33** was also replaced with a pyrazine to provide an even more hydrophilic analogue than the corresponding phenyl or pyridine analogues. Reaction of commercially available 3-bromopyrazin-2-amine **121** with 2,3-dichlorobenzene-sulfonyl chloride in pyridine gave the sulfonamide **122** in 83% yield. Displacement of

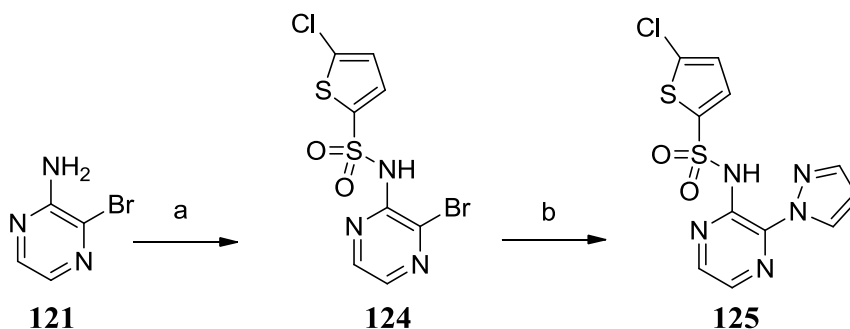
bromine of **122** with pyrazole, in the presence of sodium hydride afforded the desired pyrazine sulfonamide **123** in 71% yield (Scheme 19).



Reagents & Conditions: (a) 2,3-dichlorobenzenesulfonyl chloride, NaH, DME, rt, 73%; (b) NaH, pyrazole, NMP, 0-100 °C, 18 h, 71%.

SCHEME 19. Preparation of pyrazolyepyrazine sulfonamide 123.

The analogous 5-chlorothiophene sulfonamide compound **125** was prepared from the reaction between commercially available 3-bromopyrazin-2-amine **121** and 5-chlorothiophenesulfonyl chloride in pyridine, followed by displacement reaction of **124** with pyrazole (Scheme 20).

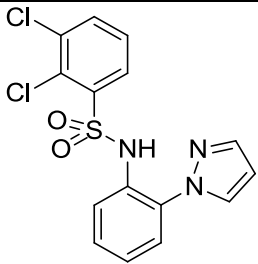
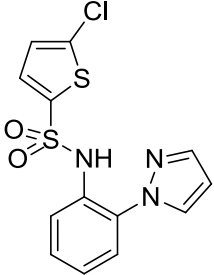
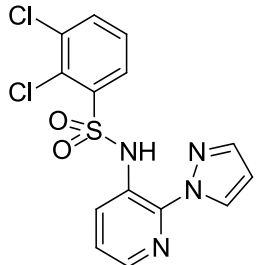
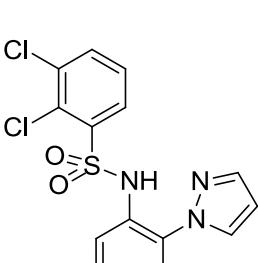
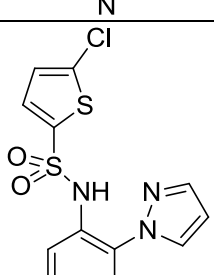


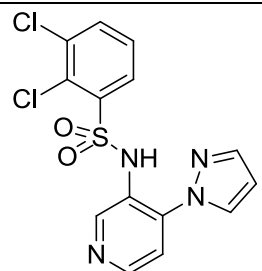
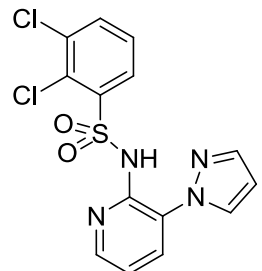
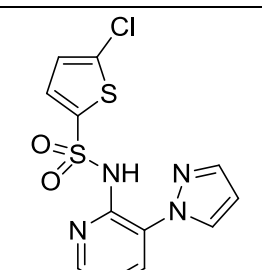
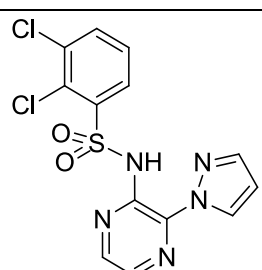
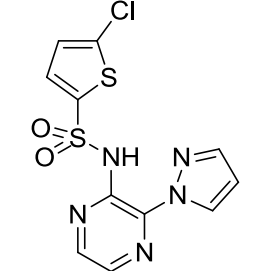
Reagents & Conditions: (a) 5-chlorothiophene-2-sulfonyl chloride, NaH, DME, rt, 80%; (b) NaH, pyrazole, NMP, 0-100 °C, 18 h, 36%.

SCHEME 20. Preparation of pyrazolyepyrazine sulfonamide 125.

The results from all these heteroaryl analogues of the phenylpyrazole **33** are shown below in Table 9.

TABLE 9. Biological data of analogues of the phenylpyrazole

Cmpd	Structure	GTPγS (pIC₅₀)	LE	LLE_{AT}	Chrom logD_{7.4}	CLND Sol. μg/mL	HWB pA2
33		6.6	0.38	0.25	6.5	48	5.3
41		6.7	0.43	0.32	6.3	80	5.2
109		5.8	0.34	0.26	6.7	34	Nd
119		6.6	0.39	0.31	3.2	76	< 5
120		5.4	0.35	0.29	2.6	180	Nd

111		5.5	0.33	0.24	2.9	164	Nd
114		7.4	0.44	0.36	3.7	203	< 5
115		7.2	0.47	0.40	2.8	133	< 5
123		6.8	0.40	0.37	2.0	181	< 5
125		6.2	0.40	0.39	2.0	162	nd

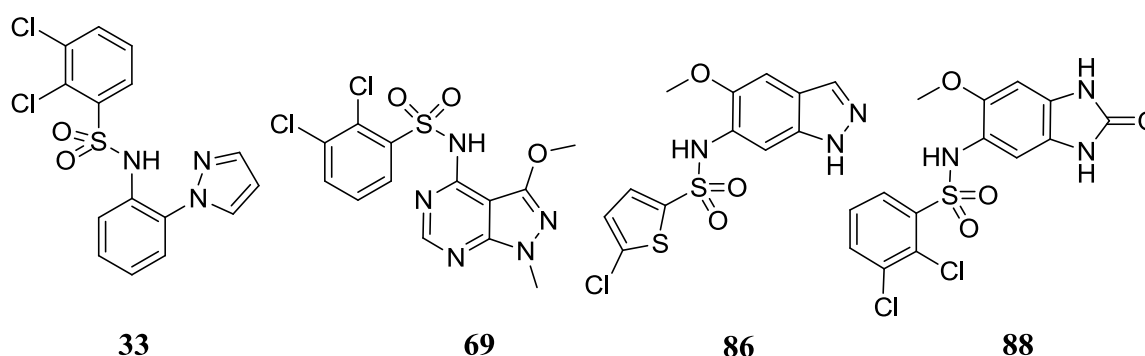
The data shows that significant improvements in potency, LE and LLE_{AT} are observed upon the introduction of a nitrogen at the 5-position (**114** and **115**) of the central phenyl ring. Both the pyridine analogues, **114** and **115** were more soluble than their phenyl analogues **33** and **41**. Nitrogen introduction at the 2- (**109**) and 4-positions (**111**) resulted in a drop in potency whereas pyridine analogue with nitrogen at the 3-position (**119**) was equipotent with phenylpyrazole **33**. Also, replacing the phenyl ring with a pyrazine (**123** and **125**) showed no

change in potency, but a significant improvement in LLE_{AT} (**123** $LLE_{AT} = 0.37$ vs **33** $LLE_{AT} = 0.25$) was observed as the $clogP$ was low. In addition, a significant drop in $chromlogD$ was observed with the pyrazinyl analogues **123** and **125**. Compared to the phenylpyrazoles **33** and **41**, the improvement of almost one log unit in activity in the $GTP\gamma S$ assay for the pyrazolyl-5-pyridines **114** and **115**, did not translate into an improvement of potency in human whole blood actin polymerisation assay. The CCR4 sulfonamides generally have high plasma protein binding ($> 90\%$). However, previous work from the lead indazole series and competitors' series has shown that high plasma protein binding does not correlate with low human whole blood activity. It is not clear why the pyrazolyl-5-pyridine sulfonamides **114** and **115** were inactive in the whole blood assay. Although, it could be that under physiological conditions, these compounds do not permeate the cell to inhibit the intracellular allosteric region of the receptor (Site 2). Both compound **114** and **115** have lower measured pK_a (5.93 and 5.65 respectively) than **33** (7.22), which suggests that **114** and **115** exists mainly as the anionic form at physiological pH. This could result in lower cellular permeation and may be a reason why no human whole blood activity is observed with both **114** and **115**.

7.7 Pharmacokinetic studies

A representative compound from each of the series (**33**, **69**, **86** and **88**) was submitted for rat and dog pharmacokinetic studies in male Wistar Han rats and male Beagle dogs (see experimental section for full detail).¹³² All the examples tested in the pharmacokinetic studies contained a 2,3-dichlorobenzenesulfonamido substituent, apart from compound **86**. The 5-chlorothiophenyl sulfonamide **86** was selected because of its higher solubility (CLND Sol = 160 $\mu g/mL$) compared to the 2,3-dichlorophenyl analogue **85** (CLND Sol = 44 $\mu g/mL$). The pharmacokinetic results are summarised in Table 10.

TABLE 10. Comparison of biological profile and rat and dog pharmacokinetic data for the new templates.



Compound No.	33	69	86	88
GTPγS (pIC₅₀):	6.5	7.1	7.3	6.6
LE / LLE _{AT} :	0.38 / 0.25	0.41 / 0.39	0.47 / 0.38	0.38 / 0.31
hWB pA2 (n):	5.3 (n=3)	< 5 (n=2)	5.4 (n=2)	5.3 (n=4)
MW / clogP:	368 / 4.5	388 / 2.2	343 / 3.1	388 / 3.1
CLND sol:	53 μ g/mL	216 μ g/mL	160 μ g/mL	42 μ g/mL
MDCK P _{ex} :	794 nm/s	422 nm/s	958 nm/s	474 nm/s
Measured pKa:	7.2	5.6	7.4	8.6
Rat PK (dose 1 mg/kg)				
Bioavailability:	Negligible	63%	60%	44%
Clearance:	40 mL/min/kg	2 mL/min/kg	14 mL/min/kg	7 mL/min/kg
V _{dss} :	2.3 L/kg	0.3 L/kg	0.8 L/kg	1.2 L/kg
t _{1/2} h:	1.1 h	1.9 h	1.3 h	2.5 h
Dog PK (PO: 1.0 mg/kg)				
Bioavailability:	nd	100%	100%	100%
(IV: 0.5 mg/kg)				
Clearance:	71 mL/min/kg	4.3 mL/min/kg	20 mL/min/kg	3.1 mL/min/kg
V _{dss} :	3.4 L/kg	0.61 L/kg	1.3 L/kg	3.0 L/kg
t _{1/2} h:	1.2 h	0.27 h	2.0 h	11 h

The passive membrane permeability (P_{ex}) of the compounds was measured across Madin Darby canine kidney – multidrug resistance 1 (MDCKII-MDR1) cells in the presence of a potent P-glycoprotein (PGP) inhibitor.¹³² PGP is an ATP-dependent protein on the cell membrane with broad specificity that pumps out various substrates and xenobiotics such as toxins or drugs out of the cell. Passive permeability in MDCK cells is measured with a PGP inhibitor to rule out any decrease of intracellular concentration due to compounds being substrates for PGP. All four compounds possessed high *in vitro* passive membrane permeability (MDCK P_{ex}), with compounds **69** and **86** showing reasonable solubility in the

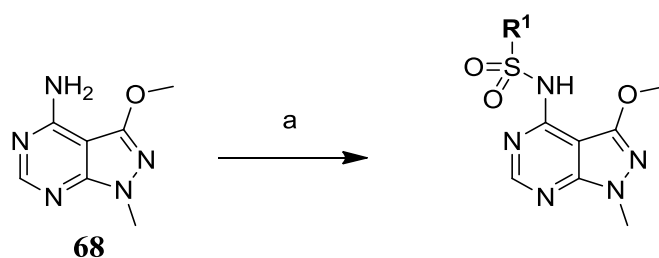
CLND assay. The blood clearance rates of compounds **69**, **86**, and **88** were low in rats, and their oral bioavailability was moderate to high. In contrast, compound **33** had a moderate blood clearance with negligible bioavailability in rat. In addition, following 0.5 mg/Kg intravenous administration to a dog, **33** showed a very high clearance. Based on both the rat and dog pharmacokinetic data, and the fact that the more potent aza analogues (**114** and **115**) from the series were inactive in the human whole blood assay, further investigation of the phenylpyrazole template was terminated. The blood clearance of **86** in the Beagle dog was also relatively high (~ 65% liver blood flow), and therefore, further progression of the 6-aminoindazole series was also terminated.

The two remaining compounds, **69** and **88**, demonstrated high oral bioavailability in dogs, with low blood clearance (< 15% liver blood flow). With the good pharmacokinetic profile of **69** and **88**, a decision was taken to investigate the pyrazolopyrimidine and the benzimidazolone series further. The main priorities for the series were to improve the human whole blood potency in the actin polymerisation assay, whilst maintaining the desired physicochemical and pharmacokinetic profile.

7.8 The pyrazolopyrimidine series

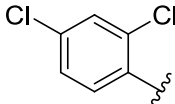
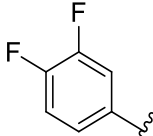
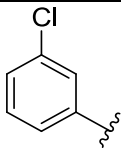
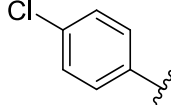
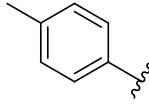
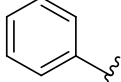
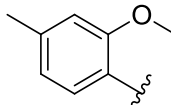
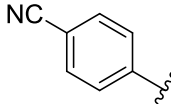
The SAR investigation of the pyrazolopyrimidine series commenced with examination of the aryl sulfonamide at the C4-position of the template. It was known from previous in-house work on the indazole series (**6**),⁶² that alkylation of the sulfonamide nitrogen was detrimental for CCR4 activity. It should also be noted from the pharmacophore of Site 2 templates and SAR of previous series,^{57,60,67} that alkyl, cycloalkyl, naphthyl or heteroaryl sulfonamides are not tolerated. Therefore, a diverse set of 30 arylsulfonyl chlorides was chosen for a sulfonamide array with desired physicochemical properties (MW < 388 and clogP < 3.0, i.e. MW and clogP lower than that of the initial lead, **69**) to examine the C4-position. The monomers and the pyrazolopyrimidine amine **68** were given to the CAT team for synthesis, where the reactions were carried out in an array format; the amine and the sulfonyl chlorides were reacted together with sodium hydride as the base. After purification, the CAT team delivered 26 compounds for screening in the GTP γ S assay and only 11 of these compounds had pIC₅₀ > 6.0. The results are shown below in Table 11 (note that not all the analogues are shown)

TABLE 11. Results from the sulfonamide array of pyrazolopyrimidine amine 160.



Reagents & Conditions: (a) ArSO₂Cl, NaH, DMF, 0 °C – rt.

Cmpd	R¹	GTP_γS (pIC₅₀)	LE	LLE_{AT}	MW	Chrom logD
69		7.1	0.41	0.39	388	2.5
70		7.1	0.44	0.45	360	1.6
126		6.7	0.38	0.35	368	2.8
127		6.7	0.38	0.37	372	1.8
128		6.4	0.40	0.42	339	1.4
129		6.5	0.39	0.40	354	1.8
130		6.2	0.35	0.35	372	2.0
131		6.4	0.37	0.37	351	2.0

132		6.2	0.35	0.33	388	2.4
133		6.1	0.35	0.38	355	1.5
134		6.2	0.37	0.36	354	1.6
135		5.9	0.35	0.35	354	1.8
136		6.0	0.36	0.37	333	1.7
137		5.9	0.37	0.40	319	1.1
138		4.8	0.26	0.30	363	2.9
139		< 4.5	-	-	344	0.8

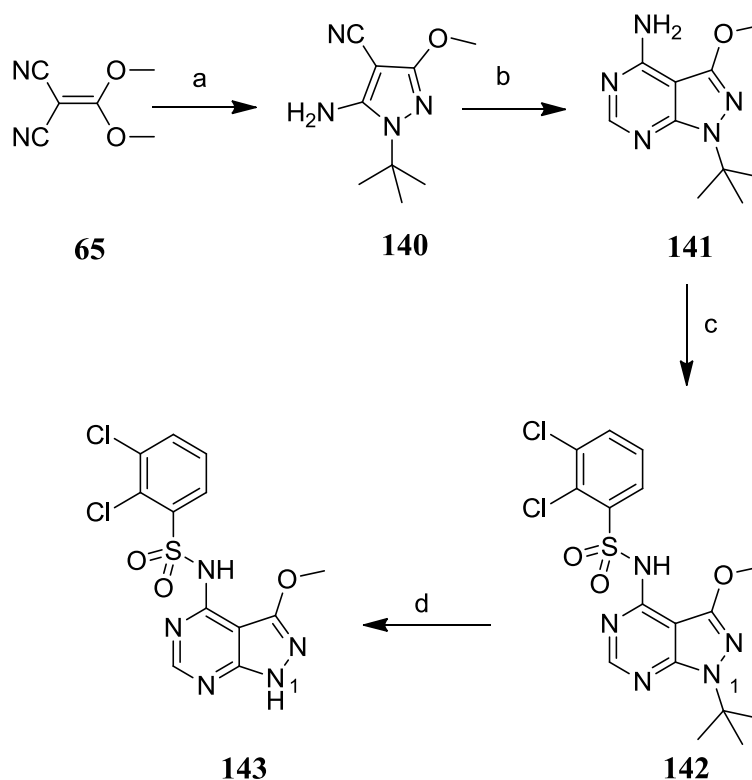
*Note. Compounds **126-139** are not in the experimental as they were prepared by the CAT team.

As expected from the previous in-house work and the competitors' series, the data confirm that the best aryl substituents are either the 2,3-dichlorophenyl or the 5-chlorothiophenyl groups. All the other analogues prepared were found to be less potent. Removal of all the substituents on the aryl ring in benzene sulfonamide **137** resulted in a marked decrease in activity. However, it is noteworthy that the LLE_{AT} of **137** is more or less identical to that of **69**, as **137** has a lower MW and clogP. The thiophene analogues **70** and **128** also demonstrated an improvement in terms of LLE_{AT} because of the lower MW and clogP. It was also observed that halogen substituents on the aryl ring were preferred to electron donating groups such as a methoxy group, or a strongly electron withdrawing group such as a nitrile; the latter modifications resulted in loss of potency.

It was concluded from this work, and SAR knowledge of the site 2 pocket from the literature,^{57,60,67} that the 2,3-dichlorobenzene or the 5-chlorothiophene sulfonamide were essential for the higher activity in the GTP γ S assay. As pharmacokinetic data were obtained with the 2,3-dichlorobenzene sulfonamide group, it was used as a reference and was retained in future modification of compound **69**.

Variation of N1, N2 and C6-substitution was then investigated. The pyrazolopyrimidine series already contains three aromatic rings, and to maintain the desired physicochemical properties by keeping the clogP and MW low, it was decided that incorporation of a third substituent on the core template should not introduce an additional aromatic ring. This will help reduce the risk of progressing the series further due to issues such as poor solubility, permeability and absorption.

The key pyrazolopyrimidine sulfonamide intermediate, **143** was prepared in order to investigate the N1-position of the pyrazolopyrimidine series (Scheme 21).



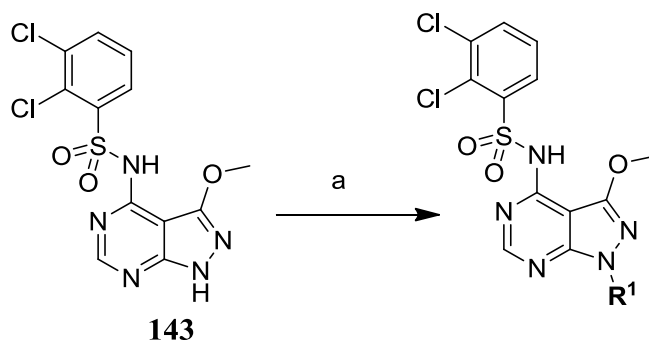
Reagents & Conditions: (a) *t*-butylhydrazine hydrochloride, MeOH, reflux, 2 h, 67%; (b) formamide, 180 °C, 2 h, 46%; (c) 2,3-dichlorobenzenesulfonyl chloride, NaH, DMF, rt, 41%; (d) conc. H₂SO₄, rt, 2 h, 80%.

SCHEME 21. Preparation of pyrazolopyrimidine sulfonamide 143.

Following a literature procedure,¹¹² reaction of **65** with *t*-butylhydrazine, followed by subsequent condensation with formamide gave the known compound, *t*-butyl pyrazolopyrimidine **141** in 46% yield. The pyrazolopyrimidine **141** was then reacted with 2,3-dichlorobenzenesulfonyl chloride, using sodium hydride as a base, to give the sulfonamide **142** in 41% yield. Finally, removal of the *t*-butyl group using concentrated sulfuric acid afforded the pyrazolopyrimidine **143** in 80% yield.

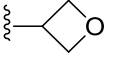
The most direct approach to investigate the SAR at the N1-position involved reaction of pyrazolopyrimidine **143** with 2 equivalents of LiHMDS, followed by addition of one equivalent of one of a range of alkylating agents (Table 12). The first equivalent of base deprotonates the more acidic sulfonamide proton (measured pK_a = 5.71) and then the second equivalent deprotonates the N1-proton. The more basic anion (the measured pK_a of the conjugate acid is 11.95) at the N1-position reacted first with the alkylating agents, affording the desired N1-alkylated products in moderate to good yield. In the reactions, a small amount of di-alkylated products (both N1 and the sulfonamide NH alkylated) were also observed in the LCMS, but were not isolated.

TABLE 12. Investigation of SAR at the N1-position of the pyrazolopyrimidine template.



Reagents & Conditions: (a) LiHMDS (2.0 equiv.), THF, RBr or RI (1.0 equiv.) -78 °C - rt.

Cmpd	R¹	GTP_γS (pIC₅₀)	LE	LLE_{AT}	MW	Chrom logD	Yield
143	H	6.9	0.40	0.37	374	1.8	-
69	Me	7.1	0.41	0.39	388	2.5	-
144	<i>i</i> -Pr	6.6	0.35	0.29	416	2.3	37%
145	<i>t</i> -Bu	5.7	0.30	0.23	416	3.4	-

146	CH ₂ CO ₂ H	6.7	0.34	0.36	432	0.8	-
147	CH ₂ CO ₂ Me	6.6	0.32	0.32	446	2.3	54%
148	CH ₂ CONH ₂	6.3	0.32	0.37	431	1.1	17%
149	CH ₂ CONHMe	6.2	0.30	0.35	445	1.3	53%
150	CH ₂ CH ₂ OMe	6.5	0.33	0.32	432	2.6	70%
151		6.6	0.33	0.35	430	2.1	56%
152	CH ₂ CH ₂ NMe ₂	5.3	0.26	0.25	445	1.6	19%

(Note. The *t*-butyl compound **145** was prepared following Scheme 21, and saponification reaction of the ester **147**, gave the acid **146**)

The data show that small groups such as a methyl group or a hydrogen atom are preferred at the N1-position. In terms of LE/LLE_{AT}, the presence of the methyl group (**69**) resulted in a small improvement over the hydrogen atom (**143**), although, the chromlogD of **143** is half a log unit lower than **69**. Any other modifications made to the N1-position reduced potency. However, it does appear that an acidic group (as in **146**) and an ester group (as in **147**) are tolerated to some extent; these groups could be used to modulate the physicochemical properties of the molecule, for example, to increase solubility or permeability.

Variation of the 6-position of the pyrazolopyrimidine series was investigated next. It should be noted that overlaying **69** with the candidate from the indazole series (**6**), using the Cresset Field Templater tool suggested that substitution at the 6-position should be tolerated (Fig. 26). The Cresset Field Templater tool produces a consensus alignment of a small number of molecules based on their molecular fields in order to gain an insight into how a ligand will interact with a protein. The molecular field is calculated from the electron distribution force field of ligands to generate field points. These field points are condensed representation of electrostatic (positive or negative charge), van der Waals, hydrophobic and shape properties of molecules, and are used to obtain the optimal overlay.

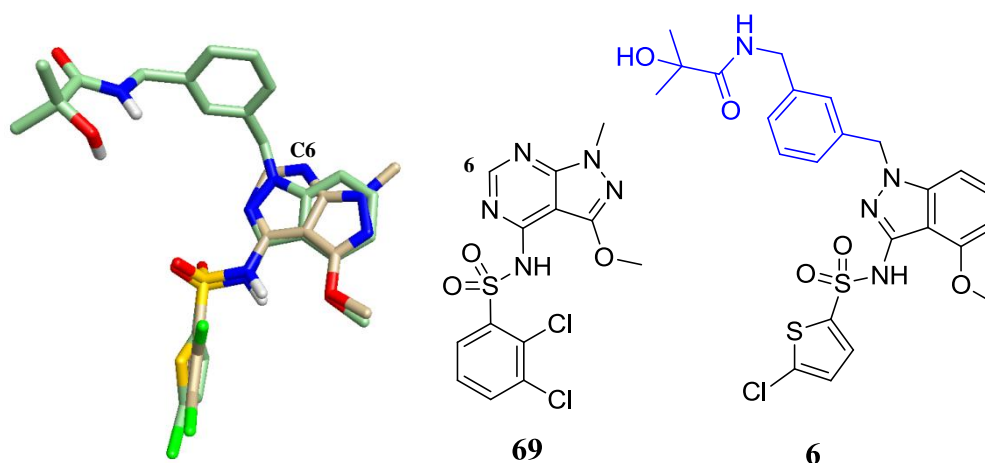


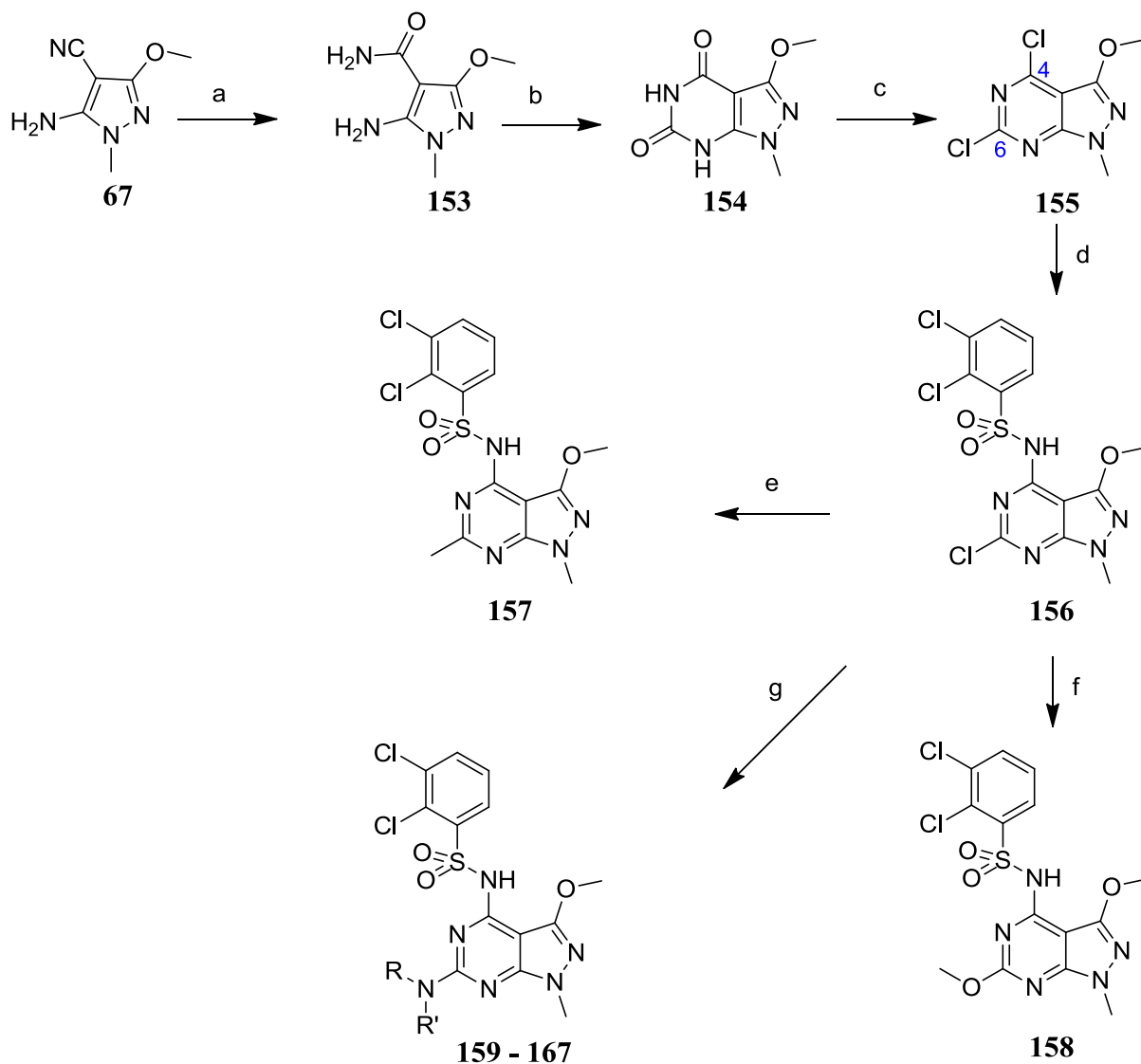
FIGURE 26. Overlay of pyrazolopyrimidine **69** with indazole **6**.

The overlay was carried out by minimising the structure of indazole **6** in 3-dimensional space, and then superimposing the pyrazolopyrimidine **69** based on the similarity in molecular field points of both of the structures. One should use these overlays with caution as there are several alternative overlays and conformers that potentially resemble how the compounds actually fit in to the allosteric site more closely. The minimum energy overlay selected here shows that the benzyl fragment from the indazole series could be incorporated at the 6-position of the pyrazolopyrimidine template. However, the fragment will not overlay perfectly, as the vector of the aryl group going out from 6-position of the pyrazolopyrimidine template will not match the direction of the indazole template. Nonetheless, introducing an aryl group will increase the aromatic ring count so it was decided not to incorporate the benzyl moiety from the indazole series but instead, to investigate the SAR with small aliphatic substituents.

The approach taken to investigate the 6-position involved preparation of key intermediate, **155**, following a modified version of the published method described by Cheng and Robins (Scheme 22).¹³³ The pyrazole nitrile, **67** was hydrolysed using concentrated sulfuric acid to give the pyrazole carboxamide, **153**. This was then reacted with CDI to give the pyrazolopyrimidone, **154**, which was heated with phosphoryl chloride, in the presence of an excess of phosphorus pentachloride, to afford the dichloropyrimidine **155**.

The selective displacement of the chlorine atoms of dichloropyrazolopyrimidine by S_NAr is well described in the literature.¹³⁴⁻¹³⁷ The chlorine atom on the 4-position was displaced first

with 2,3-dichlorobenzene sulfonamide, in the presence of NaH at 60 °C to afford the substituted intermediate, **156** in 57% yield.



Reagents & Conditions: (a) H₂SO₄, rt, 18 h, 94%; (b) CDI, DMF, 85 °C, 1 h, 68%; (c) POCl₃, PCl₅, 100 °C, 18 h, 44%; (d) 2,3-dichlorobenzene sulfonamide, NaH, THF, 0 °C - 60 °C, 57%; (e) trimethylboroxine, PdCl₂(dppf), Cs₂CO₃, 1,4-dioxane, 100 °C, μ wave, 2 h, 22%; (f) NaOMe, 130 °C, μ wave, 1 h, 52%; (g) RR'NH, neat or IPA, 100 - 130 °C, μ wave, 1 - 3 h, 25-56%.

SCHEME 22. Synthetic route to prepare pyrazolopyrimidine analogues with changes at the 6-position.

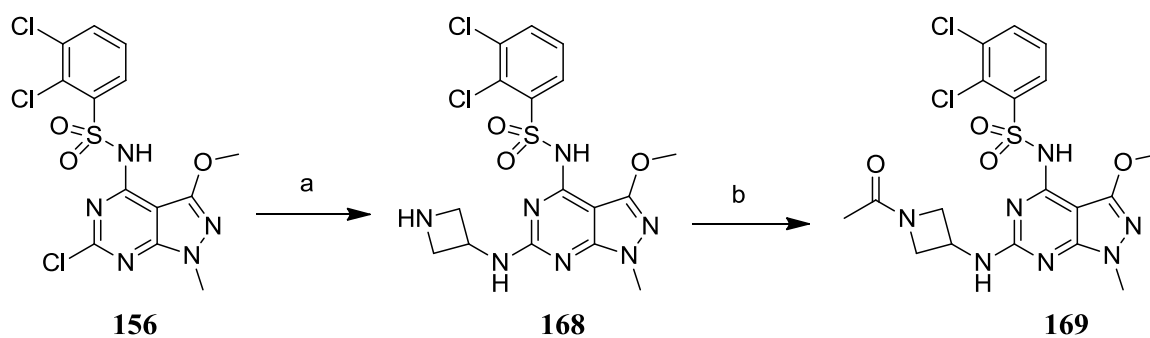
Finally, a displacement reaction of **156** with sodium methoxide, or a variety of amine nucleophiles gave the corresponding pyrazolopyrimidine analogues **158** – **167** to probe the SAR at the 6-position. Nucleophilic displacement at the 4-position is much faster than displacement at the 6-position. There is more electrostatic repulsion at the 6-position towards

the incoming nucleophile because of the two lone pairs of electrons in an sp^2 hybrid orbital on the two neighbouring nitrogens.¹³⁴ Although it does appear that the methoxy group at the 3-position could hinder the substitution at 4-position, experimentally, the 4-position was found to be the most reactive. It should be noted that there are no examples in the literature of selective displacement on 4,6-dichloropyrazolopyrimidines containing a methoxy group at the 3-position. However, there are many examples of S_NAr reaction of 2,4-dichloropyrimidines containing a small substituent at the 5-position favouring selective displacement at the 4-position.¹³⁸⁻¹⁴⁰

As expected, the second substitution reactions required higher temperatures. The methoxy group was introduced by heating **156** with sodium methoxide at 130 °C to afford **158** in 52% yield. Reactions of **156** with the corresponding amine nucleophiles were carried out either in the neat amines or with excess reagents using IPA as the solvent. The reactions were heated in the microwave at temperatures between 100 - 130 °C for 1 - 3 h to give the corresponding amino analogues.

Direct displacement reaction of the chloro pyrazolopyrimidine **156** to introduce a methyl group at the 6-position using excess methyl Grignard reagent (MeMgBr) was unsuccessful. However, a palladium-catalysed reaction with trimethylboroxine following a literature procedure afforded the methyl analogue **157** in moderate yield.¹⁴¹

The azetidine **168** was prepared by displacement of **156** with Boc protected azetidine amine, followed by deprotection with 4M HCl in dioxane (Scheme 23). Reaction of azetidine **168** with acetyl chloride afforded the acetamide **169**.

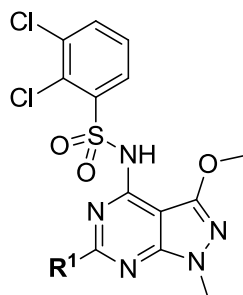


Reagents & Conditions: (a) i. 1-Boc-3-azetidine amine, IPA, 115 °C, μ wave, 2 h; ii. 4M HCl in 1,4-dioxane, 4 h, 22%; (b) AcCl, Et₃N, DCM, rt, 4 h, 40%.

SCHEME 23. Synthetic route to prepare pyrazolopyrimidine analogues **168** & **169**.

The GTP γ S data from the initial work to identify the preferred linker group and investigate the SAR at the 6-position of the pyrazolopyrimidine series are shown below in Table 13.

TABLE 13. Investigation of SAR at the 6-position of the pyrazolopyrimidine template.

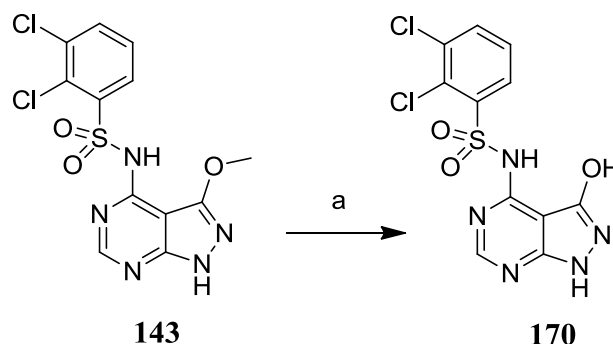


Cmpd	R ¹	GTP γ S (pIC ₅₀)	LE	LLE _{AT}	MW	Chrom logD _{7.4}
69	H	7.1	0.41	0.39	388	2.5
157	Me	6.2	0.34	0.30	402	3.4
158	OMe	6.1	0.32	0.27	418	2.0
159	NH ₂	6.5	0.35	0.34	403	2.4
160	NHMe	7.1	0.37	0.32	417	3.3
161	NMe ₂	6.2	0.31	0.27	431	4.0
162	NHEt	6.6	0.33	0.26	431	4.2
163	NHPr- <i>i</i>	5.5	0.27	0.19	445	5.0
164	N-morpholinyl	<4.5	-	-	473	2.5
165	NHCH ₂ CH ₂ OMe	5.1	0.24	0.20	461	3.3
166	NHCH ₂ CH ₂ NMe ₂	<4.5	-	-	474	1.4
167		5.0	0.23	0.21	459	2.2
168		<4.5	-	-	458	1.5
169		<4.5	-	-	506	1.5

The data show that replacing the hydrogen at the 6-position with a methyl (**157**) or a methoxy (**158**) group resulted in a log unit decrease in potency. It appears that the nitrogen is the preferred linker group, with NHMe (**160**) demonstrating similar activity to that of **69**. However, introducing the NHMe group was not beneficial in terms of LE/LLE_{AT}, as the MW

and the clogP of the compound increased. Replacing the NHMe (**160**) with NHEt (**162**) resulted in a loss in potency of 0.5 log units, and any other modifications were found to be detrimental for activity in the GTP γ S assay. Introduction of *N,N*-dimethylamino group (**161**) also resulted in almost a log unit decrease in potency suggesting that a hydrogen-bond donor (NH) may be important for interaction with the receptor. It is noteworthy that the SAR observed at the 6-position is contradictory to the suggestions from the computational overlay with the indazole candidate, **6** (Fig. 26). This could be because the two templates may bind differently in the allosteric site and therefore have different SAR. Without a protein-ligand X-ray structure it is difficult to predict how the compounds actually bind in the allosteric site.

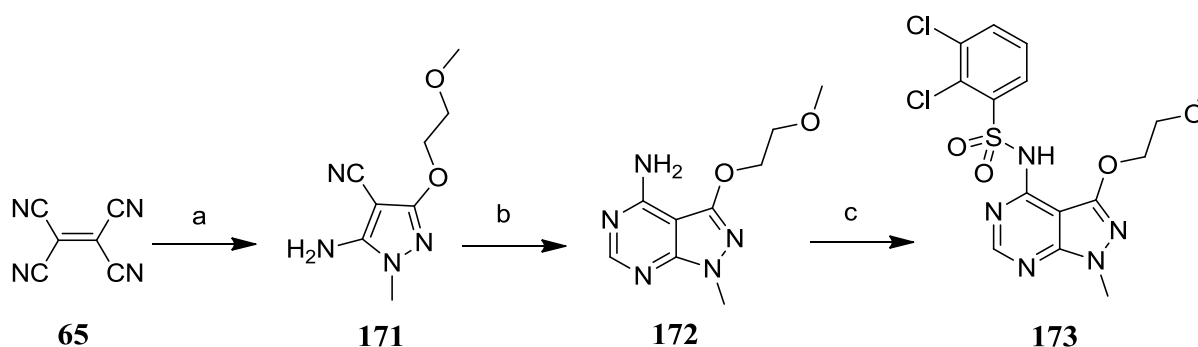
Finally, the 3-position of the pyrazolopyrimidine template was investigated. A decision was taken to introduce small changes at first in order to examine if any substitutions are tolerated at the 3-position. This included changing the methoxy group at the 3-position to hydroxy, ethoxy and 2-methoxyethoxy groups. Following a precedented procedure,¹¹² reaction of pyrazolopyrimidine **143** with TMSCl, in the presence of sodium iodide, afforded the hydroxy compound **170** in 90% yield (Scheme 24).



Reagents & Conditions: (a) TMSCl, NaI, CH₃CN, reflux, 18 h, 90%.

SCHEME 24. Synthetic route to prepare pyrazolopyrimidine analogues 170.

The preparation of the 2-methoxyethoxy analogue **173** is shown in Scheme 25. A one-pot reaction of tetracyanoethylene (**65**) with 2-methoxyethanol and urea, followed by heating with methylhydrazine at 130 °C gave the pyrazole **171** in 17% yield. Condensation of **171** with formamide gave the cyclised product **172**. Finally, deprotonation of **172** with LiHMDS, followed by reaction with 2,3-dichlorobenzenesulfonyl chloride afforded the desired target pyrazolopyrimidine **173** in 10% yield.

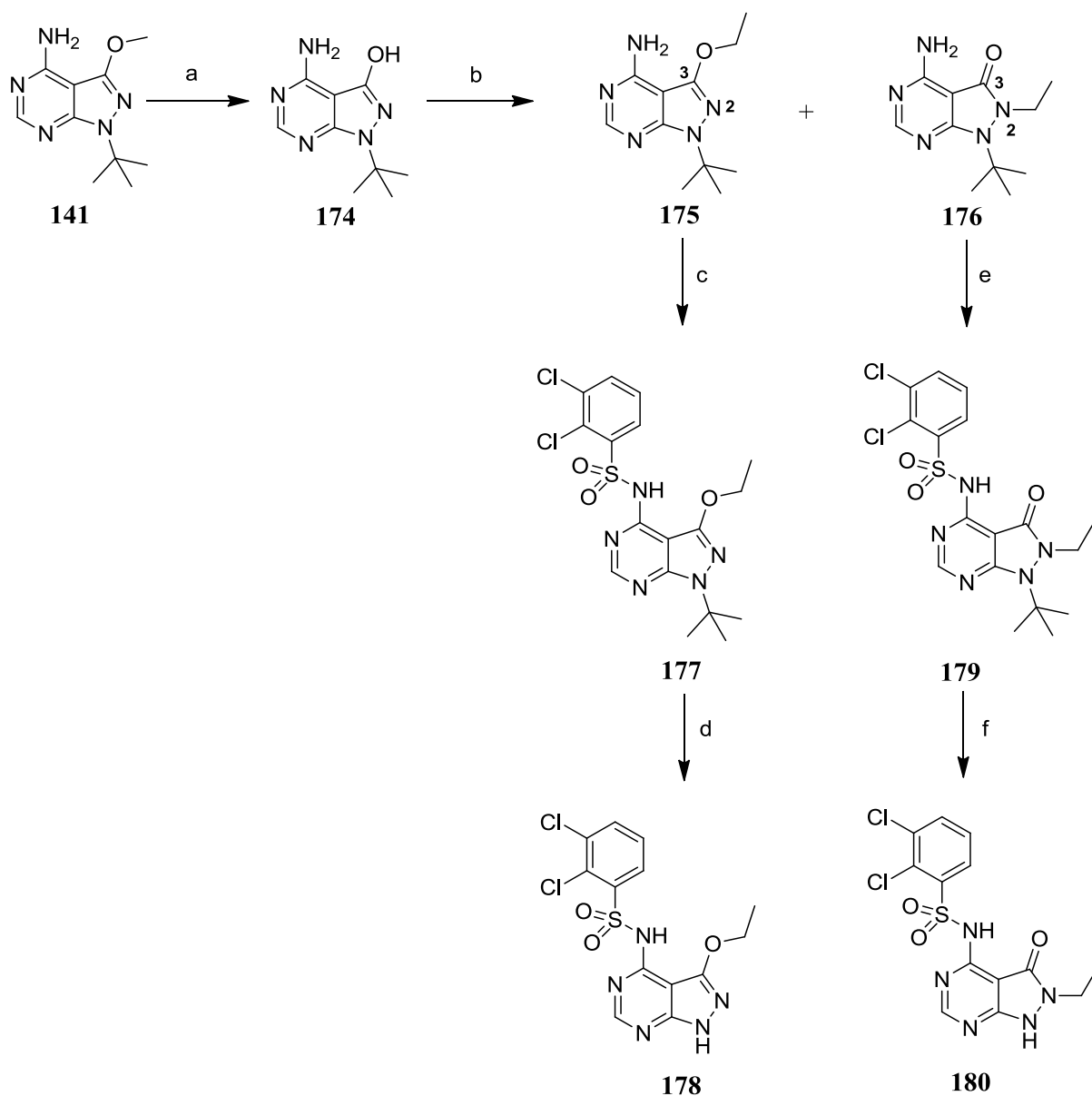


Reagents & Conditions: (a) i. 2-methoxyethanol, urea, 80 °C 15 min; ii. methylhydrazine, 80 °C 15 min, 17% (over two steps); (b) formamide, 180 °C, 3 h, 91%; (c) 2,3-dichlorobenzenesulfonyl chloride, LiHMDS, DMF, 0 °C - rt, 10%.

SCHEME 25. Synthetic route to prepare pyrazolopyrimidine sulfonamide 173.

This is a linear route and it is not ideal for late stage iterations at the 3-position. Regioselective alkylation of the hydroxy group of the pyrazolopyrimidine **170** to make C3 analogues will also be difficult. An alternative route was developed in which the changes at C3 were carried out at a later stage. This is exemplified by the preparation of the ethoxy compound **178**, which is outlined in Scheme 26.

Pyrazolopyrimidine amine **141** was reacted with TMSCl, in the presence of sodium iodide, to give the hydroxyl pyrazolopyrimidine **174** in 72% yield. Alkylation of **174** with ethyl iodide afforded **175** as the major, and **176** as the minor product. The structures of the regioisomer were confirmed by ^{13}C and ^{15}N HMBC experiments. The key correlation in an HMBC experiment from the methylene protons (4.33 ppm) of the ethoxy group to C3 (152.2 ppm) on the pyrazolopyrimidine core confirmed the structure of regioisomer **175** (Fig. 27). For regioisomer **176**, ^{15}N HMBC experiment showed a key $^3J_{\text{N-H}}$ correlation from N1 to both the *tert*-butyl protons and the methylene proton of the ethyl group, and N2 showed correlation to all the protons of the ethyl group (Fig. 27). Sulfonylation reactions of both **175** and **176** with 2,3-dichlorobenzenesulfonyl chloride, followed by hydrolysis using concentrated sulfuric acid afforded the desired target sulfonamides **178** and **180** respectively.



Reagents & Conditions: (a) TMSCl, NaI, CH₃CN, reflux, 18 h, 72%; (b) K₂CO₃, DMSO, 130 °C, 4 h, **175** 50%, **176** 6%; (c) NaH, 2,3-dichlorobenzenesulfonyl chloride, DMF, 0 °C - rt, 2 h, 31%; (d) conc. H₂SO₄, 0 °C, 1 h, 34%; (e) NaH, 2,3-dichlorobenzenesulfonyl chloride, DMF, 0 °C - rt, 2 h, 36%; (f) conc. H₂SO₄, 0 °C, 1 h, 13%.

SCHEME 26. Synthetic route to prepare pyrazolopyrimidine analogues 178 & 180.

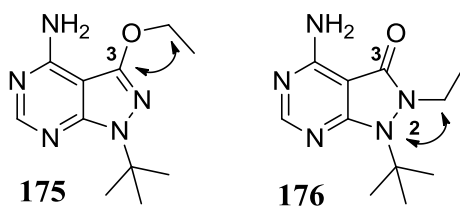
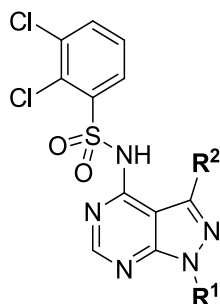


FIGURE 27. HMBC confirmation of the regioisomers 175 and 176.

The GTP γ S data from the initial work to investigate the SAR at the 3-position of the pyrazolopyrimidine series is shown below in Table 14.

TABLE 14. Initial SAR at the 3-position.



Cmpd	R ¹	R ²	GTP γ S (pIC ₅₀)	LE	LLE _{AT}	MW	Chrom logD
143	H	OMe	6.9	0.40	0.37	374	1.8
69	Me	OMe	7.1	0.41	0.39	388	2.5
170	H	OH	4.8	0.30	0.23	360	0.8
178	H	OEt	6.1	0.35	0.29	388	2.3
173	Me		5.9	0.30	0.30	432	2.3

Replacing the methoxy group (**143** or **69**) at the 3-position with a hydroxyl group (**170**) was found to be detrimental for potency. Nearly a whole log unit of potency was lost when replacing the methoxy group with an ethoxy (**178**) or with a 2-methoxyethoxy group (**173**). It appears from the data that a methoxy group is the most effective group at the 3-position.

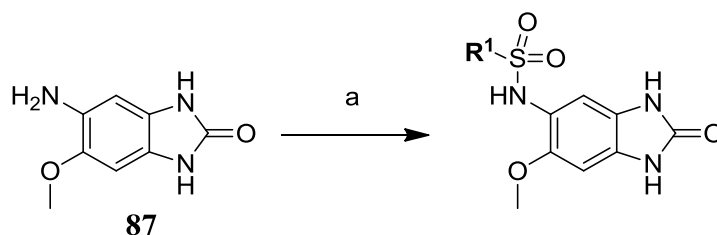
The pyrazolopyrimidine **180** with an ethyl group on N2 was also tested in the GTP γ S assay, and the compound was found to be inactive (pIC₅₀ < 4.5). As a small substitution such as an ethyl group on N2 was not tolerated, it was decided that there was no point investigating the 2-position with larger analogues.

Although the pyrazolopyrimidine template had the best pharmacokinetic profile, the GTP γ S activity could not be increased to useful levels. Five of the compounds were tested in the human whole blood assay (**69**, **143**, **158**, **159** & **162**) and all five were found to be inactive (pIC₅₀: < 5). The decision was therefore taken to terminate the series.

7.9 The benzimidazolone series

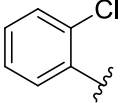
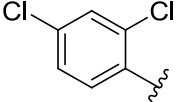
The same set of 30 diverse arylsulfonyl chlorides chosen for the pyrazolopyrimidine series (section 7.8) were given to the CAT team for a sulfonamide array for the benzimidazolone series. The reactions were carried out in an array format using pyridine as a base, and after purification, the CAT team delivered 28 compounds for screening in the GTP γ S assay. Only seven of these compounds had $\text{pIC}_{50} > 5.0$, and the data for these compounds are shown in Table 15 (note that not all the analogues are shown).

TABLE 15. Results from the sulfonamide array of benzimidazolone amine 179.



Reagents & Conditions: (a) ArSO_2Cl , pyridine, rt.

Cmpd	R ¹	GTP γ S (pIC_{50})	LE	LLE _{AT}	MW	Chrom logD
88		6.6	0.38	0.31	388	3.3
89		5.9	0.30	0.32	360	2.7
181		5.9	0.33	0.28	372	2.8
182		5.6	0.32	0.25	368	2.9
183		5.2	0.30	0.25	372	2.6

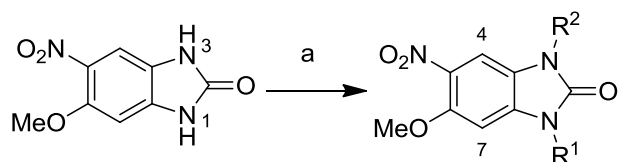
184		5.2	0.31	0.28	354	2.5
185		<4.5	-	-	388	3.2

*Note. Compounds **183-185** are not in the experimental as they were prepared by the CAT team. It should be noted that on one occasion compound **185** showed an activity of pIC₅₀: 5.1 in the GTPγS assay

As in the pyrazolopyrimidine series, the data confirm that the best aryl substituent is the 2,3-dichlorophenyl group. All the other analogues prepared were found to be less potent; even the 5-chlorothiophenyl group was found to be half a log unit less active.

The effect of substitution at the N1 and N3-positions were investigated next. In order to determine which position tolerates any substitution, a small set of compounds were initially prepared following the general method employed in Scheme 27. First, the benzimidazolone **186** was reacted with one equivalent of the various alkylating agents, using sodium hydride as a base, to give mixtures of the mono-alkylated regioisomers, and the dialkylated products. The numbering of the N1-position shown in compound **186** could change depending on the substituent used, so throughout the report, the N1-position shown in **186** is used as an arbitrary number for ease of discussion.

The N1-nitrogen was found to be the most reactive position for alkylation. For example, alkylation of **186** with one equivalent of methyl iodide gave a mixture of N1-methylated benzimidazolone, **187a** and the di-methylated benzimidazolone, **187b** in 25% and 14% yield respectively. In this particular reaction, only a trace amount of the N2-methylated product (~1%) was observed in the LCMS, with the other major peak arising from unreacted starting material. The reactivity difference between the N1- and the N3-positions could be explained by comparing the calculated pK_a values (ACD software, version 12). The N1-position is more acidic (calc. pK_a = 10.9), as it is *para*-to the nitro group compared to the N3-position (calc. pK_a = 17.1). The calculated value was correlated with benzimidazolone, which has a measured pK_a of 10.44, consistent with the calculated pK_a of **186** at the N1-position, but it is difficult to measure the pK_a of the less acidic N2-position as the in-house method only reports pK_a values in the range of 0-12.



186

187a $R^1 = \text{Me}, R^2 = \text{H};$

187b $R^1 = R^2 = \text{Me}$

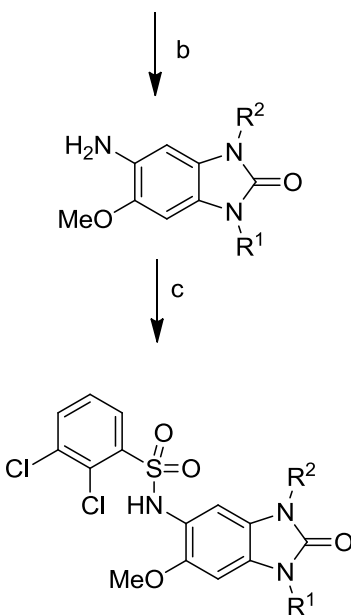
188a $R^1 = \text{CH}_2\text{CH}_2\text{OMe}, R^2 = \text{H};$

188b $R^1 = \text{H}, R^2 = \text{CH}_2\text{CH}_2\text{OMe}$

188c $R^1 = R^2 = \text{CH}_2\text{CH}_2\text{OMe}$

189a $R^1 = \text{CH}_2\text{CONH}_2, R^2 = \text{H};$

189b $R^1 = \text{H}, R^2 = \text{CH}_2\text{CONH}_2$



190a $R^1 = \text{Me}, R^2 = \text{H};$

190b $R^1 = R^2 = \text{Me}$

191a $R^1 = \text{CH}_2\text{CH}_2\text{OMe}, R^2 = \text{H};$

191b $R^1 = \text{H}, R^2 = \text{CH}_2\text{CH}_2\text{OMe}$

191c $R^1 = R^2 = \text{CH}_2\text{CH}_2\text{OMe}$

192a $R^1 = \text{CH}_2\text{CONH}_2, R^2 = \text{H};$

192b $R^1 = \text{H}, R^2 = \text{CH}_2\text{CONH}_2$

Reagents & Conditions: (a) MeI or MeOCH₂CH₂Br or NH₂COCH₂Br, NaH, DMF, rt; (b) H₂, Pd/C (10%), EtOH, 18 h; (c) 2,3-dichlorobenzenesulfonyl chloride, pyridine, rt, 20 - 38%.

SCHEME 27. Synthetic route to prepare benzimidazolone sulfonamide analogues.

The structure of the monomethyl regioisomer, **187a** was confirmed by HSQC and NOE experiments. The HSQC confirmed the chemical shifts of the aromatic protons at C4 (7.51 ppm) and C7 (7.12 ppm). Irradiating at the frequency of the *N*-methyl protons (3.34 ppm) and *O*-methyl protons (3.94 ppm), resulted in both giving an NOE for the proton at the 7-position (7.12 ppm), which is close in space, confirming the regiochemistry of the alkylation (Fig. 28). Similarly, alkylation of **186** with 2-methoxyethyl bromide and 2-bromoacetamide both gave the N1 as the major and the N3 as the minor alkylated products. The structures of the regioisomers were confirmed by HMBC and NOE experiments. The alkylated compounds,

187 - 189 were then subsequently reduced over a 10% Pd/C catalyst under a hydrogen atmosphere to give the corresponding amines, which were reacted with 2,3-dichlorobenzenesulfonyl chloride to afford the desired sulfonamides, **190 - 192**.

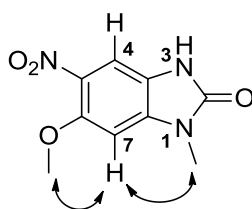


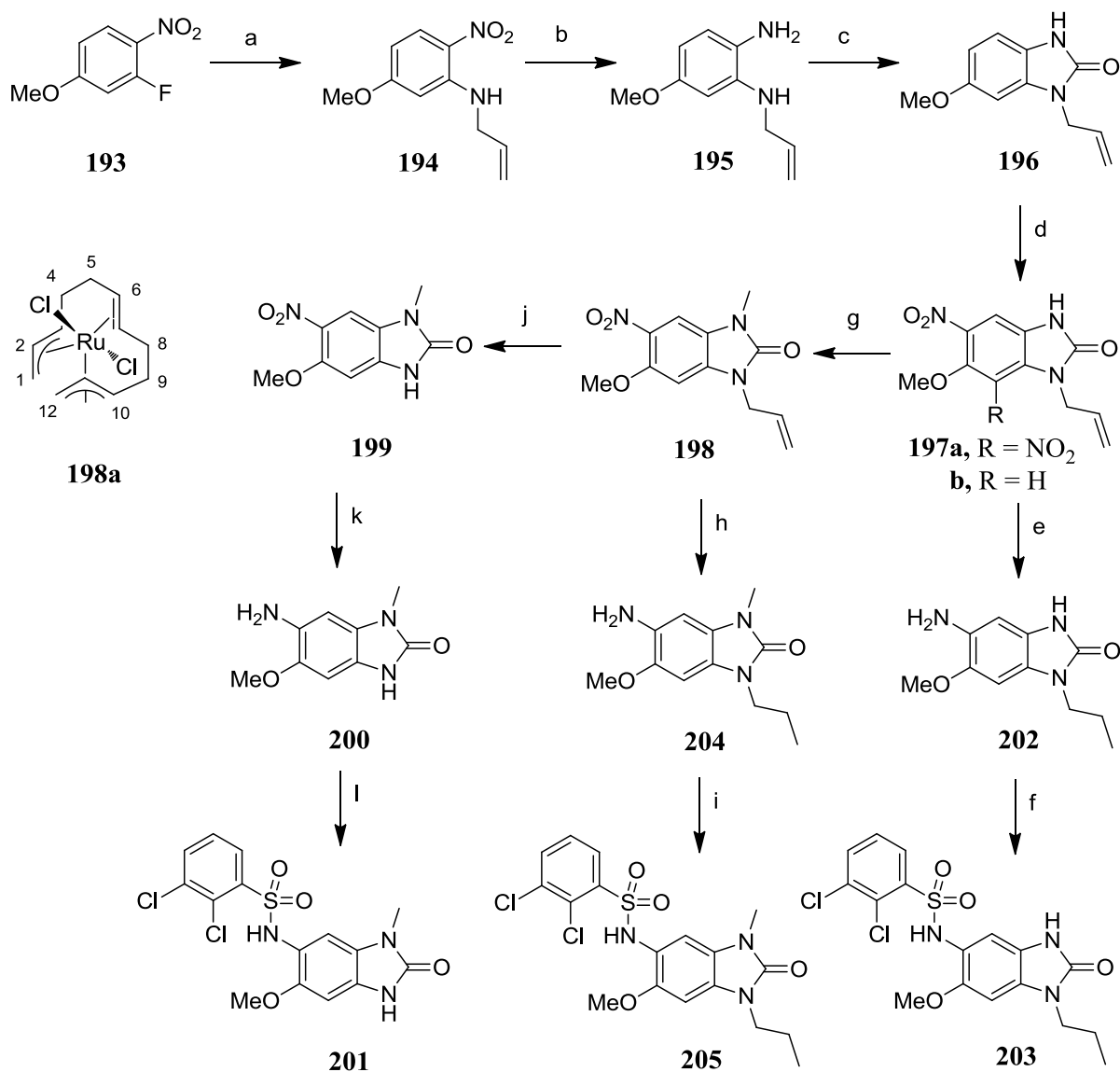
FIGURE 28. NOE confirmation of the N1-methyl regioisomer.

The general method shown in Scheme 27 was unsuccessful for the preparation of the N3-methylated regioisomer **201**, so an alternative route to explore the N3-position using an allyl protecting group was explored (Scheme 28). A number of other groups have been used to protect the benzimidazolone core; these include Boc,⁴⁶ SEM¹¹⁴ and PMB¹¹⁵ groups. However, the allyl group was chosen as it is stable to both acidic (nitric acid) and basic (sodium hydride) conditions,¹²⁶ a key requirement in the proposed synthetic route.

The reaction of commercially available 2-fluoro-4-methoxy-1-nitrobenzene with neat allylamine at room temperature afforded the nitroaniline **194** in 97% yield. The nitro group of **194** was reduced with iron and ammonium chloride to provide the phenyldiamine **195**, which was then treated with CDI to give the methoxy benzimidazolone **196** in 45% yield. Nitration of **196** using fuming nitric acid and concentrated sulfuric acid gave only the undesired dinitro product **197a**. Reaction of **196** with fuming nitric acid also gave only the undesired dinitro product. Investigation of various concentrations of nitric acid and sulfuric acid, identified 4M nitric acid as the best reagent for the preparation of the mono nitro product, **197b** (23% yield). In the reaction, a small amount of the dinitro product, **197a** (which was not isolated) and unreacted starting material was also observed by LCMS.

Alkylation of the N1-allyl protected intermediate, **197b** with methyl iodide was facile providing the methylated benzimidazolone **198** in excellent yield. However, removal of the allyl group proved to be problematic. Attempts to use palladium-catalysed conditions, involving the formation of π -allyl complex,¹¹⁶ and those based on isomerisation of the allylamine using RuCl₃ catalyst, followed by cleavage upon hydrolysis, were all found to be unsuccessful.^{126,142,143} The best method identified employed a commercially available *bis*-(allyl)-ruthenium(IV) based catalyst **198a**, utilising the one pot reaction conditions described by Nebra and co-workers.¹⁴⁴ The reaction was carried out in water, in the presence of

stoichiometric amount of potassium periodate, heating the mixture at 100 °C for 72 h to give the deprotected benzimidazolone **199** in 40% yield.



Reagents & Conditions: (a) allylamine, rt, 1.5 h, 97%; (b) Fe, NH₄Cl, EtOH, H₂O, 100 °C, 22 h, 83%; (c) CDI, THF, 50 °C, 2 h, 45%; (d) 4M HNO₃, 0 °C - rt, 4 h, 23%; (e) H₂, Pd/C, EtOH:EtOAc (1:1), 5 h, 85%; (f) 2,3-dichlorobenzene-sulfonyl chloride, pyridine, rt, 1 h, 37%; (g) NaH, MeI, DMF, 0 °C - rt, 2.5 h, 99%; (h) H₂, Pd/C, EtOH:EtOAc (1:1), 5 h, 99%; (i) 2,3-dichlorobenzene-sulfonyl chloride, pyridine, rt, 18 h, 58%; (j) dichloro(2,6,10-dodecatriene-1,12-diyl)ruthenium(IV) **198a**, KIO₄, H₂O, 100 °C, 72 h, 39%; (k) H₂, Pd/C, EtOH:EtOAc (1:1), 4 h, 92%; (l) 2,3-dichlorobenzene-sulfonyl chloride, pyridine, rt, 1 h, 22%.

SCHEME 28. Synthetic route to prepare benzimidazolone sulfonamides analogues **293**, **295** and **297**.

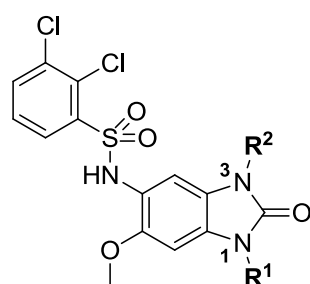
Finally, reduction of **199** using 10% Pd/C catalyst under a hydrogen atmosphere, followed by reaction with 2,3-dichlorobenzene-sulfonyl chloride in pyridine resulted in the isolation of the

desired N3-methylated sulfonamide **203**, albeit in moderate yield (37% yield). However, enough material was isolated for the GTP γ S assay and so the reaction was not investigated any further. In addition, both the nitro and allyl groups of compound **197b** and **198** were reduced using hydrogen over a 10% Pd/C catalyst, and subsequently sulfonylated with 2,3-dichlorobenzenesulfonyl chloride to afford the benzimidazolone sulfonamide analogues **203** and **205** respectively.

All of these initial analogues of the benzimidazolone series were tested in the GTP γ S assay, and the results are shown in Table 16. The biological data shows that substitution at the N1-position is preferred over the N3-position. Although no significant gain in potency or LE was observed with these initial analogues in the GTP γ S assay, the results show that activity was retained upon alkylation at the N1-position, whereas substitution at the N3-position was detrimental for potency. For example, two log unit differences in GTP γ S potency was observed between the N1-methylated compound **190a** and the N3-methylated compound **201**. Similar results were also observed with the N1-alkylated compounds, **191a** and **192a** compared to the analogous N3-alkylated compounds, **191b** and **192b** respectively.

It was encouraging to observe that an NH hydrogen bond donor from the benzimidazolone series could be removed, as this generally would aid in the permeability and absorption of molecules.^{145,146} Also, it does appear from the data that small polar groups are tolerated at the N1-position to some extent.

TABLE 16. Initial SAR at the N1 & N3-position of the benzimidazolone series.

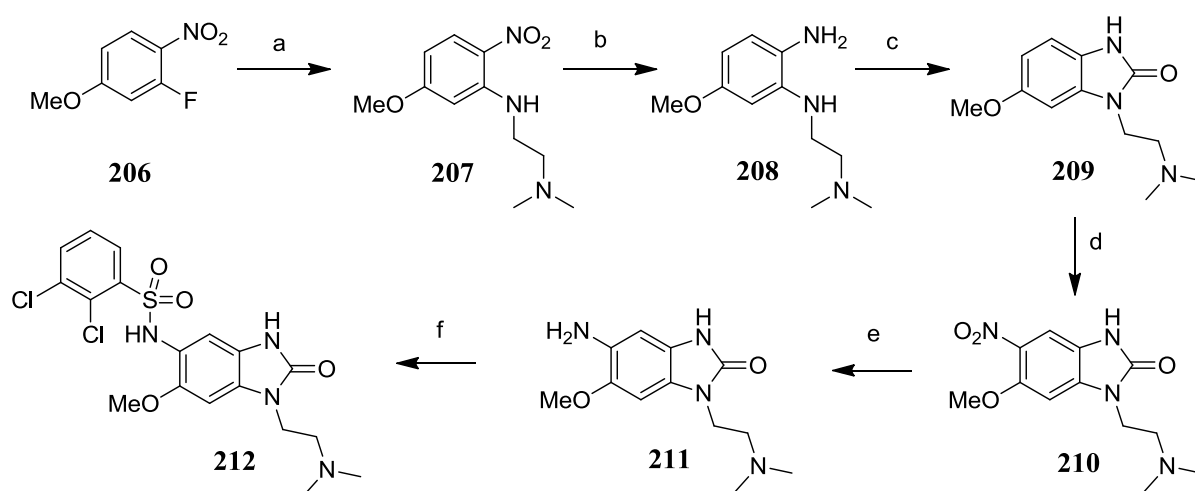


Cmpd	R¹	R²	GTPγS (pIC₅₀)	LE	LLE_{AT}	MW
88	H	H	6.5	0.38	0.31	388
190a	Me	H	6.7	0.36	0.29	402
201	H	Me	4.7	0.26	0.18	402
190b	Me	Me	5.7	0.30	0.24	416

191a	CH ₂ CH ₂ OMe	H	6.4	0.31	0.25	446
191b	H	CH ₂ CH ₂ OMe	<4.5	-	-	446
191c	CH ₂ CH ₂ OMe	CH ₂ CH ₂ OMe	<4.5	-	-	504
192a	CH ₂ CONH ₂	H	6.3	0.31	0.31	445
192b	H	CH ₂ CONH ₂	<4.5	-	-	445
203	<i>n</i> -Pr	H	6.0	0.30	0.18	430
205	<i>n</i> -Pr	Me	4.8	0.23	0.13	444

Based on these initial data, and to keep the molecular weight of the benzimidazolone analogues low, the N1-position was further explored with small lipophilic, polar and weakly basic groups in an attempt to improve the potency, solubility and physicochemical property of the series.

A regioselective route was developed for the synthesis of further N1-substituted analogues and preparation of the weakly basic *N,N*-dimethylaminoethyl compound **212** employing this method is outlined in Scheme 29.



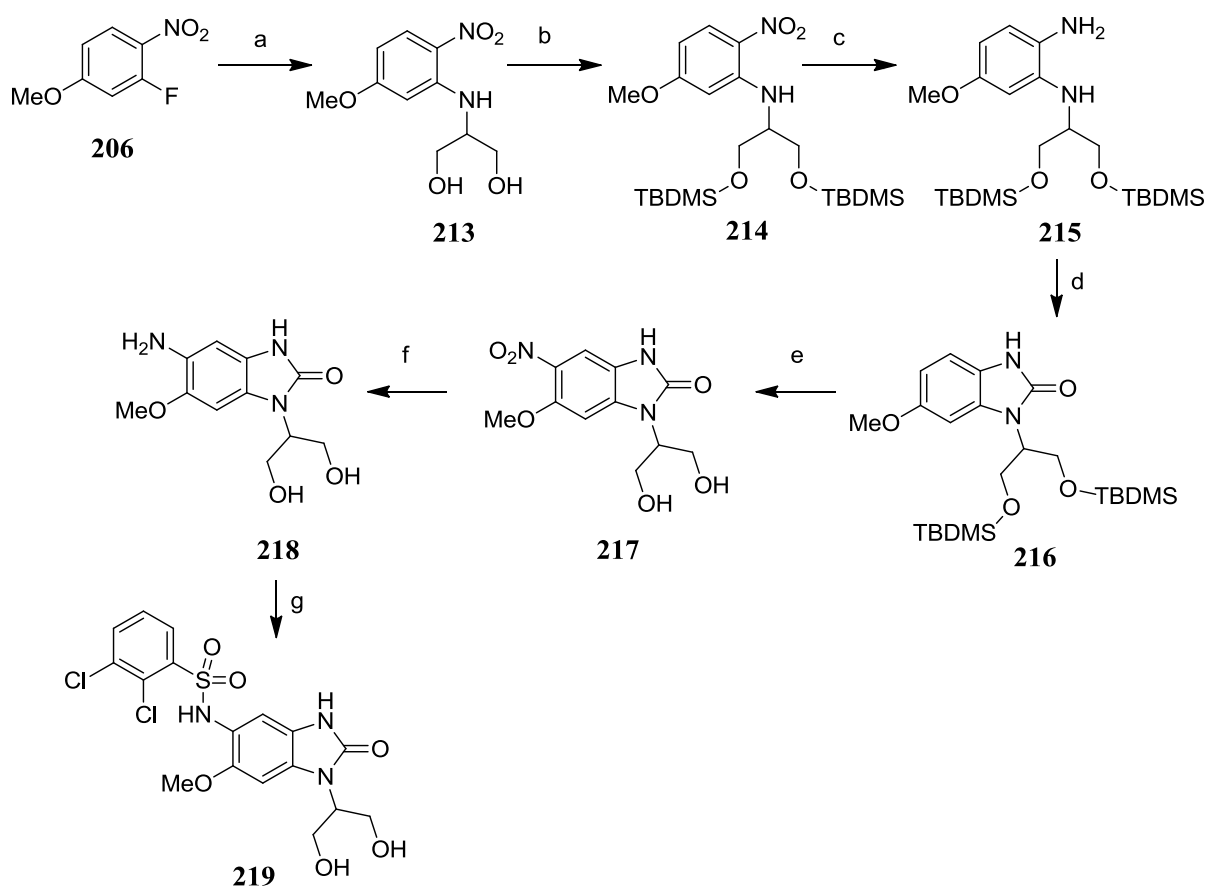
Reagents & Conditions: (a) *N,N*-dimethylethane-1,2-diamine, DIPEA, DMF, rt, 3 h, 93%; (b) H₂, Pd/C, EtOH, 18 h, 91%; (c) CDI, THF, 50 °C, 2 h, 83%; (d) 4M HNO₃, 0 °C - rt, 22 h, 53%; (e) H₂, Pd/C, EtOH:EtOAc (1:1), 18 h, 94%; (f) 2,3-dichlorobenzene sulfonamide, pyridine, rt, 1 h, 36%.

SCHEME 29. Synthetic route to prepare benzimidazolone 212.

The S_NAr displacement of commercially available 2-fluoro-4-methoxy-1-nitrobenzene with *N,N*-dimethylethane-1,2-diamine in the presence of DIPEA gave **207** in 93% yield. Reduction of the nitro group of **207** with 10% Pd/C, followed by cyclisation of the resulting diamine

208 with CDI gave the methoxy benzimidazolone **209** in 83% yield. The benzimidazolone **209** was then nitrated using 4M nitric acid to give the desired mono nitro product **210** in 53% yield. In the nitration reaction, a small amount of the dinitro product was also observed, and when the concentration of nitric acid was increased, the amount of dinitro product also increased. It should be noted that this is a much better yield than obtained for the nitration of **196** under identical conditions (Scheme 28). Finally, a second reduction with hydrogen over 10% Pd/C catalyst, followed by reaction with 2,3-dichlorobenzenesulfonyl chloride in pyridine afforded the desired sulfonamide **212** in moderate yield.

The solubility of the benzimidazolone series, as exemplified by **88**, was low. In an attempt to improve the solubility whilst retaining potency, propane-1,3-diol was introduced at the N1-position. The benzimidazolone **219** was prepared using a similar approach to that used for benzimidazolone **212** (Scheme 30).



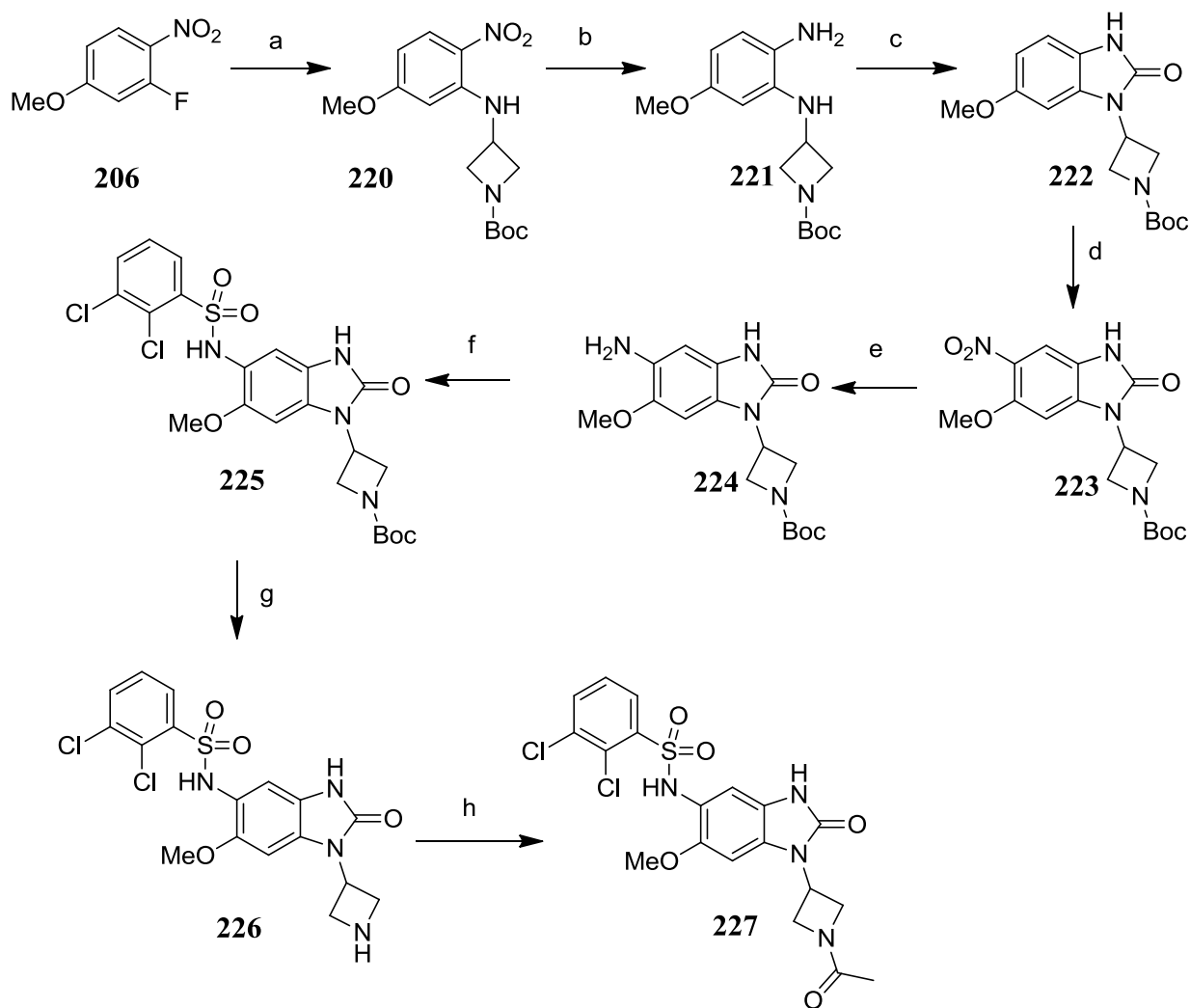
Reagents & Conditions: (a) 2-aminopropane-1,3-diol, DIPEA, DMF, rt, 48 h, 83%; (b) TBDMSCl, imidazole, DMF, rt, 3 h, 95%; (c) H₂, Pd/C, EtOH, 18 h, 70%; (d) CDI, THF, 50 °C, 3 h, 69%; (e) 4M HNO₃, 0 °C - rt, 1 h, 33%; (f) H₂, Pd/C, EtOH, 3 h, 78%; (g) 2,3-dichlorobenzenesulfonyl chloride, pyridine, rt, 1 h, 48%.

SCHEME 30. Synthetic route to prepare benzimidazolone sulfonamide 219.

Nucleophilic displacement of commercially available 2-fluoro-4-methoxy-1-nitrobenzene with 2-aminopropane-1,3-diol in the presence of DIPEA gave **213** in 83% yield. The primary alcohols of **213** were protected as the TBDMS ethers to afford **214**, which was subsequently reduced, and reacted with CDI to give the TBDMS protected diol **216** in good yield. The protected benzimidazolone **216** was then nitrated using 4M nitric acid, and concurrently under the acidic conditions, the TBDMS group cleaved to give the desired nitro benzimidazolone **217** in 33% yield. A second reduction, followed by sulfonylation with 2,3-dichlorobenzenesulfonyl chloride in pyridine afforded the desired sulfonamide **219** in moderate yield.

Introduction of a basic azetidine moiety at the N1-position could also improve the solubility of the benzimidazolone template. In addition, the NH of the azetidine group provides opportunities to carry out further SAR investigation. The azetidine benzimidazolone analogues were synthesised according to Scheme 31.

The S_NAr displacement of commercially available 2-fluoro-4-methoxy-1-nitrobenzene with *tert*-butyl 3-aminoazetidine-1-carboxylate, in the presence of DIPEA was facile, affording **220** in 93% yield. Reduction of the nitro group of **220** with hydrogen over 10% Pd/C, followed by cyclisation of the diamine with CDI gave the methoxy benzimidazolone **222** in 79% yield. The Boc protected azetidine **222** was then nitrated using 4M nitric acid. However the Boc group cleaved during the reaction, so the reaction mixture was basified to about pH 8, and reacted with Boc anhydride. After purification, the mono nitro Boc protected product **223** was isolated in 52% yield. In addition, 13% of the bis Boc protected product was also isolated. Reduction of **223** over 10% Pd/C, followed by subsequent reaction with 2,3-dichlorobenzenesulfonyl chloride in pyridine, and 4N HCl in dioxane, afforded the desired azetidine sulfonamide **226**. Treatment of azetidine **226** with one equivalent of acetic anhydride gave a mixture of mono and bis acetylated product. However, after work up of the mixture, the residue was treated with methanol and potassium carbonate to give mainly the desired mono acetylated product **227**.

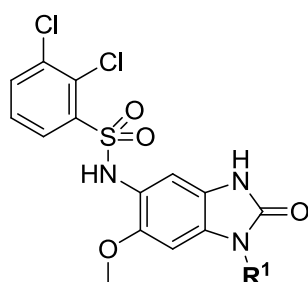


Reagents & Conditions: (a) *tert*-butyl 3-aminoazetidine-1-carboxylate, DIPEA, DMF, rt, 4 h, 84%; (b) H₂, Pd/C, EtOH, 20 h, 97%; (c) CDI, THF, 50 °C, 3 h, 79%; (d) i. 4M HNO₃, 0 °C - rt, 1 h, ii. NaHCO₃, Boc₂O, THF, 48 h, 52%; (e) H₂, Pd/C, EtOH, 3 h, 95%; (f) 2,3-dichlorobenzenesulfonyl chloride, pyridine, rt, 1 h, 57%, (g) 4N HCl in dioxane, CHCl₃, 1.5 h, 51%; (h) i. Ac₂O, pyridine, 3 h, ii. MeOH, K₂CO₃, 25%.

SCHEME 31. Synthetic route to prepare azetidine benzimidazolone sulfonamides, 226 & 227.

The results from the second iteration of analogues are shown below in Table 17. Note that the *isopropyl* analogue, **228** and the *oxetanyl* analogue, **229** were prepared following the general Scheme 27.

TABLE 17. Further SAR at the N1-position of the benzimidazolone series.



Cmpd	R ¹	GTP _γ S (pIC ₅₀)	LE	LLE _{AT}	MW	CLND Sol. μg/mL
88	H	6.5	0.38	0.31	388	44
190a	Me	6.7	0.36	0.29	402	12
191a	CH ₂ CH ₂ OMe	6.4	0.31	0.25	446	1
192a	CH ₂ CONH ₂	6.3	0.31	0.31	445	11
228	<i>i</i> -Pr	6.9	0.35	0.24	430	0
203	<i>n</i> -Pr	6.0	0.30	0.18	430	3
212	CH ₂ CH ₂ NMe ₂	5.4	0.25	0.19	459	180
219	CH(CH ₂ OH) ₂	5.7	0.27	0.26	462	176
229		6.7	0.33	0.29	444	8
226		5.8	0.28	0.25	443	82
227		6.4	0.28	0.28	485	8

The data show that small groups such as a methyl group or a hydrogen atom at the N1-position are preferred in terms of LE/LLE_{AT}. Changing the methyl group at the N1-position for an *isopropyl* group (**228**) did show a slight increase in potency. However, this could be just due to the additional hydrophobic binding (LLE_{AT} = 0.24) because of the higher lipophilicity of the molecule (clogP of **228** = 4.4, c.f. clogP of **190a** = 3.5). Despite the observed increase in potency, benzimidazolone **228** was significantly less soluble than **88** and the methyl analogue, **190a**. Replacing the methyl group of **190a** with *n*-propyl (**203**) or methoxyethyl (**191a**) reduced both potency and solubility. Introduction of solubilising groups at the N1-position, such as the basic groups in compounds **212** and **216**, and the diol in

compound **219**, helped improve the solubility but the potencies of the analogues were lower than benzimidazolone **190a**.

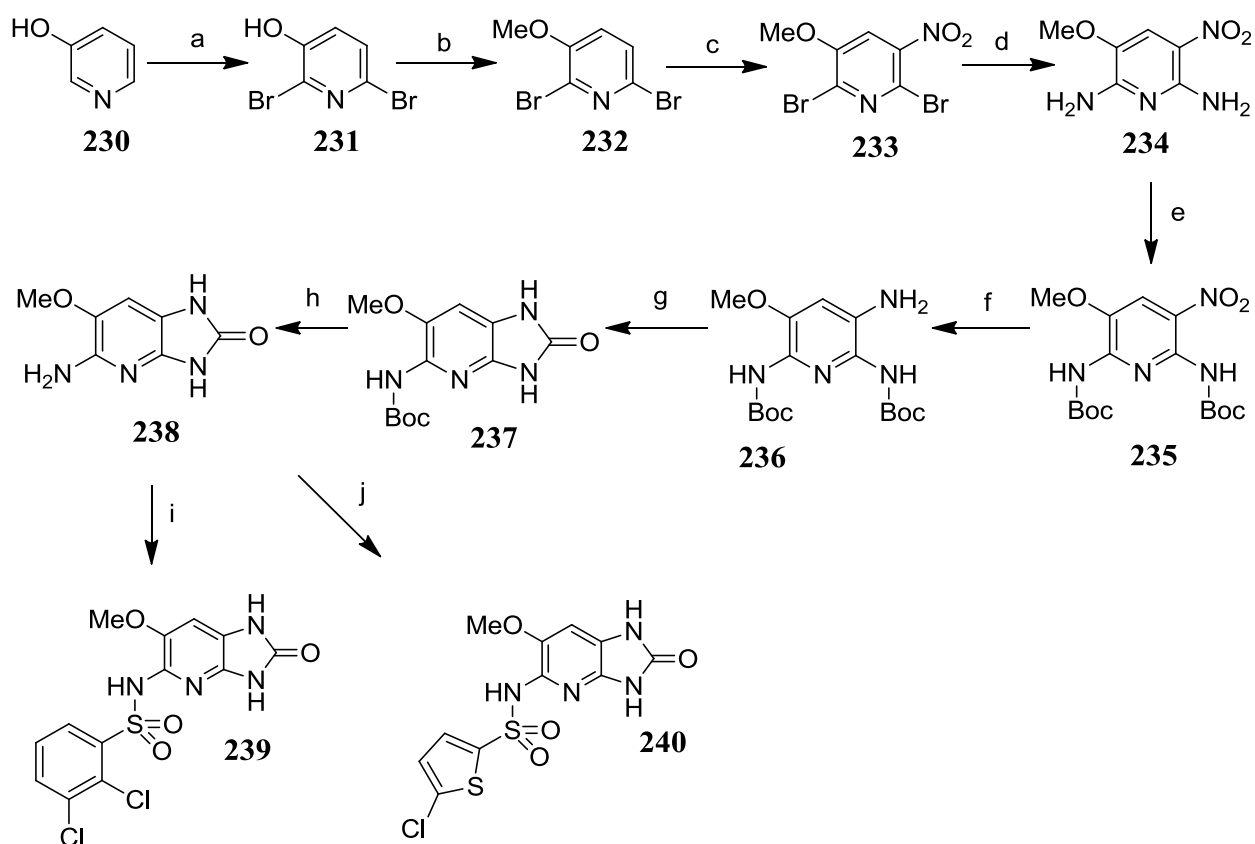
The oxetanyl compound, **229** was equipotent to **190a** in the GTP γ S assay. Compound **229** was prepared based on a paper by Muller and co-workers, who have demonstrated the utilisation of oxetane groups to improve the solubility and permeability of other scaffolds.¹⁴⁷ However, it was found that for the benzimidazolone series, the oxetane moiety did not improve the solubility (CLND solubility = 8 μ g/mL) relative to the methyl analogue **190a** (CLND solubility = 12 μ g/mL).

Any other modifications made to the N1-position reduced potency. Although, it does appear that an amide moiety (Compound **192a**) and an azetidiny amide (Compound **227**) were tolerated to some extent, which could be extended out to probe the SAR further. In addition, these positions could be used to introduce other groups to balance the solubility, permeability and absorption of the molecule. Nonetheless, as the molecular weight of the molecule was reaching 480 without a significant jump in potency, the work around the N1-position was halted.

7.10 The azabenzimidazolone series

Finally, introduction of nitrogen into the core benzimidazolone ring was investigated. This was expected to improve the solubility and physicochemical properties of the molecule. In addition, based on SAR from previous in-house series such as the aryl pyrazole series (as exemplified by **114**), it was expected that replacing the carbon adjacent to the sulfonamide substituent with nitrogen would enhance the potency.

Introduction of nitrogen at the 4-position of the benzimidazolone series is described in Scheme 32.



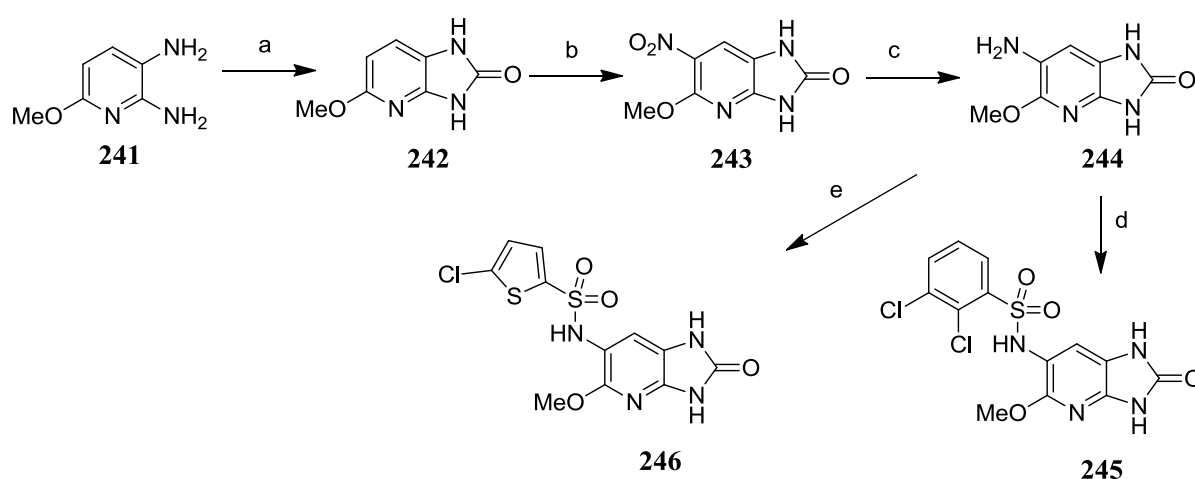
Reagents & Conditions: (a) Br₂, 10% NaOH, 0 °C, 1h, rt, 4 h, 46%; (b) MeI, K₂CO₃, DMSO, reflux, 2 h, 80%; (c) conc. HNO₃, conc. H₂SO₄, 65 °C, 36 h, 28%; (d) aq. NH₃, 90 °C, 1 h, μ wave, 78%; (e) Boc₂O, K₂CO₃, DMF, rt, 18 h, 66%; (f) Fe, AcOH, rt, 2 h, 78%; (g) pyridine, 100 °C, 1 h, μ wave, 74%; (h) TFA, rt, 30 min, 93%; (i) 2,3-dichlorobenzenesulfonyl chloride, pyridine, rt, 2 h, 30%; (j) 5-chlorothiophenesulfonyl chloride pyridine, rt, 2 h, 14%.

SCHEME 32. Synthetic route to prepare aza-benzimidazolone sulfonamides **239** & **240**.

2,6-Dibromo-3-methoxy-5-nitropyridine (**232**) was prepared following a literature procedure described by Clark and Deady.¹⁴⁸ Commercially available 3-hydroxy pyridine was reacted

with bromine under aqueous alkali conditions and then *O*-methylated to give dibromopyridinol **232** in 80% yield. Nitration of **232** occurred at the 5-position, *meta*- to the methoxy group to give **232** in 28% yield. The bromine atoms of **232** are highly activated towards nucleophilic displacement reaction by the nitro and aza functionality.¹⁴⁸ A modified version of the procedure described by Barraclough and co-workers was used for the nucleophilic displacement of **232** with ammonia to give diamine **234** in 78% yield.¹⁴⁹ Boc protection of the diamine **234**, followed by reduction of the nitro group using iron in acetic acid afforded the amino Boc-protected compound, **236** in 78% yield. This compound was then heated in a microwave at 100 °C to give the cyclised Boc protected product **237**. Finally, cleavage of the Boc group with TFA, followed by sulfonylation with either 2,3-dichlorobenzenesulfonyl chloride or 5-chlorothiophenesulfonyl chloride in pyridine afforded the desired sulfonamides **239** and **240** in moderate yield respectively.

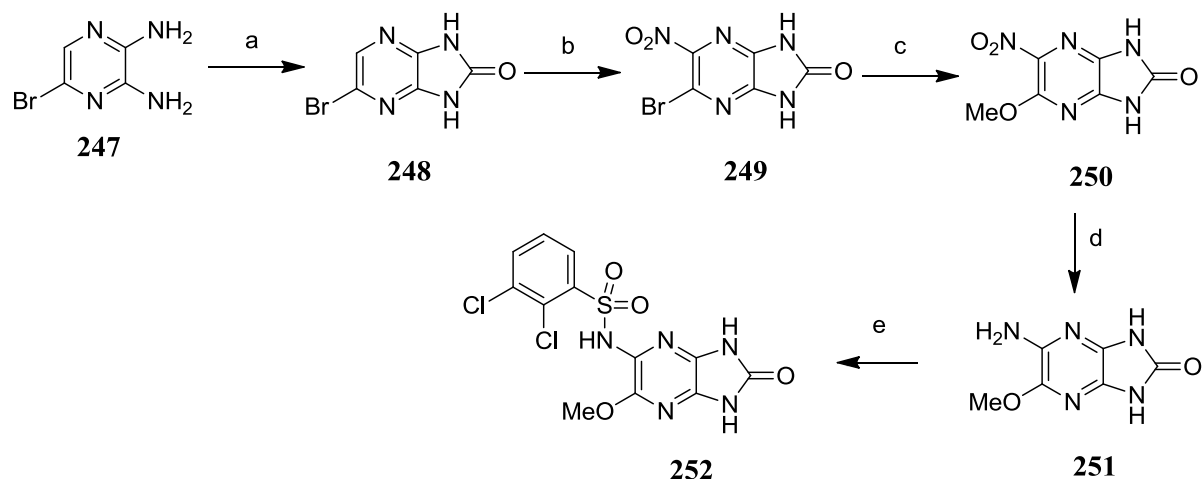
Commercially available 6-methoxypyridine-2,3-diamine (**241**) was used for the introduction of nitrogen at the 7-position of the benzimidazolone series (Scheme 33). Reaction of **242** with CDI was slow, giving the benzimidazolone in only 25% yield after 48 h. Nitration of azabenzimidazolone **242**, using triflic anhydride and fuming nitric acid gave the desired 5-nitro azabenzimidazolone **243**, which was hydrogenated over 10% Pd/C to give the amino benzimidazolone **244**. Finally, reaction with either 2,3-dichlorobenzenesulfonyl chloride or 5-chlorothiophenesulfonyl chloride afforded the target sulfonamides **245** and **246** respectively.



Reagents & Conditions: (a) CDI, Et₃N, THF, rt, 48 h, 31%; (b) Tf₂O, fuming HNO₃, rt, 3 h, 47%; (c) H₂, Pd/C, EtOH, 2 h, 76%; (d) 2,3-dichlorobenzenesulfonyl chloride, pyridine, rt, 1 h, 48%; (e) 5-chlorothiophene-2-sulfonyl chloride, pyridine, rt, 1 h, 35%;

SCHEME 33. Synthetic route to prepare benzimidazolone sulfonamide 245 & 246.

Replacing the benzene ring of the benzimidazolone core with a pyrazine ring could also help improve solubility and reduce lipophilicity of the template. The preparation of the pyrazine analogue is shown in Scheme 34.



Reagents & Conditions: (a) CDI, THF, 50 °C, 48 h, 85%; (b) NO₂BF₄, CH₃CN, rt, 1 h, 50%; (c) NaOMe, MeOH, rt – 50 °C, 20 h, 49%; (d) H₂, Pd/C, EtOH:EtOAc (1:1), 1 h, 80%; (e) 2,3-dichlorobenzenesulfonyl chloride, pyridine, rt, 1 h, 7%.

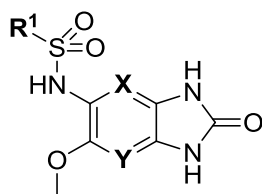
SCHEME 34. Synthetic route to prepare the pyrazine analogue for the benzimidazolone series.

Reaction of 5-bromopyrazine-2,3-diamine (**247**) with CDI gave the diaza-benzimidazolone **248** in 85% yield. Nitration, using similar conditions to AstraZeneca's for the preparation of their pyrazine analogues,⁶⁰ gave the nitro compound **249** in 50% yield. The bromine of **249** was displaced by methoxide to give the methoxy benzimidazolone **250** in 49% yield. Hydrogenation of **250** over 10% Pd/C catalyst, followed by sulfonylation with 2,3-dichlorobenzenesulfonyl chloride in pyridine afforded the desired sulfonamide **252**.

The GTP γ S assay results from the aza-benzimidazolone analogues are shown in Table 18. For the benzimidazolone series, replacing the carbon adjacent to the sulfonamide substituent with nitrogen (azabenzimidazolone **239**) resulted in more than a log unit increase in GTP γ S potency. Azabenzimidazolone **239** also demonstrated an improvement in terms of LE/LLE_{AT}, which now appears to very attractive as an efficient binder (LE = 0.43, LLE_{AT} = 0.34). Furthermore, the solubility increased; azabenzimidazolone **239** was greater than three-fold more soluble in the CLND assay compared to the benzimidazolone **88**. Even introducing nitrogen at the 7-position of the benzimidazolone core (compound **245**) showed half a log unit increase in GTP γ S potency. However, introducing two nitrogens in the benzimidazolone

core to give the pyrazine analogue **252**, did not show an additive effect in terms of potency, but it was still found to be more active than the 4-aza analogue, **245**. Furthermore, the CLND solubility of **252** was three-fold higher than that of **88**.

TABLE 18. Introduction of nitrogen to the central core of the benzimidazolone template.



Cmpd	R ¹	X	Y	GTP γ S (pIC ₅₀)	LE	LLE _{AT}	MW	CLND Sol μ g/mL
88		CH	CH	6.5	0.38	0.31	388	44
89		CH	CH	5.9	0.36	0.32	360	18
239		N	CH	7.6	0.43	0.34	389	152
240		N	CH	6.3	0.39	0.31	361	134
245		CH	N	7.1	0.40	0.29	389	126
246		CH	N	6.3	0.39	0.29	360	25
252		N	N	7.3	0.41	0.33	390	130

It should be noted that generally for CCR4 Site 2 inhibitors, replacing the 2,3-dichlorophenyl group with a 5-chlorothiophenyl group resulted in an increase in GTP γ S activity, as mentioned earlier in the report. However, the benzimidazolone series showed half a log unit reduction in potency when the 2,3-dichlorophenyl group (compound **88**) was replaced with a 5-chlorothiophenyl group (compound **89**). This trend was also observed with the azabenzimidazolone analogues with the 2,3-dichlorophenyl analogues **239** and **245** showing a greater difference in potency compared to their corresponding 5-chlorothiophenyl analogues **240** and **246** (note that the 5-chlorothiophene analogue of **252** was not prepared). This again suggests that the benzimidazolone series might bind differently at the allosteric site compared to previous in-house and competitors' series, and also could explain why modelling of the benzimidazolone series with the indazole series (**6**) did not provide comparable SAR despite a good overlay (Docking not shown).

Human whole blood actin polymerisation data and physicochemical data were obtained for a set of compounds from the benzimidazolone and azabenzimidazolone series, and the results are summarised in Table 19.

TABLE 19. Introduction of nitrogen to the central core of the benzimidazolone template.

Cmpd	GTPγS (pIC₅₀)	HWB pA₂	clogP	Chrom logP	Chrom logD_{7.4}	Sol μg/mL	PPB %	P_{ex} nm/s
88	6.5	5.3	3.1	3.2	3.3	44	93.0	474
89	5.9	nd	2.5	2.7	2.7	18	89.0	69
228	6.9	<5	4.4	4.9	4.6	0	95.2	nd
239	7.6	6.0	3.6	2.5	2.4	152	93.2	8.3
240	6.3	<5	3.0	2.0	1.4	134	92.5	0
245	7.1	5.7	4.0	3.3	3.2	126	93.3	155
246	6.3	nd	3.4	2.6	2.5	25	90.5	71
252	7.3	5.2	3.5	nd	nd	130	nd	0

The isopropyl analogue **228** was inactive in the whole blood assay. The azabenzimidazolone analogues **239**, **245** and **252** were all found to be active, with compound **239** showing activity similar to that of the indazole candidate, **6**. It should be noted that the azabenzimidazolone analogues with the 5-chlorothiophenyl group were all inactive in the whole blood assay. This is consistent with the data observed in the GTP γ S assay.

The whole blood activity data of azabenzimidazolone **239** ($pA_2 = 6.0$) is very encouraging as the molecular weight is lower than that of indazole candidate **6**, and the compound also has good LE/LLE_{AT}. In addition, the aza compounds from the benzimidazolone series all appear to have plasma protein binding around 90 - 93%, which is lower than for other CCR4 Site 2 sulfonamide antagonists. Hopefully, this will allow more unbound compounds to be available in the blood. Introduction of nitrogen into the benzimidazolone template also improved the solubility but unfortunately, it had a detrimental effect on the permeability of the molecules (e.g. P_{ex} of **239** = 8.3 nm/s, c.f. P_{ex} of **88** = 474 nm/s). It is not clear at this stage, why the permeability of the molecule has reduced so much. One initial explanation could be that the lipophilicity of the compounds has reduced. However, the clogP of the azabenzimidazolones were not consistent, as one would expect the clogP to go down when introducing nitrogen into the core. However, with the above examples, the clogP of the aza analogues appears to have increased (clogP of **88** = 3.1, c.f. clogP of **239** = 3.6). The reason for this may be that not enough examples of these types of compounds exist in the database to calculate the logP accurately. Therefore, the compounds were measured in the in-house chromatographic logP assay. The data was found to be more consistent: the aza analogues have lower chromlogP (e.g. chromlogP of **239** = 2.5) compared to the benzimidazolone **88** (chromlogP = 3.2). One could increase the lipophilicity of the azabenzimidazolones in lead optimisation by using the N1- and N3-position as a handle to balance the physicochemical properties with potency to identify a suitable candidate for the CCR4 programme.

Unfortunately, due to portfolio changes in the Respiratory CEDD, the CCR4 programme was terminated, and no further work was carried out in these series of compounds.

8.0 Extracellular allosteric CCR4 antagonists.

Efforts at GSK were also focused on identifying an extracellular allosteric CCR4 antagonist. As mentioned earlier in the thesis (Section 4.3), lipophilic amines such as Bristol Myers Squibb's (BMS) compounds **1**⁷³ and **2**,⁵⁸ Astellas' compound **3**^{59,76} and Daiichi Sankyo's compound **4**,⁷¹ bind to an extracellular allosteric region of the 7-transmembrane CCR4 receptor (termed 'Site 1' at GSK) (Fig. 29).⁶⁸

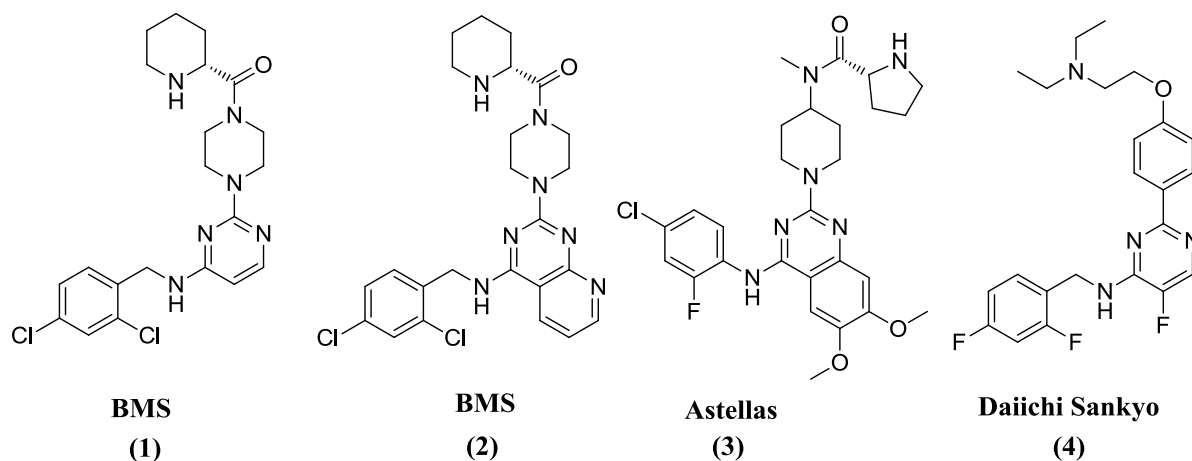


FIGURE 29. Structures of some recently published CCR4 inhibitors.

Of these Site 1 compounds, BMS's pyrimidine compound **1** was found to be a potent and selective antagonist of CCR4, demonstrating *in vivo* efficacy in a murine allergic lung inflammation model.⁷³ When compound **1** was dosed subcutaneously to mice previously challenged with ovalbumin, it caused significant reduction of eosinophilic infiltration into the bronchoalveolar lavage (BAL) fluid (ED₅₀ of 30 mg/kg).⁷³ Following further structure-activity relationship investigation of compound **1**, BMS identified and disclosed the structure of pyridopyrimidine analogue **2**, which was found to be one of the most potent CCR4 antagonists reported to date.⁵⁸ As well as showing improved *in vitro* activity, compound **2** was also found to be more efficacious than **1** in the murine allergic lung inflammation model, with an ED₅₀ of 10 mg/kg when it was administered subcutaneously to mice.⁵⁸

Both BMS compounds were synthesised in-house for assay development and they were used as standards in the primary (¹²⁵I TARC SPA and [³⁵S]-GTPγS) and the secondary (actin polymerisation human whole blood) assays. The *in vitro* potency and physicochemical properties of BMS's compounds **1** and **2** are shown in Table 20.

TABLE 20. In-house data for the BMS compounds, 1 and 2.

Compound	1	2
I¹²⁵ TARC SPA pK_i	8.6	9.1
LE / LLE _{AT} :	0.39/0.30	0.37/0.28
GTPγS (pIC₅₀):	8.1	8.3
LE / LLE _{AT} :	0.37/0.27	0.33/0.25
HWB Actin polym. (pA₂):	6.7	7.1
MW :	449	500
clogP :	4.5	4.9
Chrom logD _{7.4} :	3.5	2.8
CLND solubility:	140 μg/mL	145 μg/mL
PPB (HSA)	93.1%	92.6%

Compound **1** had a pK_i of 8.6 in the SPA and a pIC₅₀ of 8.1 in the GTPγS binding assay respectively; compound **2** is 0.5 log unit more active in the SPA assay but no real difference was observed in the GTPγS assay. Both **1** and **2** were performing close to the tight-binding limit of the GTPγS assay, so a significant difference in potency was not observed. More importantly, in the human whole blood actin polymerisation assay, compound **2** had an inhibitory activity greater than pA₂ of 7.1, depressing the maximum signal, compared to compound **1**, which had a pA₂ of 6.7. It should be noted that due to the higher molecular weight and clogP, the LE and LLE_{AT} of **2** are lower than those of **1**. Both compounds had reasonable solubility in the CLND assay, and had lower plasma protein binding (**1**, 93.1% & **2**, 92.6%) to human serum albumin (HSA) in comparison to indazole candidate **6** (96.5%). This means that a higher proportion of unbound compound will be available in the blood to exert the pharmacological effect.

Finding a potent small molecule antagonist for the Site 1 allosteric region with a good pharmacokinetic profile has proven to be challenging. The aim of this part of the programme was to discover a new Site 1 template that demonstrated good potency and pharmacokinetic properties. This posed a difficult challenge as the pharmacophore of the Site 1 antagonists suggests that an interaction between a basic moiety on the ligand and the receptor was crucial

for potency.^{73,150} Compounds with highly basic groups tend to have good solubility but very poor permeability due to the molecule existing predominantly in the charged protonated form at physiological pH of 7.4.¹⁵¹ However, it was postulated that if the basicity could be attenuated slightly without affecting the potency, then it should be possible to improve the permeability of the compounds, and hence, the oral absorption. It is worth noting that although it is less potent than the BMS's analogues **1** and **2**, Amgen have shown with their 2-aminothiazole **253** that good bioavailability (F = 63%) could be achieved in rat with Site 1 compounds containing a basic centre (calc. pK_a of **253** = 8.95) (Fig. 30).⁷²

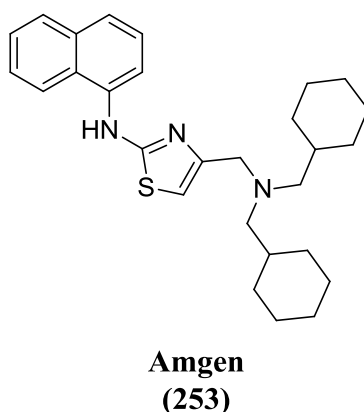


FIGURE 30. Structures of Amgen's 2-aminothiazole, 253.

The calculated pK_a of the benzylic type amine of **253** (Chemaxon software calc. pK_a = 8.95) is similar to that of the homopropylamine nitrogen of BMS compounds **1** (calc. pK_a = 8.90) and **2** (calc. pK_a = 8.89) but it should be stressed that the 2-aminothiazole **253** is much more lipophilic (clogP = 9.2, calc. chromlogD_{7.4} = 8.0) than compound **1** (clogP = 4.5, chromlogD_{7.4} = 3.5). A consequence of the high lipophilicity of **253** makes the compound more permeable and aids in oral absorption. However, molecules of high lipophilicity are generally associated with high promiscuity and off-target activity, which usually results in increased rate of attrition.⁸⁶ Leeson and co-workers have recently reported that increased promiscuity arises with basic lipophilic compounds.⁹¹ Drastic increases in lipophilicity to improve absorption should therefore be avoided when designing the inhibitors in order to reduce later problems with off-target activity.

8.1 CCR4 binding Site 1

A receptor-based drug design approach is useful when three dimensional X-ray structures of the target protein are available. Although new developments in the area of X-ray crystallography have resulted in the solutions of crystal structures of several 7-

transmembrane membrane bound receptors,^{63,66,152,153} as mentioned earlier in the thesis, the X-ray structure of CCR4 has not yet been determined. Most of the structural information of the Site 1 receptor of CCR4 has been obtained from homology models based on the solved crystal structure of rhodopsin⁶³ and β 1 and β 2 adrenergic^{64,154} 7-transmembrane receptors. Recently, Yokoyama and co-workers have used the three dimensional homology function of the Molecular Operating Environment (MOE) program to explain the binding mode and structure activity relationship of their Site 1 antagonists, the 2,4-diaminoquinazoline series, as exemplified by **254** (Fig. 31).¹⁵⁰ Yokoyama and co-workers used the resolved crystal structure of bovine rhodopsin as a template for the CCR4 receptor, and in their most favoured docking pose they have shown that in the binding pocket, the carboxyl residue on Glu-290 makes a key interaction with the terminal basic pyrrolidine nitrogen of **254**. The basic piperidine nitrogen on the of 2,4-diaminoquinazoline **254** makes a hydrogen bond with the hydroxyl residue of Tyr-258. Removal of both of these basic moieties of **254** resulted in significant loss of potency for the 2,4-diaminoquinazoline series. In addition, the NH of the nitrogen atom linked to the 4-position of the quinazoline acts as a hydrogen bond donor to form a hydrogen bond with Ser-203. These observations gave additional confidence that a homology model of CCR4 could provide useful structural insights in designing novel inhibitors.

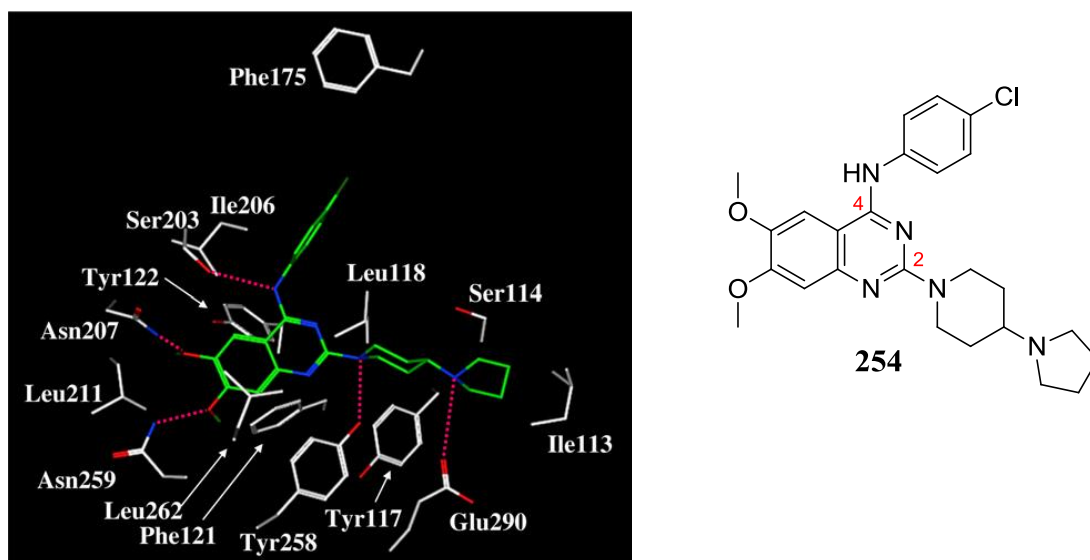


FIGURE 31. Binding interaction of **254** in a homology model of CCR4.¹⁵⁰

The BMS compound **1** was docked in the in-house homology model by an in-house computational chemist,¹⁵⁵ and the most favourable docking pose was found to be similar to that of the 2,4-diaminoquinazoline **254**, where an interaction of the terminal *R*-homoproline

nitrogen of **1** to the glutamate residue was shown to be key for binding (Fig. 32). In addition, the docking showed that the 2,4-dichlorobenzyl group of **1** occupied a hydrophobic region of the Site 1 receptor.

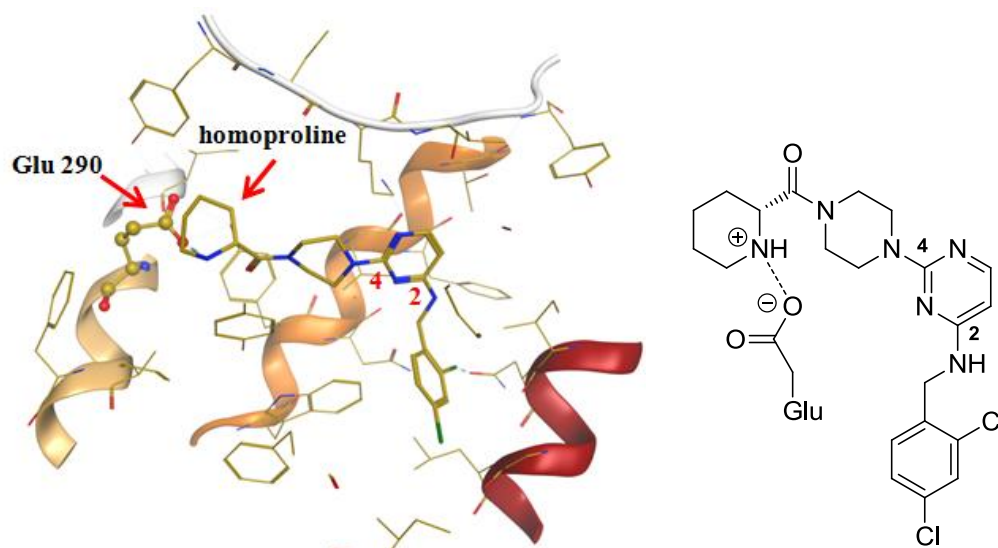


FIGURE 32. Binding interaction of BMS compound 254 in CCR4 homology model.

Although the homology model provides a putative docking mode for the binding of ligands to the receptor, the three dimensional structural information obtained must be used with caution. There could be several other docking poses for the ligand to interact with the receptor and more importantly, the sequence homology between rhodopsin and the CCR4 receptor is only about 18% in overall sequence identity, and 22% conserved in the transmembrane region (see Appendix 2). The overall sequence similarity between rhodopsin and CCR4 with amino acids possessing similar properties is 41% whilst similarity in the transmembrane region is 46% conserved. However, it is worth stressing that protein structures are more conserved than protein sequences amongst homologues and construction of homology models are carried out using structural-based alignments.¹⁵⁶ In GPCRs, the highest structural conservation is observed in the transmembrane domain and this is used for the structural-based alignments. Much more variability is observed in the intracellular and extracellular region of GPCRs¹⁵⁷ and therefore, the real three dimensional structure of the Site 1 receptor of CCR4 could be significantly different to that of the homology model, making interpretation of the structure-activity relationship observed with different templates difficult. Nonetheless, in the absence of an X-ray structure of CCR4, the homology model provides the only structural information available and with the pharmacophore of the ligands, based on known Site 1 antagonist from the literature, provides a useful starting point to design new inhibitors.

8.2 Design of novel Site 1 antagonists.

Based on literature publications and the homology model, it was proposed that the pharmacophore for a Site 1 antagonist for CCR4 consists of two ‘wings’ attached to a central core (Fig. 33).^{58,150} On the left ‘wing’ the central core has a heteroatom attached to a lipophilic group and on the opposite side, the ‘wing’ has a linker side chain attached to a terminal basic amino group. It is thought that the amino group interacts with a conserved glutamate residue located in the Site 1 pocket. During exploration of the SAR of the terminal amino group, BMS found that the *R*-enantiomers of proline or homoproline were optimal for activity in that region (in-house data for these analogues are shown in Table 23).⁷³

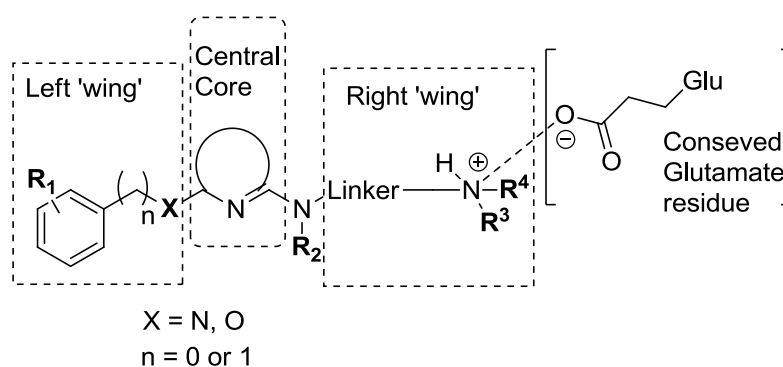


FIGURE 33. Basic pharmacophore of Site 1 inhibitors.

The linker region on the right ‘wing’ provides a ‘spacer’ between the central core and the terminal amino group. It is possible that the ‘spacer’ allows the terminal basic group to fit into the region where the conserved glutamate residue is located, allowing favourable ionic interactions to develop. Based on the homology model, the optimal distance between the terminal amino group and the glutamate carboxyl residue is expected to be around 1 - 2.5Å. It was postulated that if the ‘spacer’ residue could be fixed in a constrained conformation or extended out further, it may be possible to direct the terminal amino group to pick up stronger interactions with the glutamate residue and identify molecules with improved potency and novelty. This idea led to the investigation of several constrained diamines as well as some flexible linker groups. Figure 34 shows a selection of the diamine analogues that were investigated.

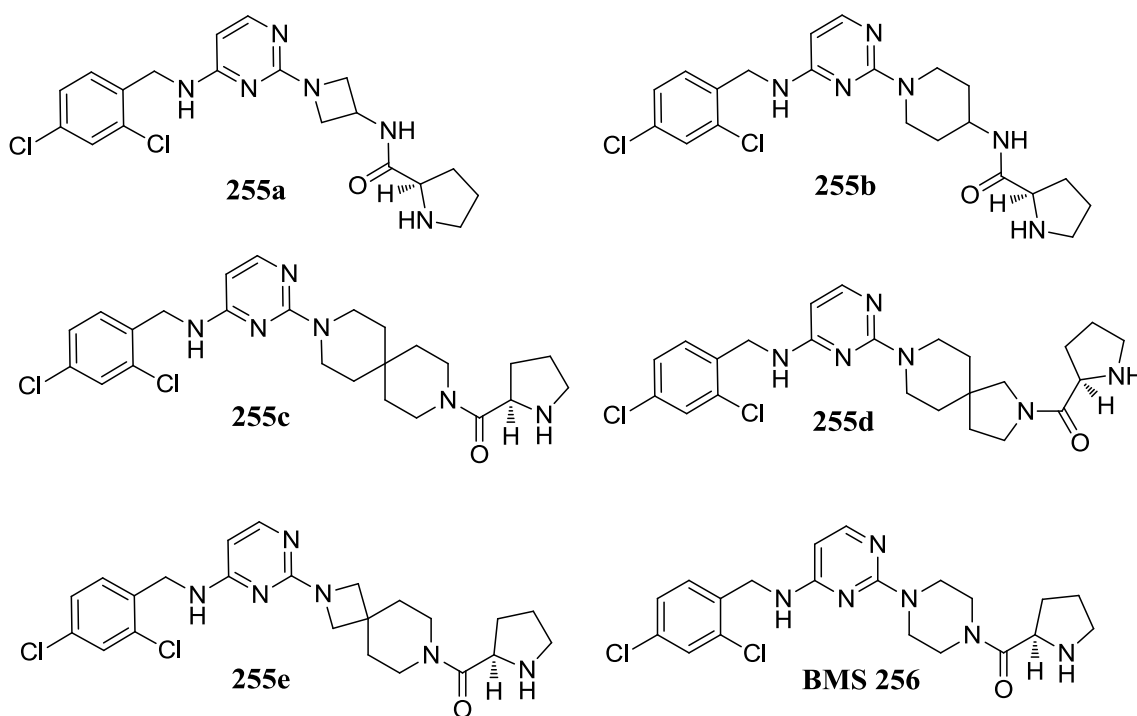


FIGURE 34. BMS compound 256 and new pyrimidine analogues 255a-255e

In these new analogues, the left wing and the central core were conserved from **1**, and only changes to the linker region were explored. In addition, *R*-proline was used as the terminal basic moiety instead of *R*-homoproline. In the BMS template, the *R*-proline analogue **256** had slightly lower activity ($pK_i = 8.2$) compared to the *R*-homoproline analogue **1** ($pK_i = 8.6$) in the in-house SPA binding assay, but it had similar LLE_{AT} (0.31) with lower $clogP$ (3.9) and $chromlogD_{7.4}$ (2.6) (c.f. **1**, $LLE_{AT} = 0.30$, $clogP = 4.5$, $chromlogD_{7.4} = 3.5$).

The new analogues with the different linkers were overlaid with the BMS compound (by an in-house computational chemist¹⁵⁵) and the structures are shown below in Figure 35. The favoured binding pose of the BMS compound **1** in the homology model was used as a template to carry out the overlays, and the new structures were then minimised and superimposed based on the similarity in their pharmacophore. The overlays show that the 2,4-dichlorobenzyl and the pyrimidine group of all the analogues superimposed very well, where the key differences were observed in the linker and the terminal amino region (Fig. 35a). The diamine compounds **255a** and **255b** overlap well in the space where the piperazine linker of BMS's compound **1** sits, but the orientation of the terminal proline group diverged significantly from compound **1**'s homoproline group (Fig. 35b and 35c). As expected with the spiro-analogues **255c**, **255d** and **255e**, the diamine linkers provide a longer spacer between the pyrimidine core and the terminal proline group but it was interesting to observe

that the terminal proline nitrogen adopts a similar position to that of the nitrogen on the BMS compound 1's homoproline group (Fig. 35d, 35e and 35f). It should be pointed out that throughout this piece of work, the fitting of the pharmacophore was prioritised over considerations of linker conformation. In the homology model, the proposed ligands were constrained to help fit in to the binding site, which will result in major entropic penalties and impact negatively on the binding energies. Electronic structure calculations were carried out for the unbound ligands; they revealed that some of the poses used to fit the homology model were strained.¹⁰⁴

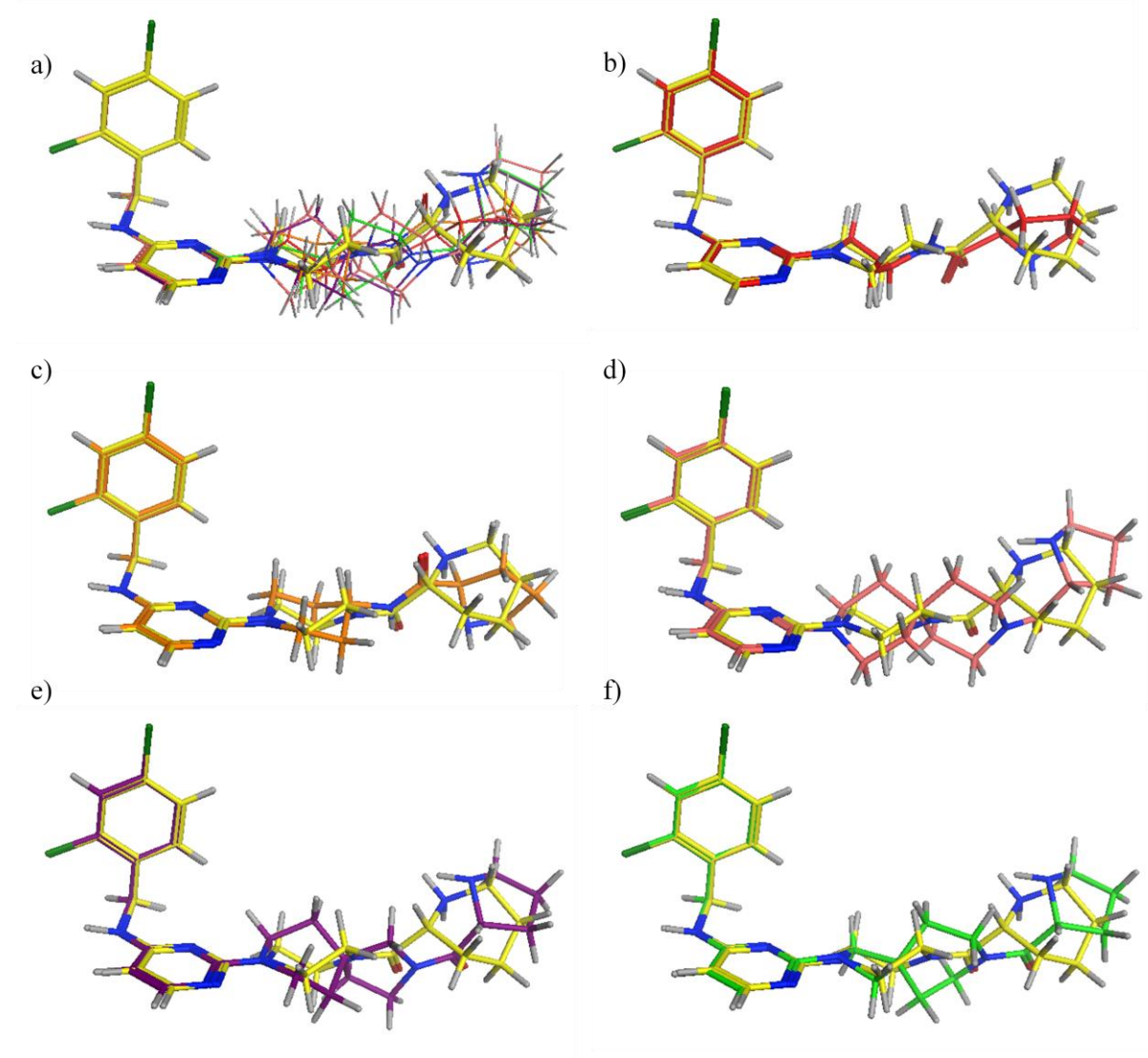
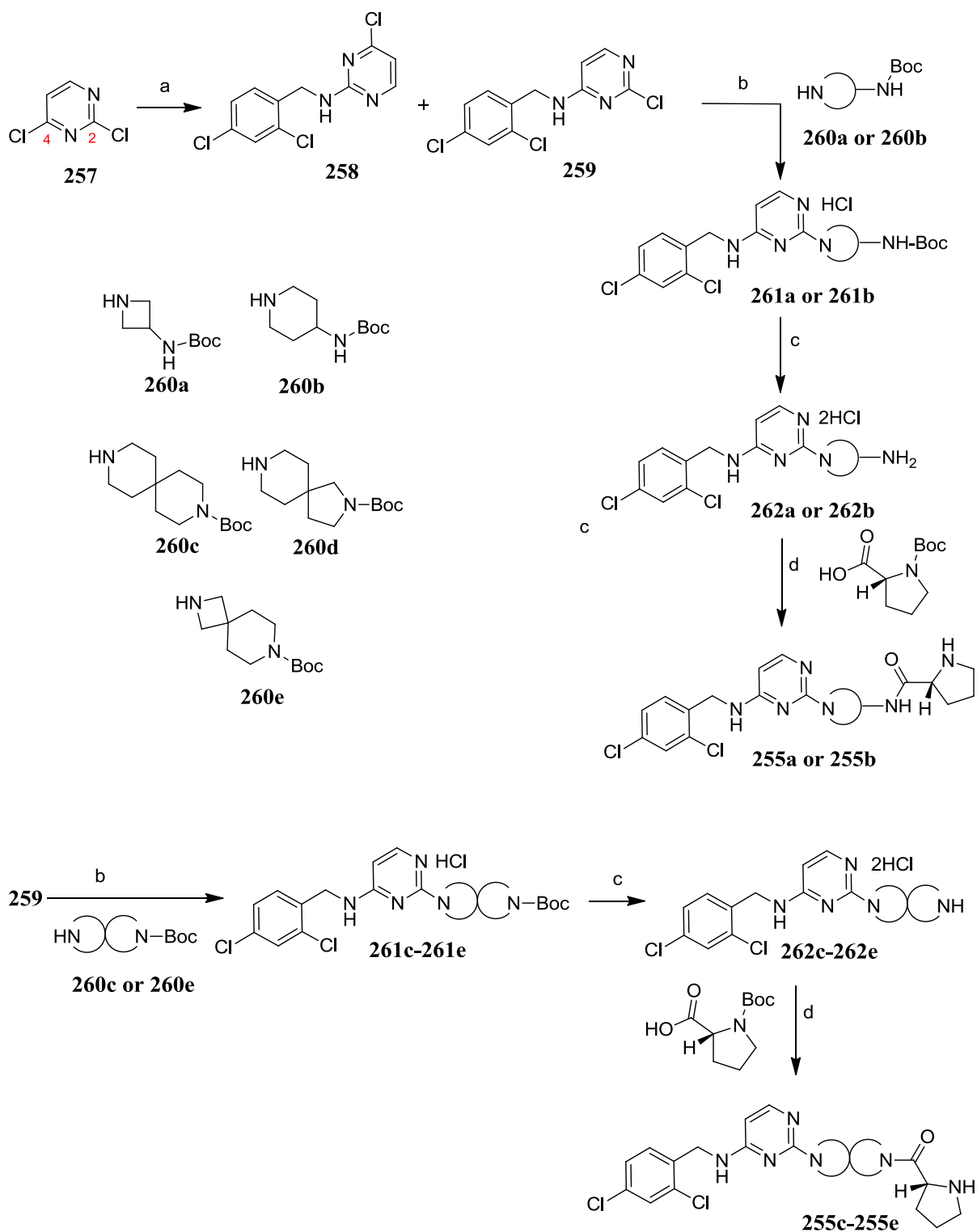


FIGURE 35. a) Overlay of BMS compound 1 (yellow) with pyrimidine analogues 255a – 255e (shown as line drawings). b) overlay of 1 and 255a. c) overlay of 1 and 255b. d) overlay of 1 and 255c. e) overlay of 1 and 255d. f) overlay of 1 and 255e.

The target analogues **255a** – **255e** were prepared by the route outlined in Scheme 35.



Reagents & Conditions: (a) 2,4-Dichlorobenzylamine, DIPEA, DCE, rt, 24 h, **258** 21%, **259** 49%; (b) Amine **260a-260e**, IPA, 90 °C, 48 h, **261a** 56%, **261b** 44%, **261c** 55%, **261d** 90%, **261e** 46%; (c) 4 M HCl in dioxane, rt, 0.5 h, **262a-262e** 97% - 99% yield; (d) i) (R)-1-(tert-butoxycarbonyl)pyrrolidine-2-carboxylic acid, HATU, DIPEA, DMF, rt, 1 h, ii) TFA, rt, 0.5 h, **255a** 85%, **255b** 68%, **255c** 44%, **255d** 79%, **255e** 50%.

SCHEME 35. Preparation of pyrimidine analogues 255a-255e.

The key steps in the synthesis were the sequential S_NAr displacement of the chlorine atoms of dichloropyrimidine **257**. The first displacement with 2,4-dichlorobenzylamine in the presence of DIPEA proceeded at room temperature to afford the 2-substituted chloropyrimidine **258** in 21% and 4-substituted chloropyrimidine **259** in 48% yield respectively. Nucleophilic displacement of halopyrimidine at the 4-position is faster than displacement at the 2-position.¹³⁴ The 2-position has slightly more electronic repulsion towards the incoming nucleophile due to two lone pairs of electrons in a sp^2 hybrid orbital on the two neighbouring nitrogens. The structure of **259** was confirmed by a 1D NOE experiment (Fig. 36), in which irradiation of the benzylic NH proton (8.42 ppm) gave an NOE enhancement of protons at the methylene position (4.54 ppm) and the pyrimidyl proton at the 5-position (6.58 ppm).

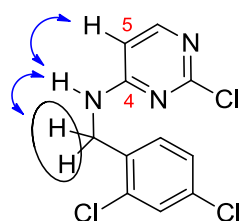


FIGURE 36. Structure of regioisomer **259** was confirmed by NOE experiment.

The substitution reaction of chloropyrimidine **259** with the mono-protected diamine reagents **260a** - **260e** at 90 °C in IPA gave the *bis*-substituted pyrimidines **261a** - **261e** respectively as hydrochloride salts (Scheme 35). Ion chromatography was carried out on a representative compound, **261d** to confirm the parent to salt ratio. The anionic chloride ion content of **261d** was measured to be 6.8% (calc. $35.5/528.9 \times 100 = 6.7\%$) confirming a 1:1 ratio between parent and the hydrochloride salt. The Boc-protected pyrimidines, **261a** - **261e** were then treated with 4 M HCl in dioxane to give the amine intermediates, **262a** - **262e** respectively as di-hydrochloride salts. Ion chromatography on a representative example (**262d**) confirmed an approximate 1:2 ratio between parent and the hydrochloride salt (measured anionic chloride ion = 13.5% vs calc. $71/465.3 \times 100 = 15\%$). Finally, amide coupling of **262a** - **262e** with Boc-protected *R*-proline, followed by deprotection with TFA gave the desired pyrimidine target compounds **255a-255e** in moderate to good yield. Some difficulty was encountered when purifying the final compounds using normal phase conventional flash chromatography or the reverse phase mass directed autoprep (MDAP) system, using formic acid as a modifier. The peaks appear to broaden in the column and final products were being recovered with 10 – 20% impurity. It was established that MDAP with a TFA modifier gives the optimum conditions for purification, and this method was used for all future purifications.

The free bases were generated by passing the TFA salts through pre-conditioned aminopropyl cartridges.

The final target compounds **255a** - **255e** were fully characterised by both 1D and 2D NMR experiments but it was observed that the ^{13}C NMR of **255d** was complex containing additional peaks, which were believed to be due to rotamers (Fig.37). In comparison to the other analogues (**255a**, **255b**, **255c** and **255e**), additional peaks for rotamers for **255d** were observed because of the unsymmetrical nature of the 6,5-spiro-diamine ring in the molecule. Two conformational isomers are possible (**255d** and **255d'**) on the NMR time scale owing to the restriction of rotation around the strained tertiary amide bond that is likely to exhibit partial double bond character (Fig. 37). It is thought that the energy barrier for rotation around the amide bond is sufficiently large to be observed on the ^{13}C NMR time scale, which results in geometrically and magnetically non-equivalent carbon peaks. Proline amides are very common structural features that exhibit rotamers due to restriction of rotation around the amide bond;^{158,159} this phenomenon is observed with many other tertiary amides.¹⁶⁰

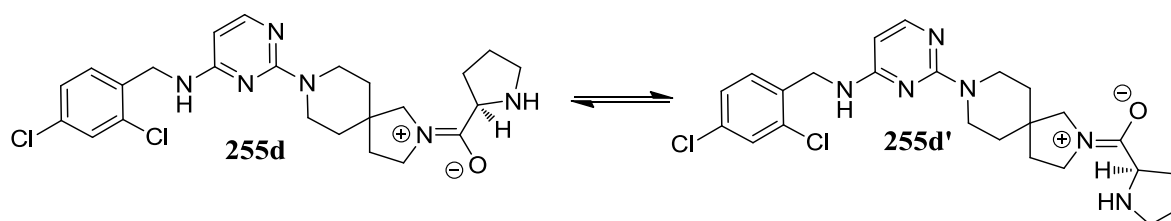


FIGURE 37. Two possible conformations of spiro-pyrimidine 255d.

Variable temperature (VT) NMR was used to confirm the presence of rotamers; at higher temperature (120 °C) the distinct peaks from the rotamers coalesced (Fig 38). It should be noted that peaks for the rotamers were not observed in the ^1H NMR of **255d**.

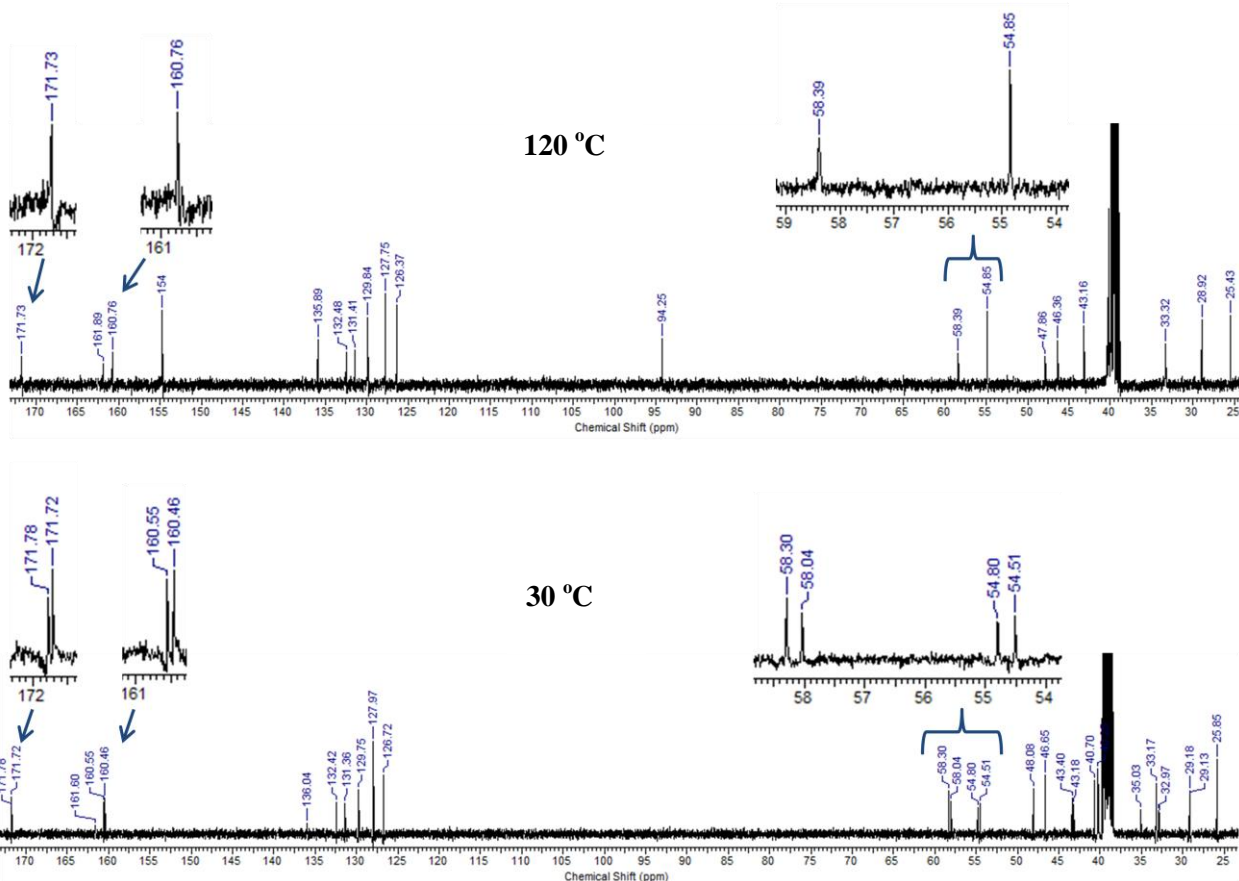


FIGURE 38. VT ^{13}C NMR of **255d** showing coalescence of the ^{13}C peaks at 120 °C.

The ^{13}C NMR of the Boc-protected intermediate **261d** also showed peaks for rotamers, whereas no additional peaks were observed for the deprotected intermediate **262d**. This confirms that the additional rotamer peaks for **255d** arise because of the slow rotation of the amide bond (see the experimental section for the ^{13}C NMR of **261d** and **262d** at room temperature in MeOD). The spiro-pyrimidine amine **262d** was further characterised by HMBC, HSQC, ROESY and ^{15}N HMBC experiments. The HMBC spectrum with the key correlations is shown in Fig. 39. The NMR experiments were carried out both in MeOD and DMSO for **262d**. In MeOD, the ^1H NMR peaks for the H13 and H15 were slightly broad, and their correlation to C2 was barely observed (see experimental section for HMBC spectrum). However, when using DMSO as the solvent, the correlations from H13 and H15 (3.69 - 3.78 ppm) to C2 (151.9 ppm) were clearly observed in the HMBC experiment (highlighted in red in Fig. 39).

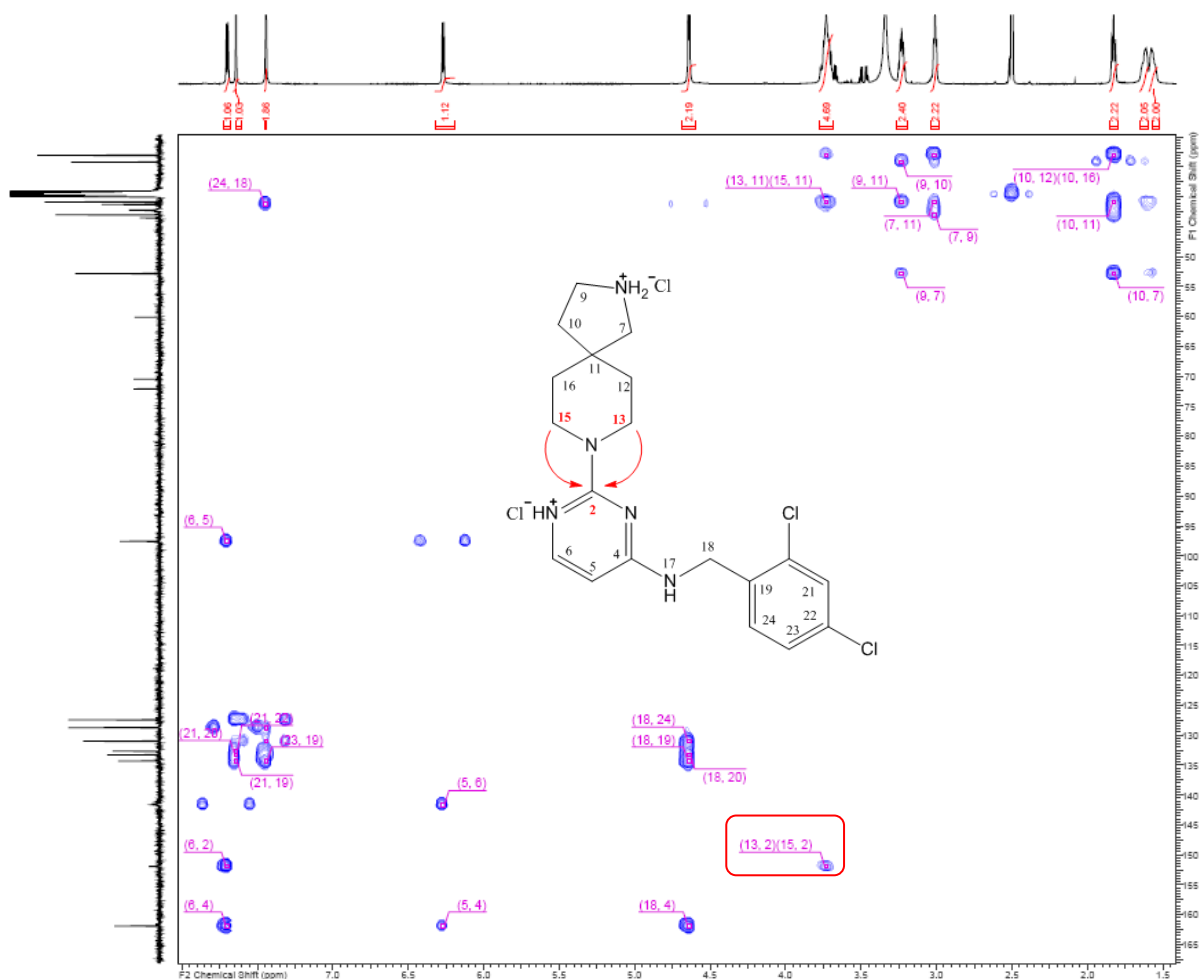


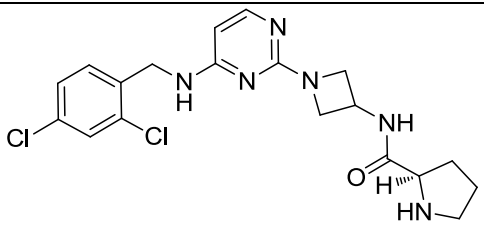
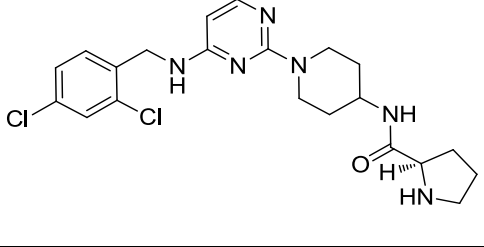
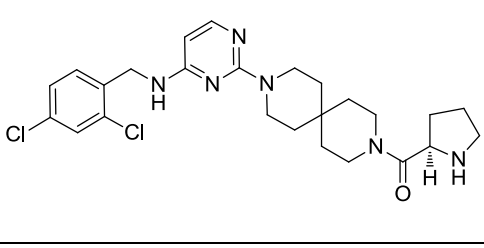
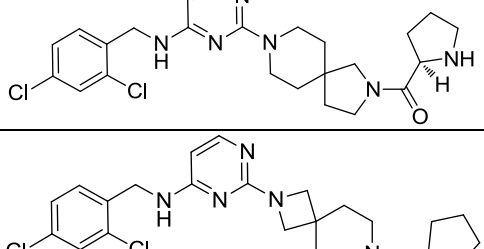
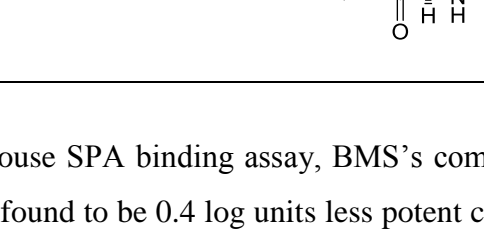
FIGURE 39. HMBC spectrum of 262d

8.3 SPA binding data of new analogues

The activity of the new compounds was measured in the SPA binding assay and the results are compared against the standard compounds **1** and **256** (Table 21).

TABLE 21. Pyrimidine analogues with changes to the linker group.

Cmpd	Structure	SPA pK _i	LE	LLE _{AT}	clogP	Chrom logD _{7.4}
1 BMS		8.6	0.39	0.30	4.5	3.5
256 BMS		8.2	0.39	0.31	3.9	2.6

255a		7.4	0.36	0.28	3.9	2.4
255b		7.7	0.35	0.32	3.0	2.7
255c		7.7	0.31	0.25	4.3	3.5
255d		7.8	0.32	0.28	3.8	3.4
255e		7.0	0.30	0.27	3.2	2.5

In the in-house SPA binding assay, BMS's compound **256** containing an *R*-proline terminal group was found to be 0.4 log units less potent compared to its corresponding *R*-homoproline compound **1**. However, compound **256** demonstrated identical LE and higher LLE_{AT} due to its lower molecular weight and clogP. In addition, the measured chromlogD_{7.4} of **256** was nearly a log unit lower than **1**.

The azetidine analogue **255a** and the spiro-azetidine **255e** were found to be much less potent than compound **256**, so these compounds were rejected at this stage. It is noteworthy that the LE and LLE_{AT} of the azetidine analogue **255a** was reasonably high; however, due to the lower potency of the compound, this template was not chosen for future SAR investigation.

For the pyrimidine analogues, **255b**, **255c** and **255d**, replacement of the linker region with the different diamines resulted in approximately half a log unit loss in potency in the SPA

binding assay ($pK_i = 7.7, 7.7$ and 7.8 respectively) compared to compound **256**. In terms of LE and LLE_{AT} , the piperidine analogue **255b** appeared to be the most attractive as a starting point; however, there were concerns around the novelty of this template, and so **255b** was also rejected.

Of the two novel spiro-pyrimidine analogues **255c** and **255d**, compound **255d** showed a better profile with higher LE, LLE_{AT} , lower MW, lower clogP and chromlogD_{7.4}, and was therefore selected for further SAR exploration in an attempt to increase the potency of the series.

It should be emphasised that the new analogues **255a** – **255e** were initially chosen for synthesis based on the overlay with the BMS compound but the inhibitory activity of the compounds in the SPA binding assay did not correlate well with the proposed binding mode. For example, a positive correlation was observed with the azetidine analogue **255a**, where overlay with the BMS compound suggested that the orientation of the basic nitrogen on the terminal proline group of **255a** was in the opposite direction to that of the terminal basic nitrogen of compound **1**, which would be expected to result in drop in potency. In the SPA assay, **255a** was over a log unit less potent than **1**. Similar to the case of the azetidine analogue **255a**, the favoured overlay of **255b** with **1** showed that the terminal proline nitrogen of **255b** projected in the opposite direction to that of **1**. The compound would therefore be expected to be much less potent but a significant drop in potency was not observed with **255b** compared to the proline analogue **256**. Although, there is no clear evidence for this, one possible explanation could be that the glutamate residue is flexible and free to move around slightly in the active site to pick up the ionic interaction with the proline nitrogen. Contrary to this hypothesis, the terminal nitrogen of the spiro-azetidine analogue **255e** was in close proximity to the basic nitrogen of the BMS compound **1** in the overlay, but **255e** was found to be more than 1.5 log units less potent in the SPA binding assay. It may be that the binding mode chosen for the overlay is not the most accurate representation of how these compounds are binding in the Site 1 allosteric site. Based on these results and the many limitations of the homology model, no further dockings or overlays were carried out to design new analogues for the spiro-pyrimidine series.

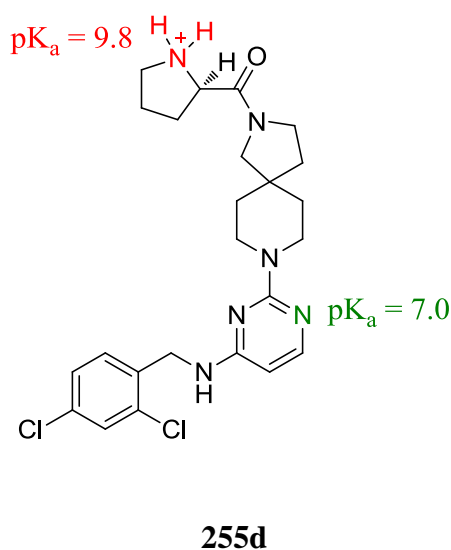
8.4 The spiro-pyrimidine template.

The biological activity, physicochemical properties and rat pharmacokinetic data of the spiro-pyrimidine **255d** were evaluated and the data are shown below in Table 22. The compound

showed good inhibitory activity in the actin human whole blood assay ($pA_2 = 6.2$) achieving potency comparable to that of the BMS compound **1** ($pA_2 = 6.6$, Table 20). Spiro-pyrimidine **255d** was also found to be selective for CCR4 against chemokine receptors, CCR1 ($pIC_{50} < 4.6$), CCR2 ($pIC_{50} < 4.6$) in radioligand $GTP\gamma S$ binding assay and CXCR2 ($pIC_{50} < 4.6$) in a FLIPR assay.

Site 1 antagonists in general tend to have poor pharmacokinetic profiles, so the compound was submitted for IV and oral PK early on in the programme. Following an IV dose (1 mg/kg) in a male rat, **255d** showed low blood clearance (9 mL/min/Kg), a good half life (4.5 h) and a moderate volume of distribution (3.7 L/Kg). However, following an oral dose, **255d** was found to have negligible bioavailability in rat.

TABLE 22. Data for the spiro-pyrimidine 255d (IV n = 4, PO n = 2).



I¹²⁵ TARC SPA pK_i	7.8
LE / LLE _{AT}	0.32/0.28
HWB Actin polym. (pA₂):	6.2
MW :	489
clogP :	3.8
Chrom logD _{7.4} :	3.4
CLND solubility:	130 µg/mL
PPB (HSA)	95.7%
Rat PK	
(dose 1 mg/kg)	
Bioavailability:	negligible
Clearance:	9 mL/min/kg
t _{1/2} median:	5.5 h
V _{dss} :	3.7 L/kg

The low bioavailability of the compound was thought to be caused by the strongly basic nature of the molecule, resulting in poor absorption. The pK_a 's calculated (for the conjugate acids, the ammonium salts) using the Chemaxon software were 9.8 for the pyrrolidine nitrogen and 7.0 for the nitrogen on the 4-position of the pyrimidine core. The measured pK_a value of the hydrogen linked to N4 was 7.39 but the pK_a of the hydrogen on the pyrrolidine

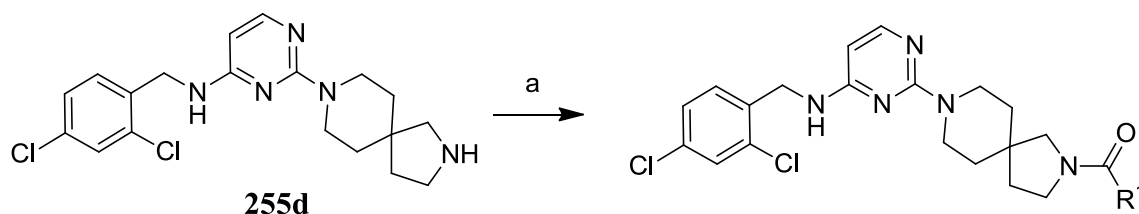
nitrogen was not detected in the spectroscopic method due to insufficient UV change during the analysis.⁹⁰ Although slightly different, it is worth highlighting that the relevant pK_a of the amino acid *L*-proline with a carboxylate group is 10.9.

In light of the *in vitro* potency, pharmacokinetic properties and the basic nature of **255d**, the chemistry strategy was focused on exploring the SAR of the template in order to increase the potency, and to understand the role of the basic centres in the molecule. Removing one of the basic centres or reducing the pK_a slightly could provide compounds with improved pharmacokinetic profiles.

8.5 Changes to the terminal proline group.

In order to understand the importance of the basic pyrrolidine nitrogen of **255d** for potency, a focused amide array around the terminal proline group was synthesised. Amide coupling of commercially available acids with the key intermediate **262d**, followed by deprotection of the relevant Boc-protected compounds with TFA afforded the desired spiro-pyrimidine amide analogues **264** - **274** (Table 23). For the preparation of **271** and **272**, the products were purified immediately after the amide coupling reaction. It should also be noted that not all the analogues are shown in the table.

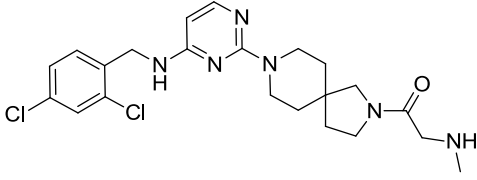
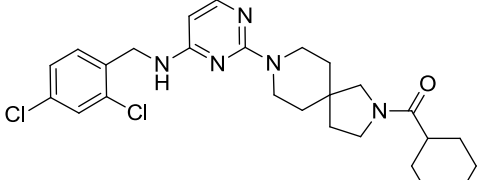
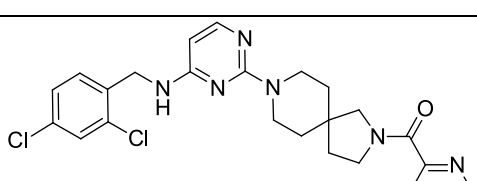
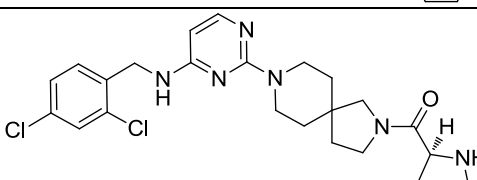
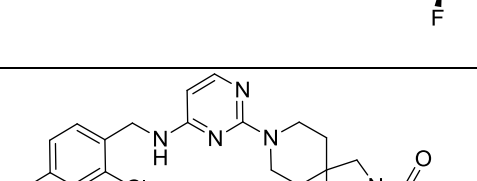
TABLE 23. Spiro-pyrimidine analogues with changes to the terminal proline group.



Reagents & Conditions: (a) i) R^1COOH , HATU, DIPEA, DMF, rt, 1 h, ii) TFA, rt, 0.5 h.

Cmpd	Structure	SPA pK_i	LE	LLE _{AT}	clogP	Chrom logD _{7.4}
1 BMS		8.6	0.39	0.30	4.5	3.5
256 BMS		8.2	0.39	0.31	3.9	2.6

263 BMS		7.6	0.35	0.25	4.5	2.7
262d		6.5	0.34	0.24	4.0	3.0
255d		7.8	0.32	0.28	3.8	3.4
264		7.0	0.29	0.24	3.8	3.9
265		7.6	0.32	0.27	3.8	3.5
266		7.6	0.31	0.24	4.3	n.d
267		7.7	0.31	0.25	4.3	3.7
268		7.3	0.30	0.28	3.3	3.3
269		7.3	0.29	0.25	3.9	3.5

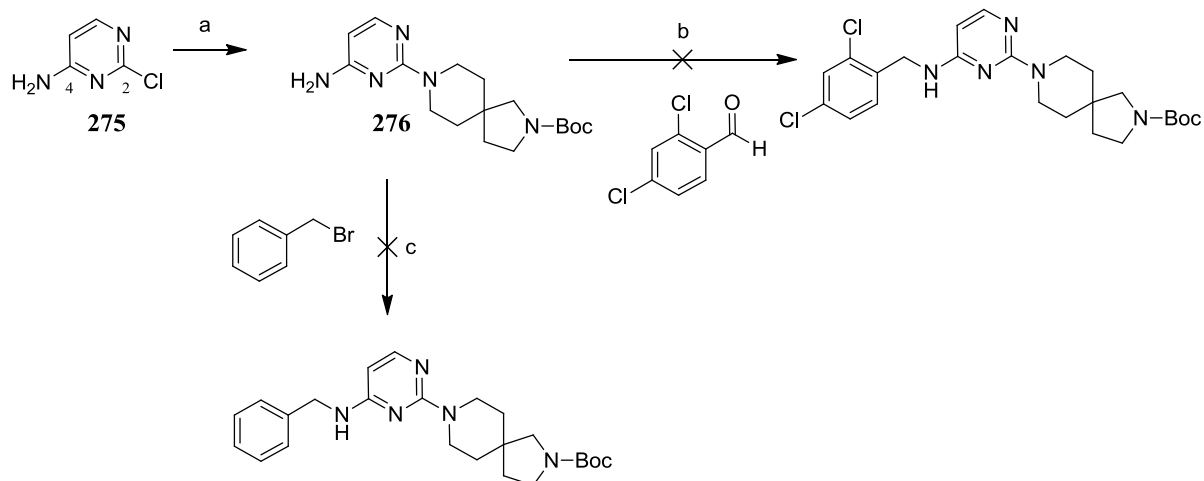
270		6.9	0.3	0.28	3.1	2.6
271		6.2	0.25	0.16	5.0	7.1
272		7.0	0.28	0.24	3.7	5.2
273		nd	nd	nd	3.6	4.2
274		nd	nd	nd	3.4	3.7

The data show that upon removal of the terminal proline group of the spiro-pyrimidine template as in **262d**, the activity in the SPA binding assay was considerably reduced ($pK_i = 6.5$). The racemic compound **265** ($pK_i = 7.6$) was found to be slightly less potent than the original 'starting hit' **255d** ($pK_i = 7.8$), whereas the *S*-enantiomer **264** was more than 0.5 log unit less potent ($pK_i = 7.0$). BMS also observed a difference in *in vitro* activities between the two enantiomers, which was reproduced in the SPA binding assay with the homoproline compounds, **1** ($pK_i = 8.6$) and **263** ($pK_i = 7.6$). In the spiro-pyrimidine series, no real difference in activity was observed (compound **255d** vs **266**) when *R*-proline was replaced with *R*-homoproline. In addition, both the *R* and *S*-homoproline analogues (compound **266** and **267**) were equipotent inhibitors of CCR4. This was surprising, as in the case of the BMS compounds, the homoproline analogue **1** was more active than the proline analogue **256**, and

a significant difference in potency was observed between the two enantiomers (compound **1** and **263**). It appears from this data that the SAR of the spiro-pyrimidine template around the terminal proline group does not follow that of BMS and other competitors' compounds that are known to bind to Site 1. Initial results also suggest that saturated heterocycles are more active than aromatic heterocycles (**272**, $pK_i = 7.0$). Moving the nitrogen from the α to the β -position (compound **268** & **229**) or removing the ring, as in the case of **270**, resulted in loss of potency. Also, replacement of the nitrogen with methylene to give the cyclohexyl analogue **271** resulted in a marked drop in potency, where **271** showed similar activity to that of the intermediate **262d**. Analogues prepared to reduce the basicity of the terminal pyrrolidine nitrogen of **255d** by introducing highly electronegative substituents such as fluorine at the position β - to the nitrogen (**273**, calc. $pK_a = 8.2$, Chemaxon software) or by changing the pyrrolidine ring to a morpholine ring (**274**, calc. $pK_a = 7.3$, Chemaxon software) also reduced the inhibitory activity of the compounds. Unfortunately, neither compound could be tested in the SPA assay due to project termination. However, both **273** and **274**, along with **255d** and compound **1** were tested in the in-house CCR4 fluorescent imaging plate reader (FLIPR) assay. The FLIPR assay measures calcium mobilisation following CCR4 activation by its orthosteric ligand TARC. Test compounds are then measured in terms of their ability to inhibit receptor activation and reduce calcium mobilisation. In the FLIPR assay, both **273** ($pIC_{50} = 5.2 \pm 0.2$) and **274** ($pIC_{50} = 5.2 \pm 0.2$) were found to be a log unit less potent than **255d** ($pIC_{50} = 6.5 \pm 0.4$) and **1** ($pIC_{50} = 7.2 \pm 0.4$). To summarise, it is quite clear from the results from both the SPA and FLIPR assay that a terminal basic nitrogen is a critical requirement for interaction with the binding site and hence for good inhibitory activity against the CCR4 receptor.

8.6 Variation of the benzyl group

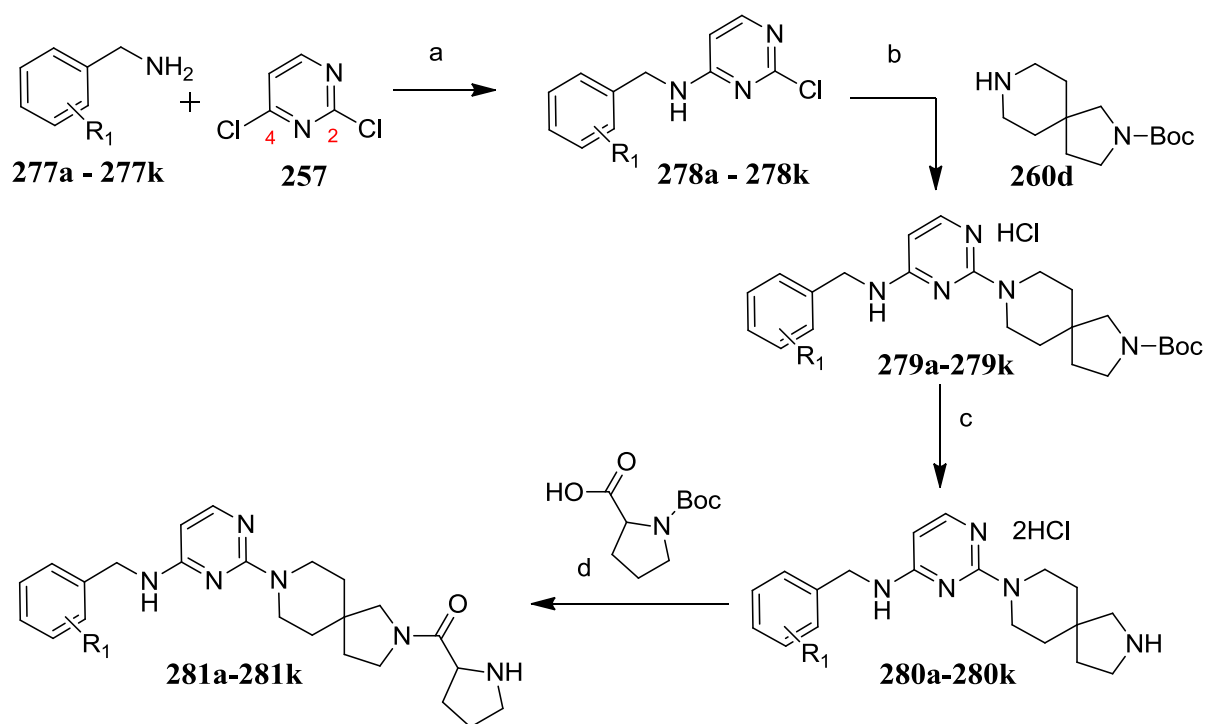
Variation around the 2,4-dichlorobenzyl substituent of **255d** was explored next. In the original synthetic route the benzyl group was introduced in the first step (Scheme 35). In order to make analogues quickly, it is better to introduce the groups that will be varied later in the synthetic route. A few synthetic routes were explored including the ones shown in Scheme 36. It was hoped that the benzyl substituent could be introduced in the synthetic sequence either *via* a reductive amination or *via* an alkylation reaction of the corresponding 4-aminopyrimidine intermediate **276**. However, both approaches failed to give the desired products.



Reagents & Conditions: (a) **260d**, DIPEA, Dioxane, 140 °C, 1 h, μ wave, 70%; (b) NaBH(OAc)₃, THF; (c) NaH, DMF, BnBr.

SCHEME 36. Attempted reductive amination or alkylation reaction of 4-aminopyrimidine 276.

It appears that the amino group is only very weakly nucleophilic and therefore not likely to react at a useful rate. Also there are no precedents in the literature to form a benzyl substituent on the 4-amino position of the pyrimidine core *via* alkylation or reductive amination when there is a nitrogen substituent on the 2-position, as in the case of **276**. Most of the literature strategies employed S_NAr reactions of 2,4-dichloropyrimidine to prepare 2,4-diamino substituted pyrimidines.^{58,134,161,162} A decision was therefore taken to employ the previously established S_NAr route to prepare a small set of spiro-pyrimidine analogues (**281a** - **281k**) containing monochloro, dichloro and difluoro substitution patterns based on the literature knowledge of the lipophilic pocket (Scheme 37).¹⁶³ Although this approach involved a number of steps to prepare the target compounds, it provided access to key intermediates for the preparation of other spiro-pyrimidine analogues (see Table 25).

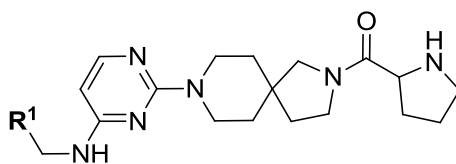


Reagents & Conditions: (a) DIPEA, DCE, rt, 24 - 48 h; (b) **260d**, IPA, 90 °C, 12 - 18 h; (c) 4 M HCl in dioxane, rt, 0.5 h or TFA, DCM, rt, 0.5 h; (d) i) 1-(*tert*-butoxycarbonyl)pyrrolidine-2-carboxylic acid, HATU, DIPEA, DMF, rt, 1 h, ii) TFA, rt, 0.5 h.

SCHEME 37. Preparation of benzyl analogues of 255d.

In the synthetic sequence, the dichloropyrimidine **257** was displaced with the substituted benzylamines **277a** – **277k** to give the 4-substituted analogues **278a** – **278k** respectively as the major isomers. The 4-substituted and 2-substituted pyrimidines were formed in an approximately 3:1 ratio, as determined in the LCMS of the crude reaction products (the minor isomers were not isolated). The pyrimidines **278a** – **278k** were then reacted with the Boc-protected spiro-pyrimidine **260d** to give the di-substituted pyrimidines, **279a** – **279k** respectively. Deprotection of the pyrimidines, **279a** - **279k** with 4 M HCl in dioxane, followed by amide coupling with Boc-protected racemic proline, and subsequent deprotection with TFA afforded the desired spiro-pyrimidines, **281a** – **281k**. These compounds were submitted for testing in the SPA binding assay and the results are shown below in Table 23.

TABLE 24. Benzyl analogues of the spiro-pyrimidine 255d



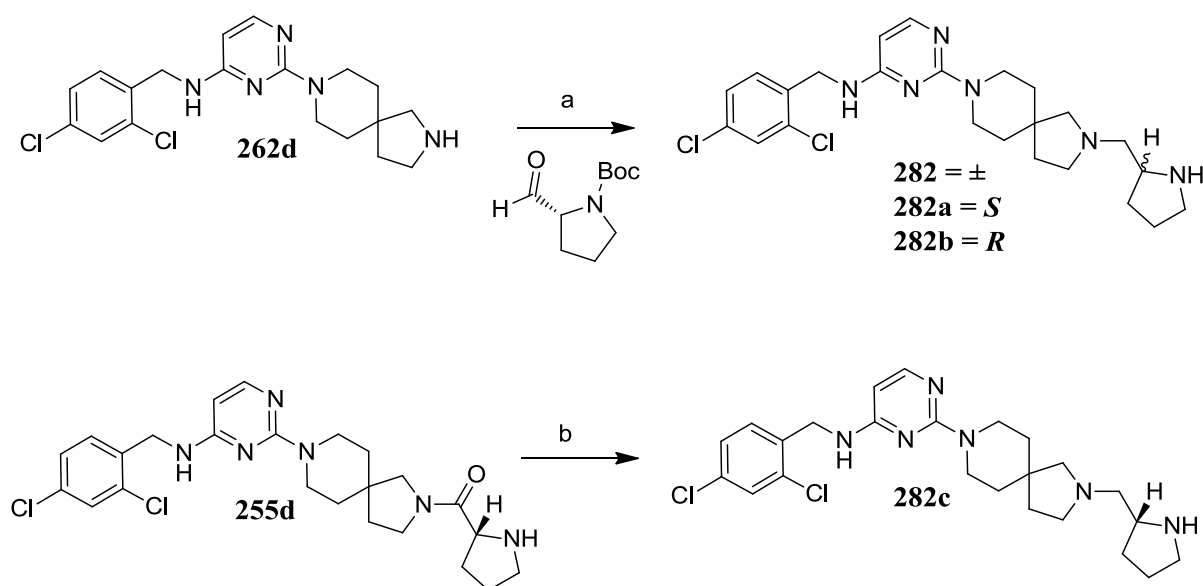
Cmpd	R ¹	SPA pK _i	LE	LLE _{AT}	Chrom logD _{7.4}
265		7.6	0.32	0.27	3.5
281a		6.1	0.26	0.24	2.8
281b		6.1	0.26	0.24	2.7
281c		6.7	0.29	0.27	2.7
281d*		5.7	0.24	0.25	2.5
281e*		7.3	0.3	0.26	3.2
281f		6.4	0.27	0.22	3.2
281g*		5.8	0.24	0.19	3.2
281h		6.5	0.27	0.22	3.3
281i		6.2	0.26	0.26	2.7
281j		6.5	0.27	0.27	2.6
281k		7.6	0.32	0.32	2.6

*compounds prepared by colleague¹⁶⁴

The data show that the best aryl groups were 2,4-dichlorophenyl (**265**, $pK_i = 7.6$) or 2,4-difluorophenyl (**281k**, $pK_i = 7.6$), which is consistent with what others have observed in the literature for Site 1 antagonists.^{73,150,163} The difluorobenzyl analogue **281k** appears to be better in terms of LLE_{AT} and has a lower molecular weight, and low $chromlogD$ than the 2,4-dichlorobenzyl analogue **265**. The results also suggest that the dichloro substituents are generally more active than the monochloro substituent, although, the *para*-chloro compound **281c** did show reasonable potency ($pK_i = 6.7$) with identical LLE_{AT} (0.27) to that of the 2,4-dichloro analogue **265**. Finally, it should be pointed out that the SAR knowledge used from the literature to select the different aryl groups to evaluate the left ‘wing’ lipophilic pocket may not be the most optimal, as SAR from one core template to another does not always correlate. For future work a more comprehensive set of aryl and none aryl group should be explored to identify the optimal interaction with the lipophilic pocket.

8.7 Removal of the proline carbonyl group.

In order to examine the role of the carbonyl group on the terminal proline, it was removed using the chemistry described in Scheme 38. It was postulated that replacing the carbonyl group with a methylene would result in increased basicity of the terminal pyrrolidine nitrogen and consequently lead to a stronger interaction with the carboxyl residue on Glu-290.



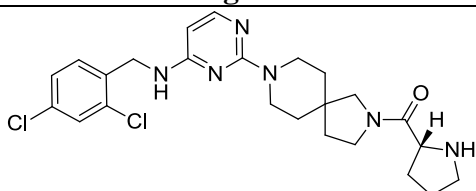
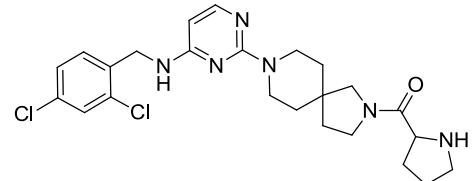
Reagents & Conditions: (a) i) $NaBH(OAc)_3$, AcOH, Molecular sieves, DCM, 3h; (ii) TFA, 1 h, 42% yield over two steps; (b) $LiAlH_4$, THF, 0 °C – rt, 18 h, 50%.

SCHEME 38. Preparation of pyrimidine analogue 282a, 282b and 282c.

Reductive amination of spiro-pyrimidine **262d** with commercially available Boc-protected *R*-proline aldehyde, followed by subsequent deprotection with TFA afforded the desired reduced amine product **282** as a racemic mixture. It appears that the product epimerised in the reaction; this was confirmed by chiral HPLC (25 cm Chiralpak AD, 5% EtOH/C7 [0.1% isopropylamine]), which showed peaks for the two enantiomers at 35.4 and 40.6 min (1:1) respectively. Enantiomers **282a** and **282b** were separated by a chiral HPLC column, and the configuration was confirmed by matching the optical rotation and the retention time of the *R*-enantiomer ($[\alpha]_D^{20} = -7.5$, $c = 0.46$ in MeOH, chiral purity = 97%) to that of a re-synthesised enantiopure sample **282c** ($[\alpha]_D^{20} = -5.1$ ($c = 0.47$ in MeOH, chiral purity 99%). The enantiopure compound **282c** was prepared employing an alternative synthetic route, which involved reduction with lithium aluminium hydride to afford the desired spiro-pyrimidine enantiomer **282c** in 50% yield (Scheme 38).

The racemic compound **282** and its enantiomers, **282a** and **282b** were tested in the SPA binding assay (Table 25). Surprisingly, the racemic spiro-pyrimidine **282** showed a log unit improvement in inhibitory activity ($pK_i = 8.6$), with very good LE (0.37) and LLE_{AT} (0.29) compared to the racemic amide analogue **265** ($pK_i = 7.6$). The separated enantiomers, **282a** and **282b** also showed similar activity to that of the racemate **282**, with no real difference observed between the two isomers in the SPA binding assay. Prompted by these results, the corresponding reduced analogues of the BMS compound **1** and the azetidine **255a** were prepared employing the same conditions described above in Scheme 38. These compounds were tested in the SPA binding assay (Table 25).

TABLE 25. Comparison of amide and the reduced analogues of spiro-pyrimidine 255d, BMS 1 and azetidine 255a.

Cmpd	Structure Reg. no.	SPA pK_i	LE	LLE_{AT}	clogP	Chrom $\log D_{7.4}$
255d		7.8	0.32	0.28	3.8	3.4
265		7.6	0.32	0.27	3.8	3.5

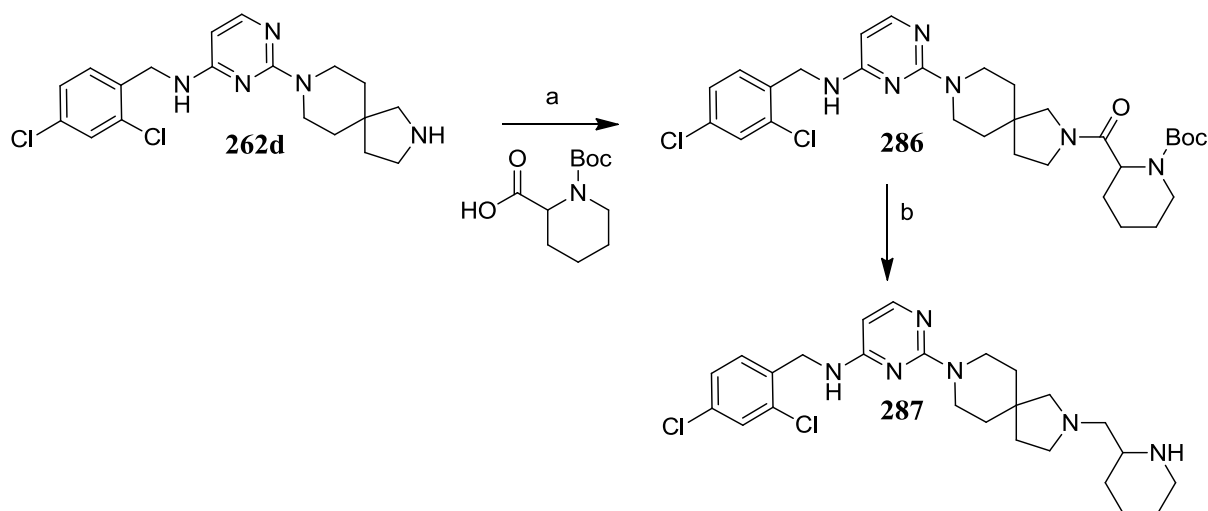
282		8.6	0.37	0.29	4.3	4.4
282a		8.4	0.36	0.28	4.3	4.3
282b		8.3	0.36	0.28	4.3	4.2
1 BMS		8.2	0.39	0.31	3.9	2.6
283		8.0	0.39	0.30	4.1	3.4
255a		7.4	0.36	0.28	3.9	2.4
284*		7.5	0.37	0.28	3.9	2.6
285*		7.9	0.40	0.29	4.3	2.7

*compounds prepared by colleague¹⁶⁴

Replacement of the carbonyl group on the BMS template with a methylene group had little effect on potency (compound **1**, $pK_i = 8.2$ vs **283**, $pK_i = 8.0$). For the azetidine analogue **285**, there was half a log unit improvement in potency compared to its corresponding amide analogues **255a** and **284**. It should be noted that the racemic amide azetidine analogue **37** and the *R*-enantiomer **255a** were equipotent in the binding assay. Interestingly, the reduced spiro-

pyrimidine analogue **282** showed a log unit improvement in potency compared to its corresponding racemic amide analogue **265**. This data again confirms that the spiro-pyrimidine template has different SAR to that of the BMS series. The significant enhancement in potency for the reduced compound **282** could be due to the increased flexibility of the terminal pyrrolidine ring, and the increase in basicity (Chemaxon software calc. $pK_a = 10.9$), which could result in the pyrrolidine nitrogen predominantly existing in the protonated form, and hence would be involved in making better interactions with the conserved glutamate residue located in the active site. In addition, the amide nitrogen on the spiro group that has been reduced will also be basic and may be involved in ionic interactions.

Encouraged by these results, reduced amine analogues of the amides were prepared; one of two methods was used depending on the availability of starting material. Reductive amination was followed by deprotection with TFA, as in Scheme 38, or amide coupling was followed by reduction of the corresponding amides with borane as in Scheme 39.



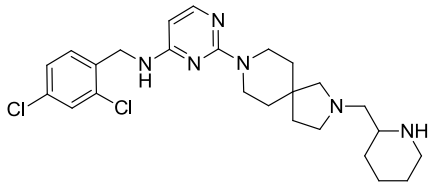
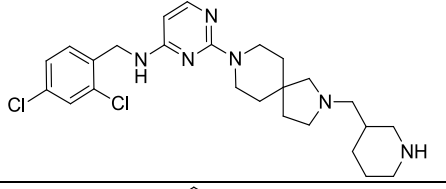
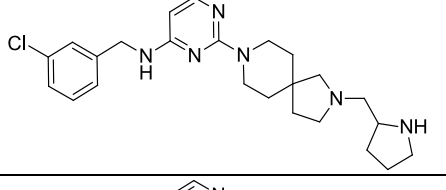
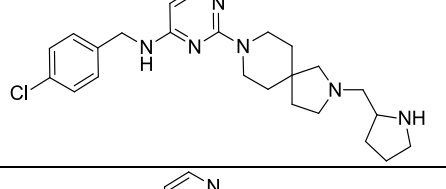
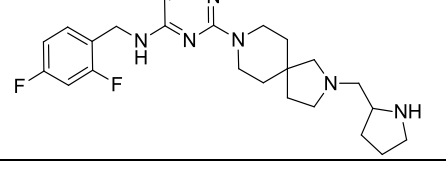
Reagents & Conditions: (a) 1-(*tert*-butoxycarbonyl)piperidine-2-carboxylic acid, HATU, DIPEA, DMF, rt, 0.5 h, 66%; (b) i) BH_3 , THF, 0 °C – rt, 1 h, ii) HCl, rt, 0.5 h, 51% over two steps.

SCHEME 39. Preparation of pyrimidine analogue **287**.

The results of the reduced amine analogues (**287 – 291**), along with their corresponding amide analogues are shown below in Table 26. As expected, apart from **288**, all the amine analogues were over a log unit more potent than the amides. The spiro-pyrimidine amine **288** has the nitrogen on the terminal piperidine ring at the β -position, and it may be that this does not allow for a favourable interaction to the receptor. The *para*-chloro pyrimidine **290** was

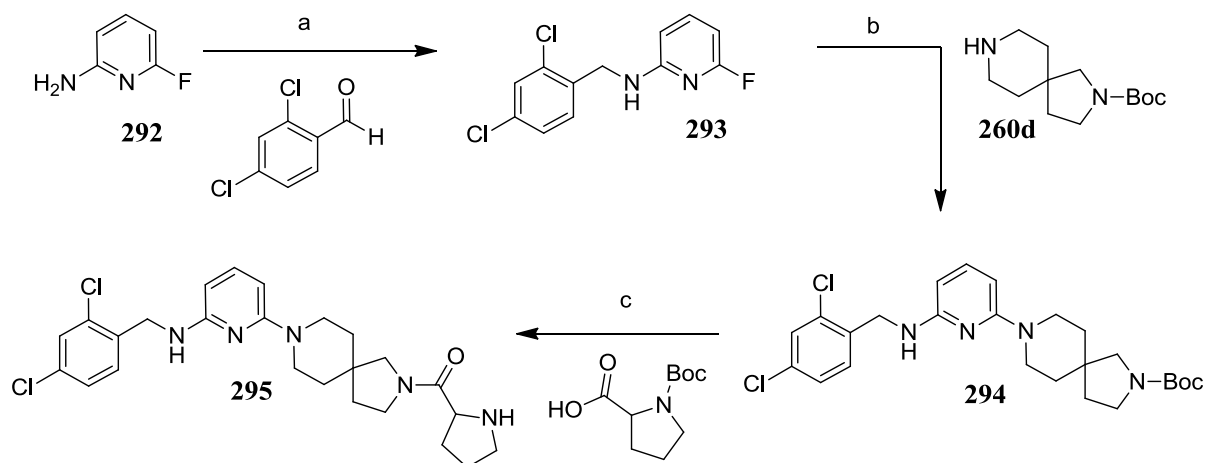
found to be equipotent with the 2,4-dichloro analogue **282**, and is nearly two log units more potent than its amide analogue **281c**. These findings indicate that the interaction of the flexible pyrrolidine amine to the receptor contributes quite significantly to the inhibitory activity of the reduced spiro-pyrimidine template.

TABLE 26. Results of amine analogues of **282**.

Reduced amine analogues				Amide analogues		
Cmpd	Structure	SPA pK _i	LE/ LLE _{AT}	Amide Cmpd	SPA pK _i	LE/ LLE _{AT}
287		8.6	0.36/ 0.26	267	7.7	0.32/ 0.25
288		7.6	0.32/ 0.24	269	7.3	0.29/ 0.25
289		7.8	0.34/ 0.30	281b	6.1	0.26/ 0.24
290		8.6	0.38/ 0.33	281c	6.7	0.29/ 0.27
291		8.5	0.36/ 0.34	281k	7.6	0.32/ 0.32

8.8 Core changes.

The SAR of the pyrimidine core was investigated next. In order to determine if the nitrogen at the 1-position was important for potency, the pyrimidine core was replaced with a pyridine. The synthetic route is shown below in Scheme 40.

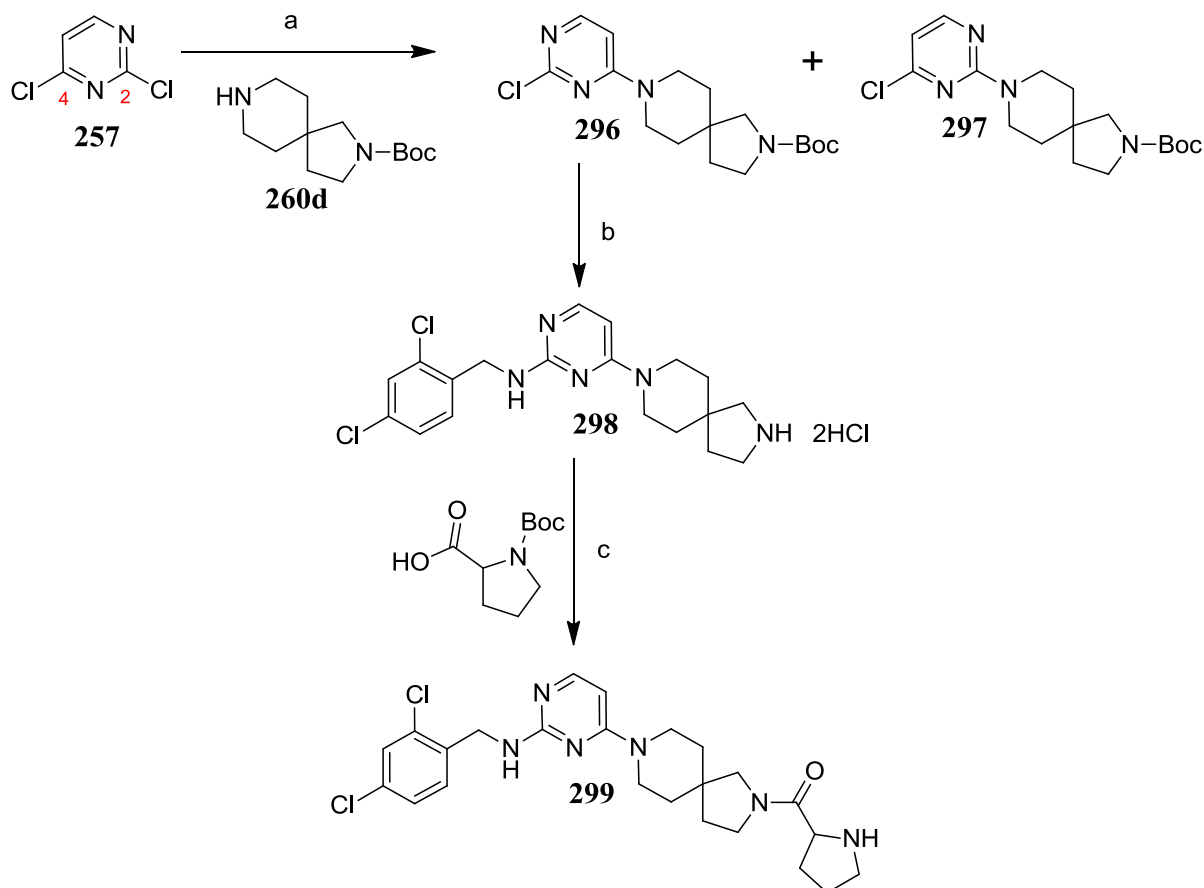


Reagents & Conditions: (a) 2,4-Dichlorobenzaldehyde, NaBH(OAc)₃, AcOH, DCM, rt, 48 h, 44%; (b) DIPEA, CH₃CN, 140 °C, 5 day, sealed vial, 24%; (c) (i) TFA, rt, 15 min, ii) HATU, DIPEA, DMF, 1-(*tert*-butoxycarbonyl)pyrrolidine-2-carboxylic acid, rt, 18 h, iii) TFA, rt, 10 min, 14% over three steps.

SCHEME 40. Preparation of pyridine analogue 295

Reductive amination of commercially available 6-fluoropyridin-2-amine (**292**) with 2,4-dichlorobenzaldehyde, followed by S_NAr reaction with spiro-amine **260d** gave the spiro-pyrimidine amine **294**. Deprotection of **294** with TFA and subsequent amide coupling with Boc-protected proline and deprotection with TFA afforded the desired pyridine compound **295**.

Purandare and co-workers reported that the second nitrogen on the pyrimidine core on the BMS template could be transposed so that the linker was attached to C2 without affecting the potency.⁷³ The pyrimidine core of the spiro-pyrimidine series was also reversed and the synthesis of the reversed pyrimidine analogue is described in Scheme 41.



Reagents & Conditions: (a) **260d**, DIPEA, DCE, rt, 24 h, **296**, 57%, **297**, 12%; (b) i) 2,4-dichlorobenzylamine, IPA, 140 °C, 1 h, μ wave, ii) 4 M HCl in dioxane, rt, 1.5 h, 74% over two steps; (c) i) 1-(*tert*-butoxycarbonyl)pyrrolidine-2-carboxylic acid, HATU, DIPEA, DMF, rt, 1 h, ii) TFA, rt, 0.5 h, 67% over two steps.

SCHEME 41. Preparation of reverse pyrimidine analogue **299**.

Nucleophilic displacement of 2,4-dichloropyrimidine **257** with the mono-protected spiroamine **260d**, gave a mixture of regioisomeric, **296** and **297**, with the desired 4-chloro substituted **296** as the major product (ratio 5:1). The excess of the major product **296** formed appears to be higher than that obtained from substitution with the benzylamines shown earlier in Scheme 35 and 37. The regiochemistry of each product was determined using ROESY experiments (Fig. 40), where for spiro-pyrimidine **296**, an NOE correlation was observed between the pyrimidine hydrogen at the 5-position (6.72 ppm) and the spiro-methylene protons at the 7 and 9-positions (chemical shifts between 3.56-3.92 ppm). For spiro-pyrimidine **297**, no NOE correlations were observed between the piperidinyl protons at the 7 and 9-positions with the protons from the pyrimidyl ring, which is indicative of the alternative regioisomer. The substitution reaction of **296** with 2,4-dichlorobenzylamine in

IPA, and subsequent deprotection with 4 M HCl in dioxane gave the amine intermediates **298** (Scheme 41). Finally, amide coupling with Boc-protected-proline, followed by deprotection with TFA afforded the desired pyrimidine **299** in good yield.

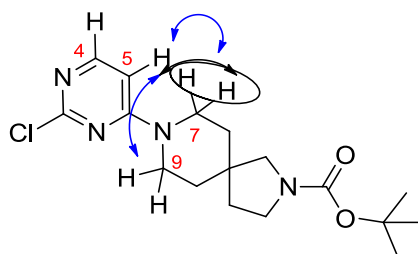


FIGURE 40. Structure of regioisomer **296** was confirmed by ROESY experiment.

The binding results of the spiro analogues with the pyridine (**295**), reverse pyrimidine (**299**), and a fused pyrido[2,3-*d*]pyrimidine (**300**) core are shown below in Table 26.

TABLE 27. Results of core changed spiro-pyrimidine analogues.

Cmpd	Structure Reg. no.	SPA pK _i	LE	LLE _{AT}	clogP	Chrom logD _{7.4}
265		7.6	0.32	0.27	3.8	3.5
295		7.0	0.29	0.23	4.2	4.5
299		7.8	0.32	0.28	3.8	3.1
300*		7.7	0.29	0.24	4.2	3.1

. *compounds prepared by colleague¹⁶⁴

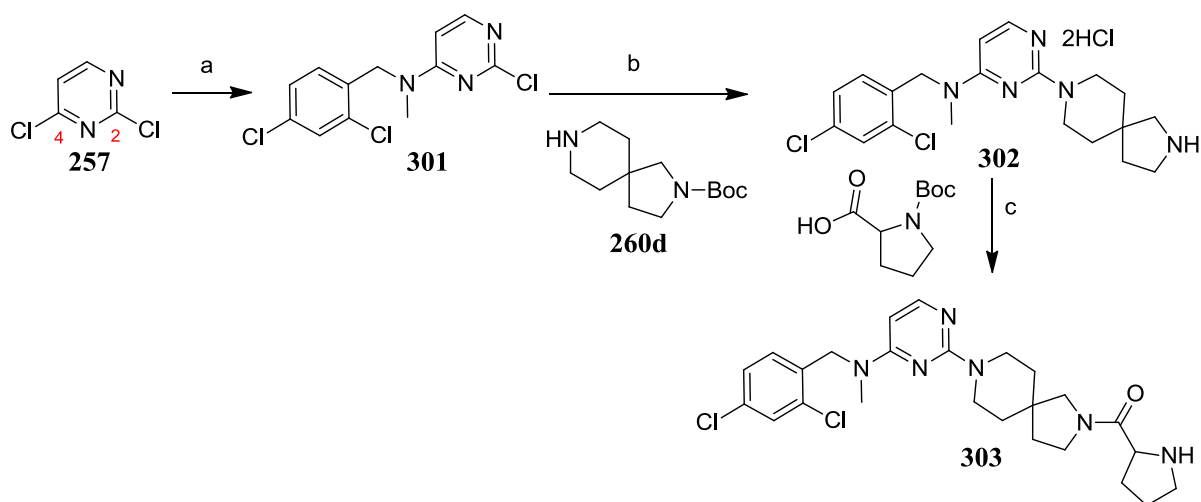
Modification of the core from pyrimidine in **265** to a pyridine in **295** resulted in loss of inhibitory activity in the SPA binding assay. It appears from this result that the nitrogen at the 1-position is important for activity and may be involved in making an interaction with a residue in the allosteric pocket. However, when the pyrimidine core was reversed, as in **299**, no significant difference in activity was observed between the two regioisomers. At this stage it is not clear why the pyridine analogue was less potent than the pyrimidine **265**.

A pyrido[2,3-*d*]pyrimidine core has shown to increase the potency of the BMS series by approximately half a log unit (pyrimidine **1** vs pyrido[2,3-*d*]pyrimidine **2**, Table 20). In an attempt to further improve the potency of the spiro-pyrimidine template, a colleague prepared a spiro analogue, **300** (Table 27) with a fused pyrido[2,3-*d*]pyrimidine core, using a route similar to the one described by Purandare and co-workers.⁵⁸ However, compared to the original pyrimidine analogue **265**, the pyrido[2,3-*d*]pyrimidine analogue **300** did not show any improvement in potency in the binding assay. Also, the molecular weight of the compound is high with low LE and LLE_{AT}, so this compound was of no further interest. Nonetheless, the result of the pyrido[2,3-*d*]pyrimidine **300** was again indicative of the fact that the SAR of the spiro-pyrimidine series is different to that of the BMS series.

8.9 Changes to the left wing benzylamine NH of the spiro-pyrimidine series.

Removal of hydrogen bond donors could enhance permeability of compounds and hence improve absorption of molecules.^{145,146,165,166} Thus, the left hand ‘wing’ NH of the spiro-pyrimidine template was replaced with NMe and oxygen. The NMe analogue was prepared using the established synthetic route and is shown in Scheme 42.

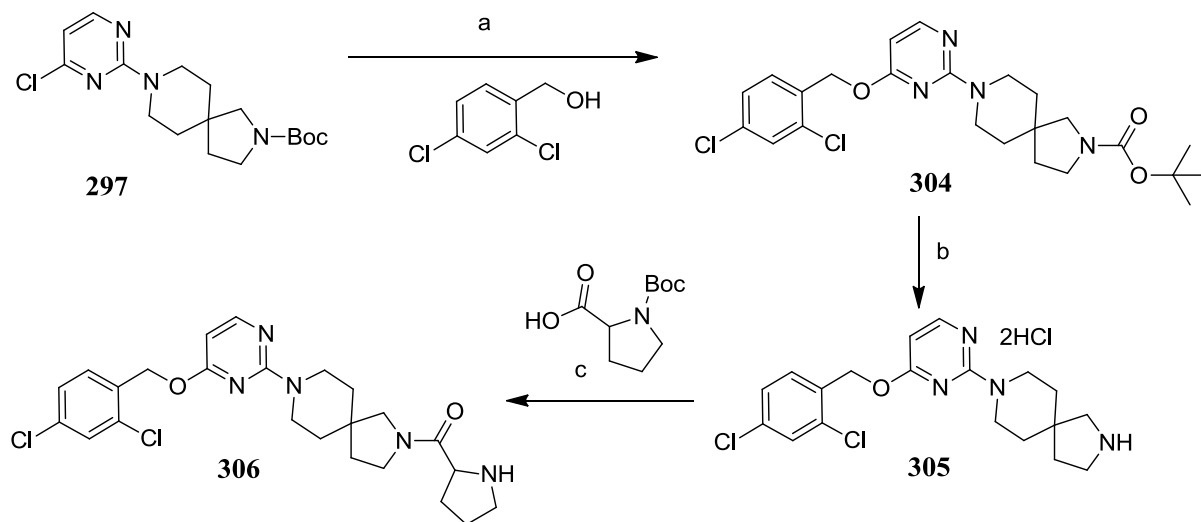
As with previous methods, the dichloropyrimidine **257** was displaced sequentially with 1-(2,4-dichlorophenyl)-*N*-methylmethanamine, then spiro-amine **260d** respectively. Deprotection under acidic conditions, followed by amide coupling with Boc-protected (\pm)-proline, and subsequent deprotection with TFA afforded the desired spiro-pyrimidine analogue **303**.



Reagents & Conditions: (a) 1-(2,4-Dichlorophenyl)-*N*-methylmethanamine, DIPEA, DCE, rt, 24 h, 38%; (b) i) **260d**, IPA, 90 °C, 24 h, ii) 4 M HCl in dioxane, rt, 0.5 h, 67% over two steps; (c) i) 1-(*tert*-butoxycarbonyl)pyrrolidine-2-carboxylic acid, HATU, DIPEA, DMF, rt, 1 h, ii) TFA, rt, 0.5 h, 26% over two steps.

SCHEME 42. Preparation of NMe pyrimidine analogue 303.

The benzyloxy analogue **306** was prepared from the spiro-pyrimidine intermediate **297** in three steps as outlined in Scheme 43.



Reagents & Conditions: (a) i) 2,4-Dichlorobenzylalcohol, NaH, DMF, 40 °C, 3 h, 51%; (b) 4 M HCl in dioxane, rt, 0.5 h, 99%; (c) i) 1-(*tert*-butoxycarbonyl)pyrrolidine-2-carboxylic acid, HATU, DIPEA, DMF, rt, 1h, ii) TFA, rt, 0.5 h, 60% over two steps.

SCHEME 43. Preparation of benzyloxy-pyrimidine analogue 306.

Displacement of **297** with 2,4-dichloro-benzylalcohol in the presence of sodium hydride, followed by deprotection with 4 M HCl gave the amine intermediate **305**. Amide coupling of **305** with Boc-protected (\pm)-proline and subsequent deprotection with TFA afforded the desired target compound **306** in good yield. The results for both the NMe and oxygen analogue are shown in Table 28.

TABLE 28. Results of core changed spiro-pyrimidine analogues.

Cmpd	Structure	SPA pK _i	LE	LLE _{AT}	clogP	Chrom logD _{7.4}
265		7.6	0.32	0.27	3.8	3.5
303		7.6	0.32	0.25	4.2	4.5
306		7.1	0.29	0.25	3.8	4.7
307		9.0	0.37	0.29	4.7	5.3

From the SPA binding data, it appears that no significant change in potency was observed when the benzyl NH group (compound **265**) was replaced with an *N*-methyl group (Compound **303**). This was encouraging as it was possible to remove a hydrogen bond donor from the series without affecting the potency, although the introduction of the methyl group did result in an increase in the clogP and chromlogD_{7.4} of the molecule. However, when the benzyl NH of spiro-pyrimidine **265** was replaced with an oxygen, half a log unit loss in potency was observed, consistent with what Purandare and co-workers observed with the BMS series.¹⁶³

Finally, the carbonyl group of the *N*-methyl analogue **306** was reduced (using previous established conditions) to give **307** (Table 28). This compound showed a significant improvement in potency ($pK_i = 9.0$) and was found to be the most potent spiro-pyrimidine analogue tested in the SPA binding assay to date, which demonstrated comparable activity to that of the more potent BMS compound **2** ($pK_i = 9.1$, Table 20).

8.10 GTP γ S and human whole blood data.

A set of potent spiro-pyrimidine compounds from the SPA assay were profiled further in the GTP γ S and actin polymerisation human whole blood assay. In addition CLND solubility and plasma protein binding data were also obtained and the results are summarised in Table 29.

TABLE 29. Additional data for spiro-pyrimidine analogues.

Cmpd	SPA pK_i	GTP γ S	HWB	clogP	Chrom $\log D_{7.4}$	CLND Sol $\mu\text{g/mL}$	PPB %
1	8.6	8.1	6.7	4.5	3.5	140	93
255d	7.8	nd	6.2	3.8	3.4	180	95
282	8.6	8.1	6.7	4.3	4.4	270	97
291	8.5	7.9	nd	3.2	3.2	160	93
307	9.0	8.0	6.0	4.7	5.3	142	97
300	7.7	7.4	5.7	4.2	3.1	174	95

As mentioned previously, the spiro-pyrimidine compound **255d** demonstrated good activity in the human whole blood assay ($pA_2 = 6.2$). Compound **282** which was a log unit more potent in the SPA binding assay was also found to be more active in the human whole blood assay ($pA_2 = 6.7$), achieving activity comparable to that of the more potent BMS compound **2** ($pA_2 > 7$). The spiro-pyrimidine **307** showed a marked improvement in the SPA binding assay ($pK_i = 9.0$); however, this observed increase in potency did not translate into the human whole blood assay, in which it was more than half a log unit less potent than **282**. The potent spiro-pyrimidine analogue **282**, **291** and **307** showed identical activity in the GTP γ S assay, similar to BMS's compound **1** and **2**. Again this could be because the compounds were reaching the binding limit of the assay. Analogues from the spiro-pyrimidine template in general demonstrated reasonable solubility in the CLND assay with good chromatographic $\log D$ values. The plasma protein binding of the compounds were low in the range of 93-95%, which means unbound compounds will be more likely to be available in the blood for

distribution to the tissues. Spiro-pyrimidine **282** was also found to be selective for CCR4 against chemokine receptors, CCR1 ($pIC_{50} < 4.6$), CCR2 ($pIC_{50} < 4.6$) in radio-ligand GTP γ S binding assay and CXCR2 ($pIC_{50} < 4.6$) in the FLIPR assay.

8.11 Pharmacokinetic studies of the spiro-pyrimidine series

Pharmacokinetic data for compound **282** and a mono basic cyclohexyl analogue **271** were generated in rat to determine if removing one of the basic centres could help to improve the absorption of these molecules (Table 30).¹³²

TABLE 30. Data for the spiro-pyrimidine compounds 255d, 282 and 271

Compound	255d	282	271
I¹²⁵ TARC SPA pK_i	7.8	8.6	6.2
LE / LLE _{AT}	0.32/0.28	0.37/0.30	0.25/0.16
HWB Actin polym. (pA₂):	6.2	6.7 (dep max)	nd
MW :	489	475	502
clogP :	3.8	4.3	5.0
Chrom logD _{7.4} :	3.4	4.4	7.1
CLND solubility:	180 μ g/mL	120 μ g/mL	5 μ g/mL
PPB (HSA)	95.7%	97.5%	97.1%
Rat PK			
(dose 1mg/kg)	(n=4)	(n=2)	(n=2)
Bioavailability:	negligible	negligible	negligible
Clearance:	9 mL/min/kg	15 mL/min/kg	53 mL/min/kg
t _{1/2} median:	4.5 h	4.0 h	1.6 h
V _{dss} :	3.7 L/kg	5.1 L/kg	4.5 L/kg

Similar to **255d**, following an IV dose (1 mg/kg) in a male rat, **282** possessed a low blood clearance (15 mL/min/Kg, 18% liver blood flow), with a good half life (4.0 h) and a moderate to high volume of distribution (5.1 L/kg). However, following an oral dose, **282** was found to have negligible bioavailability with no compound detected in the blood (C_{max} of <10 ng/mL). It should be noted that in comparison with **255d**, replacing the pyrrolidine ring with a cyclohexyl ring (in compound **271**) had a detrimental effect on potency. In rat, spiro-

pyrimidine **271** showed higher clearance and a shorter half-life compared to both **255d** and **282**. In addition, the volume of distribution was similar to **282** at 4.5 L/kg, with no improvement observed in oral exposure. Although the clearance of spiro-pyrimidine **271** was high, it appears from this study that simply removing the strongly basic centre (which has been shown to be detrimental for potency) will not improve the oral pharmacokinetic profile of the template.

From evaluation of the SAR and the pharmacokinetic data of the series, it appears that it would be very difficult to design in the required properties needed for an oral drug without diminishing the potency. The low bioavailability of the compound is thought to be caused by the strong basic nature of the molecules, resulting in poor absorption. Removing the basic centres results in significant loss in potency, and this is especially true for the terminal right ‘wing’ nitrogen that is thought to interact with a conserved glutamate residue located in the receptor. Compounds from the spiro-pyrimidine series may therefore have to be considered for topical delivery, for example using an inhaler.

8.12 Site 1 antagonists induce CCR4 internalisation

Recently, CCR4’s natural ligands were shown to induce receptor internalisation from the cell surface of human T_H2 cells into the internal cell cavity.¹⁶⁷ It is postulated that internalisation of receptors will result in less binding to the natural agonists leading to loss of functional responsiveness.

In-house work has confirmed previous observations that binding to the orthosteric site with CCL22 (MDC) or CCL17 (TARC) evoked concentration-dependent reduction in cell surface expression of CCR4 receptors ($pEC_{50} = 8.77 \pm 0.08$ and 7.98 ± 0.23 respectively) on HUT78 cells.¹⁶⁸ Begg and co-workers found that MDC was more potent and evoked almost complete internalisation, whereas TARC induced approximately 50% of receptors to internalise over the concentration range tested. More recently, Sato and co workers were the first to report a novel CCR4 small molecule antagonist K777 (Fig. 41); K777 has a Site 1 chemo-type structure that induces receptor internalisation on HUT78 cells with approximately 50% reduction of cell surface CCR4.¹⁶⁹

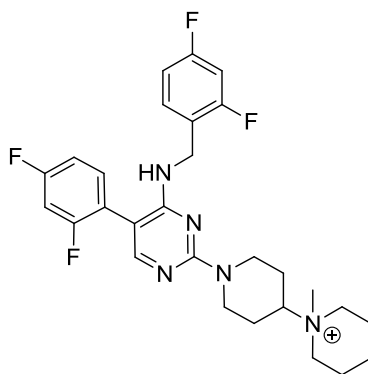


FIGURE 41. Structure of K777

Further in-house work with a set of CCR4 inhibitors has also shown that small molecule antagonists which bind to Site 1, such as Astellas compound **254** and BMS compound **2**, are capable of invoking internalisation of CCR4 receptors ($pEC_{50} = 6.4 \pm 0.2$ and 8.0 ± 0.2 respectively), while Site 2 binders, such as compound **5**, showed no internalisation on HUT78 cells.¹⁶⁸ This new understanding of the pharmacology, in which binding to the Site 1 allosteric site evokes receptor internalisation, provides a novel strategy for discovering drugs active against the chemokine receptor. It is noteworthy that receptor internalisation is not a novel pharmacological mechanism for CCR4; other chemokine receptors have been reported to internalise upon binding to their orthosteric ligands, including CCR5.¹⁷⁰

A set of compounds from the spiro-pyrimidine series were tested to assess their ability to induce internalisation of the CCR4 receptors on HUT78 cells (Table 31).¹⁷¹ The different antagonists were incubated with HUT78 cells for 30 minutes at 37 °C and the CCR4 expression levels were evaluated by flow cytometry. The pEC_{50} is the midpoint on the concentration-response curve, and the percentage value is the degree of inhibition of receptor expression. As observed previously, the natural agonist MDC inhibited cell surface expression almost completely. The two spiro-pyrimidine enantiomers, **282a** and **282b** induce receptor internalisation in equal amounts ($pEC_{50} = 7.7$ and 8.0 respectively) with over 55% reduction of cell surface CCR4. These data appear to be consistent with the SPA binding data where no significant difference was observed between the two enantiomers. The fused spiro-pyrimidine analogue **300** was slightly less potent than either enantiomer **282a** or **282b**, with a pEC_{50} value of 7.2. This is consistent with the difference in activity observed in SPA and whole blood actin polymerisation assay between the racemic compound **282** and fused spiro-pyrimidine **300**. The difluoro analogue **291** also triggered internalisation of the receptor identical to that of the enantiomers, but the NMe analogue **307**, which was the most potent

spiro-pyrimidine inhibitor in the SPA assay, had a lower pEC₅₀ value in the HUT78 cells with over 70% of cell surface CCR4 internalised.

TABLE 31. Internalisation data for the spiro-pyrimidine compounds 282a, 282b, 291, 300 and 307.

Cmpd	pEC₅₀	% of CCR4 receptors internalised
MDC	8.8	98.0
282a	7.9	56.4
282b	8.0	64.3
291	7.8	62.4
300	7.2	62.8
307	6.8	73.7

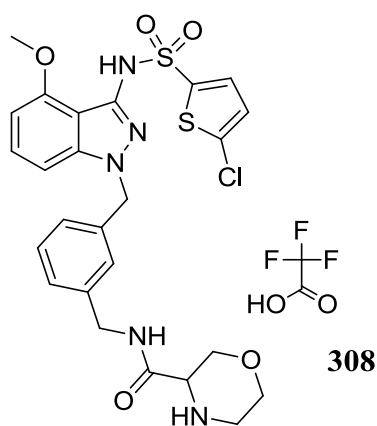
It is not yet clear why binding to Site 1 causes internalisation of the receptor, or how the binding potency affects the percentage of cell surface CCR4 to internalise, but it is widely appreciated that reducing the number of receptors expressed on the membrane will result in reduction of accessible binding sites for the natural agonist to bind. Ultimately, this will result in loss of functional responsiveness of the receptor towards chemokine, and fewer eosinophils and T_H2 cells will therefore migrate into the airways, the critical event that triggers and sustains the symptoms of allergic asthma.⁷

8.13 *In vivo* studies

Since both enantiomers **282a** and **282b** showed no real difference in binding potency and internalisation capabilities of the receptor, the racemic compound **282** was chosen for the *in vivo* studies. The details of the studies are available in the experimental section.¹⁷² The first *in vivo* experiments were carried out in the FITC (Fluorescein isothiocyanate) DTH (delayed-type hypersensitivity) female Balb/c mouse model. Cutaneous exposure of mice to FITC results in a T_H2-type immune response in which CD4⁺ cells are responsible for the delayed-type component of the dermal hypersensitivity reaction.¹⁷³ Compared to vehicle (topical dose of EtOH 20 μL/ear), dosing spiro-pyrimidine **282** at 20 mg/kg subcutaneously, resulted in a marked reduction in the ear swelling of Balb/c mouse previously sensitised with FITC (Fig. 42). The reduction of the observed FITC-induced ear thickness in the Balb/c mouse by

compound **282** suggests that inhibiting CCR4 results in the reduction of a T_H2 driven immune response. It should be noted that no significant effect was observed when the compound was dosed topically (Fig. 42), it may be that the compound was not able to reach the site of action to elicit a response via this route. Indazole **308** (Table 32),⁵⁷ a Site 2 antagonist was also dosed, 20 mg/kg subcutaneously and topically, but failed to show any positive effect on the FITC-induced female Balb/c mice (Fig. 42).

TABLE 32. Structure and biological profile of **308**



I¹²⁵ TARC SPA pK_i	8.4
GTPγS (pIC₅₀):	7.8
HWB Actin polym. (pA₂):	6.6
MW :	576
clogP :	3.2
Chrom logD _{7.4} :	3.7
CLND solubility:	286 µg/mL
PPB (HSA)	94.9%

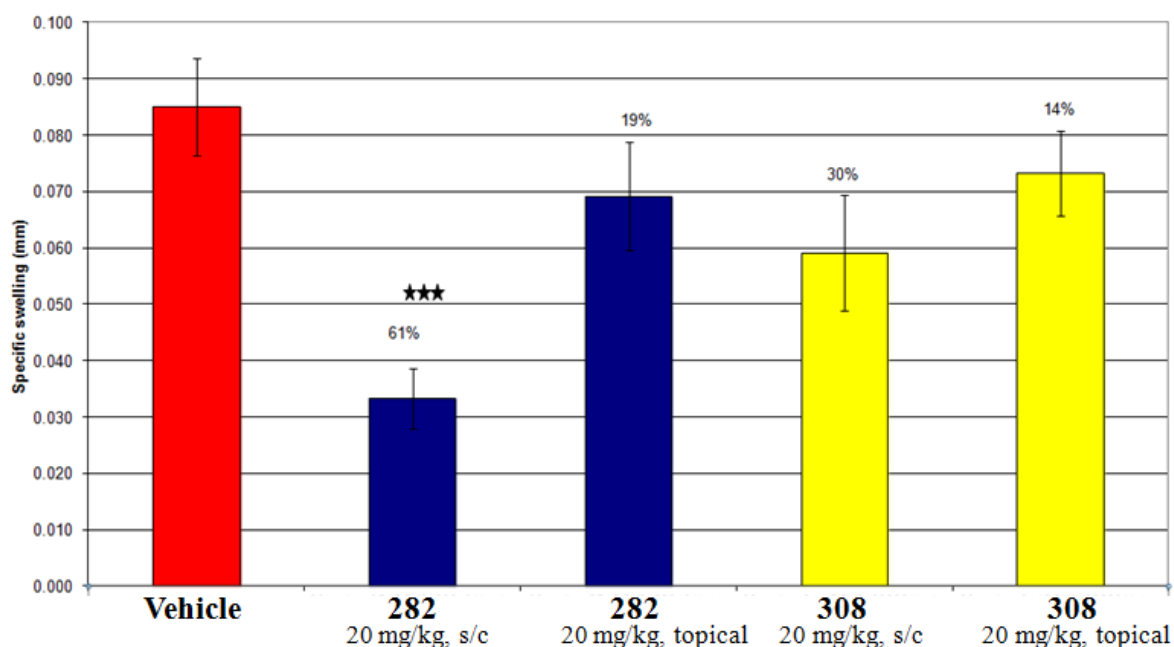


FIGURE 42. Effect of CCR4 antagonists **282** and **308** on FITC-induced ear swelling in the Balb/c mouse.

It is not clear if the *in vivo* effect observed with compound **282** arises because of the antagonist effect or the internalisation of the receptor, or a combination of both. Spiro-pyrimidine **282** and indazole **308** bind to different allosteric regions of the receptor (Site 1 and Site 2 respectively) and have similar binding activities (Table 30 and Table 32), but the fact that binding to Site 1 causes internalisation of cell surface CCR4 may be mechanistically related that an *in-vivo* effect is observed with a Site 1 antagonist and not with Site 2. Further work in biology is required to understand the pharmacological mechanism and to link the induced internalisation of cell surface CCR4 with the observed *in vivo* effect with the Site 1 compounds. Despite the lack of understanding of the mechanism of action, as far as the results with the spiro-pyrimidine compound **282** is concerned, it showed a positive effect in the *in vivo* model.

Compound **282** was evaluated in a mouse model of acute ovalbumin sensitisation and challenge, and the results are shown below in Figure 43 and 44. In this model, Balb/c mice were sensitised with ovalbumin before being dosed subcutaneously with 20 mg/kg of spiro-pyrimidine **282**. Ovalbumin is a T-cell dependent antigen commonly used to stimulate a T_H2 polarised allergic response in mice. Once the mice were sensitised, repeated dose of ovalbumin challenge leads to recruitment of leukocytes into the bronchoalveolar lavage (BAL) fluid, and increased airway hyperresponsiveness (AHR), in which the bronchioles constrict. The results show that spiro-pyrimidine **282** had an anti-inflammatory effect, demonstrating a significant reduction in eosinophil and lymphocyte infiltration into the BAL fluid after ovalbumin challenge, with no change in the macrophage and neutrophil cell counts (Fig. 43). Eosinophilic recruitment, without an increase in number of neutrophils, is a characteristic feature of allergic asthma. Chemokines play an important role in activating and recruiting particular leukocytes, including a sub-type which mediates eosinophilic migration in to the tissues.¹⁷⁴ Reduction of eosinophil infiltration in the BAL fluid observed on dosing compound **282** confirms that selective inhibition of CCR4 is a valid strategy to reduce the number of chemokines binding leading to reduced eosinophilic migration.

More significantly, spiro-pyrimidine **282** had a profound effect on airway hyperreactivity in the acute ovalbumin challenge model (Fig. 44). Animals were assessed for airway hyperresponsiveness to the spasmogen serotonin (5-hydroxytryptophan, 5HT) at concentrations of 1, 3 or 10 mg/mL. The spasmogen triggers contraction of the smooth muscle in the airways of sensitised ovalbumin challenged mice (orange line in the graph) causing difficulty in breathing, resulting in increases airway hyperresponsiveness (as

measured by Penh – derived from timing of expiration and pressure changes associated with respiration in the plethysmograph chamber). Mice dosed subcutaneously with 20 mg/kg of spiro-pyrimidine **282** showed a significant reduction of airway hyperreactivity (red line in the graph), especially at the higher concentration of 5HT, returning the levels back to the control line. The result with the spiro-pyrimidine **282** was found to compare favourably with that observed for the current gold standard corticosteroid, fluticasone propionate given intranasally (dose of 1.5 mg/kg) before ovalbumin challenge.

The *in vivo* results clearly demonstrate that binding to the Site 1 region of CCR4 receptor with a small molecule antagonist could provide an alternative therapeutic approach to treating allergic diseases such as asthma. Therapies with steroids reduce inflammation by inhibiting leukocyte recruitment indiscriminately, with significant associated side effects. Inhibiting eosinophilic recruitment without affecting other leukocytes could provide potential benefits over medications currently available in the market. Unfortunately, due to portfolio change in the GSK respiratory unit, work on the CCR4 programme was halted and no further work was carried out with the spiro-pyrimidine series.

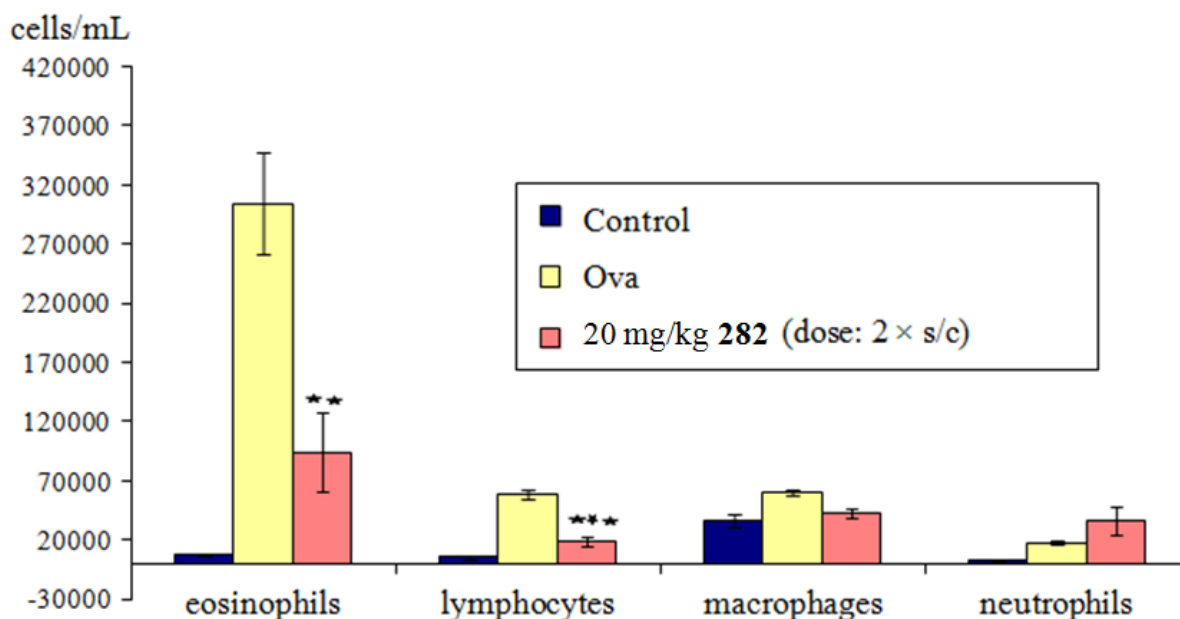


FIGURE 43. Effect of CCR4 antagonist **282** on a standard ovalbumin challenge on BAL cell influx in Balb/c mice.

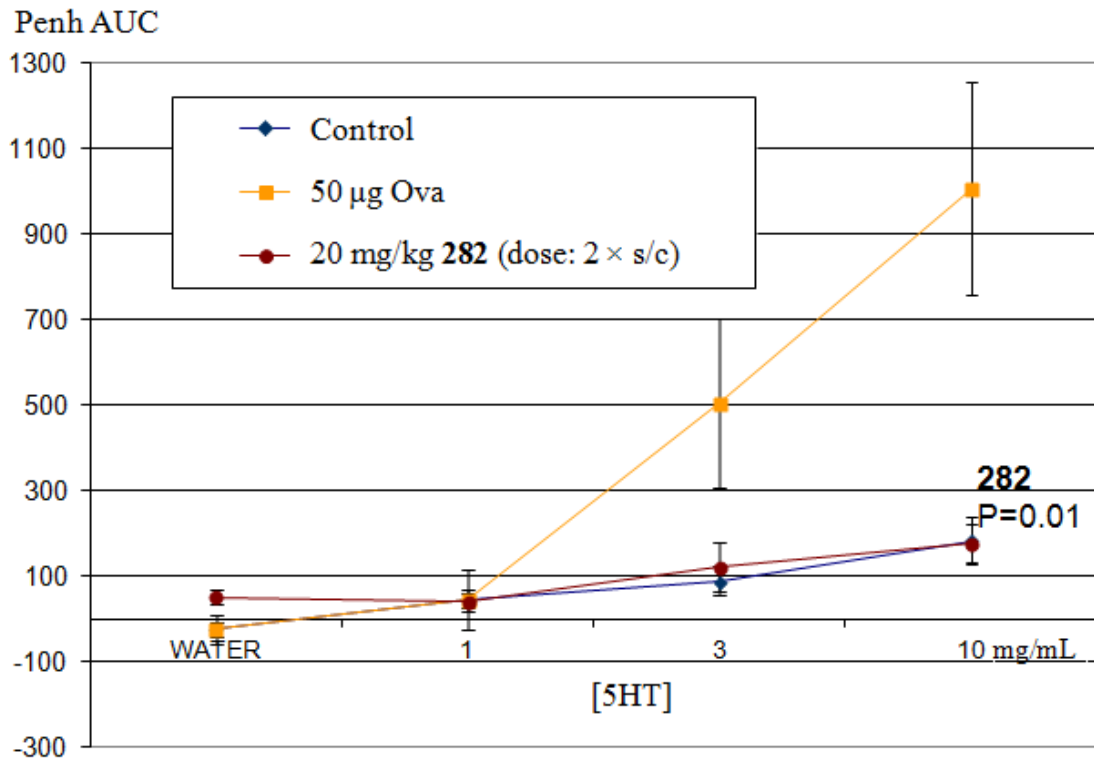


FIGURE 44. Effect of CCR4 antagonist 282 on airway hyperreactivity as measured by Penh Area Under the Curve following 5HT challenge.

9.0 Conclusion

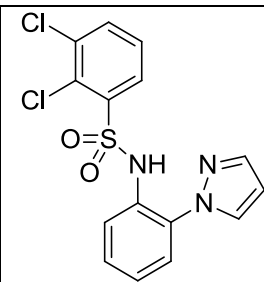
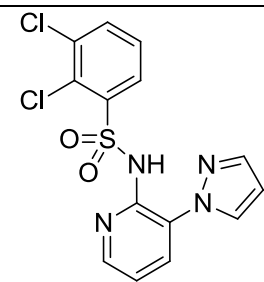
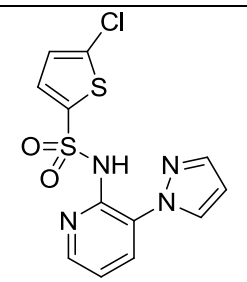
The overall aim of the project was to identify a backup template to the clinical development candidate, indazole **6**. Previous efforts to identify novel starting points for a backup series for the CCR4 programme using high throughput screening or screening of focused sets, such as the chemokine set, were all unsuccessful. In contrast, the knowledge-based approach used here, utilising the 2,3-dichlorobenzenesulfonamide moiety as an anchor to generate a virtual library of ~1600 sulfonamides, and synthesising compounds with desired drug-like properties (MW < 500, clogP < 5, H-bond donor < 5, H-bond acceptor < 10), led to the identification of several new templates with good potency and LE for the Site 2 CCR4 allosteric site. One major drawback with this protocol however, was that identification of new templates were limited to amines that were available in-house, or from commercial sources.

Previously, a small molecule X-ray crystal structure of an in-house analogue (**27**) from the candidate indazole series has shown that an intramolecular hydrogen bond allows the molecule to favour a conformation which may align favourably with the receptor binding pocket. Exploiting this theory, the potency of few of the new 'hits' were quickly enhanced by incorporating a methoxy group adjacent to the sulfonamide substituent to allow the formation of an intramolecular hydrogen bond. In addition, phenylpyrazole **33** (Table 5) was identified as a 'hit' and a small molecule X-ray structure showed that one of the nitrogen atoms of the pyrazole ring was acting as a hydrogen bond acceptor for the NH of the sulfonamide, reinforcing the hypothesis that an intramolecular hydrogen bond was important for potency. More importantly, electronic structure calculations indicated a preference for the presence of intramolecular hydrogen bonds in the global minimum of **8** and **33**, and the molecules adopting an orthogonal or clip-shaped conformation, linking the behaviour observed in the X-ray structure to those in solution.

PK studies were performed on representative compounds from four of these new templates. In two preclinical species (rat and dog), representative compounds from the 6-aminoindazole (rat clearance = 16% liver blood flow, dog = 42% liver blood flow) and the phenylpyrazole series (rat clearance = 42% liver blood flow, dog = not determined) showed high clearance and were therefore of lower interest. However, it is important to note that some of the more potent analogues from the phenylpyrazole series with lower chromlogD might have lower clearance, and therefore may still be of value. In addition, if the high clearance was due to metabolism, for example, of the pyrazole ring, then this could be reduced by introduction of

blocking groups, such as fluorine. Despite the good GTP γ S potency and ligand efficiency observed with the aza derivatives of the phenylpyrazoles, improving whole blood potency proved to be very challenging. However, the MW and chromlogD of the aza analogues (e.g. **114**, MW = 369, chromlogD = 3.7 and **115**, MW = 340, chromlogD = 2.8) are low (see Table 33) so there is potential to improve the whole blood potency by incorporating additional groups.

TABLE 33. Biological and physicochemical profile of 33, 114 and 115.

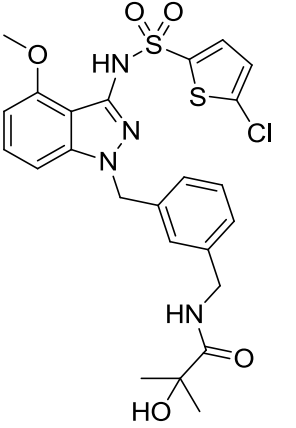
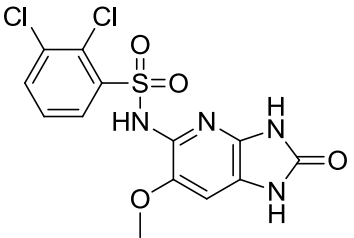
Compound No.			
	33	114	115
GTP γ S (pIC ₅₀):	6.6	7.4	7.2
LE / LLE _{AT} :	0.39/0.25	0.44/0.36	0.47/0.40
MW:	368	369	340
clogP:	4.0	3.3	2.7
ChromlogD _{7.4} :	6.4	3.7	2.8
CLND solubility:	48 μ g/mL	203 μ g/mL	133 μ g/mL

Because of time pressures, only the two templates possessing the better PK profiles were evaluated further. Investigation of the pyrazolopyrimidine series showed flat SAR with none of the analogues showing any activity in the human whole blood assay. It is not clear why these compounds were inactive, but one explanation could be that the compounds bind tightly to the plasma proteins (e.g. pyrazolopyrimidine **69**, PPB = 98.5%) and therefore are not available to inhibit the CCR4 receptor.

Interestingly, SAR studies on the benzimidazolone series and incorporation of nitrogen in the core resulted in compound **239**, with comparable potency (GTP γ S pIC₅₀ = 7.6, hWB pA₂ = 6.0) and improved physicochemical properties (MW = 389, clogP = 3.6, chromlogD = 2.4) than the candidate indazole, **6** (GTP γ S pIC₅₀ = 7.9, hWB pA₂ = 6.2, MW = 549, clogP = 3.7, chromlogD = 4.3)) (Table 34). Although PK data were not obtained, the permeability of **239**

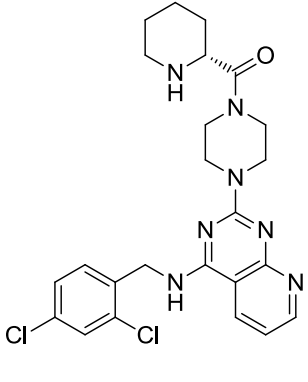
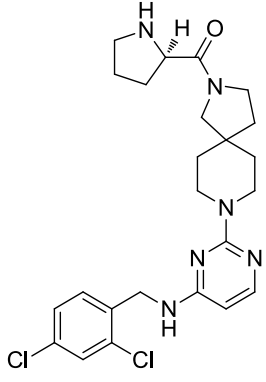
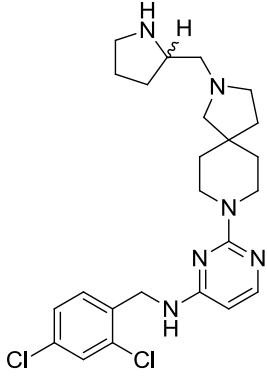
in the MDCK was low, suggesting the compound will have poor absorption. This could be addressed in a lead optimisation programme, and future work should involve investigating the SAR around the N1 and N3-position of the aza-benzimidazolone series. The main priority should be to improve the permeability of the molecule, whilst retaining the human whole blood potency. Nonetheless, azabenzimidazolone **239** is a novel allosteric CCR4 Site2 antagonist, which provides a very good starting point for further lead optimisation towards identification of a potential oral asthma drug.

TABLE 34. Biological and physicochemical data of indazole 6 and azabenzimidazolone 239.

Compound No.	 6	 239
GTPγS (pIC₅₀):	7.9	7.6
LE / LLE _{AT} :	0.30/0.27	0.43/034
hWB Actin polym (pA₂):	6.2	6.0
PPB:	96.5%	93.2%
MW :	549	389
ChromlogD _{7.4} :	4.3	2.8
CLND solubility:	162 μ g/mL	152 μ g/mL

A second objective was to design a new Site 1 inhibitor for CCR4 through a knowledge driven approach, which resulted in the identification of spiro-pyrimidine **255d** (Table 35).

TABLE 35. Biological and physicochemical data of pyrimidine 1 and spiro-pyrimidine 255d and 282.

Compound	 <p style="text-align: center;">1</p>	 <p style="text-align: center;">255d</p>	 <p style="text-align: center;">282</p>
I¹²⁵ TARC			
SPA pK_i	9.1	7.8	8.6
LE / LLE _{AT}	0.37/0.28	0.32/0.28	0.37/0.30
HWB Actin			
polym. (pA₂):	7.1	6.2	6.7
MW :	500	489	475
clogP :	4.9	3.8	4.3
ChromlogD _{7.4} :	2.8	3.4	4.4
CLND sol:	145 µg/mL	180 µg/mL	120 µg/mL
PPB (HSA)	92.6%	95.7%	97.5%

Structure activity-relationship studies were carried out in order to improve the potency, which led to the discovery of several analogues (**282**, **287**, **290**, **291** and **307**) with activities comparable to that of the leading competitor's compound **1**. Similar to the literature antagonist K777, it was also found that analogues from the spiro-pyrimidine series induced receptor internalisation on HUT78 cells with approximately 50% reduction of cell surface CCR4, whereas antagonists binding to Site-2 had no effect. This was an important finding for the group and could explain why a positive *in vivo* effect was observed with Site 1 compared to Site 2 antagonists that have similar whole blood activity. In the FITC-induced *in vivo* model when dosed subcutaneously, compound **282** demonstrated marked reductions in ear swelling in Balb/c mice. Furthermore, compound **282** showed *in vivo* efficacy in an acute ovalbumin challenge mouse model where a significant reductions in eosinophil and lymphocyte infiltration into the BAL fluid were observed after ovalbumin challenge. Most

importantly with respect to asthma, compound **282** demonstrated a profound effect on the airway hyperreactivity returning the levels back to the control line, which is comparable to the gold standard corticosteroid. These early results indicate that targeting CCR4 receptor with a small molecule antagonist could provide a potential novel opportunity for treating allergic diseases such as asthma. However, despite these encouraging data, exemplars from the spiro-pyrimidine template demonstrated poor pharmacokinetic profile for these compounds to be used as therapeutics for an oral therapy. If an inhaled delivery approach could be validated then these compounds could be potential candidates for treating asthma.

10.0 Experimental section

10.1 Biological assays

CCR4 [³⁵S]-GTP γ S binding assay⁸⁴

Membranes derived from a CHO cell line stably transfected with human CCR4 receptor (3 μ g membranes per well) were adhered to Wheat Germ Agglutinin Polystyrene LEADSeeker™ scintillation proximity assay (SPA) beads (250 μ g/well) in assay buffer containing *N*-2-hydroxyethylpiperazine-*N'*-2-ethanesulfonic acid (20 mM), MgCl₂ (10 mM), NaCl (100 mM), saponin (40 μ g/mL), bovine serum albumen (0.05% w/v), GDP (4.4 μ M), and pH adjusted to 7.4 using 1M KOH. After 1 h pre-coupling at 4 °C the bead/membrane suspension was mixed in a 4:5 ratio with [³⁵S]-GTP γ S (PerkinElmer LAS UK Ltd, radioactivity concentration 37 MBq/mL⁻¹; specific activity = 1250 Ci/mol⁻¹) made up in assay buffer containing MDC (at a concentration that results in the final assay concentration of MDC being EC₈₀) to give a final radioligand concentration of 0.6 nM. A 45 μ L/well aliquot of this reagent mixture was dispensed into white Greiner polypropylene 384-well plates containing stock solution of the test compounds in DMSO (10 mM, 0.5 μ L) or 0.5 μ L DMSO as a control, and the assay plates were sealed and centrifuged at 1000 rpm for 20 s. The plates were left to equilibrate in darkness for between 3 and 6 h before reading on a ViewLux™ luminescence imager using a 613/55 filter for 5 min/plate. Data were analyzed using a 4-parameter logistical equation to determine the antagonist IC₅₀.

[¹²⁵I]CCL17 binding studies⁸⁴

[¹²⁵I]CCL17 binding studies were performed in white, 96-well clear bottomed, SPA plates at room temperature (20–22°C) in assay buffer [mM: HEPES, 20; NaCl, 100; MgCl₂, 10; saponin, 10 mg/mL; 0.1% BSA; adjusted to pH 7.4 with KOH]. Wheatgerm agglutinin polyvinyltoluene SPA beads (SPA beads) were precoated with CCR4 cells or membranes for 30 min on ice and added to SPA plates containing CCR4 agonist, antagonist or vehicle (1% DMSO) and [¹²⁵I]CCL17 (~0.1 nM) to give 0.25 mg/well SPA beads and 2.5 mg/well membrane protein. Non-specific binding was determined in the presence of 10 nM CCL22. Plates were incubated for 4 h before detection of [¹²⁵I]CCL17 binding, using a Wallac Microbeta Trilux scintillation counter (PerkinElmer LAS UK Ltd, Beaconsfield, UK). The total amount of radioligand added to each well was calculated for data analysis using a Packard Cobra II Gamma Counter (PerkinElmer LAS UK Ltd).

Human whole blood F-actin polymerization assay⁸⁵

The human biological samples were sourced ethically and their research use was in accord with the terms of the informed consents. Volunteers gave informed consent for blood donation and denied taking any medication in the 7 days prior to donation. Blood (9 volumes) was taken from healthy human subjects into 3.8% sodium citrate solution (1 volume). The blood was incubated at room temperature with saturating concentrations of fluorescein isothiocyanate (FITC)-conjugated mouse anti-human CD4 and a non-inactivating phycoerythrin (PE)-conjugated mouse anti-human CCR4 (BD Biosciences) or appropriate isotype control antibodies for 10 min. The blood was then incubated with antagonists or vehicle (0.1% DMSO) at 37 °C for 30 min before addition of the agonist (MDC from Almac Sciences, UK; TARC from PeproTech EC, UK) for 15 sec. The assay was terminated by adding 10 volumes of FACS Lysing solution (BD Biosciences). After 30 min the cells were centrifuged (1000 g for 5 min), re-suspended in FACS Lysing solution (200 µL) and incubated at room temperature for a further 15 min. The cell suspensions were then centrifuged (1200 g for 5 min), washed twice with PBS (150 µL), centrifuging as above to recover the cells, and incubated for 20 min with lysophosphatidylcholine (100 µg.mL⁻¹) and Alexa fluor 647 phalloidin (0.075 units.mL⁻¹). The cells were centrifuged at 1200 g for 5 min and re-suspended in PBS. The F-actin content of the CD4⁺ CCR4⁺ lymphocytes in each sample was determined on a FACSCalibur flow cytometer by measuring the mean Alexa fluor 647 (FL-4) fluorescence intensity of 500 cells. This was expressed as a fraction of the Alexa fluor 647 fluorescence intensity of the CCR4⁻ lymphocytes in the same sample.

10.2 Pharmacokinetics¹³²

Pharmacokinetics were determined in male Wistar Han rats and male Beagle dogs following single oral and single intravenous administration. In the rat nominal doses of 1 mg/kg were used for intravenous (iv) and oral (po) routes. In the dog nominal doses of 0.5 and 1 mg/kg were used for iv and po routes, respectively. For all doses the compounds were formulated as solutions in DMSO-PEG 200-Water (5:45:50). Profiles were obtained by taking serial blood samples over a range of time-points up to 7 or 24 h post-dose. Blood samples were taken directly into heparinised tubes, prepared by protein precipitation and subjected to quantitative analysis by LCMS/MS using compound-specific mass transitions. Drug concentration-time profiles were generated and non-compartmental PK analysis used to generate estimates of half-life, clearance, volume of distribution and oral bioavailability.

10.3 Physicochemical assays⁹⁰

GSK in-house kinetic CLND solubility assay

5 μL of 10 mM DMSO stock solution of test compound was diluted to 100 μL with pH 7.4 phosphate buffered saline. The mixture was equilibrated for 1 h at room temperature, filtered through a Millipore Multiscreen HTS-PCF filter plates (MSSL BPC), and the eluent was quantified by suitably calibrated flow injection chemi-luminescent nitrogen detection (CLND). The upper limit of the solubility is 500 μM when working from 10 mM DMSO stock solution.

ChromlogD assay

The Chromatographic Hydrophobicity Index (CHI) values were measured using reversed phase HPLC column (50 x 2 mm 3 μM Gemini NX C18, Phenomenex, UK) with fast acetonitrile gradient at starting mobile phase of pH = 7.4. CHI values are derived directly from the gradient retention times by using a calibration line obtained for standard compounds. The CHI value approximates to the volume % organic concentration when the compound elutes. CHI is linearly transformed into ChromlogD by using the following formula: $\text{ChromlogD} = 0.0857\text{CHI} - 2.00$.

GSK pK_a measurements

The pK_a values were measured in a high throughput mode using Sirius T3 apparatus from Sirius analytical. 5 μL aliquot of 10 mM DMSO stock (plus co solvent such as MeOH for poorly soluble compounds) were titrated from pH 2.0 to pH 12.0 to give a full 40 point titration curve, which were measured using an *in situ* UV spectrometer (220 to 700 nm each point).

10.4 *In vivo* experiments¹⁷²

BALB/c mice were supplied by Charles River (Margate, UK). All animal studies were ethically reviewed and carried out in accordance with Animals (Scientific Procedures) Act 1986 and the GSK Policy on the Care, Welfare and Treatment of Animals.

For the ovalbumin-challenge model, animals were sensitised to a suspension of ovalbumin adjoined to aluminium hydroxide (10 μg OVA, 2 mg Alum, $\text{Al}(\text{OH})_3$) by intra-peritoneal administration on two occasions, 2 weeks apart. Ten days after sensitization, mice received

subcutaneous (200 µL s/c) administration of compound twice daily (5%, DMSO, 45% Peg 200, 45% H₂O) pre and post challenge with intra-nasal administration of Ovalbumin (50 µg). Dosing and challenge continued for three days, with final doses of compound the day after the final ova challenge.

Animals were assessed for airways hyperresponsiveness (AHR) to the spasmogen serotonin (5HT) using a Buxco Inc whole body plethysmography system. Animals were exposed to a nebulised solution of water or 5HT at concentrations of 1, 3 or 10 mg/mL for 2 minute periods, and lung function was assessed for a further 18 minutes. AHR is expressed as units of enhanced pause, penh, as area under the curve following each exposure.

On the day following AHR assessment the animals were killed by an overdose of anaesthetic and the lungs were lavaged *post mortem* using repeat instillations of fluid (10 mM EDTA, 0.1% BSA in PBS) that was pooled to form the bronchoalveolar lavage (BAL). BAL was assayed for inflammatory cell influx using an automated flow cytometry method based on cell size and granularity to separate different cell populations. Inflammatory cell infiltrate is expressed as cells/mL total BAL.

For delayed-type hypersensitivity assay, animals were sensitised on day 0 and 7 by topical application of 1% Fluorescein isothiocyanate (FITC) solution (10 mg/mL) in 50 µl of vehicle (1 part dibutyl phthalate/ 1 part acetone) on to each shaved flank. After fourteen days, the thickness of the animals' ears was measured using an engineer's micrometer whilst animals were under isoflurane anaesthesia, and compounds were administered either subcutaneously in 100 µl vehicle (5% DMSO, 45% Peg 200, 50% H₂O) or topically in 20 µl vehicle (EtOH) on the dorsal surface of each ear. One hour later, animals were challenged with 1% FITC solution on both sides of both ears (10 mg/mL in 1 part dibutyl phthalate/ 1 part acetone), and a second dose of compound was administered four hours post challenge. Twenty four hours after challenge animals were anaesthetised and the ears were re-measured and the thickness recorded.

10.5 Chemistry

Organic solutions were dried over anhydrous Na₂SO₄, MgSO₄ or using a hydrophobic frit. TLC was performed on Merck 0.25 mm Kieselgel 60 F₂₅₄ plates. Products were visualised under UV light and/or by staining with aqueous KMnO₄ solution.

LCMS analysis was conducted on either System A an Acquity UPLC BEH C₁₈ column (2.1 mm × 50 mm ID, 1.7 μm packing diameter) eluting with 0.1% formic acid in water (solvent A), and 0.1 % formic acid in MeCN (solvent B), using the following elution gradient 0.0 – 1.5 min 3 – 100% B, 1.5 – 1.9 min 100% B, 1.9 – 2.0 min 100 – 3% B, at a flow rate of 1 mLmin⁻¹ at 40 °C. The UV detection was an averaged signal from wavelength of 210 nm to 350 nm, and mass spectra were recorded on a mass spectrometer using alternate-scan electrospray positive and negative mode ionization (ES+ve and ES-ve); or System B an Acquity UPLC BEH C₁₈ column (50 mm × 2.1 mm ID, 1.7 μm packing diameter) eluting with 10 mM ammonium bicarbonate in water adjusted to pH10 with ammonia solution (solvent A), and MeCN (solvent B) using the following elution gradient 0.0 – 1.5 min 1 – 97% B, 1.5 – 1.9 min 97% B, 1.9 – 2.0 min 100% B at a flow rate of 1 mL min⁻¹ at 40 °C; or System C an Acquity UPLC BEH C₁₈ column (50 mm × 2.1 mm ID, 1.7 μm packing diameter) eluting with 0.1% trifluoroacetic acid in water (solvent A), and 0.1% trifluoroacetic acid in MeCN (solvent B) using the following elution gradient 0.0 – 1.5 min 3 – 100% B, 1.5 – 1.9 min 100% B, 1.9 – 2.0 min 100 – 3 %B at a flow rate of 1 mL min⁻¹ at 40 °C; or System D an Agilent Sunfire C₁₈ column (30 mm × 4.6 mm ID, 3.5 μm packing diameter) eluting with 0.1% trifluoroacetic acid in water (solvent A), and 0.1% trifluoroacetic acid in MeCN (solvent B) using the following elution gradient 0.0 – 4.2 min 3 – 100% B, 4.2 – 4.8 min 100% B, 4.8 – 5.0 min 100 – 3 % B at a flow rate of 3 mL min⁻¹ at 30 °C.

Column chromatography was performed on a Flashmaster II system. The Flashmaster II is an automated multi-user flash chromatography system, available from Argonaut Technologies Ltd, which utilizes disposable, normal phase, SPE cartridges (2 g to 100 g).

Purifications by mass-directed auto-preparative HPLC (MDAP) was conducted on either System A a Sunfire C₁₈ column (150 mm × 30 mm i.d. 5 μm packing diameter) at ambient temperature eluting with 0.1% formic acid in water (solvent A) and 0.1% formic acid in MeCN (solvent B), using an appropriate elution gradient over 15 or 25 min at a flow rate of 40 mL min⁻¹ and detecting at 210 - 350 nm at room temperature. Mass spectra were recorded on Micromass ZMD mass spectrometer using electro spray positive and negative mode, alternate scans; or System B an XBridge C₁₈ column (150 mm × 30 mm i.d. 5 μm packing diameter) at ambient temperature eluting with 10 mM ammonium bicarbonate in water adjusted to pH10 with ammonia solution (solvent A), and MeCN (solvent B), using an appropriate elution gradient over 15 or 25 min at a flow rate of 40 mL min⁻¹; or System C a

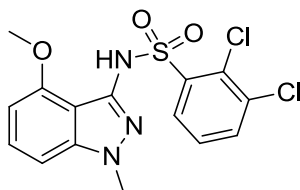
Sunfire C₁₈ column (150 mm × 30 mm i.d. 5 μm packing diameter) at ambient temperature eluting with 0.1% trifluoroacetic acid in water (solvent A), and 0.1% trifluoroacetic acid in MeCN (solvent B), using an appropriate elution gradient over 15 or 25 min at a flow rate of 40 mL min⁻¹. The software used was *MassLynx* 3.5 with *OpenLynx* and *FractionLynx* options.

Proton magnetic resonance spectra (¹H NMR) were recorded at 400, 500 or 600 MHz, unless otherwise stated. The chemical shifts (δ) are expressed in ppm relative to tetramethylsilane. Carbon magnetic resonance spectra (¹³C NMR) were recorded at 100, 126 or 150 MHz. In the cases indicated, solid NaHCO₃ was added to the NMR solution to sharpen up the line-widths of the ¹³C signals, as some signals were so broad that did not show up in the absence of base. It is assumed that the original samples had very broad signals due to inter-conversion between different forms at an intermediate rate over the NMR timescale. These different forms might be due to the zwitterionic nature of the compounds. Adding the base generated the sodium salt and created a single form with a sharp set of lines.

High resolution positive ion mass spectra were acquired on a Micromass Q-ToF 2 hybrid quadrupole time-of-flight mass spectrometer. The elemental composition was calculated using *MassLynx* v4.1 for the [M+H]⁺. All separations for HRMS were achieved using a Phenomenex Luna C₁₈ (2) reversed phase column (100 mm × 2.1 mm, 3 μm particle size). Gradient elution was carried out with the mobile phases as (A) water containing 0.1% (v/v) formic acid and (B) MeCN containing 0.1% (v/v) formic acid. The conditions for the gradient elution were initially 5% B for 2 min, increasing linearly to 100% B over 6 min, remaining at 100% B for 2.5 min then decreasing linearly to 5% B over 1 min, followed by an equilibration period of 2.5 min prior to the next injection. The flow rate was 0.5 mL/min, temperature controlled at 35 °C with an injection volume of 2 to 5 μL.

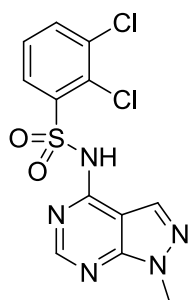
The purity of all compounds screened in the biological assays was examined by LCMS analysis and was found to be ≥ 95%, unless otherwise specified. IR spectra were recorded using a Perkin Elmer 100FT-IR spectrometer with an attenuated total reflectance (ATR) accessory. Microwave reactions were carried out using a Biotage initiator microwave with a Biotage 60 sampler. Melting points were determined on a Stuart SMP40 automatic melting point apparatus.

2,3-Dichloro-*N*-[1-methyl-4-(methoxy)-1*H*-indazol-3-yl]benzenesulfonamide (8)



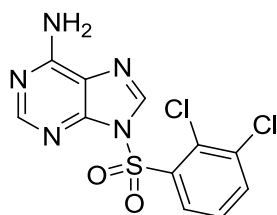
A solution of 4-methoxy-1-methyl-1*H*-indazol-3-amine¹⁷⁵ (2.38 g, 13.4 mmol) in pyridine (50 mL) was treated portionwise with 2,3-dichlorobenzenesulfonyl chloride (3.36 g, 13.7 mmol) at 20 °C, and the reaction mixture was stirred for 18 h. An additional portion of 2,3-dichlorobenzenesulfonyl chloride (1 g, 4 mmol) was added and the mixture was stirred at room temperature for 18 h. The reaction mixture was partitioned between dichloromethane (250 mL) and water (250 mL). The organic phase was washed with 2M hydrochloric acid (100 mL), dried and evaporated under reduced pressure. The residue was purified by chromatography on a silica (100 g) cartridge eluting with a gradient of 0–100% ethyl acetate–cyclohexane over 60 min. The appropriate fractions were combined and evaporated in vacuo to give **7** (2.51 g, 48%) as an off-white solid; ¹H NMR (500 MHz, DMSO-*d*₆) δ = 10.43 (s, 1H), 7.91 (dd, *J* = 8.0, 1.0 Hz, 1H), 7.85 (dd, *J* = 8.0, 1.0 Hz, 1H), 7.47 (t, *J* = 8.0 Hz, 1H), 7.26 (t, *J* = 8.0 Hz, 1H), 7.08 (d, *J* = 8.0 Hz, 1H), 6.46 (d, *J* = 8.0 Hz, 1H), 3.86 (s, 3H), 3.64 (s, 3H); ¹³C NMR (126 MHz, DMSO-*d*₆) δ = 153.5, 142.9, 141.6, 134.8, 134.5, 134.3, 129.9, 129.6, 128.6, 128.5, 110.4, 102.8, 100.4, 55.5, 36.0; IR ν_{max} (neat) 3274, 1621, 1595, 1518, 1505, 1456, 1430, 1366, 1272, 1164, 726 cm⁻¹; LCMS (Method A, UV, ES) RT = 1.05 min, [M+H]⁺ = 386, 388, 390, 100% purity. HRMS (ESI) *m/z* calculated for C₁₅H₁₄Cl₂N₃O₃S = 386.0128. Found = 386.0125 [M+H]⁺. Crystal data: C₁₅H₁₃Cl₂N₃O₃S; *M* = 386.24; colourless wedge; spontaneous crystallisation from methanol, 10% 2M HCl; 0.82 × 0.62 × 0.34 mm; triclinic; space group, *P* -1 (No. 2); unit cell dimensions, *a* = 7.9294(12) Å, *b* = 12.763(2) Å, *c* = 16.761(3) Å, α = 96.664(17) °, β = 99.981(17) °, γ = 97.378(14) °, *V* = 1640.1(5) Å³; *Z* = 4; *d*_{calc} = 1.564 Mg/m³; and μ (Mo-Kα, λ = 0.71073 Å) = 0.543 mm⁻¹.

2,3-Dichloro-*N*-(1-methyl-1*H*-pyrazolo[3,4-*d*]pyrimidin-4-yl)benzenesulfonamide (13)



Sodium hydride (10 mg of a 60% w/w dispersion in mineral oil, 0.25 mmol) was added to a stirring solution of 1-methyl-1*H*-pyrazolo[3,4-*d*]pyrimidin-4-amine (34 mg, 0.23 mmol) in anhydrous DMF (1 mL) at ambient temperature. The mixture was stirred for 5 min, then 2,3-dichlorobenzenesulfonyl chloride (61 mg, 0.25 mmol) was added and the reaction mixture was stirred at ambient temperature for 3 h. Several drops of HCl (2 M aqueous solution) were added and the mixture was concentrated under reduced pressure. The sample was taken up in DMSO (1 mL) and purified by MDAP (Method A). The solvent was evaporated under reduced pressure to afford the title product (17 mg, 21%) as a white solid; ¹H NMR (400 MHz, DMSO-*d*₆) δ = 13.18 (br.s, 1H), 8.40 (s, 1H), 8.36 (s, 1H), 8.14 (dd, *J* = 8.0, 1.5 Hz, 1H), 7.91 (dd, *J* = 8.0, 1.5 Hz, 1H), 7.57 (t, *J* = 8.0 Hz, 1H), 3.97 (s, 3H); LCMS (Method A, UV, ES) RT = 0.85 min, [M+H]⁺ = 358, 360, 362, 100% purity.

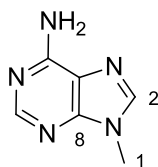
9-[(2,3-Dichlorophenyl)sulfonyl]-9*H*-purin-6-amine (17)



Sodium hydride (18 mg of a 60% w/w dispersion in mineral oil, 0.44 mmol) was added to 1*H*-purin-6-amine (50 mg, 0.37 mmol) in anhydrous DMF (1.5 mL) at ambient temperature. The mixture was stirred for 10 min, then 2,3-dichlorobenzenesulfonyl chloride (100 mg, 0.41 mmol) was added, and the reaction was stirred under nitrogen for 18 h. The reaction mixture was partitioned between ethyl acetate (15 mL) and water (15 mL). The organic layer was separated, dried using a hydrophobic frit and concentrated under reduced pressure. The crude mixture was dissolved in 1:1 DMSO-MeOH (1 mL) for MDAP purification but the product precipitated from solution. The solids were filtered, washed with cold MeOH (1 mL) and

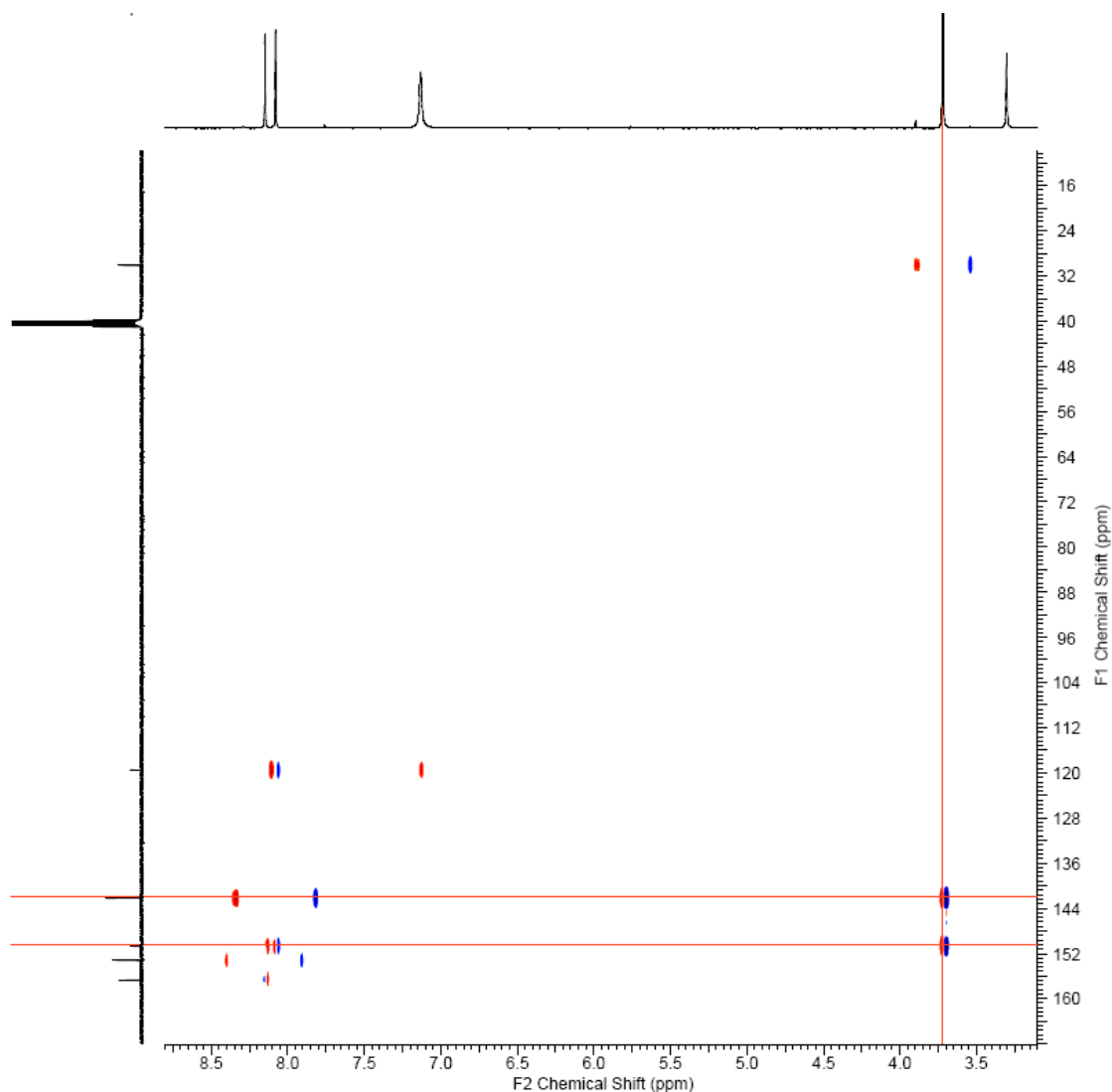
dried under reduced pressure to afford the title product (28 mg, 22%) as a white solid; ^1H NMR (600 MHz, $\text{DMSO-}d_6$) δ = 8.77 (s, 1H), 8.43 (dd, J = 8.1, 1.5 Hz, 1H), 8.12 (dd, J = 8.1, 1.5 Hz, 1H), 8.08 (s, 1H), 7.77 (t, J = 8.1 Hz, 1H), 7.70 (br.s, 2H); ^{13}C NMR (151 MHz, $\text{DMSO-}d_6$) δ = 156.3, 154.4, 148.3, 139.1, 137.4, 135.6, 134.6, 132.1, 129.4, 129.1, 118.3; HRMS (ESI) m/z calculated for $\text{C}_{11}\text{H}_8\text{Cl}_2\text{N}_5\text{O}_2\text{S}$ = 343.9776. Found = 343.9774 $[\text{M}+\text{H}]^+$; LCMS (Method A, UV, ES) RT = 0.81 min, $[\text{M}+\text{H}]^+$ = 344, 346, 348, 97% purity.

9-Methyl-9H-purin-6-amine (18)

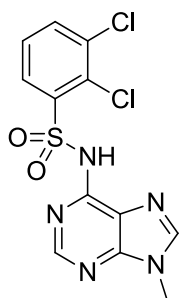


Methyl iodide (0.22 mL, 3.6 mmol) was added to a mixture of adenine (400 mg, 2.96 mmol) and cesium carbonate (1.16 g, 3.55 mmol) at ambient temperature and the reaction mixture was stirred for 48 h. The reaction was quenched with water (8 mL) and the precipitate was collected by filtration and dried under reduced pressure to afford the title product (172 mg, 39%) as a white solid; ^1H NMR (400 MHz, $\text{DMSO-}d_6$) δ = 8.14 (s, 1H), 8.08 (s, 1H), 7.15 (br.s, 2H), 3.72 (s, 3H); ^{13}C NMR (101 MHz, $\text{DMSO-}d_6$) δ = 155.8, 152.3, 149.8, 141.3, 118.6, 29.3; LCMS (Method B, UV, ES) RT = 0.39 min, $[\text{M}+\text{H}]^+$ = 150, 96% purity.

HMBC shows key correlation between the methyl protons (3.67 ppm) to C-2 (149.8) and C-8 (141.3) corresponding to $^3J_{\text{C-H}}$ couplings.



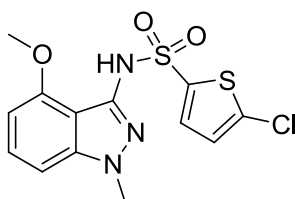
2,3-Dichloro-*N*-(9-methyl-9*H* purin-6-yl)benzenesulfonamide (19)



The title sulfonamide compound was prepared from **18** (50 mg, 0.34 mmol), 2,3-dichlorobenzenesulfonyl chloride (91 mg, 0.37 mmol) and sodium hydride (16 mg of a 60% w/w dispersion in mineral oil, 0.40 mmol) according to the procedure described for the preparation of **13**. For the work up, water (2 mL) was added and an attempt to extract the product with ethyl acetate (2 x 15 mL) failed (product insoluble). The aqueous layer was concentrated under reduced pressure. The sample was taken up in DMSO (4 mL), and the crude product was purified by MDAP (Method A). The solvent was evaporated under

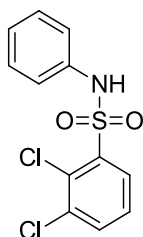
reduced pressure to afford the title product (38 mg, 32%) as a white solid; ^1H NMR (400 MHz, DMSO- d_6) δ = 13.01 (br.s, 1H), 8.36 (s, 1H), 8.26 (s, 1H), 8.14 (dd, J = 8.0, 1.5 Hz, 1H), 7.87 (dd, J = 8.0, 1.5 Hz, 1H), 7.55 (t, J = 8.0 Hz, 1H), 3.36 (s, 3H); ^{13}C NMR (151 MHz, DMSO- d_6) δ = 149.5, 148.9, 144.8, 144.0, 142.7, 133.7, 133.6, 129.2, 128.2, 122.4, 30.0; IR ν_{max} (neat) 3331, 1619, 1560, 1549, 1400, 1379, 1262, 1112, 1052, 852, 777, 701 cm^{-1} ; HRMS (ESI) m/z calculated for $\text{C}_{12}\text{H}_{10}\text{Cl}_2\text{N}_5\text{O}_2\text{S}$ = 357.9932. Found = 357.9930 $[\text{M}+\text{H}]^+$; LCMS (Method A, UV, ES) RT = 0.72 min, $[\text{M}+\text{H}]^+$ = 358, 360, 362, 99% purity.

5-Chloro-*N*-[1-methyl-4-(methoxy)-1*H*-indazol-3-yl]-2-thiophenesulfonamide (27)



The title compound was available in the GSK collection. Crystallisation solvent Acetone and water, Crystallisation method = slow evaporation. Crystal data: $\text{C}_{13}\text{H}_{12}\text{ClN}_3\text{O}_3\text{S}_2$, crystal size 0.42 x 0.12 x 0.08 mm^3 , M = 357.83, monoclinic, space group $\text{P}2_1/n$, unit cell dimensions a = 11.034(2), b = 8.6297(17), c = 16.101(3) \AA , α = 90° , β = $94.54(3)^\circ$, γ = 90° , V = 1528.3(5) \AA^3 , Z = 4, D_{calc} = 1.555 Mg/m^3 , $F(000)$ = 736, absorption coefficient = 0.538 mm^{-1} , T = 150(2) K, 9258 total reflections measured, 2646 independent, (R_{int} = 0.0360) which were used in all calculations. Final R indices (for reflections with $I > 2\sigma(I)$) were $R1$ = 0.0358, $\omega R2$ = 0.0647; R indices (all data) $R1$ = 0.0639, $\omega R2$ = 0.0733.

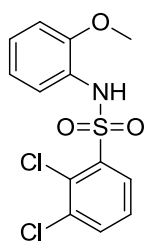
2,3-Dichloro-*N*-phenylbenzenesulfonamide (29)



2,3-Dichlorobenzenesulfonyl chloride (50 mg, 0.20 mmol) was added to a stirring solution of aniline (17 mg, 0.19 mmol) in anhydrous pyridine (0.8 mL) and the reaction mixture was stirred at ambient temperature for 4 h. The reaction mixture was evaporated under reduced pressure, and the solid was taken up in DMSO (2 mL) and purified by MDAP (Method A).

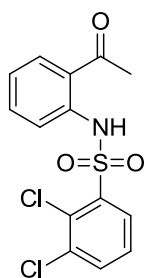
The appropriate fractions were combined and the solvent was evaporated under reduced pressure to afford the title product (40 mg, 72%) as a white solid; ^1H NMR (500 MHz, $\text{DMSO-}d_6$) δ = 10.77 (s, 1H), 8.03 (dd, J = 8.0, 1.5 Hz, 1H), 7.91 (dd, J = 8.0, 1.5 Hz, 1H), 7.53 (t, J = 8.0 Hz, 1H), 7.31 – 7.18 (m, 2H), 7.09 (d, J = 7.5 Hz, 2H), 7.02 (t, J = 7.5 Hz, 1H); ^{13}C NMR (126 MHz, $\text{DMSO-}d_6$) δ = 139.2, 137.2, 135.5, 134.7, 130.9, 129.8 (2C), 129.3, 129.1, 124.7, 119.9 (2C); IR ν_{max} (neat), 3268, 1481, 1417, 1342, 1164, 1154, 758, 697 cm^{-1} ; HRMS (ESI) m/z calculated for $\text{C}_{12}\text{H}_{10}\text{Cl}_2\text{NO}_2\text{S}$ = 301.9804. Found = 301.9800 $[\text{M}+\text{H}]^+$; LCMS (Method A, UV, ES) RT = 1.12 min, $[\text{M}+\text{H}]^+$ = 301, 303, 305, 100% purity.

2,3-Dichloro-*N*-(2-methoxyphenyl)benzenesulfonamide (30)



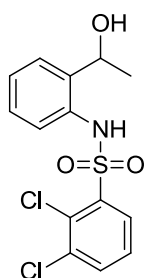
The title compound was prepared from 2-methoxyaniline (23 mg, 0.19 mmol) and 2,3-dichlorobenzenesulfonyl chloride (50 mg, 0.20 mmol) according to the procedure described for the preparation of **29**. The same work up and purification afforded **30** (45 mg, 73%) as a white solid; ^1H NMR (500 MHz, $\text{DMSO-}d_6$) δ = 9.79 (s, 1H), 7.89 (dd, J = 8.0, 1.5 Hz, 1H), 7.76 (dd, J = 8.0, 1.5 Hz, 1H), 7.44 (t, J = 8.0 Hz, 1H), 7.23 – 7.10 (m, 2H), 6.95 - 6.78 (m, 2H), 3.44 (s, 3H); ^{13}C NMR (126 MHz, $\text{DMSO-}d_6$) δ = 153.3, 140.1, 134.1, 133.7, 129.3, 129.2, 127.8, 127.6, 127.2, 124.0, 120.3, 111.6, 54.9; IR ν_{max} (neat) 3369, 1599, 1499, 1389, 1348, 1250, 1163, 1110, 751, 705 cm^{-1} ; HRMS (ESI) m/z calculated for $\text{C}_{13}\text{H}_{12}\text{Cl}_2\text{NO}_3\text{S}$ = 331.9910. Found = 331.9905 $[\text{M}+\text{H}]^+$; LCMS (Method A, UV, ES) RT = 1.18 min, $[\text{M}+\text{H}]^+$ = 330, 332, 334, 98% purity.

N-(2-Acetylphenyl)-2,3-dichlorobenzenesulfonamide (31)



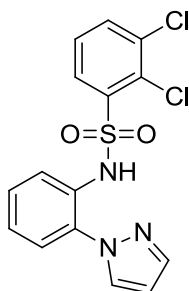
The title compound was prepared from 2-aminoacetophenone (25 mg, 0.19 mmol) and 2,3-dichlorobenzenesulfonyl chloride (50 mg, 0.20 mmol) according to the procedure described for the preparation of **29**. The same work up and purification afforded **31** (45 mg, 71%) as a white solid; ^1H NMR (500 MHz, $\text{DMSO-}d_6$) δ = 12.09 (s, 1H), 8.20 (dd, J = 8.0, 1.0 Hz, 1H), 8.05 (d, J = 8.0 Hz, 1H), 7.97 (dd, J = 8.0, 1.0 Hz, 1H), 7.61 (t, J = 8.0 Hz, 1H), 7.52 (t, J = 8.0 Hz, 1H), 7.36 (d, J = 8.0 Hz, 1H), 7.18 (t, J = 8.0 Hz, 1H), 2.67 (s, 3H); ^{13}C NMR (126 MHz, $\text{DMSO-}d_6$) δ = 203.5, 137.7, 137.7, 135.7, 135.1, 134.5, 133.1, 130.8, 128.8, 128.7, 123.4, 122.5, 117.1, 28.5; IR ν_{max} (neat) 3074, 3010, 1649, 1575, 1491, 1401, 1249, 1163, 924, 763, 707 cm^{-1} ; HRMS (ESI) m/z calculated for $\text{C}_{14}\text{H}_{12}\text{Cl}_2\text{NO}_3\text{S}$ = 343.9910. Found = 343.9909 $[\text{M}+\text{H}]^+$; LCMS (Method A, UV, ES) RT = 1.16 min, $[\text{M}+\text{H}]^+$ = 344, 346, 348, 100% purity.

2,3-Dichloro-*N*-(2-(1-hydroxyethyl)phenyl)benzenesulfonamide (**32**)



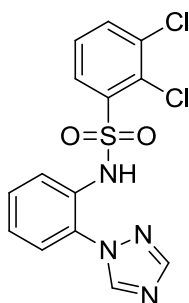
Sodium borohydride (4 mg, 0.11 mmol) was added to a stirring solution of **31** (25 mg, 0.07 mmol) in methanol (0.5 mL) and the reaction mixture was stirred at ambient temperature for 2 h. Additional sodium borohydride (4 mg, 0.11 mmol) was added and the reaction was stirred for a further 4 h. The mixture was then taken up in DMSO (1 mL) and purified by MDAP (Method A). The solvent was evaporated under reduced pressure to afford the title product (14 mg, 53%) as a colourless oil; ^1H NMR (400 MHz, $\text{MeOD-}d_4$) δ = 7.98 (dd, J = 8.0, 1.5 Hz, 1H), 7.80 (dd, J = 8.0, 1.5 Hz, 1H), 7.44 (t, J = 8.0 Hz, 1H), 7.33 (dd, J = 8.0, 1.8 Hz, 1H), 7.16 - 7.05 (m, 2H), 7.01 (dd, J = 8.0, 1.8 Hz, 1H), 5.14 (q, J = 6.5 Hz, 1H), 1.41 (d, J = 6.5 Hz, 4H) (the NH and OH exchangeable protons were not observed); ^{13}C NMR (126 MHz, $\text{DMSO-}d_6$) δ = 140.7, 139.9, 134.8, 134.3, 132.9, 129.8, 128.9, 128.7, 127.3, 126.9, 126.0, 123.5, 65.3, 24.5; LCMS (Method A, UV, ES) RT = 1.03 min, $[\text{M}+\text{H}]^+$ = 344, 346, 348, 100% purity.

***N*-(2-(1*H*-Pyrazol-1-yl)phenyl)-2,3-dichlorobenzenesulfonamide (33)**



The title compound was prepared from 2-(1*H*-pyrazol-1-yl)aniline (70 mg, 0.44 mmol) and 2,3-dichlorobenzenesulfonyl chloride (120 mg, 0.48 mmol) according to the procedure described for the preparation of **29**. The same work up and purification afforded **33** (118 mg, 71%) as a white solid; ¹H NMR (400 MHz, DMSO-*d*₆) δ = 10.9 (s, 1H), 8.23 (d, *J* = 2.0 Hz, 1H), 7.94 - 7.78 (m, 3H), 7.55 (dd, *J* = 8.0, 2.0 Hz, 1H), 7.51-7.43 (m, 2H), 7.35-7.25 (m, 2H), 6.55 (t, *J* = 2.0 Hz, 1H); ¹³C NMR (101 MHz, DMSO-*d*₆) δ = 141.1, 138.2, 135.1, 134.2, 131.4, 130.9, 130.0, 128.8, 128.4, 128.2, 127.9, 126.3, 123.6, 123.5, 107.5; IR ν_{max} (neat) 3068, 1524, 1508, 1438, 1401, 1169, 1155, 757, 704 cm⁻¹; HRMS (ESI) *m/z* calculated for C₁₅H₁₂Cl₂N₃O₂S = 368.0027. Found = 368.0028 [M+H]⁺; LCMS (Method A, UV, ES) RT = 1.23 min, [M+H]⁺ = 368, 370, 372, 100 % purity. Crystallisation solvent MeOH, Crystallisation method = slow evaporation; mp = 152 – 154 °C; Crystal data: C₁₅H₁₁Cl₂N₃O₂S, crystal size 0.44 x 0.19 x 0.11 mm³, *M* = 368.23, monoclinic, space group P2₁/*n*, unit cell dimensions *a* = 7.5758(9), *b* = 8.7573(9), *c* = 23.065(2) Å, α = 90°, β = 91.905(8)°, γ = 90°, *V* = 1529.4(3) Å³, *Z* = 4, *D*_{calc} = 1.599 Mg/m³, F(000) = 752, absorption coefficient = 0.573 mm⁻¹, *T* = 150(2) K, 4880 total reflections measured, 2872 independent, (*R*_{int} = 0.0282) which were used in all calculations. Final *R* indices (for reflections with *I* > 2σ(*I*)) were *R*1 = 0.0367, ω*R*2 = 0.0858; *R* indices (all data) *R*1 = 0.0456, ω*R*2 = 0.0949.

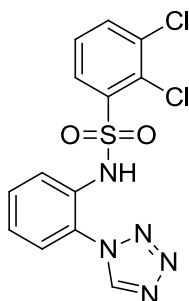
***N*-(2-(1*H*-1,2,4-Triazol-1-yl)phenyl)-2,3-dichlorobenzenesulfonamide (34)**



The title compound was prepared from 2-(1*H*-1,2,4-triazol-1-yl)aniline (54 mg, 0.34 mmol)

and 2,3-dichlorobenzenesulfonyl chloride (91 mg, 0.37 mmol) according to the procedure described for the preparation of **29**. The same work up and purification afforded **34** (76 mg, 60%) as a pale yellow solid; ^1H NMR (400 MHz, $\text{DMSO-}d_6$) δ = 10.35 (br.s, 1H), 8.81 (s, 1H), 8.12 (s, 1H), 7.90 (dd, J = 8.0, 1.5 Hz, 1H), 7.76 (dd, J = 8.0, 1.5 Hz, 1H), 7.55 - 7.51 (m, 1H), 7.49 - 7.38 (m, 3H), 7.34 - 7.28 (m, 1H); ^{13}C NMR (126 MHz, $\text{DMSO-}d_6$) δ = 152.5, 145.3, 139.5, 135.4, 134.8, 132.9, 130.2, 129.9, 129.6, 129.4, 129.0, 128.4, 128.2, 126.6; IR ν_{max} (neat) 3184, 3120, 1515, 1430, 1282, 1166, 768, 703, 675 cm^{-1} HRMS (ESI) m/z calculated for $\text{C}_{14}\text{H}_{11}\text{Cl}_2\text{N}_4\text{O}_2\text{S}$ = 368.9974. Found = 368.9974 $[\text{M}+\text{H}]^+$; LCMS (Method A, UV, ES) RT = 0.96 min, $[\text{M}+\text{H}]^+$ = 369, 371, 373, 99% purity.

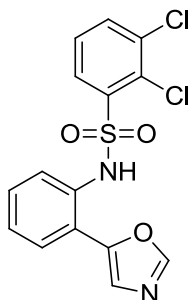
***N*-(2-(1*H*-Tetrazol-1-yl)phenyl)-2,3-dichlorobenzenesulfonamide (35)**



The title compound was prepared from 2-(1*H*-tetrazol-1-yl)aniline (84 mg, 0.34 mmol) and 2,3-dichlorobenzenesulfonyl chloride (91 mg, 0.37 mmol) according to the procedure described for the preparation of **29**. The same work up and purification afforded **35** (56 mg, 47%) as a white solid ^1H NMR (400 MHz, $\text{DMSO-}d_6$) δ = 10.56 (br.s, 1H), 9.60 (s, 1H), 7.93 (dd, J = 8.0, 1.0 Hz, 1H), 7.74 (dd, J = 8.0, 1.0 Hz, 1H), 7.64 - 7.53 (m, 2H), 7.52 - 7.42 (m, 2H), 7.34 - 7.20 (m, 1H); ^{13}C NMR (101 MHz, $\text{DMSO-}d_6$) δ = 144.6, 139.2, 134.8, 134.4, 131.4, 130.4, 130.2, 129.1, 128.9, 128.6, 128.5, 128.2, 127.5; IR ν_{max} (neat) 3149, 1509, 1408, 1352, 1168, 775, 700 cm^{-1} ; HRMS (ESI) m/z calculated for $\text{C}_{13}\text{H}_9\text{Cl}_2\text{N}_5\text{O}_2\text{S}$ = 369.9932. Found = 369.9930 $[\text{M}+\text{H}]^+$; LCMS (Method A, UV, ES) RT = 0.92 min, $[\text{M}+\text{H}]^+$ = 370, 372, 374, 95% purity. Crystallisation solvent MeOH, Crystallisation method = slow evaporation, mp = 188 – 190 $^{\circ}\text{C}$; Crystal data: $\text{C}_{13}\text{H}_9\text{Cl}_2\text{N}_5\text{O}_2\text{S}$, crystal size 0.39 x 0.10 x 0.06 mm^3 , M = 370.21, triclinic, space group $\text{P}\bar{1}$, unit cell dimensions a = 7.4390(9), b = 8.4770(12), c = 13.0579(15) \AA , α = 88.763(11) $^{\circ}$, β = 84.177(10) $^{\circ}$, γ = 64.880(13) $^{\circ}$, V = 741.50(16) \AA^3 , Z = 2, D_{calc} = 1.658 Mg/m^3 , $F(000)$ = 376, absorption coefficient = 0.595 mm^{-1} , T = 150(2) K, 8747 total reflections measured, 3152 independent, (R_{int} = 0.0377) which were used in all calculations. Final R indices (for reflections with $I > 2\sigma(I)$) were $R1$ = 0.0358,

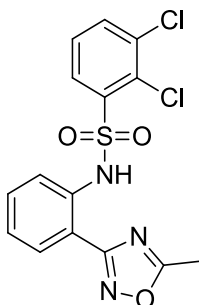
$\omega R2 = 0.0802$; R indices (all data) $R1 = 0.0461$, $\omega R2 = 0.0872$.

2,3-Dichloro-*N*-(2-(oxazol-5-yl)phenyl)benzenesulfonamide (36)



The title compound was prepared from 2-(oxazol-5-yl)aniline (54 mg, 0.34 mmol) and 2,3-dichlorobenzenesulfonyl chloride (91 mg, 0.37 mmol) according to the procedure described for the preparation of **29**. The same work up and purification afforded **36** (77 mg, 61%) as a pale yellow solid; ^1H NMR (400 MHz, $\text{DMSO-}d_6$) $\delta = 10.29$ (s, 1H), 8.39 (s, 1H), 7.92 (dd, $J = 8.0, 1.5$ Hz, 1H), 7.78 (dd, $J = 8.0, 1.5$ Hz, 1H), 7.68 (dd, $J = 7.7, 1.5$ Hz, 1H), 7.60 (s, 1H), 7.49 (t, $J = 8.0$ Hz, 1H), 7.40 (t, $J = 7.7$ Hz, 1H), 7.30 (td, $J = 7.7, 1.5$ Hz, 1H), 6.91 (dd, $J = 7.7, 1.5$ Hz, 1H); ^{13}C NMR (126 MHz, $\text{DMSO-}d_6 + \text{NaHCO}_3$) $\delta = 150.5, 149.7, 147.5, 147.1, 133.6, 131.5, 129.3, 128.9, 128.1, 127.7, 125.3, 125.0, 119.6, 119.4, 116$; HRMS (ESI) m/z calculated for $\text{C}_{15}\text{H}_{11}\text{Cl}_2\text{N}_2\text{O}_3\text{S} = 368.9862$. Found = 368.9860 $[\text{M}+\text{H}]^+$; LCMS (Method A, UV, ES) RT = 1.00 min, $[\text{M}+\text{H}]^+ = 369, 371, 373$, 100% purity.

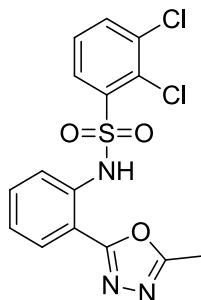
2,3-Dichloro-*N*-(2-(5-methyl-1,2,4-oxadiazol-3-yl)phenyl)benzenesulfonamide (37)



The title compound was prepared from 2-(5-methyl-1,2,4-oxadiazol-3-yl)aniline (50 mg, 0.29 mmol) and 2,3-dichlorobenzenesulfonyl chloride (77 mg, 0.31 mmol) according to the procedure described for the preparation of **29**. The same work up and purification afforded **37** (32 mg, 29%) as a white solid; ^1H NMR (400 MHz, $\text{DMSO-}d_6$) $\delta = 10.44$ (s, 1H), 8.05 (dd, $J = 8.0, 1.5$ Hz, 1H), 7.94 (d, $J = 8.0$ Hz, 2H), 7.66 - 7.37 (m, 3H), 7.28 (br.s, 1H), 2.70 (s, 3H); ^{13}C NMR (126 MHz, $\text{DMSO-}d_6$) $\delta = 177.6, 166.6, 138.7, 135.9, 135.4, 134.8, 132.9, 130.9, 130.3, 129.4, 129.2, 125.7, 121.4, 117.3, 12.5$; IR ν_{max} (neat) 3178, 1599, 1580, 1490, 1344,

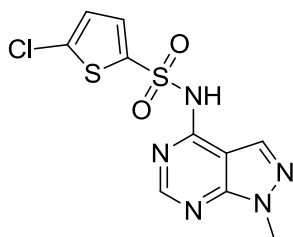
1155, 922, 753, 705 cm^{-1} ; HRMS (ESI) m/z calculated for $\text{C}_{15}\text{H}_{12}\text{Cl}_2\text{N}_3\text{O}_3\text{S}$ = 383.9975. Found = 383.9971 $[\text{M}+\text{H}]^+$; LCMS (Method A, UV, ES) RT = 1.26 min, $[\text{M}+\text{H}]^+$ = 384, 386, 388, 99% purity.

2,3-Dichloro-*N*-(2-(5-methyl-1,3,4-oxadiazol-2-yl)phenyl)benzenesulfonamide (**38**)



The title compound was prepared from 2-(5-methyl-1,3,4-oxadiazol-2-yl)aniline (59 mg, 0.34 mmol) and 2,3-dichlorobenzenesulfonyl chloride (91 mg, 0.37 mmol) according to the procedure described for the preparation of **29**. The same work up and purification afforded **38** (46 mg, 35%) as a white solid. ^1H NMR (400 MHz, $\text{DMSO}-d_6$) δ = 11.23 (s, 1H), 8.20 (dd, J = 8.0, 1.5 Hz, 1H), 7.97 (dd, J = 8.0, 1.5 Hz, 1H), 7.88 (d, J = 7.5 Hz, 1H), 7.61 (t, J = 8.0 Hz, 1H), 7.56 - 7.41 (m, 2H), 7.28 (t, J = 7.5 Hz, 1H), 2.60 (s, 3H); ^{13}C NMR (126 MHz, $\text{DMSO}-d_6$) δ = 164.1, 163.3, 138.3, 136.2, 135.6, 135.0, 133.4, 131.2, 129.4, 129.2, 129.1, 124.9, 118.7, 112.4, 11.1; IR ν_{max} (neat) 3078, 1543, 1496, 1403, 1155, 1168, 747, 705 cm^{-1} ; HRMS (ESI) m/z calculated for $\text{C}_{15}\text{H}_{12}\text{Cl}_2\text{N}_3\text{O}_3\text{S}$ = 383.9971. Found = 383.9967 $[\text{M}+\text{H}]^+$; LCMS (Method A, UV, ES) RT = 1.17 min, $[\text{M}+\text{H}]^+$ = 384, 386, 388, 100% purity.

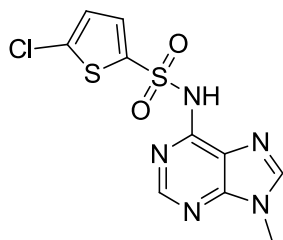
5-Chloro-*N*-(1-methyl-1*H*-pyrazolo[3,4-*d*]pyrimidin-4-yl)thiophene-2-sulfonamide (**39**)



The title compound was prepared from 1-methyl-1*H*-pyrazolo[3,4-*d*]pyrimidin-4-amine (60 mg, 0.40 mmol), 5-chlorothiophene-2-sulfonyl chloride (96 mg, 0.44 mmol) and sodium hydride (11 mg of a 60% w/w dispersion in mineral oil, 0.44 mmol) according to the procedure described for the preparation of **13**. The same work up and purification afforded **39** (21 mg, 16%) as a white solid; ^1H NMR (400 MHz, $\text{DMSO}-d_6$) δ = 13.24 (br.s, 1H), 8.42 (s, 1H), 8.38 (s, 1H), 7.59 (d, J = 4.0 Hz, 1H), 7.19 (d, J = 4.0 Hz, 1H), 3.96 (s, 3H); LCMS

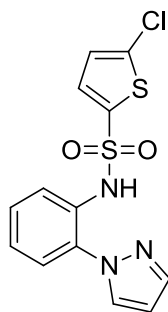
(Method A, UV, ES) RT = 0.80 min, $[M+H]^+ = 330, 332$, 100% purity.

5-Chloro-*N*-(9-methyl-9*H*-purin-6-yl)thiophene-2-sulfonamide (**40**)



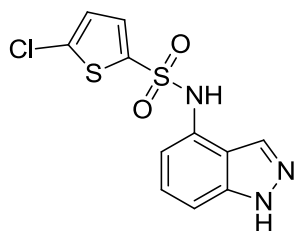
The title compound was prepared from **18** (60 mg, 0.40 mmol), 5-chlorothiophene-2-sulfonyl chloride (87 mg, 0.40 mmol) and sodium hydride (19 mg of a 60% w/w dispersion in mineral oil, 0.48 mmol) according to the procedure described for the preparation of **13**. The same work up and purification afforded **40** (64 mg, 48%) as a white solid; ^1H NMR (400 MHz, DMSO- d_6) $\delta = 12.93$ (br.s, 1H), 8.39 (s, 1H), 8.32 (s, 1H), 7.61 (d, $J = 4.0$ Hz, 1H), 7.16 (d, $J = 4.0$ Hz, 1H), 3.34 (br.s, 3H); IR ν_{max} (neat) 3262, 3086, 1636, 1569, 1411, 1265, 1130, 992, 839, 681, 658 cm^{-1} ; LCMS (Method A, UV, ES) RT = 0.68 min, $[M+H]^+ = 330, 332$, 98% purity.

5-Chloro-*N*-(2-oxo-2,3-dihydro-1*H*-benzimidazol-5-yl)-2-thiophenesulfonamide (**41**)



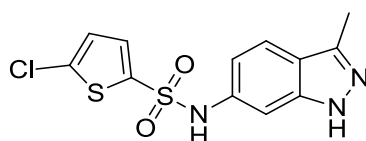
The title compound was prepared from 2-(1*H*-pyrazol-1-yl)aniline (44 mg, 0.28 mmol) and 5-chloro-2-thiophenesulfonyl chloride (60 mg, 0.28 mmol) according to the procedure described for the preparation of **29**. The same work up and purification afforded **41** (73 mg, 78%) as a colourless oil; ^1H NMR (400 MHz, DMSO- d_6) $\delta = 10.56$ (s, 1H), 8.14 (d, $J = 2.5$ Hz, 1H), 7.86 (d, $J = 2.0$ Hz, 1H), 7.65 - 7.56 (m, 1H), 7.54 - 7.47 (m, 1H), 7.46 - 7.37 (m, 2H), 7.11 - 7.06 (m, 2H), 6.55 (t, $J = 2.0$ Hz, 1H); ^{13}C NMR (101 MHz, MeOD- d_4) $\delta = 142.5, 138.7, 138.5, 134.2, 132.8, 131.5, 130.5, 129.0, 128.6, 128.3, 128.2, 123.8, 108.5$; HRMS (ESI) m/z calculated for $\text{C}_{13}\text{H}_{11}\text{Cl}_2\text{N}_3\text{O}_2\text{S} = 339.9981$. Found = 339.9978 $[M+H]^+$; LCMS (Method A, UV, ES) RT = 1.20 min, $[M+H]^+ = 340, 342$, 97% purity.

5-Chloro-*N*-(1*H*-indazol-4-yl)-2-thiophenesulfonamide (42)



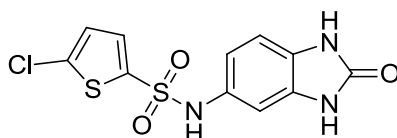
The title compound was prepared from 1*H*-indazol-4-amine (50 mg, 0.38 mmol) and 5-chloro-2-thiophenesulfonyl chloride (90 mg, 0.41 mmol) according to the procedure described for the preparation of **29**. The same work up and purification afforded **42** (81 mg, 67%) as a pale brown solid; ¹H NMR (400MHz, DMSO-*d*₆) δ = 13.12 (s, 1H), 10.83 (s, 1H), 8.14 (s, 1H), 7.40 (d, *J* = 4.0 Hz, 1H), 7.35 - 7.22 (m, 2H), 7.14 (d, *J* = 4.0 Hz, 1H), 6.96 (dd, *J* = 7.0, 1.0 Hz, 1H); LCMS (Method A, UV, ES) RT = 0.67 min, [M+H]⁺ = 314, 316, 100% purity.

5-Chloro-*N*-(3-methyl-1*H*-indazol-6-yl)-2-thiophenesulfonamide (43)



The title compound was prepared from 3-methyl-1*H*-indazol-6-amine (50 mg, 0.34 mmol) and 5-chloro-2-thiophenesulfonyl chloride (81 mg, 0.37 mmol) according to the procedure described for the preparation of **29**. The same work up and purification afforded **43** (45 mg, 40%) as a pale brown solid; ¹H NMR (400 MHz, DMSO-*d*₆) δ = 12.49 (s, 1H), 10.62 (br.s, 1H), 7.60 (d, *J* = 8.5 Hz, 1H), 7.37 (d, *J* = 4.0 Hz, 1H), 7.22 (d, *J* = 1.0 Hz, 1H), 7.16 (d, *J* = 4.0 Hz, 1H), 6.86 (dd, *J* = 8.5, 1.0 Hz, 1H), 2.42 (s, 3H); LCMS (Method A, UV, ES) RT = 0.70 min, [M+H]⁺ = 328, 330, 98% purity.

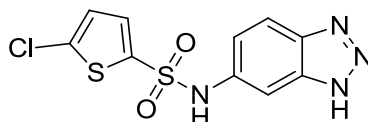
5-Chloro-*N*-(2-oxo-2,3-dihydro-1*H*-benzimidazol-5-yl)-2-thiophenesulfonamide (44)



The title compound was prepared from 5-amino-1,3-dihydro-2*H*-benzimidazol-2-one (41 mg, 0.28 mmol) and 5-chloro-2-thiophenesulfonyl chloride (60 mg, 0.28 mmol) according to the procedure described for the preparation of **29**. The same work up and purification afforded **44**

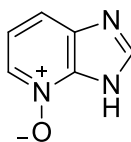
(58 mg, 64%) as a pale brown solid; $^1\text{H NMR}$ (400 MHz, $\text{DMSO-}d_6$) δ = 10.58 (s, 1H), 10.56 (s, 1H), 10.16 (s, 1H), 7.28 (d, J = 4.0 Hz, 1H), 7.17 (d, J = 4.0 Hz, 1H), 6.82 (d, J = 8.0 Hz, 1H), 6.74 (d, J = 2.0 Hz, 1H), 6.68 (dd, J = 8.0, 2.0 Hz, 1H); IR ν_{max} (neat) 3258, 1684, 1640, 1407, 1337, 1152, 796, 656 cm^{-1} ; LCMS (Method A, UV, ES) RT = 0.75 min, $[\text{M}+\text{H}]^+ = 330$, 332, 98% purity.

***N*-1*H*-1,2,3-Benzotriazol-5-yl-5-chloro-2-thiophenesulfonamide (45)**



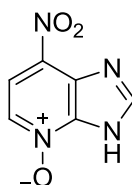
The title compound was prepared from 5-amino-1*H*-1,2,3-benzotriazole (50 mg, 0.38 mmol) and 5-chloro-2-thiophenesulfonyl chloride (90 mg, 0.41 mmol) according to the procedure described for the preparation of **29**. The same work up and purification afforded **45** (64 mg, 53%) as a pale pink solid; $^1\text{H NMR}$ (400 MHz, $\text{DMSO-}d_6$) δ = 15.61 (br.s, 1H), 10.84 (br.s, 1H), 7.88 (br.s, 1H), 7.55 (br.s, 1H), 7.41 (d, J = 4.0 Hz, 1H), 7.27 - 7.13 (m, 2H); LCMS (Method A, UV, ES) RT = 0.56 min, $[\text{M}+\text{H}]^+ = 315$, 317, 99% purity.

3*H*-Imidazo[4,5-*b*]pyridine 4-oxide (47)



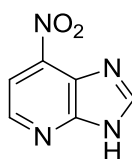
Hydrogen peroxide (43.2 mL, 423 mmol) was added to a stirring solution of 4-azabenzimidazole **46** (5.76 g, 48.4 mmol) in glacial acetic acid (43.2 mL) and the reaction mixture was stirred at 80 °C for 3 h. More hydrogen peroxide (3.6 mL, 35 mmol) was added and the reaction was heated at 80 °C for further 6 h. The mixture was concentrated under reduced pressure to about 10 mL, whereupon the product precipitated from the solution. The product was filtered, washed with water (15 mL) and dried under reduced pressure to afford the title compound (4.2 g, 64%) as a pale yellow solid; $^1\text{H NMR}$ (400 MHz, $\text{DMSO-}d_6$) δ = 10.20 (br.s, 1H), 8.41 (s, 1H), 8.18 (d, J = 6.3 Hz, 1H), 7.59 (d, J = 6.3 Hz, 1H), 7.21 (dd, J = 8.0, 6.3 Hz, 1H); LCMS (Method A, UV, ES) RT = 0.20 min, $[\text{M}+\text{H}]^+ = 135.9$, 100% purity. These data were in agreement with those reported in the literature.¹⁰⁵

7-Nitro-3*H*-imidazo[4,5-*b*]pyridine 4-oxide (48)



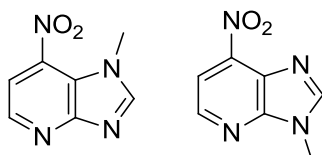
Fuming nitric acid (25 mL of a 70 wt% aqueous solution, 559 mmol) was added dropwise to a solution of **47** (4.0 g, 29.6 mmol) in TFA (28 mL) at ambient temperature. The mixture was then heated at 90 °C for 3 h, cooled and then poured onto crushed ice (50 mL). The mixture was neutralised with concentrated ammonium hydroxide while maintaining the temperature below 30 °C. The resulting solid was filtered, washed with ice water (15 mL), and dried under reduced pressure to afford the title compound (1.16 g, 22%) as a yellow solid; ¹H NMR (400 MHz, DMSO-*d*₆) δ = 8.03 (s, 1H), 7.90 (d, *J* = 7.0 Hz, 1H), 7.72 (d, *J* = 7.0 Hz, 1H), 7.0 (br.s, 1H); LCMS (Method B, UV, ES) RT = 0.30 min, [M+H]⁺ = 181, 100% purity. These data were in agreement with those reported in the literature.¹⁰⁵

7-Nitro-3*H*-imidazo[4,5-*b*]pyridine (49)



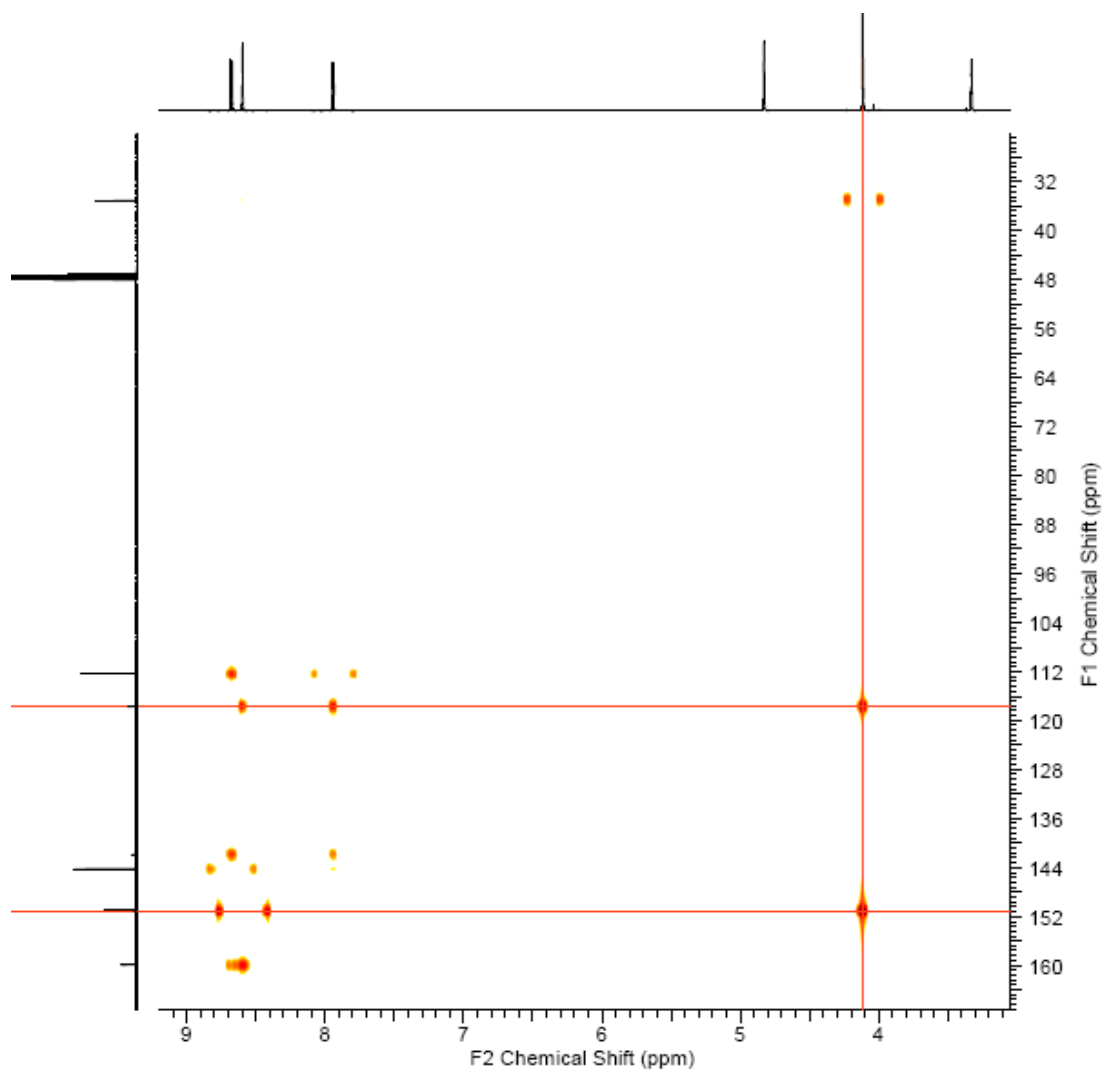
Phosphorus trichloride (4.8 mL, 55 mmol) was added dropwise to a solution of **48** (1.10g, 6.1 mmol) in anhydrous MeCN (20 mL) and the mixture was heated at 80 °C for 2 h. The reaction was cooled and the solid precipitate formed was collected by filtration, washed with ether (30 mL) and then with sodium carbonate (10 mL of a saturated aqueous solution, caution-exothermic). The solid was then crystallised from water and dried under reduced pressure to afford the title compound (400 mg, 40%) as a beige coloured solid; ¹H NMR (400 MHz, DMSO-*d*₆) δ = 13.70 (br.s, 1H), 8.78 (s, 1H), 8.68 (d, *J* = 5.0 Hz, 1H), 8.00 (d, *J* = 5.0 Hz, 1H); LCMS (Method B, UV, ES) RT = 0.42 min, [M+H]⁺ = 165, 100% purity. These data were in agreement with those reported in the literature.¹⁰⁵

1-Methyl-7-nitro-1*H*-imidazo[4,5-*b*]pyridine (50) & 3-methyl-7-nitro-3*H*-imidazo[4,5-*b*]pyridine (51)

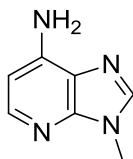


Methyl iodide (0.07 mL, 1.1 mmol) was added to a mixture of **49** (150 mg, 0.91 mmol) and cesium carbonate (357 mg, 1.1 mmol) in anhydrous DMF (1 mL), and the reaction mixture was stirred at ambient temperature for 18 h. LCMS showed peak for mixture of regioisomers. Water (10 mL) was added and the product was extracted with ethyl acetate (2 x 30 mL). The combined organic extracts were dried using a hydrophobic frit, and concentrated to afford a green coloured solid. The sample was taken up in DMSO (3 mL) and purified by MDAP (Method A). The appropriate fractions were combined and the solvent was dried under reduced pressure to give the two separated products as white solids: **50** (40 mg, 25%); ^1H NMR (600 MHz, MeOD- d_4) δ = 8.66 (d, J = 5.1 Hz, 1H), 8.58 (s, 1H), 7.92 (d, J = 5.1 Hz, 1H), 4.09 (s, 3H); ^{13}C NMR (151 MHz, MeOD- d_4) δ = 161.5, 152.6, 145.8, 143.4, 119.3, 113.9, 36.7; IR ν_{max} (neat) 1538, 1502, 1348, 1325, 1305, 847, 797, 742 cm^{-1} ; LCMS (Method A, UV, ES) RT = 0.50 min, $[\text{M}+\text{H}]^+ = 179$, 97% purity; and **51** (100 mg, 61%); ^1H NMR (600 MHz, MeOD- d_4) δ = 8.90 - 8.38 (m, 2H), 7.96 (d, J = 5.1 Hz, 1H), 3.97 (s, 3H); ^{13}C NMR (101 MHz, DMSO- d_6) δ = 151.1, 150.2, 144.2, 143.4, 126.4, 111.4, 30.1; IR ν_{max} (neat) 1525, 1504, 1474, 1354, 1325, 1262, 844, 796, 742 cm^{-1} ; LCMS (Method A, UV, ES) RT = 0.47 min, $[\text{M}+\text{H}]^+ = 179$, 100% purity.

HMBC experiment of **50** shows key ^1H - ^{13}C HMBC correlations between the *N*-methyl protons (4.09 ppm) to the carbon at the C8-position (117.6 ppm) and C2-position (151.3 ppm)



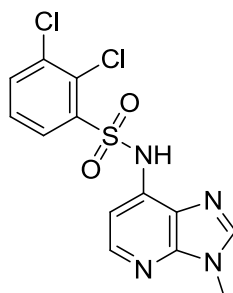
3-Methyl-3*H*-imidazo[4,5-*b*]pyridin-7-amine (**52**)



A solution of **51** (100 mg, 0.56 mmol) in ethanol (5 mL) was added to a flask containing palladium-on-carbon (60 mg of a 10% w/w, 0.56 mmol) under vacuum. The flask was back filled with N₂, evacuated and filled with H₂ using the burette apparatus. The reaction mixture was stirred under H₂ for 3 h, filtered through a celite pad, washed with ethanol (20 mL) and concentrated under reduced pressure to afford the title compound as a yellow solid (64 mg, 77%); ¹H NMR (400 MHz, MeOD-*d*₄) δ = 8.00 (s, 1H), 7.89 (d, *J* = 5.5 Hz, 1H), 6.47 (d, *J* = 5.5 Hz, 1H), 3.81 (s, 3H); the exchangeable NH₂ protons were not observed; ¹³C NMR (101 MHz, MeOD-*d*₄) δ = 148.8, 148.4, 146.0, 142.6, 123.9, 103.8, 30.2; IR ν_{max} (neat) 3337,

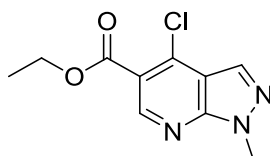
3187, 1600, 1576, 1347, 1283, 1205, 833 cm^{-1} ; HRMS (ESI) m/z calculated for $\text{C}_7\text{H}_9\text{N}_4 = 149.0827$. Found = 149.0820 $[\text{M}+\text{H}]^+$; LCMS (Method B, UV, ES) RT = 0.42 min, $[\text{M}+\text{H}]^+ = 149$, 100% purity.

2,3-Dichloro-*N*-(3-methyl-3*H*-imidazo[4,5-*b*]pyridin-7-yl)benzenesulfonamide (53)



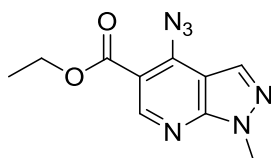
Compound **52** (30 mg, 0.20 mmol) was added to a suspension of sodium hydride (10 mg of a 60% w/w dispersion in mineral oil, 0.24 mmol) in anhydrous DMF (1 mL) at ambient temperature. Once the effervescence ceased (~5 min), 2,3-dichlorobenzenesulfonyl chloride (55 mg, 0.22 mmol) was added and the reaction mixture was stirred under nitrogen at ambient temperature for 18 h. LCMS analysis showed very small amount of the desired product. Further equivalents of sodium hydride (10 mg of a 60% w/w dispersion in mineral oil, 0.24 mmol) and 2,3-dichlorobenzenesulfonyl chloride (55 mg, 0.22 mmol) were added and the reaction was left to stir at ambient temperature for a further 18 h. No substantial improvement was observed. Water (10 mL) was added and the product was extracted with ethyl acetate (2 x 30 mL). The combined organic extracts were evaporated under reduced pressure and the sample was taken up in DMSO (1 mL) and purified by MDAP (Method B). The solvent was evaporated under reduced pressure to afford the title compound (7 mg, 10%) as a white solid; ^1H NMR (400 MHz, $\text{MeOD-}d_4$) $\delta = 8.23$ (dd, $J = 8.0, 1.5$ Hz, 1H), 8.18 (s, 1H), 8.08 (d, $J = 5.5$ Hz, 1H), 7.76 (dd, $J = 8.0, 1.5$ Hz, 1H), 7.47 (t, $J = 8.0$ Hz, 1H), 7.13 (d, $J = 5.5$ Hz, 1H), 3.84 (s, 3H); the exchangeable NH proton was not observed; LCMS (Method B, UV, ES) RT = 0.64 min, $[\text{M}+\text{H}]^+ = 357, 359, 361$, 99% purity; LCMS (Method A, UV, ES) RT = 0.85 min, $[\text{M}+\text{H}]^+ = 357, 359, 361$, 99% purity.

Ethyl 4-chloro-1-methyl-1*H*-pyrazolo[3,4-*b*]pyridine-5-carboxylate (56)



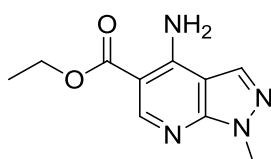
1-Methyl-1*H*-pyrazol-5-amine (4.85 g, 49.9 mmol) and diethyl ethoxymethylenemalonate (10 mL, 50 mmol) were heated at 110 °C for 1.5 h. The ethanol by-product was removed by evaporation under reduced pressure. Phosphoryl trichloride (12.1 mL, 130 mmol) was added and the mixture was heated at 110 °C for 3.5 h. The mixture was cooled to room temperature and MeCN (5 mL) was added, and then the solution was further cooled down to 10 °C. Water (80 mL) was slowly added maintaining the temperature below 10 °C and the suspension was stirred at ambient temperature overnight. The resultant solid was collected by filtration, washed with minimum amount of water and dried under reduced pressure to afford the title compound (6.7 g, 54%) as a white solid; ¹H NMR (400 MHz, DMSO-*d*₆) δ = 8.96 (s, 1H), 8.40 (s, 1H), 4.38 (q, *J* = 7.0 Hz, 2H), 4.10 (s, 3H), 1.36 (t, *J* = 7.0 Hz, 3H); ¹³C NMR (101 MHz, DMSO-*d*₆) δ = 163.6, 151.0, 150.7, 137.8, 132.2, 118.0, 115.1, 61.5, 34.2, 14.0. LCMS (Method A, UV, ES): RT = 1.00 min, [M+H]⁺ = 240, 242, 97% purity. These data were in agreement with those reported in the literature.¹⁰⁹

Ethyl 4-azido-1-methyl-1*H*-pyrazolo[3,4-*b*]pyridine-5-carboxylate (**57**)



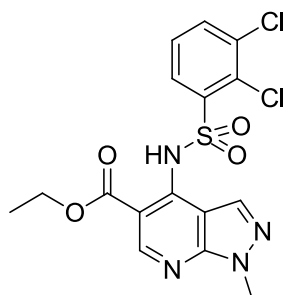
Sodium azide (0.56 g, 8.7 mmol) was added to a stirred solution of **56** (1.97 g, 8.2 mmol) in anhydrous DMF (100 mL) and the mixture was stirred at ambient temperature for 72 h. The solution was concentrated under reduced pressure, and the residue was partitioned between ether (50 mL) and water (40 mL). The ether layer was separated, washed with water (2 x 30 mL), dried using a hydrophobic frit, and evaporated under reduced pressure to afford the title compound (1.91 g, 89%) as a yellow solid; ¹H NMR (400 MHz, DMSO-*d*₆) δ = 8.87 (s, 1H), 8.40 (s, 1H), 4.35 (q, *J* = 7.0 Hz, 2H), 4.07 (s, 3H), 1.35 (t, *J* = 7.0 Hz, 3H); LCMS (Method A, UV, ES) RT = 0.88 min, [M+H]⁺ = 247, 95% purity. These data were in agreement with those reported in the literature.¹⁰⁹

Ethyl 4-amino-1-methyl-1*H*-pyrazolo[3,4-*b*]pyridine-5-carboxylate, Hydrochloride (**59**)



A solution of **57** (1.91 g, 7.8 mmol) in dry THF (100 mL) was treated slowly with triphenylphosphine (2.04 g, 7.8 mmol) and the mixture was stirred at ambient temperature for 2.5 h. The mixture was concentrated under reduced pressure and the residue was then dissolved in a mixture of ethanol (95 mL) and water (45 mL). The solution was allowed to stand at ambient temperature overnight, then concentrated HCl (4.7 mL of a 37 wt% aqueous solution) was added and the mixture was left to stir for 4 h. The mixture was concentrated under reduced pressure, and the pale yellow residue was triturated with DCM (60 mL) to afford the title compound (1.36 g, 68%) as a white solid; $^1\text{H NMR}$ (400 MHz, $\text{DMSO-}d_6$) δ = 8.84 (br.s, 1H), 8.69 (s, 1H), 8.53 (br.s, 1H), 8.41 (s, 1H), 4.32 (q, J = 7.0 Hz, 2H), 3.99 (s, 3H), 1.34 (t, J = 7.0 Hz, 3H); ^{13}C (100 MHz, $\text{DMSO-}d_6$) δ = 165.9, 152.6, 147.4, 145.9, 133.9, 105.3, 99.7, 60.7, 35.2, 14.1. LCMS (Method A, UV, ES) RT = 0.62 min, $[\text{M}+\text{H}]^+ = 221$, 100% purity. These data were in agreement with those reported in the literature.¹⁰⁹

Ethyl 4-(2,3-dichlorophenylsulfonamido)-1-methyl-1*H*-pyrazolo[3,4-*b*]pyridine-5-carboxylate (**60**)



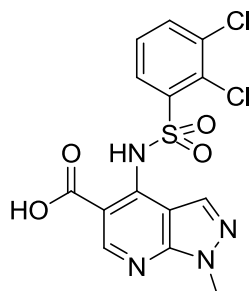
Method 1.

2,3-Dichlorobenzenesulfonamide (47 mg, 0.21 mmol) was added to a stirred solution of **59** (50 mg, 0.21 mmol) in anhydrous DMF (1 mL). Potassium carbonate (32 mg, 0.23 mmol) was added and the reaction mixture was stirred at ambient temperature for 24 h, then heated at 50 °C for a further 48 h. The mixture was concentrated and then taken up in ethyl acetate (10 mL). The organic phase was washed with HCl (5 mL of a 2 M aqueous solution), dried using a hydrophobic frit and concentrated under reduced pressure. The sample was taken up in 1:1 DMSO-MeOH (1 mL) and purified by MDAP (Method A). The solvent was evaporated under reduced pressure to afford the title compound (34 mg, 37%) as a white solid; $^1\text{H NMR}$ (400 MHz, $\text{DMSO-}d_6$) δ = 12.4 (br.s, 1H), 8.92 (s, 1H), 8.34 (dd, J = 8.0, 1.0 Hz, 1H), 8.28 (s, 1H), 7.96 (dd, J = 8.0, 1.0 Hz, 1H), 7.59 (t, J = 8.0 Hz, 1H), 4.37 (q, J = 7.0 Hz, 2H), 3.98 (s, 3H), 1.32 (t, J = 7.0 Hz, 3H); LCMS (Method A, UV, ES) RT = 1.26 min, $[\text{M}+\text{H}]^+ = 429, 431, 433$, 98% purity.

Method 2.

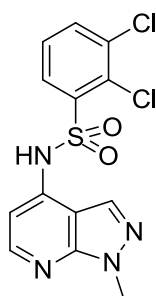
A mixture of **56** (40 mg, 0.17 mmol), 2,3-dichlorobenzene sulfonamide (42 mg, 0.18 mmol), Xantphos (19 mg, 0.03 mmol), cesium carbonate (110 mg, 0.34 mmol) and palladium(II)acetate (4 mg, 0.02 mmol) were degassed with N₂ for 5 min and was then heated at 150 °C in a microwave for 30 min. The mixture was filtered through celite, rinsed with methanol in DCM (10 mL of a 1:10 mixture), and the filtrate was concentrated under reduced pressure. The sample was taken up in 1:1 MeOH-DMSO (1 mL) and purified by MDAP (Method A). The solvent was evaporated under reduced pressure to afford the title compound (46 mg, 63%) as a white solid; mp = 178 – 179 °C; ¹H NMR (400 MHz, DMSO-*d*₆) δ = 12.4 (br.s, 1H), 8.92 (s, 1H), 8.34 (dd, *J* = 8.0, 1.0 Hz, 1H), 8.28 (s, 1H), 7.96 (dd, *J* = 8.0, 1.0 Hz, 1H), 7.59 (t, *J* = 8.0 Hz, 1H), 4.37 (q, *J* = 7.0 Hz, 2H), 3.98 (s, 3H), 1.32 (t, *J* = 7.0 Hz, 3H); HRMS (ESI) *m/z* calculated for C₁₆H₁₅Cl₂N₄O₄S = 429.0191. Found = 429.0191 [M+H]⁺; LCMS (Method A, UV, ES) RT = 1.26 min, [M+H]⁺ = 429, 431, 433, 99% purity.

4-(2,3-Dichlorophenylsulfonamido)-1-methyl-1*H*-pyrazolo[3,4-*b*]pyridine-5-carboxylic acid (**61**)



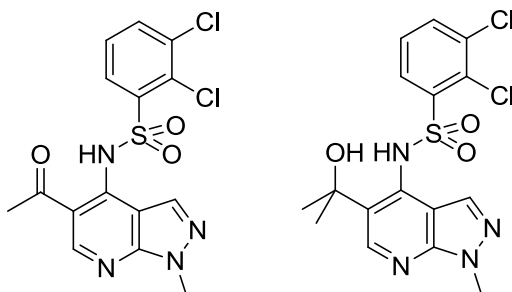
Sodium hydroxide (1.34 mL of a 2 M aqueous solution, 2.68 mmol) was added to a stirred solution of **60** (115 mg, 0.27 mmol) in ethanol (2.5 mL) and the reaction was stirred at ambient temperature for 18 h. The reaction mixture was evaporated under reduced pressure and was treated with HCl (2 M aqueous solution) until a precipitate formed. The solid was collected by filtration, washed with water and dried under reduced pressure at 40 °C to afford the title compound (93 mg, 82%) as a pale brown solid; ¹H NMR (400 MHz, DMSO-*d*₆) δ = 14.5 (br.s, 1H), 8.92 (s, 1H), 8.30 (s, 1H), 8.25 (dd, *J* = 8.0, 2.0 Hz, 1H), 7.90 (dd, *J* = 8.0, 2.0 Hz, 1H), 7.55 (t, *J* = 8.0 Hz, 1H), 3.95 (s, 3H); the exchangeable COOH proton was not observed; LCMS (Method A, UV, ES) RT = 0.84 min, [M+H]⁺ = 401, 403, 405, 100% purity.

2,3-Dichloro-*N*-(1-methyl-1*H*-pyrazolo[3,4-*b*]pyridin-4-yl)benzenesulfonamide (62)



A solution of **61** (50 mg, 0.13 mmol) in anhydrous DMF (0.5 mL) was heated in the microwave at 190 °C for 3 h. The crude sample was concentrated and taken up in 1:1 MeOH-DMSO (1 mL) and purified by MDAP (Method B). The solvent was evaporated under reduced pressure to afford the title compound (13 mg, 28%) as a white solid; ¹H NMR (400 MHz, MeOD-*d*₄) δ = 8.19 (s, 1H), 8.11 (d, *J* = 8.0 Hz, 1H), 7.98 (d, *J* = 5.5 Hz, 1H), 7.64 (d, *J* = 8.0 Hz, 1H), 7.37 (t, *J* = 8.0 Hz, 1H), 6.76 (d, *J* = 5.5 Hz, 1H), 3.96 (s, 3H); LCMS (Method B, UV, ES) RT = 0.70 min, [M+H]⁺ = 357, 359, 361, 98% purity.

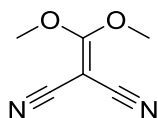
N-(5-Acetyl-1-methyl-1*H*-pyrazolo[3,4-*b*]pyridin-4-yl)-2,3-dichlorobenzenesulfonamide (63) & 2,3-dichloro-*N*-(5-(2-hydroxypropan-2-yl)-1-methyl-1*H*-pyrazolo[3,4-*b*]pyridin-4-yl)benzenesulfonamide (64)



Sodium hydride (9 mg of a 60% w/w dispersion in mineral oil, 0.23 mmol) was added to a stirred solution of **60** (100 mg, 0.23 mmol) in anhydrous THF (1 mL) at 0 °C. The mixture was stirred for 10 min and was then cooled to -78 °C. Methylmagnesium bromide in dibutyl ether (0.23 mL of a 1 M solution, 0.23 mmol) was added dropwise and the reaction was allowed to stir for 2 h. LCMS showed major peak for starting material along with two small peaks for the ketone and alcohol products. The reaction vessel was warmed to 0 °C and left to stir for an hour. LCMS showed no change in the composition of the reaction mixture. The mixture was cooled to -78 °C and a further equivalent of methylmagnesium bromide in dibutyl ether (0.23 mL of a 1 M solution, 0.23 mmol) was added to the solution. The reaction was left to warm to ambient temperature over 4 h. LCMS analysis showed significant

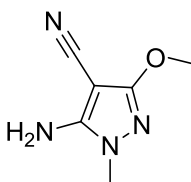
amounts of both the ketone and alcohol products. The reaction mixture was quenched with ammonium chloride (10 mL of a saturated aqueous solution) and extracted with ethyl acetate (2 x 30 mL). The combined organic extracts were dried using a hydrophobic frit, and concentrated under reduced pressure. The sample was taken up in DMSO (1 mL), and then purified by MDAP (Method A). The appropriate fractions were combined and the solvent was evaporated under reduced pressure to afford two products as white solids: **63** (8 mg, 8%); $^1\text{H NMR}$ (400 MHz, CDCl_3) δ = 13.9 (s, 1H), 8.98 (s, 1H), 8.54 (s, 1H), 8.24 (dd, J = 8.0, 2.0 Hz, 1H), 7.67 (dd, J = 8.0, 2.0 Hz, 1H), 7.38 (t, J = 8.0 Hz, 1H), 4.06 (s, 3H), 2.78 (s, 3H); LCMS (Method A, UV, ES) RT = 1.09 min, $[\text{M}+\text{H}]^+$ = 399, 401, 403, 95% purity; and **64** (23 mg, 23%); $^1\text{H NMR}$ (400 MHz, $\text{DMSO}-d_6$) δ = 12.7 (br.s, 1H), 8.34 (s, 1H), 8.16 (s, 1H), 8.09 (dd, J = 8.0, 1.0 Hz, 1H), 7.88 (dd, J = 8.0, 1.0 Hz, 1H), 7.55 (t, J = 8.0 Hz, 1H), 3.96 (s, 3H), 1.47 (s, 6H); the exchangeable OH proton was not observed; LCMS (Method A, UV, ES) RT = 0.88 min, $[\text{M}+\text{H}]^+$ = 415, 417, 419, 98% purity

2-(Dimethoxymethylene)malononitrile (**66**)¹¹²



A mixture of tetracyanoethylene (6.4 g, 50 mmol) and urea (1.0 g, 17 mmol) in MeOH (25 mL) was stirred at 50 °C for 0.5 h. Ether (250 mL) was added and the solution was chilled to -78 °C. The precipitate formed was separated by filtration while cold, and dried to afford the title compound (2.0 g, 29%) as an off-white solid; $^1\text{H NMR}$ (400 MHz, $\text{MeOD}-d_4$) δ = 4.20 (s, 6H); LCMS (Method A, UV, ES) RT = 0.52 min, $[\text{M}+\text{H}]^+$ = 139, 100% purity. These data were in agreement with those reported in the literature.¹¹²

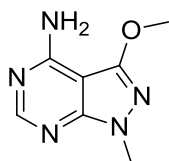
5-Amino-3-methoxy-1-methyl-1H-pyrazole-4-carbonitrile (**67**)¹¹²



Methylhydrazine (0.38 mL, 7.2 mmol) was added to a stirred solution of **66** (1.0 g, 7.2 mmol) in MeOH (25 mL) and the reaction mixture was heated at reflux for 2.5 h. The solvent was evaporated under reduced pressure. The solid residue was loaded preabsorbed on Florisil and

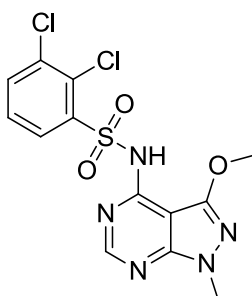
purified on a 70 g silica column using a gradient of 0-100% ethyl acetate-cyclohexane over 40 min. The appropriate fractions were combined and evaporated under reduced pressure to afford the title compound (640 mg, 58%) as a white solid; ^1H NMR (400 MHz, $\text{DMSO-}d_6$) δ = 6.54 (s, 2H), 3.75 (s, 3H), 3.38 (s, 3H); LCMS (Method A, UV, ES) RT = 0.47 min, $[\text{M}+\text{H}]^+ = 153$, 96% purity. These data were in agreement with those reported in the literature.¹¹²

3-Methoxy-1-methyl-1*H*-pyrazolo[3,4-*d*]pyrimidin-4-amine (68)



A mixture of **67** (550 mg, 3.61 mmol) and formamide (10 mL, 251 mmol) was heated at 185 °C for 4 h. The mixture was cooled to ambient temperature and was diluted with ethyl acetate (100 mL) and water (100 mL). The organic phase was separated, dried using a hydrophobic frit and evaporated under reduced pressure to give the crude product. The samples was taken up in DMSO (4 mL) and purified by MDAP (Method A). The appropriate fractions were combined and the solvent was evaporated under reduced pressure to afford the title compound (250 mg 39%) as a white solid; ^1H NMR (400 MHz, $\text{DMSO-}d_6$) δ = 8.10 (s, 1H), 7.09 (br.s., 2H), 3.96 (s, 3H), 3.71 (s, 3H); LCMS (Method A, UV, ES) RT = 0.35 min, $[\text{M}+\text{H}]^+ = 180$, 100% purity.

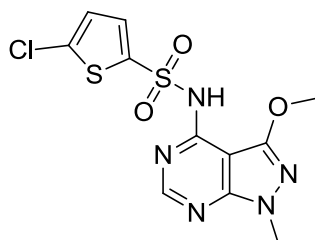
2,3-Dichloro-*N*-(3-methoxy-1-methyl-1*H*-pyrazolo[3,4-*d*]pyrimidin-4-yl)benzenesulfonamide (69)



The title compound was prepared from **68** (50 mg, 0.28 mmol), 2,3-dichlorobenzenesulfonyl chloride (75 mg, 0.31 mmol) and sodium hydride (13 mg of a 60% w/w dispersion in mineral oil, 0.34 mmol) according to the procedure described for the preparation of **105**. The same work up and purification afforded **69** (42 mg, 39%) as a white solid; ^1H NMR (400 MHz,

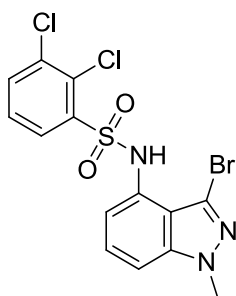
DMSO- d_6) δ = 12.37 (br.s, 1H), 8.26 (s, 1H), 8.11 (dd, J = 8.0, 1.5 Hz, 1H), 7.91 (dd, J = 8.0, 1.5 Hz, 1H), 7.57 (t, J = 8.0 Hz, 1H), 3.89 (s, 3H), 3.80 (s, 3H); ^{13}C NMR (151 MHz, DMSO- d_6) δ = 156.5, 150.9, 150.4, 148.1, 142.3, 133.8, 133.8, 129.3, 128.3, 128.0, 91.3, 56.0, 33.4; HRMS (ESI) m/z calculated for $\text{C}_{13}\text{H}_{12}\text{Cl}_2\text{N}_5\text{O}_3\text{S}$ = 388.0038. Found = 388.0033 $[\text{M}+\text{H}]^+$; LCMS (Method A, UV, ES) RT = 0.96 min, $[\text{M}+\text{H}]^+$ = 388, 390, 392, 100% purity.

5-Chloro-*N*-(3-methoxy-1-methyl-1*H*-pyrazolo[3,4-*d*]pyrimidin-4-yl)thiophene-2-sulfonamide (70)



The title compound was prepared from **68** (50 mg, 0.28 mmol), 5-chlorothiophene-2-sulfonyl chloride (67 mg, 0.31 mmol) and sodium hydride (13 mg of a 60% w/w dispersion in mineral oil, 0.34 mmol) according to the procedure described for the preparation of **105**. The same work up and purification afforded **70** (47 mg, 47%) as a white solid; ^1H NMR (400 MHz, DMSO- d_6) δ = 12.26 (br.s, 1H), 8.24 (s, 1H), 7.62 (d, J = 4.0 Hz, 1H), 7.20 (d, J = 4.0 Hz, 1H), 3.94 (s, 3H), 3.79 (s, 3H); LCMS (Method A, UV, ES) RT = 0.91 min, $[\text{M}+\text{H}]^+$ = 360, 362, 100% purity.

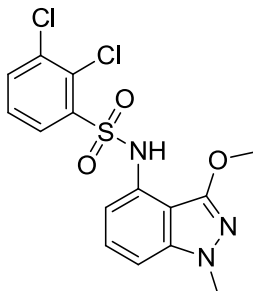
***N*-(3-Bromo-1-methyl-1*H*-indazol-4-yl)-2,3-dichlorobenzenesulfonamide (72)**



The title compound was prepared from 3-bromo-1-methyl-1*H*-indazol-4-amine (150 mg, 0.66 mmol) and 2,3-dichlorobenzenesulfonyl chloride (180 mg, 0.73 mmol) according to the procedure described for the preparation of **29**. The same work up, followed by purification on a 20 g silica column, using a gradient of 0-100% ethyl acetate-cyclohexane over 30 min, and evaporation of the solvent under reduced pressure afforded **72** (192 mg, 67%) as a yellow solid; ^1H NMR (400 MHz, MeOD- d_4) δ = 8.00 (dd, J = 8.0, 1.5 Hz, 1H), 7.78 (dd, J = 8.0, 1.5

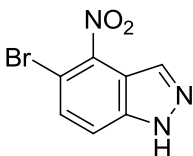
Hz, 1H), 7.42 (t, $J = 8.0$ Hz, 1H), 7.35 (d, $J = 7.5$ Hz, 1H), 7.26 (t, $J = 7.5$ Hz, 1H), 6.85 (d, $J = 7.5$ Hz, 1H), 3.99 (s, 3H); LCMS (Method A, UV, ES) RT = 1.17 min, $[M+H]^+ = 434, 436, 438, 440, 99\%$ purity.

2,3-Dichloro-*N*-(3-methoxy-1-methyl-1*H*-indazol-4-yl)benzenesulfonamide (73)



A suspension of **72** (40 mg, 0.09 mmol), sodium *tert*-butoxide (27 mg, 0.28 mmol) and copper powder (2 mg, 0.03 mmol) in anhydrous MeOH (1 mL) was sealed in a Reacti-VialTM and heated to 150 °C for 18 h. The reaction was allowed to cool to ambient temperature. Several drops of HCl (2 M aqueous solution) were added and the reaction mixture was diluted with DMSO (1 mL) and filtered through a small pad of celite. The filtrate was purified on the MDAP (Method B), and the appropriate fractions were combined and dried under reduced pressure to afford the title compound (14 mg, 39%) as a brown gum; ¹H NMR (400 MHz, CDCl₃) $\delta = 8.32$ (br.s, 1H), 8.14 (dd, $J = 8.0, 1.0$ Hz, 1H), 7.61 (dd, $J = 8.0, 1.0$ Hz, 1H), 7.32 (t, $J = 8.0$ Hz, 1H), 7.15 (t, $J = 8.0$ Hz, 1H), 6.97 (d, $J = 8.0$ Hz, 1H), 6.82 (d, $J = 8.0$ Hz, 1H), 4.13 (s, 3H), 3.80 (s, 3H); ¹³C NMR (101 MHz, CDCl₃) $\delta = 154.9, 142.9, 138.4, 135.7, 134.8, 130.6, 130.5, 130.2, 128.6, 127.1, 105.1, 104.1, 102.9, 56.6, 35.2$; IR ν_{\max} (neat) 3347, 1542, 1392, 1333, 1168, 1121, 956, 735, 701 cm⁻¹; HRMS (ESI) m/z calculated for C₁₅H₁₄Cl₂N₃O₃S = 386.0133. Found = 386.0135 $[M+H]^+$; LCMS (Method A, UV, ES) RT = 1.19 min, $[M+H]^+ = 386, 388, 390$ 100% purity.

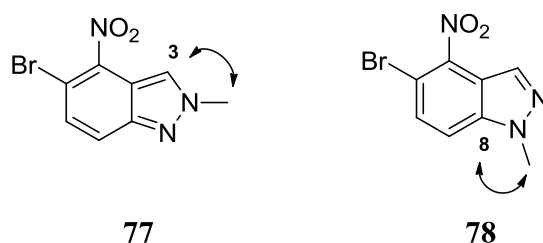
5-Bromo-4-nitro-1*H*-indazole (75)



5-Bromo-1*H*-indazole (1 g, 5.1 mmol) was dissolved in concentrated sulfuric acid (20 mL of 98 wt% aqueous solution, 380 mmol) and was cooled to 0 °C. Fuming nitric acid (1.0 mL of a 70 wt% aqueous solution, 22.6 mmol) was added dropwise and the reaction was maintained

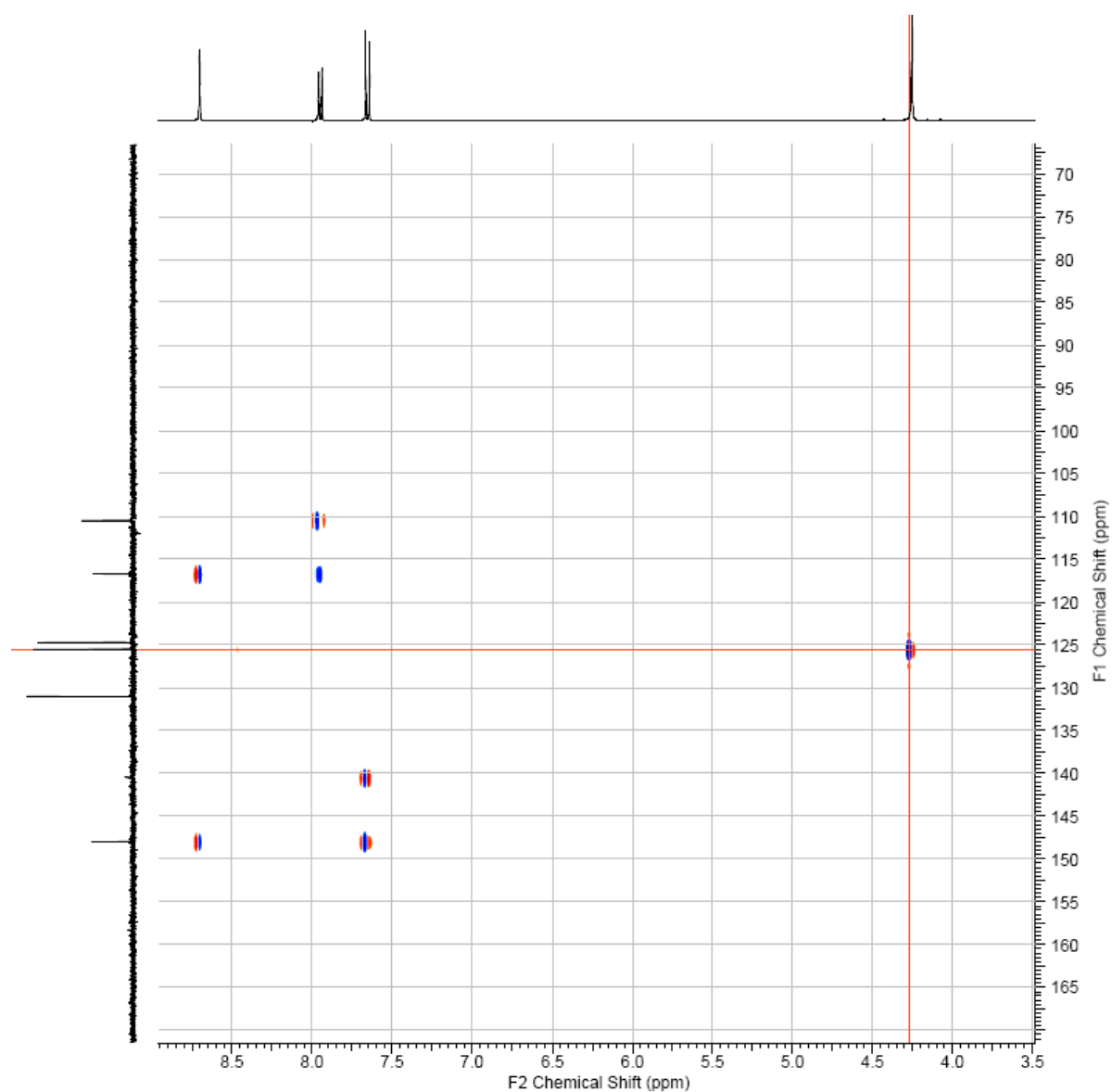
for 1 h at 0 °C. The reaction mixture was poured onto ice water (100 mL) and the precipitate was collected by filtration, washed with water (30 mL) and dried at 50 °C under reduced pressure to afford the title compound (1.1 g, 90%) as a yellow solid; ^1H NMR (600 MHz, $\text{DMSO-}d_6$): δ = 8.28 (d, $J=0.7$ Hz, 1H), 7.87 (dd, $J = 8.8$, $^4J = 0.9$ Hz, 1H), 7.77 (d, $J = 8.8$ Hz, 1H); the exchangeable NH proton was not observed; ^{13}C NMR (151 MHz, $\text{DMSO-}d_6$): δ = 140.5, 140.3, 131.2, 131.2, 117.4, 117.0, 107.1; LCMS (UV, ES) RT = 0.88 min, $[\text{M}+\text{H}]^+ = 242, 244$, 100% purity; LCMS (Method B, UV, ES) RT = 0.93 min, $[\text{M}+\text{H}]^+ = 242, 244$, 100% purity.

5-Bromo-2-methyl-4-nitro-2*H*-indazole (77) & 5-bromo-1-methyl-4-nitro-1*H*-indazole (78)

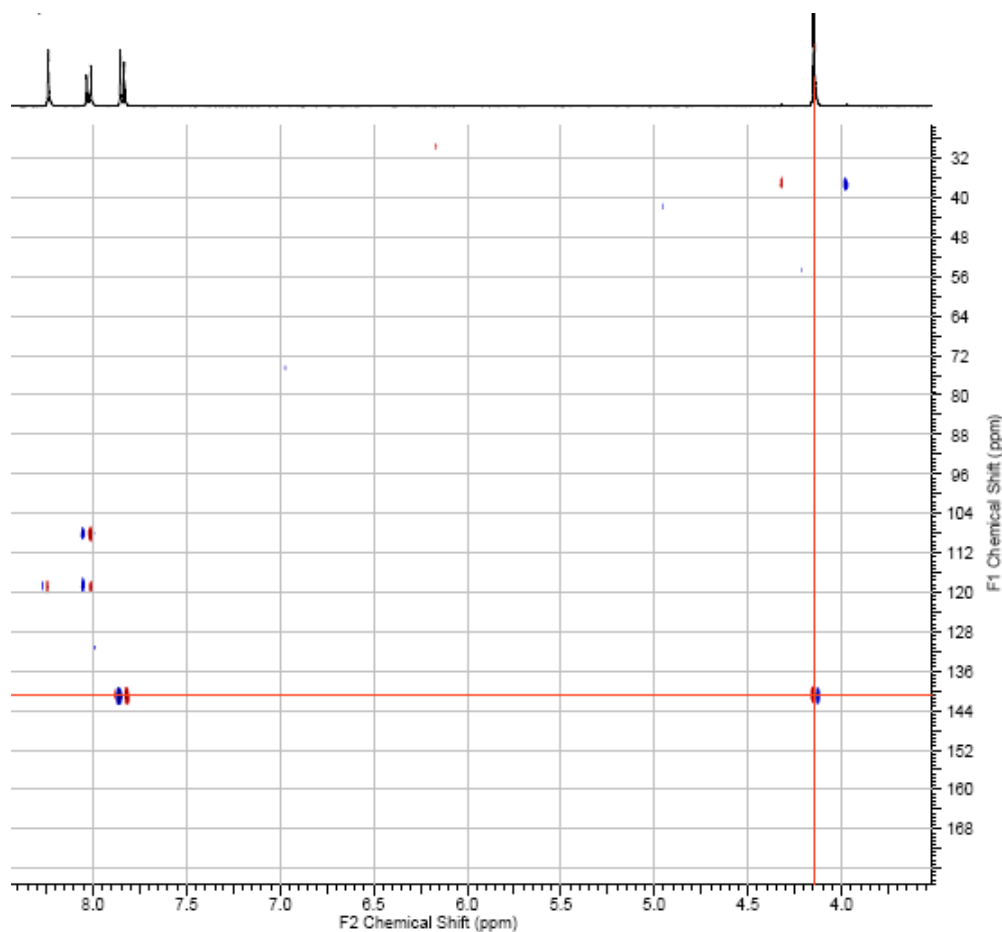


Sodium hydride (43 mg of a 60% w/w dispersion in mineral oil, 1.07 mmol) was added to a solution of **75** (200 mg, 0.83 mmol) in anhydrous DMF (2 mL). The mixture was stirred for 10 minutes, then methyl iodide (0.067 mL, 1.07 mmol) was added and the reaction mixture was stirred at room temperature for 18 h. Several drops of HCl (2 M aqueous solution) were added and the reaction mixture was concentrated under reduced pressure. The residue was taken up in DMSO (2 mL) and purified by MDAP (Method A). The appropriate fractions were combined and dried under reduced pressure to afford the two regioisomers as yellow solids: **77** (49 mg, 23%); ^1H NMR (400 MHz, $\text{DMSO-}d_6$) δ = 8.70 (s, 1H), 7.95 (dd, $J = 8.0$, 1.0 Hz, 1H), 7.65 (d, $J = 8.0$ Hz, 1H), 4.24 (s, 3H); ^{13}C NMR (101 MHz, $\text{DMSO-}d_6$) δ = 148.0, 140.4, 131.1, 125.6, 124.7, 116.7, 110.5, 41.1; IR ν_{max} (neat) 3173, 3077, 1515, 1331, 1312, 807 cm^{-1} ; LCMS (UV, ES) RT = 0.93 min, $[\text{M}+\text{H}]^+ = 256, 258$ 100% purity, and **78** (98 mg, 46%); ^1H NMR (400 MHz, $\text{DMSO-}d_6$) δ = 8.24 (s, 1H), 8.02 (dd, $J = 8.0$, 1.0 Hz, 1H), 7.84 (d, $J = 8.0$ Hz, 1H), 4.14 (s, 3H); IR ν_{max} (neat) 3175, 1520, 1328, 1320, 800 cm^{-1} ; LCMS (Method A, UV, ES) RT = 0.98 min, $[\text{M}+\text{H}]^+ = 256, 258$, 100% purity.

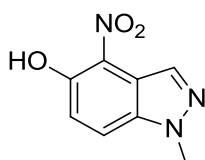
HMBC experiment for regioisomer **77** shows a correlation between the *N*-methyl protons (4.24 ppm) and the carbon at the 3-position (125.6 ppm) corresponding to $^3J_{\text{C-H}}$ couplings.



HMBC experiment for regioisomer **78** shows a correlation between between the *N*-methyl protons (4.14 ppm) and the carbon at the 8-position (141.4 ppm) corresponding to ³J_{C-H} couplings.



1-Methyl-4-nitro-1H-indazol-5-ol (79)



Method 1

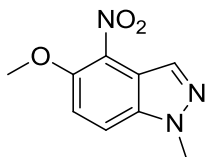
A mixture of **78** (70 mg, 0.27 mmol), sodium *tert*-butoxide (79 mg, 0.82 mmol) and copper powder (7 mg, 0.1 mmol) were dissolved in MeOH (1.5 mL) and was heated to 150 °C for 30 min. The reaction was allowed to cool to ambient temperature. LCMS showed no peak for the methoxy product but a peak for the hydroxy product was observed at RT = 0.79 min. The reaction mixture was diluted with DMSO (1 mL) and filtered through a pad of celite. The filtrate was purified on MDAP (Method A), and the solvent was dried under reduced pressure to afford the title compound (33 mg, 56%) as a yellow solid. (The desired methoxy product was not formed). ^1H NMR (400 MHz, DMSO- d_6) δ = 11.26 (br.s, 1H), 8.25 (s, 1H), 8.07 (d, J = 9.0 Hz, 1H), 7.25 (d, J = 9.0 Hz, 1H), 4.10 (s, 3H); ^1H NMR (400 MHz, MeOD- d_4) δ =

8.35 (s, 1H), 7.96 (d, $J = 8.0$ Hz, 1H), 7.23 (d, $J = 8.0$ Hz, 1H), 4.10 (s, 3H); LCMS (Method A, UV, ES) RT = 0.79 min, $[M+H]^+ = 194$, 90% purity.

Method 2

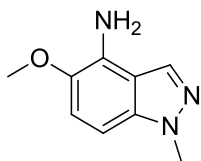
A mixture of **78** (30 mg, 0.12 mmol), 2-di-tert-butylphosphino-2',4',6'-triisopropylbiphenyl **9.52** (4 mg, 9.4 μ mol), Pd₂(dba)₃ (2 mg, 2.2 μ mol), potassium hydroxide (20 mg, 0.35 mmol) in 1,4-dioxane (0.25 mL) and water (0.25 mL) were heated in the microwave at 110 °C for 30 min. The reaction mixture was concentrated under reduced pressure, HCl (10 mL of a 1 M aqueous solution) was added and the product was extracted with ethyl acetate (2 x 15 mL). The combined organic extracts were dried using a hydrophobic frit and concentrated under reduced pressure. The crude sample was taken up in DMSO (2 mL) and purified by MDAP (Method A). The solvent was dried under reduced pressure to afford the title compound (18 mg, 80%) as a yellow solid; ¹H NMR (400 MHz, DMSO-*d*₆) $\delta = 11.26$ (br.s, 1H), 8.25 (s, 1H), 8.07 (d, $J = 9.0$ Hz, 1H), 7.25 (d, $J = 9.0$ Hz, 1H), 4.10 (s, 3H); LCMS (Method A, UV, ES) RT = 0.78 min, $[M+H]^+ = 194$, 98% purity.

5-Methoxy-1-methyl-4-nitro-1H-indazole (80)



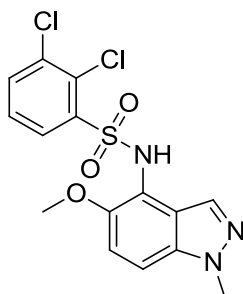
Potassium carbonate (28 mg, 0.20 mmol) was added to a solution of **79** (30 mg, 0.16 mmol) in anhydrous DMF (0.4 mL) and the mixture was stirred for 10 minutes. Methyl iodide (0.013 mL, 0.20 mmol) was then added and the mixture was stirred at ambient temperature for 18 h. The reaction mixture was diluted with ethyl acetate (30 mL) and water (20 mL). The organic phase was separated, and the aqueous layer was extracted further with ethyl acetate (2 x 30 mL). The organic extracts were combined, washed with brine (20 mL), dried using a hydrophobic frit and evaporated under reduced pressure to afford the title compound (35 mg, 98%) as a pale green solid; ¹H NMR (400 MHz, DMSO-*d*₆) $\delta = 8.18$ (s, 1H), 8.11 (d, $J = 9.0$ Hz, 1H), 7.58 (d, $J = 9.0$ Hz, 1H), 4.11 (s, 3H), 4.02 (s, 3H); LCMS (Method A, UV, ES) RT = 0.75 min, $[M+H]^+ = 208$, 90% purity.

5-Methoxy-1-methyl-1*H*-indazol-4-amine (**81**)



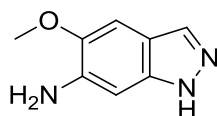
Tin(II) chloride (180 mg, 0.97 mmol) was added to a solution of **80** (40 mg, 0.19 mmol) in MeOH (1 mL). Concentrated HCl (0.08 mL of a 37 wt% aqueous solution, 0.97 mmol) was added and the reaction mixture was allowed to stir at ambient temperature for 4 h. The reaction mixture was neutralised by the addition of solid sodium carbonate. The solution was then diluted with ethyl acetate (20 mL), washed with sodium hydroxide (15 mL of a 1 M aqueous solution), followed by sodium bicarbonate (20 mL of a saturated aqueous solution), dried using a hydrophobic frit, and concentrated under reduced pressure to afford the title compound (23 mg, 52%) as a brown gum. ¹H NMR (400 MHz, MeOD-*d*₄) δ = 7.98 (s, 1 H), 7.13 (d, *J* = 8.8 Hz, 1 H), 6.73 (d, *J* = 8.8 Hz, 1 H), 3.93 (s, 3 H), 3.84 (s, 3 H); the exchangeable NH₂ protons were not observed; LCMS (Method A, UV, ES) RT = 0.57 min, [M+H]⁺ = 178, 80% purity.

2,3-Dichloro-*N*-(5-methoxy-1-methyl-1*H*-indazol-4-yl)benzenesulfonamide (**82**)



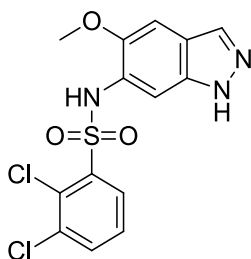
The title compound was prepared from **81** (20 mg, 0.11 mmol) and 2,3-dichlorobenzenesulfonyl chloride (33 mg, 0.14 mmol) according to the procedure described for the preparation of **29**. The same work up and purification afforded **82** as a white solid (19 mg, 43%); ¹H NMR (400 MHz, MeOD-*d*₄) δ = 8.01 (s, 1H), 7.73 (dd, *J* = 8.0 1.5 Hz, 1H), 7.63 (dd, *J* = 8.0, 1.5 Hz, 1H), 7.38 (d, *J* = 9.0 Hz, 1H), 7.28 - 7.18 (m, 1H), 7.09 (d, *J* = 9.0 Hz, 1H), 3.99 (s, 3H), 3.46 (s, 3H); the exchangeable NH proton was not observed; LCMS (Method A, UV, ES) RT = 1.02 min, [M+H]⁺ = 386, 388, 390, 100% purity.

5-methoxy-1*H*-indazol-6-amine (**84**)



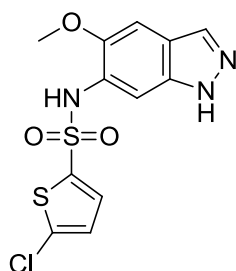
A solution of 5-methoxy-6-nitro-1*H*-indazole (500 mg, 2.59 mmol) in ethanol (15 ml) was added to a flask containing palladium-on-carbon (275 mg of a 10% w/w, 0.26 mmol) under vacuum. The flask was back filled with N₂, evacuated and filled with H₂ using the burette apparatus. The reaction mixture was stirred under H₂ for 18 h. The reaction mixture was filtered through a celite pad, washed with ethanol (50 mL) and concentrated under reduced pressure to afford the title compound (410 mg, 97%) as a brown solid; ¹H NMR (400 MHz, DMSO-*d*₆) δ = 12.20 (s, 1H), 7.68 (s, 1H), 6.96 (s, 1H), 6.63 (s, 1H), 4.97 (br.s, 2H), 3.79 (s, 3H); LCMS (Method B, UV, ES) RT = 0.58 min, [M+H]⁺ = 164, 100% purity.

2,3-Dichloro-*N*-(5-methoxy-1*H*-indazol-6-yl)benzenesulfonamide (**85**)



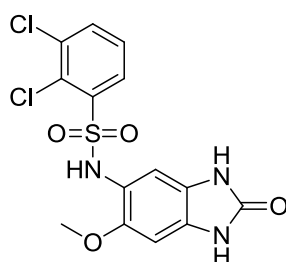
The title compound was prepared from **84** (75 mg, 0.46 mmol) and 2,3-dichlorobenzenesulfonyl chloride (124 mg, 0.51 mmol) according to the procedure described for the preparation of **29**. The same work up and purification afforded **85** (105 mg, 61%) as a white solid; ¹H NMR (400 MHz, DMSO-*d*₆) δ = 12.84 (s, 1H), 9.83 (s, 1H), 7.94 - 7.84 (m, 2H), 7.78 (dd, *J* = 8.0, 1.5 Hz, 1H), 7.43 (t, *J* = 8.0 Hz, 1H), 7.38 (s, 1H), 7.12 (s, 1H), 3.30 (s, 3H); ¹³C NMR (101 MHz, DMSO-*d*₆) δ = 148.0, 139.9, 134.6, 134.3, 134.0, 132.8, 129.4, 129.3, 128.0, 125.2, 120.6, 107.1, 100.0, 55.4; HRMS (ESI) *m/z* calculated for C₁₄H₁₂Cl₂N₃O₃S = 371.9976. Found = 371.9965 [M+H]⁺; LCMS (Method A, UV, ES) RT = 0.98 min, [M+H]⁺ = 372, 374, 376, 100% purity.

5-Chloro-*N*-(5-methoxy-1*H*-indazol-6-yl)thiophene-2-sulfonamide (**86**)



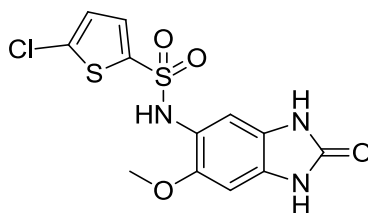
The title compound was prepared from **84** (75 mg, 0.46 mmol) and 5-chlorothiophene-2-sulfonyl chloride (100 mg, 0.46 mmol) according to the procedure described for the preparation of **29**. The same work up and purification afforded **86** (65 mg, 42%) as a beige coloured solid; ^1H NMR (400 MHz, $\text{DMSO-}d_6$) δ = 12.87 (br.s, 1H), 9.93 (br.s, 1H), 7.92 (s, 1H), 7.44 (s, 1H), 7.30 (d, J = 4.0 Hz, 1H), 7.19 (s, 1H), 7.17 (d, J = 4.0 Hz, 1H), 3.63 (s, 3H); LCMS (Method A, UV, ES) RT = 0.90 min, $[\text{M}+\text{H}]^+ = 344, 346$, 100% purity.

2,3-Dichloro-*N*-(6-methoxy-2-oxo-2,3-dihydro-1*H*-benzo[d]imidazol-5-yl)benzenesulfonamide (**88**)



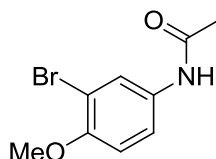
The title compound was prepared from 5-amino-6-methoxy-1,3-dihydro-2*H*-benzimidazol-2-one (57 mg, 0.31 mmol) and 2,3-dichlorobenzenesulfonyl chloride (76 mg, 0.31 mmol) according to the procedure described for the preparation of **29**. The same work up and purification afforded **88** (65 mg, 54%) as a brown solid; ^1H NMR (400 MHz, $\text{DMSO-}d_6$) δ = 10.55 (s, 1H), 10.36 (s, 1H), 9.56 (s, 1H), 7.87 (dd, J = 8.0, 2.0 Hz, 1H), 7.70 (dd, J = 8.0, 2.0 Hz, 1H), 7.40 (t, J = 8.0 Hz, 1H), 6.75 (s, 1H), 6.44 (s, 1H), 3.33 (s, 3H); ^{13}C NMR (101 MHz, $\text{DMSO-}d_6$) δ = 155.5, 149.6, 140.3, 134.0, 133.8, 129.7, 129.4, 129.2, 127.7, 122.6, 116.4, 109.4, 93.6, 55.5; IR ν_{max} (neat) 3379, 3276, 3084, 1698, 1667, 1495, 1166, 709 cm^{-1} ; HRMS (ESI) m/z calculated for $\text{C}_{14}\text{H}_{12}\text{Cl}_2\text{N}_3\text{O}_4\text{S}$ = 387.9920. Found = 387.9927 $[\text{M}+\text{H}]^+$; LCMS (Method A, UV, ES) RT = 0.85 min, $[\text{M}+\text{H}]^+ = 388, 390, 392$, 95% purity.

5-Chloro-*N*-(6-methoxy-2-oxo-2,3-dihydro-1*H*-benzo[*d*]imidazol-5-yl)thiophene-2-sulfonamide (89)



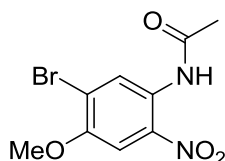
The title compound was prepared from 5-amino-6-methoxy-1,3-dihydro-2*H*-benzimidazol-2-one (50 mg, 0.28 mmol) and 5-chlorothiophene-2-sulfonyl chloride (61 mg, 0.28 mmol) according to the procedure described for the preparation of **29**. The same work up and purification afforded **89** (70 mg, 70%) as a beige coloured solid; ^1H NMR (400 MHz, $\text{DMSO-}d_6$) δ = 10.59 (br.s, 1H), 10.39 (br.s, 1H), 9.59 (br.s, 1H), 7.43 - 6.97 (m, 2H), 6.78 (br.s, 1H), 6.55 (br.s, 1H), 3.48 (br.s, 3H); IR ν_{max} (neat) 3285, 3094, 1700, 1494, 1403, 1160, 806, 704, 685 cm^{-1} ; LCMS (Method A, UV, ES) RT = 0.77 min, $[\text{M}+\text{H}]^+ = 400, 402, 100\%$ purity.

***N*-(3-Bromo-4-methoxyphenyl)acetamide (91)**



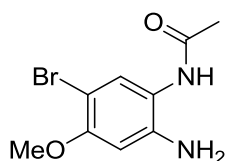
A solution of 3-bromo-4-methoxyaniline (1.0 g, 5 mmol) in DCM (10 mL) and triethylamine (1.0 mL, 7.2 mmol) was treated with acetic anhydride (0.47 mL, 5 mmol). The mixture was diluted with DCM (40 mL) and washed with HCl (30 mL of a 1 M aqueous solution), sodium bicarbonate (30 mL of a saturated aqueous solution), dried using a hydrophobic frit, and evaporated under reduced pressure to afford the title product (1.15 g, 94%) as a white solid; ^1H NMR (400 MHz, CDCl_3) δ = 7.86 (br.s, 1H), 7.68 (d, $J = 2.0$ Hz, 1H), 7.41 (dd, $J = 8.0, 2.0$ Hz, 1H), 6.81 (d, $J = 8.0$ Hz, 1H), 3.84 (s, 3H), 2.14 (3H, s); LCMS (Method A, UV, ES) RT = 0.73 min, $[\text{M}+\text{H}]^+ = 244, 246, 97\%$ purity.

***N*-(5-Bromo-4-methoxy-2-nitrophenyl)acetamide (92)**



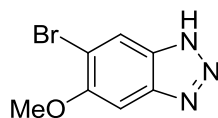
A solution of **91** (1.14 g, 4.67 mmol) in MeCN (25 mL) at 0 °C was treated with nitronium tetrafluoroborate (0.65 g, 4.89 mmol), and the mixture was stirred for 5 min whereupon a yellow solid precipitated out of solution. The reaction was stirred for a further 2 h, and was then diluted with water (50 mL). The precipitated solid was collected by filtration, washed with water, and dried under reduced pressure to afford the title compound (1.18 g, 87%) as a yellow solid; ¹H NMR (400 MHz, CDCl₃) δ = 10.7 (s, 1H), 9.08 (s, 1H), 7.67 (s, 1H), 3.95 (s, 3H), 2.28 (s, 3H); LCMS (Method A, UV, ES) RT = 0.86 min, [M+H]⁺ = 289, 291, 100% purity.

***N*-(2-Amino-5-bromo-4-methoxyphenyl)acetamide (93)**



A solution of **92** (800 mg, 2.77 mmol) in glacial acetic acid (12 mL) was treated with iron powder (927 mg, 16.6 mmol) and the mixture was stirred at 50 °C for 1 h. The reaction mixture was concentrated under reduced pressure and the residue was partitioned between water (30 mL) and ethyl acetate (50 mL). The aqueous layer was separated and extracted with more ethyl acetate (3 x 50 mL). The combined organic extracts were washed with brine (30 mL), dried using a hydrophobic frit, and evaporated under reduced pressure to afford the title compound (0.9 g, 99 %) as a pale brown solid; ¹H NMR (400 MHz, DMSO-*d*₆) δ = 11.95 (br.s, 1H), 7.27 (s, 1H), 6.46 (s, 1H), 5.13 (br.s, 2H), 3.72 (s, 3H), 2.00 (s, 3H); LCMS (Method A, UV, ES) RT = 0.60 min, [M+H]⁺ = 259, 261, 80% purity.

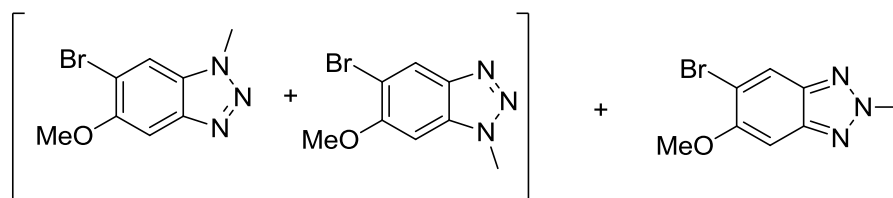
6-Bromo-5-methoxy-1*H*-benzo[*d*][1,2,3]triazole (94)



A suspension of **93** (450 mg, 1.74 mmol) in HCl (3 mL of a 6 M aqueous solution, 18 mmol) was slowly treated with solid sodium nitrite (144 mg, 2.08 mmol), and was then diluted with water (3 mL). After stirring the mixture for 1 h, ethanol (3 mL) was added, and the reaction was basified carefully to pH 9 by the addition of sodium hydroxide (10.5 mL of a 2 M aqueous solution, 21.0 mmol). LCMS showed the acetyl group has been cleaved. The

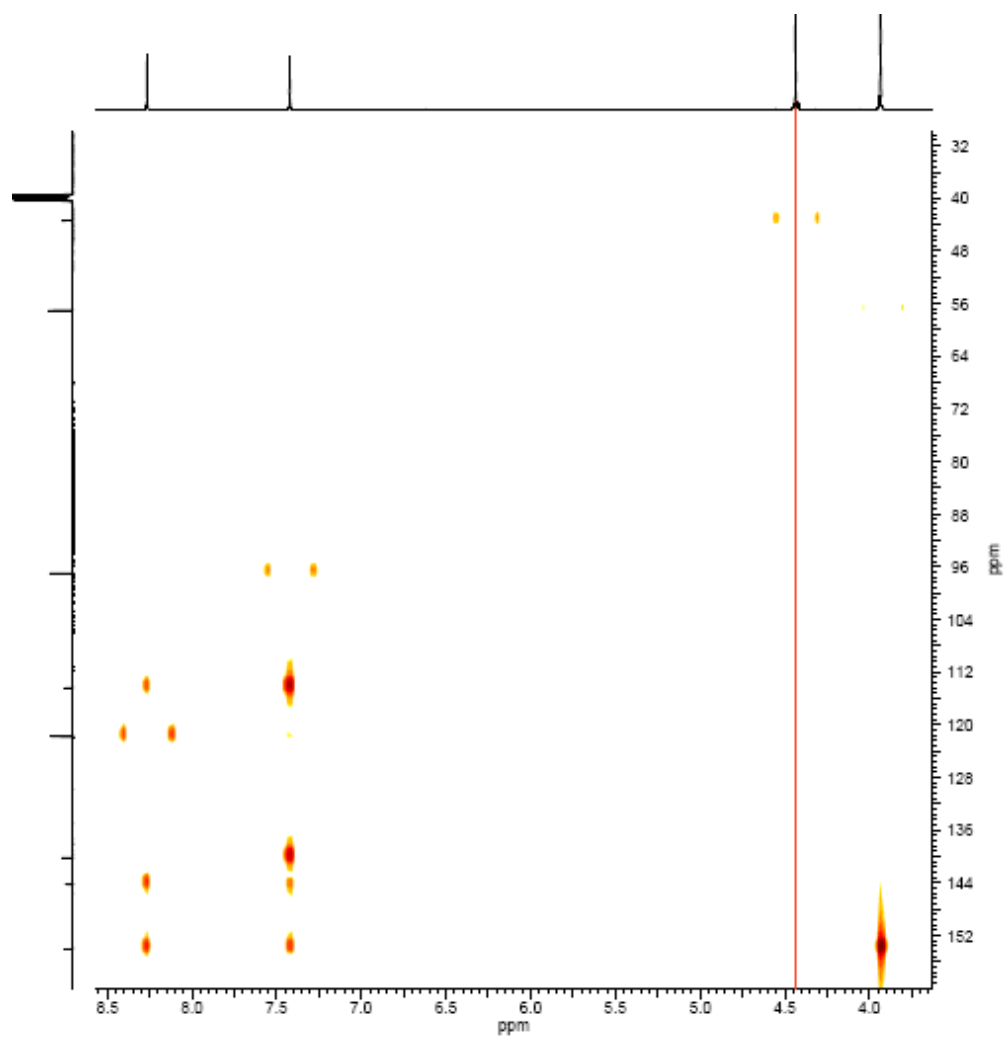
solution was concentrated under reduced pressure to remove ethanol, and the aqueous phase was extracted with ethyl acetate (3 x 50 mL). The combined organic extracts were washed with brine (25 mL), dried using a hydrophobic frit and evaporated under reduced pressure to afford the title compound (370 mg, 89%) as an off-white solid; ^1H NMR (400 MHz, DMSO- d_6) δ = 8.26 (s, 1H), 7.38 (s, 1H), 3.94 (s, 3H); the exchangeable NH proton was not observed; LCMS (Method A, UV, ES) RT = 0.72 min, $[\text{M}+\text{H}]^+ = 228, 230, 95\%$ purity.

5-Bromo-6-methoxy-1-methyl-1*H*-benzo[*d*][1,2,3]triazole with 6-bromo-5-methoxy-1-methyl-1*H*-benzo[*d*][1,2,3]triazole (3:2) (96:95) and 5-bromo-6-methoxy-2-methyl-2*H*-benzo[*d*][1,2,3]triazole (97)

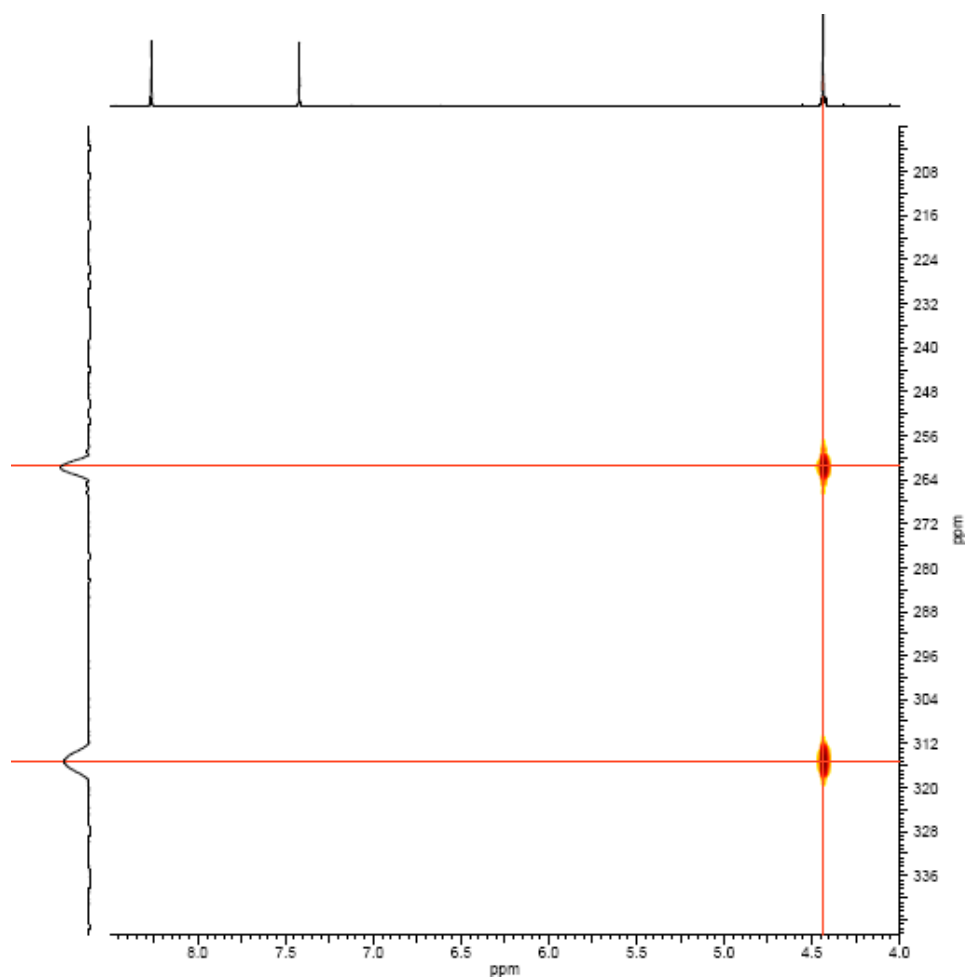


A solution of **94** (370 mg, 1.62 mmol) in DMSO (3 mL) was treated with potassium hydroxide (273 mg, 4.87 mmol) and the mixture was stirred for 5 min before methyl iodide (0.30 mL, 4.9 mmol) was added. The mixture was stirred for 1 h and was then filtered. The DMSO solutions were purified on the MDAP (Method A), and the appropriate fractions were combined and evaporated under reduced pressure to afford an inseparable (3:2) mixture of **95** and **96** (110 mg, 14%) as a white solid; ^1H NMR (600 MHz, DMSO- d_6) δ = major 8.32 (s, 1H), 7.49 (s, 1H), 4.26 (s, 3H), 3.97 (s, 3H) and minor 8.27 (s, 1H), 7.61 (s, 1H), 4.26 (s, 3H), 3.93 (s, 3H); LCMS (Method A, UV, ES) RT = 0.79 min, $[\text{M}+\text{H}]^+ = 242, 244, 100\%$ purity; and the separated **97** (45 mg, 12%); ^1H NMR (600 MHz, DMSO- d_6) δ = 8.25 (s, 1H), 7.41 (s, 1H), 4.43 (s, 3H), 3.92 (s, 3H); LCMS (Method A, UV, ES) RT = 0.91 min, $[\text{M}+\text{H}]^+ = 224, 244, 97\%$ purity.

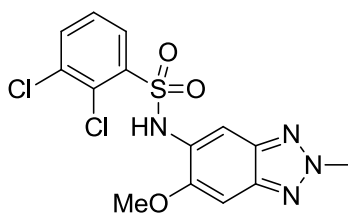
HMBC experiment of **97** shows no correlation from the methyl protons (4.43 ppm) to any of the carbon atoms (other than the 1J).



^1H - ^{15}N HMBC of regioisomer **97** shows key correlations between the *N*-methyl protons (4.43 ppm) and all three nitrogens of the triazole.



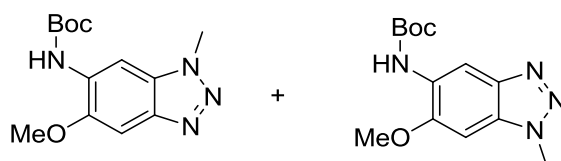
2,3-Dichloro-*N*-(6-methoxy-2-methyl-2*H*-benzo[*d*][1,2,3]triazol-5-yl)benzenesulfonamide (98**)**



A mixture of 2,3-dichlorobenzenesulfonamide (19 mg, 0.08 mmol), **97** (20 mg, 0.08 mmol), $\text{Pd}_2(\text{dba})_3$ (3.8 mg, 4.1 μmol), Xantphos (7 mg, 0.01 mmol), cesium carbonate (40 mg, 0.12 mmol) and 1,4-dioxane (0.4 mL) in a sealed vial was de-gassed with nitrogen for 5 min before being heated at 100 $^\circ\text{C}$ for 48 h. The reaction was diluted with DCM (15 mL) and ethyl acetate (10 mL), filtered through a celite pad and the solvent was evaporated under reduced pressure. The solid residue was taken up in DMSO (1 mL) and purified by MDAP (Method A). The solvent was evaporated under reduced pressure to afford the title compound

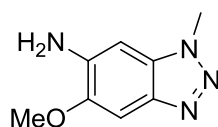
(11 mg, 34%) as a white solid; $^1\text{H NMR}$ (400 MHz, CDCl_3) δ = 8.06 (dd, J = 8.0, 1.5 Hz, 1H), 7.88 (br.s, 1H), 7.81 (s, 1H), 7.60 (dd, J = 8.0, 1.5 Hz, 1H), 7.27 (t, J = 8.0 Hz, 1H), 7.01 (s, 1H), 4.39 (s, 3H), 3.89 (s, 3H); LCMS (UV, ES) RT = 0.92 min, $[\text{M}+\text{H}]^+ = 387, 389, 391$, 90% purity.

***Tert*-butyl (6-methoxy-1-methyl-1*H*-benzo[*d*][1,2,3]triazol-5-yl)carbamate (99) and *tert*-butyl (5-methoxy-1-methyl-1*H*-benzo[*d*][1,2,3]triazol-6-yl)carbamate (100)**



A mixture of triazole **95** and **96** (30 mg, 0.12 mmol), *tert*-butyl carbamate (17 mg, 0.15 mmol), $\text{Pd}_2(\text{dba})_3$ (5.7 mg, 6.2 μmol), Xantphos (10.8 mg, 0.019 mmol) and cesium carbonate (61 mg, 0.19 mmol) were added to a 2 mL Reacti-VialTM. 1,4-dioxane (0.3 mL) was added to the mixture and the resulting suspension was de-gassed with nitrogen for 5 min. The reaction was sealed and heated at 100 $^\circ\text{C}$ for 18 hour. The reaction mixture was diluted with DCM (15 mL), filtered through a celite pad, and the solvent was evaporated under reduced pressure. The sample was then taken up in DMSO (1 mL) and purified by MDAP (Method A). The appropriate fractions were combined and the solvent was evaporated under reduced pressure to give the separated regioisomers, **99** (11.4 mg, 33%) as a beige coloured solid; $^1\text{H NMR}$ (600 MHz, CDCl_3) δ = 8.67 (br.s, 1H), 7.17 (br.s, 1H), 6.77 (s, 1H), 4.22 (s, 3H), 4.00 (s, 3H), 1.57 (s, 9H); LCMS (Method A, UV, ES) RT = 0.93 min, $[\text{M}+\text{H}]^+ = 279$, 95% purity; and **100** (11.1 mg, 32%) as a beige coloured solid; $^1\text{H NMR}$ (600 MHz, CDCl_3) δ = 8.30 (s, 1H), 7.45 (br.s, 1H), 7.35 (s, 1H), 4.24 (s, 3H), 3.99 (s, 3H), 1.57 (s, 9H); LCMS (Method A, UV, ES) RT = 0.99 min, $[\text{M}+\text{H}]^+ = 279$, 95% purity.

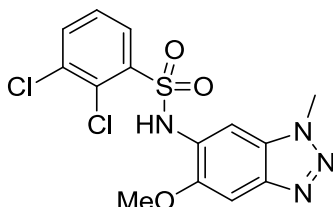
5-Methoxy-1-methyl-1*H*-benzo[*d*][1,2,3]triazol-6-amine (101)



HCl (0.2 mL of a 4 M solution in 1,4-dioxane, 0.8 mmol) was added to **99** (11 mg, 0.04

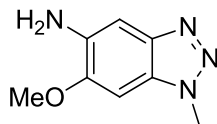
mmol), and the reaction was stirred at ambient temperature for 18 h. The reaction mixture was concentrated under reduced pressure, diluted with MeOH (2 mL) and loaded onto a 500 mg aminopropyl (NH₂) cartridge. The product was eluted with MeOH (10 mL), and the solvent was dried under reduced pressure to afford the title compound (7 mg, 99%) as a colourless oil; ¹H NMR (400 MHz, CDCl₃) δ = 7.26 (s, 1H), 6.60 (s, 1H), 4.24 (br.s, 2H), 4.14 (s, 3H), 3.95 (s, 3H); LCMS (Method A, UV, ES) RT = 0.48 min, [M+H]⁺ = 179, 100% purity.

2,3-Dichloro-N-(5-methoxy-1-methyl-1H-benzo[d][1,2,3]triazol-6-yl)benzenesulfonamide (102)



The title compound was prepared from **101** (7 mg, 0.04 mmol) and 2,3-dichlorobenzenesulfonyl chloride (11.6 mg, 0.047 mmol) according to the procedure described for the preparation of **29**. The same work up and purification afforded **102** (8 mg, 52%) as a white solid; ¹H NMR (400 MHz, CDCl₃) δ = 8.07 - 7.88 (m, 2H), 7.74 - 7.51 (m, 2H), 7.44 - 7.03 (m, 2H), 4.22 (s, 3H), 3.89 (s, 3H); LCMS (Method A, UV, ES) RT = 0.96 min, [M+H]⁺ = 387, 389, 391, 100% purity.

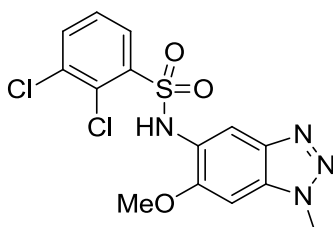
6-Methoxy-1-methyl-1H-benzo[d][1,2,3]triazol-5-amine (103)



HCl (0.2 mL of a 4 M solution in 1,4-dioxane, 0.8 mmol) was added to **100** (11 mg, 0.04 mmol), and the reaction was stirred at ambient temperature for 18 h. The reaction mixture was concentrated under reduced pressure, diluted with MeOH (2 mL) and loaded onto a 500 mg aminopropyl (NH₂) cartridge. The product was eluted with MeOH (10 mL), and the solvent was dried under reduced pressure to afford the title compound (7 mg, 99%) as a colourless oil; ¹H NMR (400 MHz, CDCl₃) δ = 7.20 (s, 1H), 6.72 (s, 1H), 4.20 (s, 3H), 3.98

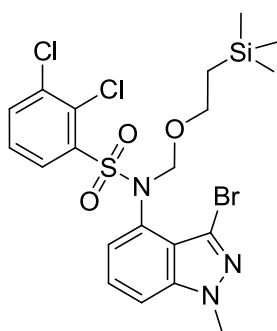
(s, 3H); the exchangeable NH₂ protons were not observed; LCMS (Method A, UV, ES) RT = 0.40 min, [M+H]⁺ = 179, 94% purity.

2,3-Dichloro-N-(6-methoxy-1-methyl-1H-benzo[d][1,2,3]triazol-5-yl)benzenesulfonamide (104)



The title compound was prepared from **103** (7 mg, 0.04 mmol) and 2,3-dichlorobenzenesulfonyl chloride (11.6 mg, 0.047 mmol) according to the procedure described for the preparation of **29**. The same work up and purification afforded **104** (9 mg, 59%) as a white solid; ¹H NMR (400 MHz, CDCl₃) δ = 8.27 - 7.97 (m, 2H), 7.73 (s, 1H), 7.61 (dd, *J* = 8.0, 1.5 Hz, 1H), 7.27 (t, *J* = 8.0 Hz, 1H), 6.73 (s, 1H), 4.19 (s, 3H), 3.93 (s, 3H); LCMS (Method A, UV, ES) RT = 0.94 min, [M+H]⁺ = 387, 389, 391, 100% purity.

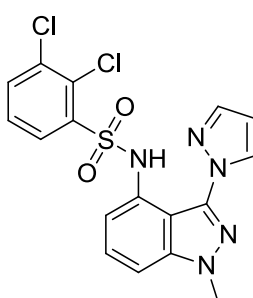
N-(3-Bromo-1-methyl-1H-indazol-4-yl)-2,3-dichloro-N-((2-(trimethylsilyl)ethoxy)methyl)benzenesulfonamide (106)



Sodium hydride (4 mg of a 60% w/w dispersion in mineral oil, 0.10 mmol) was added to a stirred solution of **72** (40 mg, 0.09 mmol) in THF (2 mL), and the effervescent mixture was stirred at ambient temperature for 30 min. The mixture was cooled to 0 °C and SEM chloride (0.017 ml, 0.097 mmol) was added dropwise. After 15 min, the cooling bath was removed and the mixture was stirred at ambient temperature for a further 3 h. MeOH (5 ml) was added and the solvent was evaporated under reduced pressure to give a residue that was partitioned between ethyl acetate (20 ml) and water (5 ml). The organic layer was separated, washed

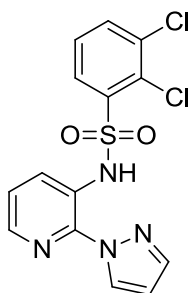
with sodium bicarbonate (15 mL of a saturated aqueous solution), dried by passing through a hydrophobic frit and evaporated under reduced pressure to afford the title compound (51 mg, 98%) as a yellow oil; ^1H NMR (400 MHz, MeOD- d_4) δ = 7.84 - 7.74 (m, 2H), 7.63 (d, J = 8.0 Hz, 1H), 7.40 (dd, J = 9.0, 7.0 Hz, 1H), 7.35 (t, J = 8.0 Hz, 1H), 7.01 (d, J = 7.0 Hz, 1 H), 5.56 (d, J = 11.0 Hz, 1H), 4.95 (d, J = 11.0 Hz, 1 H), 4.04 (s, 3H), 3.75 - 3.54 (m, 2H), 0.78 - 0.89 (m, 2H), -0.05 (s, 9H); LCMS (Method A, UV, ES) RT = 1.50 min, $[\text{M}+\text{H}]^+$ = 546, 566, 568, 570, 92% purity.

2,3-Dichloro-*N*-(1-methyl-3-(1*H*-pyrazol-1-yl)-1*H*-indazol-4-yl)benzenesulfonamide (107)



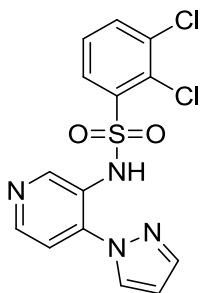
A mixture of sulfonamide **106** (50 mg, 0.09 mmol), 1*H*-pyrazole (12 mg, 0.18 mmol), potassium carbonate (59 mg, 0.40 mmol), CuI (4 mg, 0.02 mmol) and *L*-proline (4 mg, 0.04 mmol) in DMSO (0.2 mL) was heated at 110 °C in a sealed vial for 72 h. The reaction mixture was diluted with water (10 mL) and IPA in DCM (30 mL of a 1:10 mixture). The resultant slurry was filtered through celite and the organic layer was separated. The aqueous layer was extracted with another portion of IPA in DCM (30 mL of a 1:10 mixture). The combined organic extracts were washed with brine (20 mL), dried using a hydrophobic frit and concentrated under reduced pressure to afford a brown oil, (58 mg). LCMS showed no peak for the SEM protected product but a peak was observed for the SEM deprotected product (RT = 1.28 min, $[\text{M}+\text{H}]^+$ = 422, 424, 426). The sample was taken up in DMSO (1 mL) and purified by MDAP (Method B). The solvent was dried under reduced pressure to afford the title compound (4.1 mg, 11%) as a pale brown gum; ^1H NMR (400 MHz, MeOD- d_4) δ = 8.47 (d, J = 2.0 Hz, 1H), 8.18 (dd, J = 8.0, 1.5 Hz, 1H), 7.94 (d, J = 2.0 Hz, 1H), 7.68 (dd, J = 8.0, 1.5 Hz, 1H), 7.42 (t, J = 8.0 Hz, 1H), 7.32 - 7.19 (m, 1H), 7.17 - 7.06 (m, 2H), 6.64 (t, J = 2.0 Hz, 1H), 3.98 (s, 3H); the exchangeable NH proton was not observed; LCMS (Method A, UV, ES) RT = 1.29 min, $[\text{M}+\text{H}]^+$ = 422, 424, 426, 96% purity.

2,3-Dichloro-*N*-[2-(1*H*-pyrazol-1-yl)-3-pyridinyl]benzenesulfonamide (**109**)



The title compound was prepared from 2-(1*H*-pyrazol-1-yl)-3-pyridinamine (59 mg, 0.37 mmol) and 2,3-dichlorobenzenesulfonyl chloride (100 mg, 0.41 mmol) according to the procedure described for the preparation of **29**. The same work up and purification afforded **109** (83 mg, 60%) as a white solid; ¹H NMR (400 MHz, DMSO-*d*₆) δ = 12.06 (s, 1H), 8.61 (d, *J* = 2.0 Hz, 1H), 8.21 (d, *J* = 4.0 Hz, 1H), 8.09 (dd, *J* = 8.0, 1.0 Hz, 1H), 8.03 (s, 1H), 8.00–7.86 (m, 2H), 7.55 (t, *J* = 8.0 Hz, 1H), 7.34 (dd, *J* = 8.0, 4.0 Hz, 1H), 6.67 (d, *J* = 2.0 Hz, 1H); ¹³C NMR (101 MHz, DMSO-*d*₆) δ = 143.3, 141.7, 138.6, 137.4, 135.6, 134.4, 130.5, 129.6, 128.9, 128.8, 128.7, 123.6, 122.8, 107.7; IR ν_{max} (neat) 2852, 1466, 1432, 1405, 1168, 907, 750 cm⁻¹; HRMS (ESI) *m/z* calculated for C₁₄H₁₁Cl₂N₄O₂S = 368.9980. Found = 368.9971 [M+H]⁺; LCMS (Method A, UV, ES) RT = 0.80 min, [M+H]⁺ = 369, 371, 373, 98% purity.

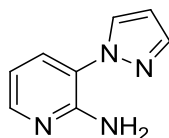
N-[4-(1*H*-Pyrazol-1-yl)pyridin-3-yl]-2,3-dichlorobenzenesulfonamide (**111**)



The title compound was prepared from 4-(1*H*-pyrazol-1-yl)pyridin-3-amine (50 mg, 0.31 mmol) and 2,3-dichlorobenzenesulfonyl chloride (84 mg, 0.34 mmol) according to the procedure described for the preparation of **29**. The same work up and purification afforded **111** (57 mg, 47%) as a pale brown solid; ¹H NMR (500 MHz, DMSO-*d*₆ + NaHCO₃) δ = 9.43 (d, *J* = 2.5 Hz, 1H), 8.34 (s, 1H), 8.03 (dd, *J* = 8.0, 1.5 Hz, 1H), 7.79 (d, *J* = 8.0 Hz, 1H), 7.71 - 7.57 (m, 3H), 7.41 (t, *J* = 8.0 Hz, 1H), 6.44 (t, *J* = 2.1 Hz, 1H); the exchangeable NH proton was not observed; ¹³C NMR (126 MHz, DMSO-*d*₆ + NaHCO₃) δ = 146.5, 143.0, 139.6,

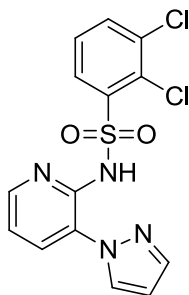
137.9, 135.7, 135.5, 133.3, 132.7, 131.5, 128.8, 128.6, 127.5, 115.2, 105.8; IR ν_{\max} (neat) 3171, 3080, 1588, 1528, 1400, 1377, 1346, 1318, 1171, 1157, 916, 763 cm^{-1} ; HRMS (ESI) m/z calculated for $\text{C}_{14}\text{H}_{11}\text{Cl}_2\text{N}_4\text{O}_2\text{S}$ = 368.9974. Found = 368.9974 $[\text{M}+\text{H}]^+$; LCMS (Method A, UV, ES) RT = 0.98 min, $[\text{M}+\text{H}]^+$ = 369, 371, 373, 95% purity.

3-(1*H*-Pyrazol-1-yl)pyridin-2-amine (113)



A mixture of 3-bromopyridin-2-amine (500 mg, 2.89 mmol), potassium carbonate (839 mg, 6.07 mmol), *N,N'*-dimethylethylenediamine (0.092 mL, 0.87 mmol), pyrazole (236 mg, 3.47 mmol) and CuI (83 mg, 0.43 mmol) in *p*-xylene (8 mL) was heated under nitrogen at 142 °C for 72 h. The mixture was partitioned between ethyl acetate (100 mL) and water (50 mL). The organic layer was separated, washed with brine (50 mL), dried using a hydrophobic frit and evaporated under reduced pressure. The sample was evaporated onto Florisil, dry loaded and purified on a 100 g silica column, using a gradient of 0-50% ethyl acetate-cyclohexane over 40 min. The appropriate fractions were combined and the solvent was evaporated under reduced pressure to afford the title compound (230 mg, 50%) as a beige coloured solid; ^1H NMR (400 MHz, CDCl_3) δ = 8.07 (d, J = 5.0 Hz, 1H), 7.85 - 7.65 (m, 2H), 7.44 (dd, J = 8.0, 1.5 Hz, 1H), 6.71 (dd, J = 8.0, 5.0 Hz, 1H), 6.47 (t, J = 2.0 Hz, 1 H), 5.75 (br.s, 2H); LCMS (Method B, UV, ES) RT = 0.61 min, $[\text{M}+\text{H}]^+$ = 161, 100% purity.

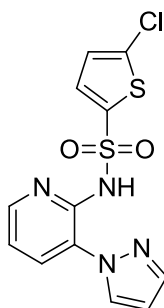
N-(3-(1*H*-Pyrazol-1-yl)pyridin-2-yl)-2,3-dichlorobenzenesulfonamide (114)



The title compound was prepared from **113** (15 mg, 0.09 mmol) and 2,3-dichlorobenzenesulfonyl chloride (25 mg, 0.10 mmol) according to the procedure described for the preparation of **29**. The same work up and purification afforded **114** (14 mg, 41%) as a white solid; ^1H NMR (400 MHz, $\text{DMSO}-d_6$, 393 K) δ = 8.48 (s, 1H), 8.23 - 8.04 (m, 2H), 7.99 (d, J = 5.0 Hz, 1H), 7.87 - 7.74 (m, 2H), 7.52 (t, J = 8.0 Hz, 1H), 7.06 (t, J = 5.0 Hz,

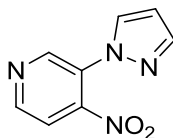
1H), 6.53 (br.s, 1H); the exchangeable NH proton was not observed; ¹H NMR (500 MHz, DMSO-*d*₆ + NaHCO₃) δ = 9.10 (d, *J* = 2.0 Hz, 1H), 8.03 (dd, *J* = 8.0, 1.5 Hz, 1H), 7.77 (dd, *J* = 8.0, 1.5 Hz, 1H), 7.66 - 7.52 (m, 3H), 7.36 (t, *J* = 8.0 Hz, 1H), 6.52 (dd, *J* = 8.0, 5.0 Hz, 1H), 6.40 (t, *J* = 2.0 Hz, 1H); the exchangeable NH proton was not observed; ¹³C NMR (126 MHz, DMSO-*d*₆ + NaHCO₃) δ = 152.2, 147.7, 144.8, 139.3, 132.6, 131.9, 131.0, 130.1, 128.8, 128.5, 127.1, 126.0, 112.0, 105.3; HRMS (ESI) *m/z* calculated for C₁₄H₁₁Cl₂N₄O₂S = 368.9974. Found = 368.9974 [M+H]⁺; LCMS (Method A, UV, ES) RT = 1.02 min, [M+H]⁺ = 369, 371, 373, 100% purity.

***N*-(3-(1*H*-Pyrazol-1-yl)pyridin-2-yl)-5-chlorothiophene-2-sulfonamide (115)**



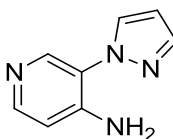
The title compound was prepared from **113** (40 mg, 0.25 mmol) and 5-chlorothiophene-2-sulfonyl chloride (60 mg, 0.28 mmol) according to the procedure described for the preparation of **29**. The same work up and purification afforded **115** (26 mg, 57%) as a brown solid; ¹H NMR (400 MHz, CDCl₃) δ = 11.20 (br.s, 1H), 8.34 (d, *J* = 4.0 Hz, 1H), 7.94 - 7.80 (m, 2H), 7.73 (d, *J* = 4.0 Hz, 1H), 7.70 - 7.60 (m, 1H), 7.10 (dd, *J* = 7.0, 4.5 Hz, 1 H), 6.90 (d, *J* = 4.5 Hz, 1H), 6.56 (br.s, 1H); ¹H NMR (500 MHz, DMSO-*d*₆ + NaHCO₃) δ = 8.91 (d, *J* = 2.0 Hz, 1H), 7.98 (dd, *J* = 5.0, 2.0 Hz, 1H), 7.82 (dd, *J* = 8.0, 2.0 Hz, 1H), 7.61 (d, *J* = 2.0 Hz, 1H), 7.30 (d, *J* = 4.0 Hz, 1H), 6.94 (d, *J* = 4.0 Hz, 1H), 6.65 (dd, *J* = 8.0, 5.0 Hz, 1H), 6.39 (t, *J* = 2.0 Hz, 1H), the exchangeable NH proton was not observed; ¹³C NMR (126 MHz, DMSO-*d*₆ + NaHCO₃) δ = 152.4, 148.8, 144.8, 139.6, 132.1, 130.3, 129.4, 127.6, 126.3, 125.7, 112.6, 105.6; HRMS (ESI) *m/z* calculated for C₁₂H₁₀ClN₄O₂S₂ = 340.9928. Found = 340.9928 [M+H]⁺; LCMS (Method A, UV, ES) RT = 1.00 min, [M+H]⁺ = 341, 343, 95% purity.

4-Nitro-3-(1*H*-pyrazol-1-yl)pyridine (**117**)



Sodium hydride (113 mg of a 60% w/w dispersion in mineral oil, 2.82 mmol) was added to a stirred solution of 1*H*-pyrazole (287 mg, 4.22 mmol) in NMP (5 mL) at 0 °C. The mixture was stirred for 5 min, then 3-fluoro-4-nitropyridine (200 mg, 1.41 mmol) was added and the reaction was heated to 100 °C for 18 h. After cooling, ethyl acetate (50 mL) and water (50 mL) were poured into the mixture. The organic layer was separated, washed with water (50 mL), brine (30 mL), dried using a hydrophobic frit, and evaporated under reduced pressure. The sample was loaded onto a 70 g silica column and purified using a gradient of 25-100% ethyl acetate-cyclohexane over 40 min. The appropriate fractions were combined and evaporated under reduced pressure to afford the title compound (173 mg, 64%) as a white solid; ¹H NMR (500 MHz, DMSO-*d*₆) δ = 9.19 (d, *J* = 2.5 Hz, 1H), 8.81 (d, *J* = 2.5 Hz, 1H), 8.62 (dd, *J* = 8.8, 2.5 Hz, 1H), 8.48 (d, *J* = 8.8 Hz, 1H), 7.96 (d, *J* = 1.5 Hz, 1H), 6.72 (t, *J* = 1.5 Hz, 1H); ¹³C NMR (126 MHz, DMSO-*d*₆) δ = 153.8, 143.9, 140.3, 138.6, 129.9, 129.0, 120.3, 110.3; IR ν_{max} (neat) 3132, 3079, 1578, 1539, 1523, 1483, 1340, 1276, 854, 755 cm⁻¹; HRMS (ESI) *m/z* calculated for C₈H₇N₄O₂ = 191.0564. Found = 191.0560 [M+H]⁺; LCMS (Method A, UV, ES) RT = 0.70 min, [M+H]⁺ = 191, 98% purity.

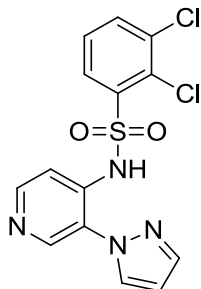
3-(1*H*-Pyrazol-1-yl)pyridin-4-amine (**118**)



Tin(II) chloride (449 mg, 2.37 mmol) was added to a solution of **117** (90 mg, 0.47 mmol) in MeOH (1.5 mL). Concentrated HCl (0.2 mL of a 37 wt% aqueous solution, 2.4 mmol) was added and the reaction mixture was allowed to stir at ambient temperature for 48 h. The reaction mixture was neutralised by the addition of solid sodium carbonate. The solution was diluted with ethyl acetate (100 mL), washed with sodium hydroxide (20 mL of a 1 M aqueous solution), followed by sodium bicarbonate (40 mL of a saturated aqueous solution), dried using a hydrophobic frit, and concentrated under reduced pressure to afford the title compound (55 mg, 68%) as a white solid; ¹H NMR (400 MHz, DMSO-*d*₆) δ = 8.32 (d, *J* = 3.0 Hz, 1H), 8.23 (d, *J* = 3.0 Hz, 1H), 7.77 (dd, *J* = 8.0, 2.0 Hz, 1H), 7.65 (d, *J* = 2.0 Hz, 1H),

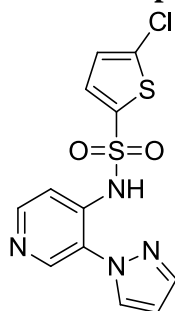
6.54 (d, $J = 8.0$ Hz, 1H), 6.46 (t, $J = 2.0$ Hz, 1H), 6.06 (br.s, 2H); LCMS (Method A, UV, ES) RT = 0.33 min, $[M+H]^+ = 161$, 93% purity.

***N*-(3-(1*H*-Pyrazol-1-yl)pyridin-4-yl)-2,3-dichlorobenzenesulfonamide (119)**



The title compound was prepared from **118** (35 mg, 0.22 mmol) and 2,3-dichlorobenzenesulfonyl chloride (70 mg, 0.28 mmol) according to the procedure described for the preparation of **29**. The same work up and purification afforded **119** (42 mg, 51%) as a pale brown solid; ^1H NMR (400 MHz, DMSO- d_6) $\delta = 12.04$ (br.s, 1H), 8.52 (d, $J = 2.5$ Hz, 1H), 8.41 (d, $J = 2.5$ Hz, 1H), 8.24 - 8.07 (m, 2H), 7.92 (dd, $J = 8.0, 1.0$ Hz, 1H), 7.73 (d, $J = 1.5$ Hz, 1H), 7.59 (t, $J = 8.0$ Hz, 1H), 7.18 (d, $J = 9.0$ Hz, 1H), 6.52 (t, $J = 2.0$ Hz, 1H); ^{13}C NMR (126 MHz, DMSO- d_6 + NaHCO $_3$) $\delta = 160.2, 147.5, 140.5, 138.8, 133.2, 131.5, 129.7, 129.2, 128.4, 128.1, 127.8, 127.5, 114.8, 107.4$; HRMS (ESI) m/z calculated for C $_{14}$ H $_{11}$ Cl $_2$ N $_4$ O $_2$ S = 368.9974. Found = 368.9974 $[M+H]^+$; IR ν_{max} (neat) 2684, 1651, 1622, 1548, 1400, 1369, 1347, 1150, 975, 800, 706 cm $^{-1}$; LCMS (Method A, UV, ES) RT = 0.94 min, $[M+H]^+ = 369, 371, 373$, 98% purity.

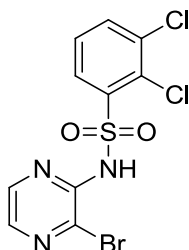
***N*-(3-(1*H*-Pyrazol-1-yl)pyridin-4-yl)-5-chlorothiophene-2-sulfonamide (120)**



The title compound was prepared from **118** (20 mg, 0.13 mmol) and 5-chlorothiophene-2-sulfonyl chloride (33 mg, 0.15 mmol) according to the procedure described for the preparation of **29**. The same work up and purification afforded **120** (23 mg, 53%) as a pale brown solid; ^1H NMR (400 MHz, CDCl $_3$) $\delta = 10.20$ (br.s, 1H), 8.75 (d, $J = 2.5$ Hz, 1H), 8.17 (dd, $J = 9.0, 2.5$ Hz, 1H), 7.92 (d, $J = 2.5$ Hz, 1H), 7.76 (d, $J = 2.5$ Hz, 1H), 7.63 (d, $J = 9.0$

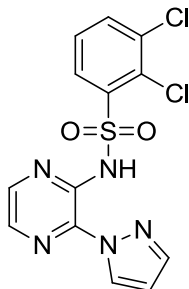
Hz, 1H), 7.42 (d, $J = 4.0$ Hz, 1H), 6.87 (d, $J = 4.0$ Hz, 1H), 6.53 (d, $J = 2.5$ Hz, 1H); IR ν_{\max} (neat) 3126, 2689, 1622, 1553, 1371, 1279, 1132, 992, 798, 691 cm^{-1} ; LCMS (Method A, UV, ES) RT = 0.92 min, $[\text{M}+\text{H}]^+ = 341, 343, 98\%$ purity.

***N*-(3-Bromopyrazin-2-yl)-2,3-dichlorobenzenesulfonamide (122)**



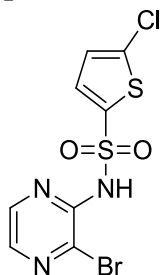
Sodium hydride (575 mg of a 60% w/w dispersion in mineral oil, 14.4 mmol) was added to a stirred solution of 3-bromopyrazin-2-amine (commercially available from Manchester Organics or Fluorochem) (500 mg, 2.87 mmol) in anhydrous DME (6 mL) at 0 °C. The mixture was stirred for 30 min and then 2,3-dichlorobenzenesulfonyl chloride (776 mg, 3.16 mmol) was added. The reaction was warmed to ambient temperature and stirred for 18 h. The reaction mixture was quenched by the addition of HCl (20 ml of a 2 M aqueous solution) and the product was extracted with ethyl acetate (3 x 50 mL). The organic extracts were combined, dried using a hydrophobic frit and evaporated under reduced pressure to give the crude product. The sample was evaporated onto Florisil, dry loaded and purified on a 50 g silica column using a gradient of 0-100% ethyl acetate-cyclohexane over 40 min. The appropriate fractions were combined and evaporated under reduced pressure to afford the title compound (800 mg, 73%) as a beige coloured solid; ^1H NMR (600 MHz, $\text{DMSO-}d_6$) $\delta = 8.15$ (br.s, 1H), 8.12 (br.s, 1H), 8.06 (dd, $J = 8.1, 1.5$ Hz, 1H), 7.93 (dd, $J = 8.1, 1.5$ Hz, 1H), 7.58 (t, $J = 8.1$ Hz, 1H); the exchangeable NH proton was not observed; ^{13}C NMR (151 MHz, $\text{CD}_3\text{OD} + \text{DCl}$) $\delta = 146.6, 141.4, 141.1, 139.3, 138.5, 136.1, 136.0, 132.3, 131.0, 128.9$; HRMS (ESI) m/z calculated for $\text{C}_{10}\text{H}_7\text{BrCl}_2\text{N}_3\text{O}_2\text{S} = 381.8814$. Found = 381.8819, $[\text{M}+\text{H}]^+$; LCMS: RT = 0.98 mins, $[\text{M}+\text{H}]^+ = 382, 384, 386, 388, 91\%$ purity.

***N*-(3-(1*H*-Pyrazol-1-yl)pyrazin-2-yl)-2,3-dichlorobenzenesulfonamide (123)**



Sodium hydride (52 mg of a 60% w/w dispersion in mineral oil, 1.3 mmol) was added to a stirred solution of 1*H*-pyrazole (107 mg, 1.57 mmol) in NMP (1.0 ml) at 0 °C. The mixture was stirred for 5 min, then **122** (100 mg, 0.261 mmol) was added and the reaction was heated to 100 °C for 18 h. After cooling, the mixture was poured into water (20 mL), acidified to pH 5 with HCl (2 M aqueous solution). Ethyl acetate (20 mL) was poured into the mixture, and the organic layer was separated, washed with water (20 mL), brine (20 mL), dried using a hydrophobic frit and evaporated under reduced pressure. The crude product was triturated with MeOH to afford the title compound (68 mg, 71%) as a white solid; ¹H NMR (400 MHz, DMSO-*d*₆) δ = 12.32 (br.s, 1H), 8.77 (d, *J* = 2.5 Hz, 1H), 8.28 (dd, *J* = 8.0, 1.5 Hz, 1H), 8.19 (d, *J* = 2.5 Hz, 1H), 8.15 (d, *J* = 1.5 Hz, 1H), 8.12 (d, *J* = 2.5 Hz, 1H), 7.98 (dd, *J* = 8.0, 1.5 Hz, 1H), 7.65 (t, *J* = 8.0 Hz, 1H), 6.80 - 6.75 (m, 1H); ¹³C NMR (126 MHz, DMSO-*d*₆) δ = 142.9, 140.0, 139.1, 138.0, 136.8, 135.9, 134.5, 134.2, 131.9, 130.1, 129.2, 129.1, 109.3; HRMS (ESI) *m/z* calculated for C₁₃H₁₀Cl₂N₅O₂S = 369.9927. Found = 369.9931, [M+H]⁺; LCMS (Method A, UV, ES) RT = 1.18 min, [M+H]⁺ = 370, 372, 374, 100% purity.

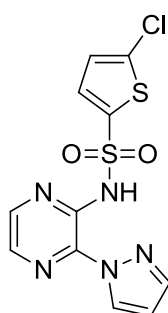
***N*-(3-Bromopyrazin-2-yl)-5-chlorothiophene-2-sulfonamide (124)**



Sodium hydride (575 mg of a 60% w/w dispersion in mineral oil, 14.4 mmol) was added to a stirred solution of 3-bromopyrazin-2-amine (500 mg, 2.87 mmol) in anhydrous DME (6 mL) at 0 °C. The mixture was stirred for 30 min and then 5-chloro-2-thiophenesulfonyl chloride (686 mg, 3.16 mmol) was added. The reaction was warmed to ambient temperature and stirred for 18 h. The reaction mixture was quenched by the addition of HCl (20 ml of a 2 M aqueous solution) and the product was extracted with ethyl acetate (2 x 100 mL). The organic extracts were combined, dried using a hydrophobic frit and evaporated under reduced

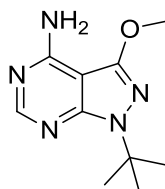
pressure to give the crude product. The sample was evaporated onto Florisil, dry loaded and purified on a 50 g silica column using a gradient of 0-100% ethyl acetate-cyclohexane over 40 min. The appropriate fractions were combined and evaporated under reduced pressure to afford the title compound (815 mg, 80%) as a pale yellow solid; $^1\text{H NMR}$ (400 MHz, $\text{DMSO-}d_6$) $\delta = 8.36$ (d, $J = 2.0$ Hz, 1H), 8.13 (d, $J = 2.0$ Hz, 1H), 7.67 (d, $J = 4.0$ Hz, 1H), 7.23 (d, $J = 4.0$ Hz, 1H); the exchangeable NH proton was not observed; LCMS (Method A, UV, ES) RT = 0.95 min, $[\text{M}+\text{H}]^+ = 354, 356, 358, 90\%$ purity.

***N*-(3-(1*H*-Pyrazol-1-yl)pyrazin-2-yl)-5-chlorothiophene-2-sulfonamide (125)**



The title compound was prepared from 1*H*-pyrazole (115 mg, 1.69 mmol), **124** (100 mg, 0.28 mmol) and sodium hydride (56 mg, of a 60% w/w dispersion in mineral oil, 1.40 mmol) according to the procedure described for the preparation of **123**. The same work up and purification using MDAP (Method A) afforded **125** (35 mg, 36%) as a white solid; $^1\text{H NMR}$ (400 MHz, $\text{DMSO-}d_6$) $\delta = 11.99$ (br.s, 1H), 8.74 (d, $J = 2.5$ Hz, 1H), 8.37 (d, $J = 2.5$ Hz, 1H), 8.26 (d, $J = 3.0$ Hz, 1H), 8.09 (d, $J = 1.0$ Hz, 1H), 7.83 (d, $J = 4.0$ Hz, 1H), 7.27 (d, $J = 4.0$ Hz, 1H), 6.74 (dd, $J = 3.0, 1.0$ Hz, 1H); LCMS (Method A, UV, ES) RT = 1.19 min, $[\text{M}+\text{H}]^+ = 342, 344, 100\%$ purity.

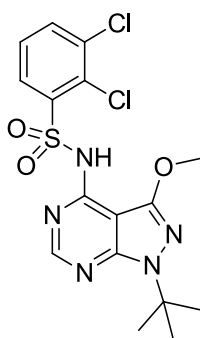
1-(*Tert*-butyl)-3-methoxy-1*H*-pyrazolo[3,4-*d*]pyrimidin-4-amine (141)



5-Amino-1-*tert*-butyl-3-methoxy-1*H*-pyrazole-4-carbonitrile **140** (52 g, 0.2 mol) and formamide (250 mL) were stirred at 180 °C for 2 h. The reaction was cooled and poured into water (2.5 L). The product was extracted into ethyl acetate (2 x 1 L), washed with water (1 L), brine (200 mL), dried (MgSO_4) and concentrated under reduced pressure to give a beige

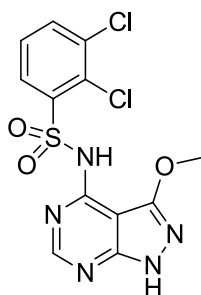
coloured solid. This was slurried with hexane, filtered, washed with hexane and dried to afford the title compound (27.2 g, 46%) as an off-white solid; ^1H NMR (400 MHz, $\text{DMSO-}d_6$) δ = 8.08 (s, 1H), 6.93 (br.s, 2H), 3.95 (s, 3H), 1.64 (s, 9H); ^{13}C NMR (101 MHz, $\text{DMSO-}d_6$) δ = 157.6, 155.8, 153.4, 153.0, 88.9, 58.7, 55.5, 28.8; IR ν_{max} (neat) 3197, 1632, 1582, 1261, 1106, 1079, 933, 718 cm^{-1} ; HRMS (ESI) m/z calculated for $\text{C}_{10}\text{H}_{16}\text{N}_5\text{O}$ = 222.1355. Found = 222.1345 $[\text{M}+\text{H}]^+$; LCMS (Method A, UV, ES) RT = 0.70 min, $[\text{M}+\text{H}]^+$ = 222, 96% purity.

***N*-(1-*tert*-butyl-3-methoxy-1*H*-pyrazolo[3,4-*d*]pyrimidin-4-yl)-2,3-dichlorobenzene sulfonamide (142)**



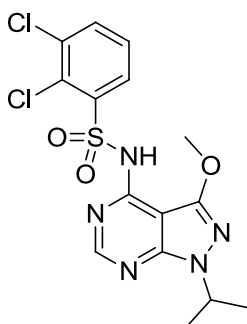
Sodium hydride (7.0 g of a 60% w/w dispersion in mineral oil, 0.18 mol) was added portion-wise to a solution of **141** (32.2 g, 0.15 mol) in anhydrous DMF (300 mL) at ambient temperature under a nitrogen atmosphere. On stirring for 0.5 h, 2,3-dichlorobenzenesulfonyl chloride (39.3 g, 0.16 mol) was added portion-wise. After stirring for 0.5 h, the mixture was poured into water (2 L) and the solid was collected by filtration then washed with water, slurried with IPA (200 mL), filtered, washed with IPA (50 mL) then hexane (50 mL) and dried to afford the title compound (25.5 g, 41%) as a white solid. ^1H NMR (400 MHz, $\text{DMSO-}d_6$) δ = 12.36 (br.s, 1H), 8.24 (s, 1H), 8.11 (dd, J = 8.0, 1.5 Hz, 1H), 7.90 (dd, J = 8.0, 1.5 Hz, 1H), 7.57 (t, J = 8.0 Hz, 1H), 3.89 (s, 3H), 1.67 (s, 9H); LCMS (Method A, UV, ES) RT = 1.27 min, $[\text{M}+\text{H}]^+$ = 430, 432, 434, 100% purity.

2,3-Dichloro-*N*-(3-methoxy-1*H*-pyrazolo[3,4-*d*]pyrimidin-4-yl)benzenesulfonamide (143)



Compound **142** (29.0 g, 0.07 mol) was added portion-wise to concentrated sulfuric acid (450 mL of a 98 wt% aqueous solution), and the reaction was stirred at ambient temperature for 2 h. The solution was then poured into ice-water (2 L). The product was filtered, washed with water, slurried with IPA (100 mL), filtered, washed with IPA (50 mL) then hexane (50 mL) and dried under reduced pressure to afford the title compound (20.0 g, 80%) as a white solid; ^1H NMR (400 MHz, DMSO- d_6) δ = 13.34 (br.s, 1H), 12.34 (br.s, 1H), 8.24 (br.s, 1H), 8.11 (dd, J = 8.0, 1.5 Hz, 1H), 7.90 (dd, J = 8.0, 1.5 Hz, 1H), 7.57 (t, J = 8.0 Hz, 1H), 3.89 (s, 3H); ^{13}C NMR (101 MHz, DMSO- d_6) δ = 157.6, 152.3, 151.2, 149.8, 147.4, 142.0, 134.0, 129.4, 128.4, 127.8, 91.0, 55.9; HRMS (ESI) m/z calculated for $\text{C}_{12}\text{H}_{10}\text{Cl}_2\text{N}_5\text{O}_3\text{S}$ = 373.9881. Found = 373.9867 $[\text{M}+\text{H}]^+$; LCMS (Method A, UV, ES) RT = 0.84 min, $[\text{M}+\text{H}]^+$ = 373, 375, 377, 99% purity.

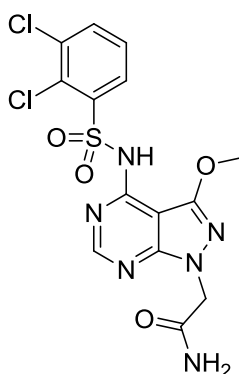
2,3-Dichloro-*N*-(1-isopropyl-3-methoxy-1*H*-pyrazolo[3,4-*d*]pyrimidin-4-yl)benzenesulfonamide (144)



LiHMDS (0.59 mL of a 1 M solution in THF, 0.59 mmol) was added to a solution of **143** (100 mg, 0.27 mmol) in anhydrous THF (1 mL) and DMF (1 mL) at 0 °C, under a nitrogen atmosphere. After stirring for 15 min, 2-bromopropane and sodium iodide (40 mg, 0.27 mmol) were added. The reaction was warmed to ambient temperature, stirred for 4 h, and was then heated at 55 °C for 18 h. The reaction mixture was quenched with HCl (10 mL of a 1 M aqueous solution) and extracted with ethyl acetate (3 x 20 mL). The combined organic extracts were washed with brine, dried using a hydrophobic frit, and concentrated under reduced

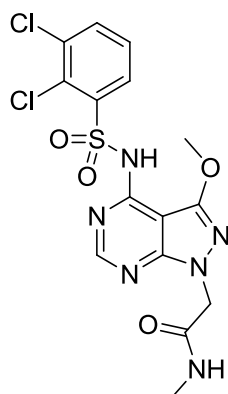
pressure. The sample was dissolved in DMSO (2 mL) and purified by MDAP (Method A). The appropriate fractions were combined and concentrated under reduced pressure to afford the title compound (43 mg, 37%) as a white solid; ^1H NMR (400 MHz, DMSO- d_6) δ = 12.34 (br.s, 1H), 8.24 (s, 1H), 8.11 (dd, J = 8.0, 1.5 Hz, 1H), 7.90 (dd, J = 8.0, 1.5 Hz, 1H), 7.57 (t, J = 8.0 Hz, 1H), 4.92 (sep, J = 7.0 Hz, 1H), 3.90 (s, 3H), 1.41 (d, J = 7.0 Hz, 6H); LCMS (Method A, UV, ES) RT = 1.20 min, $[\text{M}+\text{H}]^+$ = 416, 418, 420, 98% purity.

2,3-Dichloro-*N*-(3-methoxy-1*H*-pyrazolo[3,4-*d*]pyrimidin-4-yl)benzenesulfonamide (148)



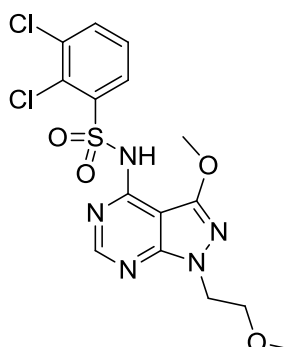
LiHMDS (0.59 mL of a 1 M solution in THF, 0.59 mmol) was added to a solution of **143** (100 mg, 0.27 mmol) in anhydrous THF (1 mL) and DMF (1 mL) at 0 °C, under a nitrogen atmosphere. After 15 min, 2-bromoacetamide (37 mg, 0.27 mmol) was added. The reaction was stirred at 0 °C for 15 min, slowly warmed to ambient temperature, and stirred for 5 h. The reaction mixture was quenched with HCl (10 ml of a 1 M aqueous solution) and extracted with ethyl acetate (3 x 20 ml). The combined organic extracts were washed with brine, dried using a hydrophobic frit and concentrated under reduced pressure. The sample was dissolved in DMSO (2 mL) and purified on the MDAP (Method A). The appropriate fractions were combined and concentrated under reduced pressure to afford the title compound (21 mg, 17%) as a white solid; ^1H NMR (400 MHz, DMSO- d_6) δ = 12.41 (br.s, 1H), 8.27 (s, 1H), 8.12 (dd, J = 8.0, 1.5 Hz, 1H), 7.91 (dd, J = 8.0, 1.5 Hz, 1H), 7.58 (t, J = 8.0 Hz, 1H), 7.52 (br.s, 1H), 7.29 (br.s, 1H), 4.78 (s, 2H), 3.88 (s, 3H); LCMS (Method A, UV, ES) RT = 0.79 min, $[\text{M}+\text{H}]^+$ = 431, 433, 435, 98% purity.

2-(4-(2,3-Dichlorophenylsulfonamido)-3-methoxy-1H-pyrazolo[3,4-d]pyrimidin-1-yl)-N-methylacetamide (149)



The title compound was prepared from **143** (100 mg, 0.27 mmol), 2-bromo-N-methylacetamide (41 mg, 0.27 mmol) and LiHMDS (0.59 mL of a 1 M solution in THF, 0.59 mmol) according to the procedure described for the preparation of **148**. The same work up and purification afforded **149** (66 mg, 53%) as a white solid; ^1H NMR (400 MHz, DMSO- d_6) δ = 12.42 (br.s, 1H), 8.27 (s, 1H), 8.12 (dd, J = 8.0, 1.5 Hz, 1H), 8.02 - 7.82 (m, 2H), 7.58 (t, J = 8.0 Hz, 1H), 4.80 (s, 2H), 3.88 (s, 3H), 2.60 (d, J = 4.5 Hz, 3H); ^{13}C NMR (101 MHz, DMSO- d_6) δ = 166.1, 157.0, 151.8, 147.9, 134.1, 134.0, 129.4, 128.5, , 128.0, 91.8, 56.2, 49.1, 25.6; peaks for 2 quaternary carbons were not observed; IR ν_{max} (neat) 3257, 1667, 1618, 1587, 1541, 1266, 1119, 1082, 855, 710, 675 cm^{-1} ; HRMS (ESI) m/z calculated for $\text{C}_{15}\text{H}_{15}\text{Cl}_2\text{N}_6\text{O}_4\text{S}$ = 445.0253. Found = 445.0254 $[\text{M}+\text{H}]^+$; LCMS (Method A, UV, ES) RT = 0.83 min, $[\text{M}+\text{H}]^+$ = 445, 447, 449, 95% purity.

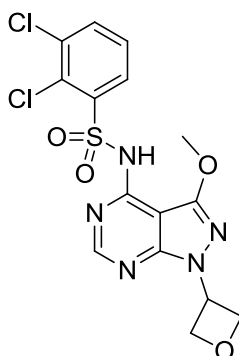
2,3-Dichloro-N-(3-methoxy-1-(2-methoxyethyl)-1H-pyrazolo[3,4-d]pyrimidin-4-yl)benzenesulfonamide (150)



The title compound was prepared from **143** (100 mg, 0.27 mmol), 1-bromo-2-methoxyethane (0.025 mL, 0.27 mmol) and LiHMDS (0.59 mL of a 1 M solution in THF, 0.59 mmol), according to the procedure described for the preparation of **144**. The same work up and

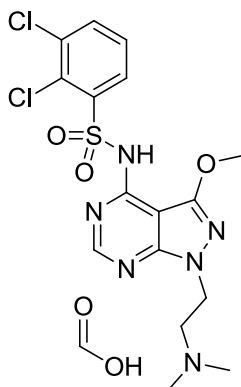
purification afforded **150** (87 mg, 70%) as a white solid; ^1H NMR (400 MHz, $\text{DMSO-}d_6$) δ = 12.37 (br.s, 1H), 8.25 (s, 1H), 8.11 (dd, J = 8.0, 1.5 Hz, 1H), 7.90 (dd, J = 8.0, 1.5 Hz, 1H), 7.57 (t, J = 8.0 Hz, 1H), 4.33 (t, J = 5.4 Hz, 2H), 3.90 (s, 3H), 3.73 (t, J = 5.4 Hz, 2H), 3.21 (s, 3H); HRMS (ESI) m/z calculated for $\text{C}_{15}\text{H}_{16}\text{Cl}_2\text{N}_5\text{O}_4\text{S}$ = 432.0300. Found = 432.0282 $[\text{M}+\text{H}]^+$; LCMS (Method A, UV, ES) RT = 0.96 min, $[\text{M}+\text{H}]^+$ = 432, 434, 436, 95% purity.

2,3-Dichloro-*N*-(3-methoxy-1-(oxetan-3-yl)-1*H*-pyrazolo[3,4-*d*]pyrimidin-4-yl)benzenesulfonamide (151)



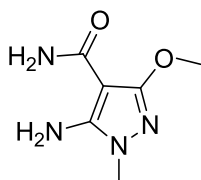
The title compound was prepared from **143** (100 mg, 0.27 mmol), 3-iodooxetane (49 mg, 0.27 mmol) and LiHMDS (0.59 mL of a 1 M solution in THF, 0.59 mmol) according to the procedure described for the preparation of **144**. The same work up and purification afforded **151** (69 mg, 56%) as a white solid; ^1H NMR (400 MHz, $\text{DMSO-}d_6$) δ = 12.42 (br.s, 1H), 8.26 (s, 1H), 8.11 (dd, J = 8.0, 1.5 Hz, 1H), 7.90 (dd, J = 8.0, 1.5 Hz, 1H), 7.57 (t, J = 8.0 Hz, 1H), 5.93 - 5.84 (m, 1H), 5.04 - 4.95 (m, 2H), 4.95 - 4.87 (m, 2H), 3.98 (s, 3H); ^{13}C NMR (101 MHz, $\text{DMSO-}d_6$) δ = 157.2, 151.0, 149.9, 147.9, 141.9, 134.0, 133.9, 129.4, 128.4, 127.9, 92.0, 75.5, 56.3, 49.5; HRMS (ESI) m/z calculated for $\text{C}_{15}\text{H}_{14}\text{Cl}_2\text{N}_5\text{O}_4\text{S}$ = 430.0144. Found = 430.0138 $[\text{M}+\text{H}]^+$; LCMS (Method A, UV, ES) RT = 0.93 min, $[\text{M}+\text{H}]^+$ = 430, 432, 434, 95% purity.

2,3-Dichloro-*N*-(1-(2-(dimethylamino)ethyl)-3-methoxy-1*H*-pyrazolo[3,4-*d*]pyrimidin-4-yl)benzenesulfonamide, formic acid salt (152)



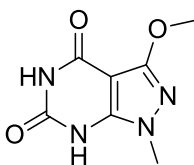
The title compound was prepared from **143** (100 mg, 0.27 mmol), 2-iodo-*N,N*-dimethylethanamine (53 mg, 0.27 mmol) and LiHMDS (0.59 mL of a 1M solution in THF, 0.59 mmol) according to the procedure described for the preparation of **144**. The same work up and purification afforded **152** (21 mg, 19%) as a white solid; ^1H NMR (600 MHz, DMSO- d_6) δ = 12.48 (br.s, 1 H), 9.13 (br.s, 1H), 8.31 (s, 1H), 8.13 (dd, J = 8.1, 1.4 Hz, 1H), 7.92 (dd, J = 8.1, 1.4 Hz, 1H), 7.59 (t, J = 8.1 Hz, 1H), 4.57 (t, J = 6.0 Hz, 2H), 3.93 (s, 3H), 3.56 (t, J = 6.0 Hz, 2H), 2.85 (s, 6H); HRMS (ESI) m/z calculated for $\text{C}_{16}\text{H}_{19}\text{Cl}_2\text{N}_6\text{O}_3\text{S}$ = 445.0616. Found = 445.0617 $[\text{M}+\text{H}]^+$; LCMS (Method A, UV, ES) RT = 0.67 min, $[\text{M}+\text{H}]^+$ = 445, 447, 449, 100% purity.

5-Amino-3-methoxy-1-methyl-1*H*-pyrazole-4-carboxamide (153)



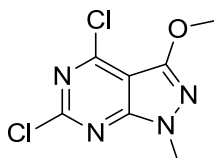
A solution of 5-amino-3-methoxy-1-methyl-1*H*-pyrazole-4-carbonitrile **67** (1.73g, 11.37 mmol) in concentrated sulfuric acid (24 ml of a 98 wt% aqueous solution, 450 mmol) was stirred at ambient temperature for 18 h. The mixture was cooled to 0 °C and neutralised by slow addition of ammonia (6 M aqueous solution). Ethyl acetate (100 mL) was added and the organic phase was separated, dried using a hydrophobic frit and evaporated under reduced pressure to afford the title compound (1.85 g, 94%) as a white solid; ^1H NMR (400 MHz, DMSO- d_6) δ = 6.71 (br.s, 1H), 6.21 (s, 2H), 6.08 (br.s, 1H), 3.81 (s, 3H), 3.38 (s, 3H); LCMS (Method A, UV, ES) RT = 0.36 min, $[\text{M}+\text{H}]^+$ = 171, 95% purity.

3-Methoxy-1-methyl-1*H*-pyrazolo[3,4-*d*]pyrimidine-4,6-diol (**154**)



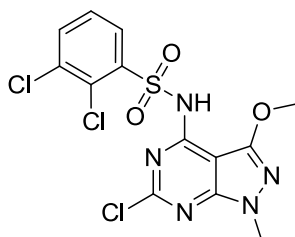
CDI (1.04 g, 6.43 mmol) was added to a solution of **153** (912 mg, 5.36 mmol) in DMF (13.5 mL), and the mixture was stirred at 85 °C for 1 h. A white precipitate formed, which was filtered, washed with diethyl ether (50 mL) and dried under reduced pressure to afford the title compound (730 g, 68%) as a white solid; ¹H NMR (400 MHz, DMSO-*d*₆) δ = 11.82 (br.s, 1H), 10.60 (br.s, 1H), 3.83 (s, 3H), 3.60 (s, 3H); LCMS (Method A, UV, ES) RT = 0.50 min, [M+H]⁺ = 197, 98% purity.

4,6-Dichloro-3-methoxy-1-methyl-1*H*-pyrazolo[3,4-*d*]pyrimidine (**155**)



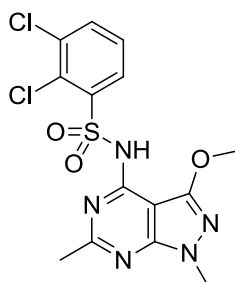
A mixture of **154** (759 mg, 3.87 mmol), phosphorus oxychloride (8 mL, 86 mmol) and phosphorus pentachloride (4.0 g, 19.4 mmol) were heated at 100 °C overnight. The reaction mixture was cooled to ambient temperature and then poured carefully onto iced water (100 mL). The aqueous phase was extracted with chloroform (2 x 100 mL). The combined organic extracts were washed with brine (50 mL), dried using a hydrophobic frit and evaporated under reduced pressure. The residue was purified on a 100 g silica column using a gradient of 0-50% ethyl acetate-cyclohexane over 60 min. The appropriate fractions were combined and evaporated under reduced pressure to afford the title compound (407 mg, 44%) as a white solid; ¹H NMR (400 MHz, DMSO-*d*₆) δ = 4.05 (s, 3H), 3.84 (s, 3H); LCMS (Method A, UV, ES) RT = 1.05 min, [M+H]⁺ = 233, 235, 237, 100% purity.

2,3-Dichloro-*N*-(6-chloro-3-methoxy-1-methyl-1*H*-pyrazolo[3,4-*d*]pyrimidin-4-yl)benzenesulfonamide (**156**)



Sodium hydride (240 mg of a 60% w/w dispersion in mineral oil, 5.98 mmol) was added to a solution of 2,3-dichlorobenzenesulfonamide (676 mg, 2.99 mmol) in anhydrous THF (6 mL). After 30 min of stirring, **155** (697 mg, 2.99 mmol) in anhydrous THF (12 mL) was added, and the reaction mixture was stirred under nitrogen at 60 °C for 18 h. The reaction was cooled to ambient temperature, ammonium chloride (20 mL of a saturated aqueous solution) was added slowly and the organic layer was separated. The aqueous layer was extracted further with ethyl acetate (2 x 40 mL), and the combined organic extracts were washed with brine (40 mL), dried using a hydrophobic frit and concentrated under reduced pressure. The residue was evaporated onto Florisil, dry loaded and purified on 100 g silica column using a gradient of 25-100% ethyl acetate-cyclohexane over 60 min. The appropriate fractions were combined and evaporated under reduced pressure to afford the title compound (760 mg, 57%) as a pale yellow solid; ¹H NMR (400 MHz, DMSO-*d*₆) δ = 8.06 (dd, *J* = 8.0, 1.5 Hz, 1H), 7.66 (dd, *J* = 8.0, 1.5 Hz, 1H), 7.42 (t, *J* = 8.0 Hz, 1H), 3.90 (s, 3H), 3.59 (s, 3H); the exchangeable NH proton was not observed; ¹³C NMR (151 MHz, DMSO-*d*₆) δ = 158.8, 156.7, 155.1, 154.7, 145.7, 132.3, 131.6, 130.2, 128.2, 127.0, 91.3, 55.5, 32.8; HRMS (ESI) *m/z* calculated for C₁₃H₁₁Cl₃N₅O₃S = 421.9648. Found = 421.9632 [M+H]⁺; LCMS (Method A, UV, ES) RT = 1.12 min, [M+H]⁺ = 422, 424, 426, 428, 94% purity.

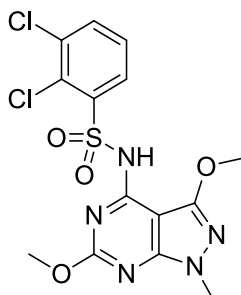
2,3-Dichloro-*N*-(3-methoxy-1,6-dimethyl-1*H*-pyrazolo[3,4-*d*]pyrimidin-4-yl)benzenesulfonamide (157)



A mixture of **156** (53 mg, 0.13 mmol), trimethylboroxine (16 mg, 0.13 mmol), Pd(dppf)Cl₂ (9 mg, 0.01 mmol) and cesium carbonate (163 mg, 0.50 mmol) in anhydrous 1,4-dioxane (0.5 mL) were heated at 100 °C for 2 h in a microwave. The mixture was diluted with MeOH (15 mL), filtered through celite, and concentrated under reduced pressure. The crude mixture was taken up in DMSO (2 mL) and purified by MDAP (Method C). The solvent was evaporated under reduced pressure to afford the title compound (15 mg, 22%) as a white solid; ¹H NMR (400 MHz, DMSO-*d*₆) δ = 11.85 (br.s, 1H), 8.10 (dd, *J* = 8.0, 1.5 Hz, 1H), 7.90 (dd, *J* = 8.0, 1.5 Hz, 1H), 7.57 (t, *J* = 8.0 Hz, 1H), 3.86 (s, 3H), 3.77 (s, 3H), 2.58 (s, 3H); HRMS (ESI)

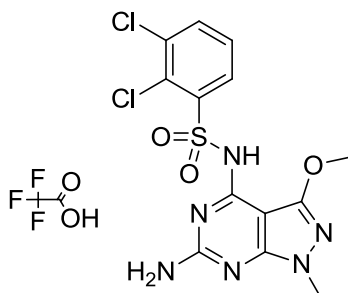
m/z calculated for $C_{14}H_{14}Cl_2N_5O_3S = 402.0194$. Found = 402.0181 $[M+H]^+$; LCMS (Method C, UV, ES) RT = 0.99 min, $[M+H]^+ = 402, 404, 406$, 100% purity.

2,3-Dichloro-*N*-(3,6-dimethoxy-1-methyl-1*H*-pyrazolo[3,4-*d*]pyrimidin-4-yl)benzenesulfonamide (158)



A mixture of sodium methoxide (0.73 mL of a 25% w/v solution in MeOH, 0.37 mmol) and **156** (31 mg, 0.07 mmol) was heated at 130 °C for 0.5 h in a microwave. The reaction was concentrated under reduced pressure, and the crude material was taken up in DMSO (1 mL) and purified by MDAP (Method C). The appropriate fractions were collected and the solvent was evaporated under reduced pressure to afford the title compound (21 mg, 52%) as a white solid; 1H NMR (400 MHz, DMSO- d_6) $\delta = 11.46$ (br.s, 1H), 8.09 (dd, $J = 8.0, 1.5$ Hz, 1H), 7.90 (dd, $J = 8.0, 1.5$ Hz, 1H), 7.57 (t, $J = 8.0$ Hz, 1H), 3.99 (br.s, 3H), 3.86 (s, 3H), 3.70 (s, 3H); HRMS (ESI) m/z calculated for $C_{14}H_{14}Cl_2N_5O_4S = 418.0144$. Found = 418.0138 $[M+H]^+$; LCMS (Method C, UV, ES) RT = 1.08 min, $[M+H]^+ = 418, 420, 422$, 100% purity.

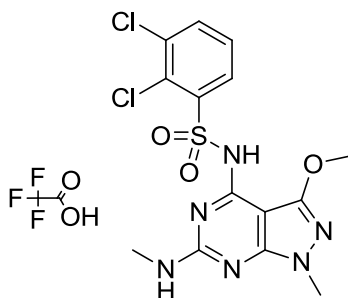
***N*-(6-amino-3-methoxy-1-methyl-1*H*-pyrazolo[3,4-*d*]pyrimidin-4-yl)-2,3-dichlorobenzenesulfonamide, trifluoroacetate (159)**



A mixture of **156** (35 mg, 0.08 mmol) and ammonia (0.18 mL, 8.28 mmol) was heated at 130 °C for 45 min in the microwave. More ammonia (0.18 mL, 8.28 mmol) was added and the reaction was reheated in the microwave at 130 °C for 2 h. The reaction mixture was concentrated under reduced pressure, and the crude material was taken up in DMSO (1 mL) and purified by MDAP (Method C). The appropriate fractions were collected and the solvent

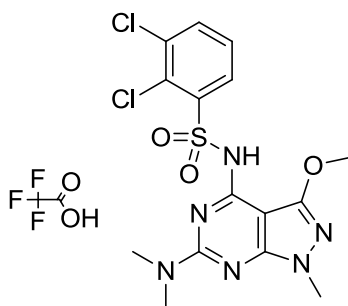
was evaporated under reduced pressure to afford the title compound (12 mg, 27%) as a white solid; ^1H NMR (400 MHz, $\text{DMSO-}d_6$) δ = 10.88 (s, 1H), 8.09 (dd, J = 8.0, 1.5 Hz, 1H), 7.90 (dd, J = 8.0, 1.5 Hz, 1H), 7.82 (s, 2H), 7.57 (t, J = 8.0 Hz, 1H), 3.81 (s, 3H), 3.56 (s, 3H); LCMS (Method C, UV, ES) RT = 0.85 min, $[\text{M}+\text{H}]^+$ = 403, 405, 407, 100% purity.

2,3-Dichloro-*N*-(3-methoxy-1-methyl-6-(methylamino)-1*H*-pyrazolo[3,4-*d*]pyrimidin-4-yl)benzenesulfonamide, trifluoroacetate (160)



The title compound was prepared from **156** (31 mg, 0.07 mmol) and methylamine (0.26 mL of a 2 M solution in THF, 0.51 mmol) according to the procedure described for the preparation of **159**. Purification using MDAP (Method C) afforded **160** (16 mg, 42%) as a white solid; ^1H NMR (400 MHz, $\text{DMSO-}d_6$) δ = 10.91 (br.s, 1H), 8.36 (br q, J = 4.5 Hz, 1H), 8.09 (dd, J = 8.0, 1.5 Hz, 1H), 7.89 (dd, J = 8.0, 1.5 Hz, 1H), 7.56 (t, J = 8.0 Hz, 1H), 3.81 (s, 3H), 3.60 (s, 3H), 2.87 (d, J = 4.5 Hz, 3H); LCMS (Method C, UV, ES) RT = 0.98 min, $[\text{M}+\text{H}]^+$ = 417, 419, 421, 100% purity.

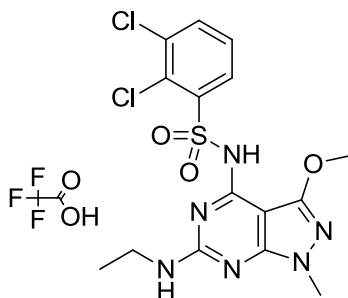
2,3-Dichloro-*N*-(6-(dimethylamino)-3-methoxy-1-methyl-1*H*-pyrazolo[3,4-*d*]pyrimidin-4-yl)benzenesulfonamide, trifluoroacetate (161)



The title compound was prepared from **156** (36 mg, 0.09 mmol) and dimethylamine (0.3 mL of a 2 M solution in THF, 0.60 mmol) according to the procedure described for the preparation of **159**. Purification using MDAP (Method C) afforded **161** (27 mg, 56%) as a white solid; ^1H NMR (400 MHz, $\text{DMSO-}d_6$) δ = 11.46 (br.s, 1H), 8.10 (dd, J = 8.0, 1.5 Hz, 1H), 7.92 (dd, J = 8.0, 1.5 Hz, 1H), 7.58 (t, J = 8.0 Hz, 1H), 3.82 (br.s, 3H), 3.61 (s, 3H), 3.16

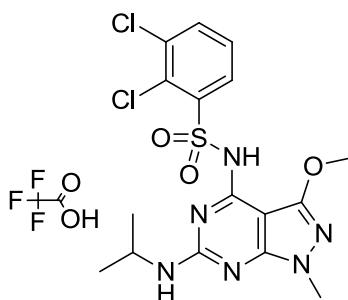
(br.s, 6H); LCMS (Method C, UV, ES) RT = 1.07 min, $[M+H]^+$ = 431, 433, 435, 100% purity.

2,3-Dichloro-*N*-(6-(ethylamino)-3-methoxy-1-methyl-1*H*-pyrazolo[3,4-*d*]pyrimidin-4-yl)benzenesulfonamide, trifluoroacetate (162)



The title compound was prepared from **156** (33 mg, 0.08 mmol) and ethylamine (0.25 mL of a 2 M solution in THF, 0.55 mmol) according to the procedure described for the preparation of **159**. Purification using MDAP (Method C) afforded **162** (20 mg, 44%) as a white solid; ^1H NMR (400 MHz, $\text{DMSO-}d_6$) δ = 10.85 (br.s, 1H), 8.41 (q, J = 4.8 Hz, 1H), 8.08 (dd, J = 8.0, 1.5 Hz, 1H), 7.90 (dd, J = 8.0, 1.5 Hz, 1H), 7.56 (t, J = 8.0 Hz, 1H), 3.81 (s, 3H), 3.59 (s, 3H), 3.38 - 3.30 (m, 2H), 1.18 (t, J = 7.0 Hz, 3H); LCMS (Method C, UV, ES) RT = 1.06 min, $[M+H]^+$ = 431, 433, 435, 100% purity

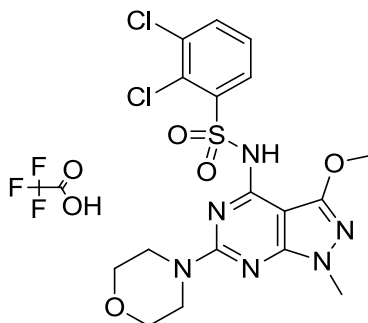
2,3-Dichloro-*N*-(6-(isopropylamino)-3-methoxy-1-methyl-1*H*-pyrazolo[3,4-*d*]pyrimidin-4-yl)benzenesulfonamide, trifluoroacetate (163)



The title compound was prepared from **156** (32 mg, 0.08 mmol) and *isopropylamine* (0.26 mL, 3.03 mmol) according to the procedure described for the preparation of **159**. Purification using MDAP (Method C) afforded **163** (18 mg, 40%) as a white solid; ^1H NMR (400 MHz, $\text{DMSO-}d_6$) δ = 10.77 (br.s, 1H), 8.37 (d, J = 6.5 Hz, 1H), 8.08 (dd, J = 8.0, 1.5 Hz, 1H), 7.89 (dd, J = 8.0, 1.5 Hz, 1H), 7.56 (t, J = 8.0 Hz, 1H), 4.09 - 3.98 (m, 1H), 3.81 (s, 3H), 3.17 (s,

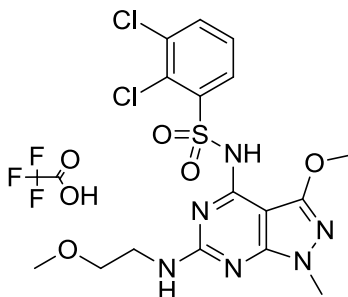
3H), 1.20 (d, $J = 6.5$ Hz, 6H); LCMS (Method C, UV, ES) RT = 1.14 min, $[M+H]^+ = 445, 447, 449, 100\%$ purity.

2,3-Dichloro-*N*-(3-methoxy-1-methyl-6-morpholino-1*H*-pyrazolo[3,4-*d*]pyrimidin-4-yl)benzenesulfonamide, trifluoroacetate (164)



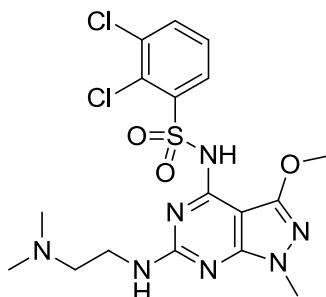
The title compound was prepared from **156** (40 mg, 0.10 mmol) and morpholine (0.25 mL, 2.84 mmol) according to the procedure described for the preparation of **159**. Purification using MDAP (Method C) afforded **164** (28 mg, 48%) as a white solid; ^1H NMR (400 MHz, DMSO- d_6) $\delta = 11.58$ (br.s, 1H), 8.12 (dd, $J = 8.0, 1.5$ Hz, 1H), 7.93 (dd, $J = 8.0, 1.5$ Hz, 1H), 7.59 (t, $J = 8.0$ Hz, 1H), 3.88 (s, 3H), 3.60 (s, 3H), 3.54 - 3.37 (m, 8H); LCMS (Method C, UV, ES) RT = 1.06 min, $[M+H]^+ = 473, 475, 477, 100\%$ purity.

2,3-Dichloro-*N*-(3-methoxy-6-((2-methoxyethyl)amino)-1-methyl-1*H*-pyrazolo[3,4-*d*]pyrimidin-4-yl)benzenesulfonamide, trifluoroacetate (165)



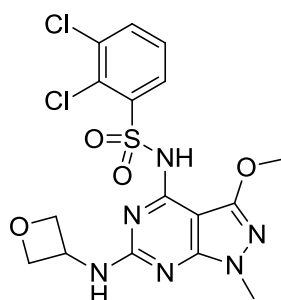
The title compound was prepared from **156** (33 mg, 0.08 mmol) and 2-methoxyethylamine (0.20 mL, 2.34 mmol) according to the procedure described for the preparation of **159**. Purification using MDAP (Method C) afforded **165** (16 mg, 34%) as a white solid; ^1H NMR (400 MHz, DMSO- d_6) $\delta = 10.91$ (s, 1H), 8.60 - 8.54 (m, 1H), 8.09 (dd, $J = 8.0, 1.5$ Hz, 1H), 7.89 (dd, $J = 8.0, 1.5$ Hz, 1H), 7.56 (t, $J = 8.0$ Hz, 1H), 3.81 (s, 3H), 3.59 (s, 3H), 3.53 - 3.48 (m, 4H), 3.31 (s, 3H); LCMS (Method C, UV, ES) RT = 1.01 min, $[M+H]^+ = 460, 462, 464, 100\%$ purity.

2,3-Dichloro-*N*-(6-((2-(dimethylamino)ethyl)amino)-3-methoxy-1-methyl-1*H*-pyrazolo[3,4-*d*]pyrimidin-4-yl)benzenesulfonamide (166)



The title compound was prepared from **156** (30 mg, 0.07 mmol) and *N,N*-dimethylethane-1,2-diamine (0.01 mL, 0.11 mmol) in IPA (0.5 mL) according to the procedure described for the preparation of **159**. Purification using MDAP (Method C) afforded the TFA salt of the product. The white solid was re-dissolved in MeOH (1 mL) and loaded on top of an aminopropyl cartridge (500 mg), previously pre-conditioned with MeOH (2 mL). The product was eluted with MeOH (10 mL) and the solvent was evaporated under reduced pressure to afford **166** (11 mg, 30%) as a white solid; ^1H NMR (400 MHz, MeOH- d_4) δ = 8.11 (dd, J = 8.0, 1.5 Hz, 1H), 7.62 (dd, J = 8.0, 1.5 Hz, 1H), 7.36 (t, J = 8.0 Hz, 1H), 3.93 (s, 3H), 3.58 (s, 3H), 3.35 - 3.31 (m, 2H), 2.89 - 2.83 (m, 2H), 2.58 (s, 6H); the two exchangeable NH protons were not observed; LCMS (Method C, UV, ES) RT = 0.75 min, $[\text{M}+\text{H}]^+ = 474, 476, 478$, 100% purity.

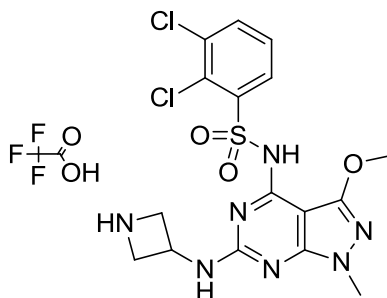
2,3-Dichloro-*N*-(3-methoxy-1-methyl-6-(oxetan-3-ylamino)-1*H*-pyrazolo[3,4-*d*]pyrimidin-4-yl)benzenesulfonamide (167)



The title compound was prepared from **156** (30 mg, 0.07 mmol) and oxetan-3-amine (0.02 mL, 0.21 mmol) in ethanol (0.5 mL) according to the procedure described for the preparation of **159**. Purification using MDAP (Method C) afforded **167** (3.5 mg, 9%) as a clear oil; ^1H NMR (400 MHz, DMSO- d_6) δ = 10.98 (s, 1H), 9.17 (d, J = 5.0 Hz, 1H), 8.09 (dd, J = 8.0, 1.5 Hz, 1H), 7.90 (dd, J = 8.0, 1.5 Hz, 1H), 7.57 (t, J = 8.0 Hz, 1H), 4.96 - 4.87 (m, 1H), 4.87 -

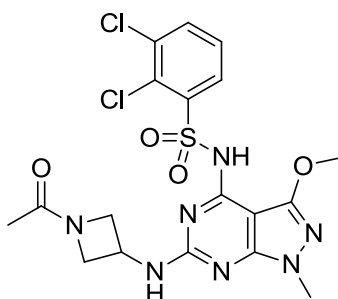
4.78 (m, 2H), 4.53 - 4.46 (m, 2H), 3.81 (s, 3H), 3.58 (s, 3H); LCMS (Method c, UV, ES) RT = 0.94 min, $[M+H]^+$ = 459, 461, 463, 100% purity.

***N*-(6-(Azetidin-3-ylamino)-3-methoxy-1-methyl-1*H*-pyrazolo[3,4-*d*]pyrimidin-4-yl)-2,3-dichlorobenzenesulfonamide, trifluoroacetate (**168**)**



A mixture of **156** (96 mg, 0.23 mmol) and 1-Boc-3-(amino)azetidine (78 mg, 0.45 mmol) in IPA (1.6 mL) was heated in a microwave at 115 °C for 2 h. The reaction mixture was concentrated under reduced pressure, and HCl (0.65 mL of a 4 M solution in 1,4-dioxane, 2.6 mmol) was added. After stirring for 4 h, the reaction was concentrated, and the crude material was taken up in DMSO (1 mL) and purified by MDAP (Method C). The appropriate fractions were collected and the solvent was evaporated under reduced pressure to afford the title compound (37 mg, 22%) as a white solid; ^1H NMR (400 MHz, DMSO- d_6) δ = 11.03 (br.s, 1H), 9.14 (br.s, 1H), 8.82 (br.s, 2H), 8.09 (dd, J = 8.0, 1.5 Hz, 1H), 7.91 (dd, J = 8.0, 1.5 Hz, 1H), 7.58 (t, J = 8.0 Hz, 1H), 4.78 - 4.68 (m, 1H), 4.30 - 4.18 (m, 2H), 4.08 - 3.96 (m, 2H), 3.82 (s, 3H), 3.62 (s, 3H); LCMS (Method C, UV, ES) RT = 0.73 min, $[M+H]^+$ = 458, 460, 462, 100% purity.

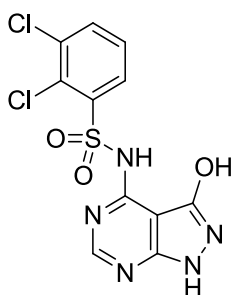
***N*-(6-((1-Acetylazetidin-3-yl)amino)-3-methoxy-1-methyl-1*H*-pyrazolo[3,4-*d*]pyrimidin-4-yl)-2,3-dichlorobenzenesulfonamide (**169**)**



Acetyl chloride (4 μL , 0.05 mmol) and triethylamine (13 μL , 0.091 mmol) were added to a solution of **168** (26 mg, 0.05 mmol) in DCM (0.5 mL), and the mixture was stirred at ambient temperature for 4 h. The reaction mixture was concentrated, and the crude material was taken

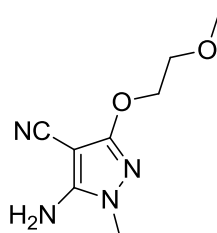
up in DMSO (1 mL) and purified by MDAP (Method B). The appropriate fractions were collected and the solvent was evaporated under reduced pressure to afford the title compound (10 mg, 40%) as a white solid; ^1H NMR (400 MHz, $\text{DMSO-}d_6$) δ = 8.12 (dd, J = 8.0, 1.5 Hz, 1H), 7.73 (dd, J = 8.0, 1.5 Hz, 1H), 7.48 (t, J = 8.0 Hz, 1H), 4.49 - 4.38 (m, 1H), 4.28 - 4.14 (m, 2H), 3.94 - 3.82 (m, 5H), 3.57 (s, 3H), 1.78 (s, 3H); the two exchangeable NH protons were not observed; LCMS (Method C, UV, ES) RT = 0.87 min, $[\text{M}+\text{H}]^+$ = 500, 502, 504, 100% purity.

2,3-Dichloro-*N*-(3-hydroxy-1*H*-pyrazolo[3,4-*d*]pyrimidin-4-yl)benzenesulfonamide (170)



TMSCl (0.22 mL, 1.68 mmol) was added to a mixture of **143** (314 mg, 0.84 mmol) and sodium iodide (252 mg, 1.68 mmol) in MeCN (11 mL). The reaction was heated to reflux and was stirred for 18 h. The suspension was cooled to ambient temperature, filtered and the solid was washed with MeCN (20 mL) and dried under reduced pressure to afford the title compound (280 mg, 90%) as a pale yellow solid; ^1H NMR (400 MHz, $\text{DMSO-}d_6$) δ = 13.09 (br.s, 1H), 12.23 (br.s, 1H), 11.19 (br.s, 1H), 8.19 (s, 1H), 8.11 (dd, J = 8.0, 1.0 Hz, 1H), 7.90 (dd, J = 8.0, 1.0 Hz, 1H), 7.57 (t, J = 8.0 Hz, 1H); ^{13}C NMR (101MHz, $\text{DMSO-}d_6$, 373 K) δ = 156.0, 151.9, 150.0, 146.5, 142.4, 133.2, 132.6, 129.1, 127.7, 127.5, 91.0; HRMS (ESI) m/z calculated for $\text{C}_{11}\text{H}_8\text{Cl}_2\text{N}_5\text{O}_3\text{S}$ = 359.9725. Found = 359.9711 $[\text{M}+\text{H}]^+$; LCMS (Method A, UV, ES) RT = 0.69 min, $[\text{M}+\text{H}]^+$ = 360, 362, 364, 100% purity.

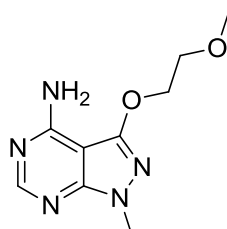
5-Amino-3-(2-methoxyethoxy)-1-methyl-1*H*-pyrazole-4-carbonitrile (171)



A mixture of 2-methoxyethanol (20 mL, 225 mmol) and urea (400 mg, 6.66 mmol) was heated to 80 °C, and treated portionwise with tetracyanoethylene (2.56 g, 20.0 mmol) over 15 min. The solution was heated for a further 5 min and cooled to ambient temperature. LCMS

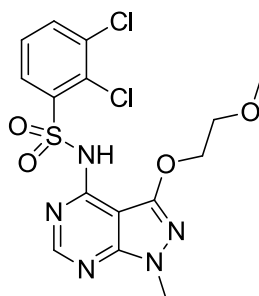
analysis shows high conversion to intermediate dialkoxycyanoethylene. Methylhydrazine (921 mg, 20.0 mmol) was added portionwise over 10 min. The red solution was heated at 80 °C for 15 min, cooled, and evaporated onto Florisil. The product was purified on a 50 g silica column, using a gradient of 0-100% ethyl acetate-cyclohexane over 40 min to give mixture of isomers (~2:1) as a cream solid. The solid (1.2 g) was crystallised from toluene (20 mL) to give a white crystalline material (0.8 g ~ 90:10 isomer ratio). Re-crystallisation from toluene (10 mL) afforded the title compound (670 mg, 17%) as a white crystalline solid. ¹H NMR (400 MHz, DMSO-*d*₆) δ = 6.54 (s, 2H), 4.23 - 4.08 (m, 2H), 3.68 - 3.50 (m, 2H), 3.37 (s, 3H), 3.28 (s, 3H); LCMS (Method A, UV, ES) RT = 0.51 min, [M+H]⁺ = 197, 90% purity.

3-(2-Methoxyethoxy)-1-methyl-1*H*-pyrazolo[3,4-*d*]pyrimidin-4-amine (172)



A mixture of **171** (520 mg, 2.65 mmol) and formamide (3 mL, 58.3 mmol) was heated at 180 °C for 3 h. The cooled suspension was diluted with IPA (3 ml) and filtered to afford the title compound (540 mg, 91%) as a beige solid; ¹H NMR (400 MHz, MeOD-*d*₄) δ = 8.10 (s, 1H), 4.51 - 4.44 (m, 2H), 3.85 - 3.79 (m, 2H), 3.77 (s, 3H), 3.45 (s, 3H); the exchangeable NH₂ protons were not observed; LCMS (Method A, UV, ES) RT = 0.39 min, [M+H]⁺ = 224, 95% purity.

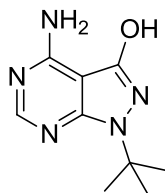
2,3-Dichloro-*N*-(3-(2-methoxyethoxy)-1-methyl-1*H*-pyrazolo[3,4-*d*]pyrimidin-4-yl)benzenesulfonamide (173)



LiHMDS (0.49 mL of a 1 M solution in THF, 0.49 mmol) was added to a solution of **172** (100 mg, 0.45 mmol) in anhydrous DMF (1 ml). The mixture was stirred for 5 min, then 2,3-dichlorobenzenesulfonyl chloride (110 mg, 0.45 mmol) was added, and the reaction was stirred under nitrogen for 1 h. LCMS analysis showed ~ 50% conversion. Further LiHMDS (0.49 mL of a 1M solution in THF, 0.49 mmol) and 2,3-dichlorobenzenesulfonyl chloride

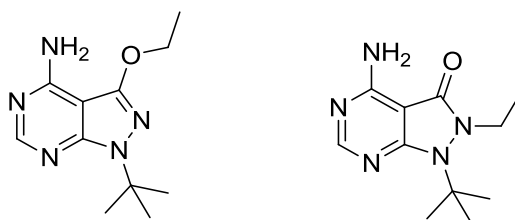
(110 mg, 0.45 mmol) was added, and the reaction was stirred for a further 1 h. The solution was concentrated under reduced pressure and the crude mixture was taken up in 1:1 DMSO-MeOH (1 mL) and purified on MDAP (Method B). The appropriate fractions were combined and the solvent was evaporated under reduced pressure to afford the title compound (19 mg, 10%) as a white solid; ^1H NMR (400 MHz, DMSO- d_6) δ = 12.38 (br.s, 1H), 8.23 (s, 1H), 8.12 (dd, J = 8.0, 1.5 Hz, 1H), 7.89 (dd, J = 8.0, 1.5 Hz, 1H), 7.55 (t, J = 8.0 Hz, 1H), 4.41 - 4.26 (m, 2H), 3.78 (s, 3H), 3.68 - 3.56 (m, 2H), 3.18 (s, 3H); ^{13}C NMR (101 MHz, DMSO- d_6) δ = 178.7, 156.0, 150.6, 147.7, 142.2, 133.9, 133.8, 129.3, 128.2, 127.8, 91.5, 69.7, 68.5, 58.2, 33.5; HRMS (ESI) m/z calculated for $\text{C}_{15}\text{H}_{16}\text{Cl}_2\text{N}_5\text{O}_4\text{S}$ = 432.0300. Found = 432.0300 $[\text{M}+\text{H}]^+$; LCMS (Method A, UV, ES) RT = 0.92 min, $[\text{M}+\text{H}]^+$ = 432, 434, 436, 100% purity.

4-Amino-1-(*tert*-butyl)-1*H*-pyrazolo[3,4-*d*]pyrimidin-3-ol (174)



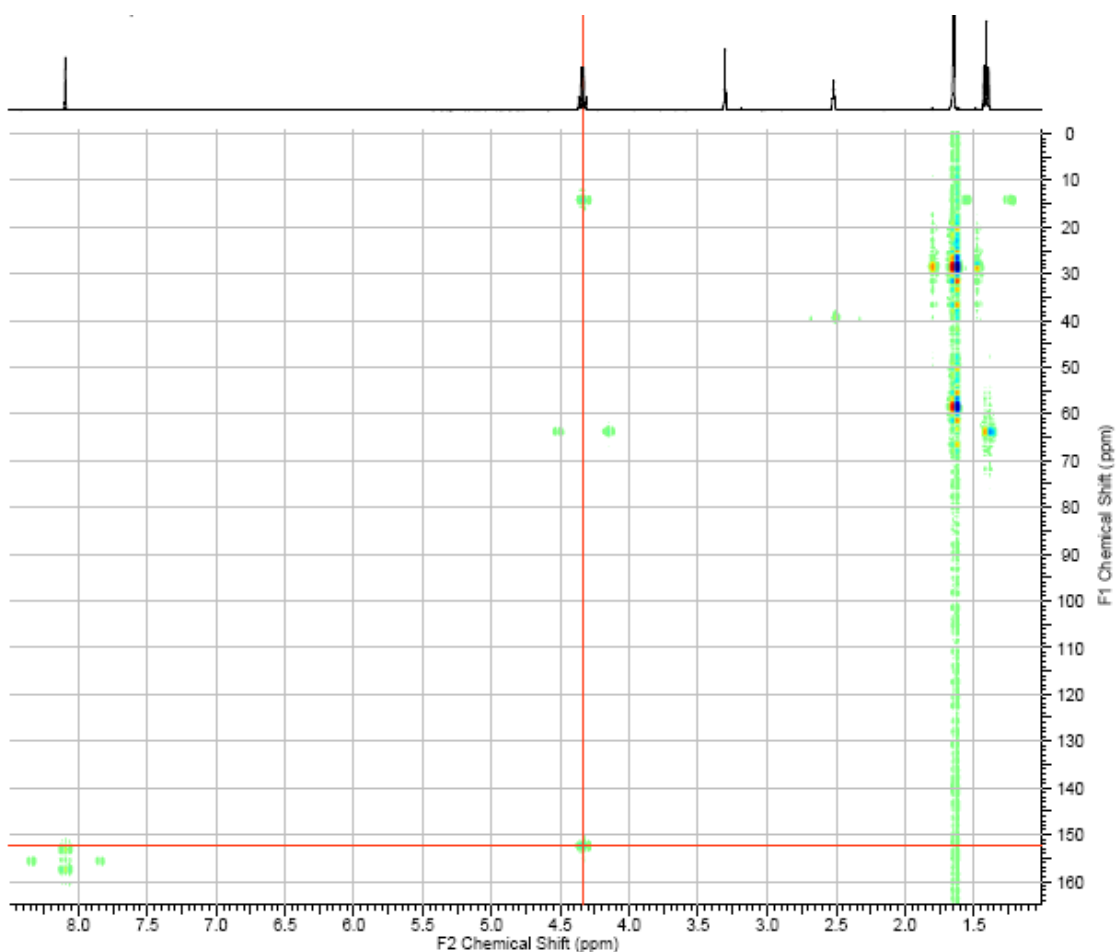
TMSCl (2.38 mL, 18.6 mmol) was added to a mixture of **141** (2.06 g, 9.31 mmol) and sodium iodide (2.79 g, 18.60 mmol) in MeCN (70 mL), and the reaction was heated at reflux under nitrogen for 18 h. More TMSCl (2.38 mL, 18.6 mmol) and sodium iodide (2.79 g, 18.60 mmol) were added, and the reaction was heated at reflux for a further 18 h. The reaction was filtered and the solid was partitioned between water (50 mL) and ethyl acetate (50 mL). The organic layer was separated and the water layer was extracted with more ethyl acetate (2 x 50 mL). The combined organic extracts were dried using a hydrophobic frit, and concentrated under reduced pressure to afford the title compound (1.42 g, 72%) as a pale yellow solid; ^1H NMR (400 MHz, DMSO- d_6) δ = 12.20 - 11.92 (br.s, 1H), 8.91 - 8.71 (m, 1H), 8.63 - 8.47 (m, 1H), 8.30 (s, 1H), 1.66 (s, 9H). LCMS (Method C, UV, ES) RT = 0.51 min, $[\text{M}+\text{H}]^+$ = 208, 96% purity.

1-(*tert*-Butyl)-3-ethoxy-1*H*-pyrazolo[3,4-*d*]pyrimidin-4-amine (175) & 4-amino-1-(*tert*-butyl)-2-ethyl-1*H*-pyrazolo[3,4-*d*]pyrimidin-3(2*H*)-one (176)

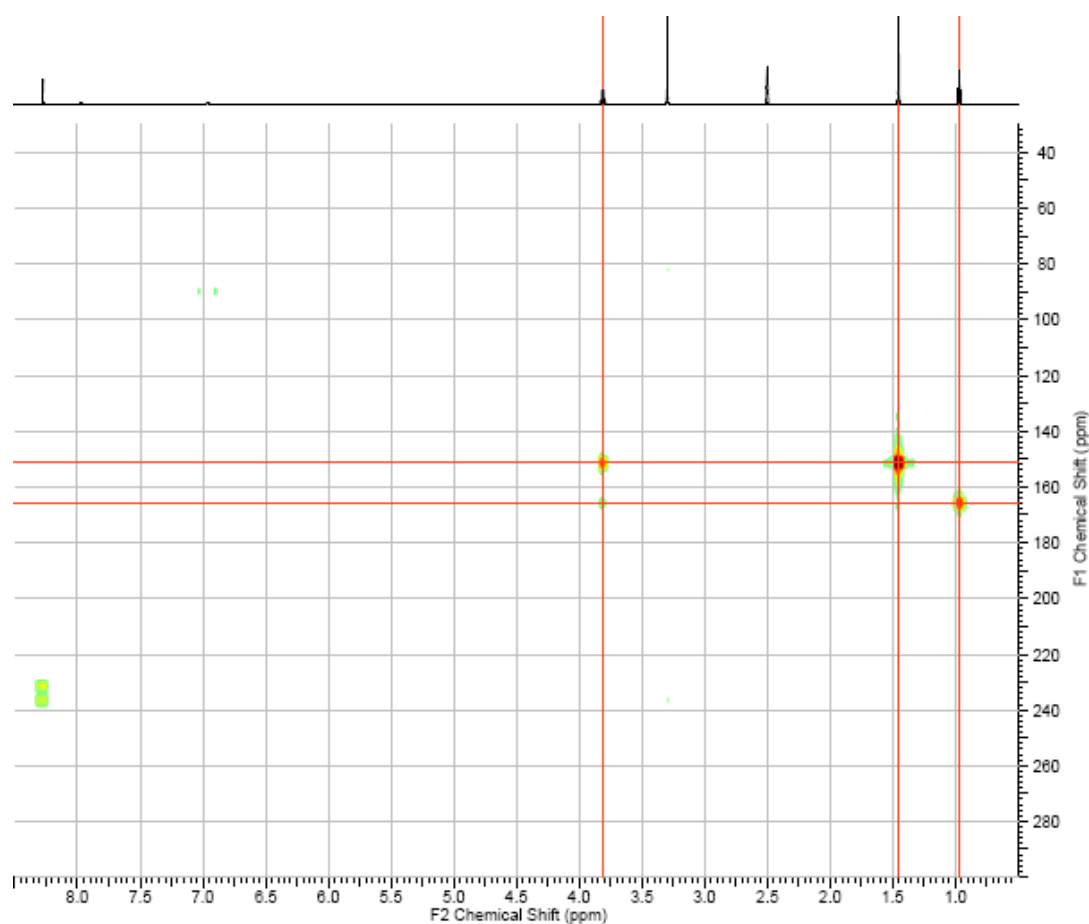


A mixture of **174** (710 mg, 3.43 mmol), iodoethane (0.33 mL, 4.11 mmol) and potassium carbonate (947 mg, 6.85 mmol) in anhydrous DMSO (14 mL) was stirred at 130 °C for 3 h. Water (30 mL) was added and the products were extracted with ethyl acetate (2 x 50 mL). The combined organic extracts were washed with water (30 mL), dried using a hydrophobic frit and concentrated under reduced pressure. The crude material was purified on a 100 g silica column, using a gradient of 0-50% ethyl acetate-cyclohexane over 40 min. The appropriate fractions were combined and the solvent was evaporated under reduced pressure to afford the two regioisomers: **175** (414 mg, 50%) as a pale brown solid; ¹H NMR (400 MHz, DMSO-*d*₆) δ = 8.08 (s, 1H), 7.70 - 6.12 (m, 2H), 4.33 (q, *J* = 7.0 Hz, 2H), 1.63 (s, 9H), 1.39 (t, *J* = 7.0 Hz, 3H); LCMS (Method B, UV, ES) RT = 1.05 min, [M+H]⁺ = 236, 98% purity; and **176** (52 mg 6%) as a white solid; ¹H NMR (400 MHz, DMSO-*d*₆) δ = 8.27 (s, 1H), 7.96 (br.s, 1H), 6.95 (br.s, 1H), 3.81 (q, *J* = 7.0 Hz, 2H), 1.46 (s, 9H), 0.97 (t, *J* = 7.0 Hz, 3H). LCMS (Method B, UV, ES) RT = 0.82 min, [M+H]⁺ = 236, 100% purity.

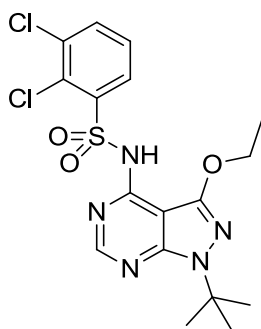
HMBC experiment of regioisomer **175** shows key correlation from the methylene protons (4.33 ppm) of the ethoxy group to the C3-carbon (152.2 ppm) on the pyrazolopyrimidine core.



^1H - ^{15}N HMBC experiment of regioisomer **176** showed a key $^3J_{\text{N-H}}$ correlation from the N1-nitrogen to both the *tert*-butyl protons and the methylene proton of the ethyl group, and the N2-nitrogen showed correlation to all the protons of the ethyl group



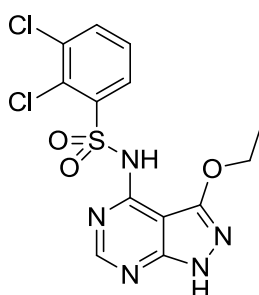
***N*-(1-(*tert*-Butyl)-3-ethoxy-1*H*-pyrazolo[3,4-*d*]pyrimidin-4-yl)-2,3-dichlorobenzenesulfonamide, trifluoroacetate (177)**



Compound **175** (414 mg, 1.76 mmol) was added to a suspension of sodium hydride (141 mg of a 60% w/w dispersion in mineral oil, 3.52 mmol) in anhydrous DMF (8 mL). After stirring at ambient temperature for 10 min, 2,3-dichlorobenzenesulfonyl chloride (475 mg, 1.94 mmol) was added, and the reaction was stirred for a further 2 h. The reaction was diluted with water (30 mL) and the product was extracted with ethyl acetate (3 x 30 mL). The combined organic extracts were dried using a hydrophobic frit and concentrated under reduced pressure. The crude material was purified on a 50 g silica column, using a gradient of 0-25% ethyl

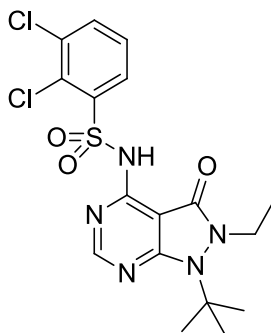
acetate-cyclohexane over 40 min. The appropriate fractions were combined and the solvent was evaporated under reduced pressure to afford the title compound (256 mg, 31%) as a white solid; $^1\text{H NMR}$ (400 MHz, $\text{DMSO-}d_6$) $\delta = 12.36$ (br.s, 1H), 8.21 (dd, $J = 8.0, 1.5$ Hz, 1H), 7.88 (dd, $J = 8.0, 1.5$ Hz, 1H), 7.55 (t, $J = 8.0$ Hz, 1H), 4.28 (q, $J = 7.0$ Hz, 2H), 1.66 (s, 9H), 1.29 (t, $J = 7.0$ Hz, 3H); the exchangeable NH proton was not observed; LCMS (Method C, UV, ES) RT = 1.31 min, $[\text{M}+\text{H}]^+ = 444, 446, 448$, 100% purity.

2,3-Dichloro-*N*-(3-ethoxy-1*H*-pyrazolo[3,4-*d*]pyrimidin-4-yl)benzenesulfonamide, trifluoroacetate (178)



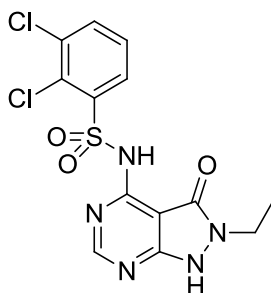
Compound **177** (97 mg, 0.22 mmol) was slowly added to a stirred solution of concentrated sulfuric acid (2 ml of a 98 wt% aqueous solution, 38 mmol) at 0 °C. The solution was stirred at this temperature for 30 min, and then neutralised carefully with sodium carbonate (saturated aqueous solution). The product was extracted with ethyl acetate (2 x 30 mL), and the combined organic extracts were dried using a hydrophobic frit and concentrated under reduced pressure. The crude material was taken up in 1:1 DMSO-MeOH (1 mL) and purified by MDAP (Method C). The appropriate fractions were combined and the solvent was evaporated under reduced pressure to afford the title compound (38 mg, 34%) as a white solid; $^1\text{H NMR}$ (400 MHz, $\text{DMSO-}d_6$) $\delta = 13.29$ (br.s, 1H), 12.34 (br.s, 1H), 8.21 (s, 1H), 8.13 (dd, $J = 8.0, 1.5$ Hz, 1H), 7.90 (dd, $J = 8.0, 1.5$ Hz, 1H), 7.56 (t, $J = 8.0$ Hz, 1H), 4.28 (q, $J = 7.0$ Hz, 2H), 1.29 (t, $J = 7.0$ Hz, 3H); LCMS (Method C, UV, ES) RT = 0.88 min, $[\text{M}+\text{H}]^+ = 388, 390, 392$, 100% purity.

***N*-(1-(*Tert*-butyl)-2-ethyl-3-oxo-2,3-dihydro-1*H*-pyrazolo[3,4-*d*]pyrimidin-4-yl)-2,3-dichlorobenzenesulfonamide, trifluoroacetate (**179**)**



The title sulfonamide compound was prepared from **176** (51 mg, 0.22 mmol), 2,3-dichlorobenzenesulfonyl chloride (59 mg, 0.24 mmol) and sodium hydride (18 mg of a 60% w/w dispersion in mineral oil, 0.44 mmol) according to the procedure described for the preparation of **177**. The same work up and purification using the MDAP (Method C) afforded **179** (46 mg, 36%) as a white solid; $^1\text{H NMR}$ (400 MHz, $\text{DMSO-}d_6$) δ = 12.59 (br.s, 1H), 8.39 (s, 1H), 8.14 (dd, J = 8.0, 1.5 Hz, 1H), 7.91 (dd, J = 8.0, 1.5 Hz, 1H), 7.58 (t, J = 8.0 Hz, 1H), 3.85 (q, J = 7.0 Hz, 2H), 1.56 (s, 9H), 0.98 (t, J = 7.0 Hz, 3H); LCMS (Method C, UV, ES) RT = 1.03 min, $[\text{M}+\text{H}]^+$ = 444, 446, 448, 100% purity.

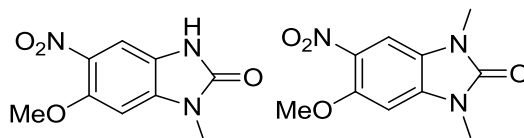
2,3-Dichloro-*N*-(2-ethyl-3-oxo-2,3-dihydro-1*H*-pyrazolo[3,4-*d*]pyrimidin-4-yl)benzenesulfonamide, trifluoroacetate (180**)**



The title sulfonamide compound was prepared from **179** (46 mg, 0.10 mmol) and concentrated sulfuric acid (1 ml of a 98 wt% aqueous solution, 18.8 mmol) according to the procedure described for the preparation of **178**. The same work up and purification afforded **180** (7 mg, 13%) as a pale yellow solid; $^1\text{H NMR}$ (400 MHz, $\text{DMSO-}d_6$) δ = 11.98 (br.s, 1H), 8.14 (s, 1H), 8.11 (dd, J = 8.0, 1.5 Hz, 1H), 7.89 (dd, J = 8.0, 1.5 Hz, 1H), 7.56 (t, J = 8.0 Hz, 1H), 3.89 (q, J = 7.0 Hz, 2H), 1.24 (t, J = 7.0 Hz, 3H); one of the exchangeable NH protons

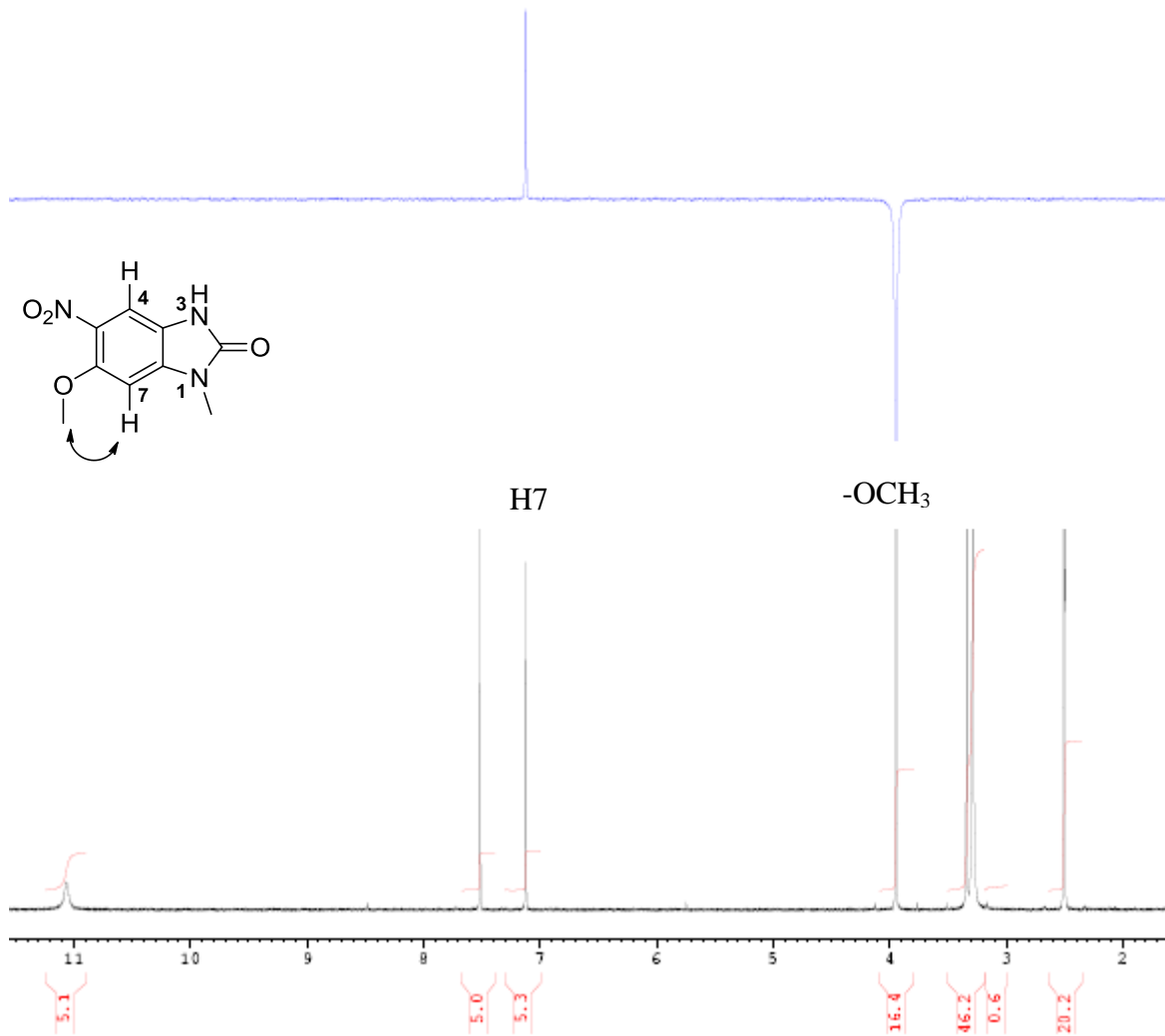
was not observed; LCMS (Method C, UV, ES) RT = 0.74 min, $[M+H]^+ = 388, 390, 392$, 100% purity.

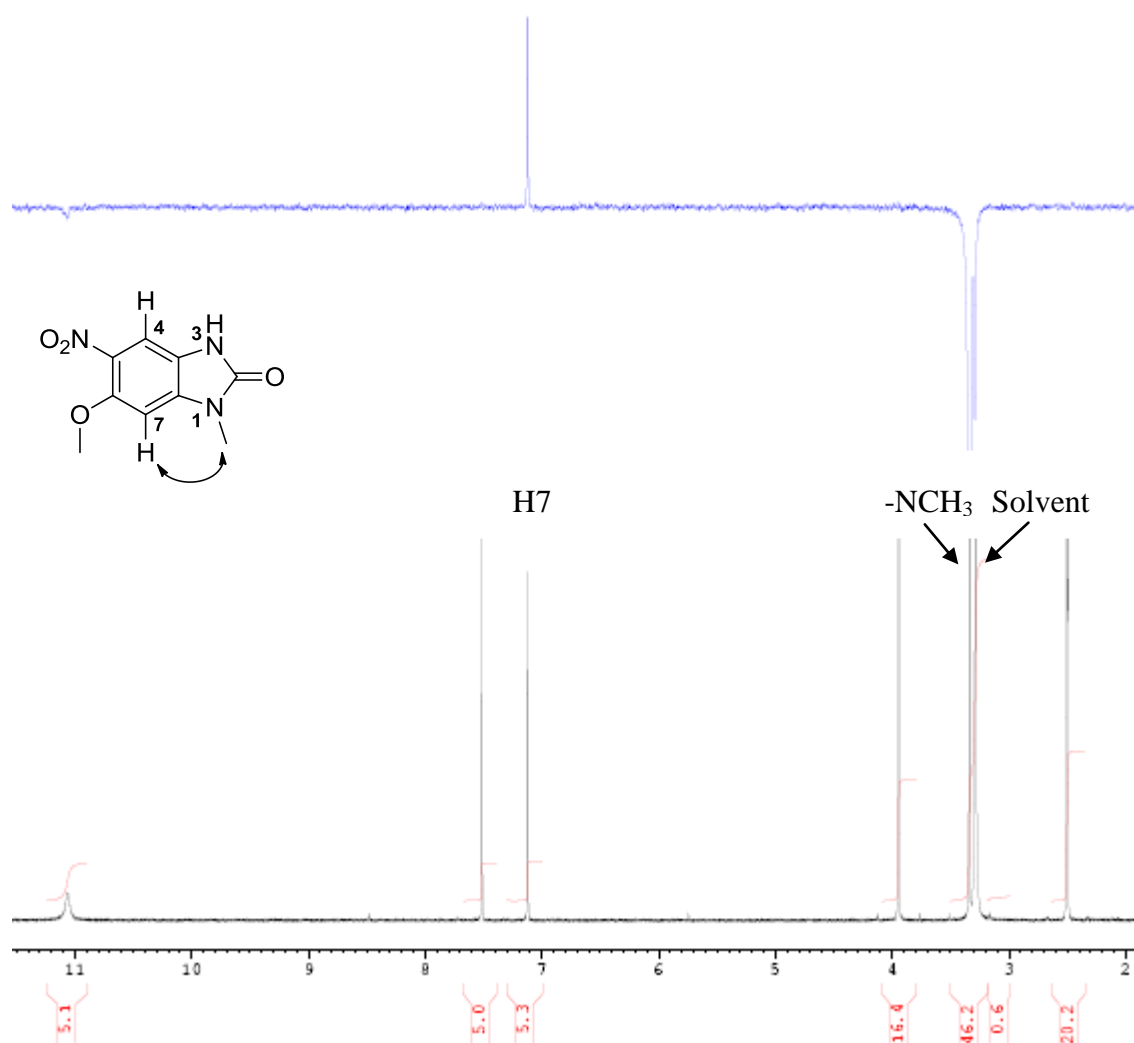
6-Methoxy-1-methyl-5-nitro-1*H*-benzo[*d*]imidazol-2(3*H*)-one (187a) and 5-methoxy-1,3-dimethyl-6-nitro-1*H*-benzo[*d*]imidazol-2(3*H*)-one (187b)



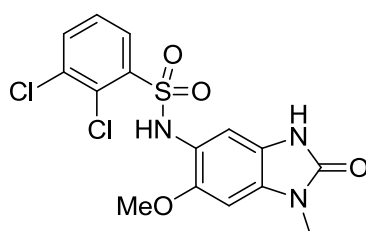
Sodium hydride (15 mg of a 60% w/w dispersion in mineral oil, 0.38 mmol) was added to a stirring solution of 5-methoxy-6-nitro-1*H*-benzo[*d*]imidazol-2(3*H*)-one (75 mg, 0.36 mmol) in anhydrous DMF (1 mL) at 0 °C. Methyl iodide (0.02 mL, 0.36 mmol) was added and the reaction mixture was stirred at ambient temperature for 4 h. The reaction mixture was then diluted with water (15 mL) and ethyl acetate (15 mL). The organic layer was separated, washed with water (10 mL), brine (10 mL), dried using a hydrophobic frit and evaporated under reduced pressure to give a brown solid. The solid was taken up in DMSO (2 mL) and purified by MDAP (Method A). The appropriate fractions were combined and the solvent was evaporated under reduced pressure to give the two separated product as yellow solids: mono alkylated product **187a** (20 mg, 25% yield); 1H NMR (400 MHz, $DMSO-d_6$) $\delta = 11.06$ (br.s, 1H), 7.51 (s, 1H), 7.12 (s, 1H), 3.94 (s, 3H), 3.34 (s, 3H); LCMS (Method A, UV, ES) RT = 0.60 min, $[M+H+MeCN]^+ = 265$, $[M+H]^+ = 222$, 95% purity; and dialkylated product **187b** (12 mg, 14%); 1H NMR (400 MHz, $DMSO-d_6$) $\delta = 7.80$ (s, 1H), 7.19 (s, 1H), 3.95 (s, 3H), 3.39 (s, 3H), 3.34 (s, 3H); 1H NMR (400 MHz, $MeOD-d_4$) $\delta = 7.74$ (s, 1H), 7.06 (s, 1H), 3.99 (s, 3H), 3.45 (s, 3H), 3.41 (s, 3H); LCMS (Method A, UV, ES) RT = 0.69 min, $[M+H+MeCN]^+ = 279$, $[M+H]^+ = 238$, 99% purity.

NOE experiment of regioisomer **187a** using $DMSO-d_6$ as a solvent showed that irradiation at the frequency of the *N*-methyl protons (3.34 ppm) and *O*-methyl protons (3.94 ppm), resulted in both giving an NOE for the proton at the C7-position (7.12 ppm), which is close in space, confirming the regiochemistry of the alkylation





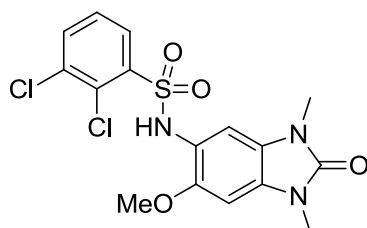
2,3-Dichloro-N-(6-methoxy-1-methyl-2-oxo-2,3-dihydro-1H-benzo[d]imidazol-5-yl)benzenesulfonamide (190a)



The benzimidazolone **187a** (20 mg, 0.09 mmol) was dissolved in a mixture of ethanol (2 mL) and ethyl acetate (2 mL), and was added to a tube containing palladium-on-carbon (5 mg of a 10% by wt, 5 μ mol) under vacuum. The tube was back filled with nitrogen, evacuated and filled with hydrogen using the burette apparatus. The reaction mixture was stirred under

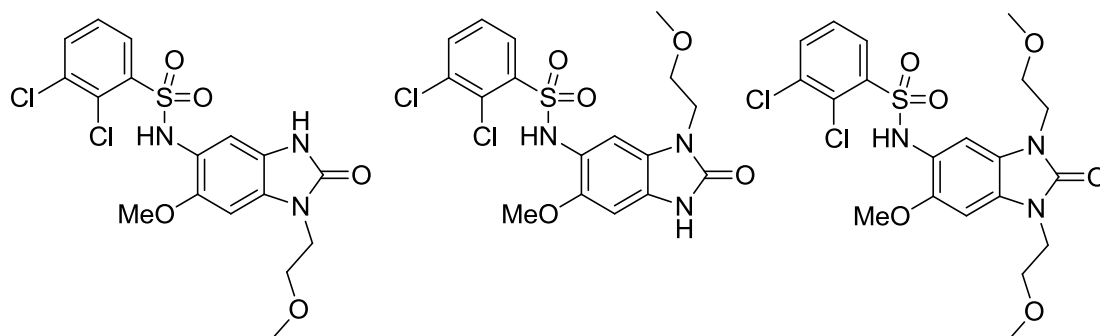
hydrogen for 18 h, and was then filtered through a celite pad. The solvent was evaporated under reduced pressure to give the crude amine intermediate, which was diluted with anhydrous pyridine (0.6 mL), and 2,3-dichlorobenzenesulfonyl chloride (20 mg, 0.09 mmol) was added. After stirring at ambient temperature for 1 h, the reaction mixture was evaporated under reduced pressure and the residue was taken up in DMSO (1 mL) and purified by MDAP (Method A). The solvent was evaporated under reduced pressure to afford the title compound (9 mg, 25 %) as a white solid. $^1\text{H NMR}$ (400 MHz, $\text{DMSO-}d_6$) δ = 10.57 (s, 1H), 9.61 (br.s, 1H), 7.86 (dd, J = 8.0, 1.5 Hz, 1H), 7.69 (dd, J = 8.0, 1.5 Hz, 1H), 7.39 (t, J = 8.0 Hz, 1H), 6.80 (s, 1H), 6.72 (s, 1H), 3.39 (s, 3H), 3.21 (s, 3H); LCMS (Method A, UV, ES) RT = 0.89 min, $[\text{M}+\text{H}]^+ = 402, 404, 406$, $[\text{M}+\text{H}+\text{MeCN}]^+ = 443, 445, 447$ 95% purity.

2,3-Dichloro-*N*-(6-methoxy-1,3-dimethyl-2-oxo-2,3-dihydro-1*H*-benzo[*d*]imidazol-5-yl)benzenesulfonamide (190b)



The title compound was prepared from **187b** (30 mg, 0.13 mmol) according to the procedure described for the preparation of **190a**. The same work up and purification afforded sulfonamide **190b** (20 mg, 38%) as a white solid: $^1\text{H NMR}$ (400 MHz, $\text{DMSO-}d_6$) δ = 9.67 (br.s, 1H), 7.87 (dd, J = 8.0, 1.5 Hz, 1H), 7.70 (dd, J = 8.0, 1.5 Hz, 1H), 7.38 (t, J = 8.0 Hz, 1H), 7.01 (s, 1H), 6.77 (s, 1H), 3.35 (s, 3H), 3.27 (s, 3H), 3.26 (s, 3H); LCMS (Method A, UV, ES) RT = 0.95 min, $[\text{M}+\text{H}]^+ = 416, 418, 420$, $[\text{M}+\text{H}+\text{MeCN}]^+ = 457, 459, 461$, 93% purity.

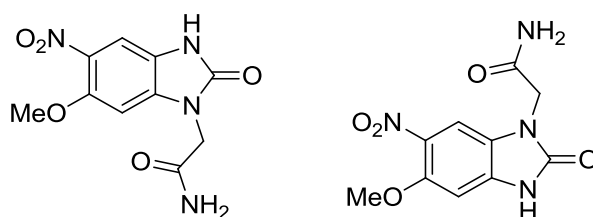
2,3-Dichloro-*N*-(6-methoxy-3-(2-methoxyethyl)-2-oxo-2,3-dihydro-1*H*-benzo[*d*]imidazol-5-yl)benzenesulfonamide (191a) and **2,3-dichloro-*N*-(6-methoxy-1-(2-methoxyethyl)-2-oxo-2,3-dihydro-1*H*-benzo[*d*]imidazol-5-yl)benzenesulfonamide (191b)** and **2,3-dichloro-*N*-(6-methoxy-1,3-bis(2-methoxyethyl)-2-oxo-2,3-dihydro-1*H*-benzo[*d*]imidazol-5-yl)benzenesulfonamide (191c)**



The title sulfonamide compounds were prepared from 5-methoxy-6-nitro-1*H*-benzo[*d*]imidazol-2(3*H*)-one (200 mg, 0.956 mmol), 1-bromo-2-methoxyethane (0.090 mL, 0.956 mmol) and 2,3-dichlorobenzoyl chloride (270 mg, 1.15 mmol) according to the procedure described for the preparation of **190a**. The same work up and purification afforded the three products: **191a** (56 mg, 22%) as a white solid; ^1H NMR (400 MHz, DMSO-*d*₆) δ = 10.58 (s, 1H), 9.60 (br.s, 1H), 7.87 (dd, J = 8.0, 1.5 Hz, 1H), 7.72 (dd, J = 8.0, 1.5 Hz, 1H), 7.40 (t, J = 8.0 Hz, 1H), 6.78 (s, 1H), 6.77 (s, 1H), 3.88 (t, J = 5.5 Hz, 2H), 3.53 (t, J = 5.5 Hz, 2H), 3.39 (s, 3H), 3.21 (s, 3H); ^{13}C NMR (101 MHz, DMSO-*d*₆) δ = 154.5, 149.8, 140.4, 134.1, 133.8, 130.1, 129.7, 129.4, 127.8, 121.0, 116.7, 109.4, 93.8, 69.3, 57.9, 55.8, 40.1; HRMS (ESI) m/z calculated for C₁₇H₁₈Cl₂N₃O₅S = 446.0344. Found = 446.0355 [M+H]⁺; LCMS (Method A, UV, ES) RT = 0.93 min, [M+H]⁺ = 446, 448, 450, 95% purity; **191b** (7 mg, 3%) as a brown solid; ^1H NMR (400 MHz, DMSO-*d*₆) δ = 10.80 (br.s, 1H), 9.48 (br.s, 1H), 7.87 (dd, J = 8.0, 1.5 Hz, 1H), 7.71 (dd, J = 8.0, 1.5 Hz, 1H), 7.40 (t, J = 8.0 Hz, 1H), 6.98 (s, 1H), 6.49 (s, 1H), 3.86 (t, J = 5.0 Hz, 2H), 3.52 (t, J = 5.0 Hz, 2H), 3.33 (s, 3H), 3.22 (s, 3H); LCMS (Method A, UV, ES) RT = 0.91 min, [M+H]⁺ = 446, 448, 450, 95% purity; **191c** (57 mg, 20%) as a white solid; ^1H NMR (400 MHz, DMSO-*d*₆) δ = 9.65 (br.s, 1H), 7.88 (d, J = 8.0 Hz, 1H), 7.73 (dd, J = 8.0, 1.5 Hz, 1H), 7.41 (t, J = 8.0 Hz, 1H), 7.02 (s, 1H), 6.82 (s, 1H), 3.94 (t, J = 6.0 Hz, 2H), 3.90 (t, J = 6.0 Hz, 2H), 3.55 (t, J = 6.0 Hz, 2H), 3.53 (t, J = 6.0 Hz, 2H), 3.38 (s, 3H), 3.22 (s, 3H), 3.20 (s, 3H); ^{13}C NMR (101 MHz, DMSO-*d*₆) δ = 153.7, 150.2, 140.5, 134.0, 133.8, 129.7, 129.4, 128.8, 127.8, 122.3, 116.9, 109.4, 93.8, 69.5,

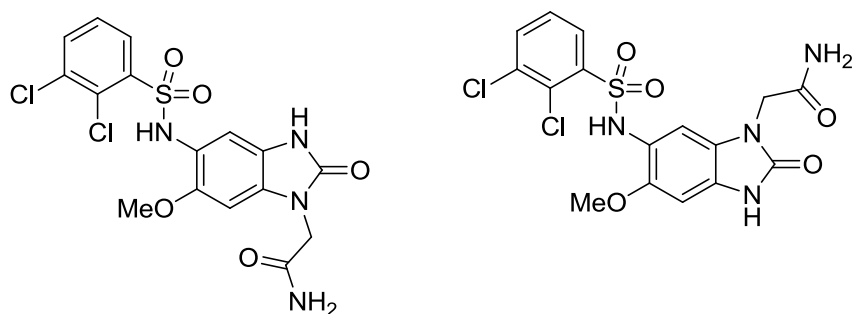
69.3, 58.0, 57.9, 55.8, 40.4 (2 peaks obscured under water); HRMS (ESI) m/z calculated for $C_{20}H_{24}Cl_2N_3O_6S$ = 504.0763. Found = 504.0764 $[M+H]^+$; LCMS (Method A, UV, ES) RT = 1.01 min, $[M+H]^+$ = 504, 506, 508, 95% purity.

2-(6-Methoxy-5-nitro-2-oxo-2,3-dihydro-1H-benzo[d]imidazol-1-yl)acetamide (189a)
and 2-(5-methoxy-6-nitro-2-oxo-2,3-dihydro-1H-benzo[d]imidazol-1-yl)acetamide (189b)



The title compounds were prepared from 5-methoxy-6-nitro-1H-benzo[d]imidazol-2(3H)-one (200 mg, 0.956 mmol) and 2-bromoacetamide (132 mg, 0.956 mmol) according to the procedure described for the preparation of **187a**. The same work up and purification afforded **189a** with **189b** (9:1) (90 mg, 32%) as a yellow solid; 1H NMR (400 MHz, DMSO- d_6) major δ = 11.11 (br.s, 1H), 7.62 (br.s, 1H), 7.52 (s, 1H), 7.22 (br.s, 1H), 7.11 (s, 1H), 4.48 (s, 2H), 3.89 (s, 3H); LCMS (Method A, UV, ES) $[M+H]^+$ = 267. A satisfactory 1H NMR spectrum could not be obtained for the minor regioisomer.

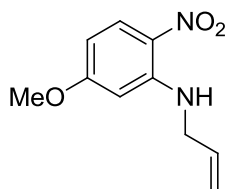
2-(5-(2,3-Dichlorophenylsulfonamido)-6-methoxy-2-oxo-2,3-dihydro-1H-benzo[d]imidazol-1-yl)acetamide (192a) & 2-(6-(2,3-dichlorophenylsulfonamido)-5-methoxy-2-oxo-2,3-dihydro-1H-benzo[d]imidazol-1-yl)acetamide (192b)



The title compounds were prepared from a mixture of **189a** and **189b** (9:1) (60 mg, 0.225 mmol) according to the procedure described for the preparation of **190a**. The same work up and purification afforded the separated **192a** (18 mg, 18%) as a white solid; 1H NMR (400 MHz, DMSO- d_6) δ = 10.59 (br.s, 1H), 9.61 (br.s, 1H), 7.87 (d, J = 8.0 Hz, 1 H), 7.72 (dd, J =

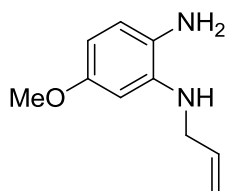
8.0, 1.5 Hz, 1H), 7.52 (br.s, 1H), 7.40 (t, $J = 8.0$ Hz, 1H), 7.11 (br.s, 1H), 6.79 (s, 1H), 6.66 (s, 1H), 4.31 (s, 2H), 3.36 (s, 3H); $^1\text{H NMR}$ (400 MHz, $\text{MeOD-}d_4$) $\delta = 7.79 - 7.66$ (m, 2H), 7.27 (t, $J = 8.0$ Hz, 1H), 7.13 (s, 1H), 6.59 (s, 1H), 4.47 (s, 2H), 3.52 (s, 3H); HRMS (ESI) m/z calculated for $\text{C}_{16}\text{H}_{15}\text{Cl}_2\text{N}_4\text{O}_5\text{S} = 445.0140$. Found = 445.0152 $[\text{M}+\text{H}]^+$; IR ν_{max} (neat) 3372, 3232, 1699, 1679, 1501, 1412, 1337, 1149, 788, 702 cm^{-1} ; LCMS (Method A, UV, ES) RT = 0.80 min, $[\text{M}+\text{H}]^+ = 445, 447, 449$, 95% purity; and **192b** (4 mg, 4% yield) as a white solid, $^1\text{H NMR}$ (400 MHz, $\text{MeOD-}d_4$) $\delta = 7.86 - 7.60$ (m, 2H), 7.27 (t, $J = 8.0$ Hz, 1H), 7.04 (s, 1H), 6.59 (s, 1H), 4.48 (s, 2H), 3.51 (s, 3H); the exchangeable NH and NH_2 protons were not observed; LCMS (Method A, UV, ES) RT = 0.79 min, $[\text{M}+\text{H}]^+ = 445, 447, 449$, 95% purity.

***N*-Allyl-5-methoxy-2-nitroaniline (194)**



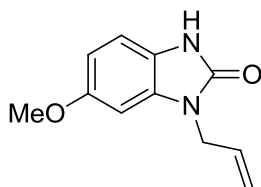
Allylamine (2.19 ml, 29.2 mmol) was added to 2-fluoro-4-methoxy-1-nitrobenzene (2.5 g, 14.6 mmol) and the reaction was stirred at ambient temperature for 1.5 h. The reaction mixture was concentrated to evaporate off any excess allylamine. The product was dissolved in ethyl acetate (300 mL) and was washed with HCl (150 mL of 1 M aqueous solution), followed by sodium bicarbonate (100 mL of a saturated aqueous solution), water (50 mL), dried using a hydrophobic frit and evaporated under reduced pressure to afford the title compound (2.94 g, 97%) as a yellow solid; $^1\text{H NMR}$ (400 MHz, $\text{DMSO-}d_6$) $\delta = 8.47$ (t, $J = 5.0$ Hz, 1H), 8.04 (d, $J = 9.0$ Hz, 1H), 6.44 - 6.19 (m, 2H), 6.08 - 5.83 (m, 1H), 5.27 (dd, $J = 17.0, 1.5$ Hz, 1H), 5.20 (dd, $J = 10.3, 1.5$ Hz, 1H), 4.12 - 4.02 (m, 2H), 3.83 (s, 3H); LCMS (Method A, UV, ES) RT = 1.07 min, $[\text{M}+\text{H}]^+ = 209$, $[\text{M}+\text{H}+\text{MeCN}]^+ = 250$, 99% purity.

***N*1-allyl-5-methoxybenzene-1,2-diamine (195)**



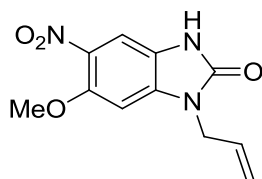
Iron powder (3.5 g of 97% w/w, 325 mesh, 62.4 mmol) was added to a solution of **194** (2.6 g, 12.5 mmol) in ethanol (70 mL) and water (35 mL). Ammonium chloride (1.8 g, 33.3 mmol) was added in one portion, and the reaction mixture was refluxed for 24 h. Ethanol was removed under reduced pressure, and the residue was partitioned between ethyl acetate (500 mL) and sodium bicarbonate (500 mL of a saturated aqueous solution). The organic layer was separated and the aqueous layer was extracted with more ethyl acetate (2 x 300 mL). The combined organic extracts were washed with brine (2 x 200 mL), dried using a hydrophobic frit and concentrated under reduced pressure to afford **195** (1.84 g, 83%) as a dark purple oil, LCMS (Method A, UV, ES) RT = 0.50 min, [M+H]⁺ 179, 80% purity. A portion of this crude material was taken to the next step without further purification. A smaller portion (40 mg) of the dark purple oil was dissolved in DMSO (1 mL) and purified by MDAP (Method A). The solvent was concentrated under reduced pressure to afford **195** (22 mg, 1 %) as a dark orange oil; ¹H NMR (400 MHz, CDCl₃) δ = 8.16 (br.s, 1H), 6.72 (d, *J* = 7.0 Hz, 1H), 6.42 - 6.15 (m, 2H), 6.11 - 5.79 (m, 1H), 5.47 - 5.24 (m, 5H), 5.19 (d, *J* = 10.0 Hz, 1H), 3.76 (s, 3H); LCMS (UV, ES) RT = 0.50 min, [M+H]⁺ = 179, 91% purity.

1-Allyl-6-methoxy-1*H*-benzo[*d*]imidazol-2(3*H*)-one (196)



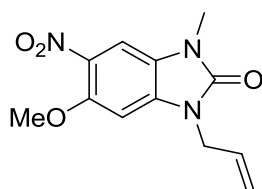
CDI (110 mg, 0.68 mmol) was added to a stirring solution of **195** (110 mg, 0.62 mmol) in THF (2 mL). The reaction mixture was heated to 50 °C and left to stir under a nitrogen atmosphere for 2 h. The reaction mixture was concentrated, dissolved in DMSO (2 mL) and purified by MDAP (Method A). The solvent was evaporated under reduced pressure to afford the title compound (57 mg, 45%) as a pale purple solid; ¹H NMR (400 MHz, DMSO-*d*₆) δ = 10.63 (br.s, 1H), 6.87 (d, *J* = 8.5 Hz, 1H), 6.67 (d, *J* = 2.5 Hz, 1H), 6.56 (dd, *J* = 8.5, 2.5 Hz, 1H), 6.04 - 5.69 (m, 1H), 5.15 (dd, *J* = 10.0, 1.5 Hz, 1H), 5.09 (dd, *J* = 17.0, 1.5 Hz, 1H), 4.38 (d, *J* = 5.0 Hz, 2H), 3.71 (s, 3H); LCMS (Method A, UV, ES) RT = 0.70 min, [M+H]⁺ = 205, [M+H+MeCN]⁺ = 250, 93% purity.

1-Allyl-6-methoxy-5-nitro-1*H*-benzo[*d*]imidazol-2(3*H*)-one (197)



A cooled solution of nitric acid (66.5 mL of a 4 N aqueous solution, 298 mmol) was added slowly to **196** (1.9 g, 9.30 mmol) at 0 °C and the reaction was stirred for 1 h. The reaction was then warmed to ambient temperature and stirred for 3 h. LCMS showed a peak for product but some of the starting material formed a gum which was not soluble in the nitration solution. Glacial acetic acid (5 mL) was added and the reaction was stirred at ambient temperature for 2 h. The reaction mixture was poured onto iced water (30 mL) and was neutralised with saturated sodium bicarbonate solution. The product was extracted with ethyl acetate (2 x 300 mL), and the combined organic extracts were washed with brine (100 mL), dried (MgSO₄) and evaporated under reduced pressure. The brown residue was purified on 100 g silica column using a gradient of 0-100% ethyl acetate-cyclohexane over 60 mins. The appropriate fractions were combined and evaporated under reduced pressure to afford the title compound (0.53 g, 23%) as a brown solid; ¹H NMR (400 MHz, DMSO-*d*₆) δ = 11.17 (br.s, 1H), 7.54 (s, 1H), 7.06 (s, 1H), 6.27 - 5.62 (m, 1H), 5.41 - 4.85 (m, 2H), 4.49 (d, *J* = 5.0 Hz, 2H), 3.91 (s, 3H); LCMS (Method A, UV, ES) RT = 0.73 min, [M+H]⁺ = 250, [M+H+MeCN]⁺ = 291, 96% purity.

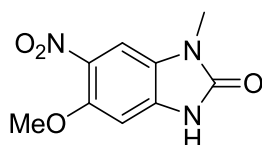
1-Allyl-6-methoxy-3-methyl-5-nitro-1*H*-benzo[*d*]imidazol-2(3*H*)-one (198)



Sodium hydride (18 mg of a 60% w/w dispersion in mineral oil, 0.46 mmol) was added to a stirring solution of **197b** (105 mg, 0.42 mmol) in anhydrous DMF (1 mL) at 0 °C. The mixture was stirred for 20 min, then methyl iodide (0.03 mL, 0.46 mmol) was added and the reaction mixture was warmed to ambient temperature and stirred for 2 h. The reaction was

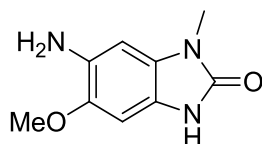
quenched with water (20 mL) and the product was extracted with ethyl acetate (3 x 20 mL). The combined organic extracts were washed with water (20 mL), brine (2 x 20 mL), dried using a hydrophobic frit and evaporated under reduced pressure to afford the title compound (110 mg, 99%) as an orange solid; $^1\text{H NMR}$ (400 MHz, $\text{DMSO-}d_6$) $\delta = 7.83$ (s, 1H), 7.13 (s, 1H), 6.12 - 5.71 (m, 1H), 5.24 - 5.07 (m, 2H), 4.54 (d, $J = 5.0$ Hz, 2H), 3.92 (s, 3H), 3.36 (s, 3H); LCMS (Method A, UV, ES) RT = 0.81 min, $[\text{M}+\text{H}]^+ = 264$, $[\text{M}+\text{H}+\text{MeCN}]^+ = 305$, 95% purity.

5-Methoxy-1-methyl-6-nitro-1*H*-benzo[*d*]imidazol-2(3*H*)-one (199)



Compound **198** (30 mg, 0.11 mmol), dichloro(2,6,10-dodecatriene-1,12-diyl)ruthenium(IV) (2.2 mg, 6.8 μmol) and potassium periodate (52 mg, 0.23 mmol) were suspended in water (1 mL) and stirred in a sealed vessel at 100 $^\circ\text{C}$ for 72 h. Ethyl acetate (10 mL) was added and the organic layer was separated, washed with brine (10 mL), dried using a hydrophobic frit and evaporated under reduced pressure to give a brown solid. The residue was taken up in DMSO (1 mL) and purified by MDAP (Method A). The solvent was evaporated under reduced pressure to afford the title compound (10 mg, 39%) as a yellow solid; $^1\text{H NMR}$ (400 MHz, $\text{MeOD-}d_4$) $\delta = 7.70$ (s, 1H), 6.93 (s, 1H), 3.94 (s, 3H), 3.38 (s, 3H); the exchangeable NH proton was not observed; LCMS (UV, ES) RT = 0.61 min, $[\text{M}+\text{H}]^+ = 224$, $[\text{M}+\text{H}+\text{MeCN}]^+ = 265$, 99% purity.

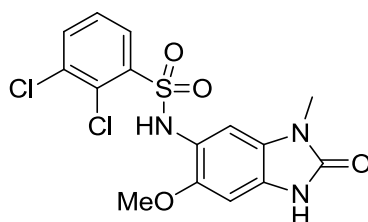
6-Amino-5-methoxy-1-methyl-1*H*-benzo[*d*]imidazol-2(3*H*)-one (200)



A solution of **199** (10 mg, 0.05 mmol) in a mixture of ethanol (1 mL) and ethyl acetate (1 mL) was added to a flask containing palladium-on-carbon (14 mg of a 10% w/w, 0.01 mmol) under vacuum. The flask was back filled with N_2 , evacuated and filled with H_2 using the burette apparatus. The reaction mixture was stirred under H_2 for 4 h, filtered through a celite pad, washed with a mixture of ethanol and ethyl acetate (30 mL of a 1:1 mixture) and

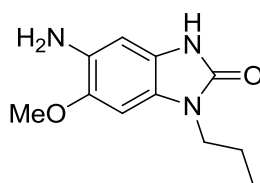
concentrated under reduced pressure to afford the title compound (8 mg, 92%) as a colourless oil; ^1H NMR (400 MHz, CDCl_3) δ = 9.13 (br.s, 1H), 6.67 (s, 1H), 6.43 (s, 1H), 3.85 (s, 3H), 3.71 (br.s, 2H), 3.35 (s, 3H); (Note: the product does not retain on the LCMS column).

2,3-Dichloro-*N*-(6-methoxy-3-methyl-2-oxo-2,3-dihydro-1*H*-benzo[*d*]imidazol-5-yl)benzenesulfonamide (201)



The title compound was prepared from **200** (8 mg, 0.04 mmol) and 2,3-dichlorobenzoyl chloride (11 mg, 0.05 mmol) according to the procedure described for the preparation of **29**. The same work up and purification using MDAP (Method A) afforded **201** (4 mg, 22%) as a white solid; ^1H NMR (400 MHz, CDCl_3) δ = 9.03 (br.s, 1H), 7.82 (dd, J = 8.0, 1.5 Hz, 1H), 7.61 (dd, J = 8.0, 1.5 Hz, 1H), 7.47 (s, 1H), 7.20 (t, J = 8.0 Hz, 1H), 7.18 (s, 1H), 6.53 (s, 1H), 3.61 (s, 3H), 3.38 (s, 3H); LCMS (Method A, UV, ES) RT = 0.88 min, $[\text{M}+\text{H}]^+ = 402, 404, [\text{M}+\text{H}+\text{MeCN}]^+ = 443, 445, 447, 96\%$ purity.

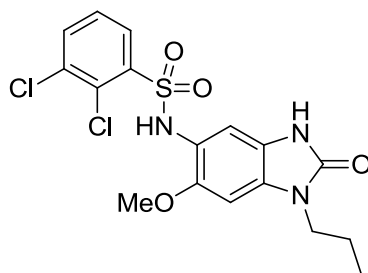
5-Amino-6-methoxy-1-propyl-1*H*-benzo[*d*]imidazol-2(3*H*)-one (202)



A solution of **197b** (40 mg, 0.16 mmol) in a mixture of ethanol (1 mL) and ethyl acetate (1 mL) was added to a flask containing palladium-on-carbon (25 mg of a 10% w/w, 0.03 mmol) under vacuum. The flask was back filled with N_2 , evacuated and filled with H_2 using the burette apparatus. The reaction mixture was stirred under H_2 for 5 h, filtered through a celite pad, washed with a mixture of ethanol and ethyl acetate (50 mL of a 1:1 mixture) and concentrated under reduced pressure to afford the title compound (30 mg, 85%) as a colourless oil; ^1H NMR (400 MHz, CDCl_3) δ = 9.73 (br.s, 1H), 6.57 (s, 1H), 6.52 (s, 1H),

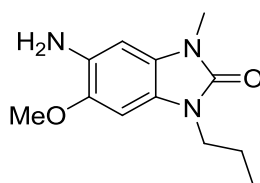
3.87 (s, 3H), 3.80 (t, $J = 7.5$ Hz, 2H), 3.67 (br.s, 2H), 1.79 (sxt, $J = 7.5$ Hz, 2H), 0.99 (t, $J = 7.5$ Hz, 3H); LCMS (Method A, UV, ES) RT = 0.40 min, $[M+H]^+ = 222$, 90% purity.

2,3-Dichloro-*N*-(6-methoxy-2-oxo-1-propyl-2,3-dihydro-1*H*-benzo[*d*]imidazol-5-yl)benzenesulfonamide (203)



The title compound was prepared from **202** (30 mg, 0.14 mmol) and 2,3-dichlorobenzenesulfonyl chloride (39 mg, 0.16 mmol) according to the procedure described for the preparation of **29**. The same work up and purification using MDAP (Method A) afforded **203** (5 mg, 7%) as a beige coloured solid; ^1H NMR (400 MHz, $\text{DMSO-}d_6$) $\delta = 10.55$ (s, 1H), 9.60 (br.s, 1H), 7.87 (dd, $J = 8.0, 1.5$ Hz, 1H), 7.72 (dd, $J = 8.0, 1.5$ Hz, 1H), 7.40 (t, $J = 8.0$ Hz, 1H), 6.79 (s, 1H), 6.74 (s, 1H), 3.67 (t, $J = 7.0$ Hz, 2H), 3.40 (s, 3H), 1.60 (sxt, $J = 7.0$ Hz, 2H), 0.83 (t, $J = 7.0$ Hz, 3H); LCMS (UV, ES) RT = 1.00 min, $[M+H]^+ = 430, 432, 434$, $[M+H+\text{MeCN}]^+ = 471, 473, 475$, 100% purity.

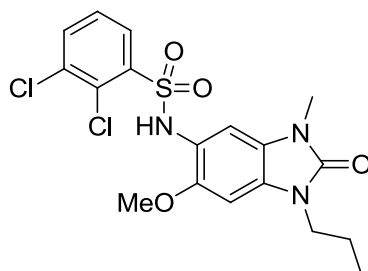
5-Amino-6-methoxy-3-methyl-1-propyl-1*H*-benzo[*d*]imidazol-2(3*H*)-one (204)



A solution of **198** (60 mg, 0.23 mmol) in a mixture of ethanol (2 mL) and ethyl acetate (2 mL) was added to a flask containing palladium-on-carbon (73 mg of a 10% w/w, 0.07 mmol) under vacuum. The flask was back filled with N_2 , evacuated and filled with H_2 using the burette apparatus. The reaction mixture was stirred under H_2 for 5 h, filtered through a celite pad, washed with a mixture of ethanol and ethyl acetate (50 mL of a 1:1 mixture) and concentrated under reduced pressure to afford the title compound (53 mg, 99%) as a colourless oil; ^1H NMR (400 MHz, CDCl_3) $\delta = 6.54$ (s, 1H), 6.43 (s, 1H), 3.88 (s, 3H), 3.79

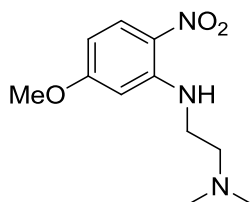
(t, $J = 7.0$ Hz, 2H), 3.70 (br.s, 2H), 3.33 (s, 3H), 3.71 (m, 2H), 0.97 (t, $J = 7.0$ Hz, 3H); LCMS (Method A, UV, ES) RT = 0.43 min, $[M+H]^+ = 236$.

2,3-Dichloro-*N*-(6-methoxy-3-methyl-2-oxo-1-propyl-2,3-dihydro-1*H*-benzo[*d*]imidazol-5-yl)benzenesulfonamide (205)



The title compound was prepared from **204** (53 mg, 0.22 mmol) and 2,3-dichlorobenzenesulfonyl chloride (56 mg, 0.23 mmol) according to the procedure described for the preparation of **29**. The same work up and purification using MDAP (Method A) afforded **205** (59 mg, 58%) as a white solid; ^1H NMR (400 MHz, CDCl_3) $\delta = 7.83$ (dd, $J = 8.0, 1.5$ Hz, 1H), 7.61 (dd, $J = 8.0, 1.5$ Hz, 1H), 7.47 (s, 1H), 7.20 (t, $J = 8.0$ Hz, 1H), 7.15 (s, 1H), 6.38 (s, 1H), 3.74 (t, $J = 7.5$ Hz, 2H), 3.64 (s, 3H), 3.37 (s, 3H), 1.71 (sxt, $J = 7.5$ Hz, 2H), 0.93 (t, $J = 7.5$ Hz, 2H); the exchangeable NH proton was not observed; ^{13}C NMR (101 MHz, $\text{DMSO-}d_6$) $\delta = 153.8, 150.4, 140.5, 134.0, 133.7, 129.8, 129.4, 128.7, 127.7, 122.7, 116.7, 109.2, 93.3, 55.8, 41.9, 26.9, 21.2, 11.0$; HRMS (ESI) m/z calculated for $\text{C}_{18}\text{H}_{20}\text{Cl}_2\text{N}_3\text{O}_4\text{S} = 444.0552$. Found = 444.0552 $[M+H]^+$; LCMS (Method A, UV, ES) RT = 1.07 min, $[M+H]^+ = 444, 446, 448, 100\%$ purity.

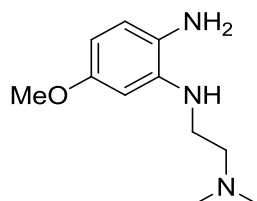
***N*1-(5-Methoxy-2-nitrophenyl)-*N*2,*N*2-dimethylethane-1,2-diamine (207)**



2-(*N,N*-dimethylamino)ethylamine (0.96 mL, 8.8 mmol) was added to a solution of 2-fluoro-4-methoxy-1-nitrobenzene (1.0 g, 5.8 mmol), in anhydrous DMF (2 mL). DIPEA (2.0 mL, 11.7 mmol) was added and the reaction mixture was stirred under nitrogen at ambient temperature for 3 h. The reaction mixture was diluted with ethyl acetate (50 mL) and the

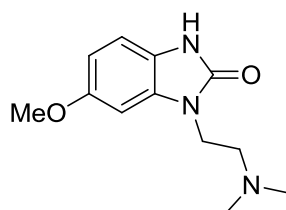
organic layer was washed with water (2 x 50 mL), brine (50 mL), dried using a hydrophobic frit and evaporated under reduced pressure to afford the title compound (1.45 g, 93%) as a yellow solid; ^1H NMR (400 MHz, $\text{DMSO-}d_6$) δ = 8.50 (br.s, 1H), 8.02 (d, J = 9.5 Hz, 1H), 6.40 - 6.18 (m, 2H), 3.87 (s, 3H), 3.48 - 3.33 (m, 2H), 2.55 (t, J = 6.0 Hz, 2H), 2.22 (s, 6H); LCMS (Method A, UV, ES) RT = 0.51 min, $[\text{M}+\text{H}]^+ = 240$, 90% purity.

N1-(2-(Dimethylamino)ethyl)-5-methoxybenzene-1,2-diamine (**208**)



A solution of **207** (1.45 g, 6.06 mmol) in ethanol (100 mL) was added to a flask containing palladium-on-carbon (0.65g of a 10% w/w, 0.61 mmol) under vacuum. The flask was back filled with N_2 , evacuated and filled with H_2 using the burette apparatus. The reaction mixture was stirred under H_2 for 18 h, filtered through a celite pad, washed with ethanol (150 mL) and concentrated under reduced pressure to afford the title compound (1.15 g, 91%) as a dark purple oil; ^1H NMR (400 MHz, $\text{DMSO-}d_6$) δ = 6.51 (d, J = 8.0 Hz, 1H), 6.08 (d, J = 2.5 Hz, 1H), 6.03 (dd, J = 8.0, 2.5 Hz, 1H), 4.46 (br.s, 1H), 3.97 (br.s, 2H), 3.64 (s, 3H), 3.17 - 2.99 (m, 2H), 2.60 - 2.42 (m, 2H), 2.21 (s, 6H); (Note: the product does not retain on the LCMS column).

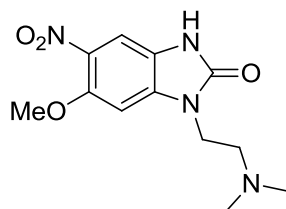
1-(2-(Dimethylamino)ethyl)-6-methoxy-1*H*-benzo[*d*]imidazol-2(3*H*)-one (**209**)



A mixture of **208** (1.15 g, 5.49 mmol) and CDI (0.89 g, 5.49 mmol) in anhydrous THF (20 mL) was heated to 50 °C for 2 h. The mixture was concentrated under reduced pressure, and the residue was taken up in ethyl acetate (40 mL). The organic layer was washed with sodium bicarbonate (40 mL of a saturated aqueous solution), brine (40 mL), dried using a hydrophobic frit and evaporated under reduced pressure to afford the title compound (1.26 g, 83%) as a dark purple solid; ^1H NMR (400 MHz, $\text{DMSO-}d_6$) δ = 10.54 (br.s, 1H), 6.85 (d, J

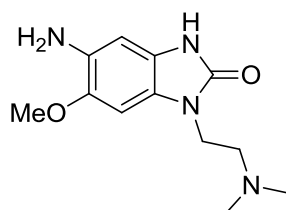
= 8.0 Hz, 1H), 6.76 (d, $J = 2.5$ Hz, 1H), 6.55 (dd, $J = 8.0, 2.5$ Hz, 1H), 3.84 (t, $J = 6.5$ Hz, 2H), 3.74 (s, 3H), 2.52 (t, $J = 6.5$ Hz, 2H), 2.18 (s, 6H); LCMS (Method A, UV, ES) RT = 0.39 min, $[M+H]^+ = 236$, 90% purity.

1-(2-(Dimethylamino)ethyl)-6-methoxy-5-nitro-1H-benzo[d]imidazol-2(3H)-one (210)



Compound **209** (1.26 g, 4.55 mmol) was treated with nitric acid (60 mL of a 4 N aqueous solution, 189 mmol) and the mixture was stirred at ambient temperature for 22 h. The reaction was poured over ice (50 mL), neutralised with solid sodium bicarbonate, and extracted with ethyl acetate (2 x 150 mL). The combined organic extracts were then washed with brine (100 mL), dried using a hydrophobic frit and evaporated under reduced pressure to afford the title compound (750 mg, 53%) as a yellow solid; ^1H NMR (400 MHz, DMSO- d_6) $\delta = 11.05$ (s, 1H), 7.51 (s, 1H), 7.15 (s, 1H), 4.00 - 3.88 (m, 5H), 2.55 (t, $J = 6.5$ Hz, 2H), 2.19 (s, 6H); LCMS (Method A, UV, ES) RT = 0.42 min, $[M+H]^+ = 281$.

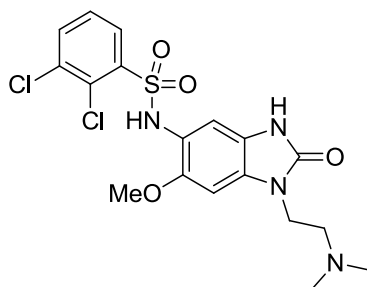
5-Amino-1-(2-(dimethylamino)ethyl)-6-methoxy-1H-benzo[d]imidazol-2(3H)-one (211)



A solution of **210** (0.75 g, 2.4 mmol) in a mixture of ethanol (50 mL) and ethyl acetate (50 mL) was added to a flask containing palladium-on-carbon (0.77g of a 10% w/w, 0.72 mmol) under vacuum. The flask was back filled with N_2 , evacuated and filled with H_2 using the burette apparatus. The reaction mixture was stirred under H_2 for 18 h, filtered through a celite pad, washed with a mixture of ethanol and ethyl acetate (100 mL of a 1:1 mixture), and concentrated under reduced pressure to afford the title compound (0.63 g, 94%) as a dark as a brown oil; ^1H NMR (400 MHz, DMSO- d_6) $\delta = 10.21$ (s, 1H), 6.70 (s, 1H), 6.38 (s, 1H), 4.40

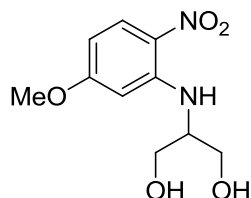
(br.s, 2H), 3.77 (t, $J = 6.5$ Hz, 2H), 3.75 (s, 3H), 2.48 (t, $J = 6.5$ Hz, 2H), 2.18 (s, 6H); LCMS (UV, ES) RT = 0.16 min, $[M+H]^+$ = no mass ion observed.

2,3-Dichloro-*N*-(1-(2-(dimethylamino)ethyl)-6-methoxy-2-oxo-2,3-dihydro-1*H*-benzo[*d*]imidazol-5-yl)benzenesulfonamide (212)



The title compound was prepared from **211** (100 mg, 0.40 mmol) and 2,3-dichlorobenzenesulfonyl chloride (108 mg, 0.44 mmol) according to the procedure described for the preparation of **29**. The same work up and purification using MDAP (Method B) afforded **212** (67 mg, 36%) as a beige coloured solid; ^1H NMR (400 MHz, DMSO- d_6) δ = 10.55 (s, 1H), 9.60 (br.s, 1H), 7.88 (d, $J = 8.0$ Hz, 1H), 7.72 (d, $J = 8.0$ Hz, 1H), 7.40 (t, $J = 8.0$ Hz, 1H), 6.78 (s, 1H), 6.74 (s, 1H), 3.80 (t, $J = 6.5$ Hz, 2H), 3.39 (s, 3H), 2.46 (t, $J = 6.5$ Hz, 2H), 2.15 (s, 6H); ^{13}C NMR (101 MHz, DMSO- d_6) δ = 154.6, 150.0, 140.7, 134.2, 134.0, 130.0, 129.9, 129.6, 128.0, 121.3, 117.3, 109.5, 93.8, 56.7, 56.0, 45.4, 38.3; HRMS (ESI) m/z calculated for $\text{C}_{18}\text{H}_{21}\text{Cl}_2\text{N}_4\text{O}_4\text{S}$ = 459.0661. Found = 459.0654 $[M+H]^+$; LCMS (Method A, UV, ES) RT = 0.69 min, $[M+H]^+$ = 459, 461, 463, 90% purity.

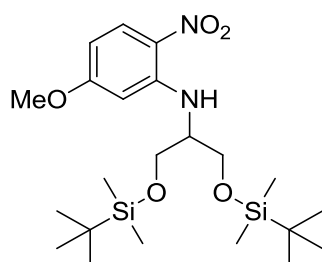
2-((5-Methoxy-2-nitrophenyl)amino)propane-1,3-diol (213)



2-Aminopropane-1,3-diol (0.8 g, 8.8 mmol) was added to a solution of 2-fluoro-4-methoxy-1-nitrobenzene (1.0 g, 5.8 mmol) in anhydrous DMF (3 mL). DIPEA (2.0 mL, 11.7 mmol) was added and the reaction mixture was stirred under nitrogen at ambient temperature for 48 h. The reaction mixture was diluted with ethyl acetate (100 mL) and the organic phase was washed with HCl (50 mL of a 1 M aqueous solution), water (50 mL), brine (50 mL), dried

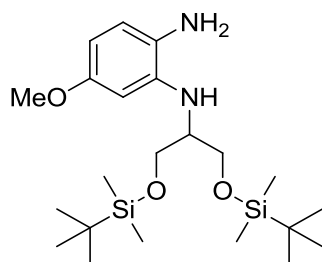
using a hydrophobic frit and evaporated under reduced pressure to afford the title compound (1.3 g, 83%) as a yellow solid; $^1\text{H NMR}$ (400 MHz, DMSO-d_6) δ = 8.02 (d, J = 9.5 Hz, 1H), 6.46 (d, J = 2.5 Hz, 1H), 6.30 (dd, J = 9.5, 2.5 Hz, 1H), 4.95 (t, J = 5.5 Hz, 2H), 3.86 (s, 3H), 3.77 - 3.68 (m, 1H), 3.67 - 3.48 (m, 4H); the exchangeable NH proton was not observed; LCMS (Method A, UV, ES) RT = 0.65 min, $[\text{M}+\text{H}]^+ = 243$, 90% purity.

***N*-(5-Methoxy-2-nitrophenyl)-2,2,3,3,9,9,10,10-octamethyl-4,8-dioxa-3,9-disilaundecan-6-amine (214)**



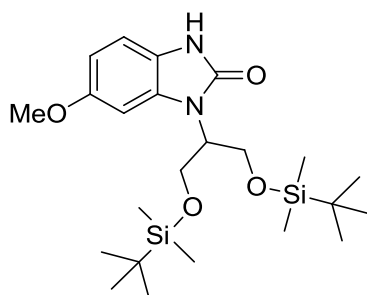
TBDMSCl (2.3 g, 15.0 mmol) and imidazole (1.0 g, 15.0 mmol) was added to a solution of **213** (1.3 g, 6.8 mmol) in anhydrous DMF (15 mL) and the reaction mixture was stirred under nitrogen at ambient temperature for 3 h. The reaction was then quenched with water (50 mL) and extracted with ethyl acetate (3 x 50 mL). The combined organic extracts were washed with brine (50 mL), dried using a hydrophobic frit and evaporated under reduced pressure to afford the title compound (3.38 g, 95%) as a yellow oil; $^1\text{H NMR}$ (400 MHz, DMSO-d_6) δ = 8.60 (d, J = 8.5 Hz, 1H), 8.02 (d, J = 9.5 Hz, 1H), 6.44 (d, J = 2.5 Hz, 1H), 6.30 (dd, J = 9.5, 2.5 Hz, 1H), 4.06 - 3.93 (m, 1H), 3.85 (s, 3H), 3.83 - 3.77 (m, 2H), 3.77 - 3.62 (m, 2H), 0.87 (s, 18 H), 0.04 (s, 6H), 0.03 (s, 6H); the exchangeable NH proton was not observed; LCMS (Method A, UV, ES) RT = 1.78 min, $[\text{M}+\text{H}]^+ = 471$, 90% purity.

5-Methoxy-*N*1-(2,2,3,3,9,9,10,10-octamethyl-4,8-dioxa-3,9-disilaundecan-6-yl)benzene-1,2-diamine (215)



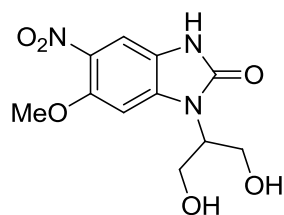
A solution of **214** (3.3 g, 7.0 mmol) in ethanol (100 mL) was added to a flask containing palladium-on-carbon (0.2 g of a 10% w/w, 2.1 mmol) under vacuum. The flask was back filled with N₂, evacuated and filled with H₂ using the burette apparatus. The reaction mixture was stirred under H₂ for 18 h, filtered through a celite pad, washed with ethanol (150 mL) and concentrated under reduced pressure to afford the title compound (2.53 g, 70%) as a dark purple oil; ¹H NMR (400 MHz, DMSO-*d*₆) δ = 6.53 (d, *J* = 8.0 Hz, 1H), 6.11 (d, *J* = 2.5 Hz, 1H), 6.03 (dd, *J* = 8.5, 2.5 Hz, 1H), 4.20 (d, *J* = 8.5 Hz, 1H), 3.87 (s, 2H), 3.72 - 3.62 (m, 4H), 3.61 (s, 3H), 3.38 (td, *J* = 8.5, 4.5 Hz, 1H), 0.88 (s, 18H), 0.04 (s, 12H); the exchangeable NH proton was not observed; LCMS (Method A, UV, ES) RT = 1.62 min, [M+H]⁺ = 441, 85% purity.

6-Methoxy-1-(2,2,3,3,9,9,10,10-octamethyl-4,8-dioxa-3,9-disilaundecan-6-yl)-1H-benzo[*d*]imidazol-2(3H)-one (216)



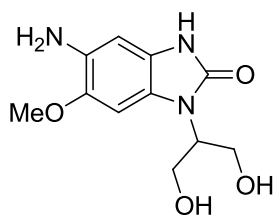
A mixture of **215** (2.50 g, 5.67 mmol) and CDI (0.92 g, 5.67 mmol) in anhydrous THF (20 mL) was heated to 50 °C for 3 h. The mixture was concentrated under reduced pressure and was taken up in ethyl acetate (60 mL). The organic layer was washed with HCl (40 mL of a 1 M aqueous solution), sodium bicarbonate (40 mL of a saturated aqueous solution), brine (40 mL), dried using a hydrophobic frit and evaporated under reduced pressure to afford the title compound (2.04 g, 69%) as a dark brown solid; ¹H NMR (400 MHz, DMSO-*d*₆) δ = 10.56 (br.s, 1H), 7.00 - 6.68 (m, 2H), 6.53 (dd, *J* = 8.5, 2.5 Hz, 1H), 4.43 - 4.27 (m, 1H), 4.12 - 4.02 (m, 2H), 4.02 - 3.93 (m, 2H), 3.71 (s, 3H), 0.75 (s, 18H), -0.04 (s, 6H), -0.11 (s, 6H); LCMS (Method A, UV, ES) RT = 1.59 min, [M+H]⁺ = 467, 90% purity.

1-(1,3-Dihydroxypropan-2-yl)-6-methoxy-5-nitro-1H-benzo[*d*]imidazol-2(3H)-one (217)



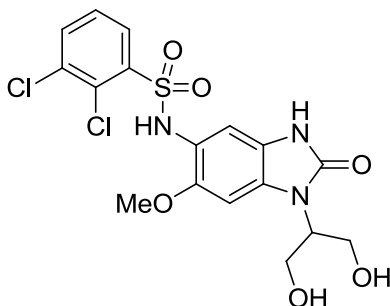
Compound **216** (200 mg, 0.43 mmol) was treated with nitric acid (4 mL of a 4 N aqueous solution, 11.1 mmol) and the mixture was stirred at ambient temperature and stirred for 1 h. The reaction was poured over ice (10 mL), and the solid was filtered, washed with water and dried under vacuum to afford a yellow solid (90 mg). The filtrate was neutralised with solid sodium bicarbonate, and extracted with ethyl acetate (2 x 20 mL). The combined organic extracts were then washed with HCl (15 mL of a 1 M aqueous solution), brine (15 mL), dried using a hydrophobic frit and evaporated under reduced pressure to afford more of the yellow solid (40 mg). The solids were combined and taken up in DMSO (2 mL) and purified by MDAP (Method A). The solvent was evaporated under reduced pressure to afford the title compound (40 mg, 33%) as a yellow solid; $^1\text{H NMR}$ (400 MHz, $\text{DMSO-}d_6$) δ = 11.03 (br.s, 1H), 7.49 (s, 1H), 7.14 (s, 1H), 4.87 (t, J = 5.5 Hz, 2H), 4.42 - 4.34 (m, 1H), 3.95 - 3.88 (m, 2H), 3.91 (s, 3H), 3.81 - 3.74 (m, 2H); LCMS (Method A, UV, ES) RT = 0.46 min, $[\text{M}+\text{H}]^+ = 284$, 100% purity.

5-Amino-1-(1,3-dihydroxypropan-2-yl)-6-methoxy-1H-benzo[*d*]imidazol-2(3H)-one (218)



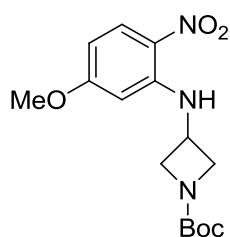
A solution of **217** (40 mg, 0.14 mmol) in ethanol (5 mL) was added to a flask containing palladium-on-carbon (15 mg of a 10% w/w, 0.14 mmol) under vacuum. The flask was back filled with N_2 , evacuated and filled with H_2 using the burette apparatus. The reaction mixture was stirred under H_2 for 3 h, filtered through a celite pad, washed with ethanol (10 mL) and concentrated under reduced pressure to afford the title compound (28 mg, 78%) as a dark purple oil; $^1\text{H NMR}$ (400 MHz, $\text{DMSO-}d_6$) δ = 10.24 (s, 1H), 6.74 (s, 1H), 6.37 (s, 1H), 4.80 (br t, J = 5.5 Hz, 2H), 4.34 (br.s, 2H), 4.19 (quin, J = 6.5 Hz, 1H), 3.88 - 3.74 (m, 4H), 3.73 (s, 3H); LCMS (Method A, UV, ES) RT = 0.17 min, $[\text{M}+\text{H}]^+ = \text{no mass ion observed}$.

2,3-Dichloro-*N*-(1-(1,3-dihydroxypropan-2-yl)-6-methoxy-2-oxo-2,3-dihydro-1*H*-benzo[*d*]imidazol-5-yl)benzenesulfonamide (219) N21778-31-1



The title compound was prepared from **218** (24 mg, 0.10 mmol) and 2,3-dichlorobenzenesulfonyl chloride (25 mg, 0.10 mmol) according to the procedure described for the preparation of **29**. The same work up and purification using MDAP (Method A) afforded **219** (21 mg, 48%) as a white solid; $^1\text{H NMR}$ (400 MHz, $\text{DMSO-}d_6$) δ = 10.55 (s, 1H), 9.59 (br.s, 1H), 7.88 (dd, J = 8.0, 1.5 Hz, 1H), 7.73 (dd, J = 8.0, 1.5 Hz, 1H), 7.41 (t, J = 8.0 Hz, 1H), 6.76 (s, 2H), 4.85 - 4.56 (m, 2H), 4.30 - 4.11 (m, 1H), 3.88 - 3.77 (m, 2H), 3.77 - 3.65 (m, 2H), 3.38 (s, 3H); HRMS (ESI) m/z calculated for $\text{C}_{17}\text{H}_{18}\text{Cl}_2\text{N}_3\text{O}_6\text{S}$ = 462.0293. Found = 462.0295 $[\text{M}+\text{H}]^+$; LCMS (Method A, UV, ES) RT = 0.77 min, $[\text{M}+\text{H}]^+$ = 462, 464, 466, 100% purity.

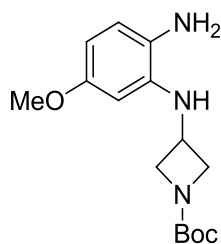
***tert*-Butyl 3-((5-methoxy-2-nitrophenyl)amino)azetidine-1-carboxylate (220)**



A solution of 3-fluoro-4-nitroanisole (513 mg, 3.00 mmol), *tert*-butyl 3-aminoazetidine-1-carboxylate (775 mg, 4.50 mmol) and DIPEA (1 mL) in DMF (1 mL) were stirred at ambient temperature for 4 h. The mixture was diluted with ethyl acetate (50 mL) and the organic phase was washed with HCl (2 x 20 mL of a 2 M aqueous solution), sodium bicarbonate (20 mL of a saturated aqueous solution), brine (20 mL), dried (MgSO_4), and evaporated under reduced pressure. The residue was purified by column chromatography on a 70 g silica column, eluting with 0-50% ethyl acetate-cyclohexane over 40 min. The solvent was removed under reduced pressure to afford the title compound (819 mg, 84%) as a yellow

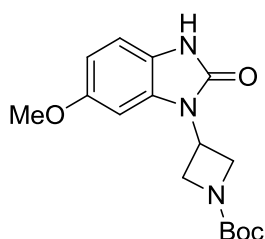
gum; $^1\text{H NMR}$ (400 MHz, CDCl_3) δ = 8.37 (d, J = 4.5 Hz, 1H), 8.16 (d, J = 9.5 Hz, 1H), 6.29 (dd, J = 9.5, 2.5 Hz, 1H), 5.83 (d, J = 2.5 Hz, 1H), 4.38-4.24 (m, 3H), 3.89-3.82 (m, 2H), 3.83 (s, 3H), 1.43 (s, 9H); LCMS (Method A, UV, ES) RT = 1.15 min, $[\text{2M+H}]^+$ = 647, 98% purity.

***tert*-Butyl 3-((2-amino-5-methoxyphenyl)amino)azetidine-1-carboxylate (221)**



A solution of **220** (819 mg, 2.53 mmol) in ethanol (100 mL) was added to a flask containing palladium-on-carbon (270 mg of a 10% w/w, 0.25 mmol) under vacuum. The flask was back filled with N_2 , evacuated and filled with H_2 using the burette apparatus. The reaction mixture was stirred under H_2 for 20 h, filtered through a celite pad, washed with ethanol (50 mL) and concentrated under reduced pressure to afford the title compound as a brown solid (723 mg, 97%); $^1\text{H NMR}$ (400 MHz, $\text{DMSO-}d_6$) δ = 9.13 (br.s, 2H), 7.05 (d, J = 8.5 Hz, 1H), 6.30 (dd, J = 8.5, 2.5 Hz, 1H), 6.20 (br.s, 1H), 6.02 (d, J = 2.5 Hz, 1H), 4.36 - 4.06 (m, 3H), 3.78 - 3.65 (m, 2H), 3.71 (s, 3H), 1.39 (s, 9H); LCMS (Method A, UV, ES) RT = 0.68 min, $[\text{M+H}]^+$ = 294, 100% purity.

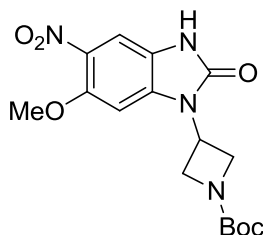
***tert*-Butyl 3-(5-methoxy-2-oxo-1*H*-benzo[d]imidazol-3(2*H*)-yl)azetidine-1-carboxylate (222)**



A mixture of **221** (723 mg, 2.46 mmol) and CDI (400 mg, 2.46 mmol) in THF (12 mL) was stirred at ambient temperature for 22 h. The mixture was concentrated under reduced pressure, and diluted with ethyl acetate (50 mL). The organic phase was washed with HCl (25 mL of a 1 M aqueous solution), sodium bicarbonate (10 mL of a saturated aqueous solution), dried using a hydrophobic frit and evaporated under reduced pressure to afford the title

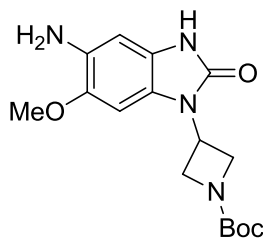
compound (620 mg, 79%) as a beige coloured solid; ^1H NMR (400 MHz, CDCl_3) δ = 8.61 (br.s, 1H), 7.01 - 6.96 (m, 2H), 6.69 (dd, J = 8.5, 2.5 Hz, 1H), 5.34 - 5.24 (m, 1H), 4.52 - 4.43 (m, 2H), 4.44 - 4.35 (m, 2H), 3.83 (s, 3H), 1.51 (s, 9H); LCMS (Method A, UV, ES) RT = 0.89 min, $[\text{M}+\text{H}]^+ = 320$, $[\text{2M}+\text{H}]^+ = 639$, 90% purity.

***tert*-Butyl 3-(6-methoxy-5-nitro-2-oxo-2,3-dihydro-1*H*-benzo[*d*]imidazol-1-yl)azetidine-1-carboxylate (223)**



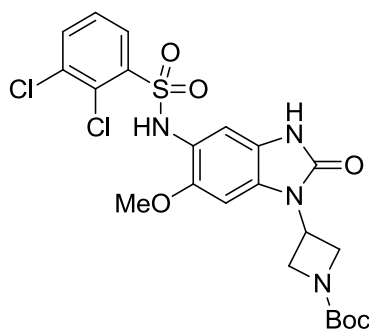
Nitric acid (30 mL of a 4 N aqueous solution, 83 mmol) was added to **222** (620 mg, 1.94 mmol) and the suspension was shaken at ambient temperature until the solid dissolved. After a couple of minutes a fine powder started to precipitate. This mixture was stirred for 4 h. The product was too water soluble to be extracted, and was thus converted to the Boc protected analogue. The mixture was treated with solid sodium bicarbonate to pH 8, and then THF (20 mL) and Boc_2O (0.76 mL, 3.27 mmol) were added. The mixture was stirred at ambient temperature for 48 h. The mixture was then extracted with ethyl acetate (3 x 50 mL), and the combined organic extracts were washed with HCl (40 mL of a 2 M aqueous solution), sodium bicarbonate (40 mL of a saturated aqueous solution), brine (40 mL), dried using a hydrophobic frit and evaporated under reduced pressure. The residue was purified using column chromatography on a 100 g silica cartridge eluting with 0-50% ethyl acetate-cyclohexane for 30 min. The solvent was evaporated under reduced pressure to afford the title compound (368 mg, 52%) as a dark yellow solid; ^1H NMR (400 MHz, CDCl_3) δ = 9.01 (s, 1H), 7.77 (s, 1H), 7.14 (s, 1H), 5.28 (m, 1H), 4.54 - 4.36 (m, 4H), 3.99 (s, 3H), 1.51 (s, 9H); LCMS (Method A, UV, ES) RT = 0.90 min, $[\text{M}+\text{H}]^+ = 365$, 95% purity.

***tert*-Butyl 3-(5-amino-6-methoxy-2-oxo-2,3-dihydro-1*H*-benzo[*d*]imidazol-1-yl)azetidine-1-carboxylate (224)**



A solution of **223** (367 mg, 1.00 mmol) in ethanol (70 mL) was added to a flask containing palladium-on-carbon (107 mg of a 10% w/w, 0.10 mmol) under vacuum. The flask was back filled with N₂, evacuated and filled with H₂ using the burette apparatus. The reaction mixture was stirred under H₂ for 20 h, filtered through a celite pad, washed with ethanol (50 mL) and concentrated under reduced pressure to afford the title compound (321 mg, 95%) as a light brown solid; ¹H NMR (400 MHz, DMSO-*d*₆) δ = 10.94 (s, 1H), 10.00 - 9.30 (br m, 2H), 7.10 (m, 2H), 5.23 - 5.14 (m, 1H), 4.49 - 4.33 (m, 2H), 4.23 (t, *J* = 9 Hz, 2H), 3.87 (s, 3H), 1.43 (s, 9H); LCMS (Method A, UV, ES) RT = 0.59 min, [M+H]⁺ = 335, [M+H+MeCN]⁺ = 376, 96% purity.

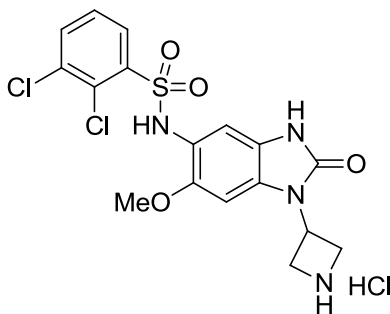
***tert*-Butyl 3-(5-(2,3-dichlorophenylsulfonamido)-6-methoxy-2-oxo-2,3-dihydro-1*H*-benzo[*d*]imidazol-1-yl)azetidine-1-carboxylate (225)**



The title compound was prepared from **224** (321 mg, 0.96 mmol) and 2,3-dichlorobenzenesulfonyl chloride (286 mg, 1.17 mmol) according to the procedure described for the preparation of **29**. The same work up and purification using column chromatography on a 70 g silica cartridge, eluting with 0-100% ethyl acetate-DCM over 30 mins afforded **225** (300 mg, 57%) as a colourless oil; ¹H NMR (400 MHz, CDCl₃) δ = 9.99 (br.s, 1H), 7.77 (d, *J* = 8.0 Hz, 1H), 7.58 (s, 1H), 7.56 (d, *J* = 8.0 Hz, 1H), 7.17 (t, *J* = 8.0 Hz, 1H), 6.77 (s, 1H),

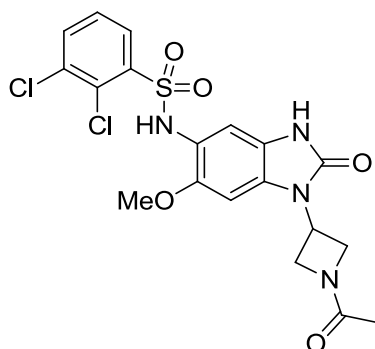
5.25 (s, 1H), 5.23 - 5.16 (m, 1H), 4.39 - 4.28 (m, 4H), 3.60 (s, 3H), 1.43 (s, 9H); LCMS (Method A, UV, ES) RT = 1.10 min, $[M+H]^+$ = 543, 545, 547, 90% purity.

***N*-(1-(Azetidin-3-yl)-6-methoxy-2-oxo-2,3-dihydro-1*H*-benzo[*d*]imidazol-5-yl)-2,3-dichlorobenzenesulfonamide hydrochloride (226)**



HCl (4 mL of a 4 M solution in dioxane, 16 mmol) was added to a solution of **225** (300 mg, 0.552 mmol) in chloroform (1 mL), and the mixture was stirred at ambient temperature for 1.5 h. A white solid which precipitated from solution was collected by filtration to afford the title compound (125 mg, 51%) as an off-white solid; ^1H NMR (400 MHz, MeOD- d_4) δ = 7.72 (br t, J = 8.0 Hz, 2H), 7.26 (t, J = 8.0 Hz, 1H), 7.14 (s, 1H), 6.75 (s, 1H), 5.31 - 5.22 (m, 1H), 4.85 - 4.79 (m, 2H), 4.45 (br t, J = 9 Hz, 2H) 3.65 (s, 3H); the four exchangeable NH protons were not observed, LCMS (Method A, UV, ES) RT = 0.68 min, $[M+H]^+$ = 443, 445, 447, 95% purity.

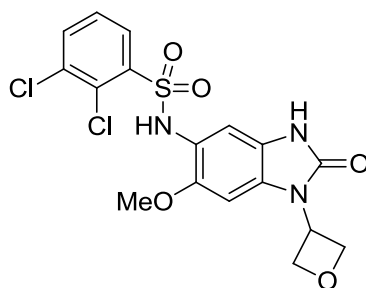
***N*-(1-(1-Acetylazetidin-3-yl)-6-methoxy-2-oxo-2,3-dihydro-1*H*-benzo[*d*]imidazol-5-yl)-2,3-dichlorobenzenesulfonamide (227)**



Acetic anhydride (50 μL , 0.53 mmol) was added to a solution of **226** (19 mg, 0.04 mmol) in pyridine (0.5 mL). The mixture was stirred at ambient temperature for 3 h; LCMS analysis showed that di-acetylation had occurred. MeOH (7.5 mL) and K_2CO_3 (60 mg 0.43 mmol)

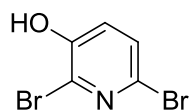
were added to the mixture, and after stirring for 24 h, HCl (2 M aqueous solution) was added to acidify the reaction. The mixture was extracted using ethyl acetate (20 mL) and the organic layer was washed with brine (20 mL), dried (MgSO₄) and concentrated under reduced pressure. The solid was taken up in DMSO (1 mL), purified by MDAP (Method A), and the solvent was evaporated under reduced pressure to afford the title compound (5 mg, 25%) as a white solid; ¹H NMR (400 MHz, MeOD-*d*₄) δ = 7.73 (m, 2H), 7.28 (t, *J* = 8.0 Hz, 1H), 7.14 (s, 1H), 6.71 (s, 1H), 5.22 – 5.14 (m, 1H), 4.75 - 4.71 (m, 1H), 4.57 (t, *J* = 9.3 Hz, 1H), 4.53 – 4.47 (m, 1H), 4.34 (t, *J* = 9.5 Hz, 1H), 3.54 (s, 3H), 1.93 (s, 3H); the two exchangeable NH protons were not observed; LCMS (Method A, UV, ES) RT = 0.82 min, [M+H]⁺ = 485, 487, 489, 98% purity.

2,3-Dichloro-*N*-(6-methoxy-1-(oxetan-3-yl)-2-oxo-2,3-dihydro-1*H*-benzo[*d*]imidazol-5-yl)benzenesulfonamide (229)



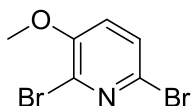
The title compound was prepared from 5-methoxy-6-nitro-1*H*-benzo[*d*]imidazol-2(3*H*)-one (128 mg, 0.612 mmol), 3-iodooxetane (135 mg, 0.734 mmol) and 2,3-dichlorobenzenesulfonyl chloride (135 mg, 0.575 mmol) according to the procedure described for the preparation of **190a**. The same work up and purification afforded **229** (7 mg, 10 % yield) as a white solid; ¹H NMR (400 MHz, DMSO-*d*₆) δ = 10.70 (br.s, 1H), 9.69 (br.s, 1H), 7.87 (d, *J* = 8.0 Hz, 1H), 7.73 (dd, *J* = 8.0, 1.5 Hz, 1H), 7.41 (t, *J* = 8.0 Hz, 1H), 6.96 (s, 1H), 6.84 (s, 1H), 5.46 - 5.33 (m, 1H), 5.05 (t, *J* = 6.5 Hz, 2H), 4.90 - 4.81 (m, 2H), 3.43 (s, 3H); LCMS (Method A, UV, ES) RT = 0.88 min, [M+H]⁺ = 444, 446, 448, 100% purity.

2,6-Dibromopyridin-3-ol (231)



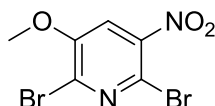
An ice-cold solution of bromine (16.2 mL, 315 mmol) in sodium hydroxide (320 mL of a 10% aqueous solution, 886 mmol) was added dropwise to a stirred solution of pyridin-3-ol (10 g, 105 mmol) in sodium hydroxide (110 mL of a 10% aqueous, 305 mmol). The solution was stirred at 0 °C for 1 h and then at room temp for 4 h. A small amount of precipitate that formed was filtered off. The filtrate was cooled, and concentrated hydrochloric acid was added until the pH reached 1. The solid was filtered, washed with water, dried, and recrystallised from carbon tetrachloride to afford the title compound (12.1 g, 46%) as a beige coloured solid; $^1\text{H NMR}$ (400 MHz, $\text{DMSO-}d_6$) δ = 11.14 (br.s, 1H), 7.47 (d, J = 8.0 Hz, 1H), 7.26 (d, J = 8.0 Hz, 1H); LCMS (UV, ES): RT = 0.79 mins, $[\text{M-H}]^-$ = 250, 252, 254, 90% purity.

2,6-Dibromo-3-methoxypyridine (232)



2,6-Dibromopyridin-3-ol (12 g, 47.5 mmol), potassium carbonate (6.0 g, 43.5 mmol), methyl iodide (10.1 mL, 162 mmol) and DMSO (20 mL) was refluxed for 2 h. The reaction mixture was poured into water (60 mL) and was warmed gently at 50 °C with stirring for 30 min. The reaction was cooled to room temp and the precipitated solid was filtered, dried under vacuum to give the crude product as a dark orange solid. Crystallisation with cyclohexane afforded the title compound (10.1 g, 80%) as a pale orange solid; $^1\text{H NMR}$ (400 MHz, $\text{DMSO-}d_6$) δ = 7.66 (d, J = 8.0 Hz, 1H), 7.52 (d, J = 8.0 Hz, 1H), 3.90 (s, 3H); LCMS (UV, ES): RT = 0.98 mins, $[\text{M+H}]^+$ = 266, 268, 270, 99% purity.

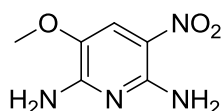
2,6-Dibromo-3-methoxy-5-nitropyridine (233)



Nitric acid (5 mL of a 70 wt% aqueous solution, 79 mmol) was added to a solution of **232** (2 g, 7.5 mmol) in sulfuric acid (18 M, 8 mL, 144 mmol) at 0 °C. The mixture was stirred and heated at 65 °C for 18 h. Additional conc. nitric acid (2.5 mL, 39.3 mmol) was added and the reaction mixture was stirred at 65 °C for a further 18 h. The reaction mixture was cooled and slowly neutralized with solid sodium carbonate. The resulting mixture was extracted with

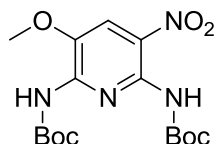
ethyl acetate (3 x 50 mL), and the combined organic extracts were dried using a hydrophobic frit and concentrated under reduced pressure. The residue was purified on 100 g silica column using a gradient of 0-25% ethyl acetate-cyclohexane over 60 min. The appropriate fractions were combined and evaporated under reduced pressure to afford the title compound (0.69 g, 28%) as a white solid; $^1\text{H NMR}$ (400 MHz, $\text{DMSO-}d_6$) δ = 8.24 (s, 1H), 3.99 (s, 3H); LCMS (UV, ES) RT = 1.05 min, $[\text{M}+\text{H}]^+$ = no mass ion found, 98% purity (Note. $^1\text{H NMR}$ Identical to that of patent WO 2010027500).

3-Methoxy-5-nitropyridine-2,6-diamine (234)



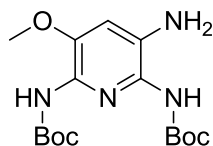
A solution of **325** (0.5 g, 1.6 mmol) in aqueous ammonia (15 M, 12.0 mL, 620 mmol) was heated at 90 °C for 1 h in the microwave oven. The reaction mixture was cooled, the yellow solid was removed by filtration, washed with a small amount of water and dried under vacuum to afford the title compound (230 mg, 78%) as a yellow solid; $^1\text{H NMR}$ (400 MHz, $\text{DMSO-}d_6$, 393 K) δ = 7.48 (br.s, 1H), 7.35 (br.s, 2H), 6.81 (br.s, 2H), 3.80 (s, 3H); LCMS (Method B, UV, ES) RT = 0.49 min, $[\text{M}+\text{H}]^+$ = 185, 98% purity.

Di-*tert*-butyl (3-methoxy-5-nitropyridine-2,6-diyl)dicarbamate (235)



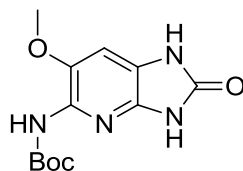
Boc-anhydride (0.76 mL, 3.3 mmol) and K_2CO_3 (560 mg, 4.10 mmol) were added to a solution of **234** (150 mg, 0.82 mmol) in DMF (4 mL). The reaction mixture was stirred at ambient temperature for 18 h, and was then diluted with water (20 mL) and ethyl acetate (40 mL). The organic layer was separated, washed with water (2 x 10 mL), brine (10 mL), dried using a hydrophobic frit, and concentrated under reduced pressure. The yellow residue was purified on a 50 g silica column using a gradient of 0-50% ethyl acetate-cyclohexane over 40 min. The appropriate fractions were combined and evaporated under reduced pressure to afford the title product (210 mg, 66%) as a yellow solid; $^1\text{H NMR}$ (400 MHz, $\text{DMSO-}d_6$) δ = 9.86 (s, 1H), 9.22 (s, 1H), 7.91 (s, 1H), 3.89 (s, 3H), 1.45 (s, 9H), 1.40 (s, 9H); LCMS (Method B, UV, ES) RT = 1.21 min, $[\text{M}+\text{H}]^+$ = 385, 98% purity.

Di-*tert*-butyl (3-amino-5-methoxypyridine-2,6-diyl)dicarbamate (236)



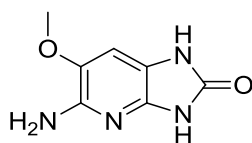
Iron powder (290 mg, 5.2 mmol) was added to a stirring solution of **235** (200 mg, 0.52 mmol) in glacial acetic acid (10 mL). The reaction mixture was stirred at ambient temperature for 2 h. The reaction mixture was concentrated under reduced pressure, and was washed with sodium bicarbonate (10 mL of a saturated aqueous solution). The washings were extracted with ethyl acetate (2 x 20 mL), and the combined organic extracts were washed with brine (20 mL), dried using a hydrophobic frit and concentrated under reduced pressure to afford the title product (170 mg, 78%) as a yellow oil; ^1H NMR (400 MHz, DMSO- d_6) δ = 8.58 (s, 1H), 8.23 (s, 1H), 6.81 (s, 1H), 4.81 (s, 2H), 3.70 (s, 3H), 1.43 (s, 9H), 1.39 (s, 9H); LCMS (Method B, UV, ES) RT = 0.94 min, $[\text{M}+\text{H}]^+ = 355$, 90% purity.

***Tert*-butyl (6-methoxy-2-oxo-2,3-dihydro-1*H*-imidazo[4,5-*b*]pyridin-5-yl)carbamate (237)**



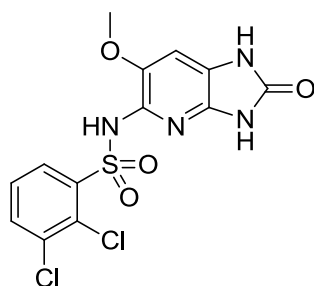
A solution of **236** (150 mg, 0.42 mmol) in dry pyridine (1.5 mL) was sealed and heated in the microwave for 1 h at 100 °C. The mixture was concentrated under reduced pressure to give the title product (110 mg, 74%) as a brown solid; ^1H NMR (400 MHz, DMSO- d_6) δ = 11.01 (br.s, 1H), 10.71 (br.s, 1H), 8.44 (s, 1H), 7.04 (s, 1H), 3.75 (s, 3H), 1.41 (s, 9H); LCMS (Method B, UV, ES) RT = 0.71 min, $[\text{M}+\text{H}]^+ = 281$, 90% purity.

5-Amino-6-methoxy-1*H*-imidazo[4,5-*b*]pyridin-2(3*H*)-one (238)



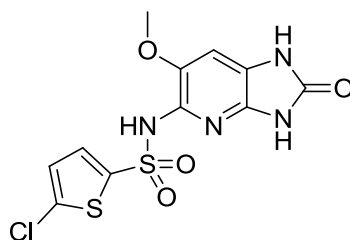
A mixture of **237** (50 mg, 0.18 mmol) and TFA (0.25 mL) was stirred at ambient temperature for 30 min. The mixture was concentrated, and the residue was dissolved in methanol and dichloromethane (1 mL of 1:1 mixture), and passed through a 500 mg aminopropyl cartridge. The cartridge was washed with more methanol and dichloromethane (10 mL of 1:1 mixture), and the filtrate was concentrated to afford the title product (30 mg, 93%) as a brown solid; ^1H NMR (400 MHz, $\text{DMSO-}d_6$) δ = 10.56 (br.s, 1H), 10.12 (s, 1H), 6.82 (s, 1H), 5.12 (s, 2H), 3.73 (s, 3H); LCMS (Method B, UV, ES) RT = 0.34 min, $[\text{M}+\text{H}]^+ = 181$, 91% purity.

2,3-Dichloro-N-(6-methoxy-2-oxo-2,3-dihydro-1H-imidazo[4,5-b]pyridin-5-yl)benzenesulfonamide (239)



The title compound was prepared from **238** (30 mg, 0.17 mmol) and 2,3-dichlorobenzenesulfonyl chloride (45 mg, 0.18 mmol) according to the procedure described for the preparation of **29**. The same work up and purification afforded **239** (20 mg, 29%) as a white solid; ^1H NMR (400 MHz, $\text{DMSO-}d_6$) δ = 11.00 (s, 1H), 10.77 (s, 1H), 10.21 (s, 1H), 7.94 (dd, $J = 8.0, 1.3$ Hz, 1H), 7.90 (dd, $J = 8.0, 1.3$ Hz, 1H), 7.51 (t, $J = 8.0$ Hz, 1H), 7.02 (s, 1H), 3.58 (s, 3H); LCMS (Method A, UV, ES) RT = 0.76 min, $[\text{M}+\text{H}]^+ = 389, 391, 393$, 95% purity.

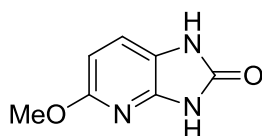
5-Chloro-N-(6-methoxy-2-oxo-2,3-dihydro-1H-imidazo[4,5-b]pyridin-5-yl)thiophene-2-sulfonamide (240)



The title compound was prepared from **238** (20 mg, 0.11 mmol) and 5-chlorothiophene-2-sulfonyl chloride (27 mg, 0.12 mmol) according to the procedure described for the

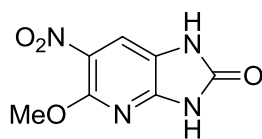
preparation of **29**. The same work up and purification afforded **240** (6 mg, 14%) as a colourless oil; ^1H NMR (400 MHz, $\text{DMSO-}d_6$) δ = 11.12 (br.s, 1H), 10.73 (br.s, 1H), 10.17 (br.s, 1H), 7.52 (d, J = 4.0 Hz, 1H), 7.17 (d, J = 4.0 Hz, 1H), 7.05 (s, 1H), 3.71 (s, 3H); LCMS (Method A, UV, ES) RT = 0.71 min, $[\text{M}+\text{H}]^+ = 361, 363$, 94% purity.

5-Methoxy-1*H*-imidazo[4,5-*b*]pyridin-2(3*H*)-one (242)



CDI (1.25 g, 7.73 mmol) was added to a solution of 6-methoxypyridine-2,3-diamine (1.0 g, 7.03 mmol) and triethylamine (2.0 mL, 14.1 mmol) in THF (13 mL), and the reaction was stirred at ambient temperature under nitrogen for 2 h. The reaction was evaporated under reduced pressure to remove THF, then triturated with ethyl acetate, and filtered to give a brown solid, which was purified on a 100 g silica column using a gradient of 0-25% methanol-dichloromethane over 40 min. The appropriate fractions were combined and evaporation under reduced pressure afforded the title product (360 mg, 31%) as a white solid; ^1H NMR (400 MHz, $\text{DMSO-}d_6$) δ = 11.18 (br.s, 1H), 10.54 (br.s, 1H), 7.21 (d, J = 8.5 Hz, 1H), 6.35 (d, J = 8.5 Hz, 1H), 3.77 (s, 3H); LCMS (UV, ES) RT = 0.45 min, $[\text{M}+\text{H}]^+ = 166$, 100% purity.

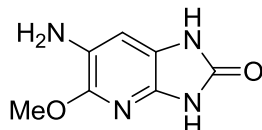
5-Methoxy-6-nitro-1*H*-imidazo[4,5-*b*]pyridin-2(3*H*)-one (243)



Compound **242** (266 mg, 1.61 mmol) was slowly added to a flask containing trifluoroacetic anhydride (5.5 mL, 39.8 mmol) at 0 °C, and the reaction was stirred at this temp for 1 h. Fuming nitric acid (0.14 mL of a 70 wt% aqueous solution, 3.21 mmol) was added dropwise and the reaction was stirred at 0 °C for a further 2 h. The reaction mixture was then slowly added to a solution of sodium metabisulphite (304 mg in 14 mL of water, 1.3 mmol) at 0 °C, and the precipitate formed was filtered under reduced pressure to afford the title product (160 mg, 47%) as a bright yellow solid; ^1H NMR (400 MHz, $\text{DMSO-}d_6$) δ = 12.09 (br.s, 1H), 11.06 (s, 1H), 7.85 (s, 1H), 3.98 (s, 3H); LCMS (Method A, UV, ES) RT = 0.52 min,

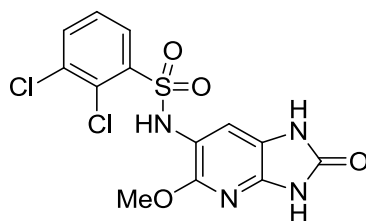
$[M+H]^+ = 211$, $[M+NH_4]^+ = 228$, 100% purity.

6-Amino-5-methoxy-1*H*-imidazo[4,5-*b*]pyridin-2(3*H*)-one (244)



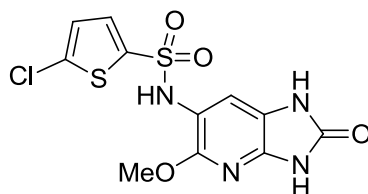
A solution of **243** (130 mg, 0.62 mmol) in ethanol (2 mL) was added to a flask containing palladium-on-carbon (66 mg of a 10% w/w, 0.06 mmol) under vacuum. The flask was back filled with N₂, evacuated and filled with H₂ using the burette apparatus. The reaction mixture was stirred under H₂ for 2 h, filtered through a celite pad, washed with ethanol (30 mL), and concentrated under reduced pressure to afford the title product (84 mg, 76% yield) as a yellow solid; ¹H NMR (400 MHz, DMSO-*d*₆) $\delta = 10.59$ (br.s, 1H), 10.14 (s, 1H), 6.69 (s, 1H), 4.38 (s, 2H), 3.80 (s, 3H); LCMS (Method A, UV, ES) RT = 0.22 min, $[M+H]^+$ = not detected, 90% purity.

2,3-Dichloro-*N*-(5-methoxy-2-oxo-2,3-dihydro-1*H*-imidazo[4,5-*b*]pyridin-6-yl)benzenesulfonamide (245)



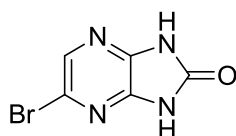
The title compound was prepared from **244** (23 mg, 0.13 mmol) and 2,3-dichlorobenzenesulfonyl chloride (35 mg, 0.14 mmol) according to the procedure described for the preparation of **29**. The same work up and purification afforded **245** (24 mg, 48%) as a white solid; ¹H NMR (400 MHz, DMSO-*d*₆) $\delta = 11.23$ (br.s, 1H), 10.52 (s, 1H), 9.90 (br.s, 1H), 7.88 (dd, *J* = 8.0, 1.5 Hz, 1H), 7.71 (dd, *J* = 8.0, 1.5 Hz, 1H), 7.41 (t, *J* = 8.0 Hz, 1H), 7.08 (s, 1H), 3.39 (s, 3H); ¹³C NMR (101 MHz, DMSO-*d*₆) $\delta = 178.8$, 154.4, 154.0, 140.4, 140.4, 134.1, 133.8, 129.7, 129.4, 127.8, 118.3, 117.1, 53.0; HRMS (ESI) *m/z* calculated for C₁₃H₁₁Cl₂N₄O₄S = 388.9878. Found = 388.9881 $[M+H]^+$; LCMS (Method A, UV, ES) RT = 0.83 min, $[M+H]^+ = 389$, 391, 393, 100% purity.

5-Chloro-*N*-(5-methoxy-2-oxo-2,3-dihydro-1*H*-imidazo[4,5-*b*]pyridin-6-yl)thiophene-2-sulfonamide (246)



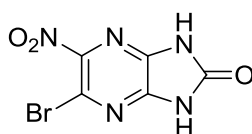
The title compound was prepared from **244** (13 mg, 0.07 mmol) and 5-chlorothiophene-2-sulfonyl chloride (17 mg, 0.08 mmol) according to the procedure described for the preparation of **29**. The same work up and purification afforded **246** (9 mg, 35% yield) as a white solid; $^1\text{H NMR}$ (400 MHz, $\text{DMSO-}d_6$) δ = 11.29 (s, 1H), 10.56 (s, 1H), 9.83 (s, 1H), 7.26 - 7.20 (m, 1H), 7.19 - 7.15 (m, 1H), 7.09 (s, 1H), 3.55 (d, 3H); HRMS (ESI) m/z calculated for $\text{C}_{11}\text{H}_{10}\text{ClN}_4\text{O}_4\text{S}_2$ = 360.9832. Found = 360.9847 $[\text{M}+\text{H}]^+$; LCMS (Method A, UV, ES) RT = 0.74 min, $[\text{M}+\text{H}]^+$ = 361, 363, 100% purity.

5-Bromo-1*H*-imidazo[4,5-*b*]pyrazin-2(3*H*)-one (248)



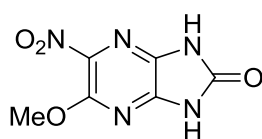
A mixture of 5-bromopyrazine-2,3-diamine (0.7 g, 3.7 mmol) and CDI (1.2 g, 7.4 mmol) in anhydrous THF (20 mL) was heated at 50 °C for 22 h. More CDI (0.7 g, 3.7 mmol) was added and the reaction was stirred at 50 °C for a further 24 h. The reaction mixture was concentrated under reduced pressure, and the sample was purified on a 100 g silica column, using a gradient of 0-100% ethyl acetate-dichloromethane over 40 min. The appropriate fractions were combined and evaporated under reduced pressure to afford the title product (0.68 g, 85%) as a white solid; $^1\text{H NMR}$ (400 MHz, $\text{DMSO-}d_6$) δ = 11.95 (br.s, 2H), 7.97 (s, 1H); LCMS (Method A, UV, ES) RT = 0.48 min, $[\text{M}+\text{H}]^+$ = 215, 217, 99% purity.

5-bromo-6-nitro-1*H*-imidazo[4,5-*b*]pyrazin-2(3*H*)-one (249)



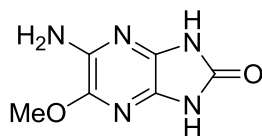
Nitronium tetrafluoroborate (1.05 g, 7.91 mmol) was added in portions over 10 min to a suspension of **248** (0.68 g, 3.16 mmol) in MeCN (10 mL) and the mixture was stirred at ambient temperature for 1 h. The reaction was poured over ice water (40 mL), and the precipitate formed was collected by filtration, washed with water and dried under reduced pressure to afford the title product (0.41 g, 50%) as a yellow solid; ^1H NMR (400 MHz, DMSO- d_6) δ = 12.67 (br.s, 1H), 12.50 (br.s, 1H); ^{13}C NMR (101 MHz, DMSO- d_6) δ = 154.4, 146.2, 143.1, 138.1, 120.0; LCMS (Method A, UV, ES) RT = 0.60 min, $[\text{M-H}]^-$ = 258, 260, 100% purity.

5-Methoxy-6-nitro-1H-imidazo[4,5-b]pyrazin-2(3H)-one (250)



Sodium methoxide (100 mg, 1.8 mmol) was added in portions to a solution of **249** (150 mg, 0.58 mmol) dissolved in MeOH (1 mL). The reaction was stirred at ambient temperature for 18 h and was then heated to 50 °C and stirred at this temperature for a further 24 h. Water was added (1 mL) and the reaction mixture was diluted with DMSO (4 mL). The solid precipitate was filtered to give a yellow solid (30 mg). LCMS and ^1H NMR showed no peak for the desired product. This material was discarded. The filtrate was diluted with more DMSO (2 mL, total of 7 mL) and purified by MDAP (7 injections on Method A). The appropriate fractions were combined and the solvent was evaporated under reduced pressure to afford the title product (60 mg, 49%) as a yellow solid; ^1H NMR (400 MHz, DMSO- d_6) δ = 12.50 (br.s, 1H), 12.01 (br.s, 1H), 4.00 (s, 3H); LCMS (Method A, UV, ES) RT = 0.47 min, $[\text{M-H}]^-$ = 210, 95% purity.

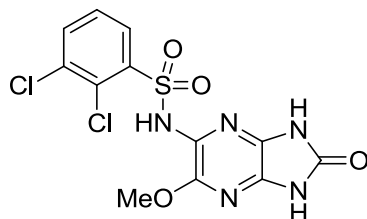
5-Amino-6-methoxy-1H-imidazo[4,5-b]pyrazin-2(3H)-one (251)



A solution of **250** (60 mg, 0.28 mmol) in ethanol (2 mL) and ethyl acetate (2 mL) was added to a flask containing palladium-on-carbon (91 mg of a 10% w/w, 0.09 mmol) under vacuum. The flask was back filled with N_2 , evacuated and filled with H_2 using the burette apparatus. The reaction mixture was stirred under H_2 for 1 h, filtered through a celite pad, washed with a

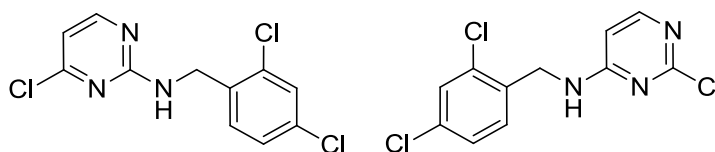
mixture of ethanol and ethyl acetate (30 mL of a 1:1 mixture), and concentrated under reduced pressure to afford the title product (41 mg, 80%) as a grey solid; $^1\text{H NMR}$ (400 MHz, $\text{DMSO-}d_6$) $\delta = 10.83$ (br.s, 1H), 10.80 (br.s, 1H), 5.53 (s, 2H), 3.83 (s, 3H); LCMS (Method A, UV, ES) RT = 0.37 min, $[\text{M}+\text{H}]^+ = 182$, 90% purity.

2,3-Dichloro-*N*-(6-methoxy-2-oxo-2,3-dihydro-1*H*-imidazo[4,5-*b*]pyrazin-5-yl)benzenesulfonamide (252)



The title compound was prepared from **251** (41 mg, 0.23 mmol) and 2,3-dichlorobenzenesulfonyl chloride (70 mg, 0.28 mmol) according to the procedure described for the preparation of **29**. The same work up and purification afforded **252** (8 mg, 7%) as a pale orange solid; $^1\text{H NMR}$ (400 MHz, $\text{MeOH-}d_4$) $\delta = 8.06$ (dd, $J = 8.0, 1.5$ Hz, 1H), 7.77 (dd, $J = 8.0, 1.5$ Hz, 1H), 7.44 (t, $J = 8.0$ Hz, 1H), 3.83 (s, 3H); the three exchangeable NH protons were not observed; LCMS (Method A, UV, ES) RT = 0.78 min, $[\text{M}+\text{H}]^+ = 390, 392, 394$, 90% purity.

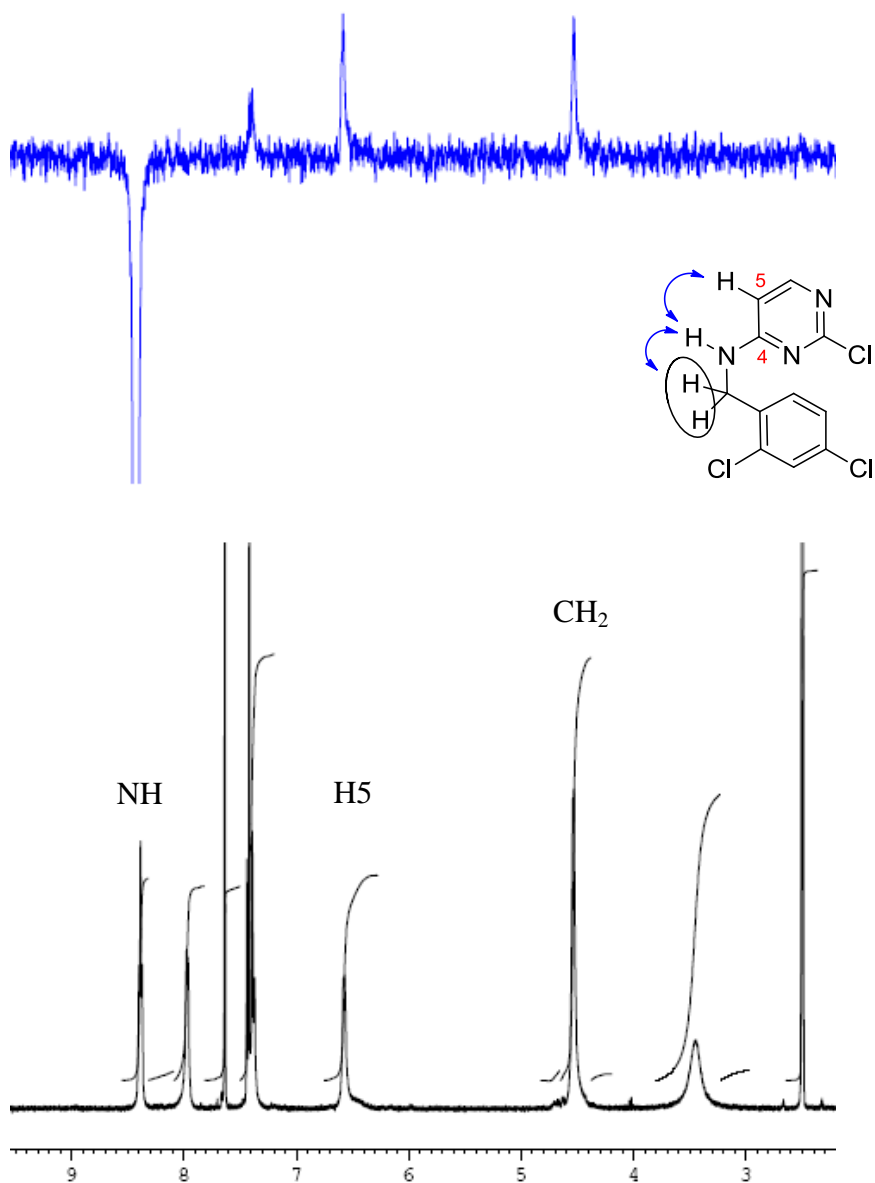
4-Chloro-*N*-(2,4-dichlorobenzyl)pyrimidin-2-amine (258) and 2-chloro-*N*-(2,4-dichlorobenzyl)pyrimidin-4-amine (259)



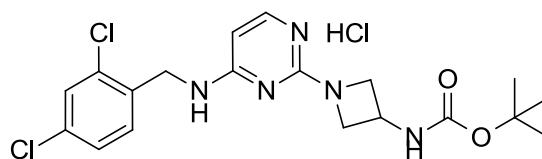
2,4-Dichlorobenzylamine (1.0 mL, 7.4 mmol) was added to a stirring solution of 2,4-dichloropyrimidine (1.0 g, 6.7 mmol) and DIPEA (1.8 mL, 10.1 mmol) in anhydrous DCE (10 mL) and the reaction mixture was stirred at ambient temperature under a nitrogen atmosphere for 24 h. LCMS showed the presence of a mixture of regioisomers (Method A, RT = 1.10 min, 63% and 1.25 min, 27%). The reaction mixture was diluted with water (50 mL) and extracted with DCM (3×50 mL). The combined organic extracts were washed with brine (50 mL), dried using a hydrophobic frit and evaporated under reduced pressure. The residue was purified by column chromatography on a silica column, using a gradient of 0-

100% ethyl acetate-cyclohexane over 40 min. The appropriate fractions were combined and evaporated under reduced pressure to afford the products as white solid: 4-chloro-*N*-(2,4-dichlorobenzyl)pyrimidin-2-amine, **258** (400 mg, 21%); ^1H NMR (400 MHz, $\text{DMSO-}d_6$) δ = 8.33 - 8.11 (m, 2H), 7.60 (d, J = 2.0 Hz, 1H), 7.43 - 7.28 (m, 2H), 6.74 (d, J = 5.0 Hz, 1H), 4.51 (d, J = 5.0 Hz, 2H); ^{13}C NMR (126 MHz, $\text{DMSO-}d_6$) δ = 162.1, 160.1, 159.9, 135.6, 132.9, 132.1, 129.6, 128.6, 127.3, 109.8, 41.7; IR ν_{max} (neat) 3269, 1597, 1561, 1531, 1449, 1412 cm^{-1} ; HRMS (ESI) m/z calculated for $\text{C}_{11}\text{H}_9\text{Cl}_3\text{N}_3$ = 287.9857. Found = 287.9860, $[\text{M}+\text{H}]^+$; LCMS (Method A, UV, ES) RT = 1.25 min, $[\text{M}+\text{H}]^+$ = 288, 290, 292, 294 100% purity; and 2-chloro-*N*-(2,4-dichlorobenzyl)pyrimidin-4-amine, **259** (950 mg, 49%); ^1H NMR (400 MHz, $\text{DMSO-}d_6$) δ = 8.42 (t, J = 4.5 Hz, 1H), 7.97 (d, J = 5.0 Hz, 1H), 7.63 (d, J = 2.0 Hz, 1H), 7.45 - 7.29 (m, 2H), 6.58 (d, J = 5.0 Hz, 1H), 4.54 (d, J = 4.5 Hz, 2H); ^{13}C NMR (101 MHz, $\text{DMSO-}d_6$) δ = 163.4, 159.7, 155.8, 134.8, 133.3, 132.5, 130.6, 128.7, 127.4, 105.2, 41.0; IR ν_{max} (neat) 3263, 1591, 1563, 1467, 1337 cm^{-1} ; HRMS (ESI) m/z calculated for $\text{C}_{11}\text{H}_9\text{Cl}_3\text{N}_3$ = 287.9857. Found = 287.9860, $[\text{M}+\text{H}]^+$; LCMS (Method A, UV, ES) RT = 1.10 min, $[\text{M}+\text{H}]^+$ = 288, 290, 292, 100% purity.

In a 1D NOE experiment of **259**, irradiation of the benzylic NH proton (8.42 ppm) gave an NOE enhancement of protons at the methylene position (4.54 ppm) and the pyrimidyl proton at the 5-position (6.58 ppm) confirming the structure.

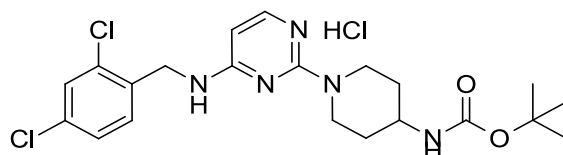


***tert*-Butyl (1-(4-((2,4-dichlorobenzyl)amino)pyrimidin-2-yl)azetidin-3-yl)carbamate, hydrochloride salt (261a)**



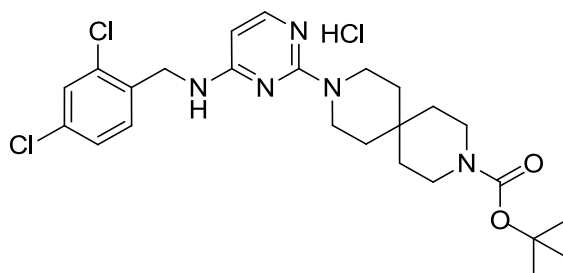
A mixture of **259** (400 mg, 1.39 mmol), *tert*-butyl azetidion-3-ylcarbamate (240 mg, 1.39 mmol) and IPA (15 mL) were stirred at 90 °C for 48 h. The reaction mixture was cooled to ambient temperature, and diethyl ether (10 mL) was added. The precipitated solid was collected by filtration, washed with diethyl ether (20 mL), and dried under reduced pressure to afford the title compound (360 mg, 56%) as a white solid; ¹H NMR (400 MHz, MeOD-*d*₄) δ = 7.59 (d, *J* = 7.0 Hz, 1H), 7.50 (d, *J* = 2.0 Hz, 1H), 7.43 (d, *J* = 8.0 Hz, 1H), 7.33 (dd, *J* = 8.0, 2.0 Hz, 1H), 6.15 (d, *J* = 7.0 Hz, 1H), 4.69 (s, 2H), 4.55 - 4.39 (m, 3H), 4.06 (dd, *J* = 9.0, 4.0 Hz, 2H), 1.45 (s, 9H); the three exchangeable protons were not observed; LCMS (Method A, UV, ES) RT = 0.95 min, [M+H]⁺ = 424, 426, 428, 97% purity.

***tert*-Butyl (1-(4-((2,4-dichlorobenzyl)amino)pyrimidin-2-yl)piperidin-4-yl)carbamate, hydrochloride salt (261b)**



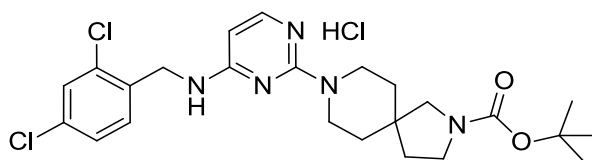
The pyrimidine **261b** was prepared from *tert*-butyl piperidin-4-ylcarbamate (290 mg, 1.46 mmol) and **259** (400 mg, 1.39 mmol) according to the procedure described for the preparation of **261a**. The same purification method afforded the title compound (300 mg, 44%) as a white solid; ¹H NMR (400 MHz, MeOD-*d*₄) δ = 7.60 (d, *J* = 7.0 Hz, 1H), 7.51 (d, *J* = 2.0 Hz, 1H), 7.40 (d, *J* = 8.0 Hz, 1H), 7.33 (dd, *J* = 8.0, 2.0 Hz, 1H), 6.17 (d, *J* = 7.0 Hz, 1H), 4.71 (s, 2H), 4.25 (d, *J* = 13.0 Hz, 2H), 3.74 - 3.58 (m, 1H), 3.28 - 3.16 (m, 2H), 1.96 (dd, *J* = 13.0, 3.0 Hz, 2H), 1.53 - 1.33 (m, 2H); 1.45 (s, 9H); the three exchangeable protons were not observed; LCMS (Method A, UV, ES) RT = 0.98 min, [M+H]⁺ = 452, 454, 546, 100% purity.

***tert*-Butyl 9-(4-((2,4-dichlorobenzyl)amino)pyrimidin-2-yl)-3,9-diazaspiro[5.5]undecane -3-carboxylate, hydrochloride salt (261c)**

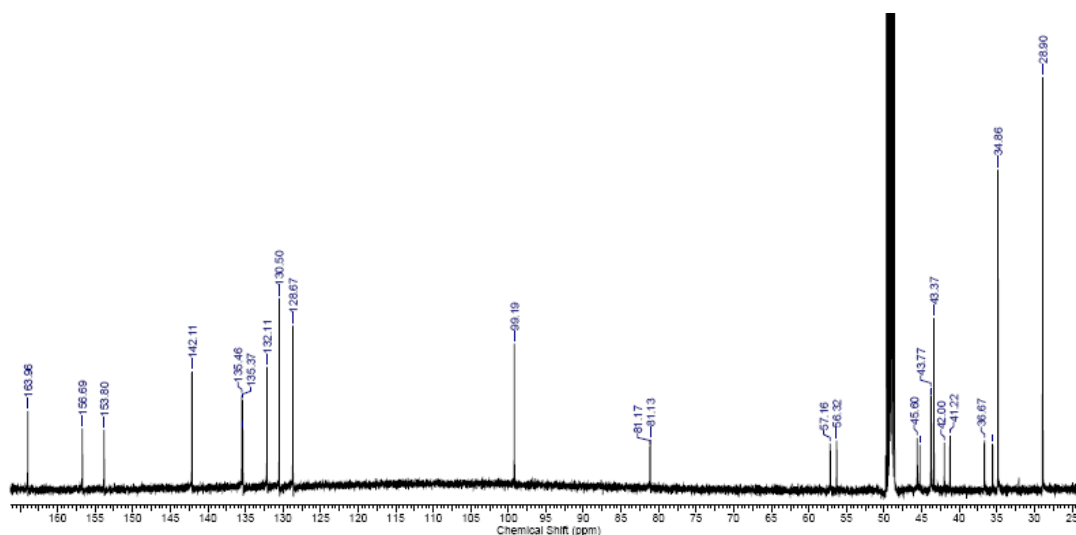


The spiro-pyrimidine **261c** was prepared from *tert*-butyl 3,9-diazaspiro[5.5]undecane-3-carboxylate (350 mg, 1.39 mmol) and **259** (400 mg, 1.39 mmol) according to the procedure described for the preparation of **261a**. The same purification method afforded the title compound (410 mg, 55%) as a white solid; ^1H NMR (400 MHz, MeOD- d_4) δ = 7.60 (d, J = 7.0 Hz, 1H), 7.51 (d, J = 2.0 Hz, 1H), 7.39 (d, J = 8.0 Hz, 1H), 7.33 (dd, J = 8.0, 2.0 Hz, 1H), 6.18 (d, J = 7.0 Hz, 1H), 4.72 (s, 2H), 3.70 (br. s, 4H), 3.43 (br. s, 4H), 1.63 - 1.56 (m, 4H), 1.55 - 1.49 (m, 4H), 1.46 (s, 9H); the two exchangeable protons were not observed; LCMS (Method A, UV, ES) RT = 1.10 min, $[\text{M}+\text{H}]^+$ = 506, 508, 510, 99% purity.

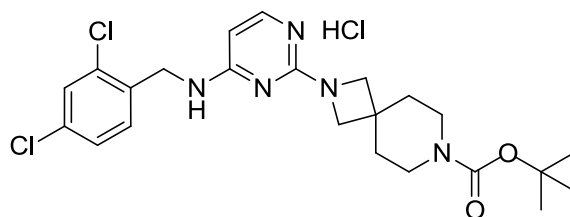
***tert*-Butyl 8-((2,4-dichlorobenzyl)amino)pyrimidin-2-yl)-2,8-diazaspiro[4.5]decane-2-carboxylate, hydrochloride salt (261d)**



The spiro-pyrimidine **261d** was prepared from *tert*-butyl 2,8-diazaspiro[4.5]decane-2-carboxylate (1.67 g, 6.93 mmol) and **259** (2.00 g, 6.93 mmol) according to the procedure described for the preparation of **261a**. The same purification method afforded the title compound (3.3 g, 90%) as a white solid; ^1H NMR (400 MHz, MeOD- d_4) δ = 7.61 (d, J = 7.0 Hz, 1H), 7.51 (d, J = 2.0 Hz, 1H), 7.41 (d, J = 8.0 Hz, 1H), 7.33 (dd, J = 8.0, 2.0 Hz, 1H), 6.20 (d, J = 7.0 Hz, 1H), 4.72 (s, 2H), 3.87 - 3.61 (m, 4H), 3.47 - 3.37 (m, 2H), 3.24 (s, 2H), 1.85 (t, J = 7.0 Hz, 2H), 1.66 - 1.58 (m, 4H), 1.47 (s, 9H); the two exchangeable protons were not observed; ^{13}C NMR (126 MHz, MeOD- d_4) δ = 164.0, 156.7, 153.8, 142.1, 135.5, 135.4, 135.3, 132.1, 130.5, 128.7, 99.2, 81.2, 81.1, 57.2, 56.3, 45.6, 45.3, 43.8, 43.7, 43.4, 42.0, 41.2, 36.7, 35.6, 34.9, 28.9 (the additional peaks were observed due to rotamers); IR ν_{max} (neat) 3230, 2922, 2962, 1687, 1655, 1619, 1581, 1406 cm^{-1} ; HRMS (ESI) m/z calculated for $\text{C}_{24}\text{H}_{32}\text{Cl}_2\text{N}_5\text{O}_2$ = 492.1928. Found = 492.1918, $[\text{M}+\text{H}]^+$; LCMS (Method A, UV, ES) RT = 1.04 min, $[\text{M}+\text{H}]^+$ = 492, 494, 496, 100% purity.

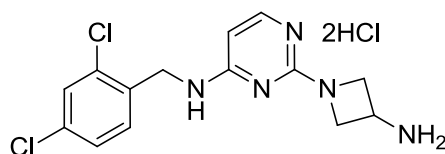


***tert*-Butyl 2-(4-((2,4-dichlorobenzyl)amino)pyrimidin-2-yl)-2,7-diazaspiro[3.5]nonane-7-carboxylate, hydrochloride salt (**261e**)**



The spiro-pyrimidine **261e** was prepared from *tert*-butyl 2,7-diazaspiro[3.5]nonane-7-carboxylate (314 mg, 1.39 mmol) and **259** (400 mg, 1.39 mmol) according to the procedure described for the preparation of **261a**. The same purification method afforded the title compound (330 mg, 46%) as a white solid; ^1H NMR (400 MHz, $\text{MeOD-}d_4$) δ = 7.59 (d, J = 7.0 Hz, 1H), 7.51 (d, J = 2.0 Hz, 1H), 7.43 (d, J = 8.0 Hz, 1H), 7.34 (dd, J = 8.0, 2.0 Hz, 1H), 6.15 (d, J = 7.0 Hz, 1H), 4.70 (s, 2H), 3.94 (s, 4H), 3.47 - 3.35 (m, 4H), 1.85 - 1.74 (m, 4H), 1.46 (s, 9H); the two exchangeable protons were not observed; LCMS (Method A, UV, ES) RT = 1.05 min, $[\text{M}+\text{H}]^+ = 478, 480, 482$, 100% purity.

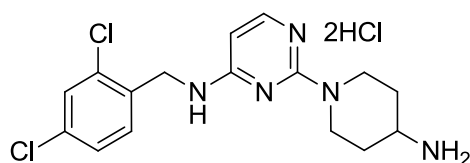
2-(3-Aminoazetidin-1-yl)-*N*-(2,4-dichlorobenzyl)pyrimidin-4-amine, di-hydrochloride salt (262a**)**



A mixture of **261a** (260 mg, 0.625 mmol) and HCl (1.6 mL of a 4 M solution in dioxane, 6.4 mmol) was stirred at ambient temperature for 0.5 h. The reaction mixture was concentrated under reduced pressure and the residue was diluted with DCM (20 mL). The solvent was

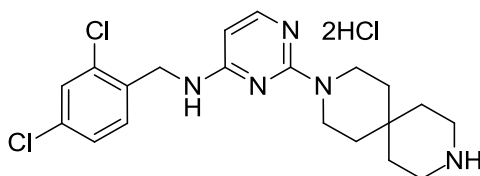
removed under reduced pressure, and dried under high vacuum to afford the title product (240 mg, 97%) as a white solid; $^1\text{H NMR}$ (400 MHz, $\text{MeOD-}d_4$) $\delta = 7.66$ (d, $J = 7.0$ Hz, 1H), 7.51 (d, $J = 2.0$ Hz, 1H), 7.43 (d, $J = 8.0$ Hz, 1H), 7.34 (dd, $J = 8.0, 2.0$ Hz, 1H), 6.25 (d, $J = 7.0$ Hz, 1H), 4.72 (s, 2H), 4.58 (dd, $J = 10.0, 7.0$ Hz, 2H), 4.36 - 4.18 (m, 3H); the five exchangeable protons were not observed; LCMS (Method A, UV, ES) RT = 0.53 min, $[\text{M}+\text{H}]^+ = 324, 326, 328$, 100% purity.

2-(4-Aminopiperidin-1-yl)-N-(2,4-dichlorobenzyl)pyrimidin-4-amine, di-hydrochloride salt (262b)



The pyrimidine **262b** was prepared from **261b** (280 mg, 0.625 mmol) and HCl (1.6 mL of a 4 M solution in dioxane, 6.4 mmol) according to the procedure described for the preparation of **262a**. The title compound was obtained as a white solid (260 mg, 98%); $^1\text{H NMR}$ (400 MHz, $\text{MeOD-}d_4$) $\delta = 7.65$ (d, $J = 7.0$ Hz, 1H), 7.52 (d, $J = 2.0$ Hz, 1H), 7.42 (d, $J = 8.0$ Hz, 1H), 7.34 (dd, $J = 8.0, 2.0$ Hz, 1H), 6.24 (d, $J = 7.0$ Hz, 1H), 4.74 (s, 2H), 4.48 (d, $J = 13.0$ Hz, 2H), 3.79 - 3.71 (m, 1H), 3.69 - 3.63 (m, 2H), 3.62 - 3.55 (m, 1H), 3.55 - 3.42 (m, 1H), 3.25 - 3.13 (m, 2H); the five exchangeable protons were not observed; LCMS (Method A, UV, ES) RT = 0.56 min, $[\text{M}+\text{H}]^+ = 352, 354, 356$, 100% purity.

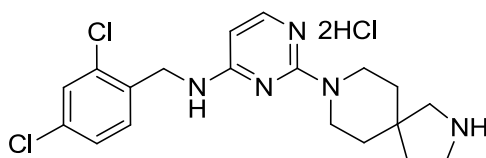
N-(2,4-Dichlorobenzyl)-2-(3,9-diazaspiro[5.5]undecan-3-yl)pyrimidin-4-amine, di-hydrochloride salt (262c)



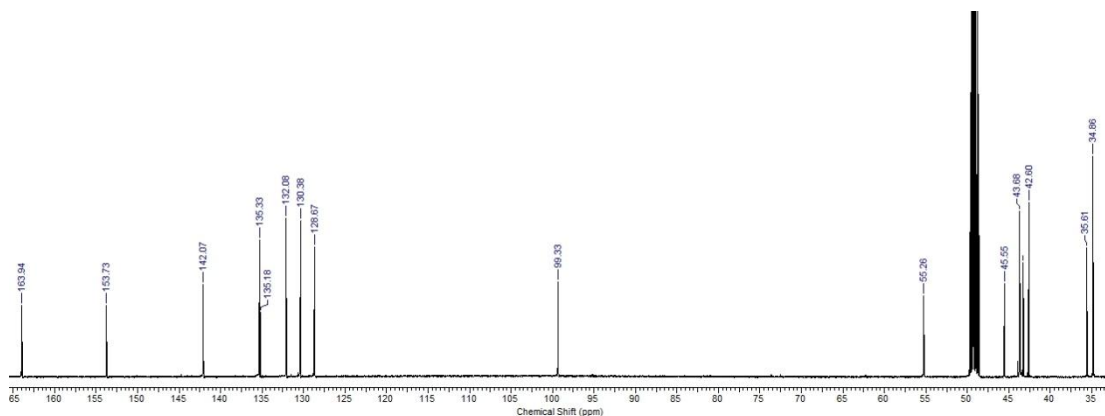
The spiro-pyrimidine **262c** was prepared from **261c** (316 mg, 0.625 mmol) and HCl (1.6 mL of a 4 M solution in dioxane, 6.4 mmol) according to the procedure described for the preparation of **262a**. The title compound was obtained as a white solid (295 mg, 99%); $^1\text{H NMR}$ (400 MHz, $\text{MeOD-}d_4$) $\delta = 7.62$ (d, $J = 7.0$ Hz, 1H), 7.51 (d, $J = 2.0$ Hz, 1H), 7.40 (d, $J = 8.0$ Hz, 1H), 7.34 (dd, $J = 8.0, 2.0$ Hz, 1H), 6.20 (d, $J = 7.0$ Hz, 1H), 4.72 (s, 2H), 3.79 - 3.70 (m, 4H), 3.25 - 3.18 (m, 4H), 1.84 - 1.75 (m, 4H), 1.70 - 1.60 (m, 4H); the four

exchangeable protons were not observed; LCMS (Method A, UV, ES) RT = 0.62 min, $[M+H]^+ = 406, 408, 410$, 99% purity.

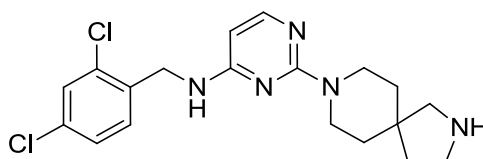
***N*-(2,4-Dichlorobenzyl)-2-(2,8-diazaspiro[4.5]decan-8-yl)pyrimidin-4-amine, dihydrochloride salt (262d)**



The spiro-pyrimidine **262d** was prepared from **261d** (455 mg, 0.860 mmol) and HCl (3.0 mL of a 4 M solution in dioxane, 12.0 mmol) according to the procedure described for the preparation of **262a**. The title compound was obtained as a white solid (400 mg, 99%); ^1H NMR (400 MHz, MeOD- d_4) $\delta = 7.67$ (d, $J = 7.0$ Hz, 1H), 7.50 (d, $J = 2.0$ Hz, 1H), 7.44 (d, $J = 8.0$ Hz, 1H), 7.35 (dd, $J = 8.0, 2.0$ Hz, 1H), 6.28 (d, $J = 7.0$ Hz, 1H), 4.74 (s, 2H), 3.92 - 3.81 (m, 2H), 3.80 - 3.71 (m, 2H), 3.47 (t, $J = 7.5$ Hz, 2H), 3.24 (s, 2H), 2.06 (t, $J = 7.5$ Hz, 2H), 1.86 - 1.66 (m, 4H); the four exchangeable protons were not observed; ^{13}C NMR (126 MHz, MeOD- d_4) $\delta = 164.0, 153.7, 142.1, 135.3, 135.2, 132.1, 130.4, 128.7, 99.3, 55.3, 45.6, 43.7, 43.3, 42.6, 35.6, 34.9$; IR ν_{max} (neat) 3431, 3355, 2869, 2827, 1650, 1617, 1574, 1467, 1410 cm^{-1} ; HRMS (ESI) m/z calculated for $\text{C}_{19}\text{H}_{24}\text{Cl}_2\text{N}_5 = 392.1403$. Found = 392.1408, $[M+H]^+$; LCMS (Method A, UV, ES) RT = 0.56 min, $[M+H]^+ = 392, 394, 396$, 100% purity.



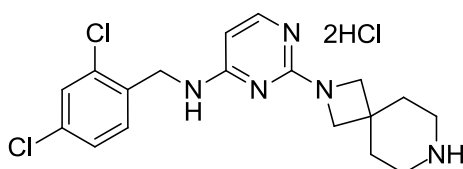
***N*-(2,4-Dichlorobenzyl)-2-(2,8-diazaspiro[4.5]decan-8-yl)pyrimidin-4-amine (262d)**



A mixture of HCl (10 mL of a 4 M solution in dioxane, 40 mmol) and **261d** (0.69 g, 1.4

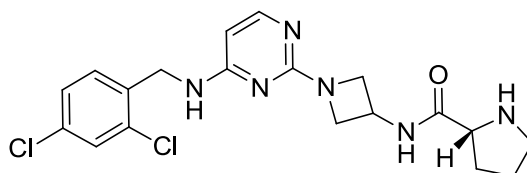
mmol) was stirred at ambient temperature for 1.5 h. The reaction mixture was concentrated under reduced pressure, and the residue was then dissolved in methanol (2 mL) and passed through an aminopropyl cartridge (40 g). The cartridge was washed with more methanol, and the filtrate was concentrated to afford the title product (0.55 g, 99%) as the free base; ^1H NMR (400 MHz, MeOD- d_4) δ = 7.71 (d, J = 6.0 Hz, 1H), 7.44 (d, J = 2.0 Hz, 1H), 7.33 (d, J = 8.0 Hz, 1H), 7.26 (dd, J = 8.0, 2.0 Hz, 1H), 5.87 (d, J = 6.0 Hz, 1H), 4.59 (s, 2H), 3.78 - 3.65 (m, 2H), 3.64 - 3.54 (m, 2H), 3.35 (s, 2H), 3.19 (t, J = 7.5 Hz, 2H), 2.93 (s, 2H), 1.82 (t, J = 7.5 Hz, 2H), 1.49 (t, J = 5.5 Hz, 4H); the two exchangeable protons were not observed; HRMS (ESI) m/z calculated for $\text{C}_{19}\text{H}_{24}\text{Cl}_2\text{N}_5$ = 392.1403. Found = 392.1408, $[\text{M}+\text{H}]^+$; LCMS (Method A, UV, ES) RT = 0.55 min, $[\text{M}+\text{H}]^+$ = 392, 394, 396, 95% purity.

***N*-(2,4-Dichlorobenzyl)-2-(2,7-diazaspiro[3.5]nonan-2-yl)pyrimidin-4-amine, di-hydrochloride salt (262e)**



The spiro-pyrimidine **262e** was prepared from **261e** (300 mg, 0.625 mmol) and HCl (1.6 mL of a 4 M solution in dioxane, 6.4 mmol) according to the procedure described for the preparation of **262a**. The title compound was obtained as a white solid (280 mg, 99%); ^1H NMR (400 MHz, MeOD- d_4) δ = 7.62 (d, J = 7.0 Hz, 1H), 7.51 (d, J = 2.0 Hz, 1H), 7.44 (d, J = 8.0 Hz, 1H), 7.35 (dd, J = 2.0, 8.0 Hz, 1H), 6.19 (d, J = 7.0 Hz, 1H), 4.72 (s, 2H), 4.04 (s, 4H), 3.26 - 3.18 (m, 4H), 2.17 - 2.03 (m, 4H); the four exchangeable protons were not observed; LCMS (Method A, UV, ES) RT = 0.58 min, $[\text{M}+\text{H}]^+$ = 378, 380, 382, 100% purity.

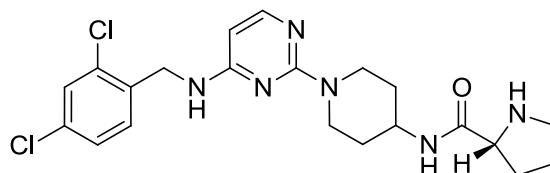
***(R)*-N-(1-(4-((2,4-Dichlorobenzyl)amino)pyrimidin-2-yl)azetididin-3-yl)pyrrolidine-2-carboxamide (255a)**



HATU (58 mg, 0.15 mmol) was added to a mixture of **262a** (47 mg, 0.12 mmol), *(R)*-1-(*tert*-butoxycarbonyl)pyrrolidine-2-carboxylic acid (25 mg, 0.12 mmol) and DIPEA (0.062 mL,

0.35 mmol) in DMF (0.8 mL), and the reaction was stirred at ambient temperature for 1 h. The reaction mixture was subjected directly to purification by MDAP (Method C). The appropriate fractions were combined and the solvent was evaporated under reduced pressure, before being taken up in DCM (0.5 mL). TFA (0.5 mL) was then added, and the mixture was stirred at ambient temperature for 30 min. The excess TFA was evaporated and the residue was then dissolved in methanol (0.5 mL) and passed through an aminopropyl cartridge (0.5 g). The cartridge was washed with additional methanol, and the filtrate was concentrated to afford the title product (42 mg, 85%) as a colourless gum; $[\alpha]_{\text{D}}^{20} = +25$ ($c = 1.00$ in MeOH); ^1H NMR (400 MHz, MeOD- d_4) $\delta = 7.67$ (d, $J = 6.0$ Hz, 1H), 7.42 (d, $J = 2.0$ Hz, 1H), 7.37 (d, $J = 8.0$ Hz, 1H), 7.26 (dd, $J = 8.0, 2.0$ Hz, 1H), 5.89 (d, $J = 6.0$ Hz, 1H), 4.64 - 4.50 (m, 3H), 4.27 (t, $J = 8.0$ Hz, 2H), 3.83 (dd, $J = 9.0, 5.0$ Hz, 2H), 3.60 (dd, $J = 9.0, 5.0$ Hz, 1H), 3.04 - 2.95 (m, 1H), 2.92 - 2.82 (m, 1H), 2.25 - 2.02 (m, 1H), 1.88 - 1.64 (m, 3H); the three exchangeable protons were not observed; ^{13}C NMR (126 MHz, MeOD- d_4) $\delta = 177.2, 164.4, 164.0, 155.1, 137.4, 135.2, 134.4, 131.9, 130.1, 128.2, 97.7, 61.7, 58.1, 48.2, 42.5, 41.3, 32.3, 27.2$; HRMS (ESI) m/z calculated for $\text{C}_{19}\text{H}_{23}\text{Cl}_2\text{N}_6\text{O} = 421.1305$. Found = 421.1298, $[\text{M}+\text{H}]^+$; LCMS (Method A, UV, ES) RT = 0.57 min, $[\text{M}+\text{H}]^+ = 421, 423, 425, 100\%$ purity.

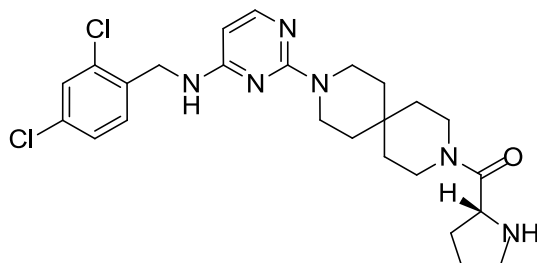
(*R*)-*N*-(1-(4-((2,4-Dichlorobenzyl)amino)pyrimidin-2-yl)piperidin-4-yl)pyrrolidine-2-carboxamide (255b)



The pyrimidine **255b** was prepared from **262b** (50 mg, 0.12 mmol) and (*R*)-1-(tert-butoxycarbonyl)pyrrolidine-2-carboxylic acid (25 mg, 0.12 mmol) according to the procedure described for the preparation of **255a**. The same work up and purification method afforded the title compound (36 mg, 68%) as a colourless gum; $[\alpha]_{\text{D}}^{20} = +25$ ($c = 1.04$ in MeOH); ^1H NMR (400 MHz, MeOD- d_4) $\delta = 7.70$ (d, $J = 6.0$ Hz, 1H), 7.42 (d, $J = 2.0$ Hz, 1H), 7.34 (d, $J = 8.0$ Hz, 1H), 7.25 (dd, $J = 8.0, 2.0$ Hz, 1H), 5.85 (d, $J = 6.0$ Hz, 1H), 4.58 (s, 2H), 4.44 (d, $J = 13.0$ Hz, 2H), 3.93 - 3.77 (m, 1H), 3.56 (dd, $J = 9.0, 6.0$ Hz, 1H), 3.06 - 2.78 (m, 4H), 2.18 - 1.99 (m, 1H), 1.90 - 1.62 (m, 5H), 1.39 - 1.21 (m, 2H); the three exchangeable protons were not observed; ^{13}C NMR (126 MHz, MeOD- d_4) $\delta = 176.4, 164.2, 162.6, 155.7, 137.6, 134.9, 134.2, 131.3, 130.1, 128.3, 96.9, 61.8, 48.4, 48.2, 44.2, 42.6, 32.6, 32.4, 27.2$; HRMS (ESI)

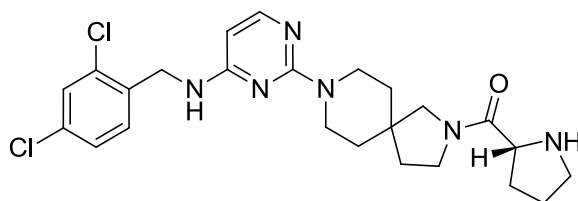
m/z calculated for $C_{21}H_{27}Cl_2N_6O = 449.1618$. Found = 449.1608, $[M+H]^+$; LCMS (Method A, UV, ES) RT = 0.57 min, $[M+H]^+ = 449, 451, 453, 100\%$ purity.

(R)-9-(4-((2,4-Dichlorobenzyl)amino)pyrimidin-2-yl)-3,9-diazaspiro[5.5]undecan-3-yl)(pyrrolidin-2-yl)methanone (255c)



The spiro-pyrimidine **255c** was prepared from **262c** (56 mg, 0.12 mmol) and (*R*)-1-(*tert*-butoxycarbonyl)pyrrolidine-2-carboxylic acid (25 mg, 0.12 mmol) according to the procedure described for the preparation of **255a**. The same work up and purification method afforded the title compound (26 mg, 44%) as a colourless gum; $[\alpha]_D^{20} = +38$ ($c = 0.86$ in MeOH); 1H NMR (400 MHz, MeOD- d_4) $\delta = 7.70$ (d, $J = 6.0$ Hz, 1H), 7.44 (d, $J = 2.0$ Hz, 1H), 7.33 (d, $J = 8.0$ Hz, 1H), 7.26 (dd, $J = 8.0, 2.0$ Hz, 1H), 5.84 (d, $J = 6.0$ Hz, 1H), 4.58 (s, 2H), 3.90 (dd, $J = 9.0, 7.0$ Hz, 1H), 3.69 - 3.61 (m, 4H), 3.59 (dd, $J = 7.0, 5.0$ Hz, 2H), 3.55 - 3.46 (m, 2H), 3.18 - 3.06 (m, 1H), 2.82 - 2.69 (m, 1H), 2.27 - 2.09 (m, 1H), 1.92 - 1.78 (m, 1H), 1.79 - 1.68 (m, 1H), 1.68 - 1.59 (m, 1H), 1.58 - 1.46 (m, 4H), 1.44 (m, 4H); the two exchangeable protons were not observed; ^{13}C NMR (126 MHz, MeOD- d_4) $\delta = 173.6, 164.3$ (weak, correlation observed from HMBC), 162.8, 155.7, 137.7, 134.9, 134.2, 131.2, 130.1, 128.3, 96.6, 59.0, 48.2, 42.2, 40.9, 39.4, 37.2, 36.4, 32.0, 31.9, 27.4; HRMS (ESI) m/z calculated for $C_{25}H_{33}Cl_2N_6O = 503.2087$. Found = 503.2076, $[M+H]^+$; LCMS (Method A, UV, ES) RT = 0.68 min, $[M+H]^+ = 503, 505, 507, 100\%$ purity.

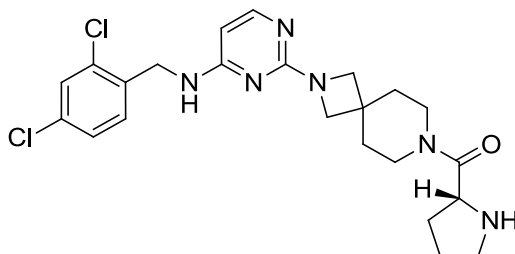
(R)-8-(4-((2,4-Dichlorobenzyl)amino)pyrimidin-2-yl)-2,8-diazaspiro[4.5]decan-2-yl)(pyrrolidin-2-yl)methanone (255d)



The spiro-pyrimidine **255d** was prepared from **262d** (100 mg, 0.22 mmol) and (*R*)-1-(*tert*-butoxycarbonyl)pyrrolidine-2-carboxylic acid (52 mg, 0.24 mmol) according to the procedure

described for the preparation of **255a**. The same work up and purification method afforded the title compound (85 mg, 79%) as a colourless gum; $[\alpha]_{\text{D}}^{20} = +36$ ($c = 0.93$ in MeOH); ^1H NMR (400 MHz, MeOD- d_4) $\delta = 7.70$ (d, $J = 6.0$ Hz, 1H), 7.43 (d, $J = 2.0$ Hz, 1H), 7.33 (d, $J = 8.0$ Hz, 1H), 7.26 (dd, $J = 8.0, 2.0$ Hz, 1H), 5.85 (d, $J = 6.0$ Hz, 1H), 4.58 (s, 2H), 3.85 - 3.41 (m, 9H), 3.20 - 3.05 (m, 1H), 2.85 - 2.69 (m, 1H), 2.28 - 2.04 (m, 1H), 1.90 (t, $J = 7.0$ Hz, 1H), 1.86 - 1.70 (m, 3H), 1.72 - 1.58 (m, 1H), 1.51 - 1.41 (m, 4H); the two exchangeable protons were not observed; ^{13}C NMR (126 MHz, MeOD- d_4) $\delta = 174.4, 174.3, 164.3, 162.7, 155.7, 137.7, 135.0, 134.9, 134.2, 131.2, 130.1, 128.3, 96.8, 60.3, 60.0, 57.2, 56.9, 48.3, 45.9, 45.8, 43.0, 42.8, 42.7, 42.6, 40.8, 37.1, 35.3, 35.2, 35.1, 35.0, 31.4, 31.3, 27.4$ (the additional peaks were observed due to rotamers); ^{13}C NMR (101 MHz, DMSO- d_6 , 393.2 K) $\delta = 171.7, 161.9, 160.8, 154.7, 135.9, 132.5, 131.4, 129.8, 127.8, 126.4, 94.3, 58.4, 54.9, 47.9, 46.4, 43.2$ (2C), 33.3 (2C), 28.9, 25.4; IR ν_{max} (neat) 3302, 2925, 2868, 1634, 1588, 1492, 1450 cm^{-1} ; HRMS (ESI) m/z calculated for $\text{C}_{24}\text{H}_{31}\text{Cl}_2\text{N}_6\text{O} = 489.1931$. Found = 489.1925 $[\text{M}+\text{H}]^+$; LCMS (Method A, UV, ES) RT = 0.67 min, $[\text{M}+\text{H}]^+ = 489, 491, 493$ 100% purity.

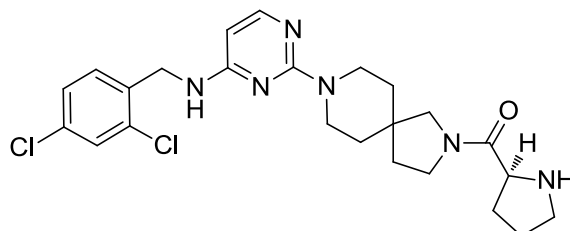
(R)-(2-(4-((2,4-Dichlorobenzyl)amino)pyrimidin-2-yl)-2,7-diazaspiro[3.5]nonan-7-yl)(pyrrolidin-2-yl)methanone (255e)



The spiro-pyrimidine **255e** was prepared from **262e** (53 mg, 0.12 mmol) and (*R*)-1-(*tert*-butoxycarbonyl)pyrrolidine-2-carboxylic acid (25 mg, 0.12 mmol) according to the procedure described for the preparation of **255a**. The same work up and purification method afforded the title compound (28 mg, 50%) as a colourless gum; $[\alpha]_{\text{D}}^{20} = +39$ ($c = 1.02$ in MeOH); ^1H NMR (400 MHz, MeOD- d_4) $\delta = 7.68$ (d, $J = 6.0$ Hz, 1H), 7.44 (d, $J = 2.0$ Hz, 1H), 7.38 (d, $J = 8.0$ Hz, 1H), 7.27 (dd, $J = 8.0, 2.0$ Hz, 1H), 5.88 (d, $J = 6.0$ Hz, 1H), 4.59 (s, 2H), 3.92 (dd, $J = 8.5, 7.0$ Hz, 1H), 3.75 (s, 4H), 3.58 (t, $J = 5.0$ Hz, 2H), 3.51 (t, $J = 5.0$ Hz, 2H), 3.13 (ddd, $J = 11.0, 7.0, 5.0$ Hz, 1H), 2.77 (td, $J = 11.0, 7.0$ Hz, 1H), 2.27 - 2.06 (m, 1H), 1.93 - 1.51 (m, 7H); the two exchangeable protons were not observed; ^{13}C NMR (126 MHz, MeOD- d_4) $\delta = 173.8, 164.2, 162.2, 155.1, 137.4, 135.2, 134.4, 131.8, 130.1, 128.3, 97.4, 60.7, 59.0, 43.6, 40.9, 37.1, 36.3, 35.5, 32.0, 27.4$; HRMS (ESI) m/z calculated for $\text{C}_{23}\text{H}_{29}\text{Cl}_2\text{N}_6\text{O} = 475.1774$.

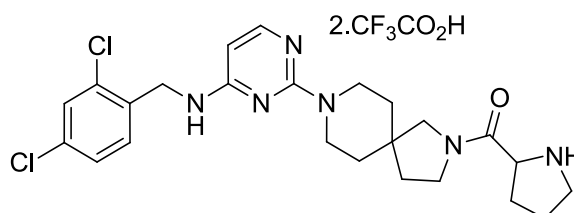
Found = 475.1767, $[M+H]^+$; LCMS (Method A, UV, ES) RT = 0.62 min, $[M+H]^+$ = 475, 477, 479, 100% purity.

(S)-8-(4-((2,4-Dichlorobenzyl)amino)pyrimidin-2-yl)-2,8-diazaspiro[4.5]decan-2-yl)(pyrrolidin-2-yl)methanone (264)



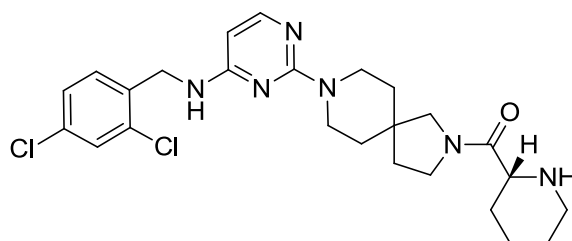
The spiro-pyrimidine **264** was prepared from **262d** (30 mg, 0.076 mmol) and (*S*)-1-(*tert*-butoxycarbonyl)pyrrolidine-2-carboxylic acid (18 mg, 0.084 mmol) according to the procedure described for the preparation of **255a**. The same work up and purification method afforded the title compound (21 mg, 56%) as a colourless gum; $[\alpha]_D^{20} = -37$ ($c = 1.08$ in MeOH); $^1\text{H NMR}$ (400 MHz, MeOD- d_4) $\delta = 7.70$ (d, $J = 6.0$ Hz, 1H), 7.43 (d, $J = 2.0$ Hz, 1H), 7.33 (d, $J = 8.0$ Hz, 1H), 7.26 (dd, $J = 8.0, 2.0$ Hz, 1H), 5.85 (d, $J = 6.0$ Hz, 1H), 4.58 (s, 2H), 3.85 - 3.41 (m, 9H), 3.20 - 3.05 (m, 1H), 2.85 - 2.69 (m, 1H), 2.28 - 2.04 (m, 1H), 1.90 (t, $J = 7.0$ Hz, 1H), 1.86 - 1.70 (m, 3H), 1.72 - 1.58 (m, 1H), 1.51 - 1.41 (m, 4H); the two exchangeable protons were not observed; $^{13}\text{C NMR}$ (126 MHz, MeOD- d_4) $\delta = 174.4, 174.3, 164.3, 162.7, 155.7, 137.7, 135.0, 134.9, 134.2, 131.2, 130.1, 128.3, 96.8, 60.3, 60.0, 57.2, 56.9, 48.3, 45.9, 45.8, 43.0, 42.8, 42.7, 42.6, 40.8, 37.1, 35.3, 35.2, 35.1, 35.0, 31.4, 31.3, 27.4$ (the additional peaks were observed due to rotamers); HRMS (ESI) m/z calculated for $\text{C}_{24}\text{H}_{31}\text{Cl}_2\text{N}_6\text{O} = 489.1931$. Found = 489.1925 $[M+H]^+$; LCMS (Method A, UV, ES) RT = 0.67 min, $[M+H]^+$ = 489, 491, 493, 100% purity.

(±)-8-(4-((2,4-Dichlorobenzyl)amino)pyrimidin-2-yl)-2,8-diazaspiro[4.5]decan-2-yl)(pyrrolidin-2-yl)methanone, di-trifluoroacetic acid salt (265)



HATU (97 mg, 0.26 mmol) was added to a mixture of **262d** (100 mg, 0.255 mmol), (\pm)-1-(*tert*-butoxycarbonyl)pyrrolidine-2-carboxylic acid (55 mg, 0.26 mmol) and DIPEA (0.13 mL, 0.77 mmol) in DMF (3 mL), and the reaction was stirred at ambient temperature for 18 h. Water (20 mL) was added and the product was extracted with EtOAc (2 \times 30 mL). The combined organic extracts were washed with brine (20 mL), filtered through a hydrophobic frit and evaporated under reduced pressure. TFA (1 mL) was then added, and the mixture was stirred at ambient temperature for a further 10 min. The excess TFA was evaporated and the residue was taken up in DMSO (3 mL) and purified by MDAP (Method C). The appropriate fractions were combined and the solvent was evaporated under reduced pressure to afford the title product (125 mg, 95%) as a white solid; $^1\text{H NMR}$ (400 MHz, MeOD- d_4) δ = 7.66 (dd, J = 7.0, 2.0 Hz, 1H), 7.50 (d, J = 2.0 Hz, 1H), 7.43 (d, J = 8.0 Hz, 1H), 7.35 (dd, J = 8.0, 2.0 Hz, 1H), 6.25 (dd, J = 7.0, 2.0 Hz, 1H), 4.75 (s, 2H), 4.64 - 4.53 (m, 1H), 3.90 - 3.37 (m, 10H), 2.63 - 2.53 (m, 1H), 2.19 - 2.08 (m, 2H), 2.07 - 1.89 (m, 3H), 1.80 - 1.57 (m, 4H); the four exchangeable protons were not observed; LCMS (Method A, UV, ES) RT = 0.68 min, $[\text{M}+\text{H}]^+ = 489, 491, 493$, 95% purity.

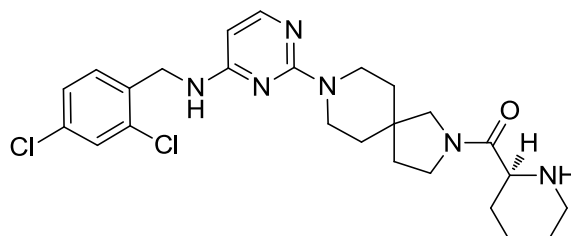
(*R*)-(8-(4-((2,4-Dichlorobenzyl)amino)pyrimidin-2-yl)-2,8-diazaspiro[4.5]decan-2-yl)(piperidin-2-yl)methanone (266)



The spiro-pyrimidine **266** was prepared from **262d** (30 mg, 0.076 mmol) and (*R*)-1-(*tert*-butoxycarbonyl)piperidine-2-carboxylic acid (19 mg, 0.084 mmol) according to the procedure described for the preparation of **255a**. The same work up and purification method afforded the title compound (15 mg, 39%) as a colourless gum; $[\alpha]_{\text{D}}^{20} = +12$ ($c = 1.03$ in MeOH); $^1\text{H NMR}$ (400 MHz, MeOD- d_4) δ = 7.71 (d, $J = 6.0$ Hz, 1H), 7.43 (t, $J = 2.0$ Hz, 1H), 7.34 (d, $J = 8.0$ Hz, 1H), 7.26 (dd, $J = 8.0, 2.0$ Hz, 1H), 5.86 (d, $J = 6.0$ Hz, 1H), 4.58 (s, 2H), 3.87 - 3.62 (m, 4H), 3.61 - 3.42 (m, 4H), 3.29 - 3.19 (m, 1H), 3.14 - 3.02 (m, 1H), 2.72 - 2.55 (m, 1H), 1.89 (t, $J = 7.0$ Hz, 2H), 1.80 (t, $J = 7.0$ Hz, 2H), 1.68 - 1.54 (m, 2H), 1.52 - 1.31 (m, 6H); the two exchangeable protons were not observed; $^{13}\text{C NMR}$ (126 MHz, MeOD- d_4) δ = 174.0, 173.9, 164.2, 162.7, 162.6, 155.7, 137.7, 134.9, 134.8, 134.2, 131.2, 130.1, 128.3, 96.8, 58.9, 58.7, 57.3, 56.5, 46.3, 46.2, 45.9, 45.5, 42.9, 42.8, 42.7, 42.6, 40.8, 37.1,

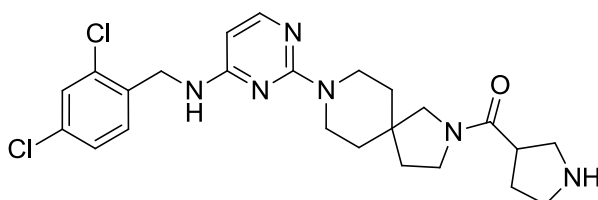
35.3, 35.2, 35.1, 35.0, 30.4, 30.3, 27.2, 25.2, 25.1 (the additional peaks were observed due to rotamers); HRMS (ESI) m/z calculated for $C_{25}H_{33}Cl_2N_6O = 503.2087$. Found = 503.2075 $[M+H]^+$; LCMS (Method A, UV, ES) RT = 0.68 min, $[M+H]^+ = 503, 505, 507, 100\%$ purity.

(S)-(8-(4-((2,4-Dichlorobenzyl)amino)pyrimidin-2-yl)-2,8-diazaspiro[4.5]decan-2-yl)(piperidin-2-yl)methanone (267)



The spiro-pyrimidine **267** was prepared from **262d** (30 mg, 0.076 mmol) and (*S*)-1-(*tert*-butoxycarbonyl)piperidine-2-carboxylic acid (19 mg, 0.084 mmol) according to the procedure described for the preparation of **255a**. The same work up and purification method afforded the title compound (14 mg, 36%) as a colourless gum; $[\alpha]_D^{20} = -11$ ($c = 1.04$ in MeOH); 1H NMR (400 MHz, MeOD- d_4) $\delta = 7.71$ (d, $J = 6.0$ Hz, 1H), 7.43 (t, $J = 2.0$ Hz, 1H), 7.34 (d, $J = 8.0$ Hz, 1H), 7.26 (dd, $J = 8.0, 2.0$ Hz, 1H), 5.86 (d, $J = 6.0$ Hz, 1H), 4.58 (s, 2H), 3.87 - 3.62 (m, 4H), 3.61 - 3.42 (m, 4H), 3.29 - 3.19 (m, 1H), 3.14 - 3.02 (m, 1H), 2.72 - 2.55 (m, 1H), 1.89 (t, $J = 7.0$ Hz, 2H), 1.80 (t, $J = 7.0$ Hz, 2H), 1.68 - 1.54 (m, 2H), 1.52 - 1.31 (m, 6H); the two exchangeable protons were not observed; ^{13}C NMR (126 MHz, MeOD- d_4) $\delta = 174.0, 173.9, 164.2, 162.7, 162.6, 155.7, 137.7, 134.9, 134.8, 134.2, 131.2, 130.1, 128.3, 96.8, 58.9, 58.7, 57.3, 56.5, 46.3, 46.2, 45.9, 45.5, 42.9, 42.8, 42.7, 42.6, 40.8, 37.1, 35.3, 35.2, 35.1, 35.0, 30.4, 30.3, 27.2, 25.2, 25.1$ (the additional peaks were observed due to rotamers); HRMS (ESI) m/z calculated for $C_{25}H_{33}Cl_2N_6O = 503.2087$. Found = 503.2075 $[M+H]^+$; LCMS (Method A, UV, ES) RT = 0.68 min, $[M+H]^+ = 503, 505, 507, 100\%$ purity.

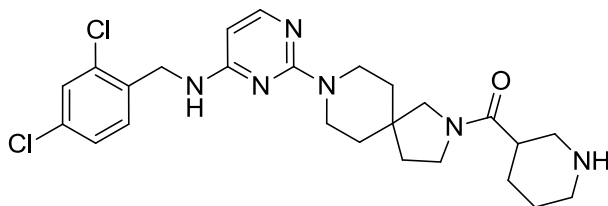
(±)-(8-(4-((2,4-Dichlorobenzyl)amino)pyrimidin-2-yl)-2,8-diazaspiro[4.5]decan-2-yl)(pyrrolidin-3-yl)methanone (268)



The spiro-pyrimidine **268** was prepared from **262d** (30 mg, 0.076 mmol) and (±)-1-(*tert*-butoxycarbonyl)pyrrolidine-3-carboxylic acid (18 mg, 0.084 mmol) according to the same procedure described for the preparation of **255a**. Similar work up and purification method

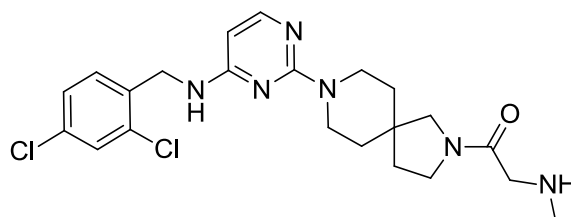
afforded the title compound (12 mg, 32%) as a colourless gum; ^1H NMR (400 MHz, MeOD- d_4) δ = 7.70 (d, J = 6.0 Hz, 1H), 7.43 (br.s, 1H), 7.33 (d, J = 8.0 Hz, 1H), 7.25 (dd, J = 8.0, 2.0 Hz, 1H), 5.85 (d, J = 6.0 Hz, 1H), 4.58 (s, 2H), 3.84 - 3.61 (m, 4H), 3.60 - 3.38 (m, 4H), 3.18 - 3.08 (m, 1H), 3.08 - 2.95 (m, 3H), 2.90 - 2.79 (m, 1H), 2.14 - 2.00 (m, 1H), 1.95 - 1.85 (m, 2H), 1.84 - 1.77 (m, 1H), 1.54 - 1.41 (m, 4H); the two exchangeable protons were not observed; ^{13}C NMR (126 MHz, MeOD- d_4) δ = 176.2, 176.0, 164.3, 162.7, 155.7, 137.7, 134.9, 134.2, 131.2, 130.1, 128.3, 96.8, 57.9, 56.7, 51.5, 51.4, 48.3, 48.2, 46.4, 45.6, 44.1, 43.8, 42.9, 42.8, 42.7, 42.6, 40.9, 37.1, 35.3, 35.3, 35.1, 35.0, 31.6 (the additional peaks were observed due to rotamers); HRMS (ESI) m/z calculated for $\text{C}_{24}\text{H}_{31}\text{Cl}_2\text{N}_6\text{O}$ = 489.1931. Found = 489.1917 $[\text{M}+\text{H}]^+$; LCMS (Method A, UV, ES) RT = 0.67 min, $[\text{M}+\text{H}]^+$ = 489, 491, 493, 100% purity.

(±)-(8-(4-((2,4-Dichlorobenzyl)amino)pyrimidin-2-yl)-2,8-diazaspiro[4.5]decan-2-yl)(piperidin-3-yl)methanone (269)



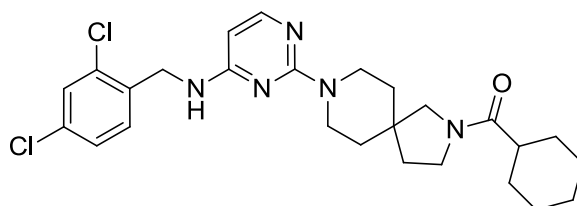
The spiro-pyrimidine **269** was prepared from **262d** (30 mg, 0.076 mmol) and (±)-1-(*tert*-butoxycarbonyl)piperidine-3-carboxylic acid (19 mg, 0.084 mmol) according to the procedure described for the preparation of **255a**. The same work up and purification method afforded the title compound (23 mg, 60%) as a colourless gum; ^1H NMR (500 MHz, MeOD- d_4) δ = 7.70 (dd, J = 6.0, 2.5 Hz, 1H), 7.43 (s, 1H), 7.37 - 7.31 (m, 1H), 7.26 (d, J = 8.0 Hz, 1H), 5.85 (br. s, 1H), 4.58 (s, 2H), 3.82 - 3.61 (m, 4H), 3.59 - 3.50 (m, 1H), 3.50 - 3.38 (m, 2H), 3.06 - 2.87 (m, 2H), 2.80 - 2.50 (m, 3H), 1.94 - 1.84 (m, 2H), 1.80 (t, J = 7.0 Hz, 1H), 1.75 - 1.59 (m, 2H), 1.58 - 1.24 (m, 5H), 1.01 - 0.81 (m, 1H); the two exchangeable protons were not observed; ^{13}C NMR (126 MHz, MeOD- d_4) δ = 175.5, 175.4, 162.7, 134.9, 134.8, 134.2, 132.6, 131.2, 130.1, 130.0, 128.3, 69.3, 57.7, 56.6, 46.9, 46.1, 45.4, 42.9, 42.8, 42.7, 42.6, 40.9, 40.3, 37.1, 35.3, 35.2, 35.1, 31.8, 30.3, 28.3, 26.2, 25.1, 24.2, 14.6, 11.6 (the additional peaks were observed due to rotamers); HRMS (ESI) m/z calculated for $\text{C}_{25}\text{H}_{33}\text{Cl}_2\text{N}_6\text{O}$ = 503.2087. Found = 503.2078 $[\text{M}+\text{H}]^+$; LCMS (Method A, UV, ES) RT = 0.65 min, $[\text{M}+\text{H}]^+$ = 503, 505, 507, 98% purity.

1-(8-(4-((2,4-Dichlorobenzyl)amino)pyrimidin-2-yl)-2,8-diazaspiro[4.5]decan-2-yl)-2-(methylamino)ethanone (270)



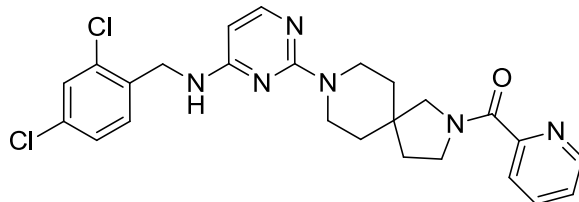
The spiro-pyrimidine **270** was prepared from **262d** (30 mg, 0.076 mmol) and 2-((*tert*-butoxycarbonyl)(methyl)amino)acetic acid (15 mg, 0.084 mmol) according to the procedure described for the preparation of **265**. Purification by MDAP (Method C, TFA modifier) afforded the title compound (23 mg, 44%) as the bis-TFA salt; $^1\text{H NMR}$ (400 MHz, $\text{MeOD-}d_4$) δ = 7.62 (dd, J = 7.0, 2.0 Hz, 1H), 7.50 (d, J = 2.0 Hz, 1H), 7.41 - 7.36 (m, 1H), 7.35 - 7.29 (m, 1H), 6.20 (dd, J = 7.0, 2.0 Hz, 1H), 4.72 (s, 2H), 3.98 (s, 2H), 3.87 - 3.63 (m, 5H), 3.63 - 3.50 (m, 2H), 3.46 - 3.35 (m, 1H), 2.75 (s, 3H), 1.99 (t, J = 7.0 Hz, 1H), 1.90 (t, J = 7.0 Hz, 1H), 1.66 (br. s, 4H); the four exchangeable protons were not observed; HRMS (ESI) m/z calculated for $\text{C}_{22}\text{H}_{29}\text{Cl}_2\text{N}_6\text{O}$ = 463.1774. Found = 463.1776 $[\text{M}+\text{H}]^+$; LCMS (Method A, UV, ES) RT = 0.60 min, $[\text{M}+\text{H}]^+$ = 463, 465, 99% purity. The free base was formed by dissolving the salt in methanol (0.5 mL) and by passing through an aminopropyl cartridge (0.5 g). The cartridge was washed with additional methanol, and the filtrate was concentrated to afford the title product, (15 mg, 42% yield) as a white solid. $^1\text{H NMR}$ (400 MHz, $\text{DMSO-}d_6$) δ = 7.74 (d, J = 4.5 Hz, 1H), 7.59 (d, J = 2.0 Hz, 2H), 7.40 (dd, J = 8.0, 2.0 Hz, 1H), 7.35 (d, J = 8.0 Hz, 1H), 5.82 (br. s, 1H), 4.50 (d, J = 5.0 Hz, 2H), 3.78 - 3.63 (m, 2H), 3.59 - 3.47 (m, 4H), 3.45 (t, J = 7.5 Hz, 2H), 3.20 (br. s, 2H), 2.27 (d, J = 2.5 Hz, 3H), 1.77 (t, J = 7.0 Hz, 1H), 1.67 (t, J = 7.0 Hz, 1H), 1.44 - 1.23 (m, 4H); HRMS (ESI) m/z calculated for $\text{C}_{22}\text{H}_{29}\text{Cl}_2\text{N}_6\text{O}$ = 463.1774. Found = 463.1776 $[\text{M}+\text{H}]^+$; LCMS (Method A, UV, ES) RT = 0.61 min, $[\text{M}+\text{H}]^+$ = 463, 465, 467, 100% purity.

Cyclohexyl(8-(4-((2,4-dichlorobenzyl)amino)pyrimidin-2-yl)-2,8-diazaspiro[4.5]decan-2-yl)methanone (271)



The spiro-pyrimidine **271** was prepared from **262d** (30 mg, 0.076 mmol) and cyclohexanecarboxylic acid (12 mg, 0.084 mmol) according to the procedure described for the preparation of **255a**. The same work up and purification method afforded the title compound (20 mg, 52%) as a colourless gum; ^1H NMR (400 MHz, MeOD- d_4) δ = 7.73 (dd, J = 6.0, 2.0 Hz, 1H), 7.46 (t, J = 2.0 Hz, 1H), 7.37 (d, J = 8.0 Hz, 1H), 7.29 (dd, J = 8.0, 2.0 Hz, 1H), 5.88 (d, J = 6.0 Hz, 1H), 4.61 (s, 2H), 3.84 - 3.63 (m, 4H), 3.62 - 3.53 (m, 1H), 3.50 (t, J = 7.0 Hz, 1H), 3.42 (s, 1H), 2.62 - 2.43 (m, 1H), 1.91 (t, J = 7.0 Hz, 1H), 1.87 - 1.67 (m, 6H), 1.59 - 1.12 (m, 10H); the exchangeable proton was not observed; ^{13}C NMR (126 MHz, MeOD- d_4) δ = 177.6, 177.5, 164.2, 162.5, 162.48 155.5, 137.6, 134.8, 134.78, 134.1, 131.1, 130.0, 128.2, 96.8, 57.7, 56.5, 45.9, 45.3, 43.8, 43.7, 42.7, 42.7, 42.6, 42.5, 40.7, 37.0, 35.2, 35.0, 34.9, 30.1, 30.0, 27.0, 26.8, 26.7 (the additional peaks were observed due to rotamers); HRMS (ESI) m/z calculated for $\text{C}_{26}\text{H}_{34}\text{Cl}_2\text{N}_5\text{O}$ = 502.2135. Found = 502.2118 $[\text{M}+\text{H}]^+$; LCMS (Method A, UV, ES) RT = 1.01 min, $[\text{M}+\text{H}]^+$ = 502, 504, 506, 100% purity.

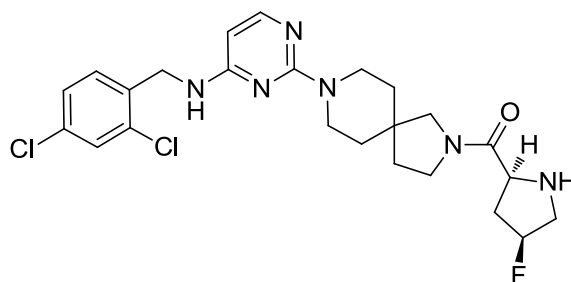
(8-(4-((2,4-Dichlorobenzyl)amino)pyrimidin-2-yl)-2,8-diazaspiro[4.5]decan-2-yl)(pyridin-2-yl)methanone (272)



The spiro-pyrimidine **272** was prepared from **262d** (30 mg, 0.076 mmol) and picolinic acid (10 mg, 0.084 mmol) according to the procedure described for the preparation of **255a**. Purification by MDAP (Method B) afforded the title compound (18 mg, 47%) as a colourless gum; ^1H NMR (500 MHz, MeOD- d_4) δ = 8.62 (d, J = 4.5 Hz, 1H), 8.04 - 7.92 (m, 1H), 7.81 - 7.65 (m, 2H), 7.55 - 7.49 (m, 1H), 7.46 (dd, J = 8.5, 2.0 Hz, 1H), 7.39 - 7.32 (m, 1H), 7.31 - 7.23 (m, 1H), 5.91 - 5.80 (m, 1H), 4.60 (d, J = 15.0 Hz, 2H), 3.84 - 3.77 (m, 1H), 3.74 (t, J = 7.0 Hz, 2H), 3.70 - 3.50 (m, 5H), 1.95 - 1.83 (m, 2H), 1.64 - 1.39 (m, 4H), the exchangeable NH proton was not observed; ^1H NMR (400 MHz, DMSO- d_6 , 393 K) δ = 8.59 (d, J = 5.0 Hz, 1H), 7.89 (dt, J = 8.0, 1.5 Hz, 1H), 7.77 (d, J = 6.0 Hz, 1H), 7.70 (d, J = 8.0 Hz, 1H), 7.48 (d, J = 2.0 Hz, 1H), 7.46 - 7.39 (m, 2H), 7.37 - 7.28 (m, 1H), 7.01 (br. s, 1H), 5.84 (d, J = 6.0 Hz, 1H), 4.55 (br. s, 2H), 3.75 - 3.57 (m, 6H), 3.50 (s, 2H), 1.82 (t, J = 7.0 Hz, 2H), 1.49 (br. s, 4H); ^{13}C NMR (126 MHz, MeOD- d_4) δ = 169.0, 168.9, 162.7, 162.6, 155.3, 149.7, 149.6,

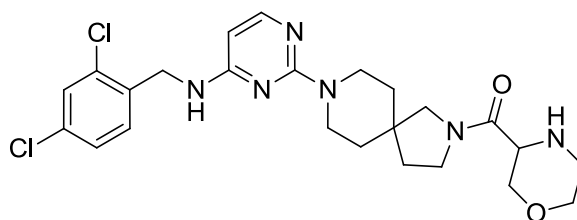
139.0, 139.0, 134.9, 134.2, 131.2, 130.1, 130.1, 128.3, 128.3, 126.7, 126.6, 124.7, 124.7, 60.0, 57.5, 46.3, 43.2, 42.8, 42.6, 40.9, 37.6, 35.4, 34.9 (the additional peaks were observed due to rotamers); HRMS (ESI) m/z calculated for $C_{25}H_{27}Cl_2N_6O = 497.1618$. Found = 497.1610 $[M+H]^+$; LCMS (Method A, UV, ES) RT = 0.86 min, $[M+H]^+ = 497, 499, 501$, 98% purity.

(8-(4-((2,4-Dichlorobenzyl)amino)pyrimidin-2-yl)-2,8-diazaspiro[4.5]decan-2-yl)((2S,4S)-4-fluoropyrrolidin-2-yl)methanone (273)



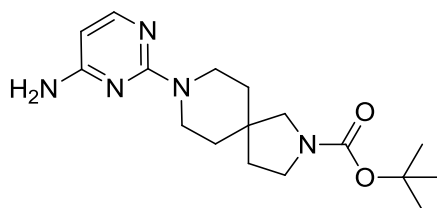
The spiro-pyrimidine **273** was prepared from **262d** (30 mg, 0.076 mmol) and (2S,4S)-1-(*tert*-butoxycarbonyl)-4-fluoropyrrolidine-2-carboxylic acid (20 mg, 0.084 mmol) according to the procedure described for the preparation of **255a**. The same work up and purification method afforded the title compound (21 mg, 54%) as a colourless oil; $[\alpha]_D^{20} = -36$ ($c = 0.75$ in MeOH); 1H NMR (400MHz, MeOD- d_4) $\delta = 7.70$ (d, $J = 5.5$ Hz, 1H), 7.43 (t, $J = 2.0$ Hz, 1H), 7.33 (d, $J = 8.0$ Hz, 1H), 7.25 (dd, $J = 8.0, 2.0$ Hz, 1H), 5.85 (d, $J = 5.5$ Hz, 1H), 5.30 - 5.03 (m, 1H), 4.58 (s, 2H), 3.88 - 3.81 (m, 1H), 3.80 - 3.61 (m, 4H), 3.60 - 3.47 (m, 2H), 3.46 - 3.24 (m, 3H), 2.87 - 2.66 (m, 1H), 2.62 - 2.39 (m, 1H), 2.04 - 1.74 (m, 3H), 1.58 - 1.39 (m, 4H); the two exchangeable protons were not observed; ^{19}F NMR (376 MHz, MeOD- d_4) $\delta = (-174.3) - (-173.6)$ (m); HRMS (ESI) m/z calculated for $C_{24}H_{30}Cl_2FN_6O = 507.1837$. Found = 507.1844 $[M+H]^+$; LCMS (Method A, UV, ES) RT = 0.62 min, $[M+H]^+ = 507, 509, 511$, 100% purity.

(±)-(8-(4-((2,4-dichlorobenzyl)amino)pyrimidin-2-yl)-2,8-diazaspiro[4.5]decan-2-yl)(morpholin-3-yl)methanone (274)



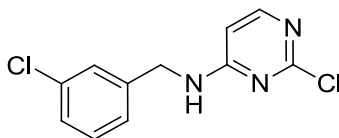
The spiro-pyrimidine **274** was prepared from **262d** (30 mg, 0.076 mmol) and (\pm)-4-(*tert*-butoxycarbonyl)morpholine-3-carboxylic acid (19 mg, 0.084 mmol) according to the procedure described for the preparation of **255a**. The same work up and purification method afforded the title compound (20 mg, 52%) as a colourless oil; ^1H NMR (400 MHz, MeOD- d_4) δ = 7.70 (d, J = 6.0 Hz, 1H), 7.44 (br. s, 1H), 7.33 (d, J = 8.0 Hz, 1H), 7.26 (dd, J = 8.0, 1.5 Hz, 1H), 5.86 (d, J = 6.0 Hz, 1H), 4.58 (br. s, 2H), 4.02 - 3.88 (m, 1H), 3.84 - 3.42 (m, 9H), 3.40 - 3.24 (m, 3H, (obscured by HOD)), 2.96 - 2.88 (m, 2H), 1.89 (t, J = 7.0 Hz, 1H), 1.80 (t, J = 7.0 Hz, 1H), 1.56 - 1.29 (m, 4H); the two exchangeable protons were not observed; ^{13}C NMR (126 MHz, MeOD- d_4) δ = 170.8, 170.7, 164.2, 162.7, 155.7, 137.7, 134.9, 134.9, 134.2, 131.2, 130.1, 128.3, 96.8, 69.8, 68.5, 57.9, 57.8, 57.4, 56.6, 46.0, 45.6, 45.4, 45.3, 43.0, 42.8, 42.7, 42.6, 40.8, 37.1, 35.3, 35.2, 35.1, 34.9 (the additional peaks were observed due to rotamers); HRMS (ESI) m/z calculated for $\text{C}_{24}\text{H}_{31}\text{Cl}_2\text{N}_6\text{O}_2$ = 505.1880. Found = 505.1878 $[\text{M}+\text{H}]^+$; LCMS (Method A, UV, ES) RT = 0.62 min, $[\text{M}+\text{H}]^+$ = 505, 507, 509, 100% purity.

***tert*-Butyl 8-(4-aminopyrimidin-2-yl)-2,8-diazaspiro[4.5]decane-2-carboxylate (276)**



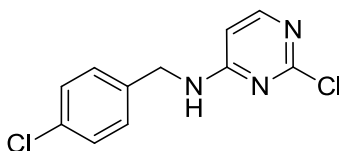
A mixture of 2-chloropyrimidin-4-amine (100 mg, 0.772 mmol), *tert*-butyl 2,8-diazaspiro[4.5]decane-2-carboxylate (220 mg, 0.926 mmol) and DIPEA (0.20 mL, 1.2 mmol) in 1,4-dioxane (0.4 mL) were heated in the microwave at 140 °C for 1 h. The reaction mixture was taken up in DMSO (1 mL) and directly purified on the MDAP (Method B). The appropriate fractions were combined and evaporated under reduced pressure to afford the title compound (180 mg, 70%) as a white solid; ^1H NMR (400 MHz, DMSO- d_6) δ = 7.72 (d, J = 5.5 Hz, 1H), 6.32 (br. s, 2H), 5.68 (d, J = 5.5 Hz, 1H), 3.76 - 3.64 (m, 2H), 3.64 - 3.51 (m, 2H), 3.36 - 3.23 (m, 2H (obscured by H_2O)), 3.11 (s, 2H), 1.72 (t, J = 6.0 Hz, 2H), 1.50 - 1.31, (m, 4H), 1.39 (s, 9H); LCMS (Method A, UV, ES) RT = 0.67 min, $[\text{M}+\text{H}]^+$ = 334, 100% purity.

2-Chloro-*N*-(3-chlorobenzyl)pyrimidin-4-amine (278b)



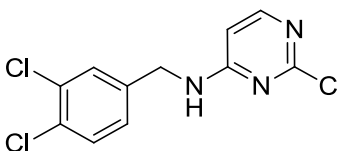
The pyrimidine **278b** was prepared from 2,4-dichloropyrimidine (1.0 g, 6.7 mmol), 3-chlorobenzylamine (0.95 g, 6.7 mmol) and DIPEA (1.8 mL, 10 mmol) according to the procedure described for the preparation of **259**. The same work up and purification method afforded the title compound (1.12 g, 66%) as a white solid; $^1\text{H NMR}$ (400 MHz, MeOD- d_4) δ = 7.88 (br. s, 1H), 7.43 - 7.13 (m, 4H), 6.46 (d, J = 5.0 Hz, 1H), 4.57 (br. s, 2H); the exchangeable NH proton was not observed; LCMS (Method A, UV, ES) RT = 0.98 min, $[\text{M}+\text{H}]^+$ = 254, 256, 258, 100% purity.

2-Chloro-*N*-(4-chlorobenzyl)pyrimidin-4-amine (278c)



The pyrimidine **278c** was prepared from 2,4-dichloropyrimidine (1.0 g, 6.7 mmol), 4-chlorobenzylamine (0.82 mL, 6.7 mmol) and DIPEA (1.8 mL, 10 mmol) according to the procedure described for the preparation of **259**. The same work up and purification method afforded the title compound (1.09 g, 64%) as a white solid; $^1\text{H NMR}$ (400 MHz, MeOD- d_4) δ = 7.87 (br. s, 1H), 7.33 (s, 4H), 6.44 (d, J = 5.0 Hz, 1H), 4.56 (br. s, 2H); the exchangeable NH proton was not observed; LCMS (Method A, UV, ES) RT = 0.98 min, $[\text{M}+\text{H}]^+$ = 254, 256, 258, 100% purity.

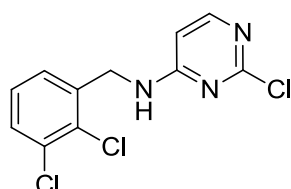
2-Chloro-*N*-(3,4-dichlorobenzyl)pyrimidin-4-amine (278e)



The pyrimidine **278e** was prepared from 2,4-dichloropyrimidine (1.0 g, 6.7 mmol) 3,4-dichlorobenzylamine (1.2 g, 6.7 mmol) and DIPEA (1.8 mL, 10 mmol) according to the procedure described for the preparation of **259**. The same work up and purification method

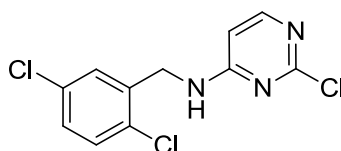
afforded the title compound (1.13 g, 58%) as a white solid; $^1\text{H NMR}$ (400 MHz, $\text{MeOD-}d_4$) δ = 7.88 (d, J = 5.0 Hz, 1H), 7.53 - 7.40 (m, 2H), 7.25 (dd, J = 8.0, 2.0 Hz, 1H), 6.45 (d, J = 5.0 Hz, 1H), 4.54 (br. s, 2H); the exchangeable NH proton was not observed; LCMS (Method A, UV, ES) RT = 1.11 min, $[\text{M}+\text{H}]^+$ = 288, 290, 292, 99% purity.

2-Chloro-*N*-(2,3-dichlorobenzyl)pyrimidin-4-amine (278f)



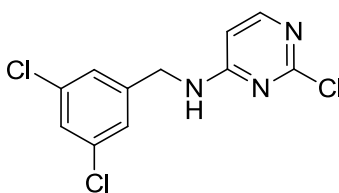
The pyrimidine **278f** was prepared from 2,4-dichloropyrimidine (1.0 g, 6.7 mmol), 2,3-dichlorobenzylamine (1.2 g, 6.7 mmol) and DIPEA (1.8 mL, 10 mmol) according to the procedure described for the preparation of **259**. The same work up and purification method afforded the title compound (0.84 g, 43%) as a pale yellow solid; $^1\text{H NMR}$ (400 MHz, $\text{MeOD-}d_4$) δ = 7.89 (d, J = 5.0 Hz, 1H), 7.50 - 7.43 (m, 1H), 7.36 (d, J = 8.0 Hz, 1H), 7.26 (t, J = 8.0 Hz, 1H), 6.50 (d, J = 5.0 Hz, 1H), 4.69 (br. s, 2H); the exchangeable NH proton was not observed; LCMS (Method A, UV, ES) RT = 1.11 min, $[\text{M}+\text{H}]^+$ = 288, 290, 292, 98% purity.

2-Chloro-*N*-(2,5-dichlorobenzyl)pyrimidin-4-amine (278g)



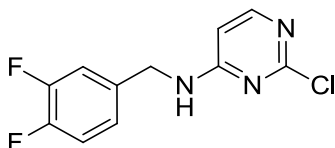
The pyrimidine **278g** was prepared from 2,4-dichloropyrimidine (200 mg, 1.34 mmol), 2,5-dichlorobenzylamine (0.22 mL, 1.3 mmol) and DIPEA (0.35 mL, 2.0 mmol) according to the procedure described for the preparation of **259**. The same work up and purification method afforded the title compound (250 mg, 65%) as a white solid; $^1\text{H NMR}$ (400 MHz, $\text{MeOD-}d_4$) δ = 7.91 (d, J = 4.5 Hz, 1H), 7.47 - 7.36 (m, 2H), 7.29 (dd, J = 8.0, 2.5 Hz, 1H), 6.52 (d, J = 4.5 Hz, 1H), 4.64 (s, 2H); the exchangeable NH proton was not observed; LCMS (Method A, UV, ES) RT = 1.07 min, $[\text{M}+\text{H}]^+$ = 288, 290, 292, 99% purity.

2-Chloro-*N*-(3,5-dichlorobenzyl)pyrimidin-4-amine (278h)



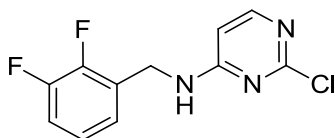
The pyrimidine **278h** was prepared from 2,4-dichloropyrimidine (1.0 g, 6.7 mmol), 3,5-dichlorobenzylamine (1.2 g, 6.7 mmol) and DIPEA (1.8 mL, 10 mmol) according to the procedure described for the preparation of **259**. The same work up and purification method afforded the title compound (0.45 g, 22%) as a white yellow solid; $^1\text{H NMR}$ (400 MHz, $\text{MeOD-}d_4$) δ = 7.91 (d, J = 5.0 Hz, 1H), 7.39 - 7.24 (m, 3H), 6.48 (d, J = 5.0 Hz, 1H), 4.56 (br. s, 2H); the exchangeable NH proton was not observed; LCMS (Method A, UV, ES) RT = 1.14 min, $[\text{M}+\text{H}]^+ = 288, 290, 292$, 95% purity.

2-Chloro-*N*-(3,4-difluorobenzyl)pyrimidin-4-amine (278i)



The pyrimidine **278i** was prepared from 2,4-dichloropyrimidine (1.0 g, 6.7 mmol), 3,4-difluorobenzylamine (0.79 mL, 6.7 mmol) and DIPEA (1.8 mL, 10 mmol) according to the procedure described for the preparation of **259**. The same work up and purification method afforded the title compound (1.2 g, 70%) as a white solid; $^1\text{H NMR}$ (400 MHz, $\text{MeOD-}d_4$) δ = 7.89 (d, J = 5.5 Hz, 1H), 7.33 - 6.99 (m, 3H), 6.45 (d, J = 5.5 Hz, 1H), 4.54 (br. s, 2H); the exchangeable NH proton was not observed; LCMS (Method A, UV, ES) RT = 0.92 min, $[\text{M}+\text{H}]^+ = 256, 258$ 100% purity.

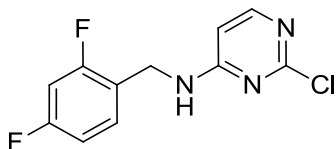
2-Chloro-*N*-(2,3-difluorobenzyl)pyrimidin-4-amine (278j)



The pyrimidine **278j** was prepared from 2,4-dichloropyrimidine (1.0 g, 6.7 mmol), 2,3-difluorobenzylamine (0.79 mL, 6.7 mmol) and DIPEA (1.8 mL, 10 mmol) according to the procedure described for the preparation of **259**. The same work up and purification method afforded the title compound (1.02 g, 59%) as a white solid; $^1\text{H NMR}$ (400 MHz, $\text{MeOD-}d_4$) δ

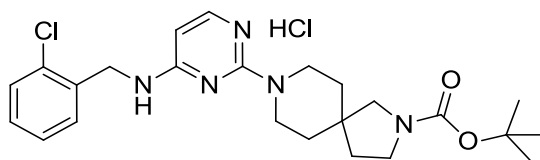
= 7.90 (br. s, 1H), 7.26 - 7.04 (m, 3H), 6.47 (d, $J = 6.0$ Hz, 1H), 4.65 (br. s, 2H); the exchangeable NH proton was not observed; LCMS (Method A, UV, ES) RT = 0.92 min, $[M+H]^+ = 256, 258$ 100% purity.

2-Chloro-*N*-(2,4-difluorobenzyl)pyrimidin-4-amine (278k)



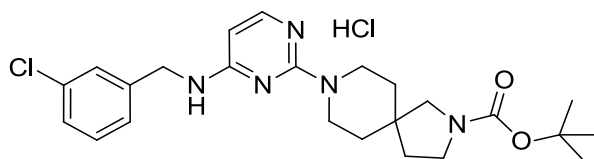
The pyrimidine **278k** was prepared from 2,4-dichloropyrimidine (1.0 g, 6.7 mmol), 2,4-difluorobenzylamine (0.79 mL, 6.7 mmol) and DIPEA (1.8 mL, 10 mmol) according to the procedure described for the preparation of **259**. The same work up and purification method afforded the title compound (1.26 g, 73%) as a white solid; ^1H NMR (400 MHz, MeOD- d_4) $\delta = 7.88$ (br. s, 1H), 7.52 - 7.34 (m, 1H), 7.03 - 6.82 (m, 2H), 6.45 (d, $J = 6.0$ Hz, 1H), 4.58 (br. s, 2H); the exchangeable NH proton was not observed; ^{19}F NMR (376 MHz, MeOD- d_4) $\delta = (-112.8)$ - (-113.5) (m, 1F), (-115.9) - (-116.4) (m, 1F); LCMS (Method A, UV, ES) RT = 0.94 min, $[M+H]^+ = 256, 258$, 100% purity. LCMS (Method A, UV, ES) RT = 0.92 min, $[M+H]^+ = 256, 258$, 100% purity.

tert-Butyl 8-(4-((2-chlorobenzyl)amino)pyrimidin-2-yl)-2,8-diazaspiro[4.5]decane-2-carboxylate, hydrochloride salt (279a)



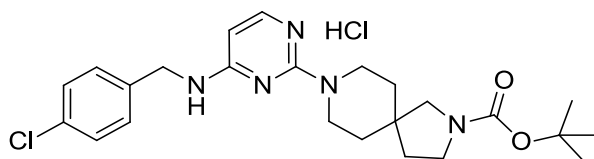
The spiro-pyrimidine **279a** was prepared from 2-chloro-*N*-(2-chlorobenzyl)pyrimidin-4-amine (commercially available from UkrOrg synthesis) (400 mg, 1.57 mmol) and *tert*-butyl 2,8-diazaspiro[4.5]decane-2-carboxylate (395 mg, 1.65 mmol) according to the procedure described for the preparation of **261a**. The same work up and purification method afforded the title compound (560 mg, 72%) as a white solid; ^1H NMR (400 MHz, MeOD- d_4) $\delta = 7.61$ (d, $J = 7.0$ Hz, 1H), 7.50 - 7.39 (m, 2H), 7.34 - 7.29 (m, 2H), 6.19 (d, $J = 7.0$ Hz, 1H), 4.76 (s, 2H), 3.88 - 3.64 (m, 4H), 3.49 - 3.39 (m, 2H), 3.26 (s, 2H), 1.87 (t, $J = 7.1$ Hz, 2H), 1.65 (br. s, 4H), 1.49 (s, 9H); the two exchangeable protons were not observed; LCMS (Method A, UV, ES) RT = 1.00 min, $[M+H]^+ = 458, 460$, 100% purity.

***tert*-Butyl 8-(4-((3-chlorobenzyl)amino)pyrimidin-2-yl)-2,8-diazaspiro[4.5]decane-2-carboxylate, hydrochloride salt (279b)**



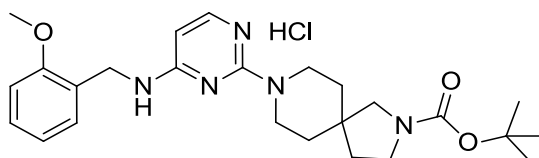
The spiro-pyrimidine **279b** was prepared from *tert*-butyl 2,8-diazaspiro[4.5]decane-2-carboxylate (190 mg, 0.787 mmol) and **278b** (200 mg, 0.787 mmol) according to the procedure described for the preparation of **261a**. The same purification method afforded the title compound (346 mg, 89%) as a white solid; ¹H NMR (400 MHz, MeOD-*d*₄) δ = 7.59 (d, *J* = 7.0 Hz, 1H), 7.42 - 7.19 (m, 4H), 6.15 (d, *J* = 7.0 Hz, 1H), 4.63 (s, 2H), 3.73 (br. s, 1H), 3.50 - 3.38 (m, 2H), 3.30 (br. s, 3H (obscured by solvent residual peak*)), 3.24 (br. s, 2H), 1.85 (t, *J* = 7.0 Hz, 2H), 1.63 (br. s, 4H), 1.47 (s, 9H); the two exchangeable protons were not observed; LCMS (Method D, UV, ES) RT = 2.55 min, [M+H]⁺ = 458, 460, 90% purity. *The presence of signal was inferred by comparison with **279a**.

***tert*-Butyl 8-(4-((4-chlorobenzyl)amino)pyrimidin-2-yl)-2,8-diazaspiro[4.5]decane-2-carboxylate, hydrochloride salt (279c)**



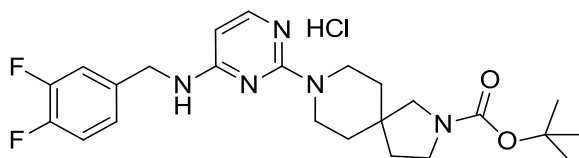
The spiro-pyrimidine **279c** was prepared from *tert*-butyl 2,8-diazaspiro[4.5]decane-2-carboxylate (190 mg, 0.787 mmol) and **278c** (200 mg, 0.787 mmol) according to the procedure described for the preparation of **261a**. The same purification method afforded the title compound (330 mg, 84%) as a white solid; ¹H NMR (400 MHz, MeOD-*d*₄) δ = 7.58 (d, *J* = 7.0 Hz, 1H), 7.42 - 7.23 (m, 4H), 6.14 (d, *J* = 7.0 Hz, 1H), 4.62 (s, 2H), 3.92 - 3.55 (m, 4H), 3.47 - 3.37 (m, 2H), 3.24 (s, 2H), 1.85 (t, *J* = 7.2 Hz, 2H), 1.62 (br. s, 4H), 1.47 (s, 9H); the two exchangeable protons were not observed; LCMS (Method D, UV, ES) RT = 2.57 min, [M+H]⁺ = 458, 460, 90% purity.

***tert*-Butyl 8-(4-((2-methoxybenzyl)amino)pyrimidin-2-yl)-2,8-diazaspiro[4.5]decane-2-carboxylate, hydrochloride salt (279d)**



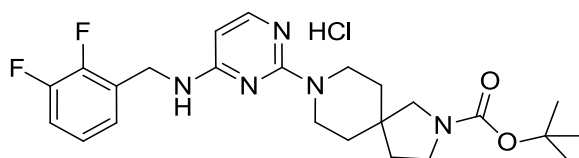
The spiro-pyrimidine **279d** was prepared from *tert*-butyl 2,8-diazaspiro[4.5]decane-2-carboxylate (397 mg, 1.65 mmol) and 2-chloro-*N*-(2-methoxybenzyl)pyrimidin-4-amine (commercially available from HDH Pharma) (393 mg, 1.57 mmol) according to the procedure described for the preparation of **261a**. The same purification method afforded the title compound (600 mg, 78%) as a white solid; ¹H NMR (400 MHz, MeOD-*d*₄) δ = 7.55 (d, *J* = 7.0 Hz, 1H), 7.39 - 7.20 (m, 2H), 7.01 (d, *J* = 8.0 Hz, 1H), 6.96 - 6.86 (m, 1H), 6.14 (d, *J* = 7.0 Hz, 1H), 4.64 (s, 2H), 3.88 (s, 3H), 3.85 - 3.65 (m, 4H), 3.51 - 3.41 (m, 2H), 3.27 (s, 2H), 1.88 (t, *J* = 7.0 Hz, 2H), 1.72 - 1.61 (m, 4H), 1.49 (s, 9H); the two exchangeable protons were not observed; LCMS (Method A, UV, ES) RT = 0.98 min, [M+H]⁺ = 454, 100% purity.

***tert*-Butyl 8-(4-((3,4-difluorobenzyl)amino)pyrimidin-2-yl)-2,8-diazaspiro[4.5]decane-2-carboxylate, hydrochloride salt (279i)**



The spiro-pyrimidine **279i** was prepared from *tert*-butyl 2,8-diazaspiro[4.5]decane-2-carboxylate (280 mg, 1.17 mmol) and **278i** (300 mg, 1.17 mmol) according to the procedure described for the preparation of **261a**. The same work up and purification method afforded the title compound (300 mg, 52%) as a white solid; ¹H NMR (400 MHz, MeOD-*d*₄) δ = 7.60 (d, *J* = 7.0 Hz, 1H), 7.34 - 7.19 (m, 2H), 7.19 - 7.08 (m, 1H), 6.14 (d, *J* = 7.0 Hz, 1H), 4.62 (s, 2H), 3.74 (br. s, 1H), 3.51 - 3.37 (m, 2H), 3.30 (br. s, 3H (obscured by solvent residual peak8)), 3.25 (s, 2H), 1.86 (t, *J* = 7.0 Hz, 2H), 1.63 (br. s, 4H), 1.47 (s, 9H); the two exchangeable protons were not observed; LCMS (Method A, UV, ES) RT = 1.07 min, [M+H]⁺ = 460, 98% purity. *The presence of signal was inferred by comparison with **279a**.

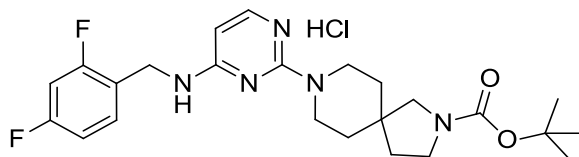
***tert*-Butyl 8-(4-((2,3-difluorobenzyl)amino)pyrimidin-2-yl)-2,8-diazaspiro[4.5]decane-2-carboxylate, hydrochloride salt (279j)**



The spiro-pyrimidine **279j** was prepared from *tert*-butyl 2,8-diazaspiro[4.5]decane-2-carboxylate (280 mg, 1.17 mmol) and **278j** (300 mg, 1.17 mmol) according to the procedure described for the preparation of **261a**. The same work up and purification method afforded

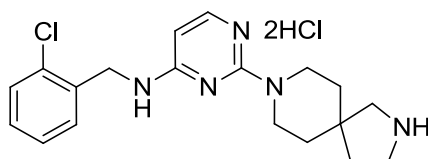
the title compound (320 mg, 55%) as a white solid; $^1\text{H NMR}$ (400 MHz, $\text{MeOD-}d_4$) $\delta = 7.60$ (d, $J = 7.0$ Hz, 1H), 7.28 - 7.05 (m, 3H), 6.13 (d, $J = 7.0$ Hz, 1H), 4.71 (s, 2H), 3.52 - 3.38 (m, 4H), 3.28 - 3.14 (m, 4H), 1.83 - 1.73 (m, 2H), 1.63 (br. s, 4H), 1.47 (s, 9H); the two exchangeable protons were not observed; LCMS (Method A, UV, ES) $\text{RT} = 1.09$ min, $[\text{M}+\text{H}]^+ = 460$, 90% purity.

***tert*-Butyl 8-((2,4-difluorobenzyl)amino)pyrimidin-2-yl)-2,8-diazaspiro[4.5]decane-2-carboxylate, hydrochloride salt (**279k**)**



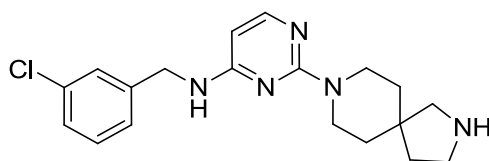
The spiro-pyrimidine **279k** was prepared from *tert*-butyl 2,8-diazaspiro[4.5]decane-2-carboxylate (188 mg, 0.782 mmol) and **278k** (200 mg, 0.782 mmol) according to the procedure described for the preparation of **261a**. The same purification method afforded the title compound (245 mg, 63%) as a white solid; $^1\text{H NMR}$ (400 MHz, $\text{MeOD-}d_4$) $\delta = 7.57$ (d, $J = 7.0$ Hz, 1H), 7.49 - 7.33 (m, 1H), 7.05 - 6.86 (m, 2H), 6.12 (d, $J = 7.0$ Hz, 1H), 4.66 (s, 2H), 3.88 - 3.60 (m, 4H), 3.48 - 3.39 (m, 2H), 3.26 (s, 2H), 1.87 (t, $J = 7.0$ Hz, 2H), 1.70 - 1.59 (m, 4H), 1.47 (s, 9H); the two exchangeable protons were not observed; $^{19}\text{F NMR}$ (376 MHz, $\text{MeOD-}d_4$) $\delta = (-112.5) - (-112.8)$ (m, 1F), $(-115.7) - (-116.0)$ (m, 1F); LCMS (Method A, UV, ES) $\text{RT} = 0.97$ min, $[\text{M}+\text{H}]^+ = 460$, 100% purity.

***N*-(2-Chlorobenzyl)-2-(2,8-diazaspiro[4.5]decan-8-yl)pyrimidin-4-amine, dihydrochloride salt (**280a**)**



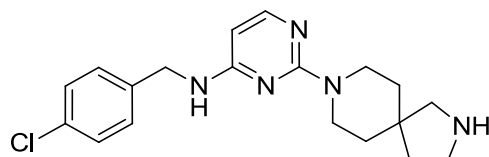
The spiro-pyrimidine **280a** was prepared from **279a** (560 mg, 1.14 mmol) and HCl (3.0 mL of a 4 M solution in dioxane, 12.0 mmol) according to the procedure described for the preparation of **262a**. The title compound was obtained (480 mg, 98%) as a white solid; $^1\text{H NMR}$ (400 MHz, $\text{MeOD-}d_4$) $\delta = 7.63$ (d, $J = 7.0$ Hz, 1H), 7.49 - 7.40 (m, 2H), 7.36 - 7.29 (m, 2H), 6.23 (d, $J = 7.0$ Hz, 1H), 4.77 (s, 2H), 3.94 - 3.82 (m, 2H), 3.78 - 3.70 (m, 2H), 3.45 (t, $J = 7.5$ Hz, 2H), 3.21 (s, 2H), 2.05 (t, $J = 7.5$ Hz, 2H), 1.76 (t, $J = 5.5$ Hz, 4H); the four exchangeable protons were not observed; LCMS (Method A, UV, ES) $\text{RT} = 0.50$ min, $[\text{M}+\text{H}]^+ = 358, 360$, 100% purity.

***N*-(3-Chlorobenzyl)-2-(2,8-diazaspiro[4.5]decan-8-yl)pyrimidin-4-amine (280b)**



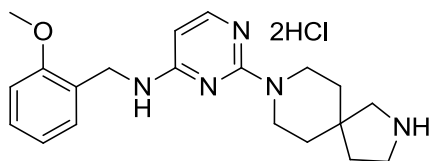
A mixture of TFA (1 mL) and **279b** (345 mg, 0.750 mmol) was stirred at ambient temperature for 0.5 h. The reaction mixture was concentrated, sodium hydroxide (20 mL of a 1 M aqueous solution) was added, and the product was extracted with EtOAc (2×20 mL). The combined organic extracts were passed through a hydrophobic frit and concentrated to afford the desired product (268 mg, 100%) as a colourless oil. LCMS showed peaks for product plus small amount of impurity. An aliquot of the crude material (80 mg) was dissolved in DMSO (1 mL) and purified by MDAP (Method B). The solvent was evaporated under reduced pressure to afford the title product (45 mg, 17%) as a colourless oil; ^1H NMR (400 MHz, MeOD- d_4) δ = 7.69 (d, J = 6.0 Hz, 1H), 7.32 (s, 1H), 7.30 - 7.13 (m, 3H), 5.82 (d, J = 6.0 Hz, 1H), 4.50 (s, 2H), 3.83 - 3.68 (m, 2H), 3.69 - 3.55 (m, 2H), 3.24 (t, J = 7.5 Hz, 2H), 2.98 (s, 2H), 1.85 (t, J = 7.5 Hz, 2H), 1.53 (t, J = 5.6 Hz, 4H); the two exchangeable NH protons were not observed; LCMS (Method A, UV, ES) RT = 0.50 min, $[\text{M}+\text{H}]^+$ = 358, 360, 94% purity.

***N*-(4-Chlorobenzyl)-2-(2,8-diazaspiro[4.5]decan-8-yl)pyrimidin-4-amine (280c)**



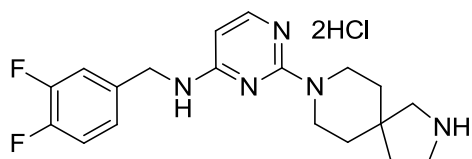
The spiro-pyrimidine **280c** was prepared from **279c** (330 mg, 0.671 mmol) and TFA (1.0 mL) according to the procedure described for the preparation of **280b**. The title compound was obtained as the TFA salt (240 mg, 100%); LCMS showed peaks for product plus small amount of impurity. An aliquot of the crude material (80 mg) was dissolved in DMSO (1 mL) and purified by MDAP (Method B, high pH). The solvent was evaporated under reduced pressure to afford the title product (32 mg, 13%) as the free base; ^1H NMR (400 MHz, MeOD- d_4) δ = 7.69 (d, J = 6.0 Hz, 1H), 7.28 (s, 4H), 5.82 (d, J = 6.0 Hz, 1H), 4.50 (s, 2H), 3.81 - 3.68 (m, 2H), 3.67 - 3.56 (m, 2H), 3.26 (t, J = 7.5 Hz, 2H), 2.99 (s, 2H), 1.86 (t, J = 7.5 Hz, 2H), 1.53 (t, J = 5.5 Hz, 4H); the two exchangeable NH protons were not observed; LCMS (Method A, UV, ES) RT = 0.51 min, $[\text{M}+\text{H}]^+$ = 358, 360, 96% purity.

***N*-(2-Methoxybenzyl)-2-(2,8-diazaspiro[4.5]decan-8-yl)pyrimidin-4-amine, dihydrochloride salt (280d)**



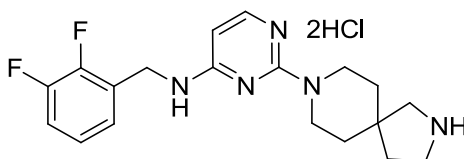
The spiro-pyrimidine **280d** was prepared from **279d** (555 mg, 1.13 mmol) and HCl (3.0 mL of a 4 M solution in dioxane, 12.0 mmol) according to the procedure described for the preparation of **262a**. The title compound was obtained as a white solid (475 mg, 98%); ^1H NMR (400 MHz, MeOD- d_4) δ = 7.57 (d, J = 7.0 Hz, 1H), 7.37 - 7.23 (m, 2H), 7.02 (d, J = 8.0 Hz, 1H), 6.93 (t, J = 8.0 Hz, 1H), 6.17 (d, J = 7.0 Hz, 1H), 4.65 (s, 2H), 3.89 (s, 3H), 3.98 - 3.82 (m, 2H), 3.82 - 3.71 (m, 2H), 3.46 (t, J = 7.5 Hz, 2H), 3.22 (s, 2H), 2.06 (t, J = 7.5 Hz, 2H), 1.78 (t, J = 5.5 Hz, 4H); the four exchangeable protons were not observed; LCMS (Method A, UV, ES) RT = 0.51 min, $[\text{M}+\text{H}]^+$ = 354, 99% purity.

***N*-(3,4-Difluorobenzyl)-2-(2,8-diazaspiro[4.5]decan-8-yl)pyrimidin-4-amine, dihydrochloride salt (280i)**



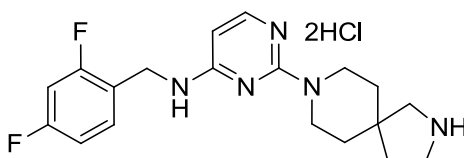
The spiro-pyrimidine **280i** was prepared from **279i** (150 mg, 0.326 mmol) and HCl (1.6 mL of a 4 M solution in dioxane, 6.4 mmol) according to the procedure described for the preparation of **262a**. The title compound was obtained as a colourless gum (140 mg, 93%); ^1H NMR (400 MHz, MeOD- d_4) δ = 7.62 (d, J = 7.0 Hz, 1H), 7.35 - 7.19 (m, 2H), 7.19 - 7.09 (m, 1H), 6.17 (d, J = 7.0 Hz, 1H), 4.62 (s, 2H), 3.92 - 3.78 (m, 2H), 3.77 - 3.66 (m, 2H), 3.43 (t, J = 7.5 Hz, 2H), 3.19 (s, 2H), 2.03 (t, J = 7.4 Hz, 2H), 1.81 - 1.67 (m, 4H); the four exchangeable NH protons were not observed; LCMS (Method D, UV, ES) RT = 1.53 min, $[\text{M}+\text{H}]^+$ = 360, 95% purity.

***N*-(2,3-Difluorobenzyl)-2-(2,8-diazaspiro[4.5]decan-8-yl)pyrimidin-4-amine, dihydrochloride salt (280j)**



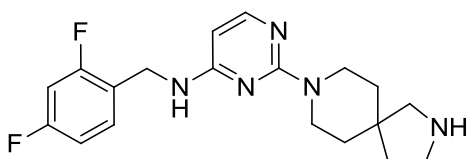
The spiro-pyrimidine **280j** was prepared from **279j** (150 mg, 0.326 mmol) and HCl (1.6 mL of a 4 M solution in dioxane, 6.4 mmol) according to the procedure described for the preparation of **262a**. The title compound was obtained as a colourless gum (142 mg, 94%); ¹H NMR (400 MHz, MeOD-*d*₄) δ = 7.62 (d, *J* = 7.0 Hz, 1H), 7.29 - 7.04 (m, 3H), 6.18 (d, *J* = 7.0 Hz, 1H), 4.73 (s, 2H), 3.94 - 3.81 (m, 2H), 3.74 - 3.63 (m, 2H), 3.44 (t, *J* = 7.5 Hz, 2H), 3.20 (s, 2H), 2.05 (t, *J* = 7.5 Hz, 2H), 1.79 - 1.69 (m, 4H); the four exchangeable protons were not observed; LCMS (Method D, UV, ES) RT = 1.53 min, [M+H]⁺ = 360, 92% purity.

***N*-(2,4-Difluorobenzyl)-2-(2,8-diazaspiro[4.5]decan-8-yl)pyrimidin-4-amine, dihydrochloride salt (280k)**



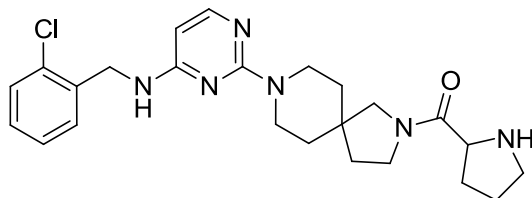
The spiro-pyrimidine **280k** was prepared from **279k** (245 mg, 0.494 mmol) and HCl (3.0 mL of a 4 M solution in dioxane, 12.0 mmol) according to the procedure described for the preparation of **262a**. The title compound was obtained as a colourless gum (213 mg, 100%); ¹H NMR (400 MHz, MeOD-*d*₄) δ = 7.60 (d, *J* = 7.0 Hz, 1H), 7.51 - 7.35 (m, 1H), 7.06 - 6.85 (m, 2H), 6.16 (d, *J* = 7.0 Hz, 1H), 4.67 (s, 2H), 3.93 - 3.82 (m, 2H), 3.80 - 3.70 (m, 2H), 3.45 (t, *J* = 7.5 Hz, 2H), 3.21 (s, 2H), 2.05 (t, *J* = 7.5 Hz, 2H), 1.77 (t, *J* = 5.6 Hz, 4H); the four exchangeable protons were not observed; ¹⁹F NMR (376 MHz, MeOD-*d*₄) δ = (-112.5) - (-112.7) (m, 1F), (-115.84) - (-116.0) (m, 1F); LCMS (Method A, UV, ES) RT = 0.50 min, [M+H]⁺ = 360, 100% purity.

***N*-(2,4-Difluorobenzyl)-2-(2,8-diazaspiro[4.5]decan-8-yl)pyrimidin-4-amine (280k)**



A mixture of TFA (0.5 mL) and **280k** (55 mg, 0.11 mmol) was stirred at ambient temperature for 0.5 h. The reaction mixture was concentrated, and was then dissolved in methanol (1 mL) and passed through an aminopropyl cartridge (500 mg). The cartridge was washed with methanol, and the filtrate was concentrated to afford the title product (36 mg, 90%) as the free base; $^1\text{H NMR}$ (400 MHz, $\text{MeOD-}d_4$) δ = 7.67 (d, J = 6.0 Hz, 1H), 7.46 - 7.27 (m, 1H), 6.99 - 6.79 (m, 2H), 5.80 (d, J = 6.0 Hz, 1H), 4.53 (br. s, 2H), 3.84 - 3.67 (m, 2H), 3.65 - 3.54 (m, 2H), 2.94 (t, J = 7.0 Hz, 2H), 2.69 (s, 2H), 1.66 (t, J = 7.0 Hz, 2H), 1.54 - 1.38 (m, 4H); the two exchangeable NH protons were not observed; LCMS (Method D, UV, ES) RT = 1.46 min, $[\text{M}+\text{H}]^+ = 360$, 90% purity.

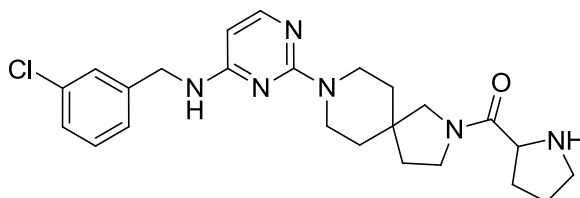
(\pm)-(8-(4-((2-Chlorobenzyl)amino)pyrimidin-2-yl)-2,8-diazaspiro[4.5]decan-2-yl)(pyrrolidin-2-yl)methanone (281a)



The spiro-pyrimidine **281a** was prepared from **280a** (50 mg, 0.14 mmol) and (\pm)-1-(*tert*-butoxycarbonyl)pyrrolidine-2-carboxylic acid (30 mg, 0.14 mmol) according to the procedure described for the preparation of **255a**. The same work up and purification method afforded the title compound (20 mg, 32%) as a colourless gum; $^1\text{H NMR}$ (400 MHz, $\text{MeOD-}d_4$) δ = 7.73 (d, J = 6.0 Hz, 1H), 7.39 (dd, J = 8.0, 1.0 Hz, 2H), 7.31 - 7.17 (m, 2H), 5.88 (d, J = 6.0 Hz, 1H), 4.65 (s, 2H), 3.94 - 3.66 (m, 4H), 3.65 - 3.44 (m, 3H), 3.41 - 3.30 (m, 2H), 3.24 - 3.05 (m, 1H), 2.91 - 2.64 (m, 1H), 2.34 - 2.11 (m, 1H), 2.01 - 1.74 (m, 4H), 1.75 - 1.60 (m, 1H), 1.58 - 1.42 (m, 4H); the two exchangeable NH protons were not observed; $^{13}\text{C NMR}$ (126 MHz, $\text{MeOD-}d_4$) δ = 174.3, 174.2, 164.4, 162.7, 155.6, 138.6, 134.2, 130.5, 130.1, 129.5, 128.1, 96.7, 60.3, 60.0, 57.2, 56.9, 48.3, 45.8, 45.7, 43.0, 42.8, 42.7, 42.6, 40.8, 37.0, 35.3, 35.3, 35.1, 35.0, 31.4, 31.3, 27.4, 27.3 (the additional peaks were observed due to

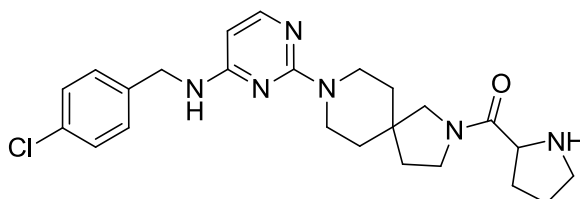
rotamers); HRMS (ESI) m/z calculated for $C_{24}H_{32}ClN_6O$ = 455.2316. Found = 455.2321, $[M+H]^+$; LCMS (UV, ES) RT = 0.59 min, $[M+H]^+$ = 455, 457, 100% purity.

(±)-(8-(4-((3-Chlorobenzyl)amino)pyrimidin-2-yl)-2,8-diazaspiro[4.5]decan-2-yl)(pyrrolidin-2-yl)methanone (281b)



The spiro-pyrimidine **281b** was prepared from **280b** (75 mg, 0.21 mmol) and (±)-1-(*tert*-butoxycarbonyl)pyrrolidine-2-carboxylic acid (45 mg, 0.21 mmol) according to the procedure described for the preparation of **255a**. The same work up and purification method afforded the title compound (30 mg, 30%) as a white solid; 1H NMR (400 MHz, MeOD- d_4) δ = 7.65 (d, J = 6.0 Hz, 1H), 7.29 (s, 1H), 7.27 - 7.10 (m, 3H), 5.78 (d, J = 6.0 Hz, 1H), 4.46 (s, 2H), 3.80 - 3.59 (m, 4H), 3.60 - 3.35 (m, 3H), 3.30 (m, 2H (obscured by solvent residual peak)), 3.15 - 3.03 (m, 1H), 2.79 - 2.67 (m, 1H), 2.23 - 2.05 (m, 1H), 1.91 - 1.68 (m, 4H), 1.67 - 1.54 (m, 1H), 1.49 - 1.41 (m, 4H); the two exchangeable NH protons were not observed; LCMS (Method A, UV, ES) RT = 0.58 min, $[M+H]^+$ = 455, 457, 96% purity. *The presence of signal was inferred by comparison with **281a**.

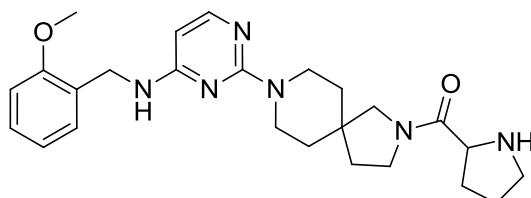
(±)-(8-(4-((4-Chlorobenzyl)amino)pyrimidin-2-yl)-2,8-diazaspiro[4.5]decan-2-yl)(pyrrolidin-2-yl)methanone (281c)



The spiro-pyrimidine **281c** was prepared from **280c** (75 mg, 0.21 mmol) and (±)-1-(*tert*-butoxycarbonyl)pyrrolidine-2-carboxylic acid (45 mg, 0.21 mmol) according to the procedure described for the preparation of **255a**. The same work up and purification method afforded the title compound (33 mg, 34%) as a white solid; 1H NMR (400 MHz, MeOD- d_4) δ = 7.70 (d, J = 6.0 Hz, 1H), 7.31 (s, 4H), 5.83 (d, J = 6.0 Hz, 1H), 4.52 (s, 2H), 3.88 - 3.76 (m, 2H), 3.75 - 3.65 (m, 2H), 3.67 - 3.43 (m, 3H), 3.30 (m, 2H (obscured by solvent residual peak*)), 3.21 - 3.07 (m, 1H), 2.83 - 2.77 (m, 1H), 2.32 - 2.12 (m, 1H), 2.00 - 1.74 (m, 4H), 1.72 - 1.59

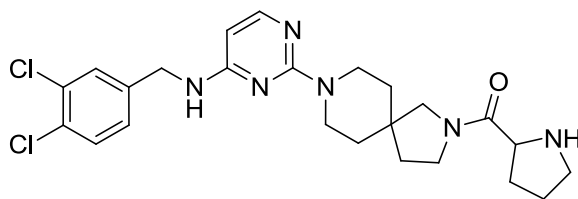
(m, 1H), 1.59 - 1.44 (m, 4H); the two exchangeable NH protons were not observed; LCMS (Method A, UV, ES) RT = 0.60 min, $[M+H]^+ = 455, 457, 100\%$ purity. *The presence of signal was inferred by comparison with **279a**.

(±)-(8-(4-((2-Methoxybenzyl)amino)pyrimidin-2-yl)-2,8-diazaspiro[4.5]decan-2-yl)(pyrrolidin-2-yl)methanone (281d)



The spiro-pyrimidine **281d** was prepared from **280d** (49 mg, 0.14 mmol) and (±)-1-(*tert*-butoxycarbonyl)pyrrolidine-2-carboxylic acid (30 mg, 0.14 mmol) according to the procedure described for the preparation of **255a**. The same work up and purification method afforded the title compound (26 mg, 41%) as a colourless gum; $^1\text{H NMR}$ (400 MHz, MeOD- d_4) $\delta = 7.69$ (d, $J = 6.0$ Hz, 1H), 7.30 - 7.18 (m, 2H), 6.96 (d, $J = 8.0$ Hz, 1H), 6.89 (dt, $J = 8.0, 1.0$ Hz, 1H), 5.83 (d, $J = 6.0$ Hz, 1H), 4.53 (br. s, 2H), 3.88 (s, 3H), 3.86 - 3.44 (m, 7H), 3.43 - 3.37 (m, 2H), 3.23 - 3.06 (m, 1H), 2.89 - 2.64 (m, 1H), 2.32 - 2.12 (m, 1H), 1.94 (t, $J = 7.0$ Hz, 1H), 1.89 - 1.74 (m, 3H), 1.74 - 1.62 (m, 1H), 1.59 - 1.47 (m, 4H); the two exchangeable NH protons were not observed; LCMS (UV, ES) RT = 0.55 min, $[M+H]^+ = 451, 99\%$ purity.

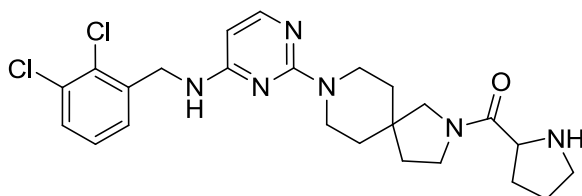
(±)-(8-(4-((3,4-Dichlorobenzyl)amino)pyrimidin-2-yl)-2,8-diazaspiro[4.5]decan-2-yl)(pyrrolidin-2-yl)methanone (281e)



A mixture of **281e** (300 mg, 1.04 mmol), *tert*-butyl 2,8-diazaspiro[4.5]decane-2-carboxylate (250 mg, 1.04 mmol) and IPA (1.5 mL) were stirred at 90 °C for 24 h. The reaction was cooled to ambient temperature, and ether (5 mL) was added. The precipitated solid was collected by filtration, washed with ether (5 mL), and dried under reduced pressure. HCl (1.6 mL of a 4 M solution in dioxane, 6.4 mmol) was added and the mixture was stirred at ambient temperature for 0.5 h. The reaction mixture was concentrated and an aliquot (120 mg) of the crude deprotected amine product was dissolved in DMF (1.5 mL). (±)-1-(*tert*-

Butoxycarbonylpyrrolidine-2-carboxylic acid (66 mg, 0.31 mmol), HATU (151 mg, 0.34 mmol) and DIPEA (0.12 ml, 0.70 mmol) were added and the reaction was stirred at ambient temperature for 18 h. The reaction mixture was partitioned between EtOAc (20 mL) and water (20 mL). The organic layer was separated, dried using a hydrophobic frit and concentrated under reduced pressure. HCl (1.6 mL of a 4 M solution in dioxane, 6.4 mmol) was added and the reaction was stirred at ambient temperature for 0.5 h. The excess HCl was evaporated and the residue was taken up in DMSO (1 mL) and purified by MDAP (Method C). The appropriate fractions were combined and the solvent was evaporated under reduced pressure to give the desired product as the TFA salt. The residue was then dissolved in methanol (0.5 mL) and passed through an aminopropyl cartridge (0.5 g). The cartridge was washed with more methanol, and the filtrate was concentrated to afford the title product (16 mg, 10%) as a colourless gum; ^1H NMR (400 MHz, MeOD- d_4) δ = 7.72 (d, J = 6.0 Hz, 1H), 7.52 - 7.39 (m, 2H), 7.25 (dd, J = 8.0, 2.0 Hz, 1H), 5.85 (d, J = 6.0 Hz, 1H), 4.50 (s, 2H), 3.84 - 3.64 (m, 4H), 3.63 - 3.44 (m, 4H), 3.43 - 3.35 (m, 1H), 3.23 - 3.09 (m, 1H), 2.79 (td, J = 10.0, 7.0 Hz, 1H), 2.32 - 2.13 (m, 1H), 1.92 (t, J = 7.0 Hz, 1H), 1.89 - 1.73 (m, 3H), 1.72 - 1.61 (m, 1H), 1.59 - 1.39 (m, 4H); the two exchangeable NH protons were not observed; LCMS (Method D, UV, ES) RT = 1.79 min, $[\text{M}+\text{H}]^+$ = 489, 491, 493, 97% purity.

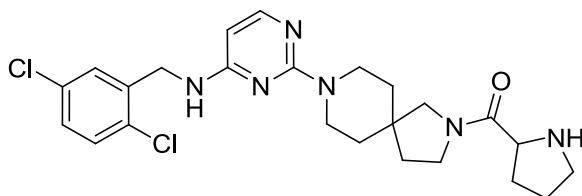
(±)-(8-(4-((2,3-Dichlorobenzyl)amino)pyrimidin-2-yl)-2,8-diazaspiro[4.5]decan-2-yl)(pyrrolidin-2-yl)methanone (281f)



The spiro-pyrimidine **281f** was prepared from **278f** (300 mg, 1.04 mmol), *tert*-butyl 2,8-diazaspiro[4.5]decan-2-carboxylate (250 mg, 1.04 mmol) and (±)-1-(*tert*-butoxycarbonyl)pyrrolidine-2-carboxylic acid (66 mg, 0.31 mmol) according to the procedure described for the preparation of **281e**. The same work up and purification method afforded the title compound (12 mg, 9%) as a colourless gum; ^1H NMR (400 MHz, MeOD- d_4) δ = 7.71 (d, J = 6.0 Hz, 1H), 7.40 (d, J = 8.0 Hz, 1H), 7.30 (d, J = 8.0 Hz, 1H), 7.22 (t, J = 8.0 Hz, 1H), 5.86 (d, J = 6.0 Hz, 1H), 4.64 (s, 2H), 3.81 - 3.75 (m, 1H), 3.74 - 3.42 (m, 6H), 3.36 - 3.33 (m, 2H), 3.20 - 3.07 (m, 1H), 2.83 - 2.71 (m, 1H), 2.27 - 2.12 (m, 1H), 1.89 (t, J = 7.2 Hz, 1H), 1.86 - 1.72 (m, 3H), 1.70 - 1.59 (m, 1H), 1.55 - 1.36 (m, 4H); the two exchangeable NH protons

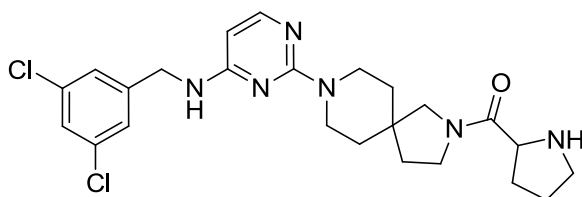
were not observed; LCMS (Method D, UV, ES) RT = 1.78 min, $[M+H]^+$ = 489, 491, 493, 100% purity.

(±)-(8-(4-((2,5-Dichlorobenzyl)amino)pyrimidin-2-yl)-2,8-diazaspiro[4.5]decan-2-yl)(pyrrolidin-2-yl)methanone (281g)



The spiro-pyrimidine **281g** was prepared from **278g** (100 mg, 0.350 mmol), *tert*-butyl 2,8-diazaspiro[4.5]decan-2-carboxylate (83 mg, 0.35 mmol) and (±)-1-(*tert*-butoxycarbonyl)pyrrolidine-2-carboxylic acid (66 mg, 0.31 mmol) according to the procedure described for the preparation of **281e**. The same work up and purification method afforded the title compound (17 mg, 10%) as a colourless gum; $^1\text{H NMR}$ (400 MHz, MeOD- d_4) δ = 7.72 (d, J = 6.0 Hz, 1H), 7.41 - 7.31 (m, 2H), 7.23 (dd, J = 8.0, 2.0 Hz, 1H), 5.87 (d, J = 6.0 Hz, 1H), 4.58 (s, 2H), 3.82 - 3.63 (m, 4H), 3.61 - 3.42 (m, 3H), 3.39 - 3.33 (m, 2H), 3.19 - 3.08 (m, 1H), 2.82 - 2.71 (m, 1H), 2.26 - 2.10 (m, 1H), 1.90 (t, J = 7.0 Hz, 1H), 1.86 - 1.71 (m, 3H), 1.71 - 1.58 (m, 1H), 1.53 - 1.42 (m, 4H); the two exchangeable NH protons were not observed; LCMS (Method D, UV, ES) RT = 1.74 min, $[M+H]^+$ = 489, 491, 493, 99% purity.

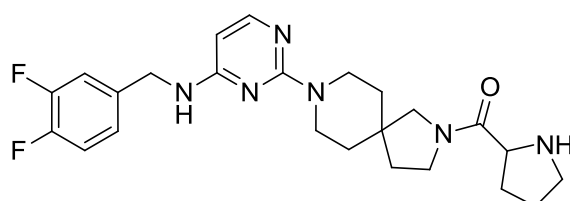
(±)-(8-(4-((3,5-Dichlorobenzyl)amino)pyrimidin-2-yl)-2,8-diazaspiro[4.5]decan-2-yl)(pyrrolidin-2-yl)methanone (281h)



The spiro-pyrimidine **281h** was prepared from **278h** (300 mg, 1.04 mmol), *tert*-butyl 2,8-diazaspiro[4.5]decan-2-carboxylate (250 mg, 1.04 mmol) and 1-(*tert*-butoxycarbonyl)pyrrolidine-2-carboxylic acid (66 mg, 0.31 mmol) according to the procedure described for the preparation of **281e**. The same work up and purification method afforded the title compound (13 mg, 9%) as a colourless gum; $^1\text{H NMR}$ (400 MHz, MeOD- d_4) δ = 7.71 (d, J = 6.0 Hz, 1H), 7.28 (s, 3H), 5.84 (d, J = 6.0 Hz, 1H), 4.48 (s, 2H), 3.87 (t, J = 7.7 Hz, 1H), 3.82 - 3.42 (m, 6H), 3.41 - 3.33 (m, 2H), 3.22 - 3.13 (m, 1H), 2.90 - 2.77 (m, 1H), 2.31 - 2.16 (m,

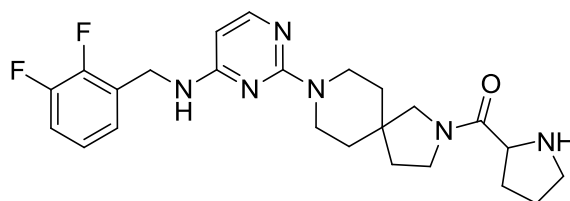
1H), 1.96 - 1.76 (m, 4H), 1.75 - 1.62 (m, 1H), 1.58 - 1.42 (m, 4H); the two exchangeable NH protons were not observed; LCMS (Method D, UV, ES) RT = 1.83 min, $[M+H]^+ = 489, 491, 493$, 99% purity.

(±)-(8-(4-((3,4-Difluorobenzyl)amino)pyrimidin-2-yl)-2,8-diazaspiro[4.5]decan-2-yl)(pyrrolidin-2-yl)methanone (281i)



The spiro-pyrimidine **281i** was prepared from **280i** (140 mg, 0.324 mmol) and (±)-1-(*tert*-butoxycarbonyl)pyrrolidine-2-carboxylic acid (70 mg, 0.33 mmol) according to the procedure described for the preparation of **255a**. The same work up and purification method afforded the title compound (29 mg, 20%) as a white solid; ^1H NMR (400 MHz, MeOD- d_4) $\delta = 7.65$ (d, $J = 6.0$ Hz, 1H), 7.24 - 6.92 (m, 3H), 5.78 (d, $J = 6.0$ Hz, 1H), 4.45 (s, 2H), 3.81 - 3.71 (m, 2H), 3.70 - 3.61 (m, 2H), 3.60 - 3.39 (m, 3H), 3.37 - 3.29 (m, 2H), 3.17 - 3.00 (m, 1H), 2.83 - 2.63 (m, 1H), 2.23 - 2.08 (m, 1H), 1.88 (t, $J = 7.0$ Hz, 1H), 1.83 - 1.70 (m, 3H), 1.68 - 1.55 (m, 1H), 1.54 - 1.37 (m, 4H); the two exchangeable NH protons were not observed; LCMS (Method D, UV, ES) RT = 1.65 min, $[M+H]^+ = 457$, 100% purity.

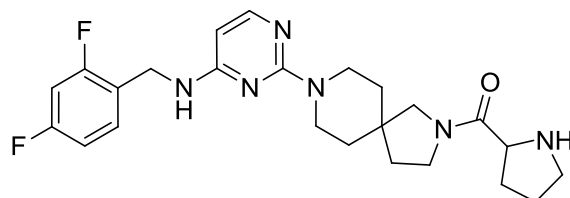
(±)-(8-(4-((2,3-Difluorobenzyl)amino)pyrimidin-2-yl)-2,8-diazaspiro[4.5]decan-2-yl)(pyrrolidin-2-yl)methanone (281j)



The spiro-pyrimidine **281j** was prepared from **280j** (140 mg, 0.324 mmol) and (±)-1-(*tert*-butoxycarbonyl)pyrrolidine-2-carboxylic acid (70 mg, 0.33 mmol) according to the procedure described for the preparation of **255a**. The same work up and purification method afforded the title compound (15 mg, 10%) as a white solid; ^1H NMR (400 MHz, MeOD- d_4) $\delta = 7.69$ (d, $J = 6.0$ Hz, 1H), 7.20 - 6.95 (m, 3H), 5.83 (d, $J = 6.0$ Hz, 1H), 4.60 (s, 2H), 3.82 - 3.65 (m, 4H), 3.64 - 3.43 (m, 3H), 3.40 - 3.34 (m, 2H), 3.14 (td, $J = 11.0, 6.0$ Hz, 1H), 2.86 - 2.70 (m, 1H), 2.28 - 2.07 (m, 1H), 1.91 (t, $J = 7.0$ Hz, 1H), 1.86 - 1.73 (m, 3H), 1.72 - 1.59 (m, 1H),

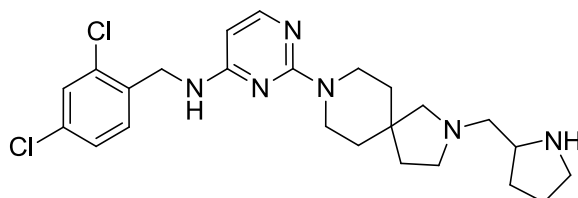
1.53 – 1.42 (m, 4H); the two exchangeable NH protons were not observed; LCMS (Method D, UV, ES) RT = 1.64 min, $[M+H]^+ = 457$, 100% purity.

(±)-**(8-(4-((2,4-Difluorobenzyl)amino)pyrimidin-2-yl)-2,8-diazaspiro[4.5]decan-2-yl)(pyrrolidin-2-yl)methanone (281k)**



The spiro-pyrimidine **281k** was prepared from **280k** (30 mg, 0.069 mmol) and (±)-1-(*tert*-butoxycarbonyl)pyrrolidine-2-carboxylic acid (15 mg, 0.069 mmol) according to the procedure described for the preparation of **255a**. The same work up and purification method afforded the title compound (19 mg, 60%) as a colourless gum; ^1H NMR (500 MHz, MeOD- d_4) $\delta = 7.68$ (d, $J = 6.0$ Hz, 1H), 7.44 - 7.32 (m, 1H), 6.97 - 6.79 (m, 2H), 5.81 (d, $J = 6.0$ Hz, 1H), 4.53 (s, 2H), 3.84 - 3.75 (m, 2H), 3.75 - 3.64 (m, 2H), 3.63 - 3.43 (m, 3H), 3.41 - 3.32 (m, 2H), 3.19 - 3.09 (m, 1H), 2.81 - 2.71 (m, 1H), 2.26 - 2.13 (m, 1H), 1.92 (t, $J = 7.0$ Hz, 1H), 1.87 - 1.71 (m, 3H), 1.70 - 1.59 (m, 1H), 1.57 - 1.46 (m, 4H); the two exchangeable NH protons were not observed; ^{13}C NMR (126 MHz, DMSO- d_6 , 393.4 K) $\delta = 171.8, 161.9, 160.8, 160.0$ (2C), 154.2, 129.9, 122.5, 109.9, 102.4, 93.9, 58.2, 54.6, 46.0, 42.8, 39.9 (2C), 36.2, 33.1 (2C), 28.6, 25.1 (2 aromatic carbon missing due to weak signal); ^{19}F NMR (376 MHz, MeOD- d_4) $\delta = (-113.5) - (-115.3)$ (m, 1F), $(-116.0) - (-117.9)$ (m, 1F); HRMS (ESI) m/z calculated for $\text{C}_{24}\text{H}_{31}\text{F}_2\text{N}_6\text{O} = 457.2522$. Found = 457.2515; $[M+H]^+$; LCMS (Method A, UV, ES) RT = 0.54 min, $[M+H]^+ = 457$, 100% purity.

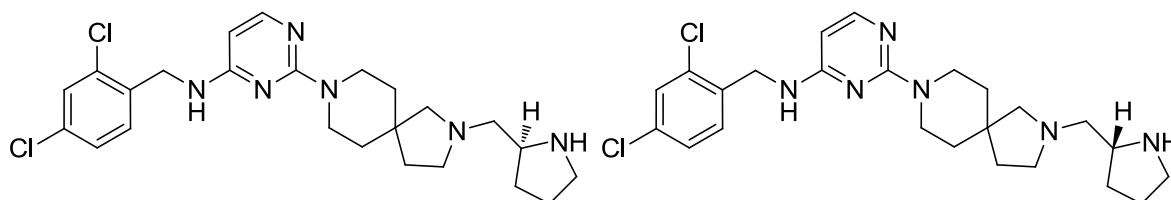
(±)-***N*-(2,4-Dichlorobenzyl)-2-(2-(pyrrolidin-2-ylmethyl)-2,8-diazaspiro[4.5]decan-8-yl)pyrimidin-4-amine (282)**



(*R*)-*tert*-Butyl 2-formylpyrrolidine-1-carboxylate (0.08 mL, 0.4 mmol) was added to a mixture of **262d** (165 mg, 0.42 mmol) and molecular sieves (100 mg) in DCM (3 mL) and the reaction was stirred at ambient temperature, under a nitrogen atmosphere for 30 min.

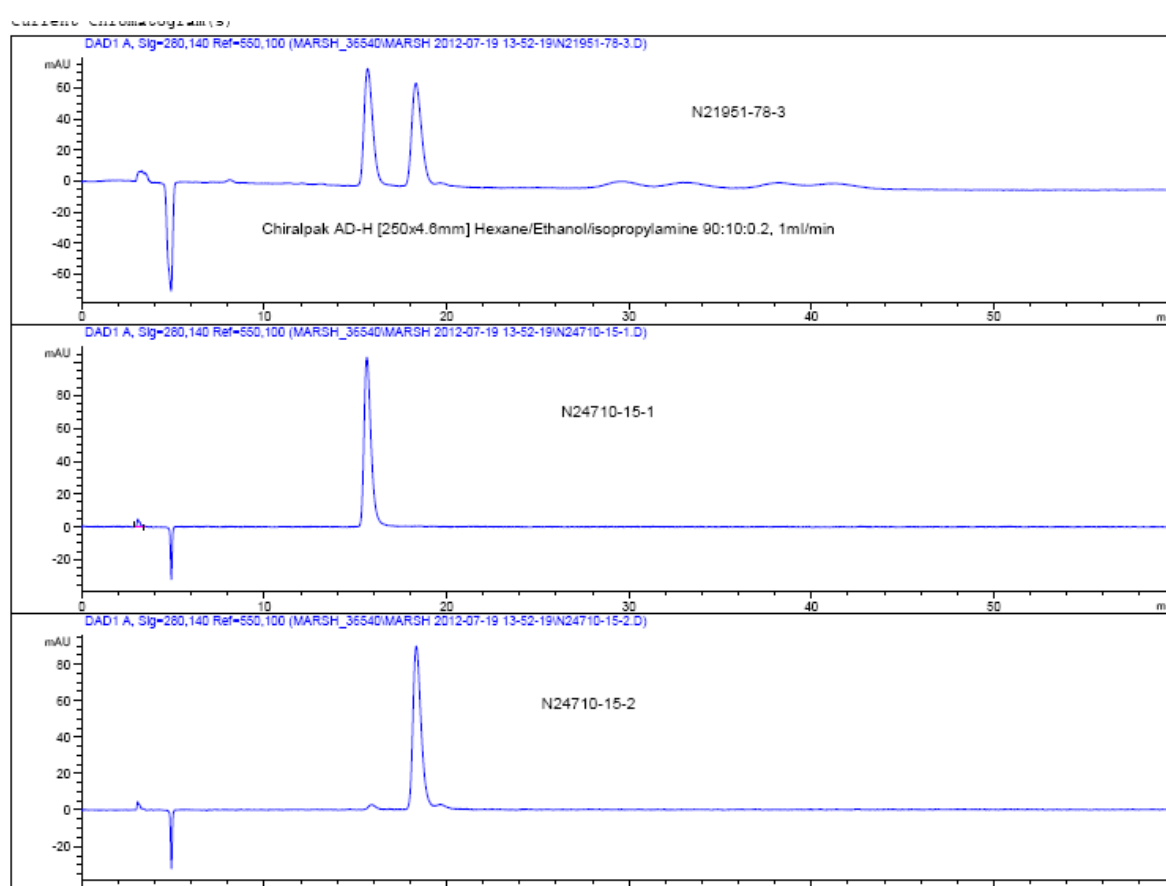
Acetic acid (3 μ L, 0.042 mmol) and sodium triacetoxyborohydride (107 mg, 0.51 mmol) were added and the reaction mixture was stirred for an additional 3 h. The mixture was partitioned between DCM (50 mL) and water (50 mL). The organic layer was separated, washed with water (3 \times 50 mL), dried using a hydrophobic frit and concentrated under reduced pressure. TFA (1.5 mL) was then added and the reaction was stirred at ambient temperature for 1 h. The mixture was concentrated, taken up in DMSO (2 mL) and purified by MDAP (Method C). The solvent was evaporated and the solid was taken up in methanol (1 mL) and passed through an aminopropyl cartridge (1 g). The cartridge was washed with additional methanol and the eluent was evaporated under reduced pressure to afford the title product (84 mg, 42%) as a white solid; $[\alpha]_D^{20} = 0$ (c = 0.50 in MeOH) ^1H NMR (400 MHz, MeOD- d_4) $\delta = 7.68$ (d, $J = 6.0$ Hz, 1H), 7.40 (d, $J = 2.0$ Hz, 1H), 7.34 - 7.30 (m, 1H), 7.25 - 7.21 (m, 1H), 5.82 (d, $J = 5.5$ Hz, 1H), 4.56 (s, 2H), 3.71 - 3.47 (m, 4H), 3.14 (dd, $J = 7.0, 6.0$ Hz, 1H), 2.98 - 2.90 (m, 1H), 2.78 (dt, $J = 10.0, 7.0$ Hz, 1H), 2.72 - 2.63 (m, 1H), 2.63 - 2.56 (m, 1H), 2.56 - 2.33 (m, 4H), 1.98 - 1.85 (m, 1H), 1.80 - 1.70 (m, 2H), 1.64 (t, $J = 7.0$ Hz, 2H), 1.45 (m, 5H); the two exchangeable NH protons were not observed; ^{13}C NMR (126 MHz, MeOD- d_4) $\delta = 164.2, 162.7, 155.7, 137.7, 134.9, 134.2, 131.2, 130.1, 128.3, 96.5, 67.5, 62.8, 58.4, 55.2, 46.8, 43.1, 43.0, 41.8, 38.8, 37.8, 31.4, 25.9$; LCMS (Method A), UV, ES) RT = 0.61 min, $[\text{M}+\text{H}]^+ = 475, 477, 479$, 96% purity. Note, the product racemised in the reaction - confirmed by chiral HPLC (Chiralpak AD, 250 \times 4.6 mm, col. no. ADOOCE-NK016, 5% ethanol/heptane [0.1% isopropylamine], flow rate of 1 mL/min), which showed peaks for the two enantiomers at 35.4 and 40.6 min (1:1) respectively.

(S)-N-(2,4-Dichlorobenzyl)-2-(2-(pyrrolidin-2-ylmethyl)-2,8-diazaspiro[4.5]decan-8-yl)pyrimidin-4-amine (282a) and (R)-N-(2,4-dichlorobenzyl)-2-(2-(pyrrolidin-2-ylmethyl)-2,8-diazaspiro[4.5]decan-8-yl)pyrimidin-4-amine (282b)

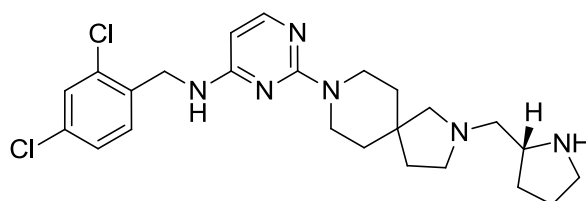


The enantiomers of the racemic spiro-pyrimidine **282** (28 mg) were separated on a Chiralpak AD-H (250 \times 30 mm, 5 μ m) column with a flow rate of 45 mL/min and an isocratic gradient system of 90:10 hexane (0.2% isopropylamine v/v): ethanol (0.2% isopropylamine v/v) over 40 min. Fractions for isomer 1 were collected between 14 and 16 min, and for isomer 2 were

collected between 17 and 19 min respectively. The appropriate fractions were combined and then evaporated to dryness to afford the two separated enantiomers as colourless gums: **282a** (5 mg), $[\alpha]_D^{20} = +8.5$ ($c = 0.50$ in MeOH) and **282b** (5 mg), $[\alpha]_D^{20} = -7.5$ ($c = 0.46$ in MeOH). The enantiomers were analysed on a Chiralpak AD-H (250 × 4.6mm, 5 micron) column with a flow rate of 1 mL/min and an isocratic gradient system of 90:10 hexane (0.2% isopropylamine v/v): ethanol (0.2% isopropylamine v/v) over 60 min. Isomer 1, **282a** (RT = 100% chiral purity by UV) and isomer 2, **282b** (97% chiral purity). The chromatogram is shown below. The stereochemistry was assigned by matching the optical rotation and the retention time of the *R*-enantiomer **282b** with that of the enantiopure **282c**.

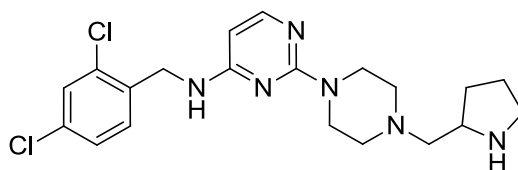


(*R*)-*N*-(2,4-dichlorobenzyl)-2-(2-(pyrrolidin-2-ylmethyl)-2,8-diazaspiro[4.5]decan-8-yl)pyrimidin-4-amine (282c)



LiAlH₄ (0.20 mL of a 1 M solution in diethyl ether, 0.20 mmol) was added to a solution of **262d** (75 mg, 0.14 mmol) in THF (1 mL) at 0 °C, and the reaction mixture was stirred at room temperature for 18 h. Water (8 µL) was added, followed by aqueous sodium hydroxide (8 µL of 2 M solution) and more water (24 µL). The reaction was stirred at room temperature for 0.5 h, anhydrous magnesium sulfate was then added and the mixture was stirred for an additional 15 min, before being filtered under vacuum. The filtrate was then partitioned between EtOAc (10 mL) and water (10 mL). The organic layer was separated, and the aqueous layer was extracted with more EtOAc (3 × 10 mL). The combined organic layers were dried using a hydrophobic frit and concentrated under reduced pressure. The crude product was taken up in DMSO (1 mL) and purified by MDAP (Method C). The solvent was evaporated and the solid was taken up in methanol (1 mL) and passed through an aminopropyl cartridge (1 g). The cartridge was washed with additional methanol and the eluent was evaporated under reduced pressure to afford the title product (34 mg, 50%) as a colourless gum; $[\alpha]_D^{20} = -5.1$ ($c = 0.47$ in MeOH); Chiral HPLC RT = 36.5 min, 99% chiral purity (Chiralpak AD, 250 × 4.6 mm, col. no. ADOOCE-NK016, 5% ethanol/heptane [0.1% isopropylamine], flow rate of 1 mL/min); ¹H NMR (500 MHz, MeOD-*d*₄) $\delta = 7.68$ (d, $J = 6.0$ Hz, 1H), 7.42 (d, $J = 1.5$ Hz, 1H), 7.33 (d, $J = 8.0$ Hz, 1H), 7.24 (dd, $J = 8.0, 1.5$ Hz, 1H), 5.83 (d, $J = 6.0$ Hz, 1H), 4.57 (s, 2H), 3.79 - 3.43 (m, 4H), 3.19 - 3.07 (m, 1H), 3.00 - 2.89 (m, 1H), 2.83 - 2.75 (m, 1H), 2.71 - 2.64 (m, 1H), 2.63 - 2.56 (m, 1H), 2.56 - 2.33 (m, 4H), 1.97 - 1.87 (m, 1H), 1.81 - 1.71 (m, 2H), 1.66 (t, $J = 7.0$ Hz, 2H), 1.56 - 1.21 (m, 5H); the two exchangeable NH protons were not observed; ¹³C NMR (126 MHz, MeOD-*d*₄) $\delta = 164.2, 162.7, 155.7, 137.7, 134.9, 134.2, 131.2, 130.1, 128.3, 96.5, 67.5, 62.8, 58.4, 55.2, 46.8, 43.1, 43.0, 41.8, 38.8, 37.8, 31.4, 25.9$; IR ν_{\max} (neat) 3300, 2922, 1587, 1491, 1448, 1338 cm⁻¹; HRMS (ESI) m/z calculated for C₂₄H₃₃Cl₂N₆ = 475.2138. Found = 457.2134; [M+H]⁺; LCMS (Method A, UV, ES) RT = 0.57 min, [M+H]⁺ = 475, 477, 479, 97% purity.

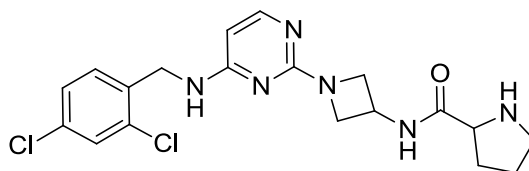
(±)-*N*-(2,4-Dichlorobenzyl)-2-(4-(pyrrolidin-2-ylmethyl)piperazin-1-yl)pyrimidin-4-amine (283)



The pyrimidine **283** was prepared from *N*-(2,4-dichlorobenzyl)-2-(piperazin-1-yl)pyrimidin-4-amine (BMS intermediate⁷³) (120 mg, 0.319 mmol) and (*R*)-*tert*-butyl 2-formylpyrrolidine-

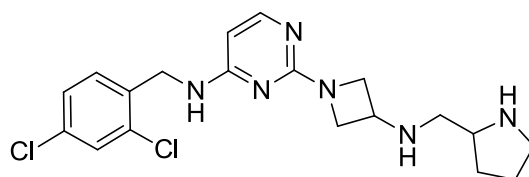
1-carboxylate (64 mg, 0.32 mmol) according to the procedure described for the preparation of **282**. The same work up and purification method afforded the title compound (115 mg, 85%) as a white solid; $[\alpha]_D^{20} = 0$ ($c = 0.50$ in MeOH) indicating that the product had racemised; ^1H NMR (400 MHz, MeOD- d_4) $\delta = 7.64$ (d, $J = 6.0$ Hz, 1H), 7.35 (d, $J = 2.0$ Hz, 1H), 7.25 (d, $J = 8.0$ Hz, 1H), 7.18 (dd, $J = 8.0, 2.0$ Hz, 1H), 5.82 (d, $J = 6.0$ Hz, 1H), 4.51 (s, 2H), 3.85 - 3.70 (m, 1H), 3.65 - 3.45 (m, 4H), 3.30 - 3.14 (m, 2H), 2.57 - 2.37 (m, 4H), 2.33 - 2.19 (m, 2H), 2.15 - 2.04 (m, 1H), 2.03 - 1.90 (m, 2H), 1.65 - 1.47 (m, 1H); the two exchangeable NH protons were not observed; LCMS (Method D, UV, ES) RT = 1.60 min, $[\text{M}+\text{H}]^+ = 421, 423, 425$, 100% purity

(±)-*N*-(1-(4-((2,4-Dichlorobenzyl)amino)pyrimidin-2-yl)azetidin-3-yl)pyrrolidine-2-carboxamide (284)



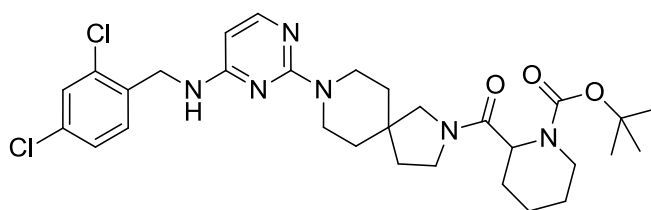
The pyrimidine **284** was prepared from **262a** (200 mg, 0.617 mmol) and (±)-1-(*tert*-butoxycarbonyl)pyrrolidine-2-carboxylic acid (159 mg, 0.740 mmol) according to the procedure described for the preparation of **255a**. The same work up and purification method afforded the title compound (41 mg, 16%) as a white solid; ^1H NMR (400 MHz, MeOD- d_4) $\delta = 7.63$ (d, $J = 6.0$ Hz, 1H), 7.39 (d, $J = 2.0$ Hz, 1H), 7.34 (d, $J = 8.0$ Hz, 1H), 7.23 (dd, $J = 8.0, 2.0$ Hz, 1H), 5.86 (d, $J = 6.0$ Hz, 1H), 4.61 - 4.48 (m, 3H), 4.23 (t, $J = 8.0$ Hz, 2H), 3.79 (dd, $J = 8.0, 6.0$ Hz, 2H), 3.58 (dd, $J = 8.0, 6.0$ Hz, 1H), 3.02 - 2.93 (m, 1H), 2.89 - 2.80 (m, 1H), 2.16 - 2.03 (m, 1H), 1.76 - 1.64 (m, 3H); the three exchangeable protons were not observed; LCMS (Method D, UV, ES) RT = 1.63 min, $[\text{M}+\text{H}]^+ = 421, 423, 425$, 100% purity.

***N*-(2,4-Dichlorobenzyl)-2-(3-((pyrrolidin-2-ylmethyl)amino)azetidin-1-yl)pyrimidin-4-amine (285)**



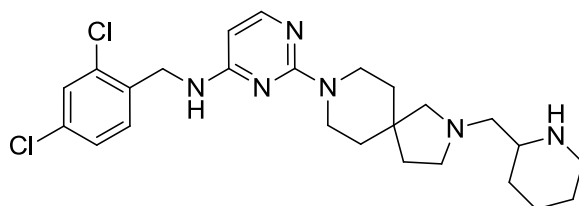
The pyrimidine **285** was prepared from **262a** (110 mg, 0.28 mmol) according to the procedure described for the preparation of **282**. The same work up and purification method afforded the title compound (40 mg, 35%) as a white solid; ^1H NMR (500 MHz, MeOH- d_4) δ = 7.66 (d, J = 5.5 Hz, 1H), 7.42 (s, 1H), 7.38 (d, J = 8.0 Hz, 1H), 7.26 (d, J = 8.0 Hz, 1H), 5.87 (d, J = 5.5 Hz, 1H), 4.58 (br. s, 2H), 4.15 (t, J = 7.0 Hz, 2H), 3.76 - 3.69 (m, 2H), 3.69 - 3.62 (m, 1H), 3.12 (quin, J = 7.0 Hz, 1H), 2.94 - 2.87 (m, 1H), 2.87 - 2.78 (m, 1H), 2.56 (d, J = 6.5 Hz, 2H), 2.01 - 1.87 (m, 1H), 1.86 - 1.67 (m, 2H), 1.45 - 1.29 (m, 1H); the three exchangeable NH protons were not observed; ^{13}C NMR (126 MHz, MeOH- d_4) δ = 164.4, 164.1, 155.1, 137.5, 135.2, 134.4, 131.8, 130.1, 128.2, 97.2, 59.4, 58.1, 58.0, 52.7, 47.0, 42.5, 30.9, 26.2; HRMS (ESI) m/z calculated for $\text{C}_{19}\text{H}_{25}\text{Cl}_2\text{N}_6$ = 407.1512. Found = 407.1514; $[\text{M}+\text{H}]^+$; LCMS (Method A, UV, ES) RT = 0.46 min, $[\text{M}+\text{H}]^+$ = 407, 409, 411, 97% purity.

(±)-tert-Butyl 2-(8-(4-((2,4-dichlorobenzyl)amino)pyrimidin-2-yl)-2,8-diazaspiro[4.5]decane-2-carbonyl)piperidine-1-carboxylate (286)



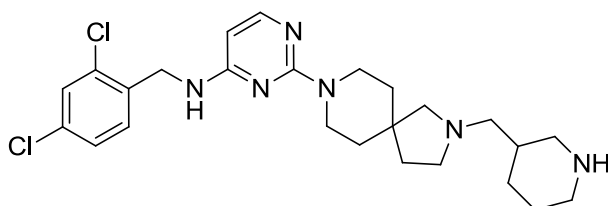
HATU (113 mg, 0.298 mmol) was added to a mixture of (±)-1-(tert-butoxy carbonyl)piperidine-2-carboxylic acid (53 mg, 0.23 mmol), **262d** (90 mg, 0.23 mmol) and DIPEA (0.12 mL, 0.69 mmol) in DMF (0.8 mL) and the reaction mixture was stirred at ambient temperature for 30 min. The reaction mixture was diluted with DMF (0.4 mL) and purified directly by MDAP (Method B). The appropriate fractions were collected and the solvent was evaporated under reduced pressure to afford the title compound (92 mg, 66%) as a white solid; ^1H NMR (400 MHz, MeOD- d_4) δ = 7.72 (d, J = 6.0, 1H), 7.45 (t, J = 2.0 Hz, 1H), 7.35 (d, J = 8.0 Hz, 1H), 7.28 (dd, J = 8.0, 2.0 Hz, 1H), 5.89 (d, J = 6.0 Hz, 1H), 4.78 (br. s, 1H), 4.60 (s, 2H), 3.94 - 3.84 (m, 1H), 3.82 - 3.72 (m, 2H), 3.64 - 3.47 (m, 4H), 3.44 - 3.35 (m, 2H), 3.30 - 3.20 (m, 1H), 1.99 - 1.88 (m, 2H), 1.86 - 1.69 (m, 3H), 1.69 - 1.58 (m, 2H), 1.56 - 1.26 (m, 14H); the exchangeable NH proton was not observed LCMS (Method A, UV, ES) RT = 1.05 min, $[\text{M}+\text{H}]^+$ = 604, 606, 608, 100% purity.

(±)-*N*-(2,4-Dichlorobenzyl)-2-(2-(piperidin-2-ylmethyl)-2,8-diazaspiro[4.5]decan-8-yl)pyrimidin-4-amine (**287**)



BH₃.THF (0.08 mL of a 1 M solution in THF, 0.08 mmol) was added to a stirring solution of **286** (16 mg, 0.016 mmol) in THF (0.2 mL) and the reaction mixture was stirred at ambient temperature for 18 h. MeOH (1 mL) and HCl (0.5 mL of a 6 M aqueous solution) were slowly added and the reaction was refluxed for 30 min. The reaction mixture was concentrated, taken up in DMSO (1 mL) and purified on the MDAP (Method B). The appropriate fractions were combined and the solvent was evaporated under reduced pressure to afford the title compound (4 mg, 51%) as a white solid; ¹H NMR (400 MHz, MeOD-*d*₄) δ = 7.70 (d, *J* = 6.0 Hz, 1H), 7.45 (d, *J* = 2.0 Hz, 1H), 7.35 (d, *J* = 8.0 Hz, 1H), 7.27 (dd, *J* = 8.0, 2.0 Hz, 1H), 5.85 (d, *J* = 6.0 Hz, 1H), 4.59 (s, 2H), 3.78 - 3.63 (m, 2H), 3.60 - 3.48 (m, 2H), 3.05 (d, *J* = 12.0 Hz, 1H), 2.77 - 2.59 (m, 3H), 2.58 - 2.35 (m, 4H), 2.24 (dd, *J* = 12.0, 4.0 Hz, 1H), 1.81 (d, *J* = 12.0 Hz, 1H), 1.73 - 1.60 (m, 4H), 1.55 - 1.37 (m, 6H), 1.18 - 1.03 (m, 1H); the two exchangeable NH protons were not observed; LCMS (Method D, UV, ES) RT = 1.69 min, [M+H]⁺ = 489, 491, 493, 100% purity.

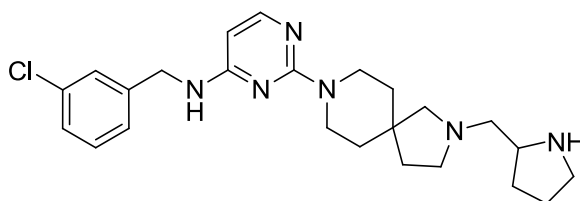
(±)-*N*-(2,4-Dichlorobenzyl)-2-(2-(piperidin-3-ylmethyl)-2,8-diazaspiro[4.5]decan-8-yl)pyrimidin-4-amine (**288**)



The spiro-pyrimidine **288** was prepared from **262d** (40 mg, 0.10 mmol) and (±)-*tert*-butyl 3-formylpiperidine-1-carboxylate (22 mg, 0.10 mmol) according to the procedure described for the preparation of **282**. The same work up and purification method afforded the title compound (14 mg, 28%) as a white solid; ¹H NMR (400 MHz, MeOD-*d*₄) δ = 7.70 (d, *J* = 6.0 Hz, 1H), 7.46 (d, *J* = 2.0 Hz, 1H), 7.35 (d, *J* = 8.0 Hz, 1H), 7.28 (dd, *J* = 8.0, 2.0 Hz, 1H),

5.85 (d, $J = 6.0$ Hz, 1H), 4.59 (s, 2H), 3.72 - 3.63 (m, 2H), 3.61 - 3.51 (m, 2H), 3.15 (d, $J = 12.0$ Hz, 1H), 3.00 (d, $J = 12.0$ Hz, 1H), 2.66 - 2.49 (m, 3H), 2.48 - 2.16 (m, 5H), 1.87 (d, $J = 12.0$ Hz, 1H), 1.77 - 1.63 (m, 4H), 1.59 - 1.50 (m, 1H), 1.47 (br. s, 4H), 1.16 - 1.01 (m, 1H); the two exchangeable NH protons were not observed; LCMS (Method D, UV, ES) RT = 1.65 min, $[M+H]^+ = 489, 491, 493$, 100% purity.

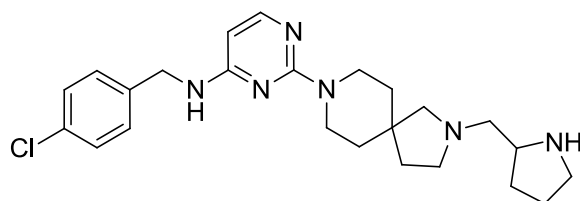
(±)-*N*-(3-Chlorobenzyl)-2-(2-(pyrrolidin-2-ylmethyl)-2,8-diazaspiro[4.5]decan-8-yl)pyrimidin-4-amine (289)



The spiro-pyrimidine **289** was prepared from **281b** (90 mg, 0.25 mmol) and (*R*)-*tert*-butyl 2-formylpyrrolidine-1-carboxylate (50 mg, 0.25 mmol) according to the same procedure described for the preparation of **282**. The same work up and purification method afforded the title compound (26 mg, 23%) as a white solid; $[\alpha]_D^{20} = 0^*$ ($c = 0.50$ in MeOH); $^1\text{H NMR}$ (400 MHz, MeOD- d_4) $\delta = 7.69$ (d, $J = 6.0$ Hz, 1H), 7.35 (s, 1H), 7.31 - 7.15 (m, 3H), 5.81 (d, $J = 6.0$ Hz, 1H), 4.51 (s, 2H), 3.76 - 3.66 (m, 2H), 3.65 - 3.54 (m, 2H), 3.28 - 3.15 (m, 1H), 2.99 (td, $J = 10.5, 7.0$ Hz, 1H), 2.91 - 2.82 (m, 1H), 2.77 - 2.37 (m, 6H), 2.03 - 1.90 (m, 1H), 1.86 - 1.76 (m, 2H), 1.73 - 1.65 (m, 2H), 1.53 (br. s, 4H), 1.47 - 1.37 (m, 1H); the two exchangeable NH protons were not observed; LCMS (Method D, UV, ES) RT = 1.51 min, $[M+H]^+ = 441, 443$, 100% purity.

*The product had racemised during synthesis.

(±)-*N*-(4-Chlorobenzyl)-2-(2-(pyrrolidin-2-ylmethyl)-2,8-diazaspiro[4.5]decan-8-yl)pyrimidin-4-amine (290)

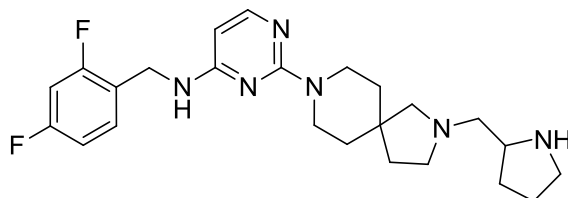


The spiro-pyrimidine **290** was prepared from **281c** (90 mg, 0.25 mmol) and (*R*)-*tert*-butyl 2-formylpyrrolidine-1-carboxylate (50 mg, 0.25 mmol) according to the procedure described

for the preparation of **282**. The same work up and purification method afforded the title compound (24 mg, 22%) as a white solid; $[\alpha]_{\text{D}}^{20} = 0^*$ ($c = 0.49$ in MeOH); $^1\text{H NMR}$ (400 MHz, MeOD- d_4) $\delta = 7.62$ (d, $J = 6.0$ Hz, 1H), 7.25 (s, 4H), 5.75 (d, $J = 6.0$ Hz, 1H), 4.45 (s, 2H), 3.69 - 3.60 (m, 2H), 3.58 - 3.49 (m, 2H), 3.17 (dd, $J = 7.5, 6.0$ Hz, 1H), 2.98 - 2.88 (m, 1H), 2.80 (td, $J = 10.5, 7.0$ Hz, 1H), 2.71 - 2.29 (m, 6H), 1.97 - 1.85 (m, 1H), 1.79 - 1.70 (m, 2H), 1.64 (t, $J = 7.0$ Hz, 2H), 1.50 - 1.42 (m, 4H), 1.42 - 1.31 (m, 1H); the two exchangeable NH protons were not observed; LCMS (Method D, UV, ES) RT = 1.57 min, $[\text{M}+\text{H}]^+ = 441, 443, 100\%$ purity.

*The product had racemised during synthesis.

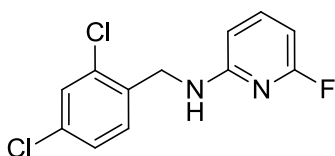
(±)-*N*-(2,4-Difluorobenzyl)-2-(2-(pyrrolidin-2-ylmethyl)-2,8-diazaspiro[4.5]decan-8-yl)pyrimidin-4-amine (291)



The spiro-pyrimidine **291** was prepared from **281k** (free base) (36 mg, 0.10 mmol) and (*R*)-*tert*-butyl 2-formylpyrrolidine-1-carboxylate (20 mg, 0.10 mmol) according to the procedure described for the preparation of **282**. The same work up and purification method afforded the title compound (20 mg, 45%) as a beige coloured solid; $[\alpha]_{\text{D}}^{20} = 0^*$ ($c = 0.46$ in MeOH); $^1\text{H NMR}$ (400 MHz, MeOD- d_4) $\delta = 7.68$ (d, $J = 6.0$ Hz, 1H), 7.45 - 7.32 (m, 1H), 7.00 - 6.80 (m, 2H), 5.81 (d, $J = 6.0$ Hz, 1H), 4.55 (s, 2H), 3.80 - 3.67 (m, 2H), 3.66 - 3.55 (m, 2H), 3.28 - 3.14 (m, 1H), 3.05 - 2.94 (m, 1H), 2.85 (td, $J = 10.0, 7.0$ Hz, 1H), 2.77 - 2.37 (m, 6H), 2.06 - 1.90 (m, 1H), 1.86 - 1.75 (m, 2H), 1.71 (t, $J = 7.0$ Hz, 2H), 1.58 - 1.46 (m, 4H), 1.46 - 1.37 (m, 1H); the two exchangeable NH protons were not observed; LCMS (Method D, UV, ES) RT = 1.45 min, $[\text{M}+\text{H}]^+ = 443, 99\%$ purity.

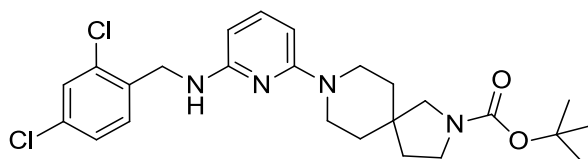
*The product had racemised during synthesis.

***N*-(2,4-Dichlorobenzyl)-6-fluoropyridin-2-amine (293)**



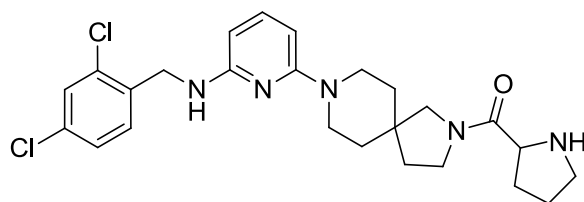
A mixture of 6-fluoro-2-pyridinamine (400 mg, 3.57 mmol) and 2,4-dichlorobenzaldehyde (624 mg, 3.57 mmol) in anhydrous DCM (3 mL) were stirred at ambient temperature, under a nitrogen atmosphere for 1 h. Acetic acid (0.020 mL, 0.36 mmol) and sodium triacetoxyborohydride (1.66 g, 7.85 mmol) were added and the reaction mixture was stirred for an additional 48 h. The reaction mixture was partitioned between DCM (30 mL) and water (30 mL), and the organic layer was separated, passed through a hydrophobic frit and concentrated under reduced pressure. The crude residue was taken up in DMSO (4 mL) and purified on the MDAP (Method A). The appropriate fractions were combined and the solvent was evaporated under reduced pressure to afford the title compound (427 mg, 44%) as a white solid; $^1\text{H NMR}$ (400 MHz, $\text{MeOD-}d_4$) δ = 7.51 - 7.44 (m, 1H), 7.43 (d, J = 2.0 Hz, 1H), 7.37 (d, J = 8.0 Hz, 1H), 7.25 (dd, J = 8.0, 2.0 Hz, 1H), 6.34 (dd, J = 8.0, 2.0 Hz, 1H), 6.09 (dd, J = 8.0, 2.0 Hz, 1H), 4.53 (s, 2H); the exchangeable NH proton was not observed; LCMS (Method B, UV, ES) RT = 1.32 min, $[\text{M}+\text{H}]^+$ = 271, 273, 275 100% purity.

***tert*-Butyl 8-((2,4-dichlorobenzyl)amino)pyridin-2-yl)-2,8-diazaspiro[4.5]decane-2-carboxylate (294)**



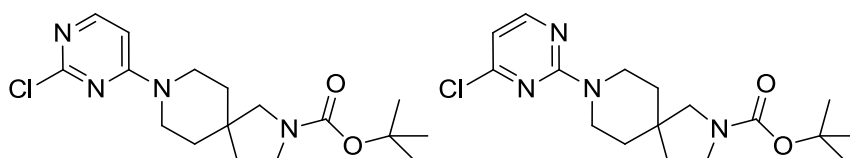
A mixture of **293** (50 mg, 0.18 mmol), *tert*-butyl 2,8-diazaspiro[4.5]decane-2-carboxylate (**260d**) (44 mg, 0.18 mmol) and DIPEA (0.1 mL, 0.57 mmol) in acetonitrile (0.1 mL) were sealed in a Reacti-VialTM and heated at 140 °C for 5 days. LCMS showed the reaction only went to 33% completion. The reaction mixture was partitioned between DCM (10 mL) and water (10 mL). The organic layer was separated, passed through a hydrophobic frit and concentrated. The crude residue was taken up in DMSO (1 mL) and purified on the MDAP (Method A). The appropriate fractions were combined and the solvent was evaporated under reduced pressure to afford the title compound (22 mg, 24%) as a colourless oil; $^1\text{H NMR}$ (400 MHz, $\text{MeOD-}d_4$) δ = 7.39 (d, J = 2.0 Hz, 1H), 7.36 (d, J = 8.0 Hz, 1H), 7.25 - 7.16 (m, 2H), 5.95 (d, J = 8.0 Hz, 1H), 5.85 (d, J = 8.0 Hz, 1H), 4.52 (s, 2H), 3.55 - 3.33 (m, 5H), 3.16 (s, 2H), 1.73 (t, J = 7.0 Hz, 2H), 1.48 - 1.39 (m, 14H); the exchangeable NH proton was not observed; LCMS (Method B, UV, ES) RT = 1.59 min, $[\text{M}+\text{H}]^+$ = 491, 493, 495, 95% purity.

(±)-8-(6-((2,4-Dichlorobenzyl)amino)pyridin-2-yl)-2,8-diazaspiro[4.5]decan-2-yl)(pyrrolidin-2-yl)methanone (295)



A mixture of **294** (19 mg, 0.039 mmol) and TFA (0.5 mL) were stirred at ambient temperature for 15 min before being concentrated under reduced pressure. DMF (0.5 mL) was then added, followed by (±)-1-(*tert*-butoxycarbonyl)pyrrolidine-2-carboxylic acid (8 mg, 0.04 mmol), HATU (15 mg, 0.039 mmol) and DIPEA (0.020 mL, 0.12 mmol), and the reaction mixture was stirred at ambient temperature for 18 h. The mixture was partitioned between EtOAc (20 mL) and water (15 mL). The organic layer was separated, passed through a hydrophobic frit and concentrated. TFA (0.5 mL) was then added and the mixture was stirred for 10 min. The reaction mixture was concentrated and the crude product was taken up in DMSO (1 mL) and purified on the MDAP (Method C). The appropriate fractions were combined and the solvent was evaporated under reduced pressure. The residue was then dissolved in methanol (0.5 mL) and passed through an aminopropyl cartridge (0.5 g). The cartridge was washed with additional methanol, and the filtrate was concentrated to afford the title product (2.7 mg, 14%) as a colourless gum; ¹H NMR (400 MHz, MeOD-*d*₄) δ = 7.40 (t, *J* = 1.5 Hz, 1H), 7.36 (d, *J* = 8.5 Hz, 1H), 7.25 - 7.17 (m, 2H), 5.97 (dd, *J* = 8.0 2.5, Hz, 1H), 5.86 (d, *J* = 8.0 Hz, 1H), 4.52 (s, 2H), 3.77 (t, *J* = 7.5 Hz, 1H), 3.71 - 3.32 (m, 8H), 3.19 - 3.08 (m, 1H), 2.82 - 2.71 (m, 1H), 2.26 - 2.12 (m, 1H), 1.91 - 1.72 (m, 4H), 1.69 - 1.58 (m, 1H), 1.50 - 1.41 (m, 4H); the two exchangeable NH protons were not observed; LCMS (Method D, UV, ES) RT = 2.00 min, [M+H]⁺ = 490, 492, 494, 100% purity.

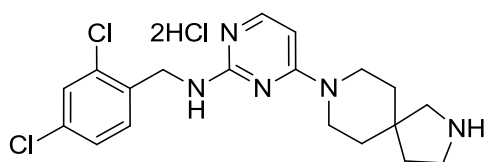
***tert*-Butyl 8-(2-chloropyrimidin-4-yl)-2,8-diazaspiro[4.5]decane-2-carboxylate (296) and *tert*-butyl 8-(4-chloropyrimidin-2-yl)-2,8-diazaspiro[4.5]decane-2-carboxylate (297)**



tert-Butyl 2,8-diazaspiro[4.5]decane-2-carboxylate, **260d** (0.40 g, 1.7 mmol) was added to a stirring solution of 2,4-dichloropyrimidine (0.25 g, 1.7 mmol) and DIPEA (0.38 mL, 2.2 mmol) in anhydrous DCE (3 mL), and the reaction was stirred at ambient temperature under a

nitrogen atmosphere for 24 h. The reaction mixture was diluted with water (20 mL) and extracted with DCM (3 × 25 mL). The combined organic layers were washed with brine (25 mL), dried using a hydrophobic frit and concentrated under reduced pressure. The crude mixture was purified by column chromatography on a silica column, using a gradient of 0-100% ethyl acetate-cyclohexane over 40 min. The appropriate fractions were combined and evaporated under reduced pressure to afford the separated regioisomers as white solids: *tert*-butyl 8-(2-chloropyrimidin-4-yl)-2,8-diazaspiro[4.5]decane-2-carboxylate **296** (335 mg, 57%); ¹H NMR (600 MHz, MeOD-*d*₄) δ = 7.98 (d, *J* = 6.2 Hz, 1H), 6.72 (d, *J* = 6.4 Hz, 1H), 3.92 - 3.56 (m, 4H), 3.49 - 3.40 (m, 2H), 3.30 - 3.23 (m, 1H), 3.27 (s, 1H), 1.87 (t, *J* = 7.2 Hz, 2H), 1.71 - 1.60 (m, 4H), 1.48 (s, 9H); LCMS (Method A, UV, ES) RT = 1.08 min, [M+H]⁺ = 353, 355, 100% purity, and *tert*-butyl 8-(4-chloropyrimidin-2-yl)-2,8-diazaspiro[4.5]decane-2-carboxylate **297** (70 mg, 12%); ¹H NMR (600 MHz, MeOD-*d*₄) δ = 8.19 (d, *J* = 5.1 Hz, 1H), 6.58 (d, *J* = 5.1 Hz, 1H), 4.00 - 3.67 (m, 4H), 3.55 - 3.36 (m, 4H), 1.86 (t, *J* = 7.2 Hz, 2H), 1.65 - 1.56 (m, 4H), 1.49 (s, 9H); LCMS (Method A, UV, ES) RT = 1.32 min, [M+H]⁺ = 353, 355.

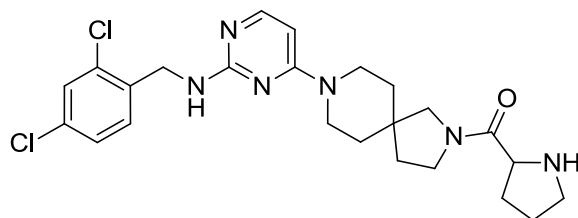
***N*-(2,4-Dichlorobenzyl)-4-(2,8-diazaspiro[4.5]decan-8-yl)pyrimidin-2-amine, dihydrochloride salt (298)**



A mixture of **296** (150 mg, 0.425 mmol), 2,4-dichlorobenzylamine (0.063 mL, 0.47 mmol) and IPA (1 mL) were heated in the microwave at 140 °C for 1 h. The reaction was cooled to ambient temperature, and ether (5 mL) was added. The precipitated solid was collected by filtration, washed with ether (10 mL), and dried under reduced pressure. HCl (1.0 mL of a 4 M solution in dioxane, 4.0 mmol) was added and the reaction was stirred at ambient temperature for 1.5 h. The reaction mixture was concentrated under reduced pressure and the residue was diluted with DCM (20 mL). The solvent was removed under reduced pressure, and dried under high vacuum to afford the title product (147 mg, 74%) as a colourless gum; ¹H NMR (400 MHz, DMSO-*d*₆) δ = 6.92 (d, *J* = 7.5 Hz, 1H), 6.70 (d, *J* = 2.0 Hz, 1H), 6.61 (d, *J* = 8.0 Hz, 1H), 6.53 (dd, *J* = 8.0, 2.0 Hz, 1H), 5.70 (d, *J* = 7.5 Hz, 1H), 3.88 (s, 2H), 3.09 - 2.78 (m, 4H), 2.62 (t, *J* = 7.5 Hz, 2H), 2.38 (s, 2H), 1.22 (t, *J* = 7.5 Hz, 2H), 0.89 (br. s, 4H);

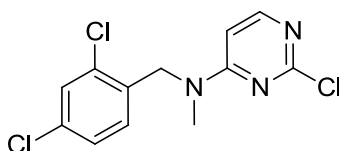
the four exchangeable protons were not observed; LCMS (Method A, UV, ES) RT = 0.54 min, $[M+H]^+ = 358, 360, 362$, 100% purity.

(±)-(8-(2-((2,4-Dichlorobenzyl)amino)pyrimidin-4-yl)-2,8-diazaspiro[4.5]decan-2-yl)(pyrrolidin-2-yl)methanone (299)



The spiro-pyrimidine **299** was prepared from **298** (110 mg, 0.236 mmol) and (±)-1-(*tert*-butoxycarbonyl)pyrrolidine-2-carboxylic acid (51 mg, 0.24 mmol) according to the procedure described for the preparation of **255a**. The same work up and purification method afforded the title compound (77 mg, 67%) as a colourless gum; $^1\text{H NMR}$ (400 MHz, $\text{MeOD-}d_4$) $\delta = 7.74$ (dd, $J = 6.0, 1.0$ Hz, 1H), 7.41 (t, $J = 2.0$ Hz, 1H), 7.34 (d, $J = 8.0$ Hz, 1H), 7.23 (dd, $J = 8.0, 2.0$ Hz, 1H), 6.05 (dd, $J = 6.0, 3.0$ Hz, 1H), 4.55 (s, 2H), 3.77 (t, $J = 7.5$ Hz, 1H), 3.70 - 3.42 (m, 6H), 3.39 - 3.33 (m, 2H), 3.19 - 3.08 (m, 1H), 2.83 - 2.70 (m, 1H), 2.24 - 2.12 (m, 1H), 1.89 (t, $J = 7.0$ Hz, 1H), 1.86 - 1.72 (m, 3H), 1.71 - 1.58 (m, 1H), 1.54 - 1.41 (m, 4H); the two exchangeable NH protons were not observed; $^{13}\text{C NMR}$ (101 MHz, $\text{MeOD-}d_4$) $\delta = 174.4, 174.3, 163.6, 163.0, 157.0, 138.3, 134.7, 134.0, 130.9, 130.0, 128.2, 94.8, 60.2, 60.0, 57.1, 56.8, 45.7, 43.4, 43.0, 42.7, 42.6, 40.8, 37.0, 35.2, 35.1, 35.0, 34.9, 34.8, 31.4, 31.3, 27.4$ (the additional peaks were observed due to rotamers); HRMS (ESI) m/z calculated for $\text{C}_{24}\text{H}_{31}\text{Cl}_2\text{N}_6\text{O} = 489.1931$. Found = 489.1920 $[M+H]^+$; LCMS (Method A, UV, ES) RT = 0.59 min, $[M+H]^+ = 489, 491, 493$, 100% purity.

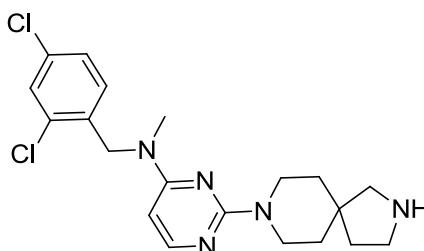
2-Chloro-*N*-(2,4-dichlorobenzyl)-*N*-methylpyrimidin-4-amine (301)



The pyrimidine **301** was prepared from 2,4-dichloropyrimidine (0.50 g, 3.4 mmol), [(2,4-dichlorophenyl)methyl]methylamine (0.64 g, 3.4 mmol) and DIPEA (1.3 mL, 7.4 mmol) according to the procedure described for the preparation of **259**. The same work up and purification afforded the title compound (0.39 g, 38%) as a white solid; $^1\text{H NMR}$ (400 MHz,

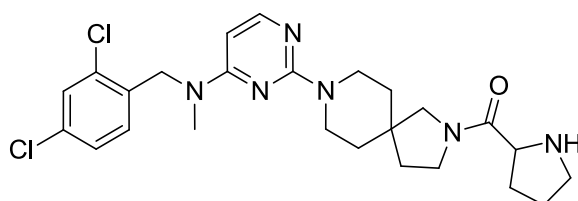
MeOD- d_4) δ = 8.04 (br. s, 1H), 7.52 (d, J = 2.0 Hz, 1H), 7.31 (dd, J = 8.0, 2.0 Hz, 1H), 7.12 (d, J = 8.0 Hz, 1H), 6.66 (br. s, 1H), 4.89 (s, 2H (obscured by HOD*)), 3.13 (br. s, 3H); LCMS (Method A, UV, ES) RT = 1.28 min, $[M+H]^+$ = 302, 304, 306, 100% purity. *The presence of signal was inferred by comparison with **259**.

***N*-(2,4-Dichlorobenzyl)-*N*-methyl-2-(2,8-diazaspiro[4.5]decan-8-yl)pyrimidin-4-amine (302)**



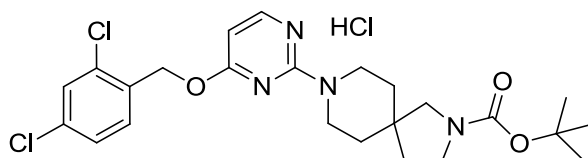
A mixture of **301** (200 mg, 0.661 mmol), *tert*-butyl 2,8-diazaspiro[4.5]decan-2-carboxylate (159 mg, 0.661 mmol) and IPA (1 mL) were stirred at 90 °C for 24 h. The reaction was cooled to ambient temperature, concentrated under reduced pressure and treated with HCl (1.0 mL of a 4 M solution in dioxane, 4.0 mmol). The reaction was stirred at ambient temperature for 30 min and was then partitioned between EtOAc (30 mL) and saturated aqueous sodium bicarbonate solution (30 mL). The organic layer was separated, dried using a hydrophobic frit and concentrated under reduced pressure to afford the title compound (180 mg, 67%) as a pale brown oil; ^1H NMR (400 MHz, MeOD- d_4) δ = 7.86 (d, J = 6.0 Hz, 1H), 7.49 (d, J = 2.0 Hz, 1H), 7.28 (dd, J = 8.0, 2.0 Hz, 1H), 7.07 (d, J = 8.0 Hz, 1H), 6.00 (d, J = 6.0 Hz, 1H), 4.84 (br. s, 2H), 3.81 - 3.66 (m, 2H), 3.65 - 3.52 (m, 2H), 3.14 (s, 3H), 2.98 (t, J = 7.0 Hz, 2H), 2.72 (s, 2H), 1.76 - 1.59 (m, 2H), 1.53 - 1.39 (m, 4H); the exchangeable NH proton was not observed; LCMS (Method D, UV, ES) RT = 1.82 min, $[M+H]^+$ = 407, 409, 411, 87% purity.

(±)-(8-(4-((2,4-Dichlorobenzyl)(methyl)amino)pyrimidin-2-yl)-2,8-diazaspiro[4.5]decan-2-yl)(pyrrolidin-2-yl)methanone (303)



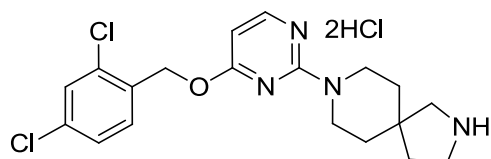
The spiro-pyrimidine **303** was prepared from **302** (94 mg, 0.23 mmol) and (\pm)-1-(*tert*-butoxycarbonyl)pyrrolidine-2-carboxylic acid (50 mg, 0.23 mmol) according to the procedure described for the preparation of **255a**. The same work up and purification method afforded the title compound (31 mg, 26%) as a colourless gum; $^1\text{H NMR}$ (400 MHz, $\text{MeOD-}d_4$) δ = 7.87 (d, J = 6.0 Hz, 1H), 7.49 (t, J = 2.0 Hz, 1H), 7.27 (dd, J = 8.0, 2.0 Hz, 1H), 7.06 (d, J = 8.0 Hz, 1H), 6.01 (d, J = 6.0 Hz, 1H), 4.84 (br. s, 2H), 3.89 - 3.43 (m, 8H), 3.23 - 3.08 (m, 4H), 2.88 - 2.72 (m, 1H), 2.28 - 2.11 (m, 1H), 1.91 (t, J = 7.0 Hz, 1H), 1.88 - 1.73 (m, 3H), 1.73 - 1.59 (m, 2H), 1.49 (br. s, 4H); the exchangeable NH proton was not observed; LCMS (Method D, UV, ES) RT = 1.86 min, $[\text{M}+\text{H}]^+$ = 503, 505, 507, 100% purity.

***tert*-Butyl 8-(4-((2,4-dichlorobenzyl)oxy)pyrimidin-2-yl)-2,8-diazaspiro[4.5]decane-2-carboxylate, hydrochloride salt (**304**)**



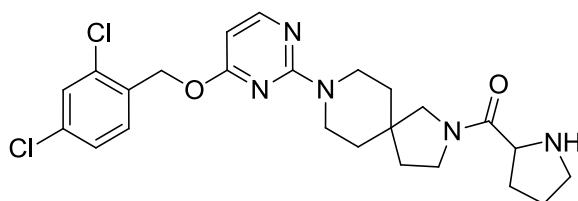
Sodium hydride (19 mg of a 60% w/w dispersion in mineral oil, 0.48 mmol) was added to a cooled (0 °C) solution of 2,4-dichlorobenzyl alcohol (42 mg, 0.24 mmol) in DMF (0.5 mL). The mixture was stirred at 0 °C for 10 min, and was then slowly warmed to 40 °C and stirred for 30 min. A solution of **297** (70 mg, 0.20 mmol) in DMF (0.5 mL) was then added, and the mixture was stirred at 40 °C for 3 h. The reaction mixture was partitioned between EtOAc (10 mL) and water (10 mL). The organic layer was separated, washed with brine, dried using a hydrophobic frit and concentrated under reduced pressure. The brown residue was then taken up in DMSO (2 mL) and purified by MDAP (Method C). The appropriate fractions were combined and the solvent was evaporated under reduced pressure to give the title product (54 mg, 51%) as a white solid. $^1\text{H NMR}$ (400 MHz, $\text{MeOD-}d_4$) δ = 8.07 (d, J = 7.0 Hz, 1H), 7.60 - 7.51 (m, 2H), 7.39 (dd, J = 8.0, 2.0 Hz, 1H), 6.45 (d, J = 7.0 Hz, 1H), 5.60 (s, 2H), 3.86 (br. s, 4H), 3.48 - 3.39 (m, 2H), 3.28 (s, 2H), 1.88 (t, J = 7.0 Hz, 2H), 1.76 - 1.67 (m, 4H), 1.47 (s, 9H); the exchangeable NH proton was not observed; LCMS (Method A, UV, ES) RT = 1.45 min, $[\text{M}+\text{H}]^+$ = 493, 495, 497, 98% purity.

8-(4-((2,4-Dichlorobenzyl)oxy)pyrimidin-2-yl)-2,8-diazaspiro[4.5]decane, dihydrochloride salt (305)



The spiro-pyrimidine **305** was prepared from **304** (54 mg, 0.10 mmol) and HCl (1.0 mL of a 4 M solution in dioxane, 4.0 mmol) according to the procedure described for the preparation of **262a**. The title compound was obtained (47 mg, 99%) as a colourless gum; ^1H NMR (400 MHz, MeOD- d_4) δ = 8.10 (d, J = 7.0 Hz, 1H), 7.63 - 7.56 (m, 2H), 7.43 (dd, J = 8.0, 2.0 Hz, 1H), 6.53 (d, J = 7.0 Hz, 1H), 5.65 (s, 2H), 3.80 - 3.73 (m, 1H), 3.72 - 3.65 (m, 2H), 3.63 - 3.57 (m, 1H), 3.48 (t, J = 7.5 Hz, 2H), 3.26 (s, 2H), 2.10 (t, J = 7.5 Hz, 2H), 1.87 (br. s, 4H); the three exchangeable protons were not observed; LCMS (Method A, UV, ES) RT = 0.82 min, $[\text{M}+\text{H}]^+$ = 393, 395, 397, 99% purity.

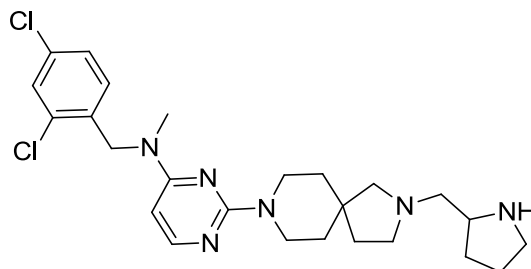
(±)-(8-(4-((2,4-Dichlorobenzyl)oxy)pyrimidin-2-yl)-2,8-diazaspiro[4.5]decan-2-yl)(pyrrolidin-2-yl)methanone (306)



The spiro-pyrimidine **306** was prepared from **305** (30 mg, 0.064 mmol) and (±)-1-(*tert*-butoxycarbonyl)pyrrolidine-2-carboxylic acid (14 mg, 0.064 mmol) according to the procedure described for the preparation of **255a**. The same work up and purification method afforded the title compound (19 mg, 60%) as a colourless gum; ^1H NMR (500 MHz, MeOD- d_4) δ = 8.04 (d, J = 6.0 Hz, 1H), 7.54 - 7.42 (m, 2H), 7.33 (dd, J = 8.0, 2.0 Hz, 1H), 6.10 (d, J = 6.0 Hz, 1H), 5.44 (s, 2H), 3.95 - 3.67 (m, 6H) 3.66 - 3.47 (m, 2H), 3.44 - 3.33 (m, 1H), 3.20 - 3.08 (m, 1H), 2.85 - 2.69 (m, 1H), 2.31 - 2.11 (m, 1H), 1.94 (t, J = 7.0 Hz, 1H), 1.88 - 1.72 (m, 3H), 1.72 - 1.62 (m, 1H), 1.60 - 1.44 (m, 4H); the exchangeable NH proton was not observed; ^{13}C NMR (126 MHz, MeOD- d_4) δ = 174.4, 174.3, 170.6, 162.7, 159.5, 135.5, 135.3, 135.0, 131.7, 130.3, 128.6, 97.6, 65.1, 60.3, 60.0, 57.1, 56.8, 48.3, 45.8, 43.0, 42.8, 42.7, 40.8, 37.0, 35.3, 35.2, 35.1, 35.0, 31.4, 31.3, 27.4 (the additional peaks were observed due to rotamers); HRMS (ESI) m/z calculated for $\text{C}_{24}\text{H}_{30}\text{Cl}_2\text{N}_5\text{O}_2$ = 490.1771. Found =

490.1771 [M+H]⁺; LCMS (Method A, UV, ES) RT = 0.84 min, [M+H]⁺ = 490, 492, 494, 100% purity.

(±)-*N*-(2,4-Dichlorobenzyl)-*N*-methyl-2-(2-(pyrrolidin-2-ylmethyl)-2,8-diazaspiro[4.5]decan-8-yl)pyrimidin-4-amine (**307**)



The spiro-pyrimidine **307** was prepared from **302** (90 mg, 0.22 mmol) and *tert*-butyl 2-formylpyrrolidine-1-carboxylate (44 mg, 0.22 mmol) according to the procedure described for the preparation of **282**. The same work up and purification method afforded the title compound (35 mg, 32%) as a white solid; ¹H NMR (400 MHz, MeOD-*d*₄) δ = 7.85 (d, *J* = 6.0 Hz, 1H), 7.49 (d, *J* = 2.0 Hz, 1H), 7.27 (dd, *J* = 8.0, 2.0 Hz, 1H), 7.06 (d, *J* = 8.0 Hz, 1H), 5.99 (d, *J* = 6.0 Hz, 1H), 4.83 (br. s, 2H), 3.74 - 3.49 (m, 4H), 3.30 - 3.19 (m, 1H), 3.13 (s, 3H), 3.01 (td, *J* = 10.0, 7.0 Hz, 1H), 2.87 (td, *J* = 10.0, 7.0 Hz, 1H), 2.77 - 2.67 (m, 1H), 2.67 - 2.35 (m, 5H), 2.03 - 1.92 (m, 1H), 1.88 - 1.76 (m, 2H), 1.69 (t, *J* = 7.0 Hz, 2H), 1.55 - 1.35 (m, 5H); the exchangeable NH proton was not observed; LCMS (Method D, UV, ES) RT = 1.72 min, [M+H]⁺ = 489, 491, 493, 100% purity.

References:

- (1) Asher, M. I.; Montefort, S.; Bjorksten, B.; Lai, C. K. W.; Strachan, P. D.; Weiland, K. S.; Williams, H. *Lancet* **2006**, *368*, 733-743.
- (2) <http://www.nhlbi.nih.gov/health/health-topics/topics/asthma> accessed on 03/2014.
- (3) Bloemen, K.; Verstraelen, S.; Van Den Heuvel, R.; Witters, H.; Nelissen, I.; Schoeters, G. *Immunol. Lett.* **2007**, *113*, 6-18.
- (4) Kim, H. Y.; De Kruyff, R. H.; Umetsu, D. T. *Nat. Immunol.* **2010**, *11*, 577-584.
- (5) Birnbaum, S.; Barreiro, T. J. *Chest* **2007**, *131*, 1932-1935.
- (6) Umetsu, D. T.; McIntire, J. J.; Akbari, O.; Macaubas, C.; DeKruyff, R. H. *Nat. Immunol.* **2002**, *3*, 715-720.
- (7) Holgate, S. T.; Polosa, R. *Nat. Rev. Immunol.* **2008**, *8*, 218-230.
- (8) Kay, A. B.; Ying, S.; Varney, V.; Gaga, M.; Durham, S. R.; Moqbel, R.; Wardlaw, A. J.; Hamid, Q. *J. Exp. Med.* **1991**, *173*, 775-778.
- (9) Hammad, H.; Lambrecht, B. N. *Nat. Rev. Immunol.* **2008**, *8*, 193-204.
- (10) Bischoff, S. C. *Nat. Rev. Immunol.* **2007**, *7*, 93-104.
- (11) Smit, J. J.; Lukacs, N. W. *Eur. J. Pharmacol.* **2006**, *533*, 277-288.
- (12) Lee, J. J.; Dimina, D.; Macias, M. P.; Ochkur, S. I.; McGarry, M. P.; O'Neill, K. R.; Protheroe, C.; Pero, R.; Nguyen, T.; Cormier, S. A.; Lenkiewicz, E.; Colbert, D.; Rinaldi, L.; Ackerman, S. J.; Irvin, C. G.; Lee, N. A. *Science* **2004**, *305*, 1773-1776.
- (13) Giembycz, M. A.; Lindsay, M. A. *Pharmacol. Rev.* **1999**, *51*, 213-339.
- (14) Procopiou, P. A.; Barrett, V. J.; Bevan, N. J.; Butchers, P. R.; Conroy, R.; Emmons, A.; Ford, A. J.; Jeulin, S.; Looker, B. E.; Lunniss, G. E.; Morrison, V. S.; Mutch, P. J.; Perciaccante, R.; Ruston, M.; Smith, C. E.; Somers, G. *Bioorg. Med. Chem.* **2011**, *19*, 4192-4201.
- (15) Matthys, H. *Respiration* **2001**, *68*, 432-437.
- (16) Barnes, P. J.; Chung, K. F.; Page, C. P. *Pharmacol. Rev.* **1998**, *50*, 515-596.
- (17) Johnson, M.; Hagan, G. W. E. *Prog. Respir. Res.* **2001**, *31*, 60-63.
- (18) Pease, J. E.; Horuk, R. *Exp Op. Drug Discov.* **2014**, *9*, 467-483.
- (19) Charo, I. F.; Ransohoff, R. M. *N. Engl. J. Med.* **2006**, *354*, 610-621.
- (20) Zlotnik, A.; Yoshie, O. *Immunity* **2000**, *12*, 121-127.
- (21) Palmqvist, C.; Wardlaw, A. J.; Bradding, P. *Br. J. Pharmacol.* **2007**, *151*, 725-736.
- (22) Bachelierie, F.; Ben-Baruch, A.; Burkhardt, A. M.; Combadiere, C.; Farber, J. M.; Graham, G. J.; Horuk, R.; Sparre-Ulrich, A. H.; Massimo, L.; Luster, A. D.;

- Mantovani, A.; Matsushima, K.; Murphy, P. M.; Nibbs, R.; Nomiyama, H.; Power, C. A.; Proudfoot, A. E. I.; Rosenkilde, M. M.; Rot, A.; Sozzani, S.; Thelen, M.; Yoshie, O.; Zlotnik, A. *Pharmacol. Rev.* **2014**, *66*, 1-79.
- (23) MacArthur, R. D.; Novak, R. M. *Clin. Infect. Dis.* **2008**, *47*, 236-241.
- (24) Brave, M.; Farrell, A.; Ching Lin, S.; Ocheltree, T.; Pope Miksinski, S.; Lee, S. L.; Saber, H.; Fourie, J.; Tornoe, C.; Booth, B.; Yuan, W.; He, K.; Justice, R.; Pazdur, R. *Oncology* **2010**, *78*, 282-288.
- (25) Lieberman-Blum, S. S.; Fung, H. B.; Bandres, J. C. *Clin. Therap.* **2008**, *30*, 1228-1250.
- (26) Westby, M.; van der Ryst, E. *Antiviral Chem. Chemotherapy.* **2005**, *16*, 339-354.
- (27) Ray, N.; Doms, R. W. *Curr. Top. Microbiol. and Immunol.* **2006**, *303*, 97-120.
- (28) Wood, A.; Armour, D. *Prog. Med. Chem.* **2005**, *43*, 239-271.
- (29) Pease, J.; Horuk, R. *J. Med. Chem.* **2012**, *55*, 9363-9392.
- (30) Choi, W.-T.; Duggineni, S.; Xu, Y.; Huang, Z.; An, J. *J. Med. Chem.* **2012**, *55*, 977-994.
- (31) De Clercq, E. *Biochem. Pharmacol.* **2009**, *77*, 1655-1664.
- (32) Peled, A.; Grabovsky, V.; Habler, L.; Sandbank, J.; Arenzana-Seisdedos, F.; Petit, I.; Ben-Hur, H.; Lapidot, T.; Alon, R. *J. Clin. Invest.* **1999**, *104*, 1199-1211.
- (33) Broxmeyer, H. E.; Orschell, C. M.; Clapp, D. W.; Hangoc, G.; Cooper, S.; Plett, P. A.; Liles, W. C.; Li, X.; Graham-Evans, B.; Campbell, T. B.; Calandra, G.; Bridger, G.; Dale, D. C.; Srouf, E. F. *J. Exp. Med.* **2005**, *201*, 1307-1318.
- (34) Bahl, A. K.; Springthorpe, B.; Riley, R. *Prog. Resp. Res.* **2010**, *39*, 153-159.
- (35) Zhang, P.; Dairaghi, D. J.; Jaen, J. C.; Powers, J. P. *Ann. Rep. Med. Chem.* **2013**, *48*, 133-147.
- (36) Neighbour, H.; Boulet, L. P.; Lemiere, C.; Sehmi, R.; Leigh, R.; Sousa, A. R.; Martin, J.; Dallow, N.; Gilbert, J.; Allen, A.; Hall, D.; Nair, P. *Clin. Exp. Allergy* **2014**, *44*, 508-516.
- (37) Barnes, P. J. *Nat. Rev. Immunol.* **2008**, *8*, 183-192.
- (38) Takeda, A.; Baffi, J. Z.; Kleinman, M. E.; Cho, W. G.; Nozaki, M.; Yamada, K.; Kaneko, H.; Albuquerque, R. J. C.; Dridi, S.; Saito, K.; Raisler, B. J.; Budd, S. J.; Geisen, P.; Munitz, A.; Ambati, B. K.; Green, M. G.; Ishibashi, T.; Wright, J. D.; Humbles, A. A.; Gerard, C. J.; Ogura, Y.; Pan, Y.; Smith, J. R.; Grisanti, S.; Hartnett, M. E.; Rothenberg, M. E.; Ambati, J. *Nature* **2009**, *460*, 225-230.

- (39) Adamson, P.; Shima, D.; Ng, Y. S. E.; GlaxoSmithKline: WO 2013079696 A1, 6 Jun. 2013
- (40) Hughes, R. O.; Rogier, D. J.; Devraj, R.; Zheng, C.; Cao, G.; Feng, H.; Xia, M.; Anand, R.; Xing, L.; Glenn, J.; Zhang, K.; Covington, M.; Morton, P. A.; Hutzler, J. M.; Davis, J. W.; Scherle, P.; Baribaud, F.; Bahinski, A.; Mo, Z.-L.; Newton, R.; Metcalf, B.; Xue, C.-B. *Bioorg. Med. Chem. Lett.* **2011**, *21*, 2626-2630.
- (41) Subramaniam, J. M.; Whiteside, G.; McKeage, K.; Croxtall, J. C. *Drugs* **2012**, *72*, 1293-1298.
- (42) <http://ir.chemocentryx.com/releasedetail.cfm?ReleaseID=877222>;-ChemoCentryx announces (Oct 2014) positive phase 1 study of oral CCR9 antagonist, CCX507: accessed on 11/2014.
- (43) Sullivan, T. J.; Dairaghi, D. J.; Krasinski, A.; Miao, Z.; Wang, Y.; Zhao, B. N.; Baumgart, T.; Berahovich, R.; Ertl, L. S.; Pennell, A.; Seitz, L.; Miao, S.; Ungashe, S.; Wei, Z.; Johnson, D.; Boring, L.; Tsou, C. L.; Charo, I. F.; Bekker, P.; Schall, T. J.; Jaen, J. C. *J. Pharmacol. Exp. Ther.* **2012**, Accessed on Feb 2012. Authours have voluntarily withdrawn this manuscript from publication as the structure of CCX2140 could not be disclosed
- (44) Hanefeld, M.; Schell, E.; Gouni-Berthold, I.; Melichar, M.; Vesela, I.; Johnson, D.; Miao, S.; Sullivan, T. J.; Jaen, J. C.; Schall, T. J.; Bekker, P.; Huttenmeister, R.; Karrasch, J. *J. Diabetes. Met.* **2012**, *3*, 1-8.
- (45) <http://ir.chemocentryx.com/releasedetail.cfm?ReleaseID=887402>;-ChemoCentryx announces (Dec 2014) positive results in phase II diabetic nephropathy trial with CCR2 Inhibitor, CCX140: accessed on 12/2014.
- (46) Klarenbeek, A.; Maussang, D.; Blanchetot, C.; Saunders, M.; van der Woning, S.; Smit, M.; de Haard, H.; Hofman, E. *Drug Discov. Today: Technol.* **2012**, *9*, 237-244.
- (47) Ishida, T.; Iida, S.; Akatsuka, Y.; Ishii, T.; Miyazaki, M.; Komatsu, H.; Inagaki, H.; Okada, N.; Fujita, T.; Shitara, K.; Akinaga, S.; Takahashi, T.; Utsunomiya, A.; Ueda, R. *Clin. Cancer Res.* **2004**, *10*, 7529-7539.
- (48) Ishida, T.; Joh, T.; Uike, N.; Yamamoto, K.; Utsunomiya, A.; Yoshida, S.; Saburi, Y.; Miyamoto, T.; Takemoto, S.; Suzushima, H.; Tsukasaki, K.; Nosaka, K.; Fujiwara, H.; Ishitsuka, K.; Inagaki, H.; Ogura, M.; Akinaga, S.; Tomonaga, M.; Tobinai, K.; Ueda, R. *J. Clin. Oncol.* **2012**, *30*, 837-842.
- (49) Owen, C. *Pulm. Pharmacol. Ther.* **2001**, *14*, 193-202.

- (50) Perros, F.; Hoogsteden, H. C.; Coyle, A. J.; Lambrecht, B. N.; Hammad, H. *Allergy* **2009**, *64*, 995-1002.
- (51) Vijayanand, P.; Durkin, K.; Hartmann, G.; Morjaria, J.; Seumois, G.; Staples, K. J.; Hall, D.; Bessant, C.; Bartholomew, M.; Howarth, P. H.; Friedmann, P. S.; Djukanovic, R. *J. Immunol.* **2010**, *184*, 4568-4574.
- (52) Kawasaki, S.; Takizawa, H.; Yoneyama, H.; Nakayama, T.; Fujisawa, R.; Izumizaki, M.; Imai, T.; Yoshie, O.; Homma, I.; Yamamoto, K.; Matsushima, K. *J. Immunol.* **2001**, *166*, 2055-2062.
- (53) Reiss, Y.; Proudfoot, A. E.; Power, C. A.; Campbell, J. J.; Butcher, E. C. *J. Exp. Med.* **2001**, *194*, 1541-1547.
- (54) Hartl, D.; Buckland, K. F.; Hogaboam, C. M. *Inflammation & Allergy Drug Targets* **2006**, *5*, 219-228.
- (55) Yuan, Q.; Bromley, S. K.; Means, T. K.; Jones, K. J.; Hayashi, F.; Bhan, A. K.; Luster, A. D. *J. Exp. Med.* **2007**, *204*, 1327-1334.
- (56) Purandare, A. V.; Somerville, J. E. *Curr. Top. Med. Chem.* **2006**, *6*, 1335-1344.
- (57) Procopiou, P. A.; Barton, N. P.; Barrett, V. J.; Begg, M.; Clapham, D.; Copley, R. C. B.; Graves, R. H.; Ford, A. J.; Hall, D. A.; Hancock, A. P.; Hill, A. P.; Hobbs, H.; Hodgson, S. T.; Jumeaux, C.; Lacroix, Y. M. L.; Miah, A. H.; Morriss, K. M. L.; Needham, D.; Sheriff, E. B.; Slack, R. J.; Smith, C. E.; Sollis, S. L.; Hugo, S. *J. Med. Chem.* **2013**, *56*, 1946-1960.
- (58) Purandare, A. V.; Wan, H.; Somerville, J. E.; Burke, C.; Vaccaro, W.; Yang, X.; McIntyre, K. W.; Poss, M. A. *Bioorg. Med. Chem. Lett.* **2007**, *17*, 679-682.
- (59) Yokoyama, K.; Ishikawa, N.; Igarashi, S.; Kawano, N.; Masuda, N.; Hamaguchi, W.; Yamasaki, S.; Koganemaru, Y.; Hattori, K.; Miyazaki, T.; Ogino, S.-i.; Matsumoto, Y.; Takeuchi, M.; Ohta, M. *Bioorg. Med. Chem.* **2009**, *17*, 64-73.
- (60) Baxter, A.; Johnson, T.; Kindon, N.; Roberts, B.; Steele, J.; Stocks, M.; Tomkinson, N.; AstraZeneca: WO 2003051870 A1, 26 June 2003.
- (61) Cahn, A.; Hodgson, S. T.; Wilson, R.; Robertson, J.; Watson, J.; Beerah, M.; Hughes, S. C.; Young, G.; Graves, R.; Hall, D.; Van Marle, S.; Solari, R. *BMC Pharmacology and Toxicology* **2013**, *14*, 1-14.
- (62) Procopiou, P. A.; Ford, A. J.; Graves, R. H.; Hall, D. A.; Hodgson, S. T.; Lacroix, Y. M. L.; Needham, D.; Slack, R. J. *Bioorg. Med. Chem. Lett.* **2012**, *22*, 2730-2733.

- (63) Palczewski, K.; Kumasaka, T.; Hori, T.; Behnke, C. A.; Motoshima, H.; Fox, B. A.; Le Trong, I.; Teller, D. C.; Okada, T.; Stenkamp, R. E.; Yamamoto, M.; Miyano, M. *Science* **2000**, *289*, 739-745.
- (64) Rasmussen, S. G. F.; Choi, H. J.; Rosenbaum, D. M.; Kobilka, T. S.; Thian, F. S.; Edwards, P. C.; Burghammer, M.; Ratnala, V. R. P.; Sanishvili, R.; Fischetti, R. F.; Schertler, G. F. X.; Weis, W. I.; Kobilka, B. K. *Nature* **2007**, *450*, 383-387.
- (65) Warne, T.; Moukhametzianov, R.; Baker, J. G.; Nehme, R.; Edwards, P. C.; Leslie, A. G. W.; Schertler, G. F. X.; Tate, C. G. *Nature* **2011**, *469*, 241-244.
- (66) Tan, Q.; Zhu, Y.; Li, J.; Chen, Z.; Han, G. W.; Kufareva, I.; Li, T.; Ma, L.; Fenalti, G.; Zhang, W.; Xie, X.; Yang, H.; Jiang, H.; Cherezov, V.; Liu, H.; Stevens, R. C.; Zhao, Q.; Wu, B. *Science* **2013**, *341*, 1387-1390.
- (67) Andrews, G.; Jones, C.; Wreggett, K. A. *Mol. Pharmacol.* **2008**, *73*, 855-867.
- (68) Slack, R. J.; Russell, L. J.; Nalesso, G.; Thompson, S. A.; Chen, Y. H.; Barnes, A.; Hall, D. A.; Barton, N. P.; Weston, C.; Allen, M.; Hodgson, S. T. *Pharmacol. Res. Per.* **2013**, *1*, 1-25.
- (69) Salchow, K.; Bond, M. E.; Evans, S. C.; Press, N. J.; Charlton, S. J.; Hunt, P. A.; Bradley, M. E. *Br. J. Pharmacol.* **2010**, *159*, 1429-1439.
- (70) Scholten, D. J.; Canals, M.; Maussang, D.; Roumen, L.; Smit, M. J.; Wijtmans, M.; de Graaf, C.; Vischer, H. F.; Leurs, R. *Br. J. Pharmacol.* **2012**, *165*, 1617-1643.
- (71) Nakagami, Y.; Kawase, Y.; Yonekubo, K.; Nosaka, E.; Etori, M.; Takahashi, S.; Takagi, N.; Fukuda, T.; Kuribayashi, T.; Nara, F.; Yamashita, M. *Biol. Pharm. Bull.* **2010**, *33*, 1067-1069.
- (72) Wang, X.; Xu, F.; Xu, Q.; Mahmud, H.; Houze, J.; Zhu, L.; Akerman, M.; Tonn, G.; Tang, L.; McMaster, B. E.; Dairaghi, D. J.; Schall, T. J.; Collins, T. L.; Medina, J. C. *Bioorg. Med. Chem. Lett.* **2006**, *16*, 2800-2803.
- (73) Purandare, A. V.; Wan, H.; Gao, A.; Somerville, J.; Burke, C.; Vaccaro, W.; Yang, X.; McIntyre, K. W.; Poss, M. A. *Bioorg. Med. Chem. Lett.* **2006**, *16*, 204-207.
- (74) Gong, H.; Qi, H.; Sun, W.; Zhang, Y.; Jiang, D.; Xiao, J.; Yang, X.; Wang, Y.; Li, S. *Molecules* **2012**, *17*, 9961-9970.
- (75) Yokoyama, K.; Ishikawa, N.; Igarashi, S.; Kawano, N.; Hattori, K.; Miyazaki, T.; Ogino, S.-i.; Matsumoto, Y.; Takeuchi, M.; Ohta, M. *Bioorg. Med. Chem.* **2008**, *16*, 7021-7032.
- (76) Toru, K.; Noriyuki, K.; Naoyuki, M.; Koji, K.; Hiroshi, N.; Hiroshi, I.; Tadashi, T.; Kazuhiro, Y.; Takahiro, M.; Astellas Pharma Inc.: WO 2007111227, 24 Oct 2007.

- (77) Hodgson, S. T.; Lacroix, Y. M.; Procopiou, P. A.; GlaxoSmithKline: WO 2010097395 A1, 2 Sept. 2010.
- (78) Habashita, H.; Kokubo, M.; Shibayama, S.; Tada, H.; Sagawa, K.; Ono Pharmaceutical Co.: WO 20030708, 2004.
- (79) Zweemer, A. J. M.; Nederpelt, I.; Vrieling, H.; Hafith, S.; Doornbos, M. L. J.; de Vries, H.; Abt, J.; Gross, R.; Stamos, D.; Saunders, J.; Smit, M. J.; IJzerman, A. P.; Heitman, L. H. *Mol. Pharmacol.* **2013**, *84*, 551-561.
- (80) Hall, S. E.; Mao, A.; Nicolaidou, V.; Finelli, M.; Wise, E. L.; Nedjai, B.; Kanjanapangka, J.; Harirchian, P.; Chen, D.; Selchau, V.; Ribeiro, S.; Schyler, S.; Pease, J. E.; Horuk, R.; Vaidehi, N. *Mol. Pharmacol.* **2009**, *75*, 1325-1336.
- (81) Allegretti, M.; Bertini, R.; Bizzarri, C.; Beccari, A.; Mantovani, A.; Locati, M. *Trends in Pharmacological Sciences* **2008**, *29*, 280-286.
- (82) Carter, P. H.; Tebben, A. J. *Methods in Enzymol.* **2009**, *461*, 249-279.
- (83) Nicholls, D. J.; Tomkinson, N. P.; Wiley, K. E.; Brammall, A.; Bowers, L.; Grahames, C.; Gaw, A.; Meghani, P.; Shelton, P.; Wright, T. J.; Mallinder, P. R. *Mol. Pharmacol.* **2008**, *74*, 1193-1202.
- (84) Browning, C.; Chowdhury, F.; Chen, Y. H.; Gordon, L.; Powney, B.; Rowedder, J.; Slack, R. J. *GlaxoSmithKline*.
- (85) Begg, M.; Hall, D. A.; Pun, T. *GlaxoSmithKline*.
- (86) Leeson, P. D.; Springthorpe, B. *Nat. Rev. Drug Disc.* **2007**, *6*, 881-890.
- (87) Hopkins, A. L.; Groom, C. R.; Alex, A. *Drug Discov. Today* **2004**, *9*, 430-431.
- (88) Mortenson, P. N.; Murray, C. W. *J. Comput.-Aided Mol. Des.* **2011**, *25*, 663-667.
- (89) Young, R. J.; Green, D. V. S.; Luscombe, C. N.; Hill, A. P. *Drug Discov. Today* **2011**, *16*, 822-830.
- (90) Brunally, S.; Hill, A. P.; Reid, I.; Clara, V. *GlaxoSmithKline*.
- (91) Leeson, P. D.; Empfield, J. R. *Ann. Rep. Med. Chem.* **2010**, *45*, 393-407.
- (92) Hann, M. M.; Keserü, G. M. *Nat. Rev. Drug. Discov.* **2012**, *11*, 355-365.
- (93) Lipinski, C. A. *Drug Discov. Today: Technol.* **2004**, *1*, 337-341.
- (94) Bemis, G. W.; Murcko, M. A. *J. Med. Chem.* **1996**, *39*, 2887-2893.
- (95) Barnett, H. *GlaxoSmithKline* **2011**, Unpublished Work.
- (96) Zinic, B.; Krizmanic, I.; Vikic-Topic, D.; Srzic, D.; Zinic, M. *Croat. Chem. Acta* **2001**, *74*, 399-414.
- (97) Megati, S.; Phadtare, S.; Zemlicka, J. *J. Org. Chem.* **1992**, *57*, 2320-2327.

- (98) Lambertucci, C.; Antonini, I.; Buccioni, M.; Ben, D. D.; Kachare, D. D.; Volpini, R.; Klotz, K.-N.; Cristalli, G. *Bioorg. Med. Chem.* **2009**, *17*, 2812-2822.
- (99) Van Zandt, M. C.; Sibley, E. O.; McCann, E. E.; Combs, K. J.; Flam, B.; Sawicki, D. R.; Sabetta, A.; Carrington, A.; Sredy, J.; Howard, E.; Mitschler, A.; Podjarny, A. D. *Bioorg. Med. Chem.* **2004**, *12*, 5661-5675.
- (100) Harter, W. G.; Albrecht, H.; Brady, K.; Caprathe, B.; Dunbar, J.; Gilmore, J.; Hays, S.; Kostlan, C. R.; Lunney, B.; Walker, N. *Bioorg. Med. Chem. Lett.* **2004**, *14*, 809-812.
- (101) Kuhn, B.; Mohr, P.; Stahl, M. *J. Med. Chem.* **2010**, *53*, 2601-2611.
- (102) Sasaki, S.; Cho, N.; Nara, Y.; Harada, M.; Endo, S.; Suzuki, N.; Furuya, S.; Fujino, M. *J. Med. Chem.* **2003**, *46*, 113-124.
- (103) Miah, A. H.; Copley, R. C. B.; O'Flynn, D.; Percy, J. M.; Procopiou, P. A. *Org. Biomol. Chem.* **2014**, *12*, 1779-1792.
- (104) Percy, J. M. *University of Strathclyde* **2014**.
- (105) Boehr, D. D.; Farley, A. R.; LaRonde, F. J.; Murdock, T. R.; Wright, G. D.; Cox, J. R. *Biochemistry* **2005**, *44*, 12445-12453.
- (106) Steglich, W.; Hoefle, G. *Angew. Chem., Int. Ed. Engl.* **1969**, *8*, 981.
- (107) Spivey, A. C.; Fekner, T.; Spey, S. E. *J. Org. Chem.* **2000**, *65*, 3154-3159.
- (108) Priem, G.; Pelotier, B.; Macdonald, S. J. F.; Anson, M. S.; Campbell, I. B. *J. Org. Chem.* **2003**, *68*, 3844-3848.
- (109) Hamblin, J. N.; Angell, T. D. R.; Ballantine, S. P.; Cook, C. M.; Cooper, A. W. J.; Dawson, J.; Delves, C. J.; Jones, P. S.; Lindvall, M.; Lucas, F. S.; Mitchell, C. J.; Neu, M. Y.; Ranshaw, L. E.; Solanke, Y. E.; Somers, D. O.; Wiseman, J. O. *Bioorg. Med. Chem. Lett.* **2008**, *18*, 4237-4241.
- (110) Vaultier, M.; Knouzi, N.; Carrie, R. *Tetrahedron Lett.* **1983**, *24*, 763-764.
- (111) Dupouy, G.; Marchivie, M.; Triki, S.; Sala-Pala, J.; Salaun, J.-Y.; Gomez-Garcia, C. J.; Guionneau, P. *Inorg. Chem.* **2008**, *47*, 8921-8931.
- (112) Bulawa, C. E.; Devit, M.; Elbaum, D.; FoldRx Pharmaceuticals, Inc.: WO 2009062118 A2, 14 May 2009.
- (113) Middleton, W. J.; Engelhardt, V. A. *J. Am. Chem. Soc.* **1958**, *80*, 2788-2795.
- (114) Wolter, M.; Nordmann, G.; Job, G. E.; Buchwald, S. L. *Org. Lett.* **2002**, *4*, 973-976.
- (115) Altman, R. A.; Shafir, A.; Choi, A.; Lichtor, P. A.; Buchwald, S. L. *J. Org. Chem.* **2008**, *73*, 284-286.
- (116) Naidu, A. B.; Sekar, G. *Tetrahedron Lett.* **2008**, *49*, 3147-3151.
- (117) Zhang, H.; Ma, D.; Cao, W. *Synlett* **2007**, 243-246.

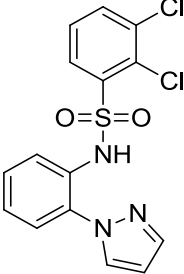
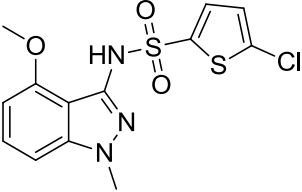
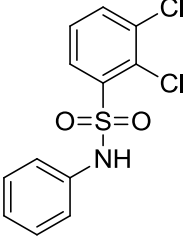
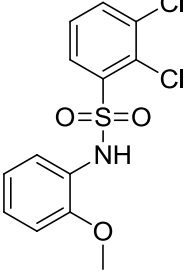
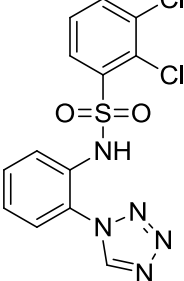
- (118) Chang, J. W. W.; Xu, X.; Chan, P. W. H. *Tetrahedron Lett.* **2007**, *48*, 245-248.
- (119) Ley, S. V.; Thomas, A. W. *Angew. Chem., Int. Ed.* **2003**, *42*, 5400-5449.
- (120) Monnier, F.; Taillefer, M. *Angew. Chem., Int. Ed.* **2009**, *48*, 6954-6971.
- (121) Antilla, J. C.; Baskin, J. M.; Barder, T. E.; Buchwald, S. L. *J. Org. Chem.* **2004**, *69*, 5578-5587.
- (122) Anderson, K. W.; Ikawa, T.; Tundel, R. E.; Buchwald, S. L. *J. Am. Chem. Soc.* **2006**, *128*, 10694-10695.
- (123) Shi, A.; Nguyen, T. A.; Battina, S. K.; Rana, S.; Takemoto, D. J.; Chiang, P. K.; Hua, D. H. *Bioorg. Med. Chem. Lett.* **2008**, *18*, 3364-3368.
- (124) Iley, J.; Carvalho, E.; Norberto, F.; Rosa, E. *J. Chem. Soc., Perkin Trans. 2* **1992**, 281-289.
- (125) Lu, Y.; Li, Y.; Zhang, R.; Jin, K.; Duan, C. *Tetrahedron* **2013**, *69*, 9422-9427.
- (126) Green, T. W.; Wuts, P. G. M. *Protective Groups in Organic Synthesis*; 2nd ed.; John Wiley and Sons: New York, 1991.
- (127) Bomhard, E. M.; Herbold, B. A. *Crit. Rev. Toxicol.* **2005**, *35*, 783-835.
- (128) Culshaw Janet, D.; Eden, J. M.; Ford, S. J.; Hayter, B.; Perkins, D. R.; Pike, K. G. *Synlett* **2012**, *23*, 1816-1820.
- (129) Lemoine, R. C.; Petersen, A. C.; Setti, L.; Jekle, A.; Heilek, G.; de Rosier, A.; Ji, C.; Berry, P.; Rotstein, D. M. *Bioorg. Med. Chem. Lett.* **2010**, *20*, 4753-4756.
- (130) Bittner, A. R.; Sinz, C. J.; Chang, J.; Kim, R. M.; Mirc, J. W.; Parmee, E. R.; Tan, Q.; Merck & Co.: WO2009032249 A1, 12 Mar. 2009.
- (131) Smith, C. J.; Ali, A.; Chen, L.; Hammond, M. L.; Anderson, M. S.; Chen, Y.; Eveland, S. S.; Guo, Q.; Hyland, S. A.; Milot, D. P.; Sparrow, C. P.; Wright, S. D.; Sinclair, P. J. *Bioorg. Med. Chem. Lett.* **2010**, *20*, 346-349.
- (132) Barrett, J.; Eddershaw, P.; Graves, R. *GlaxoSmithKline* **2012**, Unpublished work.
- (133) Cheng, C. C.; Robins, R. K. *J. Org. Chem.* **1958**, *23*, 852-861.
- (134) Joule, J. A.; Mills, K. *Heterocyclic Chemistry*; 4th ed.; Blackwell, 2000.
- (135) Senga, K.; Robins, R. K. *J. Heterocycl. Chem.* **1982**, *19*, 1565-1567.
- (136) Link, W.; Oyarzabal, J.; Serelde, B. G.; Albarran, M. I.; Rabal, O.; Cebria, A.; Alfonso, P.; Fominaya, J.; Renner, O.; Peregrina, S.; Soilan, D.; Ceballos, P. A.; Hernandez, A.-I.; Lorenzo, M.; Pevarello, P.; Granda, T. G.; Kurz, G.; Carnero, A.; Bischoff, J. R. *J. Biol. Chem.* **2009**, *284*, 28392-28400.
- (137) Peet, N. P.; Lentz, N. L.; Sunder, S.; Dudley, M. W.; Ogden, A. M. L. *J. Med. Chem.* **1992**, *35*, 3263-3269.

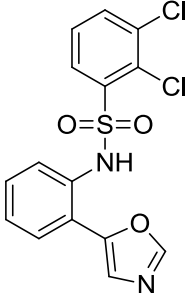
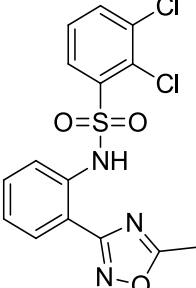
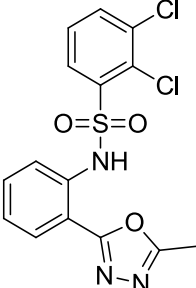
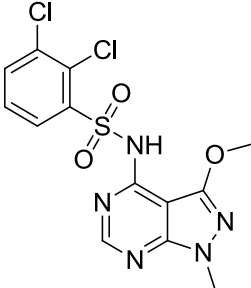
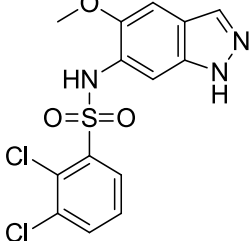
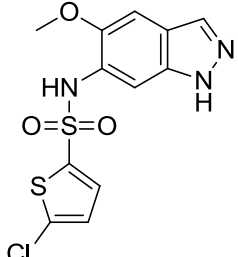
- (138) Mao, Y.; Lin, N.; Tian, W.; Han, X.; Han, X.; Huang, Z.; An, J. *J. Med. Chem.* **2012**, *55*, 1346-1359.
- (139) Nagashima, S.; Nagata, H.; Iwata, M.; Yokota, M.; Moritomo, H.; Orita, M.; Kuromitsu, S.; Koakutsu, A.; Ohga, K.; Takeuchi, M.; Ohta, M.; Tsukamoto, S.-i. *Bioorg. Med. Chem.* **2008**, *16*, 6509-6521.
- (140) Cantin, L.-D.; Liang, S.; Ogutu, H.; Iwuagwu, C. I.; Boakye, K.; Bullock, W. H.; Burns, M.; Clark, R.; Claus, T.; delaCruz, F. E.; Daly, M.; Ehrgott, F. J.; Johnson, J. S.; Keiper, C.; Livingston, J. N.; Schoenleber, R. W.; Shapiro, J.; Town, C.; Yang, L.; Tsutsumi, M.; Ma, X. *Bioorg. Med. Chem. Lett.* **2007**, *17*, 1056-1061.
- (141) McNaughton-Smith, G. A.; Amato, G. S.; Fritch, P. C.; Icagen, Inc., USA.: WO 2003068767 A1, 21 Aug. 2003.
- (142) Guibe, F. *Tetrahedron* **1998**, *54*, 2967-3042.
- (143) Escoubet, S.; Gastaldi, S.; Bertrand, M. *Eur. J. Org. Chem.* **2005**, 3855-3873.
- (144) Cadierno, V.; Gimeno, J.; Nebra, N. *Chem. Eur. J.* **2007**, *13*, 6590-6594.
- (145) Walker, D. K.; Dack, K. N.; Dickinson, R. P.; Fenner, K. S.; James, K.; Rawson, D. J.; Smith, D. A. *Drug Metab. Dispos.* **2001**, *29*, 1424-1431.
- (146) Von Geldern, T. W.; Hoffman, D. J.; Kester, J. A.; Nellans, H. N.; Dayton, B. D.; Calzadilla, S. V.; Marsh, K. C.; Hernandez, L.; Chiou, W. *J. Med. Chem.* **1996**, *39*, 982-991.
- (147) Wuitschik, G.; Carreira, E. M.; Wagner, B.; Fischer, H.; Parrilla, I.; Schuler, F.; Rogers-Evans, M.; Muller, K. *J. Med. Chem.* **2010**, *53*, 3227-3246.
- (148) Clark, G. J.; Deady, L. W. *Aust. J. Chem.* **1981**, *34*, 927-932.
- (149) Barraclough, P.; Black, J. W.; Cambridge, D.; Collard, D.; Firmin, D.; Gerskowitch, V. P.; Glen, R. C.; Giles, H.; Hill, A. P. *J. Med. Chem.* **1990**, *33*, 2231-2239.
- (150) Yokoyama, K.; Ishikawa, N.; Igarashi, S.; Kawano, N.; Masuda, N.; Hattori, K.; Miyazaki, T.; Ogino, S.-i.; Orita, M.; Matsumoto, Y.; Takeuchi, M.; Ohta, M. *Bioorg. Med. Chem.* **2008**, *16*, 7968-7974.
- (151) Gleeson, M. P. *J. Med. Chem.* **2008**, *51*, 817-834.
- (152) Zhu, L.; Zhao, Q.; Wu, B. *Curr. Op. Struct. Bio.* **2013**, *23*, 539-546.
- (153) Jacobson, K. A.; Costanzi, S. *Mol. Pharmacol.* **2012**, *82*, 361-371.
- (154) Warne, T.; Moukhametzianov, R.; Baker, J. G.; Nehme, R.; Edwards, P. C.; Leslie, A. G. W.; Schertler, G. F. X.; Tate, C. G. *Nature* **2011**, *469*, 241-244.
- (155) Barton, N. P. *GlaxoSmithKline* **2013**, Unpublished Work.
- (156) Costanzi, S. *Methods Mol. Biol.* **2012**, *857*, 259-279.

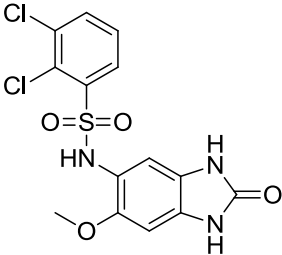
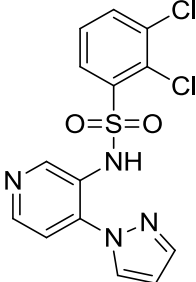
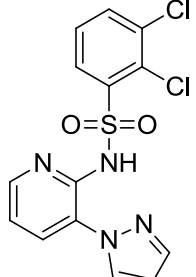
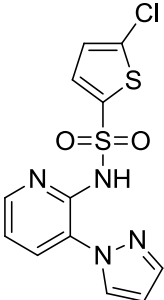
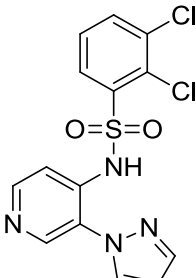
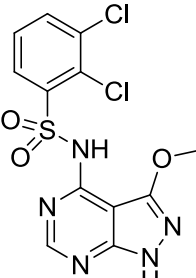
- (157) Hanson, M. A.; Stevens, R. C. *Structure* **2009**, *17*, 8-14.
- (158) Deng, S.; Taunton, J. *J. Am. Chem. Soc.* **2002**, *124*, 916-917.
- (159) Croft, A. K.; Foley, M. K. *Org. Biomol. Chem.* **2008**, *6*, 1594-1600.
- (160) Dugave, C.; Demange, L. *Chem. Rev.* **2003**, *103*, 2475-2532.
- (161) Mohamed, T.; Zhao, X.; Habib, L. K.; Yang, J.; Rao, P. P. N. *Bioorg. Med. Chem.* **2011**, *19*, 2269-2281.
- (162) Bregman, H.; Berry, L.; Buchanan, J. L.; Chen, A.; Du, B.; Feric, E.; Hierl, M.; Huang, L.; Immke, D.; Janosky, B.; Johnson, D.; Li, X.; Ligutti, J.; Liu, D.; Malmberg, A.; Matson, D.; McDermott, J.; Miu, P.; Nguyen, H. N.; Patel, V. F.; Waldon, D.; Wilenkin, B.; Zheng, X. M.; Zou, A.; McDonough, S. I.; DiMauro, E. F. *J. Med. Chem.* **2011**, *54*, 4427-4445.
- (163) Purandare, A. V.; Gao, A.; Wan, H.; Somerville, J.; Burke, C.; Seachord, C.; Vaccaro, W.; Wityak, J.; Poss, M. A. *Bioorg. Med. Chem. Lett.* **2005**, *15*, 2669-2672.
- (164) Shula, L. *GlaxoSmithKline* **2011**, Unpublished Work.
- (165) Veber, D. F.; Johnson, S. R.; Cheng, H.-Y.; Smith, B. R.; Ward, K. W.; Kopple, K. D. *J. Med. Chem.* **2002**, *45*, 2615-2623.
- (166) Scott, J. S.; Berry, D. J.; Brown, H. S.; Buckett, L.; Clarke, D. S.; Goldberg, K.; Hudson, J. A.; Leach, A. G.; MacFaul, P. A.; Raubo, P.; Robb, G. *MedChemComm* **2013**, *4*, 1305-1311.
- (167) Mariani, M.; Lang, R.; Binda, E.; Panina-Bordignon, P.; D'Ambrosio, D. *Eur. J. Immunol.* **2004**, *34*, 231-240.
- (168) Ajram, L.; Begg, M.; Slack, R.; Cryan, J.; Hall, D.; Hodgson, S.; Ford, A.; Barnes, A.; Swieboda, D.; Mousnier, A.; Solari, R. *Eur. J. Pharmacol.* **2014**, *729*, 75-85.
- (169) Sato, T.; Iwase, M.; Miyama, M.; Komai, M.; Ohshima, E.; Asai, A.; Yano, H.; Miki, I. *Pharmacol.* **2013**, *91*, 305-313.
- (170) Howard, O. M.; Korte, T.; Tarasova, N. I.; Grimm, M.; Turpin, I. A.; Rice, W. G.; Michejda, C. J.; Blumenthal, R.; Oppenheim, J. J. *J. Leukoc. Biol.* **1998**, *64*, 6-13.
- (171) Ford, A.; Begg, M.; Slack, R. J. *GlaxoSmithKline* **2014**, Unpublished Work.
- (172) Ford, A.; Haase, M. *GlaxoSmithKline* **2014**, Unpublished Work.
- (173) Dearman, R. J.; Kimber, I. *Immunol.* **2000**, *101*, 442-451.
- (174) Teixeira, M. M.; Wells, T. N. C.; Lukacs, N. W.; Proudfoot, A. E. I.; Kunkel, S. L.; Williams, T. J.; Hellewell, P. G. *J. Clin. Invest.* **1997**, *100*, 1657-1666.
- (175) Liu, H.-J.; Hung, S.-F.; Chen, C.-L.; Lin, M.-H. *Tetrahedron* **2013**, *69*, 3907-3912.

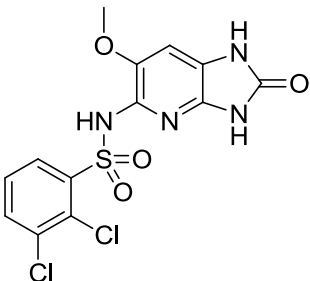
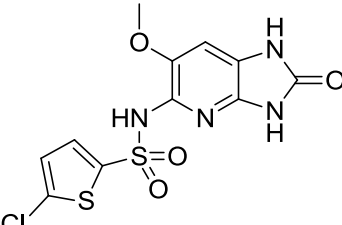
Appendix 1

Correlation of measured pK_a with ACD v.12 calculated pK_a .

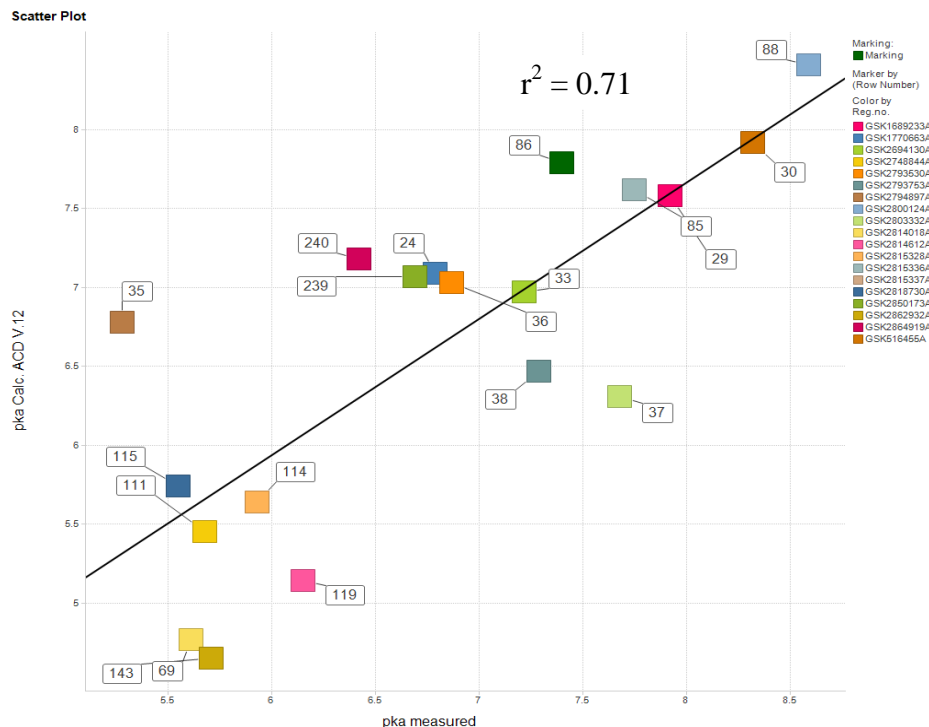
Compound no.	Structure	pK_a Calc. ACD V.12	pK_a measured
33	 <chem>Clc1cc(Cl)ccc1NS1=CN=C1</chem>	6.97	7.22
27	 <chem>COC1=CC=C(C=C1)N2C=NC(C2)S(=O)(=O)C3=CC(=C(S3)Cl)</chem>	7.39	6.79
29	 <chem>Clc1cc(Cl)ccc1NS(=O)(=O)c2ccccc2</chem>	7.58	7.92
30	 <chem>Clc1cc(Cl)ccc1NS(=O)(=O)c2cc(OC)ccc2</chem>	7.92	8.32
35	 <chem>Clc1cc(Cl)ccc1NS(=O)(=O)c2ccccc2N3=NN=CN3</chem>	6.78	5.28

36		7.03	6.87
37		6.31	7.68
38		6.47	7.29
69		4.77	5.61
85		7.62	7.75
86		7.79	7.4

88		8.41	8.59
111		5.45	5.68
114		5.64	5.93
115		5.74	5.55
119		5.14	6.15
143		4.65	5.71

239		7.07	6.69
240		7.18	6.42

Graph showing a good trend between measured pK_a with ACD v.12 calculated pK_a . The graph yields an r^2 value of 0.71 with a fairly good correlation. It should be noted that there are a few points on the graph, which show a large deviation between measured and calculated pK_a . For example, compounds **35**, **37**, **69**, **119** and **143** have greater than a log unit difference between measured and calculated pK_a .



Appendix 2

The sequence alignment of CCR4 with bovine rhodopsin (1F88). The highlighted sections are the seven transmembrane region of the two different GPCR.

Consensus	5 10 15 20 25 30 35 40 45 50	MNGTEGPNFYVPFSNKTGYVVRSPFEAPQYYLAEPWQFSMLAAYMFLLIMLG
1F88:1		MNGTEGPNFYVPFSNKTG · · VVRSPFEAPQYYLAEPWQFSMLAAYMFLLIMLG
CCR4h:4		MNPTDIADTTLDES IYSNYYLYES I PKPCTKEG I KAFGELFLPPLYSLVFVFG
Consensus	58 63 68 73 78 83 88 93 98 103	FPINFLTLYVTVQHKKLRTPLNY I LLNLAVADLFMVFGGFTTTLYTSLHGYFV
1F88:1		FPINFLTLYVTVQHKKLRTPLNY I LLNLAVADLFMVFGGFTTTLYTSLHGYFV
CCR4h:4		LLGNSVVVLLVLFKYKRLRSMTDVYLLNLA I SDLLFVFSLPFWGYAADQ · · WV
Consensus	111 116 121 126 131 136 141 146 151 156	FGPTGCNLEGGFATLGG E I ALWSLVLLA I ERYVVVCKPMSNFRFGTENHAIMG
1F88:1		FGPTGCNLEGGFATLGG E I ALWSLVLLA I ERYVVVCKPMSNFRFG · ENHAIMG
CCR4h:4		FGLGLCKM I SWMYLVGFYSG I FVVMLMS I DRYLA I VHAVFSLRARTLT YGVIT
Consensus	164 169 174 179 184 189 194 199 204 209	VAF TWMALACAAPPLVGWSRY I PEGMQCSCG I DYYTPHEETNNESFV I YMFV
1F88:1		VAF TWMALACAAPPLVGWSRY I PEGMQCSCG I DYYTPHEETNNESFV I YMFV
CCR4h:4		SLATWSVAVFASLPGEL · FSTCYTERNHTYCKTKY · SLNSTTWKVLSSLEINI
Consensus	217 222 227 232 237 242 247 252 257 262	VHFI I PLIV I FFCY GQLVFTVKEAAAQQQESATTQKAEKEVTRMVI I MVIAFL
1F88:1		VHFI I PLIV I FFCY GQLVFTVKEAAAQQQESATTQKAEKEVTRMVI I MVIAFL
CCR4h:4		I GLV I PLG I M LFCYSM I I RTLQHCKNEKKN · · · · · KAVKMIFAVVVLEL
Consensus	270 275 280 285 290 295 300 305 310 315	ICWLPYAGVAFY I FTHQLEVLQDCTGSDFGPI FMT I PAFFAKTSAVYNPVIY I
1F88:1		ICWLPYAGVAFY I FTHQ · · · · · GSDFGPI FMT I PAFFAKTSAVYNPVIY I
CCR4h:4		GEWTPYNI V LFL ETL V E L V L Q D C T F E R Y L D Y A I Q A T E T L A F V H C C L N P I I Y F
Consensus	323 328 333 338 341 348 351 358 363 368	MMNKQFRNCMVTT LCCGKNPLGDDEASTTVSKTETSQVAPAYTQSTMDHDLHD
1F88:1		MMNKQFRNCMVTT LCCGKNPLGDDEASTTVSKTETSQVAPA
CCR4h:4		FLGEKFRKY I LQLFKTCRGLFVLCQYCGLLQIYSADTPSSSYTQSTMDHDLHD
Consensus	376 381 386 391 396 401 406 411 416 421	AL
1F88:1		
CCR4h:4		A L